PALLADIUM-CATALYZED DIRECT REGIOSELECTIVE C–H ACYLATION OF OXIMES AND ANILIDES AND COPPER-CATALYZED TRICHLOROMETHYLATION OF *N*-ARYL-ACRYLAMIDES

CHAN CHUN WO

Ph.D

The Hong Kong Polytechnic University

2015

The Hong Kong Polytechnic University

Department of Applied Biology and Chemical Technology

Palladium-Catalyzed Direct Regioselective C–H Acylation of Oximes and Anilides and Copper-Catalyzed Trichloromethylation of *N*-Aryl-Acrylamides

CHAN Chun Wo

A thesis submitted in partial fulfillment

of the requirements for the degree of

Doctor of Philosophy

December 2014

CERTIFICATION OF ORIGINALITY

I hereby declare that this thesis is my own work and that, to the best of my knowledge and belief, it reproduces no material previously published or written, nor material that has been accepted for the award of any other degree or diploma, except where due acknowledgement has been made in the text.

_____

CHAN Chun Wo

ABSTRACT

Abstract of the thesis entitled

Palladium-Catalyzed Direct Regioselective C–H Acylation of Oximes and Anilides and Copper-Catalyzed Trichloromethylation of *N*-Aryl-Acrylamides

Submitted by CHAN Chun Wo

for the degree of Doctor of Philosophy

at The Hong Kong Polytechnic University in Demcember 2014

Palladium-catalyzed *ortho*-selective arene C–H functionalizations are promising approach for developing sustainable organic synthesis. Most successful examples involve alkenes/alkynes and organometallic reagents for C–C bond formation. This thesis explores the catalytic coupling of arenes with aldehydes and chloroform for regioselective C–C bond formation. Our study showed the principal step involves transforming the aldehydes and chloroform to carboradicals, which are key intermediates for the coupling reactions.

To begin, direct acylation of acetophenones with aldehydes to afford 1,2-diacylbenzenes was examined. Treating acetophenone *O*-methyloxime with

4-chlorobenzaldehyde (**2a**), TBHP and $Pd(OAc)_2$ (5 mol%) in toluene at 100 ^oC furnished the desired benzophenone (**3a**) in 71% yield. This acylation reaction exhibits excellent *ortho*-selectivity; functional groups such as methoxy, sulfonyl, halogen and amide were tolerated. Apart from benzaldehyde, aliphatic and heteroaromatic aldehydes are also effective partners with 55-95% product yields being achieved. In this work, **3a** was deoximinated to give diketone (**4a**) which was converted to phthalazines - a medicinally useful heterocycle.

The related *ortho*-selective acylation of anilides was examined for synthesis of 2-aminobenzophenones. Treating *N*-pivalanilides (**6a**) with 4-chlorobenzaldehyde, TBHP, TFA (1 equiv) and $Pd(OAc)_2$ (5 mol%) in toluene at 40 ^oC for 3 h, produced the corresponding *ortho*-acylated anilide in 80% yield. This anilide acylation also displayed excellent *ortho*-selectivity and functional group tolerance for a wide range of substrates. For example, aldehydes containing heteroaromatic rings and strained cyclopropanes have been successfully coupled to anilides.

Kinetic study on the acylation of 2-phenylpyridine (**8a**) with 4-chlorobenzaldehyde (**2a**) with TBHP revealed an experimental rate law: rate = $k[\mathbf{8a}]^{-1}[\mathbf{Pd}]^2$. The inverse first-order dependence of [**8a**] suggests that the turnover-limiting step should involve substrate dissociation. The second-order dependence on [**Pd**] suggests the involvement of dinuclear palladium complex in the

turnover-limiting step. With **8a**-d_5 as substrate, significant primary kinetic isotope effect (k_H / k_D = 5.6) is consistent with substantial C–H bond cleavage at the turnover-limiting step. A Hammett correlation study on a series of *meta*-substituted pivalanilides (**6**) (Y = OMe, Me, Ph, H, Cl and Br) revealed a linear free energy relationship (R = 0.96) and small ρ^+ value of -0.74. The small negative ρ^+ value implies that the Pd(II)-mediated C–H cleavage should not proceed through an cationic arene intermediate. Reacting the cyclopalladated complex $[Pd(C\sim N)(OAc)]_2$ (C~N = 2-phenylpyridine) (**8a-Pd**) with **2a** (3 equiv) and TBHP (2 equiv) afforded the coupled ketone in 42% yield. The catalytic C–H acylation was suppressed by radical scavengers such as ascorbic acid in a dose-dependent manner. When 2,2,6,6-tetramethylpiperidine *N*-oxide (TEMPO) (1 equiv) was employed as additives, the ketones formation was completely suppressed and the 2,2,6,6-tetramethylpiperidino-4-chlorobenzoate was isolated in 78% yield. These finding are compatible to intermediacy of carboradicals in the acylation reaction. The catalytic acylation is probably mediated by coupling of the carboradicals with the arylpalladium(II) complexes.

Trichloromethyl moiety is prevalent to many medicinally useful molecules such as dysamide, barbamide and muironolide. In this work, we examined trichloromethyl [$^{\cdot}CCl_3$] radical generated from chloroform for C–H coupling reactions. Treating

cyclopalladated complex **8a-Pd** with di-*tert*-butylperoxide in chloroform at 120 ^{o}C failed to afford any trichloromethylated arenes. However, treating *N*-arylacrylamides (1 equiv) with di-*tert*-butylperoxide in chloroform in 120 ^{o}C furnished the carbocyclized 2-oxindoles (**10a**) in 68% yield. In the presence of $CuBr_2$ (5 mol%), this reaction proceeded to give the 2-oxindole up to 87% yield. Functional groups such as methoxy, halogen and ketone groups are well tolerated.

PUBLICATIONS AND CONFERENCE

PUBLICATIONS

Chan, C.-W.; Lee, P.-Y.; Yu, W.-Y. "Copper-catalyzed cross-dehydrogenative coupling of *N*-arylacrylamides with chloroform using *tert*-butyl peroxybenzoate as oxidant for the synthesis of trichloromethylated 2-oxindoles", *Tetrahedron Lett.*, **2015**, *56*, 2559.

Sit, W.-N.; Chan, C.-W.; Yu, W.-Y. "Palladium(II)-Catalyzed *ortho*-C–H Benzoxylation of 2-Arylpyridines by Oxidative Coupling with Aryl Acylperoxides", *Molecules*, **2013**, *18*, 4403.

Chan, C.-W.; Zhou, Z.; Yu, W.-Y. "Palladium(II)-Catalyzed Direct *ortho*-C–H Acylation of Anilides by Oxidative Cross-Coupling with Aldehydes using *tert*-Butyl Hydroperoxide as Oxidant", *Adv. Synth. Catal.*, **2011**, *353*, 2999.

Chan, C.-W.; Zhou, Z.; Chan. A. S. C.; Yu, W.-Y. "Pd-Catalyzed *ortho*-C–H Acylation / Cross Coupling Of Aryl Ketone *O*-Methyl Oximes with Aldehydes Using *tert*-Butyl Hydroperoxide as Oxidant", *Organic Letter*, **2010**, *12*, 3926.

CONFERENCE

Chan, C.-W.; Zhou, Z.; Yu, W.-Y. "Palladium(II)-Catalyzed Direct *ortho*-C–H Acylation of Anilides by Oxidative Cross-Coupling with Aldehydes using *tert*-Butyl

Hydroperoxide as Oxidant", 16th Belgian Organic Synthesis Symposium, Sapporo, Japan, 4-9 August, 2013.

SYMPOSIUMS

Chan, C.-W.; Lee, P.-Y.; Zhou, Z.; Yu, W.-Y. "Copper-Catalyzed Cross-Dehydrogenative Coupling of *N*-arylacrylamides with Chloroform Using *tert*-Butyl Peroxybenzoate as Oxidant for the Synthesis of Trichloromethylated 2-Oxindoles", The 22nd Symposium on Chemistry Postgraduate Research in Hong Kong, 18 April, 2014.

Chan, C.-W.; Wang, H.; Zhou, Z.; Yu, W.-Y. "Palladium-Catalyzed C2-Acylation of Indoles by Oxidative Cross Coupling with Aldehydes Using *tert*-Butyl Hydroperoxide as Oxidant", The 21st Symposium on Chemistry Postgraduate Research in Hong Kong, 12 April, 2014.

Chan, C.-W.; Zhou, Z.; Yu, W.-Y. "Palladium(II)-Catalyzed Direct *ortho*-C–H Acylation of Anilides by Oxidative Cross-Coupling with Aldehydes using *tert*-Butyl Hydroperoxide as Oxidant", The 19th Symposium on Chemistry Postgraduate Research in Hong Kong, 14 April, 2012.

Chan, C.-W.; Zhou, Z.; Chan. A. S. C.; Yu, W.-Y. "Pd-Catalyzed *ortho*-C–H Acylation / Cross Coupling Of Aryl Ketone *O*-Methyl Oximes with Aldehydes Using *tert*-Butyl Hydroperoxide as Oxidant", The 18th Symposium on Chemistry Postgraduate Research in Hong Kong, 30 April, 2011.

TABLE OF CONTENTS

ABBREVIATIONS AND SYMBOLS

AcOH	Acetic acid
Ac	Acetyl
Ad	1-Adamantyl
Ar	Aryl
Å	Angstrom
BDE	Bond dissociation energy
Bn	Benzoyl
BQ	Benzoquinone
Bz	Benzyl
CDC	Cross-dehydrogenative coupling
CO	Carbon monoxide
CMD	Concerted-metalation deprotonation
DCE	1,2-Dichloroethane
DCM	Dichloromethane
DEAD	Diethyl azodicarboxylate
DMA	N,N-Dimethylacetamide
DMF	N,N-Dimethylformamide
DMSO	Dimethyl sulfoxide
EA	Ethyl acetate
ESI	Electrospray-ionization
GC	Gas chromatography
GC-FID	Gas chromatography – flame ionization detector
GC-MS	Gas chromatography – mass spectroscopy

IR	Infrared spectroscopy
KIE	Kinetic isotope effect
MeCN	Acetonitrile
MO	Molecular orbital
MS	Mass spectroscopy
NEt_3	Triethylamine
NMR	Nuclear magnetic resonance
NHC	N-heterocyclic carbene
OAc	Acetate ion
OPiv	2,2,2-trimethylacetate
OTf	Trifluoromethanesulfonate ion
OTs	*p*-toluenesulfonate
phen	1,10-Phenanthroline
PPh_3	Triphenylphosphine
rt	Room temperature
THF	Tetrahydrofuran
TLC	Thin layer chromatography
p-tol-BINASO	1,1'-Binaphthalene-2,2'-diyl-bis-(*p*-tolylsulfoxide) ligand
Tp	Hydrotrispyrazolyborate ligand
p-TsOH	*p*-Toluenesulfonic acid
TEMPO	2,2,6,6-Tetramethyl-1-piperidinyloxy
TFA	Trifluoroacetic acid
s	Singlet
d	Doublet
t	Triplet

q	Quartet
m	Multiplet
δ	Chemical shift in NMR
J	Coupling constant
k	Rate constant
ν	IR absorption
ρ	Hammett rho value

LIST OF FIGURES

APPENDICES

LIST OF SCHEMES

LIST OF TABLES

Chapter 1

Introduction

1.1 General background

Carbon-carbon (C–C) bond formation is of fundamental significance in synthetic organic chemistry.[1] Advancement in the methodologies of C–C bond forming processes enables the construction of complex architecture of natural products, medicinal useful compounds and supramolecules from simple precursors.[2] Conventionally, Lewis acid-mediated Friedel-Crafts reactions have been established for C–C bonds formation on arenes with organohalides (e.g. alkyl halides, acyl chlorides) as coupling partners.[3] Indeed, the Friedel-Crafts method necessitates an over-stoichiometric amount of hazardous Lewis acid reagents. In most cases, the reactions suffer from poor regioselectivity as well as over-alkylations.

Recently, the advent of palladium-catalyzed cross coupling reactions such as Heck, Suzuki, and Negishi reactions has revolutionized the C–C bond formation chemistry on arenes. Development of a wide range of ligands has allowed highly efficient catalytic coupling of aryl halides or pseudohalides with various nucleophiles

such as alkenes and organometallic reagents (Scheme 1.1). Notably, Pd-catalyzed cross coupling reaction has been extensively applied for total synthesis of natural products such as calcidol, singulair, halenaquinone and dragmacidin F (Figure 1.1).[5]

Scheme 1.1 Examples of palladium catalyzed-cross coupling reactions

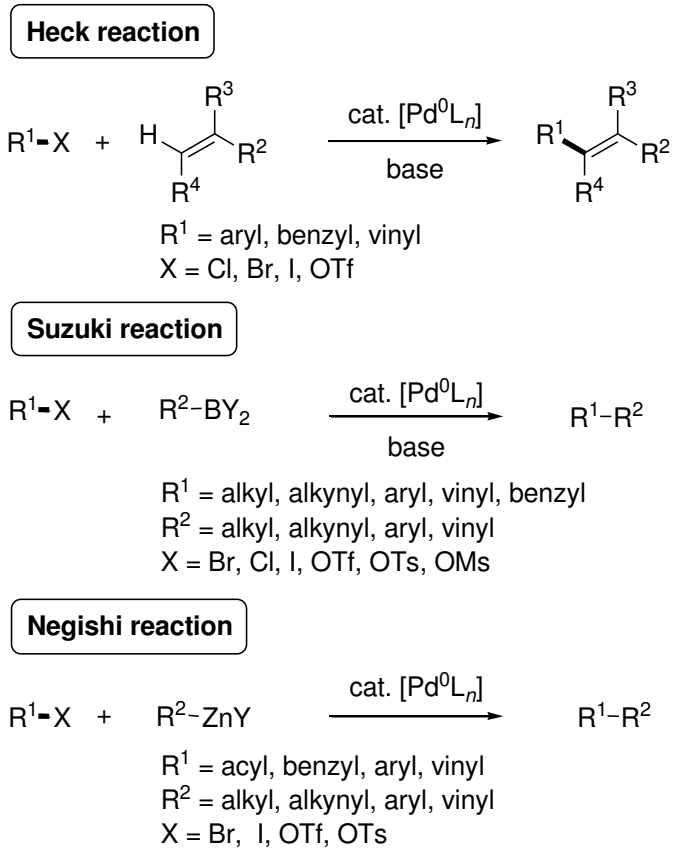

Figure 1.1 Synthetic examples of Pd-catalyzed cross-coupling reactions

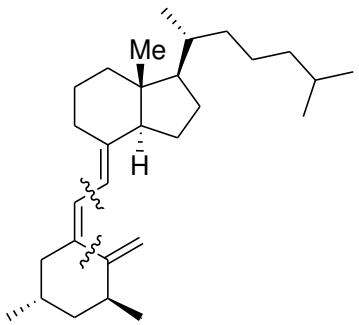

(+)-calcidol (Trost, 1995)

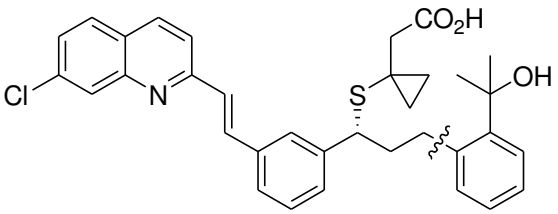

Singulair (Merck, 1993)

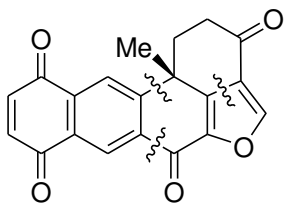

Halenaquinone (Shibasaki, 1996)

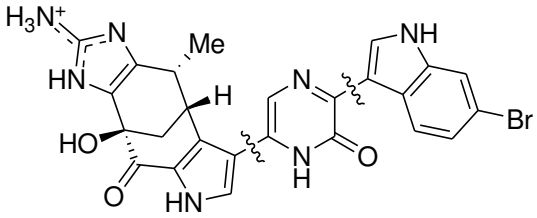

Dragmacidin F (Stoltz, 2004)

Irrespective to those apparent successes, the current coupling technology requires the use of pre-functionalized substrates and limited substrate scope. In view of atom economy and synthetic efficiency, development of effective C–C bond forming reactions through regioselective direct functionalization of unactivated carbon-hydrogen (C–H) bonds is the most desirable goal for contemporary catalysis research.

1.2 Challenges of C–H bond functionalization

C–H bond is the most ubiquitous chemical moieties found in Nature. From the perspective of synthetic simplicity, utilizing C–H bonds directly as functionalization

partners has been a subject of extensive investigation over the past decades.[6] However, utilizing C–H bonds for cross-coupling reaction are challenging under most reaction conditions for two reasons.[6c,7] First, C–H bonds are strong with high dissociation energy (BDE). For instance, BDE values of the C–H bond in methane and benzene are 104 and 112 kcal/mol respectively. Compared to carbon-halogen (C–X) bonds (e.g. BDE of C–Br in bromobenzene = 84 kcal/mol), the relatively strong C–H bond constitutes a large kinetic barrier for the direct C–H bond cleavage (Table 1.1).[8] Second, the acidity of a C–H bond is extremely low with pK_a values in the range of 45–60, implies that heterolytic cleavage of C–H bonds by strong bases is not feasible.[1b]

Table 1.1 Experimental bond dissociation energies (BDE) based on radical heats of formation [RX → R• + H•]

bond type	BDE (kcal mol^{-1})	bond type	BDE (kcal mol^{-1})
Ph–I	67	CH_3–H	105
Ph–Br	84	$(CH_3)_3$–H	97
Ph–Cl	97	Ph–H	112

In systems where C–H functionalizations are feasible, another challenge is to control the selectivity. For example, with regard to chemoselectivity, the C–H bonds in functionalized compounds are easily over-oxidized to form C–O bond under

strongly oxidizing conditions. Typically example of this problem is the hydrocarbon (C_nH_{2n+2}) combustion. Tolerance of functional group with relatively weaker bonds (e.g. C–X bond) during the activation of strong C–H bond is also a concern. Furthermore, the problems of regioselective functionalization of a compound with more than one C–H bond is also manifest.

1.3 Pathways for transition metal-mediatied C–H activation

In the past several decades, extensive investigation has been directed to transition metal-mediated C–H activation. As illustrated in Scheme 1.2, there are two major pathways for transition metal-mediated C–H activation: (1) the outer-sphere pathway and (2) the inner-sphere pathway. [6c, 9]

Scheme 1.2 Two general pathways for transition metal-mediated C–H activation

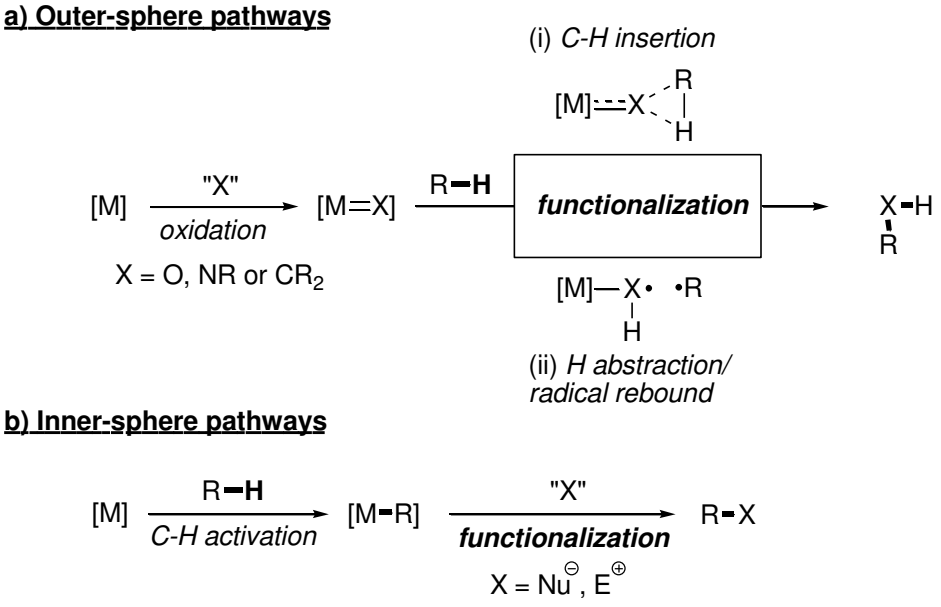

The outer-sphere pathway does not involve the direct interaction of the C–H bond with the metal center. Instead the transition metal would first be oxidized to form a highly reactive [M]=X species where X can be O (oxo), NR (nitrenoid) or CR_2 (carbenoid). The C–H bond would then react with the reactive [M]=X species *via* either direct C–H insertion, or a stepwise hydrogen atom abstraction – organic radical recombination sequence to afford the C–H functionalized product. The preference of C–H bond cleavage for this pathway is generally determined by the BDE of the C–H bond; therefore, the selectivity favors to the weaker C–H bonds (e.g. benzylic, allylic or alpha). Moreover, over-oxidation can be a problem due to the weaker C–H bond in highly functionalized products.

The inner-sphere pathway involves initial C–H bond cleavage by transition metal ions to afford an organometallic species [M]–R. The C–H bond cleavage process can occur through (1) oxidative addition, (2) electrophilic metalation, (3) concerted metalation deprotonation and (4) agostic C–H complex formation followed by deprotonation. The selectivity of the inner-sphere pathway is generally related to the propensity of the metal center to bind a particular C–H bond. Being less dependent on the BDE of C–H bond for the selectivity, the inner-sphere pathway is more often be utilized for functionalization of strong C–H bonds (e.g. arene C–H bonds) to aviod

over-oxidation. The metalated complex would then be functionalized by treatment of either nucleophiles of electrophiles to afford the cross-coupled products.

1.4 Early work in transition metal-mediated arene C–H activation

Apart from the outer-sphere pathway for C–H insertion, the transition metal-mediated C–H activation *via* the inner-sphere pathway is an attractive alternative and has been extensively investigated for many years. While the outer-sphere pathway generally involves functionalization of secondary and tertiary C–H bonds, the inner-sphere pathway is typically characterized by the high affinity towards arene C–H bonds.

In some earlier examples of transition metal-mediated C–H activation, electron-rich arenes were found to react with Lewis acidic transition metals to form organometallic complexes. For example, electron-rich arenes were found to undergo direct mecuration with HgX_2 (Scheme 1.3). In 1982, Pesci and co-workers discovered that anilines would react with $Hg(OAc)_2$ to form a new [Hg(II)-Ar] species (Scheme 1.3, a).[10a] Volhard and co-workers showed that thiophene could be directly mecurated at the C2-position with $HgCl_2$ in the presence of NaOAc, which would then react as a nucleophile with benzoyl chloride to form phenyl 2-thienyl ketone (Scheme 1.3, b). [10b]

Dimroh and co-workers later found that benzene can also be mecurated with $Hg(OAc)_2$ led to phenylmercuric acetate complex (Scheme 1.3, c) [10c].

Scheme 1.3 Early works on Metallation of arenes with HgX_2[10]

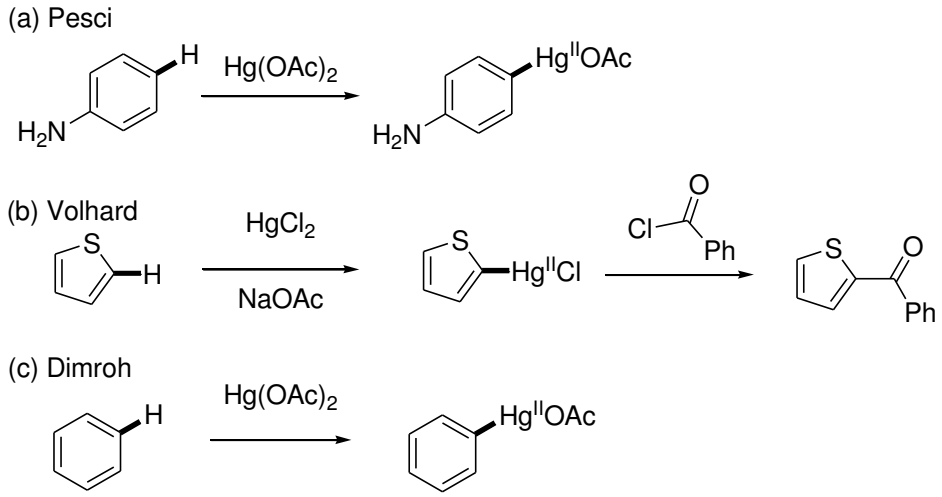

In 1931, Kharasch and co-workers described the first example of direct C–H auration (Scheme 1.4)[10d]. By reacting $AuCl_3$ with benzene and the corresponding phenylauric(III) chloride was obtained in 78% yield. Although the reaction occurred under mild conditions, the resulting organometallic complexes were too unstable and that it limited the synthetic application of the phenylauric complexes.

Scheme 1.4 Auration of benzene by $AuCl_3$ by Kharasch and co-workers[10d]

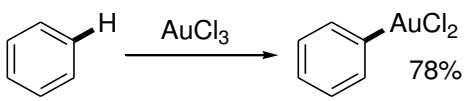

In 1967, a groundbreaking study by Fujiwara and co-workers described a series of transformations *via* palladium(II)-mediated C–H activation of aromatic solvents. It was found that refluxing dimeric styrene Pd(II) chloride with benzene solvent in the presence of AcOH (benzene:AcOH = 4:1) afforded *trans*-stilbene in 56% yield (Scheme 1.5, a). In their later reports, $Pd(OAc)_2$ was found to be able to mediate the coupling of styrene and arene solvents to afford the corresponding *trans*-stilbene in up to 90% yield. Structurally defined arylpalladium(II) complexes could be isolated with dialkyl sulfide as ligands. Notably, a regioisomeric mixture of products was obtained for mono-substituted arenes (Scheme 1.5, b).

Scheme 1.5 Palladium(II)-mediated C–H activation of aromatic solvents by Fujiwara and co-workers

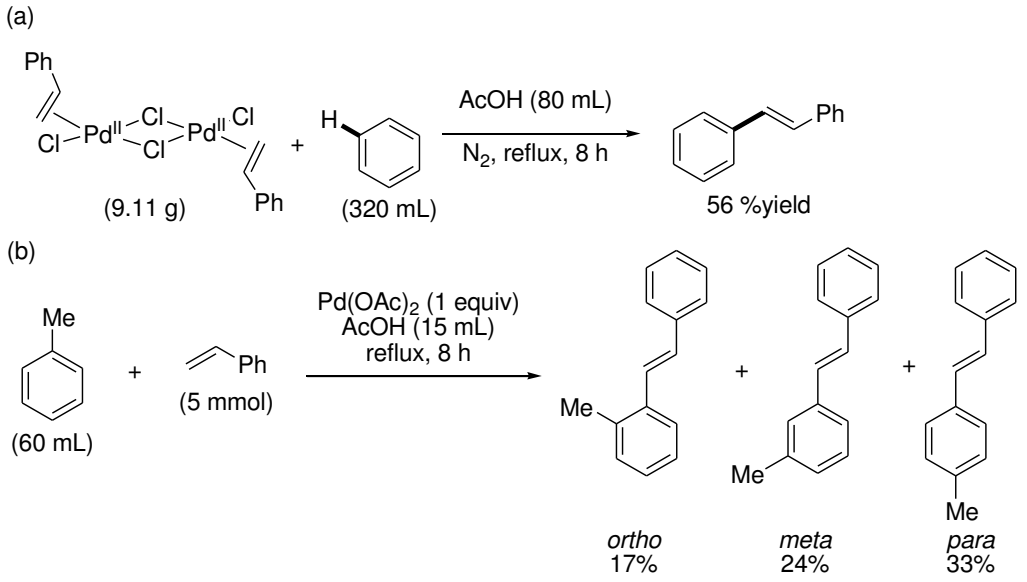

1.5 Arene C–H activation *via* chelation-assisted *ortho*-C–H metallation

In developing synthetically useful transformations *via* transition metal mediated C–H activation, two major limitations in Fujiwara's Pd(II) catalysis are (1) the use of arenes substrates in excess (normally as solvent) and (2) the lack of regioselectivity. To overcome these limitations, chelation-assisted *ortho*-C–H metallation pathway has been extensively investigated in recent years (Scheme 1.6).[6] By employing a proximal donor group such as nitrogen atoms to direct the transition metal ion to *ortho*-C–H bond, this would result in cyclometallated arylmetal complex formation. The cyclometallation could be facilitated towards the *ortho*-C–H bond in two folds.[1b] Kinetically, the coordinated directing group can guide the metal catalyst closer to the *ortho*-C–H bond. Also, the resulting cyclometallated intermediates can be stabilized thermodynamically.

Scheme 1.6 General depiction of chelation-assisted *ortho*-C–H metallation pathway

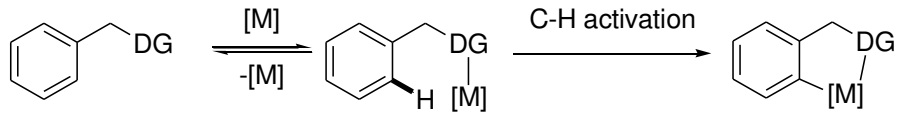

DG = donor group (e.g. N)

Scheme 1.7 Early examples of preparation of cyclonickelated complex of azobenzene

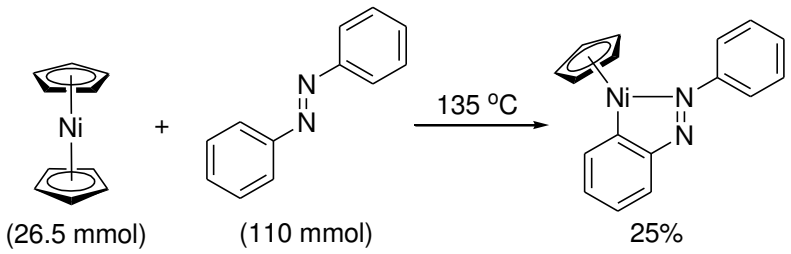

The first example of cyclometallation was reported by Kleiman and co-workers in 1963. By refluxing dicyclopentyldienyl nickel(II) in neat azobenzene at 135 ^{o}C for 4 h, a five-membered cyclonickelated complex was obtained and characterized (Scheme 1.7).[12] Later, Cope and co-workers demonstrated an analogous reactions with other metals such as platinum(II)[13] and palladium (II)[13] to afford some well-defined dinuclear cyclometallated complexes (Scheme 1.8). In their works, potassium tetrachloropalladate(II) was treated with azobenzene (1 equiv) in methanol at room temperature for 2 h to afford the cyclopalladated complex in 95% yield.

Scheme 1.8 Preparation of the palladacycle of azobenzene

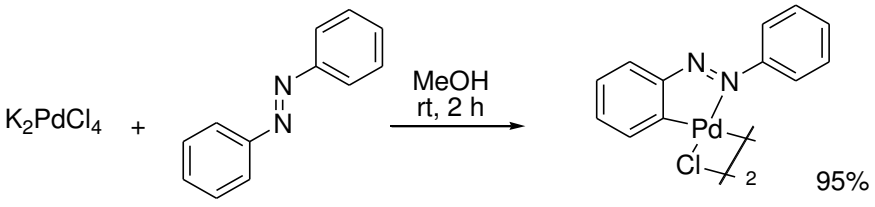

After these pioneering works, enormous examples of palladated complexes with different directing group were reported in the past several decades (Scheme 1.9).[14] Despite the apparent success of the cyclopalladated complex synthesis, little attention was directed to further functionalization of the corresponding cyclopalladated complexes was sparse in this early stage of development.

Scheme 1.9 Selected examples of cyclopalladated complexes[14]

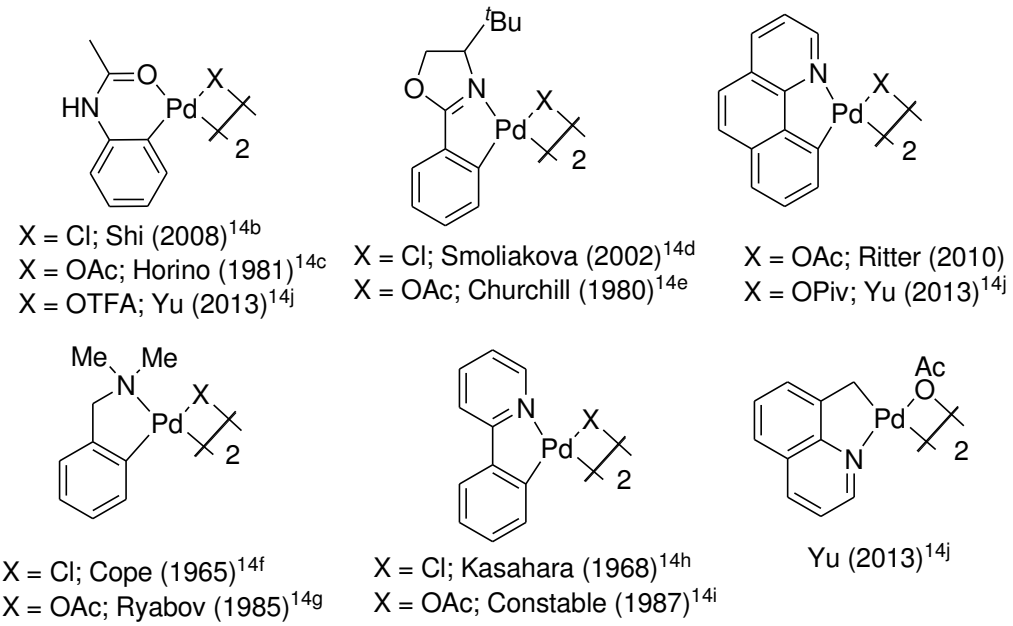

In 1971, Fahey and co-workers reported a pioneering work on Pd(II)-catalyzed *ortho*-selective arene C–H functionalization (Scheme 1.10).[15] In Fahey's work, when azobenzene (5.5 mmol) was treated with $PdCl_2$ (20 mol%) in dioxane / H_2O (2:1) with

slowly bubbling chlorine gas at 85 ^{o}C for 16 h, only *ortho*-chlorinated azobenzenes were isolated in 68% yield. The author proposed that the C–H chlorination should proceed *via* initial cyclopalladation of azobenzene followed by oxidative addition of chlorine to form a putative Pd(III) or Pd(IV) intermediate. The Pd(III) or Pd(IV) intermediate would then undergo C–Cl reductive elimination to release the product. Notably, in the absence of $PdCl_2$ the azobenzene chlorination predominantly observed at the *para*-position (71% yield). This observation was consistent with classical aromatic chlorination *via* electrophilic aromatic substitution mechanism. Tremont and co-workers reported another important finding that acetanilides could undergo *ortho*-methylation with MeI in the presence of a stoichiometric amount of $Pd(OAc)_2$.[16] Again, the oxidation of the cyclopalladated complex to putative Pd(IV) intermediate was proposed to be the key step in this transformation.

Scheme 1.10 Pd(II)-catalyzed *ortho*-C–H chlorination of azobenzene (Fahey)

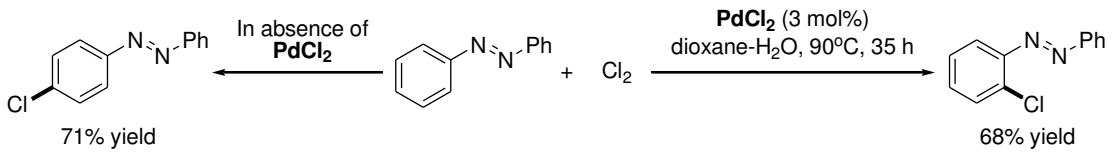

1.6 Palladium-catalyzed *ortho*-selective arene C–H activation for C–C bond formation

In 1998, Miura and co-workers reported a highly efficient, regioselective Pd(II)-catalyzed *ortho*-C–H cross coupling of benzoic acids with alkenes using $Cu(OAc)_2$ as oxidant (Scheme 1.11). Despite the moderate product yields, the excellent *ortho*-selectivity set the stage for further investigation of the field of palladium-catalyzed chelation-assisted *ortho*-C–H functionalization.

Scheme 1.11 Pd-catalyzed C–H coupling of benzoic acids with alkenes (Miura and co-workers)

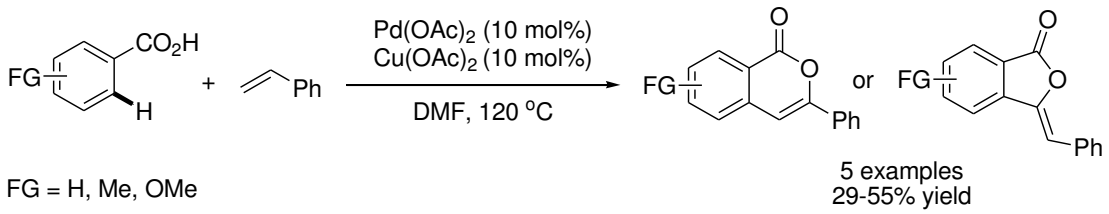

1.6.1 Mechanism of chelation-assisted arene C–H activation by Pd(II) catalysis

Scheme 1.12 Various proposed mechanisms for Pd-catalyzed chelation-assisted arene C–H activation

[1] Electrophilic Metalation

Ryabov (1985)

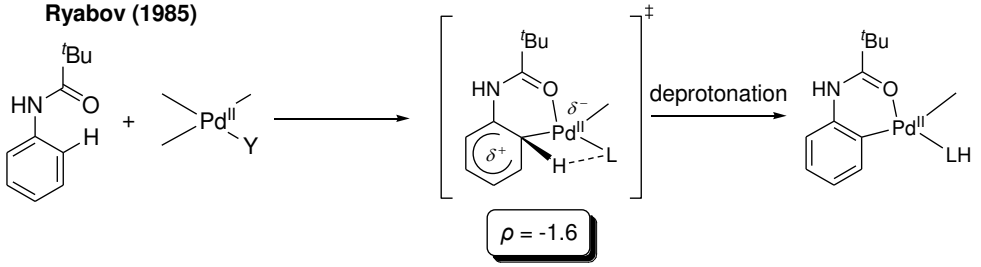

Wheland intermediate

[2] Formation of agostic C-H complex

Davies and Macgregor (2005)

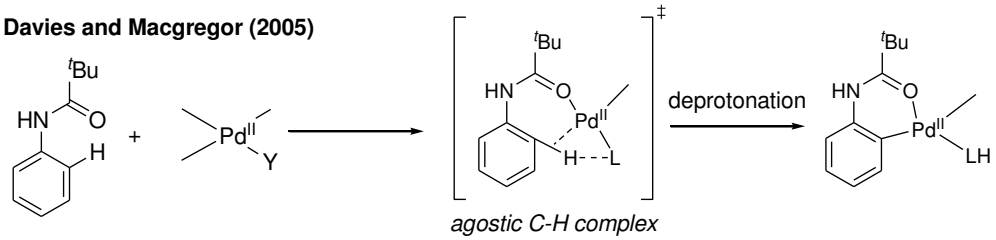

agostic C-H complex

[3] Oxidative Addition (OA)

Canty and van Koten (1995)

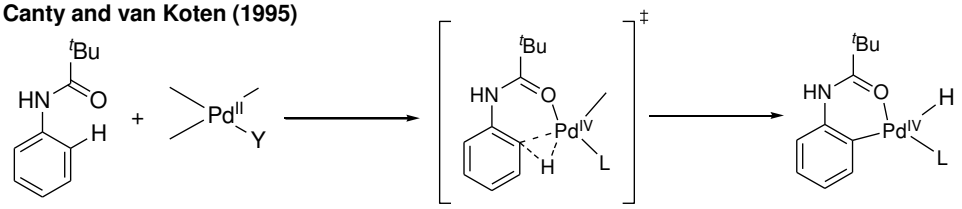

[4] Concerted Metalation Deprotonation (CMD)

Fagnou (2006)

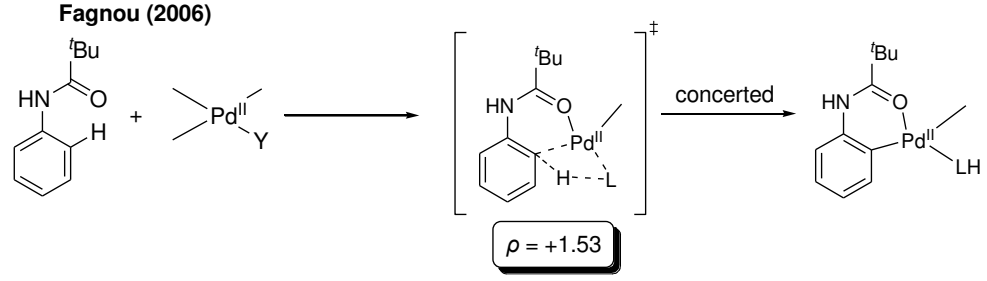

In the development of Pd(II)-catalyzed *ortho*-selective arene C–H functionalization, a great deal of attention has been focused on the mechanism of C–H bond cleavage, which led to the formation of cyclopalladated complexes. As depicted in Scheme 1.12, generally four transition state models were proposed in the recent decade.

Ryabov and co-workers proposed a mechanism for the cyclopalladation of *N,N*-dimethylbenzylamine involving the formation of an arenium intermediate through "electrophilic metallation" (Scheme 1.12, [1]).[19] The primary kinetic isotopic effect (k_H / k_D) of 2.2 and the negative slope of the Hammett plot (ρ = -1.6) indicated that the cyclopalladation is rate-limiting and electrophilic in nature. Based on these results, Ryabov and co-workers have proposed the cyclopalladation of *N,N*-dimethylbenzylamine by $Pd(OAc)_2$ should proceed through electrophilic aromatic substitution *via* the Wheland intermediate (arenium intermediate). The rate of electrophilic cyclopalladation increases with the electron-releasing substituents on the arene.

Davies and Macgregor performed a DFT calculation study on the cyclopalladation with $Pd(OAc)_2$ of *N,N*-dimethylbenzylamine (Scheme 1.12, [2]).[20] Their results showed that the reaction goes by an electrophilic like activation, but *via*

the agnostic C–H complex rather than the traditionally assumed Wheland intermediate. Also, the author suggested that the acetate play an important role to stabilize the six-membered agnostic transition state through hydrogen bonding. Koten and Canty proposed another mechanism called "oxidative addition" (Scheme 1.12, [3]).[21] Oxidative addition is a mechanism where an electron rich metal (e.g. Pt(II), Ir(I), Rh(I) and Ru(0)) reacts with a C–H bond to form a M–C and M–H bond *via* a three-membered transition state.

Recently, Fagnou and co-workers proposed the concerted metalation deprotonation (CMD) for direct arylation on perfluorobenzenes with aryl halide in the presence of $Pd(OAc)_2$ (Scheme 1.12, [4]).[22] The term "concerted" is used to describe the process that the hydrogen is abstracted by the coordinated base (L) at the same time as the M–C bond is formed. It is noteworthy that the reaction exhibited a linear Hammett correlation with a positive slope (ρ = +1.53) for the arylation of C-4 substituted substituted pyridine *N*-oxide. The positive ρ value indicated a negative charge implied the developing negative charge at the CMD transition state for C–H bond cleavage.

1.6.2 Palladium-catalyzed *ortho*-selective arene C–H activation for C–C bond formation

To date, Pd-catalyzed arene C–H functionalization has been attracting widespread attention from the chemical community. In particular, C–C bond formation reactions such as alkenylation, alkylation, alkynylation, arylation and carbonylation have been extensively investigated.[18]

1.6.2.1 Pd-catalyzed *ortho*-C–H alkenylation

An early example reported by van Leeuwen and co-workers involved *ortho*-C–H alkenylation of acetanilides with *n*-butyl acrylate (1.1 equiv) in AcOH at room temperature with $Pd(OAc)_2$ (5 mol%) as catalyst (Scheme 1.13).[23a] Lloyd-Jones and co-workers demonstrated the analogous oxidative coupling between *N*,*N*-dimethyl-*N*'-aryl ureas and dienes affords indolines products by *ortho*-C–H alkenylation followed by cyclization (Scheme 1.14).[23b] Recently, Ge and co-workers described *ortho*-C–H alkenylation of toluene derived silanols with AgOAc as oxidant (Scheme 1.15).[23c] The dialkylsilanol group can be easily removed by treatment of TBAF in good yield.

Scheme 1.13 Pd-catalyzed acetanilides *ortho*-C–H alkenylation (van Leeuwen and co-workers)

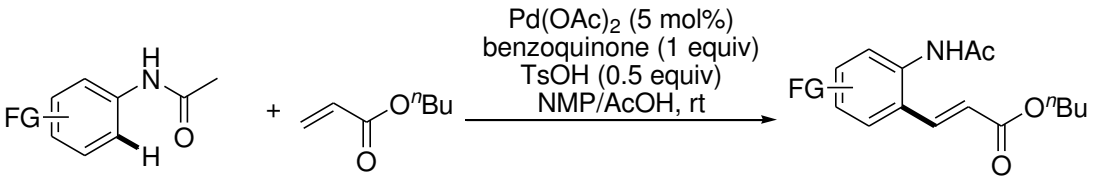

FG = Me, MeO, Br, CF_3

Scheme 1.14 Pd-catalyzed *N*,*N*-dimethyl-*N*'-aryl ureas *ortho*-C–H alkenylation (Lloyd-Jones and co-workers)

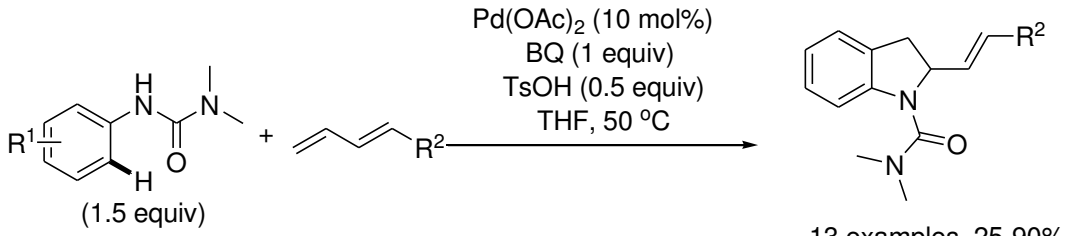

R^1 = H, alkyl, OMe, halo, CF_3
R^2 = CO_2nBu, Ph, CO_2Et, NO_2

Scheme 1.15 Pd-catalyzed silanol group assisted *ortho*-C–H alkenylation toluene (Ge and co-workers)

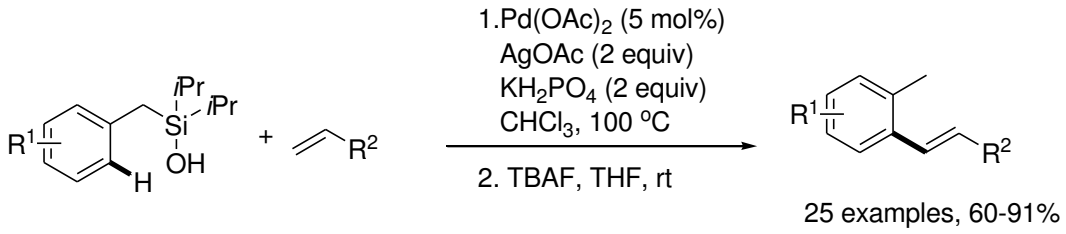

R^1 = H, alkyl, OMe, halo
R^2 = CO_2nBu, SO_2Me, CO_2Et

In general, a stoichiometric amount of re-oxidant such as benzoquinone (BQ), AgOAc and $Cu(OAc)_2$ was required for regeneration of the active Pd(II) species from Pd(0). An alternative pathway to bypass the requirement for using stoichiometric re-oxidants was reported by Daugulis and co-workers (Scheme 1.16).[23d] In this system,

3-bromo-acrylates were used as coupling partners for the anilide-directed *ortho*-C–H alkenylation.

Scheme 1.16 Pd-catalyzed pivalanilide *ortho*-C–H alkenylation with 3-bromo-acrylate (Daugulis and co-workers)

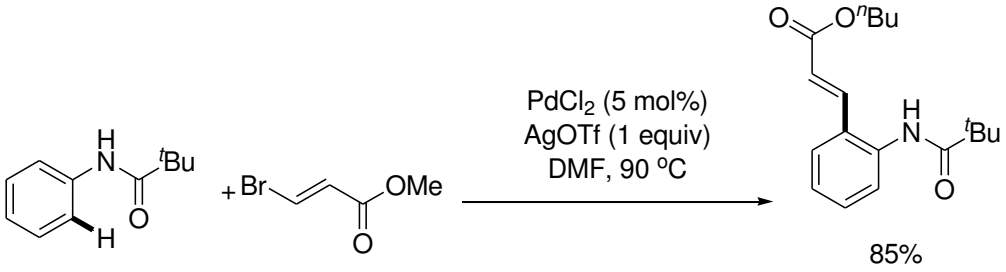

1.6.2.2 Pd-catalyzed *ortho*-C–H alkylation

The pioneering work of $Pd(OAc)_2$-catalyzed *ortho*-C–H alkylation was reported by Yu and co-workers.[24] With 4,4-dimethyloxazoline as directing group, the *ortho*-C–H alkylation was accomplished by using tetraalkyl tin (0.075 equiv x 10), in the presence of $Pd(OAc)_2$ (10 mol%) in acetonitrile at 100 °C (Scheme 1.17). In this system, $Cu(OAc)_2$ (1 equiv) was used as terminal oxidant and BQ (1 equiv) was a key promoter.[24a] More recently, the same group reported the analogous Pd-catalyzed *ortho*-C–H alkylation of 2-arylpyridines with alkyl boronic acid (Scheme 1.18).[24b]

Scheme 1.17 Pd-catalyzed oxazoline *ortho*-C–H alkylation with tetraalkyl tin reagents (Yu and co-workers)

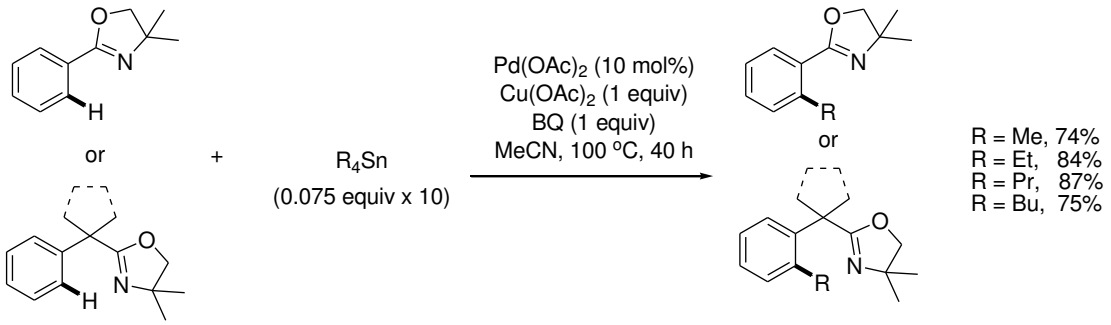

Scheme 1.18 Pd-catalyzed 2-arylpyridine *ortho*-C–H alkylation with alkyl boronic acids (Yu and co-workers)

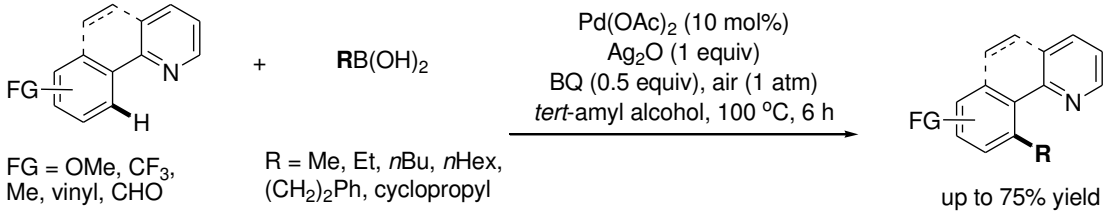

Apart from using organometallic reagents, our group devised a C–H / C–H coupling reaction for Pd-catalyzed *ortho*-C–H alkylation of anilides using β-keto esters as coupling partners (Scheme 1.19).[25] It was found that treatment of *N*-pivalanilides with dimethyl malonate (3 x 3 equiv / 4 h) in the presence of $Pd(OAc)_2$ (10 mol%), $Mn(OAc)_3 \cdot 2H_2O$ (3 x 0.5 equiv / 4 h) and TFA (3 x 3 equiv / 4 h) in toluene at room temperature afforded the *othro*-alkylation product in 25 – 94% yield.

Scheme 1.19 Pd-catalyzed *ortho*-C–H alkylation of anilides with β-keto esters by Yu (W. –Y.) and co-workers

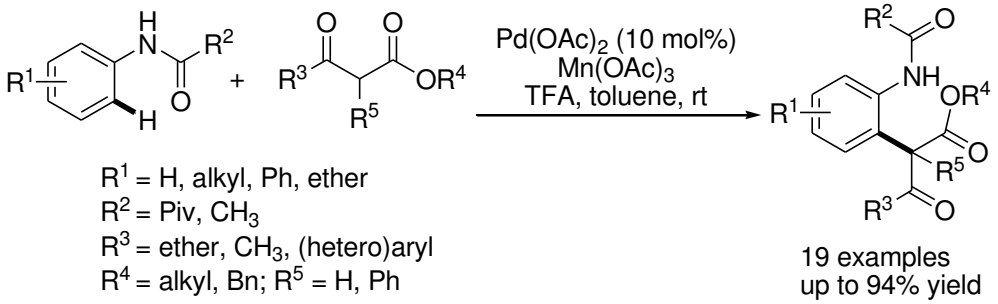

1.6.2.3 Pd-catalyzed *ortho*-C–H alkynylation

Chatani and co-workers reported the first example of Pd-catalyzed *ortho*-C–H alkynylation of anilides with bromoalkynes (Scheme 1.20).[26] Employing $Pd(OAc)_2$ (10 mol%) along with silyl-protected bromoalkynes, AgOTf and K_2CO_3, *ortho*-alkynylated anilides were produced in 71 – 93% yield. This reaction represents a powerful analogue to the Sonogashira reaction which involved the coupling of aryl halides with the C–H bond of terminal alkynes.

Scheme 1.20 Pd-catalyzed *ortho*-C–H alkynylation of anilides with bromoalkynes (Chatani and co-workers)

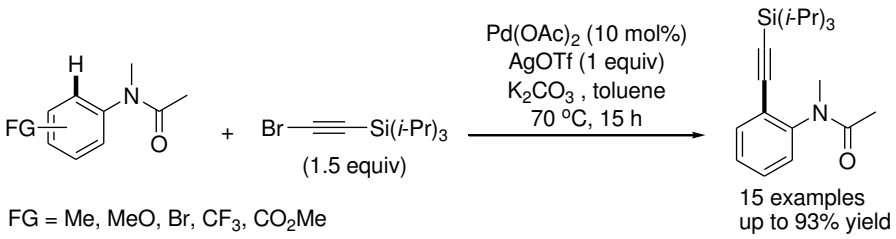

1.6.2.4 Pd-catalyzed *ortho*-C–H arylation

In 2005, Sanford and co-workers reported a key development of $Pd(OAc)_2$-catalyzed *ortho*-C–H arylation of arenes using unsymmetrical mesityl/aryl-substituted iodinium(III) reagents ([Mes-I-Ar]BF_4) (Scheme 1.21).[27a,b] It was found that diverse directing group such as 2-pyridyl, quinolinyl, pyrrolidinyl, acetamide were effectively arylated with excellent *ortho*-selectivity. Daugulis and co-workers reported the $Pd(OAc)_2$-catalyzed *ortho*-C–H arylation using stoichiometric AgOAc in conjunction with aryl iodides as reagents (Scheme 1.22).[27c] Initially, *N*-pivalanilide was treated with $Pd(OAc)_2$ (1.5 mol%), phenyl iodide (2.2 equiv) and AgOAc (2 equiv) in TFA at 120 ^oC for 3 h afforded the 2,6-diarylated anilides in 91% yield. Yu (W. –Y.) and co-workers also demonstrated the use of aryl acylperoxides for the $Pd(OAc)_2$-catalyzed *ortho*-C–H arylation (Scheme 1.23).[27d] Employing $Pd(OAc)_2$ (5 mol%) as catalyst along with aryl acylperoxides in AcOH : CH_3CN (1 mL : 1 mL) at 100 ^oC for 2 h, substrate containing pyridyl, oxime, oxazoline undergo *ortho*-selective C–H arylation in 46 – 87% yield. The arylation protocol of azoarenes[27e] and anilides[27f] with aryl acylperoxides was also investigated by other group.

Scheme 1.21 $Pd(OAc)_2$-catalyzed *othro*-C–H arylation of arenes using $[Mes\text{-}I\text{-}Ar]BF_4$ (Sanford and co-workers)

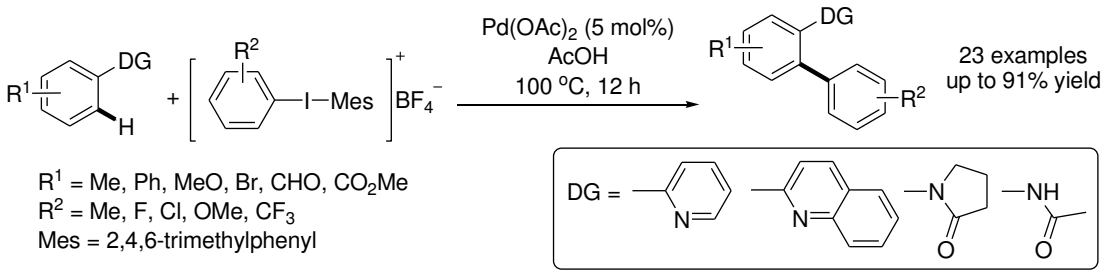

Scheme 1.22 $Pd(OAc)_2$-catalyzed *othro*-C–H arylation of anilides with aryl iodides (Daugulis and co-workers)

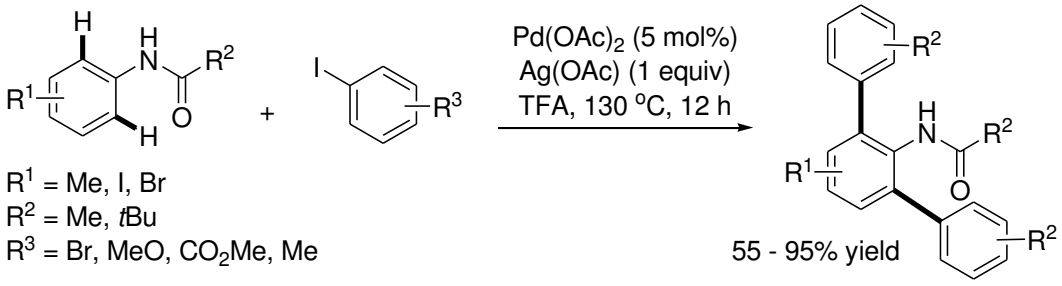

Scheme 1.23 $Pd(OAc)_2$-catalyzed *othro*-C–H arylation of anilides with aryl acylperoxides by Yu (W. –Y.) and co-workers

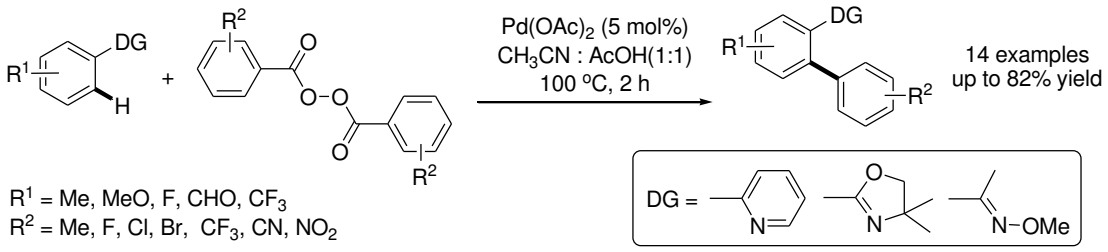

Apart from the arylation reactions employing pre-functionalized arylation

reagents, another strategy involved the Pd(II)-catalyzed *ortho*-selective C–H coupling with unactivated arene C–H bonds has also been extensively explored in recent years.[28] The first general example was reported by Sanford and co-workers with $Pd(OAc)_2$ (10 mol%), BQ (0.5 equiv) and Ag_2CO_3 (2 equiv) as stoichiometric oxidant, 2-phenylpyridines can effectively couple with various substituted arenes to give the *ortho*-arylation products in up to 93% yield. [28a] Similar transformations employing anilides as substrates were also investigated by research groups of Shi[28b,c] and Buchwald[28d] subsequently (Scheme 1.24).

Scheme 1.24 Pd(II)-catalyzed *ortho*-C–H coupling with arene C–H bonds

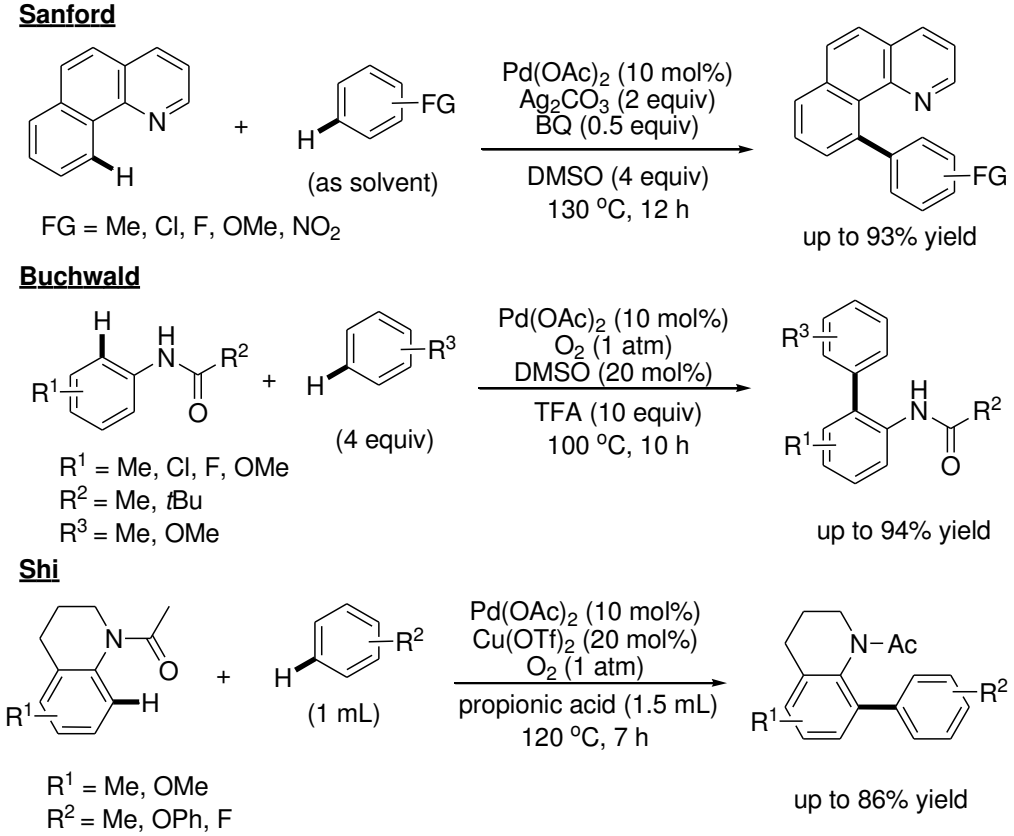

1.6.2.5 Pd-catalyzed *ortho*-C–H carbonylation

An early example of Pd(II)-catalyzed *othro*-C–H carbonylation using carbon monoxide (CO) as coupling partner involved the formation of benzolactam derivatives from benzylamines (Scheme 1.25).[29a] Yu and co-workers achieved the Pd-catalyzed *ortho*-C–H carbonylation of carboxylates (e.g. benzoic acid and phenylacetic acid) and acetanilides (Scheme 1.26). [29b] More recently, Lloyd-Jones and co-workers demonstrated that *N*-alkyl-*N'*-aryl urea and *N,N*-dialkyl-*N'*-aryl urea were effective substrates for Pd-catalyzed *ortho*-C–H carboxylation to construct cyclic imidates (Scheme 1.27).[29c]

Scheme 1.25 Pd-catalyzed *othro*-C–H carbonylation of benzylamines using carbon monoxide for benzolactam syntheses (Orito and co-workers)

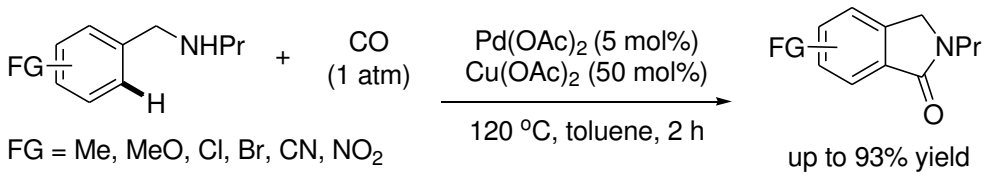

FG = Me, MeO, Cl, Br, CN, NO_2

up to 93% yield

Scheme 1.26 Pd-catalyzed *othro*-C–H carbonylation of anilides and carboxlates with CO (Yu and co-workers)

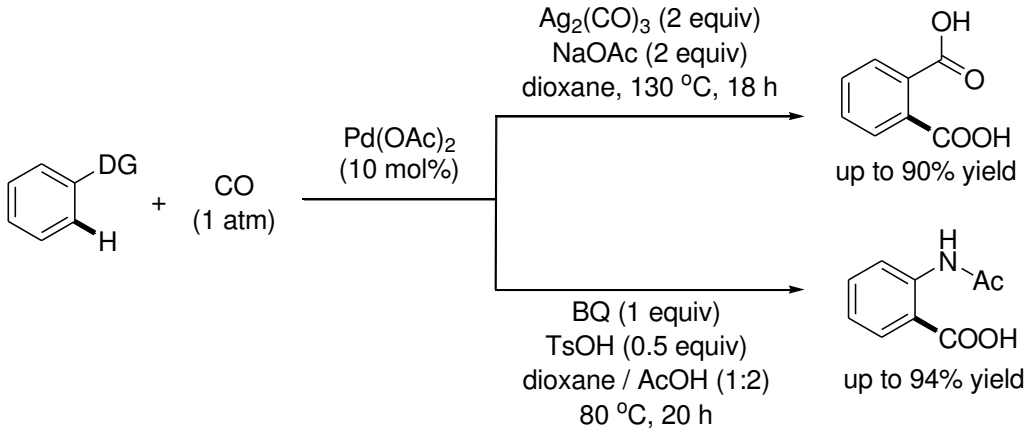

Scheme 1.27 Pd-catalyzed *othro*-C–H carbonylation of urea-directed for cyclic imidates syntheses (Lloyd-Jones and co-workers)

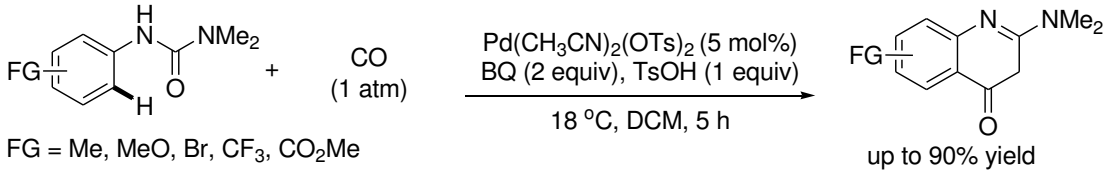

FG = Me, MeO, Br, CF_3, CO_2Me

Yu (W. -Y) and co-workers employed an alternative strategy for Pd-catalyzed *othro*-C–H carbonylation (Scheme 1.28).[29d] Instead of using carbon monoxide, diethyl azodicarboxylate (DEAD) was found to be an effective reagent for C–H ethoxycarbonylation. In this work, employing $Pd(OAc)_2$ (5 mol%), DEAD (0.5 equiv x 4), oxone (2 equiv) in DCE at 100 °C for 3 h, arenes with a variety of directing

group such as pyridine, amide and oxime ether are effective substrates.

Scheme 1.28 $Pd(OAc)_2$-catalyzed *othro*-C–H ethoxycarbonylation of arenes with diethyl azodicarboxylate (DEAD) by Yu (W. -Y) and co-workers

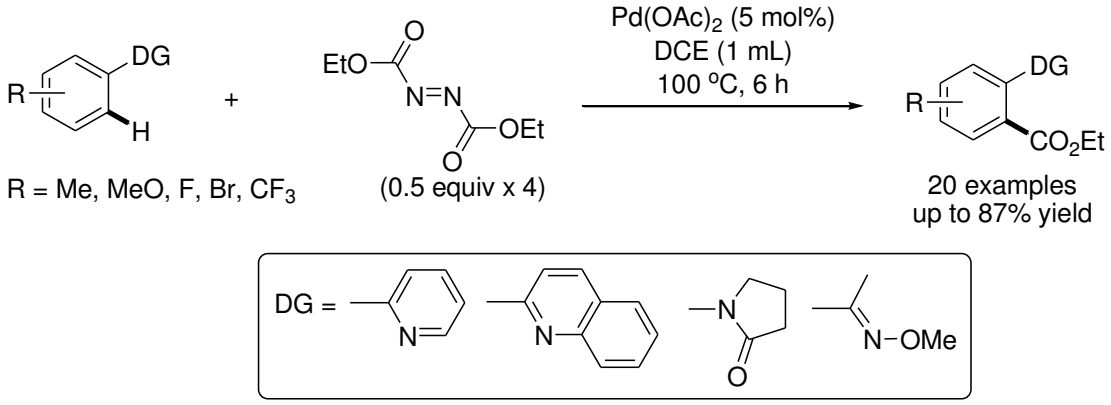

1.6.3 Palladium-catalyzed oxidative cross coupling for C–C bond formation *via* two-fold direct C–H activation – cross-dehydrogenative coupling

Scheme 1.29 Pd-catalyzed cross-dehydrogenative coupling of aryl C–H bonds

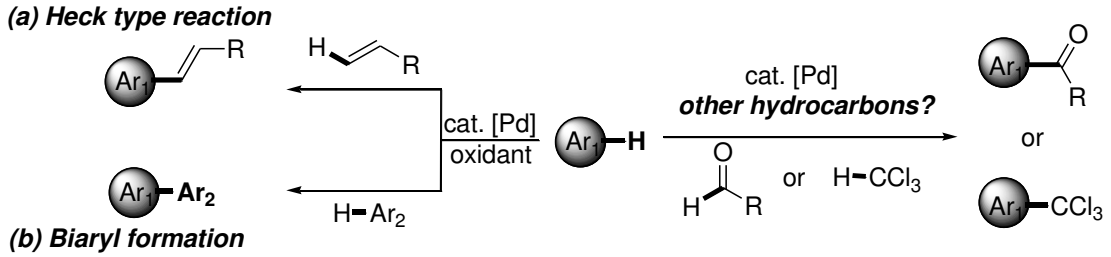

Recently, building C–C bonds *via* two-fold direct C–H activation has emerged as an attracting and challenging goal in catalysis [termed cross-dehydrogenative

coupling (CDC)] (Scheme 1.29).[30] Pd-catalyzed CDC reactions have been extensively studied. Since the pioneering work by both research group of Miura[17] and Fujiwara[11b] on the Pd-catalyzed oxidative aromatic C–H alkenylations, numerous successful examples have been developed in CDC between arenes and alkenes based on Pd(II)/Pd(0) catalysis to afford the Heck-type reaction products. Biaryl bond formations have also been achieved through CDC reaction involving *ortho*-selective cyclopalladation, followed by coupling with a range of functionalized or simple arenes. However, the analogous examples of structural different hydrocarbons are sparse in the literature.

1.7 Aims and objectives

Formation of C–C bond through regioselective direct functionalization of unactivated C–H bonds is of significant in sustainable organic synthesis. In this research, we aim to develop catalytic cross-dehydrogenative coupling of arenes (**H**-Ar) with hydrocarbons such as aldehydes (**H**–C(O)R) and chloroform (**H**–CCl_3) for regioselective C–C formation.

Conventional acylation of arenes such as Friedel-Craft reaction have been extensively investigated; however, these pathways suffer from poor regioselectivity and atom-efficiency. Our initial attention is directed to Pd-catalyzed *ortho*-C-H bond acylation of arenes with aldehydes. The first part of this research is to achieve the synthesis of 1,2-diacylbenzenes *via* a Pd-catalyzed direct acylation of acetophenones with aldehydes. Development of the catalytic C–H acylation for the synthesis of medicinally useful building blocks is a subject of interest. In this research, we will also explore Pd-catalyzed direct acylation of anilides for the synthesis of 2-aminobenzophenones.

Understanding the mechanism is a critical step towards developing broadly applicable catalytic C–H cross coupling reactions. In this regard, a detailed

investigation of the mechanism of the Pd-catalyzed *ortho*-C–H acylation of 2-phenylpyridine was conducted. Reaction rate order of each reactant will be determined. In this research, the evidence of acyl radical intermediacy in the catalytic reactions will also be investigated. We desire to propose a possible mechanism based on our mechanistic study.

Selective trichloromethylation of hydrocarbons is of fundamental interest for organic synthesis. In the final part of this research, we plan to achieve facile synthesis of trichloromethylated 2-oxindoles *via* Cu-catalyzed cross-dehydrogenative coupling (CDC) of *N*-arylacrylamides with chloroform.

Chapter 2

Palladium-catalyzed oxidative aromatic C–H acylation with aldehydes using tert-butyl hydroperoxide as oxidant

2.1 Palladium-catalyzed direct C-H acylation of oximes

2.1.1 Background

1,2-Diacylbenzenes are versatile precursors for syntheses of some medicinal valuable heterocycles such as phthalazines, isoquinolines, isobenzofurans and isoindoles (Scheme 2.1).[31] Moreover, 1,2-diacylbenzenes are employed as fluorescence reagents for highly selective analysis of amino acids and peptides.[32]

Conventionally, 1,2-diacylbenzenes are prepared by oxidative cleavage of *N*-acylhydrazones of *O*-hydroxyaryl ketones with $Pb(OAc)_4$[33] or hypervalent iodine reagents[34], and oxidation of 1,2-aryldimethanol by SeO_2[35]. However, apart from requiring of pre-functionalized starting materials, these methods suffer from narrow substrate scopes, harsh reaction conditions and the use of toxic reagents.

Scheme 2.1 Some heterocyclic compounds derived from 1,2-diacylbenzenes

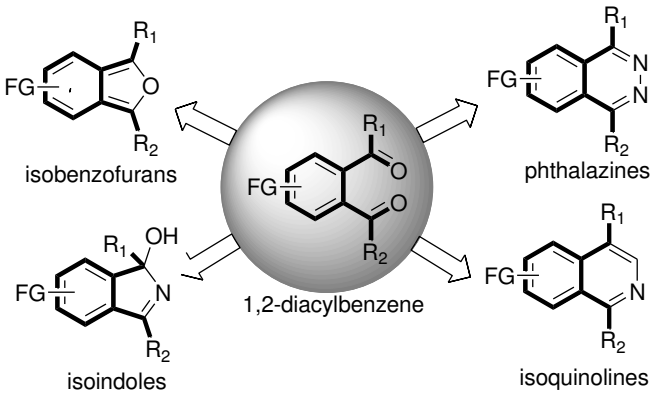

Catalytic dehydrogenative cross-coupling (CDC) reactions involving activation of two C–H bonds are attractive, and yet challenging, approach for C–C bond formation[30]. In this regard, recent advances have been made in Pd-catalyzed *ortho*-C–H functionalizations.[18] With imine as directing group, acetophenone oximes have been frequently employed as substrates for alkenylation, arylation and cycloaddition. Yet, the analogous direct C–H acylation with aldehydes are far less established.

In this work, we investigated the Pd-catalyzed *ortho*-C–H acylation of oximes by oxidative coupling with aldehydes. Simple deprotection of the oxime group would afford structural diverse 1,2-diacylbenzenes, which is a versatile precursor to many heterocyclic compounds.

2.1.2 Results and discussion

Initially, acetophenone *O*-methyl oxime **1a** (1 equiv) and 4-chlorobenzaldehyde **2a** (3 equiv) were treated with TBHP (2 equiv) and $Pd(OAc)_2$ (5 mol%) in a toluene-AcOH mixture (1 mL, 2:1 v/v) at 100 °C for 12 h. Aldehyde **2a** was chosen for study because it is a commercially available crystalline solid, while other liquid aldehydes may contain acid impurities. In our initial study, product **3a** was obtained in 47% yield (Scheme 2.2). The molecular structure of **3a** has been established by X-ray crystallography (Figure 2.1).

Scheme 2.2 Preliminary study

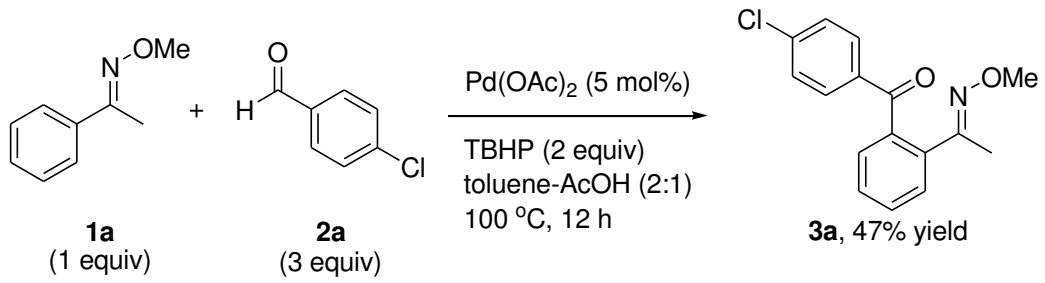

1a (1 equiv) + **2a** (3 equiv) → **3a**, 47% yield

Figure 2.1 Molecular structure of (4-chlorophenyl)(2-((E)-1-methoxyiminoethyl) phenyl)methanone (**3a**)

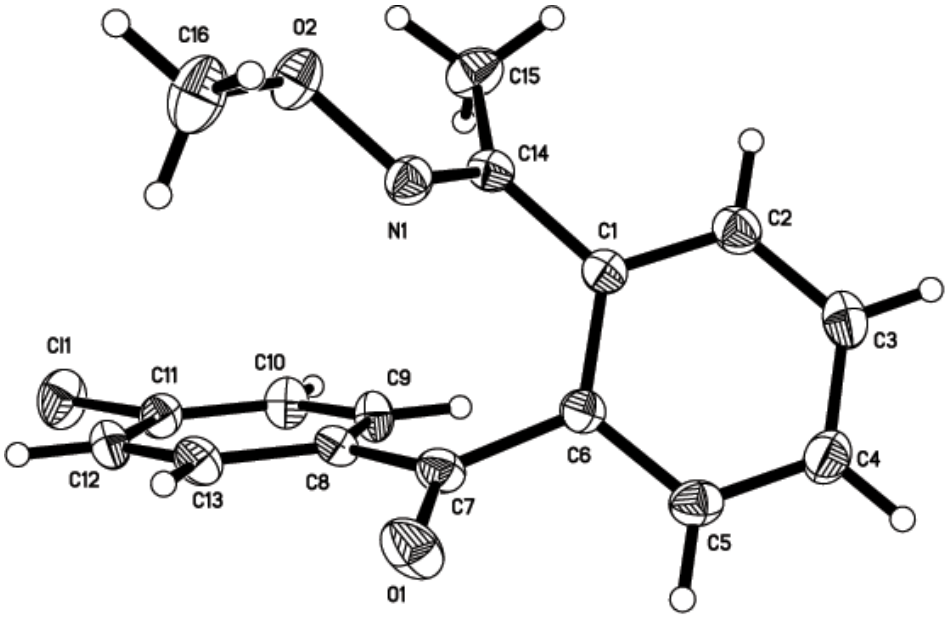

Table 2.1 Selected bond distances and angles for **3a**

bond distances [Å]	
C(6)-C(7)	1.487(4)
O(1)-C(7)	1.217(3)
C(7)-C(8)	1.490(4)
Cl(1)-C(11)	1.738(3)
N(1)-C(14)	1.278(3)

bond angles [^{o}]	
O(1)-C(7)-C(6)	120.6(3)
O(1)-C(7)-C(8)	120.2(3)

Table 2.2 Crystal data and structure refinement for **3a**

Empirical formula	$C_{16}H_{14}ClNO_2$
Formula weight	287.73
Temperature	296(2) K
Wavelength	0.71073 Å
Crystal system	Orthorhombic
Space group	Pbca
Unit cell dimensions	a = 11.7356(5) Å □= 90°.
	b = 5.8444(7) Å □= 90°.
	c = 16.8878(7) Å □= 90°.
Volume	2957.3(2) $Å^3$
Z	8
Density (calculated)	1.292 mg/m^3
Absorption coefficient	0.258 mm^{-1}
F(000)	1200
Crystal size	0.30 x 0.24 x 0.18 mm^3
Theta range for data collection	2.41 to 27.12°.
Index ranges	-10<=h<=15,-15<=k<=19,-21<=l<=21
Reflections collected	13901
Independent reflections	3260 [R(int) = 0.0821]
Completeness to theta = 27.31°	99.9 %
Absorption correction	Semi-empirical from equivalents
Max. and min. transmission	1 and 0.689
Refinement method	Full-matrix least-squares on F^2
Data / restraints / parameters	3260 / 0 / 182
Goodness-of-fit on F^2	1.002
Final R indices [I>2sigma(I)]	R1 = 0.0533, wR2 = 0.1198
R indices (all data)	R1 = 0.1528, wR2 = 0.1549
Extinction coefficient	0.0019(7)
Largest diff. peak and hole	0.229 and -0.224 $e.Å^{-3}$

2.1.2.1 Reaction optimization

We began by examining the effect of acid additives. When the amount of AcOH was decreased from 35 equiv to 2 equiv, comparable yield was obtained (entries 1 and 2; Table 2.3). This result shows that a sub-stoichiometric amount of AcOH would be enough to promote the oxidative C–H acylation. A slightly better yield of **3a** was achieved with the use of 0.5 equiv of AcOH as additives (entry 4).

Table 2.3 Effect of acid quantity[a]

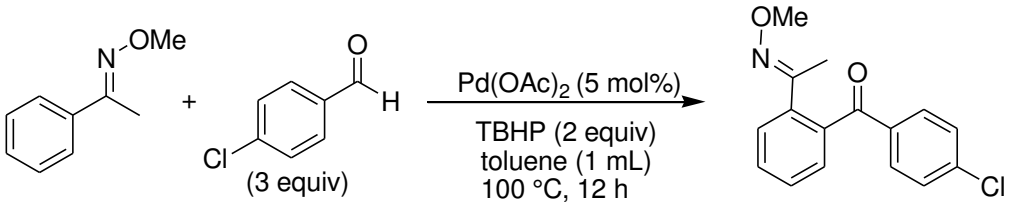

1a **2a** **3a**

entry	AcOH (equiv)	yield (%)[b]
1	35 (0.5 mL)	47
2	2	48
3	1	53
4	0.5	58
5	0.1	50
6	10 mol%	43

[a]Reaction conditions: **1a** (0.25 mmol), **2a** (0.75 mmol), $Pd(OAc)_2$ (5 mol%), TBHP (0.5 mmol), AcOH and undegassed toluene (1 mL) at 100 °C for 12 h. [b]Yields were determined by ^1H NMR with 1,2-dibromomethane as internal standard.

We also examined the effect of different acids in the acylation reactions (Table 2.4). With TFA as additive, **3a** was obtained in only 23% with substantial substrate decomposition being observed (entry 2). Notably, the use of TsOH led to serious substrate decomposition without any product formation (entry 3). Steric bulky 1-adamantanecarboxylic acid gave a slightly lower yield (entry 4); whereas employing proprionic acid or some benzoic acids as additives produced comparable results as AcOH (entries 5 – 8).

Table 2.4 Effect of acid[a]

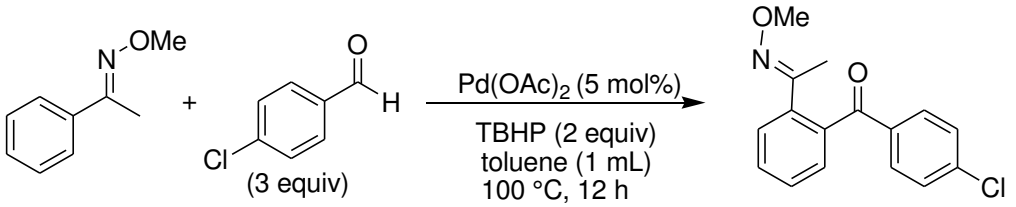

1a **2a** **3a**

entry	acid (0.5 equiv)	yield (%)[b]
1	AcOH	58
2	TFA	23
3	TsOH	0
4	1-AdCO_2H	48
5	EtCO_2H	53
6	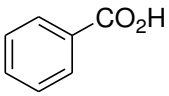	57

7	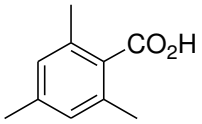	52
8	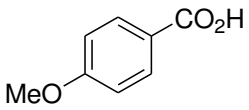	55

[a]Reaction conditions: **1a** (0.25 mmol), **2a** (0.75 mmol), $Pd(OAc)_2$ (5 mol%), TBHP (0.5 mmol), acid (0.125 mmol) and undegassed toluene (1 mL) at 100 °C for 12 h. [b]Yields were determined by ^1H NMR with 1,2-dibromomethane as internal standard.

Apart from $Pd(OAc)_2$, other Pd(II) complexes were evaluated for the catalytic C–H acylation (Table 2.5). Notably, in the absence of $Pd(OAc)_2$, no product formation was observed with full recovery of the starting materials (entry 2). The Pd(II) complexes with chloride ligands such as $[PdCl_2(PhCN)_2]$ and $[PdCl_2(PPh_3)_2]$ produced **3a** in around 55% yields (entries 3 and 4). Yet, employing $[Pd(CH_3CN)_2(OTs)_2]$ as catalyst resulted in no detectable product formation with substantial decomposition of the starting oximes (entry 5). This result is consistent with our previous finding with TsOH as additives (Table 2.4). Increasing the $Pd(OAc)_2$ loading to 10 mol% did not give significant improvement in the product yield (entry 6).

Table 2.5 Effect of the Pd catalyst[a]

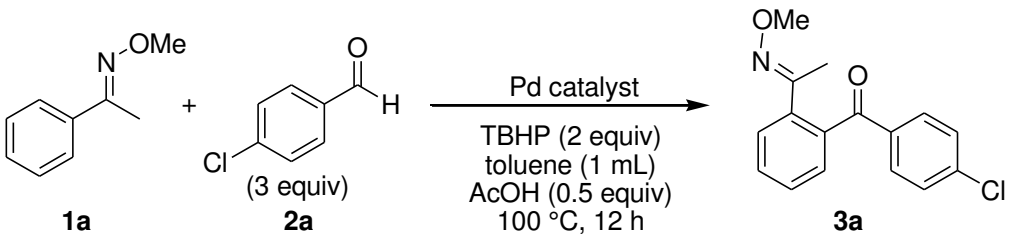

1a **2a** **3a**

entry	Pd catalyst	yield (%)[b]
1	$Pd(OAc)_2$	58
2	-	0
3	$[PdCl_2(PhCN)_2]$	53
4	$[PdCl_2(PPh_3)_2]$	63
5	$[Pd(CH_3CN)_2(OTs)_2]$	0
6[c]	$Pd(OAc)_2$	55

[a]Reaction conditions: **1a** (0.25 mmol), **2a** (0.75 mmol), Pd catalyst (5 mol%), TBHP (0.5 mmol), AcOH (0.125 mmol) and undegassed toluene (1 mL) at 100 ^{o}C for 12 h. [b]Yields were determined by ^{1}H NMR with 1,2-dibromomethane as internal standard. [c]10 mol% $Pd(OAc)_2$ was used.

Effect of the amount of the aldehyde (**2a**) and TBHP was examined (Table 2.6). When the amount of **2a** increased to 6 equiv, **3a** was obtained in 76% (entry 2). However, further increase the aldehyde amount to 10 equiv failed to give better results (67% yield, entry 3). Varying the amount of TBHP from 1 to 3 equiv only gave **3a** in 45% and 58% yield, respectively (entries 4 and 5).

Table 2.6 Effect of the aldehyde and TBHP quantity[a]

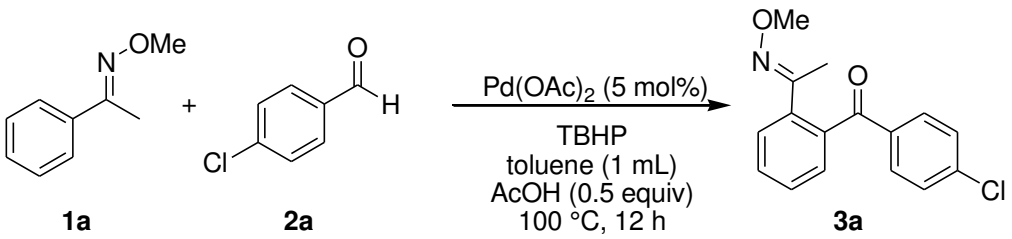

1a **2a** **3a**

entry	aldehyde (equiv)	TBHP (equiv)	yield (%)[b]
1	3	2	58
2	6	2	76
3	10	2	67
4	6	1	45
5	6	3	58

[a]Reaction conditions: **1a** (0.25 mmol), **2a**, $Pd(OAc)_2$ (5 mol%), TBHP, AcOH (0.125 mmol) and undegassed toluene (1 mL) at 100 ^{o}C for 12 h. [b]Yields were determined by ^{1}H NMR with 1,2-dibromomethane as internal standard.

Temperature effect on the acylation reaction was also investigated (Table 2.7). By TLC monitoring, the reaction was found to be completed in 2 h at 100 ^{o}C (entry 2). When the reaction was performed at 120 ^{o}C, a diminished yield (65%) was obtained (entry 3). At 80 ^{o}C, the reaction only produced **3a** in 37% yield after four hours of reaction (entry 4).

Table 2.7 Effect of temperature and reaction time[a]

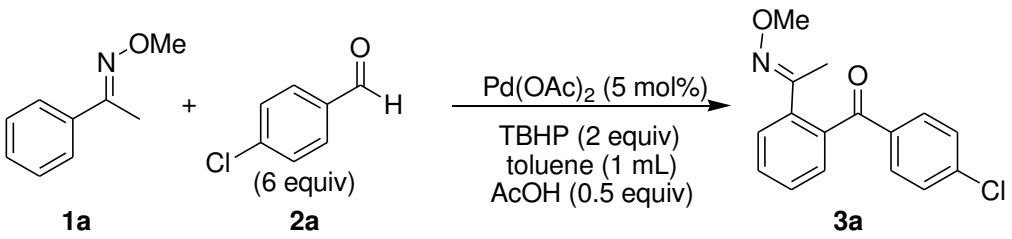

1a **2a** **3a**

entry	temp (^{o}C)	time (h)	yield (%)[b]
1	100	12	76
2	100	2	73
3	120	0.5	65
4	80	4	37

[a]Reaction conditions: **1a** (0.25 mmol), **2a** (1.5 mmol), $Pd(OAc)_2$ (5 mol%), TBHP (0.5 mmol), AcOH (0.125 mmol) and undegassed toluene (1 mL). [b]Yields were determined by ^{1}H NMR with 1,2-dibromomethane as internal standard.

Finally, we examined the effect of solvents (Table 2.8). Donor solvents such as THF, CH_3CN, DMF and DMA were all undesirable for the acylation, and **3a** was formed in 7-19% yields (entries 1 – 4). Dioxane was an effective solvent for this reaction, albeit with a slightly lower product yield of 51% being obtained (entry 5). Other non-polar solvents DCE and xylene failed to afford better results (entries 6 and 7). Eventually, toluene was still considered the best solvent based on the product yield (73%, entry 8). Thus, the optimal conditions were found to be: **1a** (0.25 mmol), **2a** (1.5 mmol), $Pd(OAc)_2$ (5 mol%), TBHP (0.5 mmol), AcOH (0.125 mmol) and

undegassed toluene (1 mL) at 100 °C for 2 h, and **3a** was produced in 71% isolated yield.

Table 2.8 Effect of solvents[a]

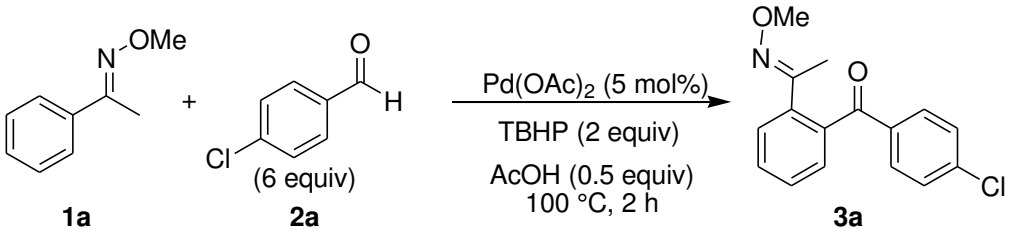

1a **2a** **3a**

entry	solvent (1 mL)	yield (%)[b]
1	THF	7
2	CH_3CN	18
3	DMA	19
4	DMF	11
5	dioxane	51
6	DCE	56
7	xylene	47
8	toluene	73, 71[c]

[a]Reaction conditions: **1a** (0.25 mmol), **2a** (1.5 mmol), $Pd(OAc)_2$ (5 mol%), TBHP (0.5 mmol), AcOH (0.125 mmol) and undegassed solvent (1 mL) at 100 °C for 2 h. [b]Yields were determined by ^1H NMR with 1,2-dibromomethane as internal standard. [c]Isolated yield.

2.1.2.2 Scopes and limitations

With the optimized conditions in hand, we turned to examine the substrate scope

of the Pd-catalyzed acylation reaction, and the results were depicted in Table 2.9. With 4-chlorobenzaldehyde as coupling partner, the substituted acetophenone oximes were transformed to the corresponding ketones **3b**, **3c** and **3g** in 50-88% yields. In general, electron-withdrawing (F, Cl, Br, $MeSO_2$) and -donating groups (OMe, amide) were tolerated (**3a**-**3f**). For **3e**, the aldehyde coupling was selectively directed to the *ortho*-position of the oxime group, rather than the amide group. This result reflects the stronger donor ability of the nitrogen than the oxygen atom.[36] Consistent with many related studies,[37] the Pd-catalyzed C–H acylation of *meta*-substituted arenes was favored at the less hindered site of the aromatic ring (**3c** and **3f**).

Oximes with a bicyclic scaffold would also undergo facile C–H acylation reactions. For instance, 4-chromanone *O*-methyl oxime would react with 4-chlorobezaldehyde (6 equiv) under the Pd-catalyzed conditions to furnish ketone **3g** in 88% yield. Likewise, effective transformations of the tetralone analogues to **3h** (75%) and **3i** (87%) were also accomplished with piperonal and 2-naphthaldehyde as the coupling partners. Aliphatic aldehydes such as 3-phenylpropanal, 1-hexanal and cyclohexylcarboxyaldehyde can be coupled to the oximes under our optimized conditions to afford ketones **3j** (90%), **3k** (87%) and **3l** (77%) respectively.

Scheme 2.3 Synthesis of Aroylindoles

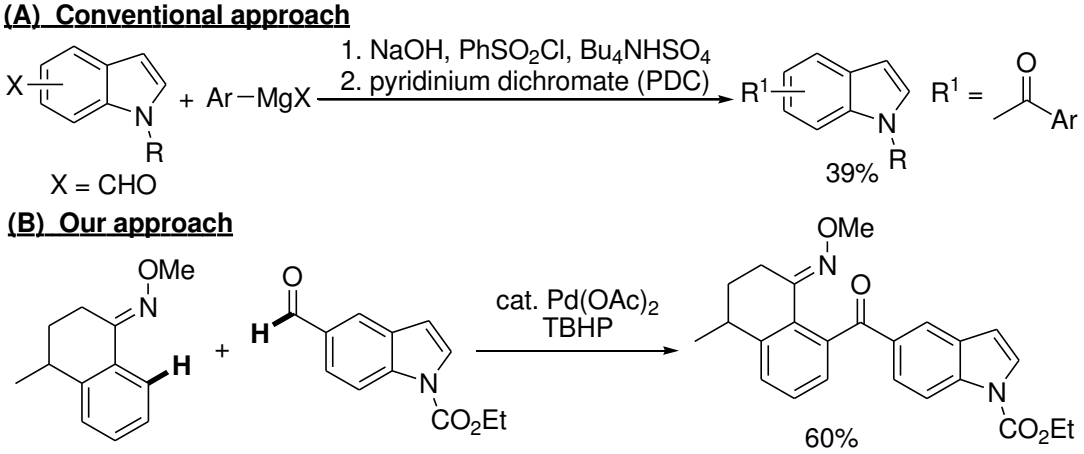

Heteroaromatic rings such as indoles are important scaffords of many pharmaceutically active compounds;[38] 1-aryoylindoles can be readily prepared by direct acylation of the N–H free indole precursors. Conventionally, other regioisomers can be prepared from the indole-carboxyaldehydes by Grignard addition, followed by PDC oxidation with only 39% overall yield (Scheme 2.3).[39] In our approach, when the tetralone *O*-methyl oxime was treated with ethyl 5-formyl-1*H*-indole-1-carboxylate under the Pd-catalyzed conditions, ketone **3p** was exclusively isolated in 60% yield and C3-functionalized products were not detected. Similarly, effective couplings with furfural and 5-chloro-2-thiophenecarboxyaldehyde were also accomplished in 55% (**3n**) and 95% (**3o**) yields. As expected, the catalytic coupling of 4-chromanone oxime with 2-benzofurancarboxyaldehyde gave ketone **3m** in 72% yield. In all cases, no

significant oxidation to the heterocycles was observed under our experimental conditions.

In this work, the direct acylation of the sp^3 C–H bond has also been examined. Treatment of 8-methylquinoline with 4-chlorobenzaldehyde using the Pd-catalyzed protocol afforded ketone **3q** in 42% yield. 8-Quinolyl benzyl (**3q'**) was obtained as side product (22%) due to over-oxidation.

Scheme 2.4 *O*-Acetyl oximes as removable directing group

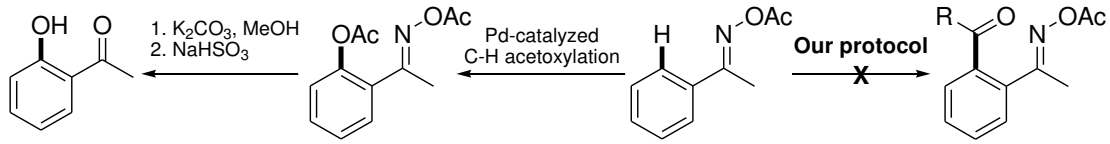

According to Sanford and co-workers, *O*-acetyl oximes were effective directing groups for the Pd-catalyzed C–H acetoxylations and that they can be removed more readily than the oxime ether groups (Scheme 2.4).[40] Despite this apparent advantage, our Pd-catalyzed protocol failed to give ketone products when acetophenone *O*-acetyl oxime was employed as substrate. NMR analysis of the reaction mixture revealed substantial decomposition of the starting oximes.

Table 2.9 Substrate scope study for the Pd-catalyzed cross coupling reaction of oximes with aldehydes[a,b]

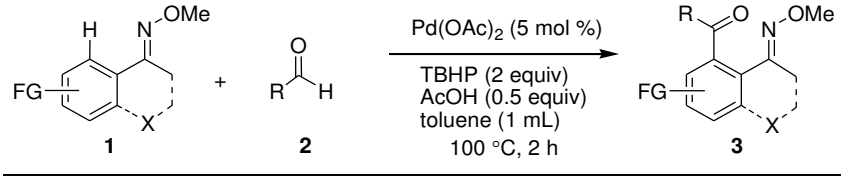

1 **2** **3**

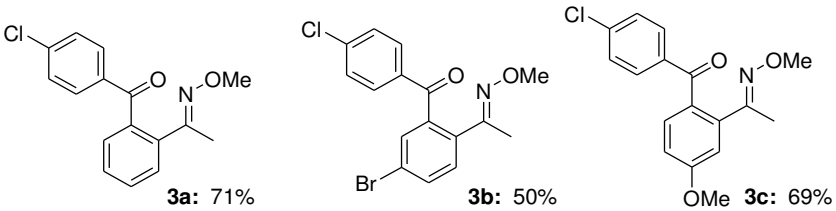

3a: 71%

3b: 50%

3c: 69%

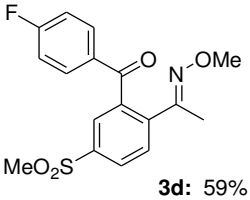

3d: 59%

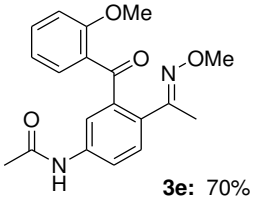

3e: 70%

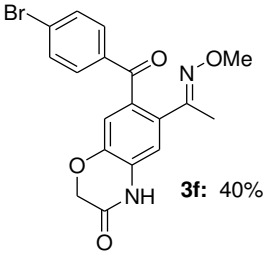

3f: 40%

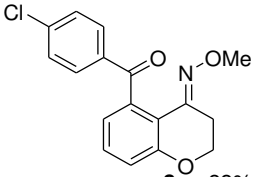

3g: 88%

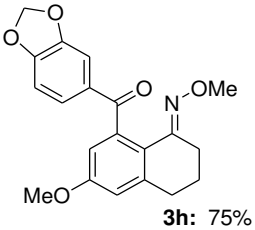

3h: 75%

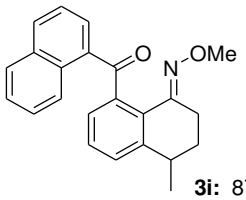

3i: 87%

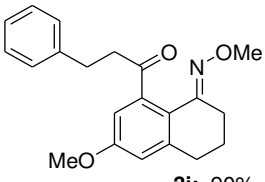

3j: 90%

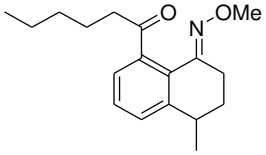

3k:[c] 87%

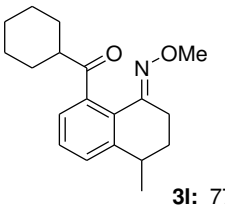

3l: 77%

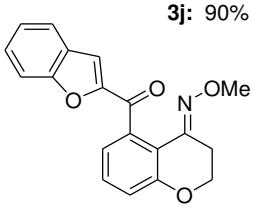

3m: 72%

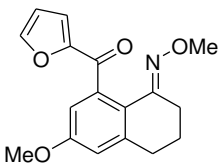

3n: 55%

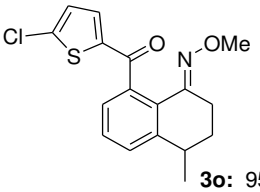

3o: 95%

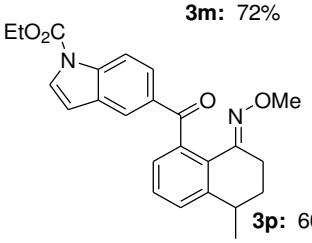

3p: 60%

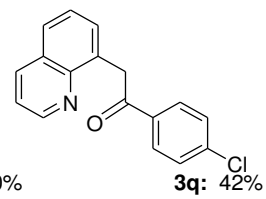

3q: 42%

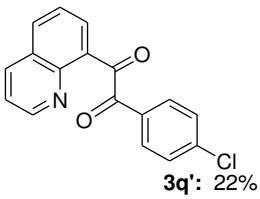

3q': 22%

[a]Reaction conditions: **1** (0.25 mmol), **2** (1.5 mmol), $Pd(OAc)_2$ (5 mol%), TBHP (0.5 mmol), AcOH (0.125 mmol) and undegassed toluene (1 mL) at 100 °C for 2 h. [b]Isolated yields. [c]DCE as solvent.

2.1.2.3 Synthetic applications

Having established the catalytic direct acylation reaction, we hoped to explore the synthetic application of this acylation reaction. *O*-Methyloxime group serves as excellent directing group due to easy formation and chemical stability. However, unlike oximes (=NOH), *O*-methyloximes are particularly unreactive toward acid hydrolysis. Thus, we began to investigate deprotection of *O*-methyloximes to ketones.

Table 2.10 Screening conditions for the deoximation of **2a**[a]

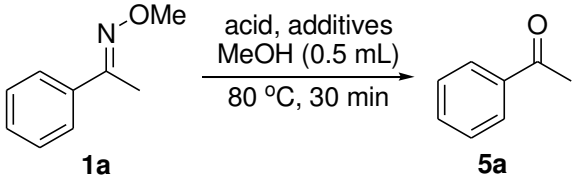

1a **5a**

entry	acid (0.5 mL)	additives (equiv)	yield (%)[b]
1	AcOH	---	0
2	1M HCl	---	0
3	3M HCl	---	10
4	6M HCl	---	44
5	12M HCl	---	48
6	6M HCl	Fe (2)	60

7	6M HCl	Zn (2)	29[c]
8	6M HCl	Cu (2)	62
9	6M HCl	Cu (2)	60[d]
10	6M HCl	Cu (2)	56[e]
11	6M HCl	Cu (1)	58
12	6M HCl	Cu (4)	61
13	6M HCl	Cu (2)	70[f]

[a]Reaction conditions: **1a** (0.25 mmol), acid (0.5 mL), additive, MeOH (0.5 mL), 80 ^{o}C, 30 min. [b]Yields were determined by GC with tetradecane as internal standard. [c]Ethyl benzene as over reduced product is observed. [d]Reaction run for 1.5 h. [e]Reaction run at 60 ^{o}C. [f]Dioxane (0.5 mL) as solvent.

Initially, we employed the readily available acetophenone *O*-methyl oxime **1a** as model substrate (Table 2.10). Treating **1a** with AcOH and 1M HCl solution (0.5 mL) in MeOH (0.5 mL) at 80 ^{o}C failed to give the desired **5a** (entries 1 and 2). Yet, using 3M HCl solution afforded **5a** in 10% yield (entry 3). Preliminary results indicated that the use of concentrated HCl solution is crucial to the deprotection. Thus HCl solution with various concentrations was tested, and the formation of **5a** increased to 44% with 6M HCl (entries 4 and 5). Employing a modified procedure of Giri and co-workers,[41] we treated **1a** with a mixture of iron powder and HCl, and **5a** was obtained in 60% yield (entry 6). Finally, employment of 6M HCl with copper powder with dioxane as solvent led to better result (70%) (entry 13).

Scheme 2.5 Phthalazine synthesis

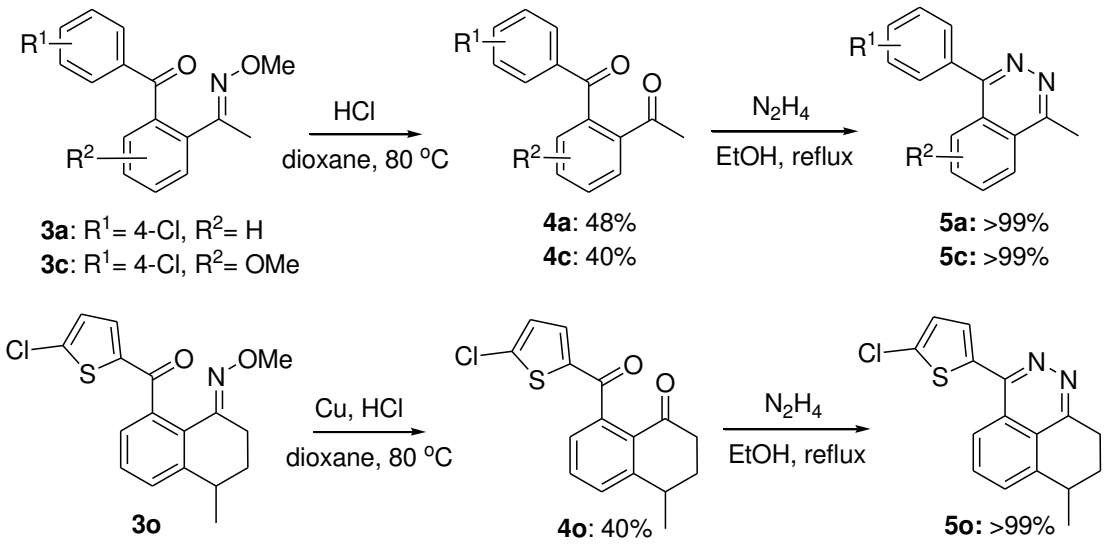

With the optimized conditions in hand, we turned to develop a straightforward synthesis of phthalazines (Scheme 2.5). Phthalazines and derivatives are known to exhibit interesting luminescent[42] and anticancer activities[43]. In this work, the oxime deprotection for **3a** and **3c** was performed well in HCl/dioxane mixture (2 mL, 1:1 v/v). After hydrazine condensation, **5a** and **5c** were obtained in around 45% overall yield. Yet, treating of **3o** with the HCl/dioxane protocol produced a complicated mixture. However, successful oxime deprotection was achieved in the presence of copper powder, and subsequent hydrazine condensation afforded **5o** in 40% overall yield.

2.2 Palladium-catalyzed direct C-H acylation of anlides

2.2.1 Background

Scheme 2.6 Some medicinally useful heterocycles derived from 2-aminobenzophenones

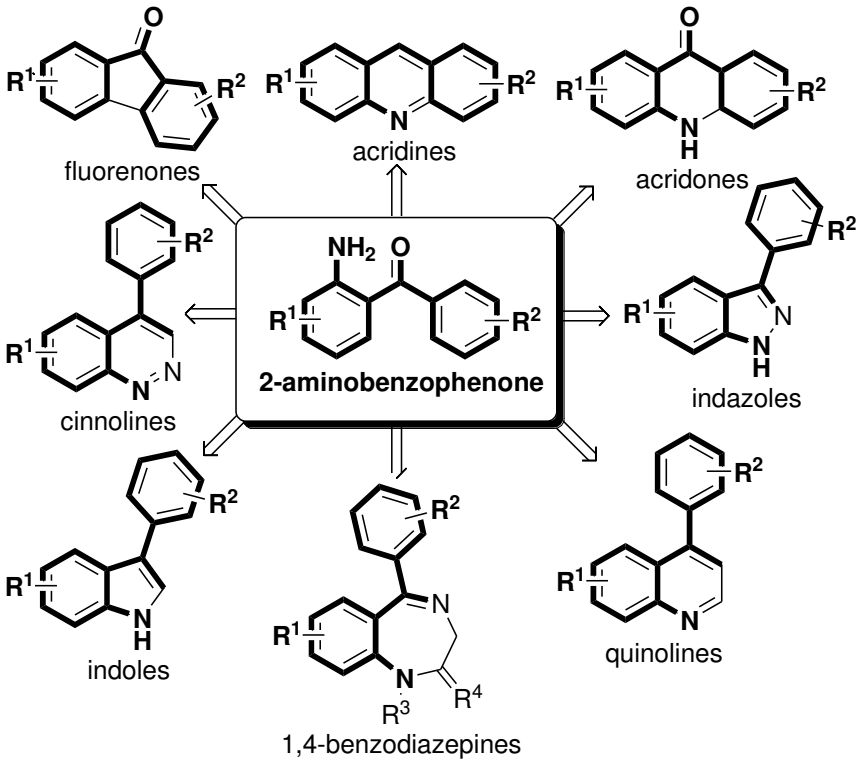

With the success in the catalytic C–H acylation of oximes, we were prompted to extend this reaction to the synthesis of other important organic molecules. 2-Aminobenzophenones are important precursors to many medicinally useful heterocycles such as fluorenones, cinnoline, acridones, indazoles, indoles, quinolines and benzodiazepines (Scheme 2.6).[44,45] Conventionally, 2-aminobenzophenones are

prepared by Friedel-Crafts acylation of anthranilic acids with arenes (Scheme 2.7, route A).[44b] However, the Friedel-Crafts acylations suffer from poor regioselectivity using an over-stoichiometric amount of Lewis acid catalyst. While direct Friedel-Crafts acylation of anilines with acyl chlorides is problematic, 2-aminobenzophenones can be prepared by directly reacting anilines with benzonitriles promoted by the stoichiometric amounts of BCl_3 and $AlCl_3$ (the Sugasawa reaction) (Scheme 2.7, route B).[46]

Scheme 2.7 Synthesis of 2-aminobenzophenones

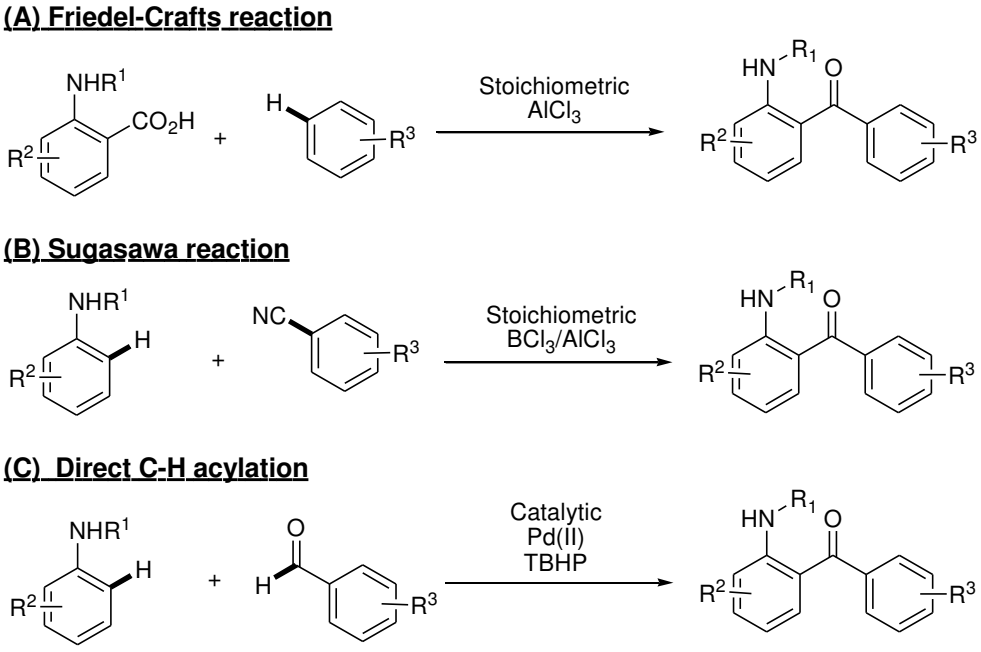

Notwithstanding, with the growing demand for sustainable chemical synthesis, direct catalytic C–H functionalization of anilines by employing non-hazardous acylating reagents under mild conditions are highly desirable.[47] In this work, we describe a highly versatile 2-aminobenzophenone synthesis by Pd-catalyzed oxidative *ortho*-C–H bond cross coupling of anilides[48] with aldehydes using TBHP as oxidant (Scheme 2.7, route C). Unlike the Friedel-Crafts reactions, the catalytic anilide coupling reactions proceed at 40 ^{o}C and exhibit excellent regiocontrol and functional group tolerance; aliphatic, aromatic and heteroaromatic aldehydes are effective coupling partners to generate structurally diverse 2-aminobenzophenone derivatives.

2.2.2 Results and discussion

Initially, we examined the reaction of 3,4-dimethyl-*N*-pivalanilide **6a** (0.25 mmol) and 4-chlorobenzaldehyde **2a** (0.75 mmol) in the presence of TBHP (0.5 mmol), TFA (0.25 mmol) and $Pd(TFA)_2$ (10 mol %) in undegassed DCE (1 mL) at 100 ^oC for 3 h. We were gratified that **7a** was obtained in 50% yield (Scheme 2.8). The molecular structure of **7a** has been established by X-ray crystallography (Figure 2.2). Under our experimental conditions, formation of *ortho*-arylation products was not observed.

Scheme 2.8 Preliminary study

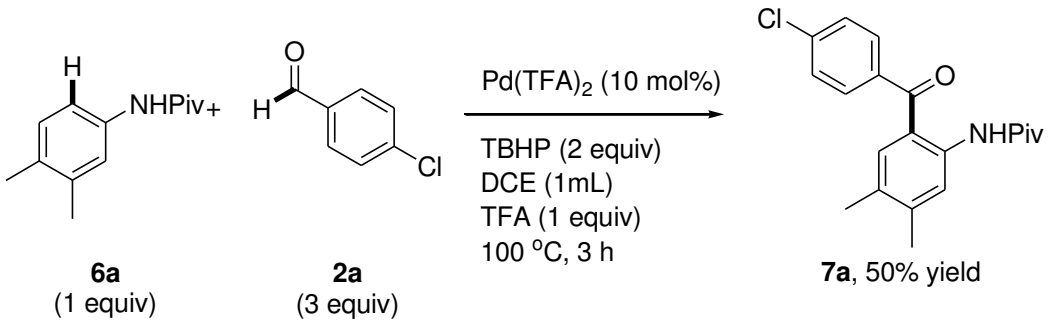

Figure 2.2 Molecular structure of **7a**

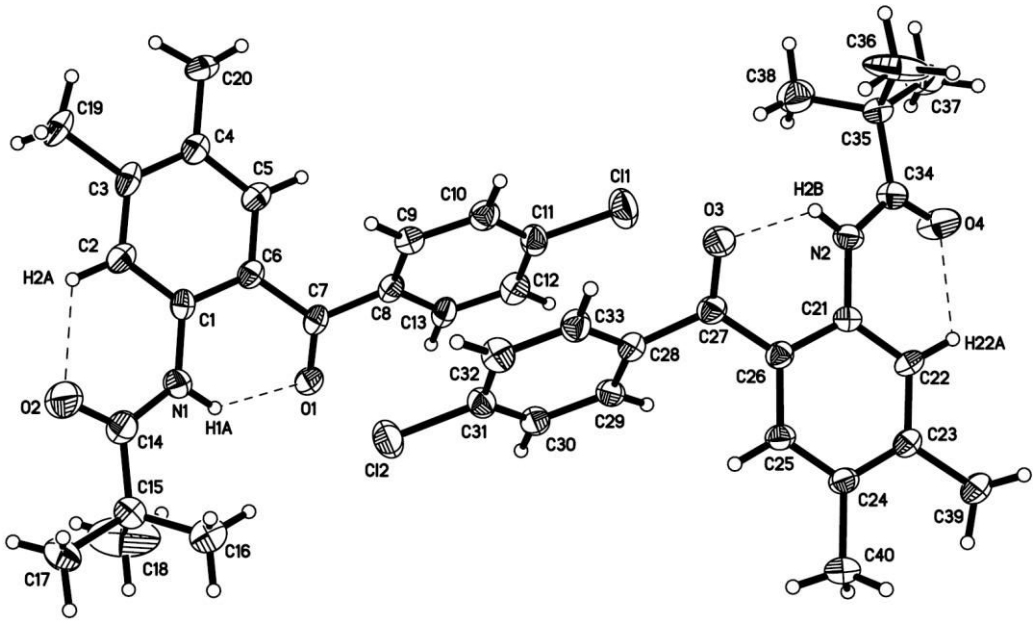

Table 2.11 Selected bond distances and angles of **7a**

bond distances [Å]	
C(6)-C(7)	1.473(2)
O(1)-C(7)	1.230(2)
C(7)-C(8)	1.493(3)
Cl(1)-C(11)	1.735(2)
N(1)-C(14)	1.343(2)

bond angles [^{o}]	
O(1)-C(7)-C(6)	121.59(17)
O(1)-C(7)-C(8)	119.37(16)

Table 2.12 Crystal data and structure refinement for **7a**

Empirical formula	$C_{20}H_{22}NO_2Cl$
Formula weight	343.84
Temperature	296(2) K
Wavelength	0.71073 Å
Crystal system	monoclinic
Space group	P2(1)/c
Unit cell dimensions	a = 18.5793(7) Å □= 90°.
	b = 11.4493(4) Å □= 114°.
	c = 19.7532(9) Å □= 90°.
Volume	3829.7(3) $Å^3$
Z	8
Density (calculated)	1.193 mg/m^3
Absorption coefficient	0.210 mm^{-1}
F(000)	1456
Crystal size	0.50 x 0.40 x 0.36 mm^3
Theta range for data collection	2.08 to 27.54°.
Index ranges	-24<=h<=24,-14<=k<=14, -25<=l<=21
Reflections collected	49384
Independent reflections	8802 [R(int) = 0.1050]
Completeness to theta = 27.31°	99.7 %
Absorption correction	Semi-empirical from equivalents
Max. and min. transmission	0.746 and 0.623
Refinement method	Full-matrix least-squares on F^2
Data / restraints / parameters	8802 / 21 / 490
Goodness-of-fit on F^2	1.004
Final R indices [I>2sigma(I)]	R1 = 0.0663, wR2 = 0.1647
R indices (all data)	R1 = 0.2132, wR2 = 0.2239
Extinction coefficient	0.0013(2)
Largest diff. peak and hole	0.235 and -0.211 $e.Å^{-3}$

2.2.2.1 Reaction optimization

To begin, the effect of temperature was examined (Table 2.13). The reaction was found to be completed in 3 h at 100 °C and **3a** was formed in only 50% yield (entry 1). When the reaction was lower to 40 °C, a better yield of 80% was obtained (entry 2). Performing the reaction under a nitrogen atmosphere further improved the product yield to 90% (entry 3). We found that effective acylation also occurred even at room temperature with an extended reaction time (12 h), with **7a** being obtained in 77% yield (entry 4).

Table 2.13 Effect of temperature and reaction time[a]

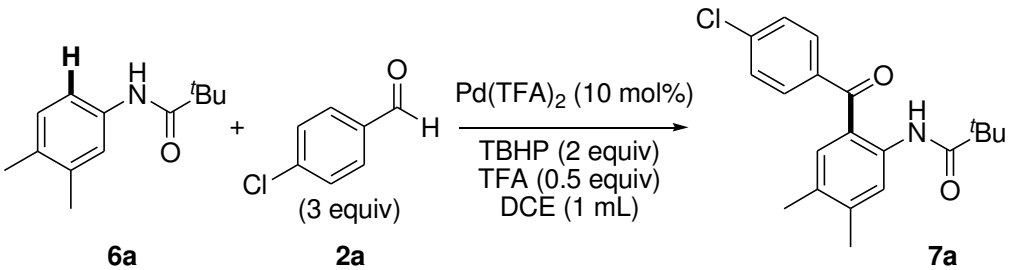

6a **2a** **7a**

entry	temp (°C)	time (h)	conv (%)[b]	yield (%)[b]
1	100	3	100	50
2	40	3	95	80
3[c]	40	3	10	90
4	rt	12	79	77

[a]Reaction conditions: **6a** (0.25 mmol), **2a** (0.75 mmol), $Pd(TFA)_2$ (10 mol%), TBHP (0.5 mmol), TFA (0.125 mmol) and undegassed DCE (1 mL). [b]Yields were determined by ^1H NMR with 1,2-dibromomethane as internal standard. [c]Under N_2.

Table 2.14 Effect of solvents[a]

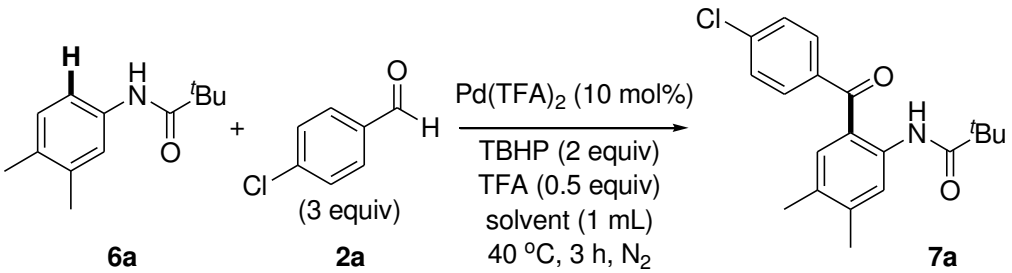

6a **2a** **7a**

entry	solvent	conv (%)[b]	yield (%)[b]
1	DCE	100	90
2	dioxane	54	34
3[c]	CH_3CN	60	31
4	DME	70	56
5	toluene	100	94

[a]Reaction conditions: **6a** (0.25 mmol), **2a** (0.75 mmol), $Pd(TFA)_2$ (10 mol%), TBHP (0.5 mmol), TFA (0.125 mmol) and solvent (1 mL), 40 °C, 3 h, under nitrogen. [b]Yields and conversion were determined by ^1H NMR with 1,2-dibromomethane as internal standard.

Commonly used organic solvents were screened (Table 2.14). Donor solvents such as dioxane, CH_3CN and DME were undesirable solvents for the acylation, and **3a** was formed in 34-56% yields (entries 2 – 4). When toluene was employed as solvent, the best result was achieved (94%) (entry 5).

Table 2.15 Effect of the Pd catalyst[a]

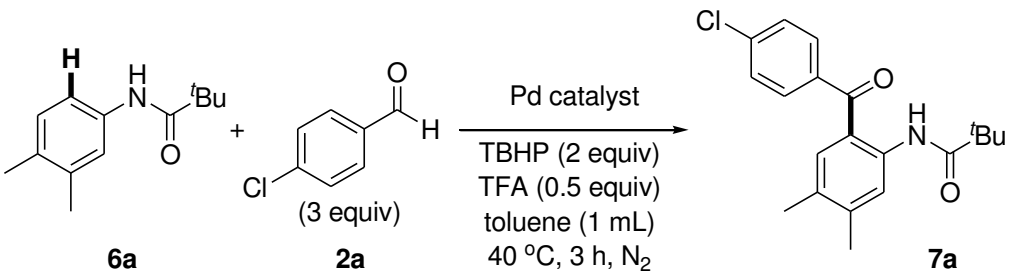

6a **2a** **7a**

entry	Pd catalyst (mol%)	conv (%)[b]	yield (%)[b]
1	$Pd(TFA)_2$ (10)	100	94
2	---	0	0
3	$Pd(OAc)_2$ (10)	100	88
4	$Pd(OAc)_2$ (5)	100	86
5	$Pd(OTs)_2(CH_3CN)_2$	100	67
6	$PdCl_2(CH_3CN)_2$ (5)	30	<5
7	$PdCl_2(PPh_3)_2$ (5)	60	39

[a]Reaction conditions: **6a** (0.25 mmol), **2a** (0.75 mmol), Pd catalyst, TBHP (0.5 mmol), TFA (0.125 mmol) and toluene (1 mL), 40 °C, 3 h under nitrogen. [b]Yields and conversion were determined by ^{1}H NMR with 1,2-dibromomethane as internal standard.

Apart from $Pd(TFA)_2$, we evaluated other Pd(II) complexes for the catalytic C–H acylation (Table 2.15). As anticipated, there was no product formation with full recovery of starting materials in the absence of Pd complex (entry 2). $Pd(OAc)_2$ exhibits comparable activity, and 88% of **7a** was formed. Notably, lower catalyst loading of $Pd(OAc)_2$ of 5 mol% gave comparable yield (entry 4). Employing

$[Pd(OTs)_2(CH_3CN)_2]$ as catalyst gave no improvement of the product formation (entry 5). Pd(II) complexes with chloride ligands like $[PdCl_2(CH_3CN)_2]$ and $[PdCl_2(PPh_3)_2]$ produced poor results (entries 6 and 7).

Table 2.16 Effect of TFA loading[a]

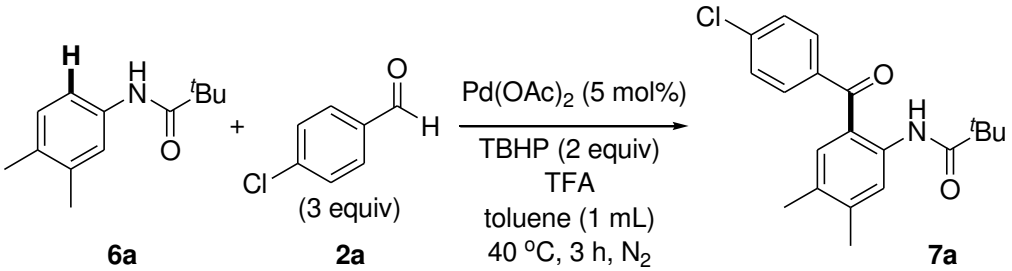

6a **2a** **7a**

entry	TFA (equiv)	conv (%)[b]	yield (%)[b]
1	---	0	0
2	10	83	<5
3	5	73	<5
4	1	100	86
5	0.5	95	80
6	0.1	40	36

[a]Reaction conditions: **6a** (0.25 mmol), **2a** (0.75 mmol), $Pd(OAc)_2$ (5 mol%), TBHP (0.5 mmol), TFA and toluene (1 mL), 40 °C for 3 h under nitrogen. [b]Yields and conversion were determined by ^1H NMR with 1,2-dibromomethane as internal standard.

The amount of TFA was examined for the C–H acylation of anilides (Table 2.16). In the absence of TFA, **7a** was not obtained with full recovery of the starting materials

(entry 1). Applying 5-10 equiv of TFA for the acylation reaction, **7a** was obtained in less than 5% yield and substantial decomposition of **6a** was observed (entries 2 and 3). Gratifyingly when 1 equiv of TFA was used, **7a** was obtained in 86% yield (entry 4). Yet, employing 0.1 equiv TFA resulted in poor conversion of substrate **6a**, and **7a** was obtained in 36% yield (entry 6).

Table 2.17 Effect of acids[a]

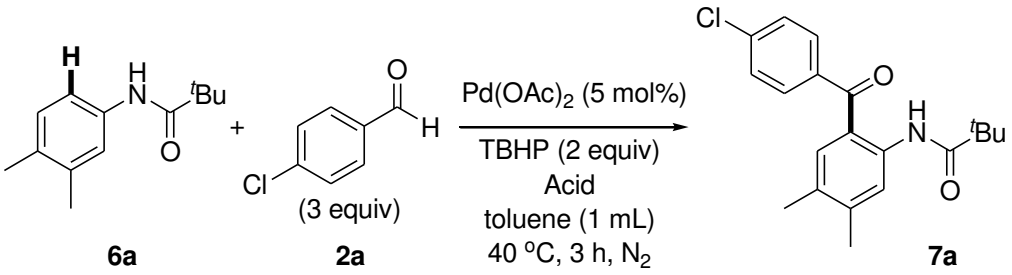

6a **2a** **7a**

entry	acid (1 equiv)	conv (%)[b]	yield (%)[b]
1	AcOH	15	<5
2	PivOH	0	0
3	$PhCO_2H$	10	10
4	$C_5H_{11}CO_2H$	0	0
5	TsOH	100	48
6	TFA	100	86

[a]Reaction conditions: **6a** (0.25 mmol), **2a** (0.75 mmol), $Pd(OAc)_2$ (5 mol%), TBHP (0.5 mmol), acid additive (0.25 mmol) and toluene (1 mL), 40 °C for 3 h under nitrogen. [b]Yields and conversion were determined by ^1H NMR with 1,2-dibromomethane as internal standard.

For comparison, we also examined the effect of different acids for the C–H acylation reactions (Table 2.17). With AcOH as additive, **7a** was obtained in only 15% (entry 1). Employing other carboxylic acids such as PivOH, $PhCO_2H$ and $C_5H_{11}CO_2H$ as additives failed to give better product yields (entries 2 – 4). Notably, the use of TsOH as additives led to serious substrate decomposition, and **7a** was obtained in only 48% yield (entry 5). In this work, TFA was the most effective additives for the acylation, and **7a** was formed in 86% yield (entry 6).

Table 2.18 Effect of aldehyde and TBHP quantity[a]

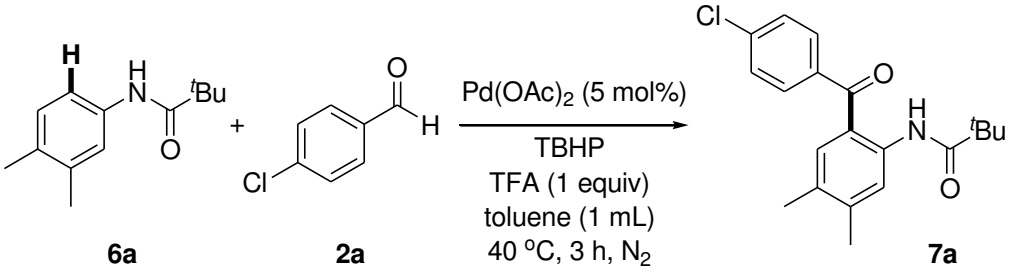

6a **2a** **7a**

entry	**2a** (equiv)	TBHP (equiv)	conv (%)[b]	yield (%)[b]
1	3	2	100	86
2	3	1.5	78	61
3	3	1	70	50
4	6	2	100	88
5	1.5	2	88	68

[a]Reaction conditions: **6a** (0.25 mmol), **2a**, $Pd(OAc)_2$ (5 mol%), TBHP, TFA (0.25 mmol) and toluene (1 mL), 40 °C for 3 h under nitrogen. [b]Yields and conversion were determined by ^1H NMR with 1,2-dibromomethane as internal standard.

The amount of **2a** and TBHP was also examined (Table 2.18). Reducing the amount of TBHP to 1.5 and 1 equiv resulted in 61% and 50% product yield respectively (entries 2 and 3). When the amount of **2a** was increased to 6 equiv, formation of **3a** was slightly increased to 88% (entry 4). However, employing 1.5 equiv of **2a** resulted in only 68% of **7a** being formed (entry 5).

Table 2.19 Effect of oxidants[a]

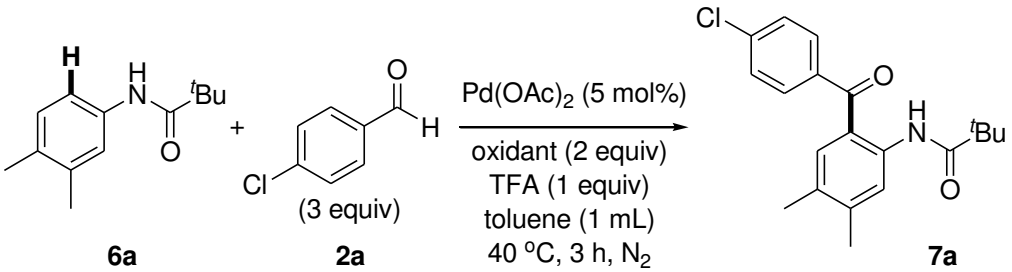

6a **2a** **7a**

entry	oxidant (2 equiv)	conv (%)[b]	yield (%)[b]
1	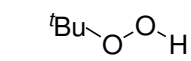	100	86[c]
2	---	0	0
3	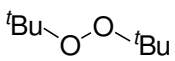	0	0
4	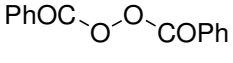	60	0
5	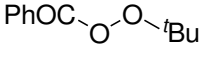	0	0
6	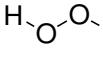	20	0
7	$K_2S_2O_8$	20	trace
8	$Cu(OAc)_2$	0	0

9	BQ	0	0

[a]Reaction conditions: **6a** (0.25 mmol), **2a** (0.75 mmol), $Pd(OAc)_2$ (5 mol%), oxidant (0.5 mmol), TFA (1 equiv) and toluene (1 mL), 40 ^oC for 3 h under nitrogen. [b]Yields and conversion were determined by ^1H NMR with 1,2-dibromomethane as internal standard. [c]Isolated yield.

Finally, the effectiveness of oxidants was also examined (Table 2.19). Apart from TBHP, other peroxide-type oxidants (e.g. *tert*-butyl peroxide, benzoyl peroxide, *tert*-butyl peroxybenzoate, $K_2S_2O_8$ and H_2O_2) failed to produce any significant product formation. BQ and $Cu(OAc)_2$, which are common oxidants for Pd(0) regeneration to Pd(II), are also failed to effect any desirable product.

Thus, the optimal conditions were found to be: **6a** (0.25 mmol), **2a** (0.75 mmol), $Pd(OAc)_2$ (5 mol%), TFA (0.125 mmol), TBHP (0.5 mmol) and toluene (1 mL) under nitrogen at 40 ^oC for 3 h, and **7a** was obtained in 86% isolated yield (Table 2.19, entry 1).

2.2.2.2 Scopes and limitations

With the optimized conditions in hand, we turned to examine the substrate scope for the acylation of anilides, and the results were depicted in Table 2.20. Treating 4-chlorobenzaldehyde (**2a**, 3 equiv) and 3-methoxypivalanilide (**6b**) in the Pd-catalyzed conditions [$Pd(OAc)_2$ (5 mol%), TBHP (2 equiv), TFA (1 equiv), N_2, toluene, 40 ^oC, 3 h (method A)] afforded **7b** in 71% yield. However, method A was less effective for the analogous reaction of 3-tosyloxypivalanilide (**6c**) with **7c** being formed in 28% yield. After several attempts, effective cross coupling of **6c** was achieved when TBHP was added in a batchwise fashion (method B); product **7c** was obtained in 74% yield. Similarly, other substituted pivalanilides (Y = 3-$OCHF_2$, 4-C(O)Me and 4-Br) would undergo facile cross-coupling with method B: **7d** (70%), **7e** (52%), **7f** (45%). Acetamido, benzamido and tertiary amide groups are effective directing groups for the *ortho*-C–H coupling reactions to give arylketones **7g**-**k** in 64-55% yields.

As expected, other substituted benzaldehydes are effective coupling partners for the Pd-catalyzed acylation of pivalanildes, and the ketones **7l**-**n** were produced in 87 – 72% yields. Likewise, the coupling with aliphatic aldehydes such as pentanal, cyclohexane-carboxyaldehyde, 3-phenylpropanal and phenylacetaldehyde furnished

ketones **7o** (72%), **7p** (76%), **7q** (70%) and **7r** (48%), respectively. In this work, facile coupling of cyclopropane-carboxyaldehyde with acetanilide afforded exclusively cyclopropyl arylketone **7s** in 64% yield. Furthermore, the reaction of (*tert*-butyldimethylsilyloxy)acetaldehyde with acetanilde gave **7t** in 61% yield, and the silyloxy group was well tolerated. Similarly *N*-Cbz-protected 2-aminopropanal reacted with pivalanilide to afford **7u** in 64% yield. It was reported that amino-functionalized ketones such as **7u** are useful precursors for the *N*-alkylaminoethylcamptothecin analogues.[49] According to the literature, the amino-functionalized aryl-ketones were prepared in four steps involving Freidel-Craft acylation and Michael addition with appropriate alkylamines in 7 – 44% yields (Scheme 2.9).[50]

Scheme 2.9 Synthesis of *N*-alkylaminoethylcamptothecin prescursors

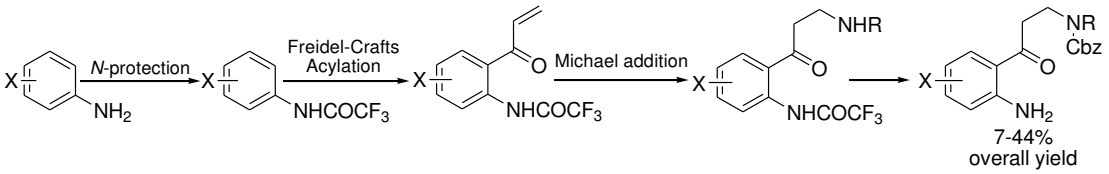

Heteroaromatic rings such as indoles are important scaffolds for many pharmaceutically active compounds. In this work, when pivalanilide **6a** was treated

with ethyl-5-formyl-1-*H*-indole-1-carboxylate under the Pd-catalyzed conditions, ketone **7v** was exclusively isolated in 60% yield. The couplings with furfural, 5-chloro-2-thiophenecarboxyaldehyde and 2-benzothiophene-carboxyaldehyde were also accomplished: **7w** (62%), **7x** (75%) and **7y** (76%). In all cases, no significant oxidation to the heterocycles was observed under our experimental conditions.

2.3 Proposed mechanism for palladium-catalyzed direct C-H acylation

A plausible mechanism is shown in Scheme 2.10. The acylation may be initiated by arene C–H bond palladation to form cyclopalladated complex **A**. Then complex **A** would couple with the acyl radicals, which were generated *in situ* by hydrogen atom abstraction of the aldehydes, to give either the putative palladium (III) or (IV) intermediate **B**. Subsequently, C–C bond formation through reductive elimination affords the ketones and regenerates the Pd(II) species for the next catalytic run.

A more detailed mechanistic investigation of Pd(II)-catalyzed arene C–H acylation will be presented in the next chapter.

Table 2.20 Substrate scope study for the Pd-catalyzed cross coupling reaction of anilides with aldehydes[a,b]

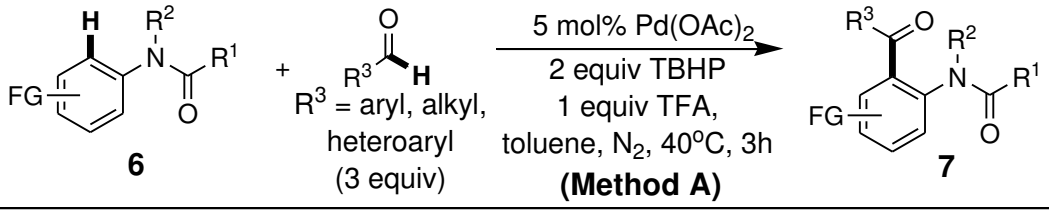

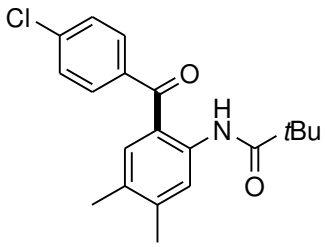

7a: 80%

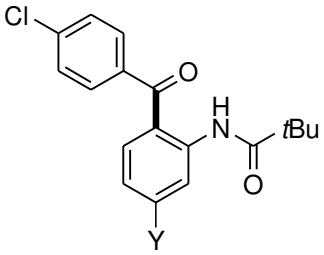

7b: **Y** = OMe, 71%
7c: **Y** = OTs, 74%[c]
7d: **Y** = $OCHF_2$, 70%[c]

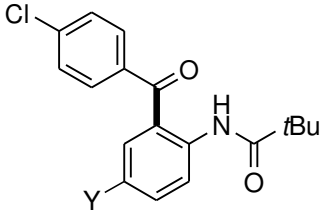

7e: **Y** = C(O)Me, 52%
7f: **Y** = Br, 45%

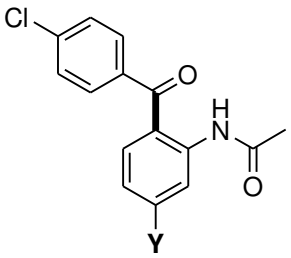

7g: **Y** = H, 59%[c]
7h: **Y** = Me, 63%[c]

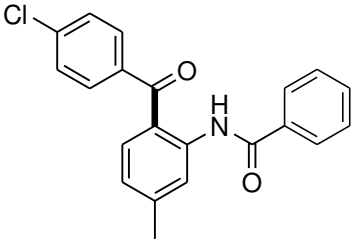

7i: 55%[c]

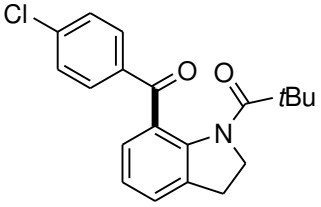

7j: 58%

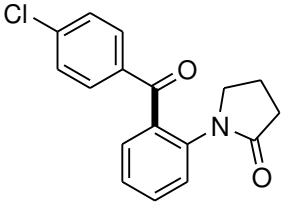

7k: 64%

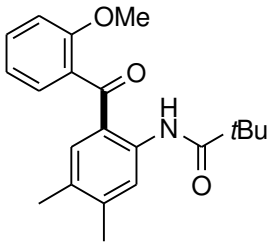

7l: 72%

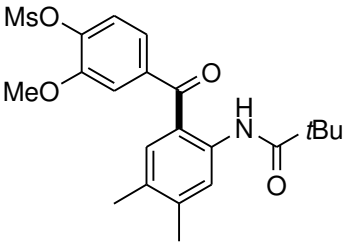

7m: 72%

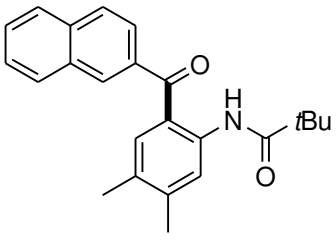

7n: 87%

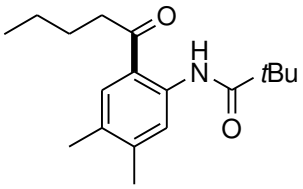

7o: 72%

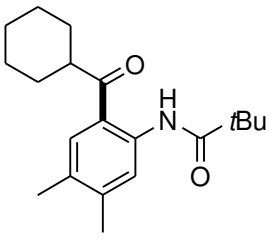

7p: 76%

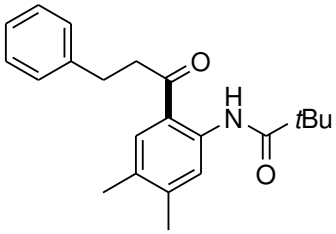

7q: 70%

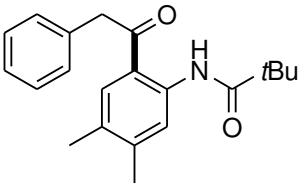

7r: 48%[c]

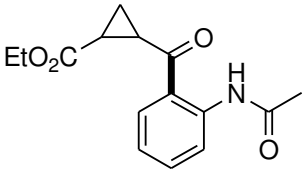

7s: 64%[c]

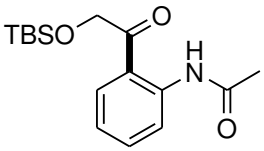

7t: 61%

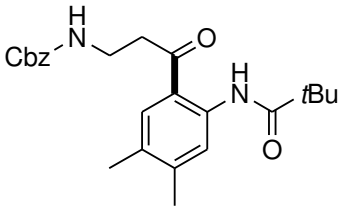

7u: 64%

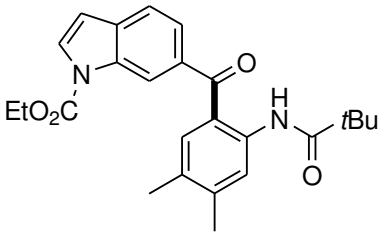

7v: 60%[c]

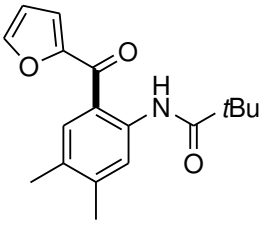

7w: 62%

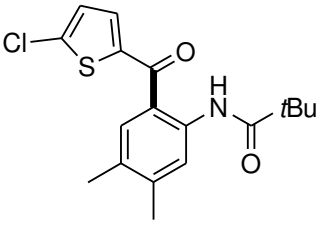

7x: 75%

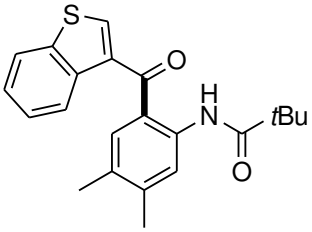

7y: 76%

[a]Reaction conditions: **6** (0.25 mmol), **2** (0.75 mmol), $Pd(OAc)_2$ (5 mol%), TBHP (0.5 mmol), TFA (0.25 mmol) and toluene (1 mL) under nitrogen at 40 °C for 3 h. [b]Isolated yields. [c]**Method B**: $Pd(OAc)_2$ (10 mol%), TBHP (2 x 0.25 mmol; addition interval 6 h).

Scheme 2.10 Proposed mechanism

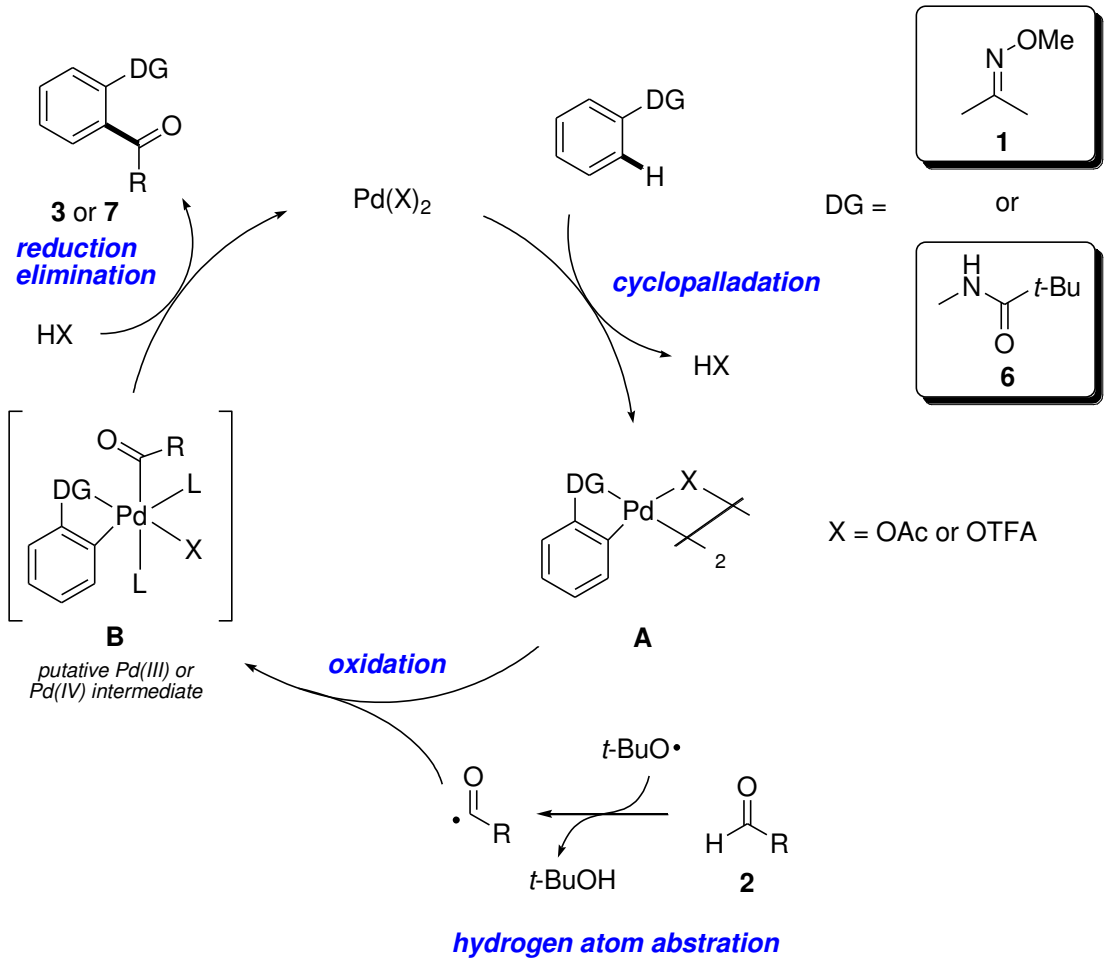

2.4 Concluding summary

In conclusion, we accomplished the Pd(II)-catalyzed *ortho*-C–H acylation of acetophenone oximes and anilides with aldehydes using tert-butyl hydroperoxide (TBHP) as benign oxidant for the synthesis of 1,2-diacylbenzenes and 2-aminobenzophenones.

For the acylation of oximes, functional groups such as halogens, methoxy, sulfonyl and amido groups were well tolerated, and the corresponding acylation products were formed in good yields and remarkable *ortho*-selectivity. Apart from benzaldehydes, aliphatic and heteroaryl aldehydes can be effectively coupled to the oximes. Deoximination of the acylation products produced 1,2-diacylbenzenes, which furnished phthalazine by condensation with hydrazine.

For the acylation of anilides, substrates bearing electron-releasing groups generally produced the desired product in good yields with excellent regioselectivity. Yet, substrates bearing electron-withdrawing group are less effective substrates with only moderate yields. A broad variety of aldehydes including aryl, aliphatic and heteroaryl aldehydes can be employed. The acylation of anilides occurred smoothly at

mild conditions (40 ^{o}C, 3 h).

The reactions were proposed to be initiated by Pd(II)-catalyzed *ortho*-C–H bond cleavage to generate a cyclopalladated complex. The cyclopalladated complex would react with the acyl radical, which is generate by hydrogen atom abstraction of aldehyde, to give putative Pd(III) or (IV) intermediate. Subsequent reductive elimination would furnish the acylation product and the active Pd(II) species.

2.5 Experimental section

All the solvents were freshly distilled and dried according to the standard methods prior to use. Oximes were prepared by reacting the aldehydes or ketones with $MeONH_2$. HCl in H_2O or MeOH for overnight, followed by 20% NaOH work-up then extraction with diethyl ether.[51a] Anilides were obtained from commercial suppliers (Aldrich) or synthesized by the reaction of the corresponding anilines with pivaloyl chloride.[23a] Aldehydes were obtained commercially and purified by vacuum distillation if necessary. 4.8M TBHP in DCE is prepared by the reported procedure.[51b]

Thin layer chromatography was performed on silica gel plates. Flash column chromatography was performed on silica gel (Merck, 230-400 mesh). ^{1}H and ^{13}C NMR spectra were recorded on a Bruker DPX-400 MHz spectrometer. The chemical shift (δ) values are given in ppm and are referenced to residual solvent peaks; carbon multiplicities were determined by DEPT-135 and DEPT-90 experiments. Coupling constants (*J*) were reported in hertz (Hz). Multiplicity abbreviations are: s = singlet, d= doublet, t = triplet, q = quartet, m = multiplet, dt = doublet of triplets, td = triplet of doublets, and br = broad. Mass spectra and high resolution mass spectra (HRMS) were obtained on a VG MICROMASS Fison VG platform, a Finnigan Model Mat 95 ST instrument, or a Bruker APEX 47e FT-ICR mass spectrometer. Infra-red spectra were obtained by a Bruker Vector 22 FT-IR spectrometer. Optical rotations were recorded on a Perkin-Elmer 341 polarimeter in a 10 mm cell. Melting points were measured on a BUCHI Melting Point B-545 machine. X-ray crystallographic study was performed by a Brüker CCD area detector diffractometer.

2.5.1 General procedures for palladium-catalyzed direct C–H acylation of oximes

A mixture of oxime **1** (0.25 mmol), $Pd(OAc)_2$ (0.0125 mmol, 5 mol%), TBHP (0.5 mmol;4.8M in DCE) in toluene (1mL) and acetic acid (0.5 equiv) was sealed in a 8 mL-vial with a Teflon lined cap. The mixture was heated at 100 ^{o}C (oil bath temperature) for 2 h. After cooling to room temperature, the reaction mixture was filtered through Celite, and the filtrate was concentrated under vacuum to afford an oily substance. The crude product was loaded onto a silica gel column for flash column chromatography.

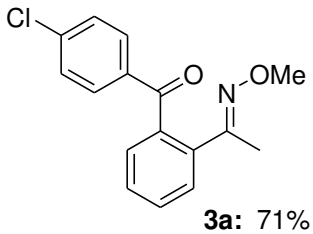

3a: 71%

Eluant: 80% *n*-hexane/20% EA. The product was obtained as a pale yellow solid. Melting point: 106.6-107.1^{o}C ^{1}H NMR (400 MHz, CD_2Cl_2): δ_H 7.63 (d, J = 8.0 Hz, 2H), 7.59-7.45 (m, 4H), 7.41 (d, J = 8.0 Hz, 2H), 3.66 (s, 3H), 3.48 (s, 3H). ^{13}C NMR (100 MHz, CD_2Cl_2): δ_C 196.0 (C), 153.7 (C), 138.5 (C), 138.4 (C), 136.9 (C), 136.1 (C), 130.4 (C-H), 130.3 (C-H), 128.8 (C-H), 128.7 (C-H), 128.5 (C-H), 127.6 (C-H), 61.6 (CH_3), 13.9 (CH_3). IR (KBr, cm^{-1}): 1672.1. HRMS (ESI): calcd. for $C_{16}H_{15}NO_2Cl$: 288.0791, found: 288.0786.

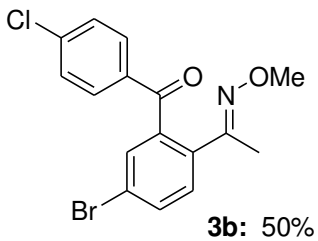

3b: 50%

Eluant: 66% *n*-hexane/33% DCM. The product was obtained as a pale yellow solid. Melting point: 106.4-107.7°C ^{1}H NMR (400 MHz, CD_2Cl_2): δ_H 7.67-7.62 (m, 3H), 7.55 (s, 1H) 7.39-7.36 (m, 3H), 3.63 (s, 3H), 2.02 (s, 3H). ^{13}C NMR (100 MHz, CD_2Cl_2): δ_C 194.6 (C), 152.5 (C), 140.0 (C), 139.2 (C), 136.0 (C), 134.8 (C), 133.2 (C-H), 131.5 (C-H), 130.5 (C-H), 129.1 (C-H), 128.7 (C-H), 123.0 (C), 61.8 (CH_3), 13.8 (CH_3). IR (KBr, cm^{-1}): 1666.5. HRMS (ESI): calcd. for $C_{16}H_{14}NO_2ClBr$: 365.9896, found: 365.9912.

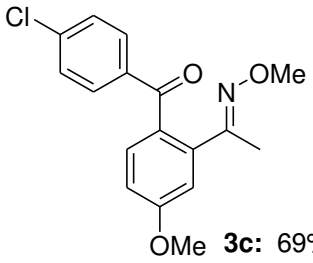

3c: 69%

Eluant: 90% *n*-hexane/10% EA. The product was obtained as pale yellow oil. ^{1}H NMR (400 MHz, CD_2Cl_2): δ_H 7.60 (d, J = 8.0 Hz, 2H), 7.45-748 (m, 1H), 7.40 (d, J = 8.0 Hz, 2H), 7.02-7.00 (m, 2H), 3.91 (s, 3H), 3.70 (s, 3H), 2.00 (s, 3H) ^{13}C NMR (100 MHz, CD_2Cl_2): δ_C 195.4 (C), 161.4 (C), 154.3 (C), 138.8 (C), 138.2 (C), 137.5 (C), 131.3 (C-H), 130.8 (C), 130.4 (C-H), 128.4 (C-H), 113.8 (C-H), 113.5 (C-H), 61.8 (CH_3), 55.6 (CH_3), 14.4 (CH_3). IR (neat, cm^{-1}): 1662.4. HRMS (ESI): calcd. for $C_{17}H_{17}NO_3Cl$: 318.0897, found: 318.0911.

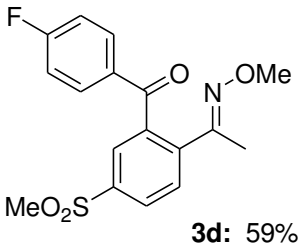

3d: 59%

Eluant: 80% *n*-hexane/20% EA. The product was obtained as yellow oil. ^{1}H NMR (400 MHz, CD_2Cl_2): δ_H 8.10 (d, J = 4.0, 1H), 7.99 (s, 1H), 7.77-7.69 (m, 3H),

7.16-7.11 (m, 2H), 3.67 (s, 3H), 3.10 (s, 3H), 2.09 (s, 3H). ^{13}C NMR (100 MHz, CD_2Cl_2): δ_C 193.9 (C), 166.9 (C), 164.3 (C), 152.5 (C), 140.9 (C), 139.7 (C), 133.9 (C), 131.7 (C-H), 128.9 (C-H), 127.5 (C-H), 115.7 (C-H), 115.5 (C-H), 61.9 (CH_3), 44.3 (CH_3), 13.6 (CH_3). HRMS (ESI): calcd. for $C_{17}H_{16}FNO_4S$: 349.0824, found: 349.1823.

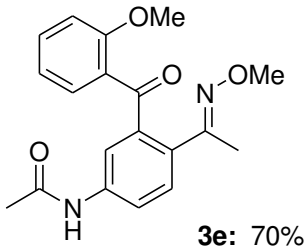

3e: 70%

Eluant: 50% *n*-hexane/50% DCM. The product was obtained as pale yellow oil. ^{1}H NMR (400 MHz, CD_2Cl_2): δ_H 8.63 (s, 1H), 7.94 (d, J = 2.0, 1H), 7.55 (s, 1H), 7.55-7.44 (m, 2H), 7.34 (d, J=8, 1H), 6.98-6.92 (m, 2H), 3.74 (s, 3H), 3.64 (s, 3H), 2.13 (s, 3H), 1.89 (s, 3H). ^{13}C NMR (100 MHz, CD_2Cl_2): δ_C 196.6 (C), 169.0 (C), 158.3 (C), 154.7 (C), 141.2 (C), 139.0 (C), 133.4 (C-H), 131.9 (C), 131.1 (C-H), 128.4 (C-H), 128.3 (C), 121.2 (C-H), 120.1 (C-H), 120.0 (C-H), 111.7 (C-H), 61.4 (CH_3), 55.4 (CH_3), 22.4 (CH_3), 14.7 (CH_3). HRMS (ESI): calcd. For $C_{17}H_{18}N_2O_3$: 298.1314, found: 298.1316.

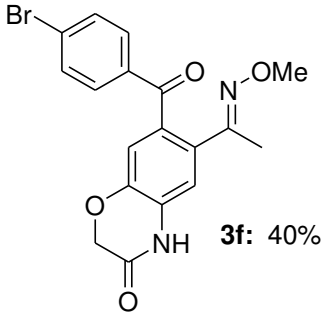

3f: 40%

Eluant: 50% *n*-hexane/50% DCM. The product was obtained as yellow oil. ^{1}H NMR (400 MHz, CD_2Cl_2): δ_H 8.57 (bs, 1H), 7.57 (d, J = 1.6, 2H), 7.55 (d, J = 1.6, 2H),

7.46-7.15 (m, 2H), 4.65 (s, 2H), 3.67 (s, 3H), 1.94 (s, 3H). ^{13}C NMR (100 MHz, CD_2Cl_2): δ_C 194.7 (C), 164.1 (C), 153.5 (C), 144.8 (C), 138.0 (C), 131.7 (C-H), 131.4 (C), 129.9 (C-H), 127.6 (C), 126.3 (C), 123.0 (C), 122.5 (C-H), 118.5 (C-H), 67.3 (CH_2), 61.6 (CH_3), 13.7 (CH_3). HRMS (ESI): calcd. for $C_{18}H_{15}BrN_2O_4$: 402.0233, found: 402.0239.

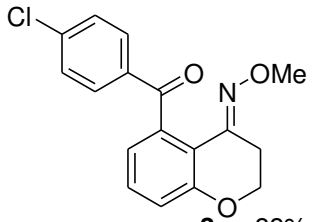

3g: 88%

Eluant: 95% *n*-hexane/5% EA. The product was obtained as a pale yellow solid. Melting point: 103.6-104.1°C ^{1}H NMR (400 MHz, CD_2Cl_2): δ_H 7.68 (d, J = 8.6 Hz, 2H), 7.35 (d, J = 8.4 Hz, 2H), 7.32-7.30 (m, 1H), 7.01 (d, J = 8.0 Hz, 1H), 6.86 (d, J = 8.0 Hz, 1H), 4.21 (t, J = 4.0 Hz, 2H), 3.53 (s, 3H), 2.79 (t, J = 4.0 Hz, 2H). ^{13}C NMR (100 MHz, CD_2Cl_2): δ_C 195.9 (C), 156.9 (C), 146.0 (C), 138.6 (C), 138.3 (C), 136.4 (C), 130.4 (C-H), 130.3 (C-H), 128.6 (C-H), 120.8 (C-H), 119.0 (C-H), 116.1 (C), 64.9 (CH_2), 61.8 (CH_3), 24.0(CH_2). IR (KBr, cm^{-1}): 1672.6. HRMS (ESI):calcd. for $C_{17}H_{17}NO_3Cl$: 316.0740, found: 316.0755.

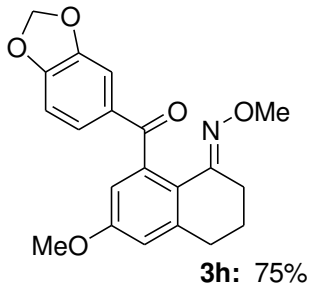

3h: 75%

Eluant: 85% *n*-hexane/15% EA. The product was obtained as a yellow solid. Melting point:118.4-119.2°C ^{1}H NMR (400 MHz, $CDCl_3$): δ_H 7.30 (s, 1H), 7.19 (d, J = 8.0

Hz, 1H), 6.76-6.69 (m, 3H), 6.00 (s, 2H), 3.80 (s, 3H), 3.56 (s, 3H), 2.74 (t, J =6.0, 2H), 2.56 (t, J =6.6, 2H), 1.82 (t, J =6.2, 2H). ^{13}C NMR (100 MHz, $CDCl_3$): δ_C 195.9 (C), 159.5 (C), 151.4 (C), 151.0 (C), 147.8 (C), 142.4 (C), 140.3 (C), 133.1 (C), 125.2 (C-H), 121.3 (C), 114.5 (C-H), 112.1 (C-H), 108.6 (C-H), 107.6 (C-H), 101.6 (CH_2), 61.5 (CH_3), 55.4 (CH_3), 30.7 (CH_2), 24.1 (CH_2), 21.1 (CH_2). IR (KBr, cm^{-1}): 1662.8. HRMS (ESI): calcd. for $C_{20}H_{20}NO_5$: 354.1341, found: 354.1348.

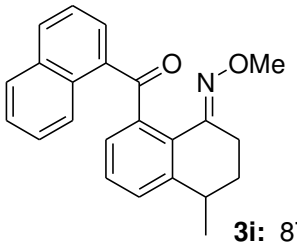

3i: 87%

Eluant: 95% *n*-hexane/5% EA. The product was obtained as an orange solid. Melting point: 123.3-123.9°C. ^{1}H NMR (400 MHz, CD_2Cl_2): δ_H 8.04-7.83 (m, 5H), 7.61-7.48 (m, 4H) 7.35-7.33 (m, 1H), 3.57 (s, 3H), 3.03-2.99 (m, 1H), 2.63-2.58 (m, 2H), 2.01-1.95 (m, 1H), 1.80-1.69 (m, 1H), 1.36 (d, J =7.0, 3H). ^{13}C NMR (100 MHz, CD_2Cl_2): δ_C 197.5 (C), 152.2 (C), 145.6 (C), 138.7 (C), 136.1 (C), 135.2 (C), 132.6 (C), 129.9 (C-H), 129.3 (C-H), 128.8 (C-H), 128.5 (C), 128.2 (C-H), 128.0 (C-H), 127.9 (C-H), 127.7 (C-H), 126.5 (C-H), 124.9 (C-H), 61.6 (C-H), 33.7 (C-H), 28.1 (CH_2), 21.6 (CH_2), 20.0 (CH_3). IR (KBr, cm^{-1}): 1663.6. HRMS (ESI): calcd. for $C_{23}H_{21}NO_2$: 344.1763, found: 344.1761.

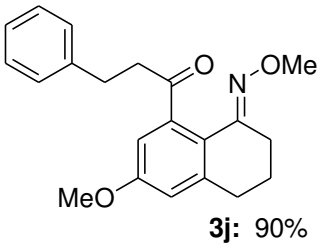

3j: 90%

Eluant: 95% *n*-hexane/5% EA. The product was obtained as a yellow solid. Melting

point: 102.6-103.3°C. ^{1}H NMR (400 MHz, $CDCl_3$): δ_H 7.30-7.20 (m, 5H), 6.77 (d, J = 2.6, 1H), 6.57 (d, J = 2.6, 1H), 3.95 (s, 3H), 3.82 (s, 3H), 3.05-3.00 (m, 4H), 2.76-2.73 (m, 4H), 1.88-1.84 (m, 2H). ^{13}C NMR (100 MHz, $CDCl_3$): δ_C 205.7 (C), 159.7 (C), 153.0 (C), 143.2 (C), 142.7 (C), 141.6 (C), 128.4 (C-H), 128.3 (C-H), 125.9 (C-H), 120.0 (C), 114.2 (C-H), 110.8 (C-H), 61.8 (CH_3), 55.4 (CH_3), 44.9 (CH_2), 30.9 (CH_2), 30.6 (CH_2), 24.5 (CH_2), 21.1 (CH_2). IR (KBr, cm^{-1}): 1701.0. HRMS (ESI): calcd. for $C_{21}H_{24}NO_3$: 338.1756, found: 338.1763.

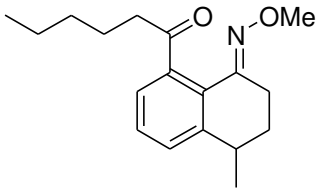

3k:[c] 87%

Eluant: 95% *n*-hexane/5% EA. The product was obtained as orange oil. ^{1}H NMR (400 MHz, CD_2Cl_2): δ_H 7.32-7.30 (m, 2H), 7.06-7.04 (m, 1H), 3.92 (s, 3H), 2.94-2.90 (m, 1H), 2.81-2.76 (m, 2H), 2.68-2.64 (m, 2H), 1.97-1.92 (m, 1H), 1.73-1.63 (m, 3H), 1.36-1.28 (m, 7H), 0.91 (t, J = 4.8, 3H). ^{13}C NMR (100 MHz, CD_2Cl_2): δ_C 207.2 (C), 153.0 (C), 145.7 (C), 141.6 (C), 128.7 (C-H), 127.7 (C-H), 126.8 (C), 124.7 (C-H), 61.9 (C-H), 43.4 (CH_2), 33.6 (CH_3), 31.5 (CH_2), 27.9 (CH_2), 24.5 (CH_2), 22.5 (CH_2), 21.7 (CH_2), 19.8 (CH_3), 13.7 (CH_3). IR (neat, cm^{-1}): 1697.6. HRMS (ESI): calcd. for $C_{18}H_{26}NO_2$: 288.1965, found: 288.1964.

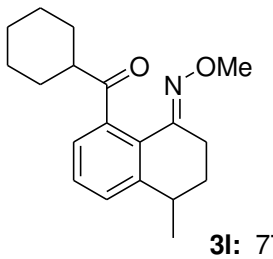

3l: 77%

Eluant: 95% *n*-hexane/5% EA. The product was obtained as yellow oil. ^{1}H NMR (400 MHz, CD_2Cl_2): δ_H 7.33-7.31 (m, 2H), 7.01 (d, J = 6.8, 1H), 3.92 (s, 3H), 2.93-2.91 (m,

1H), 2.90-2.80 (m, 2H), 2.79-2.60 (m, 1H), 1.97-1.95 (m, 1H), 1.84-1.65 (m, 6H), 1.45-1.43 (m, 1H), 1.28 (d, J = 8.0, 3H), 1.27-1.23 (m, 3H). ^{13}C NMR (100 MHz, CD_2Cl_2): δ_C 210.2 (C), 153.5 (C), 145.7 (C), 140.5 (C), 128.5 (C-H), 127.6 (C-H), 127.0 (C), 125.7 (C-H), 61.9 (C-H), 50.6 (C-H), 33.7 (CH_3), 29.6 (CH_2), 29.4 (CH_2), 27.9 (CH_2), 26.0 (CH_2), 25.9 (CH_2), 25.8 (CH_2), 21.9 (CH_2), 19.8 (CH_3). HRMS (ESI): calcd. for $C_{19}H_{25}NO_2$: 299.4112, found: 299.1917.

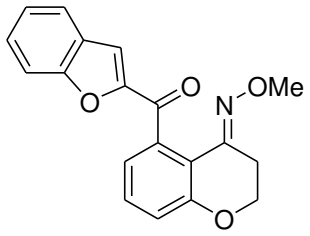

3m: 72%

Eluant: 95% *n*-hexane/5% EA. The product was obtained as a yellow solid. Melting point: 151.1-152.0 ^{o}C. ^{1}H NMR (400 MHz, CD_2Cl_2): δ_H 7.66 (d, J = 8.0 Hz, 1H), 7.59 (d, J = 8.0 Hz, 1H), 7.47 (t, J = 4.0 Hz, 1H), 7.39 (t, J = 8.0 Hz, 1H), 7.29 (t, J = 4.0 Hz, 1H), 7.11-7.09 (m, 2H), 7.01 (d, J = 8.0 Hz, 1H), 4.27 (t, J = 4.0 Hz, 2H), 3.59 (s, 3H), 2.86 (t, J = 4.0 Hz, 2H). ^{13}C NMR (100 MHz, CD_2Cl_2): δ_C 186.3 (C), 157.1 (C), 155.6 (C), 153.6 (C), 146.7 (C), 137.6 (C), 130.4 (C-H), 127.6 (C-H), 127.3 (C), 123.7 (C-H), 123.1 (C-H), 121.1 (C-H), 119.5 (C-H), 116.8 (C), 113.0 (C-H), 112.2 (C-H), 65.0 (CH_2), 61.9 (CH_3), 24.1 (CH_2). IR (KBr, cm^{-1}): 1647.0. HRMS (ESI): calcd. for $C_{19}H_{16}NO_4$: 322.1079, found: 322.1086.

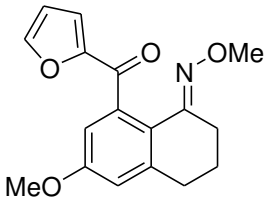

3n: 55%

Eluant: 95% *n*-hexane/5% EA. The product was obtained as brown solid. Melting point: 82.7-83.6^{o}C. ^{1}H NMR (400 MHz, CD_2Cl_2): δ_H 7.56 (q, J = 1.0, 1H), 6.84 (d, J =

2.7, 1H) 6.81-6.78 (m, 2H), 6.49 (t, J = 1.7, 1H), 3.84 (s, 3H), 3.60 (s, 3H), 2.77 (t, J = 6.2, 2H), 2.61 (t, J = 6.7, 2H), 1.85 (t, J = 6.3, 2H). ^{13}C NMR (100 MHz, CD_2Cl_2): δ_C 184.9 (C), 159.5 (C), 153.5 (C), 152.1 (C), 145.6 (C-H), 142.9 (C), 139.2 (C), 121.7 (C), 116.7 (C-H), 114.9 (C-H), 112.3 (C-H), 111.8 (C-H), 61.4 (CH_3), 55.5 (CH_3), 30.5 (CH_2), 24.2 (CH_2), 21.1 (CH_2). IR (KBr, cm^{-1}): 1655.3. HRMS (ESI): calcd. for $C_{21}H_{24}NO_3$: 300.1236, found: 300.1236.

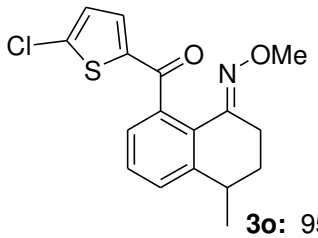

3o: 95%

Eluant: 66% *n*-hexane/33% DCM. The product was obtained as yellow oil. ^{1}H NMR (400 MHz, CD_2Cl_2): δ_H 7.41 (d, J = 4.9, 2H), 7.22 (t, J = 4.5, 1H), 6.93 (d, J = 4.0, 1H), 6.87 (d, J = 4.0, 1H) 3.71 (s, 3H), 2.96 (bs, 1H), 2.70-2.66 (m, 2H), 2.00-1.92 (m, 1H), 1.72-1.67 (m, 1H), 1.32 (d, J = 7.0, 3H). ^{13}C NMR (100 MHz, CD2Cl_2): δ_C 189.2 (C), 152.0 (C), 145.8 (C), 144.5 (C), 137.7 (C), 137.3 (C), 131.8 (C-H), 128.7 (C-H), 128.6 (C-H), 128.2 (C), 127.3 (C-H), 126.1 (C-H), 61.8 (C-H), 33.6 (CH_3), 28.0 (CH_2), 21.6 (CH_2), 19.9 (CH_3). IR (neat, cm^{-1}): 1648.9. HRMS (ESI): calcd. for $C_{17}H_{16}NO_2ClS$: 333.8365, found: 333.8364.

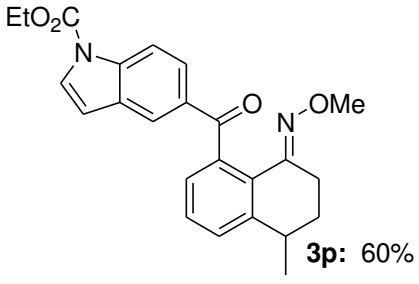

3p: 60%

Eluant: 90% *n*-hexane/10% EA. The product was obtained as a white solid. Melting point: 135.7-136.8°C. ^{1}H NMR (400 MHz, CD_2Cl_2): δ_H 8.20 (d, J = 8.7, 1H), 7.86 (s,

1H), 7.75 (d, *J* = 8.7, 1H), 7.69 (d, *J* = 3.7, 1H), 7.47-7.42 (m, 2H), 7.27 (d, *J* = 6.0, 1H), 6.63 (d, *J* = 3.6, 1H), 4.50 (q, *J* = 7.1, 2H) 3.54 (s, 3H), 2.98 (bs, 1H), 2.60-2.58 (m, 2H), 1.99-1.92 (m, 1H), 1.72-1.67 (m, 1H), 1.47 (t, *J* = 7.1, 3H), 1.34 (d, *J* = 7.0, 3H) ^{13}C NMR (100 MHz, CD_2Cl_2): δ_C 197.3 (C), 152.1 (C), 150.7 (C), 145.5 (C), 139.1 (C), 137.4 (C), 133.7 (C), 130.1 (C), 128.6 (C-H), 128.3 (C), 127.9 (C-H), 126.8 (C-H), 126.4 (C-H), 125.2 (C-H), 122.5 (C-H), 112.6 (C-H), 108.3 (C-H), 63.6 (CH_2), 61.5 (C-H), 33.7 (CH_3), 28.1 (CH_2), 21.5 (CH_2), 19.9(CH_3), 14.2(CH_3) IR (KBr, cm^{-1}): 1730.2, 1669.4. HRMS (ESI): calcd. for $C_{24}H_{25}N2O_4$: 405.1814, found: 405.1797.

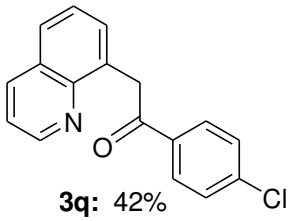

3q: 42%

Eluant: 80% *n*-hexane/ 20% EA. The product was obtained as yellow oi. ^{1}H NMR (400 MHz, CD_2Cl_2): δ_H 8.88-8.87 (m, 1H), 8.17-8.16 (m, 1H), 8.15 (d, *J* = 1.0, 2H), 8.10-8.07 (m, 1H), 7.77-7.75 (m, 1H), 7.43-7.51 (m, 1H), 7.40-7.38 (m, 3H), 4.93 (s, 2H). ^{13}C NMR (100 MHz, CD_2Cl_2): δ_C 197.4 (C), 149.6 (C-H), 146.4 (C), 139.3 (C), 136.3 (C-H), 135.4 (C), 134.0 (C), 130.4 (C-H), 130.1 (C-H), 128.8 (C-H), 128.5 (C), 127.3 (C-H), 126.3 (C-H), 121.1 (C-H), 40.8 (CH_2). HRMS (ESI): calcd. for $C_{17}H_{12}ClNO$: 281.0625, found: 281.0623.

2.5.2 General procedures for the oxime deprotection

Ketone **3a/3c/3o** was added to a mixture of dioxane (0.5 mL) and 6M HCl (0.5 mL) in an 8-mL vial with a Teflon lined cap. For **3o**, copper powder (2 equiv) was added to the mixture. Then the mixture was heated to 80 ^{o}C for 2 h (0.5 h for **3o**). After cooling to room temperature, the reaction mixture was filtered through Celite, and the filtrate was concentrated under vacuum to afford an oily substance. The crude product was loaded onto a silica gel column for flash column chromatography.

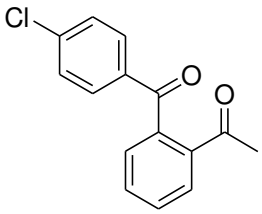

4a: 48%

Eluant: 80% *n*-hexane/20% EA. The product was obtained as red oil. ^{1}H NMR (400 MHz, CD_2Cl_2): δ_H 7.93 (d, J = 4.0, 1H), 7.69-7.63 (m, 4H), 7.43-7.39 (m, 3H), 2.53 (s, 3H). ^{13}C NMR (100 MHz, CD_2Cl_2): δ_C 198.2 (C), 196.2 (C), 140.4 (C), 139.0 (C), 137.1 (C), 135.8 (C), 132.5 (C-H), 130.3 (C-H), 129.8 (C-H), 129.6 (C-H), 128.7 (C-H), 128.0 (C-H), 27.0 (CH_3). HRMS (ESI): calcd. for $C_{15}H_{11}ClO_4$: 258.0424, found: 258.0428.

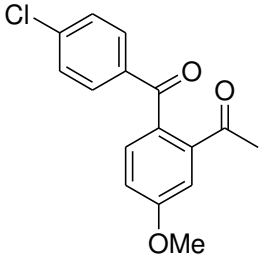

4c: 40%

Eluant: 80% *n*-hexane/20% EA. The product was obtained as red oil. ^{1}H NMR (400 MHz, CD_2Cl_2): δ_H 7.65 (d, J = 4.0, 2H), 7.43-7.38 (m, 3H), 7.30-7.29 (m, 1H),

7.13-7.10 (m, 1H), 3.93 (s, 3H), 2.47 (s, 3H). ^{13}C NMR (100 MHz, CD_2Cl_2): δ_C 199.4 (C), 195.4 (C), 161.2 (C), 141.1 (C), 138.8 (C), 136.3 (C), 131.5 (C), 130.6 (C-H), 130.5 (C-H), 128.6 (C-H), 115.9 (C-H), 115.1 (C-H), 55.8 (CH_3), 27.9 (CH_3). HRMS (ESI): calcd. for $C_{16}H_{13}ClO_3$: 288.0624, found: 288.0621.

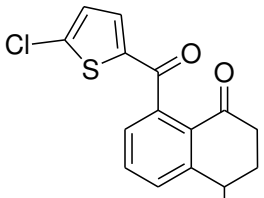

4o: 40%

Eluant: 80% *n*-hexane/20% EA. The product was obtained as yellow oil. ^{1}H NMR (400 MHz, CD_2Cl_2): δ_H 7.60-7.53 (m, 1H), 7.51 (d, J = 2.0, 1H), 7.23-7.21 (m, 1H), 6.90-6.88 (m, 2H), 3.21-3.16(m, 1H), 2.79-2.76 (m, 1H), 2.60-2.52 (m, 1H), 2.32-2.24 (m, 1H), 2.01-1.91 (m, 1H), 1.44 (d, J = 7.0, 3H). ^{13}C NMR (100 MHz, CD_2Cl_2): δ_C 197.4 (C), 189.4 (C), 150.4 (C), 143.6 (C), 139.9 (C), 138.6 (C), 133.1 (C-H), 132.4 (C-H), 130.4 (C), 129.3 (C-H), 127.4 (C-H), 125.5 (C-H), 36.0 (CH_2), 33.1 (C-H), 29.9 (CH_2), 20.5 (CH_3). HRMS (ESI): calcd. for $C_{16}H_{13}ClO_2S$: 304.0356, found: 304.0359.

2.5.3 General procedures for the phthalazine synthesis

The diacyl compounds **4a/4c/4o** and hydrazine (5 equiv.) were added to ethanol (1 mL) in an 8 mL-vial with a Teflon lined cap. Then the mixture was heated to reflux for 2 h. After cooling to room temperature, the reaction mixture was filtered through Celite, and the filtrate was concentrated under vacuum to afford an oily substance. The crude product was loaded onto a silica gel column for flash column chromatography.

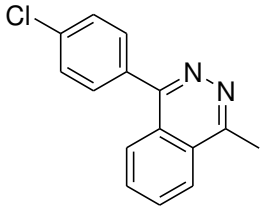

5a: >99%

Eluant: 100% EA. The product was obtained as yellow oil. ^{1}H NMR (400 MHz, CD_2Cl_2): δ_H 8.18 (d, J = 8.2, 1H), 8.04-7.89 (m, 3H), 7.67 (d, J = 8.4, 2H), 7.57 (d, J = 8.3, 2H), 3.09 (s, 3H). ^{13}C NMR (100 MHz, CD_2Cl_2): δ_C 158.3 (C), 156.9 (C), 135.4 (C), 134.8 (C), 132.6 (C-H), 132.4 (C-H), 131.4 (C-H), 128.7 (C-H), 126.6 (C), 126.3 (C-H), 125.0 (C-H), 19.4 (CH_3). HRMS (ESI): calcd. for $C_{15}H_{11}ClN_2$: 254.0623, found: 254.0630.

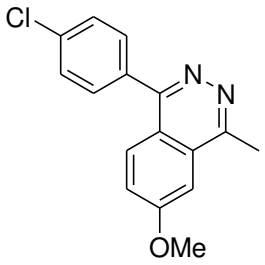

5c: > 99%

Eluant: 100% EA. The product was obtained as a yellow oil. ^{1}H NMR (400 MHz, CD_2Cl_2): δ_H 7.91 (d, J = 9.1, 1H), 7.66 (d, J = 8.4, 2H), 7.55 (d, J = 8.1, 2H), 7.46-7.44 (m, 1H), 7.36 (s, 1H), 4.03 (s, 3H), 3.00 (s, 3H). ^{13}C NMR (100 MHz, CD_2Cl_2): δ_C 162.0 (C), 157.2 (C), 156.1 (C), 135.4 (C), 135.1 (C), 131.3 (C-H), 128.6 (C-H), 128.3 (C-H), 123.5 (C-H), 120.1 (C), 103.3 (C-H), 55.8 (CH_3), 29.7 (C), 19.8 (CH_3). HRMS (ESI): calcd. for $C_{16}H_{13}ClN_2O$: 284.0768, found: 284.0769.

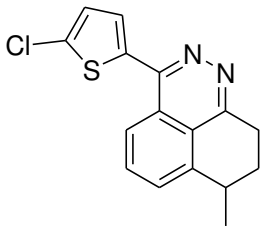

5o: > 99%

Eluant: 100% EA. The product was obtained as yellow oil. ^{1}H NMR (400 MHz, CD_2Cl_2): δ_H 8.2 (d, J = 7.0, 1H), 7.91-7.87 (m, 1H), 7.81-7.79 (m, 1H), 7.48 (d, J = 4.0, 1H), 7.09 (d, J = 3.9, 1H) , 3.48-3.41 (m, 1H), 3.34-3.27 (m, 2H), 2.34-2.27 (m, 1H), 2.04-1.95 (m, 1H), 1.47 (d, J = 7.0, 3H). ^{13}C NMR (100 MHz, CD_2Cl_2): δ_C 157.4 (C), 151.5 (C), 143.2 (C), 139.0 (C), 132.9 (C), 132.5 (C-H), 129.2 (C-H), 128.4 (C-H), 126.9 (C-H), 124.0 (C), 123.4 (C), 122.4 (C-H), 33.4 (C-H), 30.4 (CH_2), 28.8 (CH_2), 20.5 (CH_3). HRMS (ESI): calcd. for $C_{16}H_{13}ClN_2S$: 300.0567, found: 300.0568.

2.5.4 General procedures for palladium-catalyzed direct C–H acylation of anilides

A 10 mL Schlenk-type test tube (with a Quick-fit stopper and side arm) equipped with a magnetic stir bar was charged with the anilides substrate **6** (0.25 mmol), $Pd(OAc)_2$ (2.8 mg, 0.0125 mmol), aldehyde **2** (0.75 mmol). The reaction tube was stoppered, then evacuated and charged with N_2 (repeated three times). Subsequently, dry toluene (1 mL), TFA (0.0192 mL, 0.25 mmol), TBHP (5 M in DCE, 0.1 mL, 0.5 mmol) was added under a flow of N_2. The reaction mixture was stirred at 40 ^{o}C for 3 h. The reaction mixture was filtered over a plug of celite and the solvent was removed under vacuum. The resulting residue was purified by silica gel flash column chromatography using hexanes/EtOAc as the eluent.

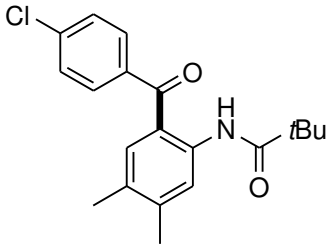

7a: 80%

Eluent: 100% *n*-hexane/33.3% Ether. ^{1}H NMR (400 MHz, $CDCl_3$): δ_H 11.15 (bs, NH), 8.55(s, 1H), 7.62-7.60 (d, J = 8.8, 2H), 7.46-7.44 (d, J = 8.8, 2H), 7.24 (s, 1H), 2.32 (s, 3H), 2.18(s, 3H), 1.34 (s, 9H). ^{13}C NMR (100 MHz, $CDCl_3$): δ_C 198.4 (C), 178.1 (C), 144.9 (C), 139.3 (C), 138.4 (C), 137.6 (C), 134.3 (C-H), 131.1 (C-H), 130.3 (C), 128.6 (C-H), 122.4 (C-H), 120.7 (C), 40.2 (C), 27.6 (CH_3), 20.5 (CH_3), 19.2 (CH_3). IR (KBr, cm^{-1}): 1681.2. HRMS (ESI): calcd. for $C_{20}H_{22}NO_2NaCl$: 366.1256, found: 366.1258.

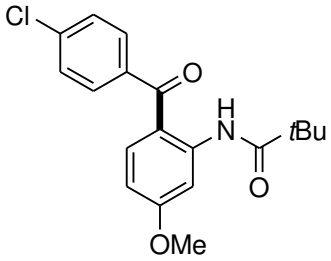

7b: 71%

Eluent: 95% *n*-hexane/5% EA. ^{1}H NMR (400 MHz, $CDCl_3$): δ_H 11.83 (bs, NH), 8.50 (d, J = 2.3, 1H), 7.57 (d, J = 8.4, 2H), 7.48 (s, 1H), 7.46-7.43 (m, 2H), 6.57-6.54 (m, 1H), 3.90 (s, 3H), 1.36 (s, 9H). ^{13}C NMR (100 MHz, $CDCl_3$): δ_C 197.8 (C), 178.9 (C), 165.1 (C), 144.7 (C), 138.1 (C), 138.0 (C), 136.2 (C-H), 130.9 (C-H), 128.7 (C-H), 115.3 (C), 109.6 (C-H), 104.4 (C-H), 55.8 (CH_3), 40.6 (C), 27.7 (CH_3). IR (KBr, cm^{-1}): 1683.1. HRMS (ESI): calcd. for $C_{19}H_{20}NO_3NaCl$: 368.1015, found: 368.1029.

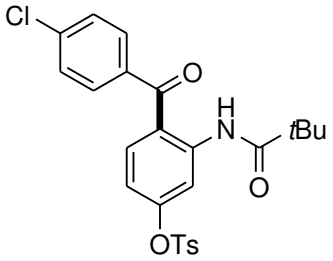

7c: 74%

Eluent: 80% *n*-hexane/20% EA. ^{1}H NMR (400 MHz, $CDCl_3$): δ_H 11.24 (bs, NH), 8.42 (d, J = 2.4, 1H), 7.80 (d, J = 8.3, 2H), 7.59 (d, J = 8.5, 2H), 7.52 (d, J = 8.8, 1H), 7.46 (d, J = 8.5, 2H), 7.34 (d, J = 8.1, 2H), 6.88-6.86 (m, 1H), 2.45 (s, 3H), 1.30 (s, 9H). ^{13}C NMR (100 MHz, $CDCl_3$): δ_C 197.7 (C), 177.9 (C), 153.8 (C), 145.8 (C), 143.1 (C), 139.1 (C), 136.8 (C), 135.1 (C-H), 132.4 (C), 131.1 (C-H), 130.0 (C-H), 128.8 (C-H), 128.5 (C-H), 120.7 (C), 115.3 (C-H), 114.8 (C-H), 40.3 (C), 27.4 (CH_3), 21.7 (CH_3). IR (neat, cm^{-1}): 1690.8. HRMS (ESI): calcd. For $C_{25}H_{24}NO_5NaSCl$: 508.0951 found: 508.0916.

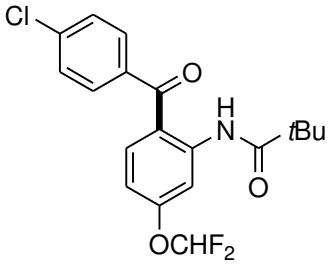

7d: 70%

Eluent: 94% *n*-hexane/6% EA. ^{1}H NMR (400 MHz, $CDCl_3$): δ_H 11.48 (bs, NH), 8.65 (s, 1H), 7.61 (d, J = 8.2, 2H), 7.56 (d, J = 8.8, 1H), 7.47 (d, J = 7.9, 2H), 6.78 (d, J = 8.6, 1H), 6.68 (t, J = 80.0), 1.35 (s, 9H). ^{13}C NMR (100 MHz, $CDCl_3$): δ_C 197.7 (C), 178.5 (C), 155.9 (C), 143.7 (C), 138.8 (C), 137.1 (C), 135.7 (C-H), 131.0 (C-H), 128.7 (C-H), 118.9 (C), 117.8 (C), 115.2 (C-H), 112.6 (C), 111.8 (C-H), 110.1 (C-H), 40.4 (C), 27.5 (CH_3). IR (KBr, cm^{-1}): 1675.1. HRMS (ESI): calcd. for $C_{19}H_{18}NO_3NaClF_2$: 404.0832, found: 404.0841.

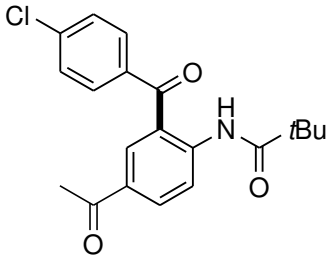

7e: 52%

Eluent: 90% *n*-hexane/10% EA. ^{1}H NMR (400 MHz, $CDCl_3$): δ_H 11.33 (bs, NH), 8.85 (d, J = 8.8, 1H), 8.18 (s, 1H), 8.13 (d, J = 8.9, 2H), 7.65 (d, J = 8.2, 2H), 7.49 (d, J = 8.2, 2H), 2.54 (s, 3H), 1.36 (s, 9H). ^{13}C NMR (100 MHz, $CDCl_3$): δ_C 198.3 (C), 195.9 (C), 178.5 (C), 145.1 (C), 139.6 (C), 136.6 (C), 134.7 (C-H), 133.8 (C-H), 131.5 (C-H), 130.6 (C), 129.1 (C-H), 122.2 (C), 120.1 (C-H), 40.6 (C), 27.6 (CH_3), 26.5 (CH_3). IR (KBr, cm^{-1}): 1693.4. HRMS (ESI): calcd. for $C_{20}H_{20}NO_3NaCl$: 380.1029, found: 380.1014.

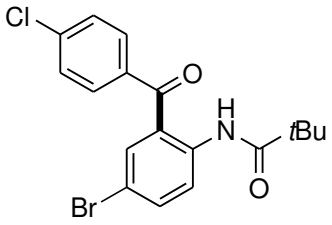

7f: 45%

Eluent: 90% *n*-hexane/10% EA. ^{1}H NMR (400 MHz, $CDCl_3$): δ_H 10.96 (s, NH), 8.63 (d, J = 8.9, 1H), 7.67-7.62 (m, 4H), 7.50 (d, J = 7.9, 2H), 1.33 (s, 9H). ^{13}C NMR (100 MHz, $CDCl_3$): δ_C 197.3 (C), 178.1 (C), 140.2 (C), 139.6 (C), 137.3 (C-H), 136.4 (C), 135.5 (C-H), 131.4 (C-H), 129.0 (C-H), 124.6 (C), 123.4 (C-H), 114.4 (C), 40.4 (C), 27.6 (CH_3). IR (KBr, cm^{-1}): 1698.3. HRMS (ESI): calcd. for $C_{18}H_{17}NO_2NaClBr$: 416.0029, found: 416.0033.

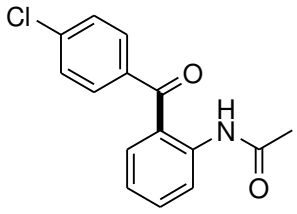

7g: 59%

Eluent: 90% *n*-hexane/10% EA. ^{1}H NMR (400 MHz, $CDCl_3$): δ_H 10.69 (bs, NH), 8.61 (d, J = 8.4, 1H), 7.66-7.63 (m, 2H), 7.59-7.55 (m, 1H), 7.51-7.45 (m, 3H), 7.08 (t, J = 7.4, 1H), 2.22 (s, 3H). ^{13}C NMR (100 MHz, $CDCl_3$): δ_C 198.4 (C), 169.3 (C), 140.6 (C), 139.2 (C), 137.0 (C), 134.6 (C-H), 133.3 (C-H), 131.4 (C-H), 128.8 (C-H), 123.2 (C), 122.3 (C-H), 121.9 (C-H), 25.4 (CH_3). IR (KBr, cm^{-1}): 1701.6. HRMS (ESI): calcd. for $C_{15}H_{12}NO_2NaCl$: 296.0457, found: 296.0454.

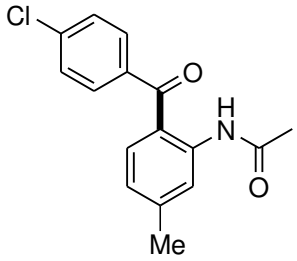

7h: 63%

Eluent: 90% *n*-hexane/10% EA. ^{1}H NMR (400 MHz, $CDCl_3$): δ_H 10.89 (bs, NH), 8.49 (s, 1H), 7.62 (d, J = 8.3, 2H), 7.46 (d, J = 8.3, 2H), 7.22 (d, J = 8.0, 1H), 6.89 (d, J = 7.9, 1H), 2.43 (s, 3H), 2.22 (s, 3H). ^{13}C NMR (100 MHz, $CDCl_3$): δ_C 198.3 (C), 169.3 (C), 146.4 (C), 140.9 (C), 138.8 (C), 137.4 (C), 133.6 (C-H), 131.3 (C-H), 128.7 (C-H), 123.1 (C-H), 122.0 (C-H), 120.4 (C), 25.5 (CH_3), 22.3 (CH_3). IR (KBr, cm^{-1}): 1734.8. HRMS (ESI): calcd. for $C_{15}H_{12}NO_2NaCl$: 310.0611, found: 310.0607.

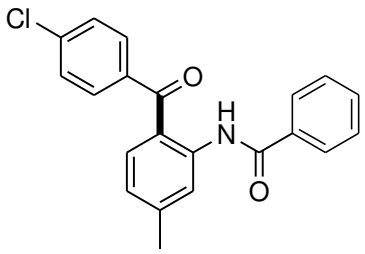

7i: 55%

Eluent: 98% *n*-hexane/2% EA. ^{1}H NMR (400 MHz, $CDCl_3$): δ_H 12.03 (bs, NH), 8.77 (s, 1H), 8.07 (d, *J* = 6.6, 2H), 7.64 (d, *J* = 8.5, 2H), 7.53-7.51 (m, 3H), 7.47-7.45 (m, 3H), 6.94 (d, *J* = 8.1, 2H), 2.47 (s, 3H). ^{13}C NMR (100 MHz, $CDCl_3$): δ_C 198.7 (C), 165.9 (C), 146.6 (C), 141.4 (C), 138.6 (C), 137.4 (C), 134.6 (C), 134.0 (C-H), 132.1 (C-H), 131.1 (C-H), 128.8 (C-H), 128.6 (C-H), 127.4 (C-H), 123.2 (C-H), 121.8 (C-H), 120.3 (C), 22.3 (CH_3). IR (Kbr, cm^{-1}): 1690.7. HRMS (ESI): calcd. for $C_{21}H_{16}NO_2NaCl$: 372.0767, found: 372.0757.

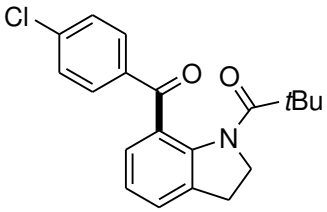

7j: 58%

Eluent: 80% *n*-hexane/20% EA. ^{1}H NMR (400 MHz, $CDCl_3$): δ_H 7.68 (d, *J* = 6.7, 2H), 7.37-7.33 (m, 4H), 7.12(t, *J* = 6.8, 1H), 4.18 (t, *J* = 7.7, 2H), 3.13 (t, *J* = 7.6, 2H), 1.04 (s, 9H). ^{13}C NMR (100 MHz, $CDCl_3$): δ_C 192.4 (C), 176.8 (C), 141.5 (C), 138.3 (C), 136.5 (C), 133.3 (C), 130.9 (C-H), 128.5 (C), 128.3 (C-H), 127.8 (C-H), 127.0 (C-H), 124.6 (C-H), 50.4 (CH_2), 39.3 (C), 30.3 (CH_2), 27.6 (CH_3). IR (KBr, cm^{-1}): 1660.3. HRMS (ESI): calcd. for $C_{20}H_{20}NO_2NaCl$: 364.1087, found: 364.1080.

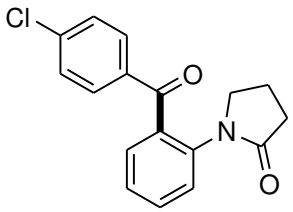

7k: 64%

Eluent: 67% *n*-hexane/33% EA. ^{1}H NMR (400 MHz, $CDCl_3$): δ_H 7.76 (d, J = 8.4, 2H), 7.55 (t, J =7.5, 1H), 7.45-7.40 (m, 3H), 7.35-7.28 (d, J = 8.5, 2H), 3.82 (t, J = 6.9, 2H), 2.27 (t, J = 7.9, 2H), 1.98 (t, J = 7.6, 2H). ^{13}C NMR (100 MHz, $CDCl_3$): δ_C 194.4 (C), 174.6 (C), 139.2 (C), 137.1 (C), 135.6 (C), 135.2 (C), 131.7 (C-H), 131.4 (C-H), 129.8 (C-H), 128.5 (C-H), 126.3 (C-H), 125.0 (C-H), 50.6 (CH_2), 31.2 (CH_2), 18.6 (CH_2). IR (neat, cm^{-1}): 1680.5. HRMS (ESI): calcd. for $C_{17}H_{14}NO_2NaCl$: 322.0600, found: 322.0611.

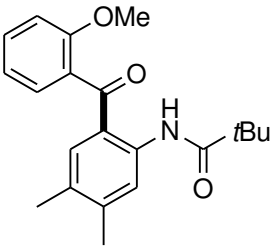

7l: 72%

Eluent: 80% *n*-hexane/20% EA. ^{1}H NMR (400 MHz, $CDCl_3$): δ_H 11.83 (bs, NH), 8.65 (s, 1H), 7.47-7.43 (m, 1H), 7.25-7.23 (m, 1H), 7.16 (s, 1H), 7.04-6.98 (m, 2H), 3.76 (s, 3H), 2.30 (s, 3H), 2.11 (s, 3H), 1.37 (s, 9H). ^{13}C NMR (100 MHz, $CDCl_3$): δ_C 200.3 (C), 178.6 (C), 156.8 (C), 145.5 (C), 140.1 (C), 135.4 (C-H), 131.7 (C-H), 130.3 (C), 129.7 (C), 129.1 (C-H), 121.6 (C-H), 121.0 (C), 120.5 (C-H), 111.6 (C-H), 55.8 (CH_3), 40.5 (C), 27.8 (CH_3), 20.7 (CH_3), 19.2 (CH_3). IR (KBr, cm^{-1}): 1681.0. HRMS (ESI): calcd. for $C_{21}H_{25}NO_3Na$: 362.1730, found: 362.1732.

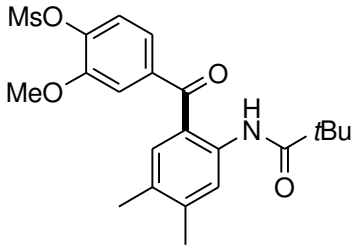

7m: 72%

Eluent: 80% *n*-hexane/20% EA. ^{1}H NMR (400 MHz, $CDCl_3$): δ_H 11.01 (bs, NH), 8.53 (s, 1H), 7.39-7.37 (m, 2H), 7.30 (s, 1H), 7.24-7.21 (m, 1H), 3.93 (s, 3H), 3.24 (s, 3H), 2.32 (s, 3H), 2.19 (s, 3H), 1.33 (s, 9H). ^{13}C NMR (100 MHz, $CDCl_3$): δ_C 198.1 (C), 178.1 (C), 151.7 (C), 145.2 (C), 141.1 (C), 139.4 (C), 139.1 (C), 134.4 (C-H), 130.5 (C), 124.2 (C-H), 123.2 (C-H), 122.6 (C-H), 120.8 (C), 114.0 (C-H), 56.4 (CH_3), 40.3 (C), 38.8 (CH_3), 27.7 (CH_3), 20.7(CH_3), 19.3(CH_3). IR (neat, cm^{-1}): 1681.0. HRMS (ESI): calcd. for $C_{22}H_{27}NO_6NaS$: 456.1469, found: 456.1457.

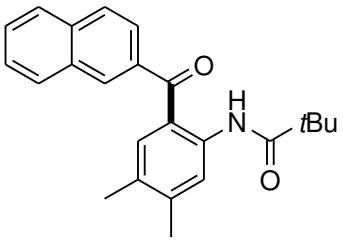

7n: 87%

Eluent: 94% *n*-hexane/6% EA. ^{1}H NMR (400 MHz, $CDCl_3$): δ_H 11.27 (bs, NH), 8.61 (s, 1H), 8.16 (s, 1H), 7.94-7.89 (m, 3H), 7.79 (d, *J*= 8.5, 1H), 7.61-7.53 (m, 2H), 7.38 (s, 1H), 2.35 (s, 3H), 2.17 (s, 3H), 1.37 (s, 9H). ^{13}C NMR (100 MHz, $CDCl_3$): δ_C 199.7 (C), 178.0 (C), 144.5 (C), 139.3 (C), 136.6 (C), 135.0 (C), 134,7 (C-H), 132.2 (C), 131.1 (C-H), 130.3 (C), 129.3 (C-H), 128.2 (C-H), 128.2 (C-H), 127.8 (C-H), 126.9 (C-H), 125.7 (C-H), 122.4 (C-H), 121.3 (C), 40.2 (C), 27.6 (CH_3), 20.5 (CH_3), 19.2 (CH_3). IR (KBr, cm^{-1}): 1681.4. HRMS (ESI): calcd. for $C_{24}H_{25}NO_2Na$: 382.1782, found: 382.1783.

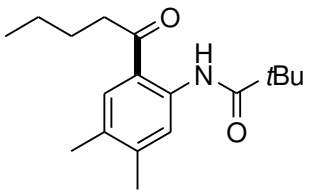

7o: 72%

Eluent: 80% *n*-hexane/20% EA. ^{1}H NMR (400 MHz, $CDCl_3$): δ_H 11.90 (bs, NH), 8.62 (s, 1H), 7.62 (s, 1H), 2.96 (t, J = 7.5,2H), 2.28 (s, 3H), 2.24 (s, 3H), 1.72-1.65 (m, 2H), 1.42-1.36 (m, 2H), 1.33 (s, 9H), 0.94 (t, J = 7.3, 3H).^{13}C NMR (100 MHz, $CDCl_3$): 204.7 (C), 178.3 (C), 144.7 (C), 139.4 (C), 131.5 (C-H), 130.3 (C), 121.7 (C-H), 120.0 (C), 40.3 (C), 39.6 (CH_2), 27.6 (CH_3), 27.0 (CH_2), 22.4 (CH_2), 20.4 (CH_3), 19.3 (CH_3), 13.9 (CH_3). IR (KBr, cm^{-1}): 1682.2. HRMS (ESI): calcd. for $C_{18}H_{27}NO_2Na$: 312.1937, found: 312.1939.

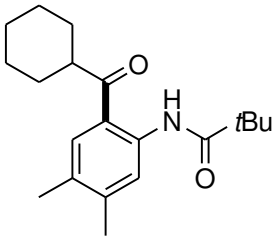

7p: 76%

Eluent: 91% *n*-hexane/ 9% EA. ^{1}H NMR (400 MHz, $CDCl_3$): δ_H 11.9 (bs, NH), 8.62 (s, 1H), 7.62 (s, 1H), 3.30 (t, J = 11.2, 1H), 2.28 (s, 3H), 2.26 (s, 3H), 1.85-1.83 (d, J = 10.5, 2H), 1.75 (d, J = 12.5, 3H), 1.54-1.37 (m, 5H), 1.32 (s, 9H), 1.27-1.24 (m, 1H). ^{13}C NMR (100 MHz, $CDCl_3$): δ_C 208.1(C), 178.3 (C), 144.6 (C), 139.8 (C), 131.1 (C-H), 130.3 (C), 122.0 (C-H), 119.3 (C), 46.4 (C-H), 40.3 (C), 29.9 (CH_2), 27.6 (CH_3), 25.9 (CH_2), 25.8 (CH_2), 20.4 (CH_3), 19.4 (CH_3). IR (neat, cm^{-1}): 1679.6. HRMS (ESI): calcd. for $C_{20}H_{29}NO_2Na$: 338.2098, found: 338.2096.

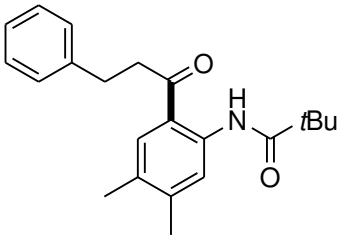

7q: 70%

Eluent: 98% *n*-hexane/2% EA. ^{1}H NMR (400 MHz, $CDCl_3$): δ_H 11.88 (bs, NH), 8.66 (s, 1H), 7.62 (s, 1H), 7.32-7.24 (m, 5H), 3.33 (t, J = 7.3, 2H), 3.05 (t, J = 8.2, 2H), 2.30 (s, 3H), 2.24 (s, 3H), 1.36 (s, 9H). ^{13}C NMR (100 MHz, $CDCl_3$): δ_C 203.2 (C), 178.3 (C), 145.0 (C), 141.1 (C), 139.5 (C), 131.4 (C-H), 130.4 (C), 128.6 (C-H), 128.5 (C-H), 126.3 (C-H), 121.8 (C-H), 120.0 (C), 41.8 (CH_2), 40.3 (C), 30.6 (CH_2), 27.7 (CH_3), 20.5 (CH_3), 19.3 (CH_3). IR (KBr, cm^{-1}): 1677.1. HRMS (ESI): calcd. for $C_{22}H_{27}NO_2Na$: 360.1928, found: 360.1939.

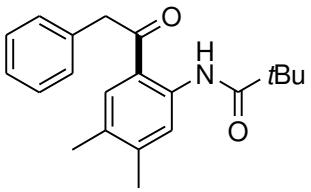

7r: 48%

Eluent: 95% *n*-hexane/5% EA. ^{1}H NMR (400 MHz, $CDCl_3$): δ_H 11.83 (bs, NH), 8.66 (s, 1H), 7.76 (s, 1H), 7.34-7.25 (m, 5H), 4.30 (s, 2H), 2.30 (s, 3H), 2.25 (s, 3H), 1.33 (s, 9H). ^{13}C NMR (100 MHz, $CDCl_3$): δ_C 201.7 (C), 178.5 (C), 145.4 (C), 140.1 (C), 134.9 (C), 132.2 (C-H), 130.5 (C), 129.5 (C-H), 128.9 (C-H), 127.1 (C-H), 122.0 (C-H), 119.8 (C), 46.8 (CH_2), 40.5(C), 27.8 (CH_3), 20.6 (CH_3), 19.5 (CH_3). IR (KBr, cm^{-1}): 1685.8. HRMS (ESI): calcd. for $C_{21}H_{25}NO_2NaCl$: 346.2040, found: 346.2045.

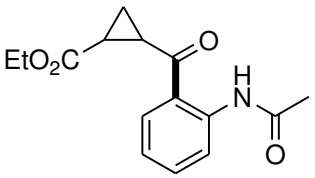

7s: 64%

Eluent: 90% *n*-hexane/10% EA. ^{1}H NMR (400 MHz, $CDCl_3$): δ_H 11.38 (bs, NH), 8.69 (d, J = 8.4, 1H), 8.06 (d, J = 8.0, 1H), 7.55 (t, J = 7.5, 1H), 7.14 (t, J = 7.4, 1H), 4.18 (q, J = 6.4, 2H), 3.20-3.16 (m, 1H), 2.39-2.34 (m, 1H), 2.19 (s, 3H), 1.61 (t, J = 6.6, 2H), 1.28 (t, J = 7.1, 3H). ^{13}C NMR (100 MHz, $CDCl_3$): δ_C 200.6 (C), 172.0 (C), 169.4 (C), 140.8 (C), 135.3 (C-H), 131.1 (C-H), 122.6 (C-H), 122.3 (C), 121.0 (C-H), 61.4 (CH_2), 27.2 (CH_3), 25.6 (CH_3), 25.1 (CH_3), 18.2 (CH_2), 14.3 (CH_3). IR (neat, cm^{-1}): 1697.2. HRMS (ESI): calcd. for $C_{15}H_{17}NO_4Na$: 298.1220, found: 298.1221.

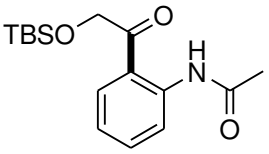

7t: 61%

Eluent: 91% *n*-hexane/9% EA. ^{1}H NMR (400 MHz, $CDCl_3$): δ_H 11.5 (bs, NH), 8.73 (d, J = 8.5, 1H), 7.78 (d, J = 8.0, 1H), 7.55 (t, J = 7.5, 1H), 7.08 (t, J = 7.4, 1H), 4.94 (s, 2H), 2.23 (s, 3H), 0.94 (s, 9H), 0.14 (s, 6H). ^{13}C NMR (100 MHz, $CDCl_3$): δ_C 201.0 (C), 169.5 (C), 141.0 (C), 135.2 (C-H), 129.4 (C-H), 122.2 (C-H), 121.0 (C-H), 119.5 (C), 67.5 (CH_2), 25.8 (CH_3), 25.5 (CH_3), 18.5 (C), -5.3 (Si-CH_3). IR (neat, cm^{-1}): 1666.2. HRMS (ESI): calcd. for $C_{16}H_{25}NO_3NaSi$: 330.1597, found: 330.1604.

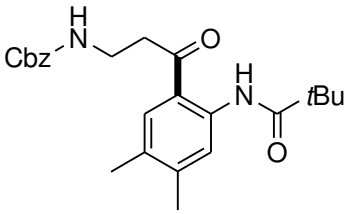

7u: 64%

Eluent: 100% *n*-hexane/20% EA. ^{1}H NMR (400 MHz, $CDCl_3$): δ_H 11.80 (bs, NH), 8.66 (s, 1H), 7.61 (s, 1H), 7.34-7.33 (m, 5H), 5.08 (s, 2H), 3.59 (t, *J* = 5.8, 2H), 3.26 (t, *J* = 5.6, 2H), 2.29 (s, 3H), 2.24 (s, 3H), 1.34 (s, 9H).^{13}C NMR (100 MHz, $CDCl_3$): δ_C 202.9 (C), 178.5 (C), 156.5 (C), 145.7 (C), 139.7 (C), 136.6 (C), 131.7 (C), 130.7 (C-H), 128.7 (C-H), 128.3 (C-H), 121.8 (C-H), 119.7 (C), 66.9 (CH_2), 40.5 (C), 39.8 (CH_2), 36.2 (CH_2), 27.8 (CH_3), 20.7 (CH_3), 19.4 (CH_3). IR (neat, cm^{-1}): 1718.0. HRMS (ESI): calcd. for $C_{24}H_{30}N_2O_4Na$: 433.2101, found: 433.2103.

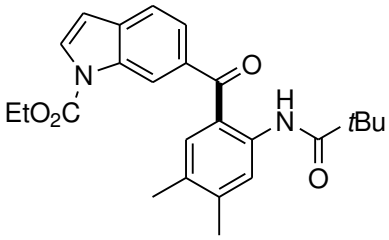

7v: 60%

Eluent: 94% *n*-hexane/6% EA. ^{1}H NMR (400 MHz, $CDCl_3$): δ_H 11.16 (bs, NH), 8.55 (s, 1H), 8.27 (d, *J* = 8.5 , 1H), 7.93 (s, 1H), 7.71-7.68 (m, 2H), 7.34 (s, 1H), 6.67 (d, *J* = 3.5, 1H), 4.53 (q, *J* = 7.1, 2H), 2.34 (s, 3H), 2.18 (s, 3H), 1.51-1.48 (t, *J* = 7.1, 3H), 1.34 (s, 9H). ^{13}C NMR (100 MHz, $CDCl_3$): δ_C 199.7 (C), 178.1 (C), 150.8 (C), 144.1 (C), 139.2 (C), 137.5 (C), 134.7 (C-H), 134.3 (C), 130.2 (C), 130.2 (C), 127.2 (C-H), 126.5 (C-H), 123.6 (C-H), 122.4 (C-H), 121.8 (C), 114.9 (C-H), 108.5 (C-H), 63.8 (CH_2), 40.3 (C), 27.7 (CH_3), 20.6 (CH_3), 19.3 (CH_3), 14.5 (CH_3). IR (neat, cm^{-1}): 1743.1. HRMS (ESI): calcd. for $C_{25}H_{28}N_2O_4Na$: 443.1940, found: 443.1947.

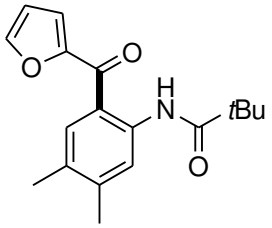

7w: 62%

Eluent: 95% *n*-hexane/5% EA. ^{1}H NMR (400 MHz, $CDCl_3$): δ_H 10.95 (bs, NH), 8.50 (s, 1H), 7.71-7.69 (m, 2H), 7.15-7.14 (m, 1H), 6.60-6.59 (m, 1H), 2.32 (s, 3H), 2.26 (s, 3H), 1.32 (s, 9H). ^{13}C NMR (100 MHz, $CDCl_3$): δ_C 184.3 (C), 177.9 (C), 152.1 (C), 147.3 (C-H), 144.3 (C), 138.7 (C), 132.4 (C-H), 130.5 (C), 122.5 (C-H), 121.2 (C-H), 121.0 (C), 112.2 (C-H), 40.1 (C), 27.6 (CH_3), 20.5 (CH_3), 19.3 (CH_3). IR (KBr, cm^{-1}): 1676.0. HRMS (ESI): calcd. for $C_{18}H_{21}NO_3Na$: 322.1420, found: 322.1419.

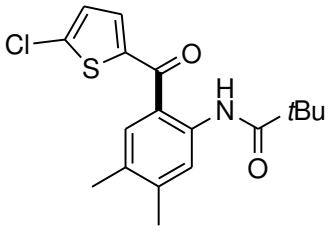

7x: 75%

Eluent: 96% *n*-hexane/4% EA. ^{1}H NMR (400 MHz, $CDCl_3$): δ_H 10.6 (bs, NH), 8.45 (s, 1H), 7.54 (s, 1H), 7.36 (d, J = 4.0, 1H), 6.98 (d, J = 4.0, 1H), 2.32 (s, 3H), 2.25 (s, 3H), 1.31 (s, 9H). ^{13}C NMR (100 MHz, $CDCl_3$): δ_C 188.6 (C), 177.7 (C), 144.1 (C), 142.8 (C), 139.9 (C), 138.1 (C), 134.6 (C-H), 132.5 (C-H), 130.6 (C), 127.4 (C-H), 122.8 (C-H), 121.3 (C), 40.1 (C), 27.5 (CH_3), 20.4 (CH_3), 19.2 (CH_3). IR (KBr, cm^{-1}): 1686.6. HRMS (ESI): calcd. for $C_{18}H_{20}NO_2NaSCl$: 372.0800, found: 372.0801.

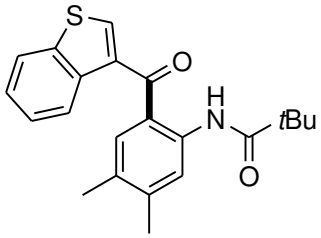

7y: 76%

Eluent: 98% *n*-hexane/2% EA. ^{1}H NMR (400 MHz, $CDCl_3$): δ_H 11.14 (bs, NH), 8.56 (s, 1H), 8.32 (d, J = 8.1, 1H), 7.92-7.87 (m, 2H), 7.51-7.42 (m, 3H), 2.35 (s, 3H), 2.20 (s, 3H), 1.35 (s, 9H). ^{13}C NMR (100 MHz, $CDCl_3$): δ_C 193.3 (C), 178.0 (C), 144.3 (C), 140.0 (C), 138.8 (C), 137.4 (C), 136.5 (C-H), 135.9 (C), 133.8 (C-H), 130.5 (C), 125.5 (C-H), 124.7 (C-H), 122.8 (C), 122.5 (C-H), 122.4 (C-H), 53.5 (CH_2), 40.2 (C), 27.6 (CH_3), 20.5 (CH_3), 19.2 (CH_3). IR (neat, cm^{-1}): 1681.3. HRMS (ESI): calcd. for $C_{22}H_{23}NO_2NaS$: 388.1348, found: 388.1347.

Chapter 3

Mechanistic investigation on the Palladium-catalyzed ortho-selective C–H acylation

3.1 Introduction

In chapter 2, we described the Pd(II)-catalyzed aromatic C–H acylation of oximes and anilides with aldehydes and TBHP as oxidant. The catalytic reaction was proposed to proceed through (Scheme 3.1): (1) directing group-assisted *ortho*-C–H bond cleavage by Pd(II) to form palladacyclic complex **A**; (2) coupling of **A** with acyl radicals to form a putative palladium (III)[53] or (IV)[52] intermediate **B**, and (3) C–C bond formation via reductive elimination of **B** with regeneration of Pd(II) catalyst. However, there are several mechanistic issues remain outstanding: (1) what is the catalyst resting state? (2) What is the nature of the turnover-limiting step? (3) What is the mechanistic underpinning associated with the carboradical coupling step?

In this chapter, we will disclose our kinetic investigation of the dehydrogenative arene C–H acylation, and this includes kinetic rate order determination, primary kinetic H/D isotope effect and Hammett correlation study. Effort to characterize the

acyl radical mediated mechanism will also be discussed.

Scheme 3.1 Previously proposed catalytic cycle

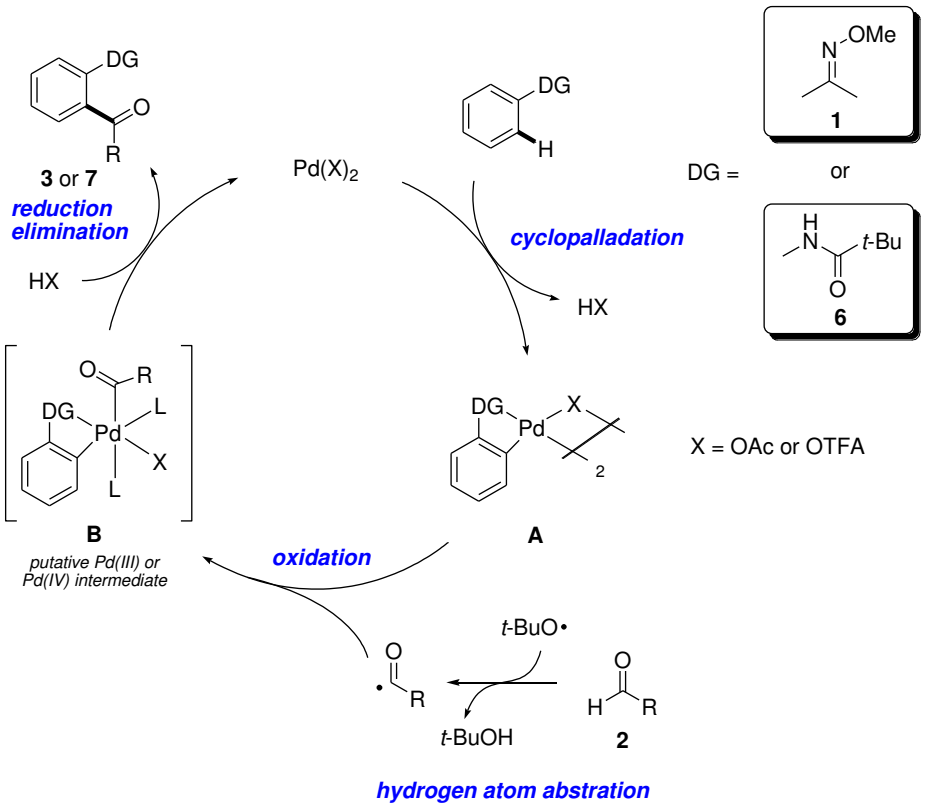

3.2 Results

3.2.1 Reaction rate order

Our kinetic studies on the C–H acylation were conducted by employing 2-phenylpyridine (**8a**) and 4-chlorobenzaldehyde (**2a**) as model substrates with TBHP as oxidant and $Pd(OAc)_2$ as catalyst. Substrate **8a** displays several desirable features: (1) it undergoes selective mono-acylation with excellent mass balance; (2) facile acylation occurs within a reasonable time at 60 ^oC and no reaction at room temperature. Thus, complete reaction quenching can be achieved by immersing the reaction mixture into ice-bath temperature. Moreover, **8a** has already been employed as model substrate for other related C–H functionalization reactions (e.g. acetoxylation,[52a,b,c] chlorination[52c,d] and arylation[52e,f]); thus, comparisons of our findings with other literature data become possible.

We began our investigation by monitoring the reaction profile with GC-FID under the following conditions: **8a** (200 mM), **2a** (600 mM), $Pd(OAc)_2$ (10 mM), TBHP (300 mM), AcOH (175 mM) in toluene at 60 ^oC (Scheme 3.2). The kinetic profile of **9a** formation was obtained by determining the **9a** formation in regular quenching at every 5 min interval. The experimental data were successfully fitted by nonlinear regression techniques (Graphpad Prism Version 5) (Figure 3.1). Initial rate of the reaction was established by linear regression of the data below 60 mM **9a**

(>30% conversion of **8a**) (Figure 3.2).

Scheme 3.2 Typical conditions for kinetic studies

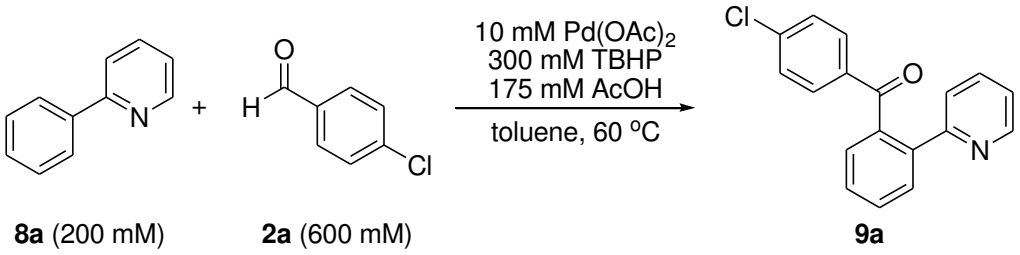

Figure 3.1 Time-dependent increase of **9a** for the Pd-catalyzed C–H acylation

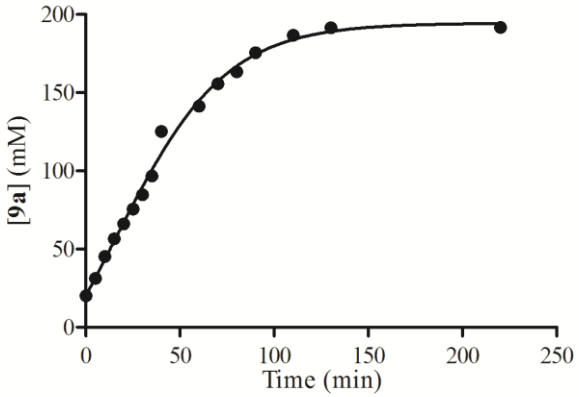

Figure 3.2 Initial rate of the acylation with the data below 60 mM **9a** formation

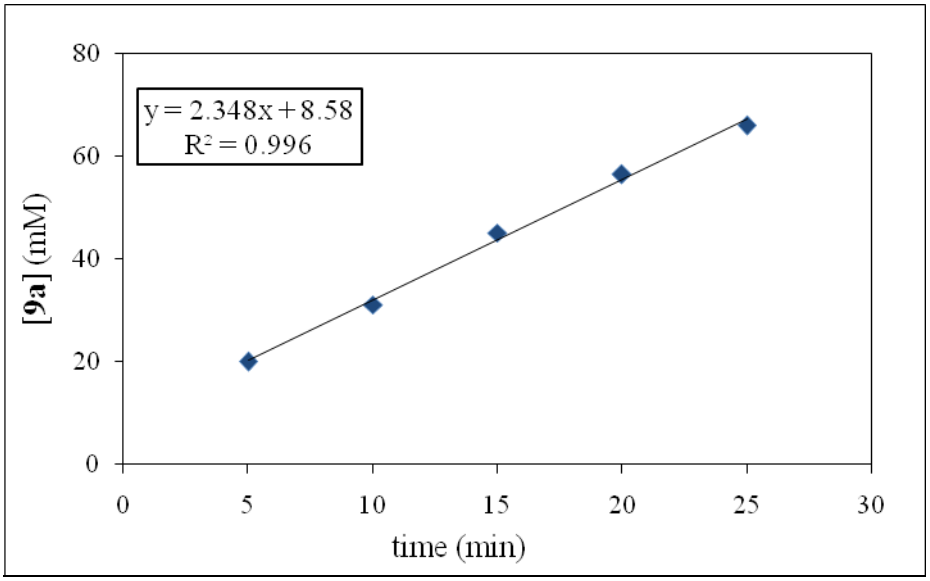

We next sought to establish the kinetic order in each reaction component of the acylation reaction.

At first, the rate order of **8a** was ascertained by varying **8a**'s concentration (80 to 300 mM) in the presence of **2a** (600 mM), TBHP (300 mM), AcOH (175 mM) and $Pd(OAc)_2$ (10 mM) in toluene at 60 ^oC (Table 3.1). It is necessary to keep **8a** as the limiting reagent for reproducible results (i.e. [**2a**] > [**8a**]). Each experiment was run in triplicate in a parallel manner, and each kinetic result represents an average of three runs. The reaction mixtures were stirred at room temperature for 5 min to ensure complete mixing of all stock solutions. The reactions were run for a certain amount of time with **8a** conversion being kept below 30%, which is within the linear range of the product formation curve (Figure 3.1). The reactions were then quenched by immersing the reaction mixtures into an ice-water bath for 5 min. The amount of **9a** being formed was determined by gas chromatography; method of initial rates was employed to determine the reaction rate at each [**8a**], and a plot of the initial rate (Δ[**9a**] /Δt) versus [**8a**] was linear. Intriguingly the reaction demonstrated an inverse dependence on [**8a**] (Figue 3.3). Next, the initial rate (Δ[**9a**] /Δt) was plotted versus $[\mathbf{8a}]^{-1}$ to show a linear relationship (R^2 = 0.99), confirming an inverse first-order dependence on [**8a**] (Figure 3.4). The inverse first-order relationship was further

verified by plotting log (Δ[**9a**] /Δt) against log ([**8a**]), and a linear plot with a slope of -0.95 (R^2 = 0.84) was obtained. These findings strongly suggest that one equivalent of **8a** must be lost in order to progress from the resting state to the transition state at the turnover-limiting step.

Table 3.1 Initial rate as a function of [**8a**]

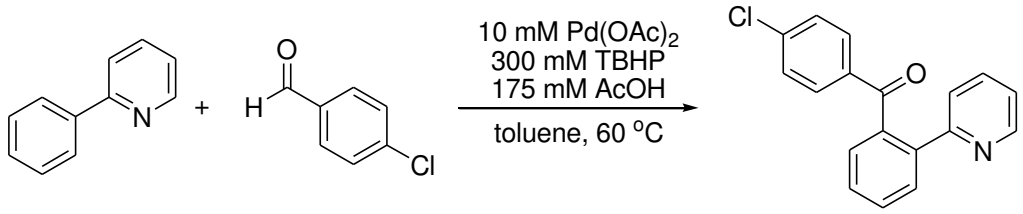

8a (80 - 300 mM) **2a** (600 mM) **9a**

[**8a**] mM	average initial rate (mM/min)
80	3.13 ± 0.27
120	2.91 ± 0.12
200	1.91 ± 0.13
240	1.51 ± 0.45
300	0.97 ± 0.21

Figure 3.3 Plot of the initial rate (Δ[**9a**] /Δt) versus [**8a**]

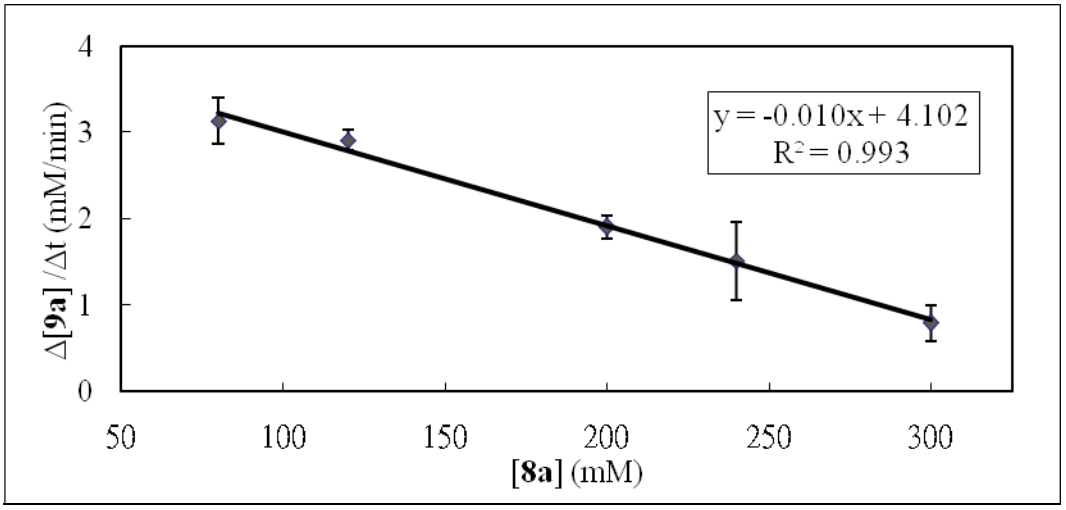

Figure 3.4 Plot of log (Δ[**9a**] /Δt) versus log [**8a**]

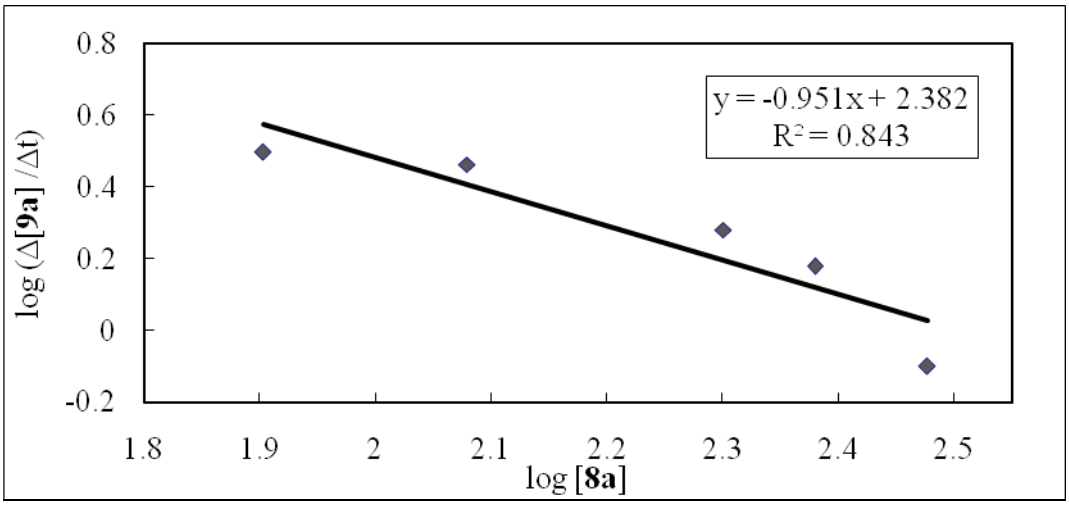

The kinetic order of **2a** was determined by conducting the experiments under similar conditions (i.e., [**2a**] > [**8a**]) (Table 3.2). This was performed with a fixed concentration of **8a** (200 mM), [$Pd(OAc)_2$] (10 mM), [TBHP] (300 mM) and [AcOH] (175 mM), and varying the concentration of **2a** (400 – 650 mM) in toluene at 60 ^{o}C. A plot of initial rate (Δ[**9a**] /Δt) versus [**2a**] as shown below (Figue 3.5). The initial rates

were found to be zeroth-order with respect to [**2a**] over a range of concentration. The zeroth-order relationship was further confirmed by plotting log (Δ[**9a**] /Δt) versus log ([**2a**]) giving a straight line with a slope of -0.18 (Figure 3.6).

Table 3.2 Initial rate as a function of [**2a**]

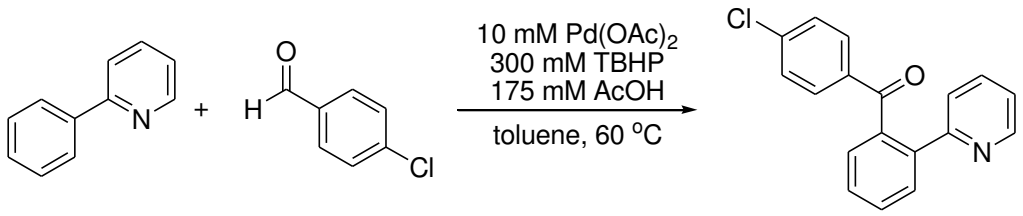

8a (200 mM) **2a** (400 - 650 mM) **9a**

[**2a**] mM	average initial rate (mM/min)
400	2.07 ± 0.47
450	2.29 ± 0.42
500	1.78 ± 0.27
550	2.36 ± 0.20
600	2.23 ± 0.45
650	1.74 ± 0.10

Figure 3.5 Plot of the initial rate (Δ[**9a**] /Δt) versus [**2a**]

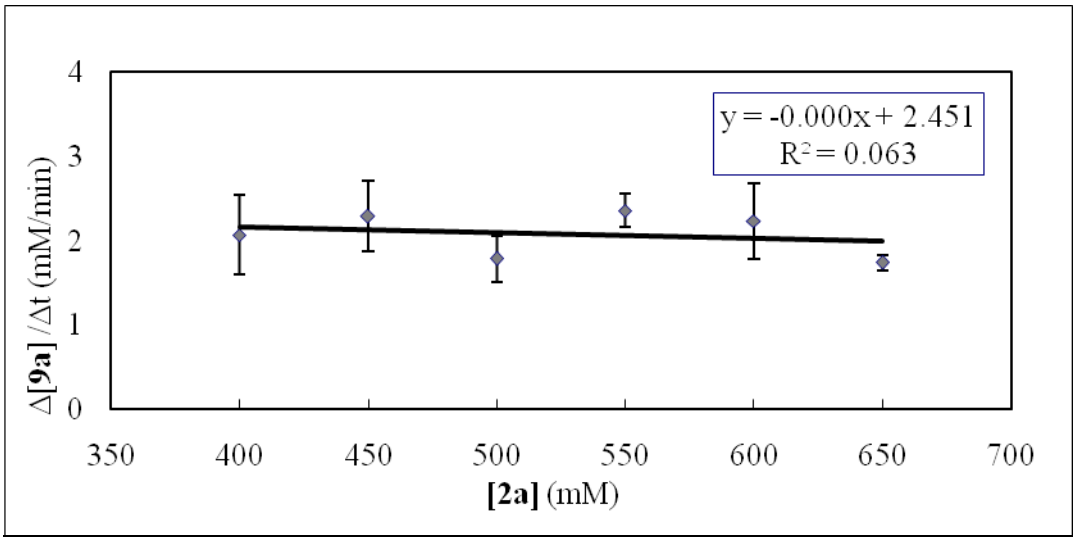

Figure 3.6 Plot of log (Δ[**9a**] /Δt) versus log [**2a**]

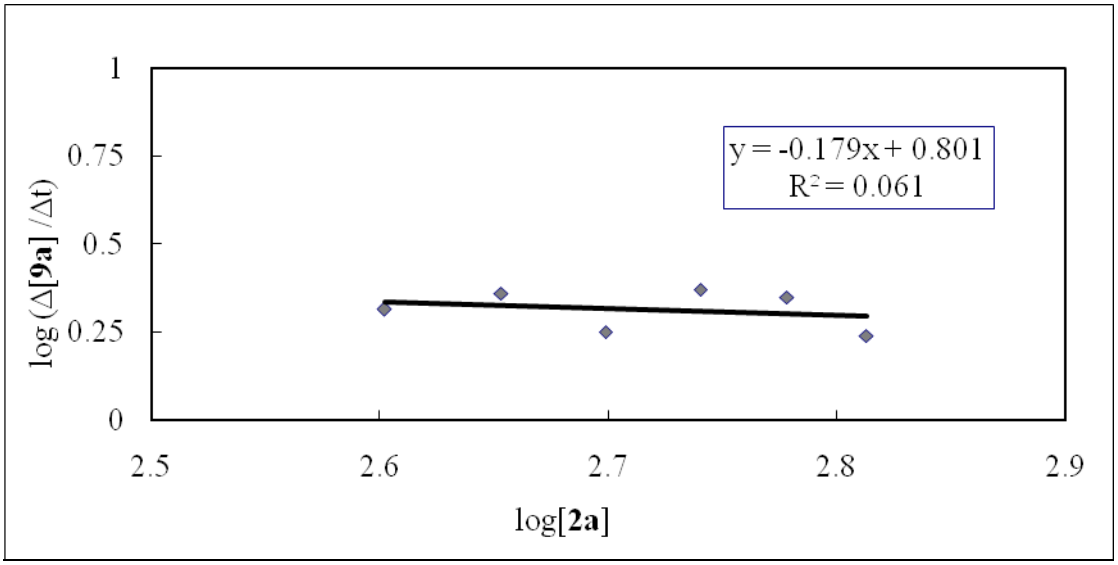

Likewise, the kinetic order of TBHP was determined by conducting the experiments with a fixed concentration of **8a** (200 mM), [$Pd(OAc)_2$] (10 mM), [**2a**] (600 mM) and [AcOH] (175 mM), and varying the concentration of TBHP (300 – 600 mM) in toluene at 60 ^{o}C (Table 3.3). A plot of initial rate (Δ[**9a**] /Δt) versus [TBHP] as shown below (Figue 3.7). The initial rates were found to be zeroth-order with respect to [TBHP] over a range of concentration (300 – 600 mM). The zeroth-order relationship was further confirmed by plotting log (Δ[**9a**] /Δt) versus log ([TBHP]) giving a straight line with a slope of -0.14 (Figure 3.8).

Table 3.3 Initial rate as a function of [TBHP]

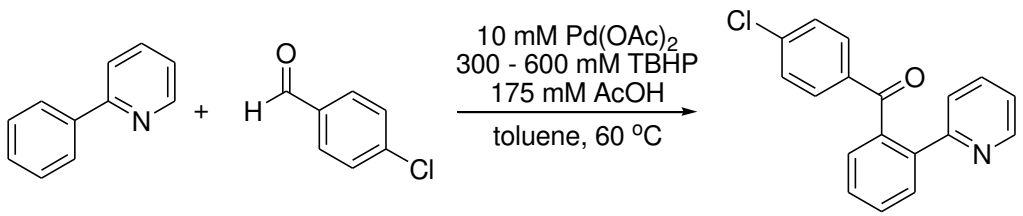

8a (200 mM) **2a** (600 mM) **9a**

[TBHP] mM	average initial rate (mM/min)
300	1.10 ± 0.13
350	1.19 ± 0.19
400	1.06 ± 0.19
450	1.18 ± 0.21
500	0.91 ± 0.14
600	1.09 ± 0.22

Figure 3.7 Plot of the initial rate (Δ[**9a**] /Δt) versus [TBHP]

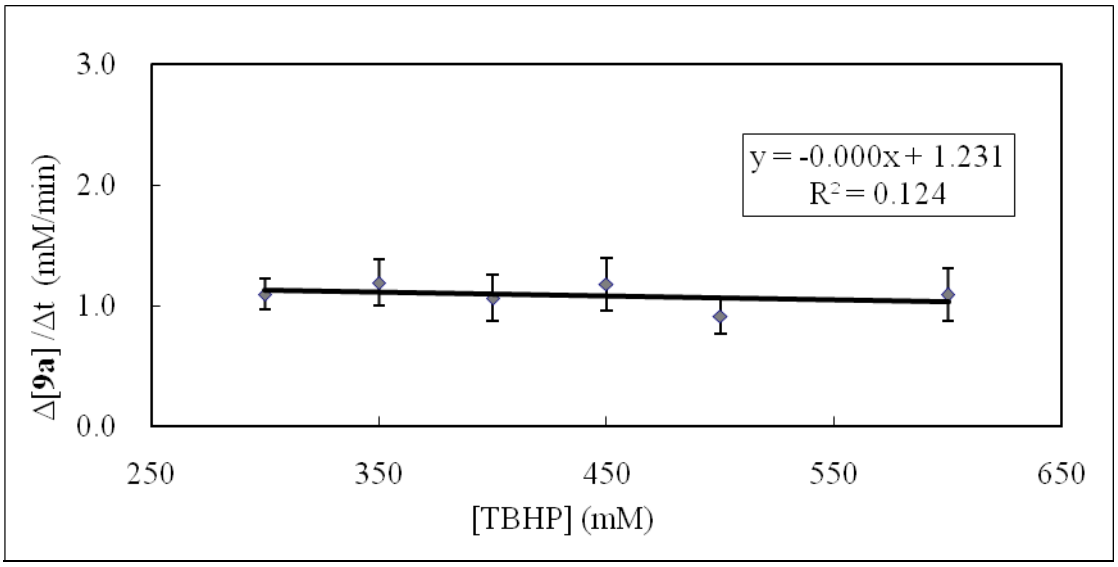

Figure 3.8 Plot of log (Δ[**9a**] /Δt) versus log [TBHP]

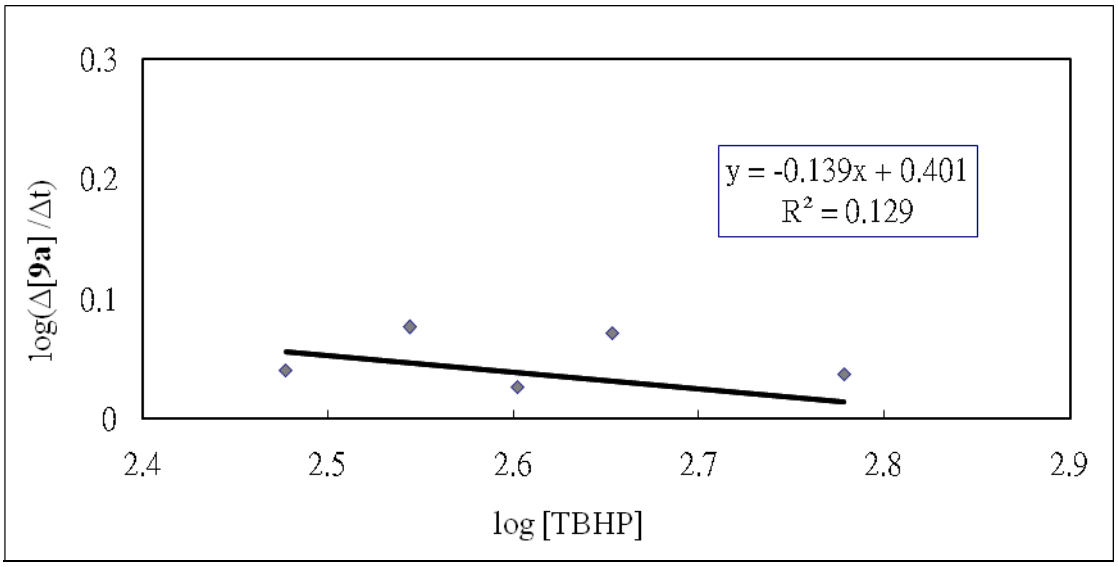

The kinetic rate order of $Pd(OAc)_2$ was determined by conducting the experiments with a fixed concentration of **8a** (200 mM), [TBHP] (300 mM), [**2a**] (600 mM) and [AcOH] (175 mM), and varying the concentration of [$Pd(OAc)_2$] (2.5 – 15 mM) in toluene at 60 °C (Table 3.4). A plot of the initial rate (Δ[**9a**] /Δt) versus [$Pd(OAc)_2$] displayed a non-linear relationship (Figure 3.9). However, a plot of initial rate versus $[Pd(OAc)_2]^2$ afford a straight line (R^2 = 0.98) (Figure 3.10). This result is indicative of a second-order dependence on [$Pd(OAc)_2$]. The second-order dependence was further confirmed by plotting log (Δ[**9a**] / Δt) versus log ([$Pd(OAc)_2$]) giving a straight line with a slope of 1.95 (R^2 = 0.88) (Figure 3.11). The observed second-order dependence of [$Pd(OAc)_2$] suggests that the acylation reaction would probably involve a dinuclear palladium intermediate at the turnover-limiting step.

Table 3.4 Initial rate as a function of $[Pd(OAc)_2]$

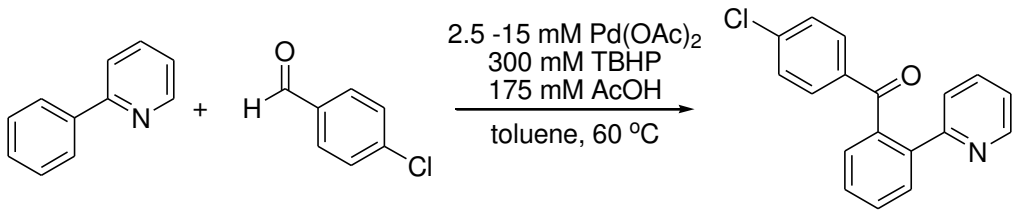

8a (200 mM) **2a** (600 mM) **9a**

$[Pd(OAc)_2]$ mM	average initial rate (mM/min)
2.5	0.11 ± 0.03
5	0.15 ± 0.09
7.5	0.36 ± 0.16
10	1.32 ± 0.20
15	3.03 ± 0.41

Figure 3.9 Plot of the initial rate (Δ[**9a**] /Δt) versus $[Pd(OAc)_2]$

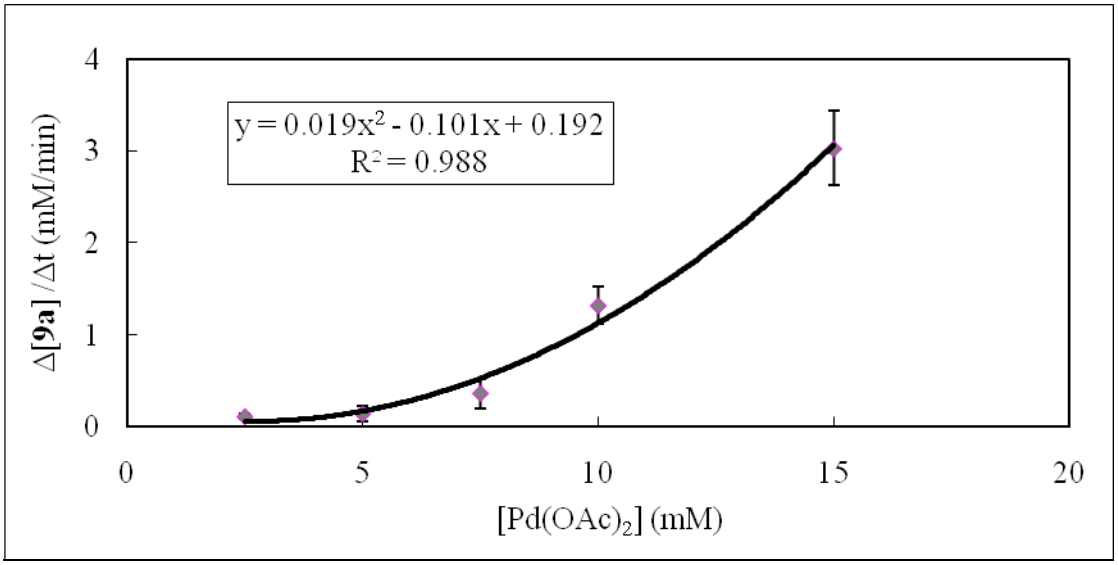

Figure 3.10 Plot of the initial rate (Δ[**9a**] /Δt) versus $[Pd(OAc)_2]^2$

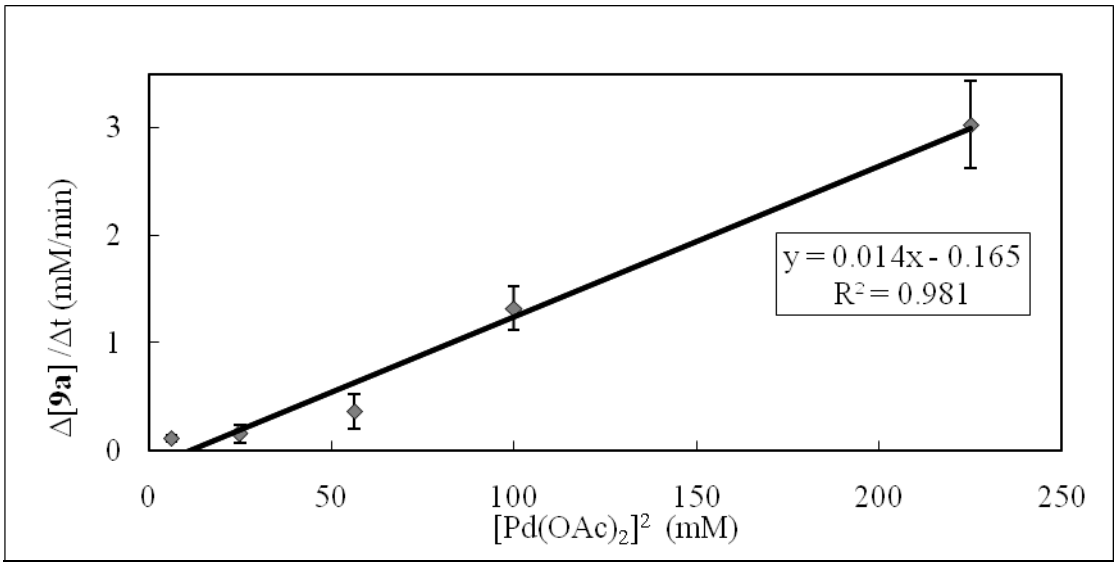

Figure 3.11 Plot of log (Δ[**9a**] /Δt) versus log $[Pd(OAc)_2]$

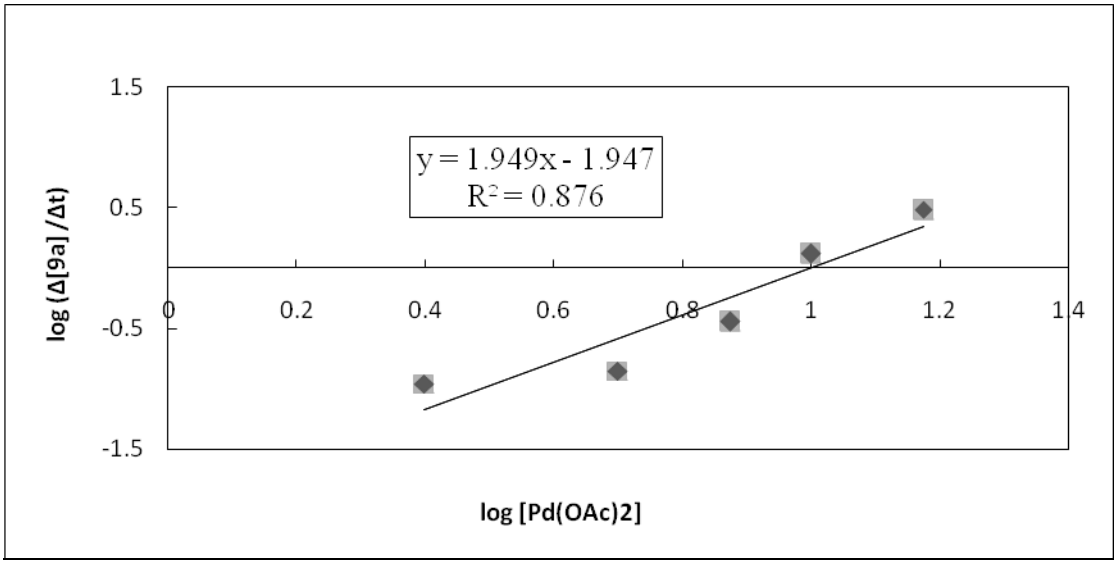

The kinetic rate order of **13b** was determined by the conducting experiments with a fixed concentration of **8a** (200 mM), [TBHP] (300 mM), [**2a**] (600 mM) and [AcOH] (175 mM), and varying the concentration of [**13b**] (6 – 14 mM) in toluene at 60 ^{o}C (Table 3.5). A plot of initial rate (Δ[**9a**] /Δt) versus [**13b**] displayed a non-linear relationship (Figure 3.12). A plot of the initial rate versus [**13b**]^2 afforded a straight line (R^2 = 0.98) (Figure 3.13). This result is consistent with of a second-order dependence on [**13b**]. The second-order dependence was further confirmed by plotting log (Δ[**9a**] /Δt) versus log ([**13b**]) giving a straight line with a slope of 1.93 (R^2 = 0.97) (Figure 3.14). The observed second-order dependence of [**13b**] suggests that the dinuclear cyclopalladated complex may be dissociated into a monomer, and a recombination of two monomers is required before the turnover-limiting step. Thus, the acylation reaction would probably involve a dinuclear palladium intermediate at the turnover-limiting step.

Table 3.5 Initial rate as a function of [**13b**]

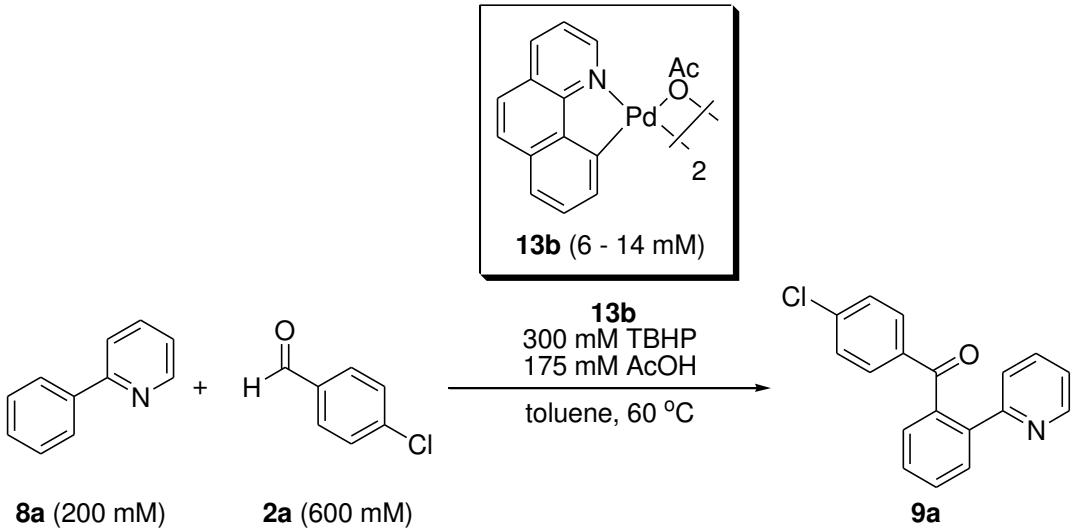

[**13b**] mM	average initial rate (mM/min)
6	1.70 ± 0.36
8	3.55 ± 0.14
10	4.38 ± 0.43
12	6.36 ± 0.88
14	10.41 ± 0.04

Figure 3.12 Plot of the Initial Rate (Δ[**9a**] /Δt) versus [**13b**]

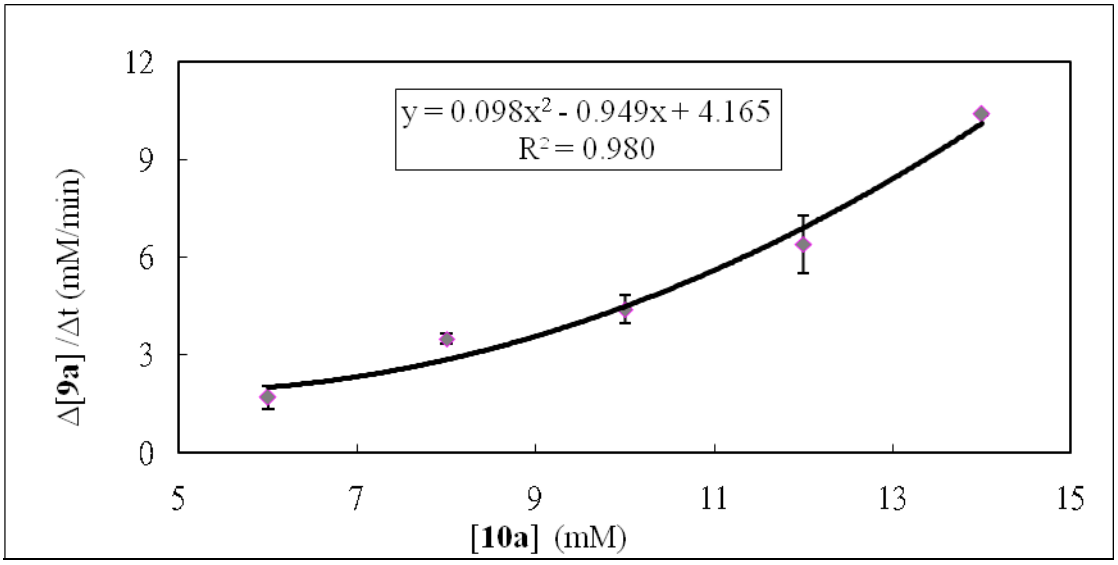

Figure 3.13 Plot of the initial rate (Δ[**9a**] /Δt) versus [**13b**]^2

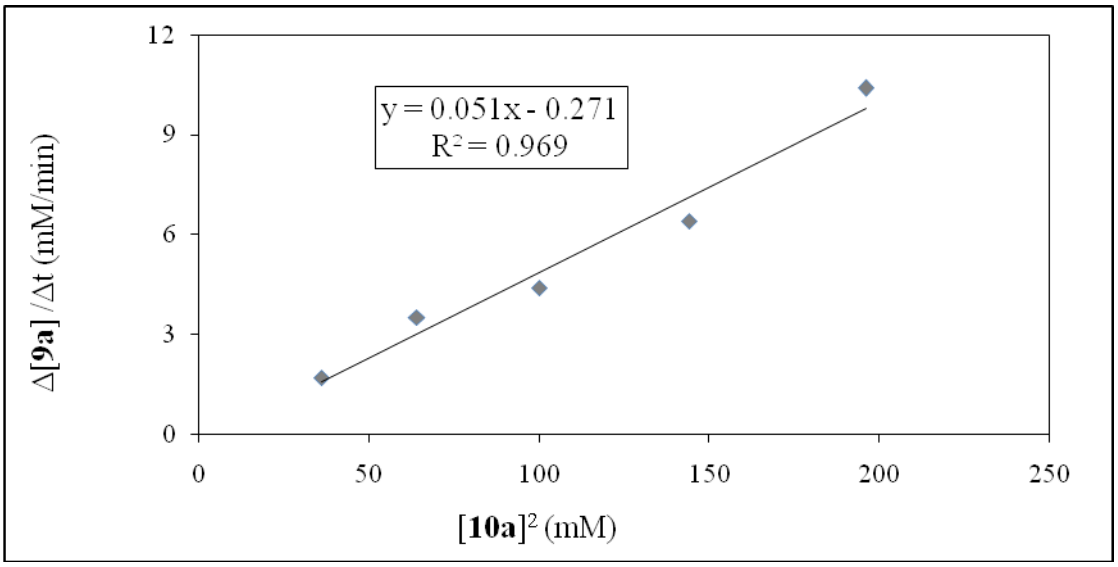

Figure 3.14 Plot of log (Δ[**9a**] /Δt) versus log [**13b**]

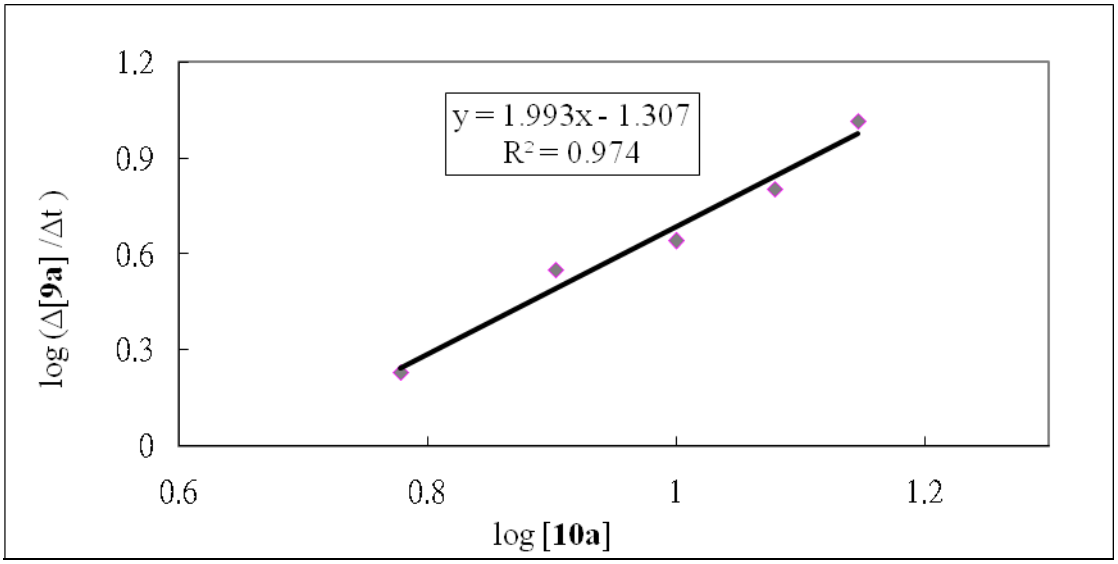

3.2.2 Kinetic isotope effect studies

In this work, intermolecular KIE was performed by determining the initial rates of acylation of 2-phenylpyridine (**8a**) and d_5-2-phenylpyridine (**8a**-d_5) separately (Scheme 3.3). The reaction was repeated for three times, and an average kinetic isotope effect (KIE) of k_H/k_D = 5.6 based on initial reaction rate measurement (conversion of 20%) was obtained. The k_H/k_D value was comparable to the reported Pd-catalyzed directing group-assisted *ortho*-C–H functionalization reactions, which typically exhibit primary intermolecular KIE values ranging from 2.2 to 6.7. The significant KIE obtained in this work strongly suggests that the C–H cleavage should be a turnover-limiting step for acylation of 2-phenylpyridines.

Scheme 3.3 KIE studies on the parallel reactions of **8a** and **8a**-d_5 with **2a**

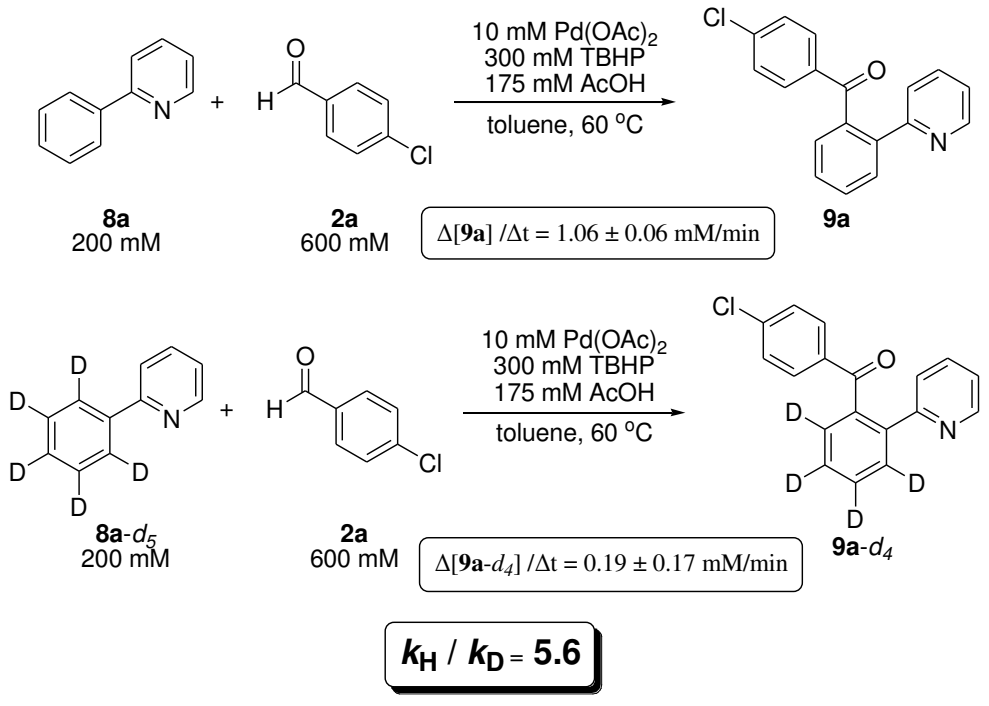

3.2.3 Hammett correlation study

In this work, a Hammett correlation study on a series of *meta*-substituted pivalanilides (**6-Y**) was examined. In this work, an equimolar amount of competitive pivalanilides (0.2 mmol in total), $Pd(OAc)_2$ (4 mol%), 4-chlorobenzaldehyde **2a** (6 mmol), TBHP (0.4 mmol), TFA (0.2 mmol) in toluene (1mL) under nitrogen atmosphere at 40 ^{o}C for 4 min (around 10-20 % of pivalanilide conversion). The reaction mixture was cooled with ice-bath and quenched by saturated sodium bisulfate solution (2 mL). The resulting residue was analyzed by GC/FID for determination of conversion using a calibration curve (3 points) with tetradecane (0.1 mmol) as the internal standard. Each result was triplicated and an average value was reported in each case. By plotting log (k_Y / k_H) versus the Hammett σ_p^+ constant, we obtained a straight line (R^2 = 0.96) with ρ^+ was found to be -0.74 (Figure 3.15). The small negative ρ^+ value implies that the Pd(II)-mediated C–H cleavage should not proceed through an cationic arene species such as Wheland intermediate.

Figure 3.15 Linear free energy correlation study for the Pd(II)-catalyzed acylation of *meta*-substituted pivalanilides

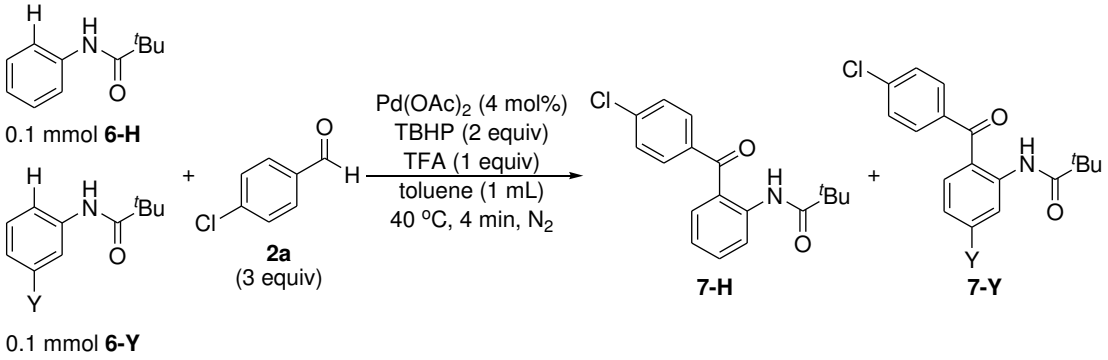

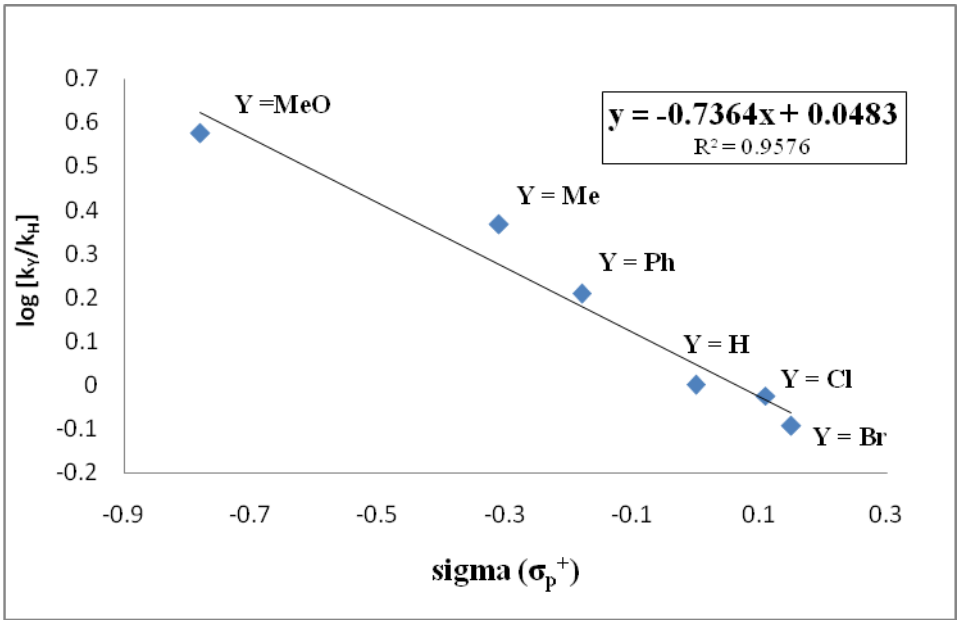

3.2.4 Stoichiometric reactions of cyclopalladated complexes with aldehyde

On the basis of observed *ortho*-selectivity, we proposed that the Pd-catalyzed acylation should be initiated by an *ortho*-C–H cyclopalladation. To ascertain the intermediacy of the arylpalladium(II) complex, we have examined the stoichiometric reaction of 4-chlorobenzaldehyde (**2a**) with the cyclopalladated complexes of 2-phenylpyridine (**8a-Pd**). The crystal structure of **8a-Pd** was obtained by Yu (W. –Y.) and co-workers.[29d] In the work, cyclopalladated complex **8a-Pd** was prepared by treating **8a** (1 mmol) and $Pd(OAc)_2$ (1 mmol) in methanol (10 mL) at room temperature, the dinuclear cyclopalladated complexes $[Pd(C\sim N)(OAc)]_2$ (C~N = 2-phenylpyridine) (**8a-Pd**) was obtained in 81% yield as a bright yellow solid (Scheme 3.4, eq 1). X-ray crystallographic analysis (see figure 3.16) revealed complex **8a-Pd** does not display the expected planar geometry (approximate D_{2h} symmetry) but an open "clamshell" structure. The acetate ligands are perpendicular to the plane of the Pd atoms and 2-phenylpyridine ligands. The Pd atoms are quite close to each other with Pd–Pd bond distance of 2.86 Å. The analogous dinuclear palladium complex containing different cyclometalated ligands has also been prepared and structurally characterized by other research groups, which most adopted the characteristic open "clamshell" structure features Pd–Pd distance of 2.8–2.9 Å (Figure 3.17).[54]

Scheme 3.4 Synthesis of cyclopalladated complex **8a-Pd** and the stoichiometric reaction with **2a**

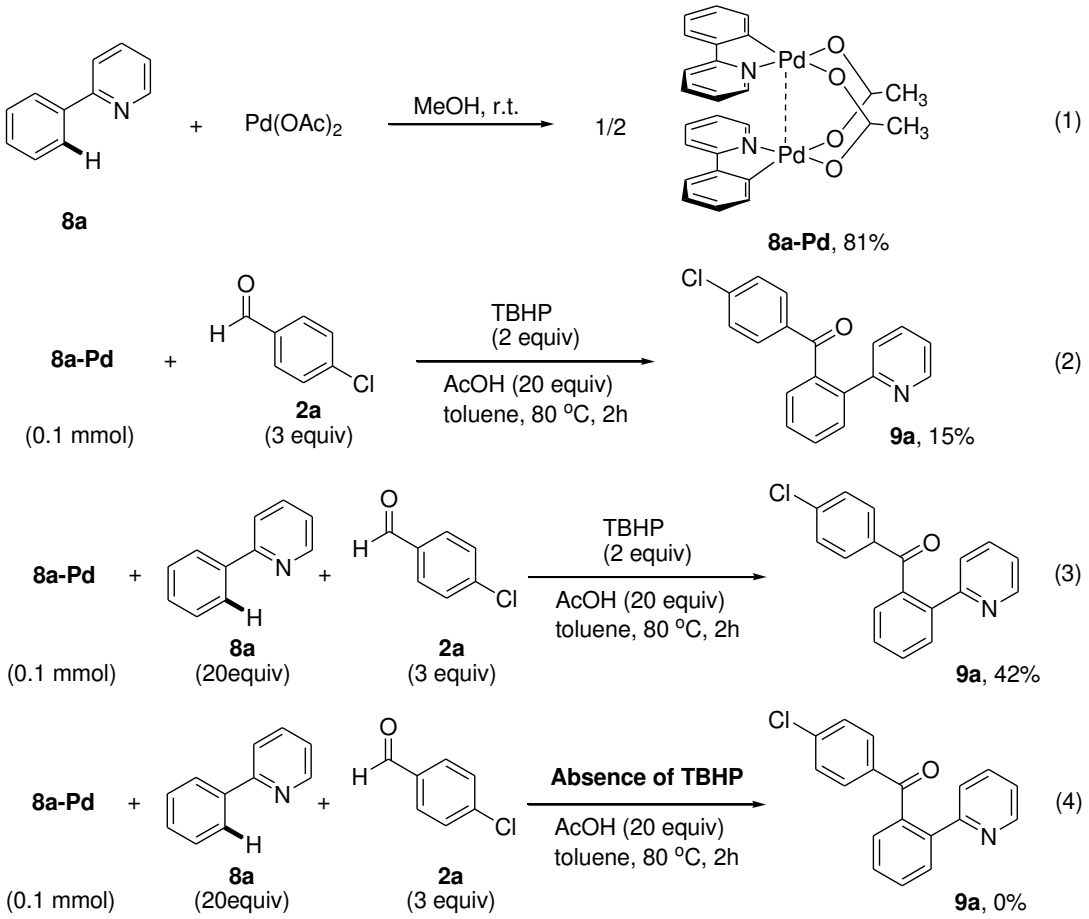

Figure 3.16 X-ray Structure of [(2-phenylpyridine)Pd(μ-OAc)]$_2$ (**8a-Pd**) reported by Yu (W. –Y.) and co-workers

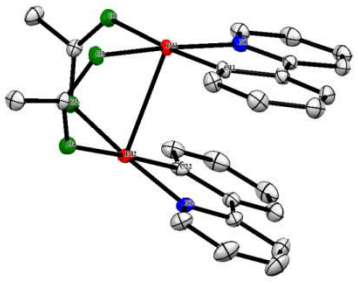

Pd–Pd = 2.862 Å

Figure 3.17 Collection of dinuclear Pd(II) acetate complexes with Pd–Pd bond distances 2.8-2.9 Å

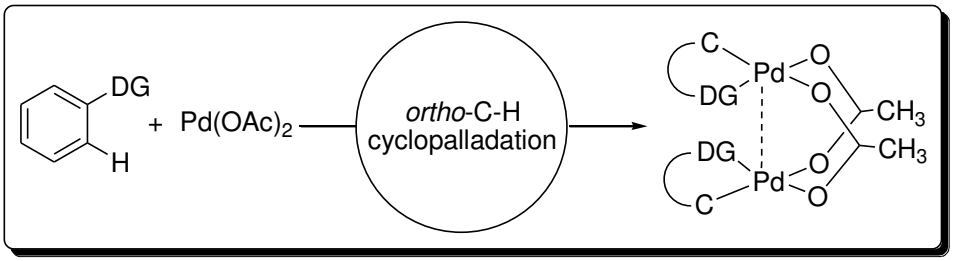

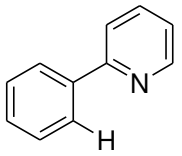

Yu (W. -Y) (2006)[29d]
Pd-Pd = 2.862

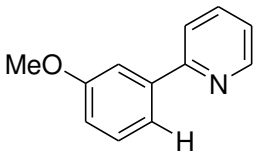

Yu (W. -Y) (2008)[29d]
Pd-Pd = 2.845

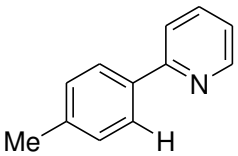

Gray (2010)[64]
Pd-Pd = 2.857

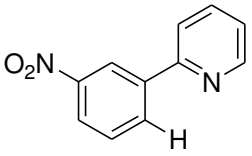

Fronczek (1983)[54a]
Pd-Pd = 2.822

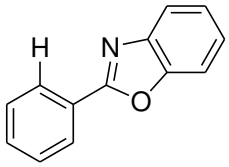

Churchill (1980)[14e]
Pd-Pd = 2.871

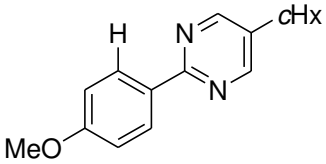

Ghedini (1990)[54b]
Pd-Pd = 2.871

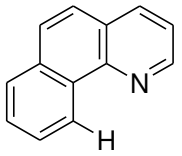

Ritter (2010)[53a]
Pd-Pd = 2.842

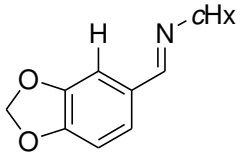

Vila (2010)[54c]
Pd-Pd = 2.865

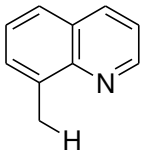

Yu (W. -Y) (2013)[14j]
Pd-Pd = 2.890 A

In this work, when **8a-Pd** (0.1 mmol) was treated with **2a** (0.3 mmol), TBHP (0.3 mmol), AcOH (20 equiv) in toluene (1 mL) at 80 ^{o}C, the coupled ketone **9a** was obtained in only 15% yield (Scheme 3.4, eq 2). However, when 20 equivalent of **8a** (2 mmol) was employed, the stoichiometric reaction of **8a-Pd** with **2a** afforded **9a** in

42% yield (eq 3). It is plausible that the addition of 2-phenylpyridine was needed to release the coupled ketone through ligand exchange. Notably, in the absence of TBHP, no ketone **9a** was formed (eq 4). Thus, a direct nucleophilic-type reaction of the cyclopalladated complex with aldehyde can be ruled.

Apart from being a potent stoichiometric reagent, **8a-Pd** is a kinetically competent catalyst for the C–H acylation (Table 3.6). For example, **8a-Pd** (5 mol%) effectively catalyzed the acylation of **8a** (0.2 mmol) with **2a** (0.6 mmol), TBHP (0.4 mmol) and AcOH (0.2 mmol) in toluene (1 mL) at 60 ^{o}C for 3 h to furnish **9a** in 88% yield (Table 3.6, entry 1), which is comparable to the analogous reaction with $Pd(OAc)_2$ as catalyst (entry 2, 90 %).

Table 3.6 Kinetic competence of cyclometallated **8a-Pd** for C–H acylation[a]

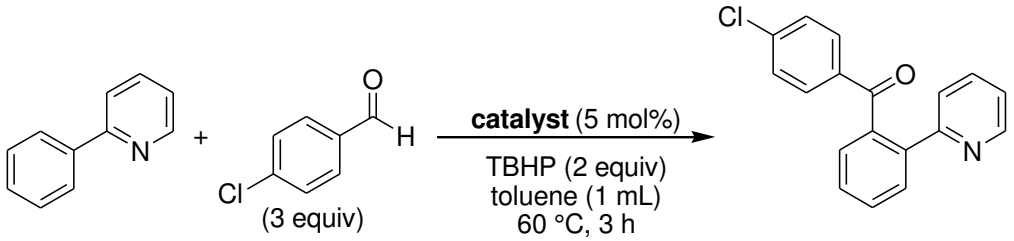

8a **2a** **9a**

entry	catalyst (5 mol%)	yield (%)[b]
1	**8a-Pd**	88
2	$Pd(OAc)_2$	90
3	**10**	0

[a]Reaction conditions: **8a** (0.2 mmol), **2a** (0.6 mmol), catalyst (5 mol%), TBHP (0.5 mmol), AcOH (0.2 mmol) and toluene (1 mL) under air at 60 ^{o}C for 3 h. [b]Yields were determined by GC-FID with tetradecane as internal standard.

Scheme 3.5 Stoichiometric and catalytic acylation of mononuclear **10**

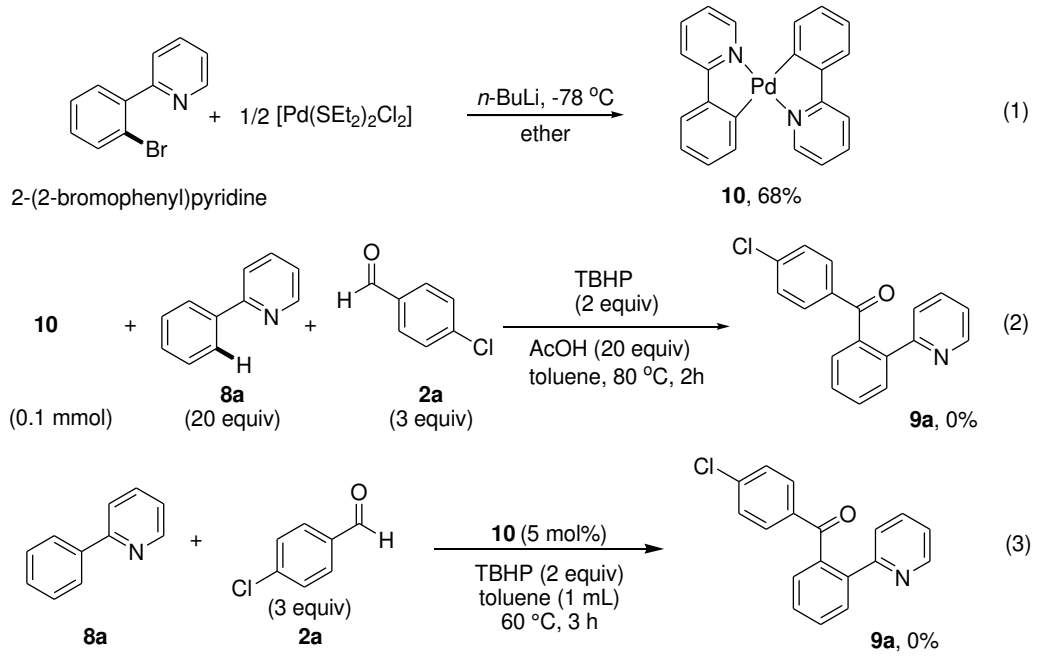

The feasibility of the involvement of mononuclear arylpalladium(II) complexes has been assessed. Mononuclear [Pd(2-phenylpyridine)$_2$] complex (**10**) was synthesized by reacting 2-(2-bromophenyl)pyridine with *n*-BuLi and Pd(Et$_2$S)$_2$Cl$_2$ and **10** was obtained in 68 % yield (Scheme 3.5, eq 1). In this work, when **10** was subjected to the stoichiometric acylation conditions: **10** (0.1 mmol), **8a** (2 mmol) **2a** (0.3 mmol), TBHP (0.3 mmol), AcOH (20 equiv) in toluene (1 mL) at 80 ^{o}C, no coupled ketone **9a** was obtained with complete recovery of complex **10** (eq 2). Similarly, mononuclear complex **10** was found to be incompetent catalyst for the acylation of **8a**. For instance, subjecting **8a** and **2a** (0.6 mmol) under the standard conditions (i.e. **10** (5 mol%), TBHP (0.5 mmol), AcOH (0.2 mmol) and toluene (1 mL) under air at 60 ^{o}C for 3 h), no desired **9a** was obtained with complete recovery of

substrate **8a**. Therefore, mononuclear arylpalladium(II) complex **10** is unlikely to be a competent intermediate for the acylation reaction.

3.2.5 Evidence for involvement of acyl radical intermediate

Table 3.7 Detrimental effect on the acylation by radical scavenger[a]

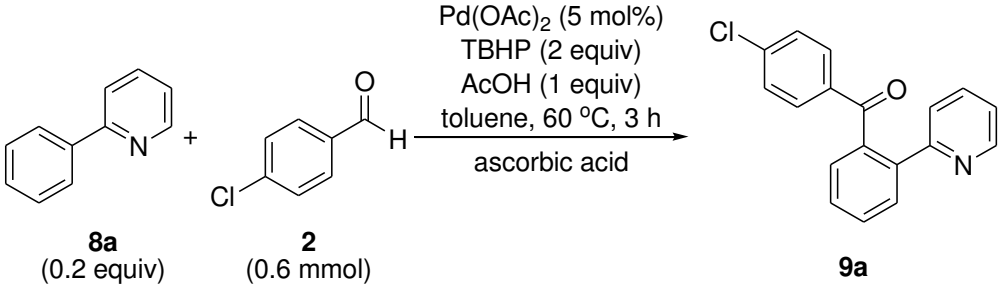

8a (0.2 equiv) **2** (0.6 mmol) **9a**

entry	ascorbic acid (mol%)	yield (%)[b]
1	0	89
2	10	60
3	25	35
4	50	19

[a]Reaction conditions: **8a** (0.2 mmol), **2a** (0.6 mmol), $Pd(OAc)_2$ (5 mol%), TBHP (0.5 mmol), AcOH (0.2 mmol), ascorbic acid and toluene (1 mL) under air at 60 °C for 3 h. [b]Yields were determined by GC-FID with tetradecane as internal standard.

Table 3.7 shows the detrimental effect of radical scanvenger on the acylation reaction.[55] Different concentration of ascorbic acid (0-50 mol%) (well-known radical scanvengers) were found to suppress catalytic acylation reaction in a dose-dependent manner. The formation of **9a** was reduced from 89% to 19% when ascorbic acid loading was increased from 0 mol% to 50 mol%. Based on this finding, the acylation is probably mediated by radicals.

Accodring to the literature, decomposition of TBHP should generate reactive *t*-BuO$^{\cdot}$ radicals,[56] which would react with aldehydes by hydrogen atom abstraction to give reactive acyl radicals[58]. It is possible to trap the active acyl radicals by TEMPO in the acylation reaction.[57] As illustrated by Scheme 3.6, when 2,2,6,6-tetramethylpiperidine *N*-oxide (TEMPO) was added to the catalytic reaction of **8a** with **2a**, no desired **9a** was obtained. Notably, 4-chlorobenzoate-2,2,6,6-tetramethylpiperidine was isolated in 65 % yield. This result is consistent with the involvement of acyl radicals in the acylation reaction.

Scheme 3.6 Trapping of the acyl radicals in catalytic condition

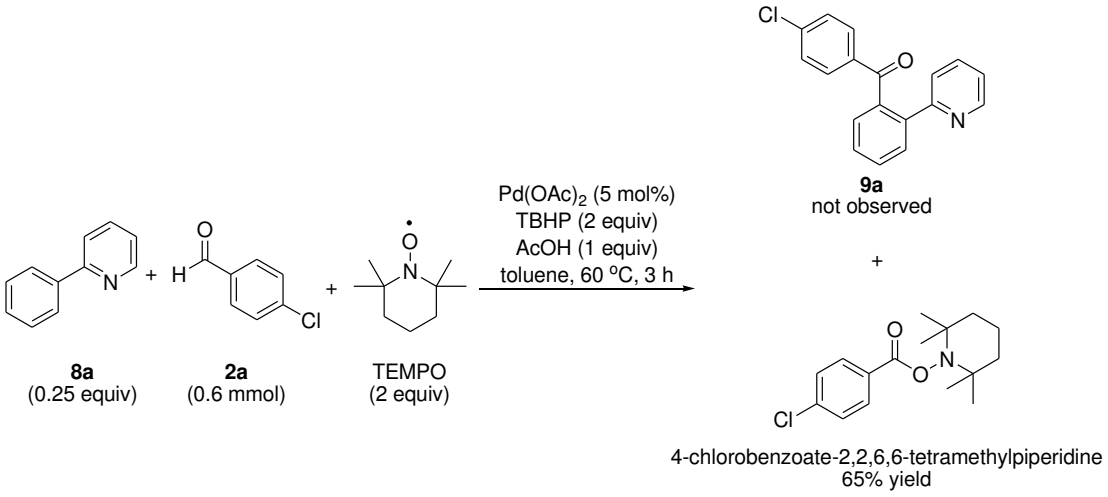

Table 3.8 Acylation with aldehydes with different decarbonylation constants[a]

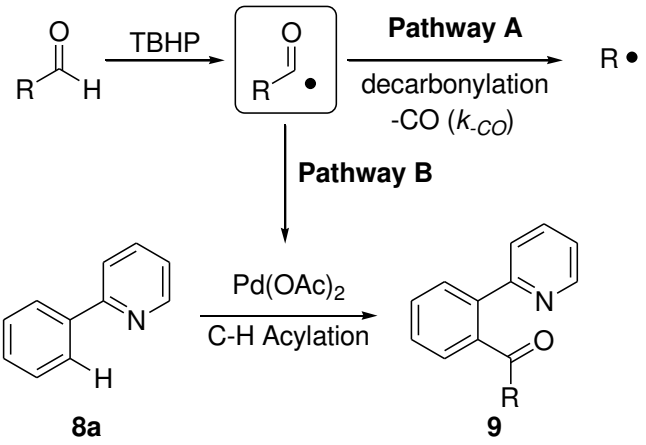

entry	acyl radical	decarbonylation constant (k_{-CO} in s^{-1})	yield (%)[b]
1	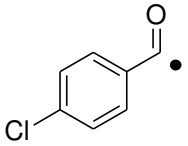	1.5×10^{-7}	89
2	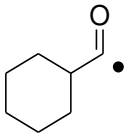	1.4×10^{4}	77
3	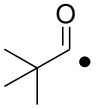	8.3×10^{5}	0

[a]Reaction conditions: **8a** (0.2 mmol), **2** (0.6 mmol), $Pd(OAc)_2$ (5 mol%), TBHP (0.5 mmol), AcOH (0.2 mmol) and toluene (1 mL) under air at 60 °C for 3 h. [b]Yields were determined by GC-FID with tetradecane as internal standard.

According to the literature, acyl radicals are known to undergo decarbonylation to afford alkylcarboradicals and CO.[58] The decarbonylative rate constants (k_{-CO}) of 4-chlorobenzoyl, cyclohexanecarbonyl and pivaloyl radical are depicted in Table 3.8. As shown in Table 3.8, alkylacyl radicals are characterized by faster decarbonylation

with larger k_{-CO} (Table 3.8, entry 2). Aroyl radicals are generally undergoing slow decarbonylation with smaller k_{-CO} (entry 1). Apparently, the decarbonylative rate become faster if the product carboradical is more stable (i.e. stability trend for 3^o radicals > 2^o radicals > aryl radicals).

As anticipated, when 4-chlorobenzaldehyde was employed as coupling partner, 89% yield coupled ketones were obtained (Table 3.8, entry 1). The relative stability of the 4-chlorobenzoyl radicals (relatively small $k_{-CO} = 1.5 \times 10^{-7}\ s^{-1}$) would be the key for effective coupling. Then we further investigated on the analogous coupling reaction by employing cyclohexanecarbaldehyde as coupling partner. While the corresponding cyclohexylacyl radicals is expected to undergo fast decarbonylation ($k_{-CO} = 1.4 \times 10^4$) versus the 4-chlorobenzoyl radicals, the coupled ketone was still obtained in 77% yield (entry 2). This result suggests the acyl radical coupling with the arylpalladium complexes is rather competitive versus the decarbonylation. However, when pivalaldehyde was employed as coupling partner, no coupled ketones were obtained with immediate palladium black formation (entry 3). Probably, the *tert*-butylacyl radicals was rapidly decarbonylated to form the *tert*-butyl radicals, which may react with the cyclopalladated complexes to form palladium black through β-hydrogen elimination.

3.3 Discussion

3.3.1 Turnover-limiting step

In this study, the first question to address is the nature of the turnover-limiting step. We first compared our results to other reported results.

Scheme 3.7 Comparison of the KIE values and the reaction order of the oxidant

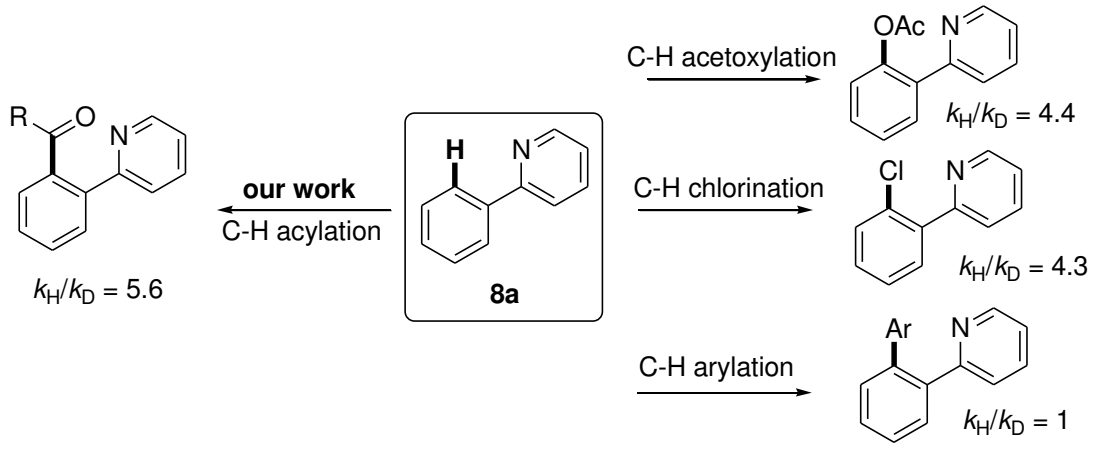

The data presented above offers valuable insights into the mechanism of Pd-catalyzed acylation. The large intermolecular KIE value (k_H/k_D = 5.6) provides a strong evidence that the C–H acylation proceeded via turnover-limiting C–H cyclopalladation (see Scheme 3.7). The KIE value is comparable to the reported Pd(II)-catalyzed oxidative C–H acetoxylation (k_H/k_D = 4.4)[52c] and chlorination (k_H/k_D = 4.3)[52s] with the C–H bond activation as turnover-limiting step. The observed intermolecular KIE value in this work is in contrast to the analogous C–H arylation reactions (k_H/k_D = 1)[52e], which involve turnover-limiting oxidation of the

cyclometalated aryl-Pd(II) complexes.

3.3.2 Catalyst resting state

Scheme 3.8 Possible mechanism for the turnover-limiting step of C–H acylation

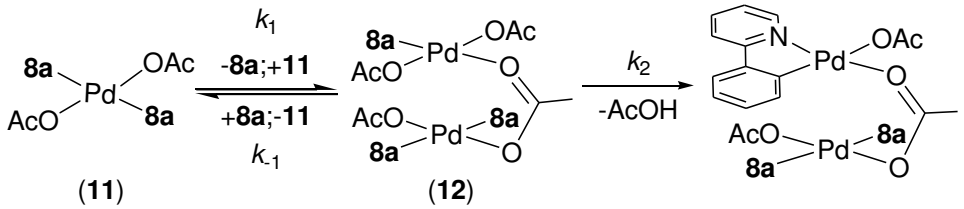

$$\text{rate} = \frac{k_1 k_2 [11]}{k_{-1}[8a]}$$

Then we would like to address another important question: what is the catalyst resting state of the acylation? Based on the experimental rate law: rate = k[**8a**]$^{-1}$[**Pd**]^2, we proposed that the catalyst resting state during C–H acylation is most likely the monometallic complex **11** (Scheme 3.8). Extensive literature precedent has shown that $Pd(X)_2$ (X = OAc or Cl) reacts rapidly and quantitatively with excess amines or pyridine derivatives (L) to form monomeric complexes of general structure $Pd(X)_2(L)_2$.[19a, 59a] For example, $Pd(OAc)_2$(benzylamine)$_2$ has been directly observed in the $Pd(OAc)_2$-mediated C–H cyclopalladation of benzylamine in acetonitrile (Scheme 3.9).[59b]

Scheme 3.9 Formation of a monomeric $Pd(X)_2(L)_2$ complex

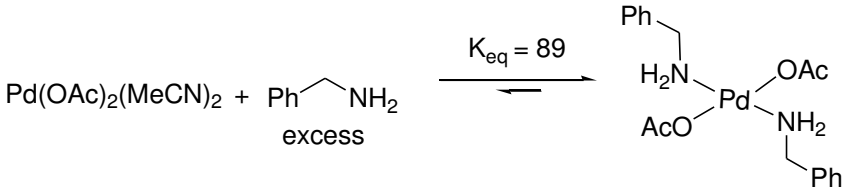

The observed inverse first-order dependence on [**8a**] implicates a pre-equilibrium dissociation step of one equivalent **8a** from **11** prior to the turnover-limiting C–H activation. Similar findings have been reported by Sanford and co-workers for their study on Pd-catalyzed C–H acetoxylation.[52c] The second-order dependence on [**Pd**] implicates that the catalyst should recombine after the dissociation of **8a** to form the bimetallic complex **12** before the turnover-limiting C–H cyclopalladation, which is comparable to the proposed intermediate in C–H arylation. Thus, the catalyst resting state is likely to be complex **12**.

3.3.3 Mechanism of Pd(II)-mediated C–H bond activation

Scheme 3.10 Proposed mechanistic models for directing group-assisted *ortho*-C–H activation

[1] Oxidative Addition (OA)

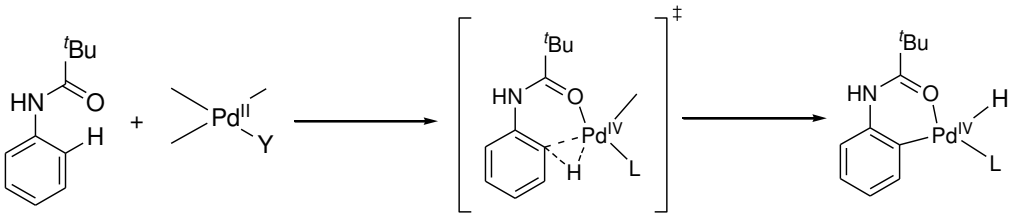

[2] Electrophilic Metalation

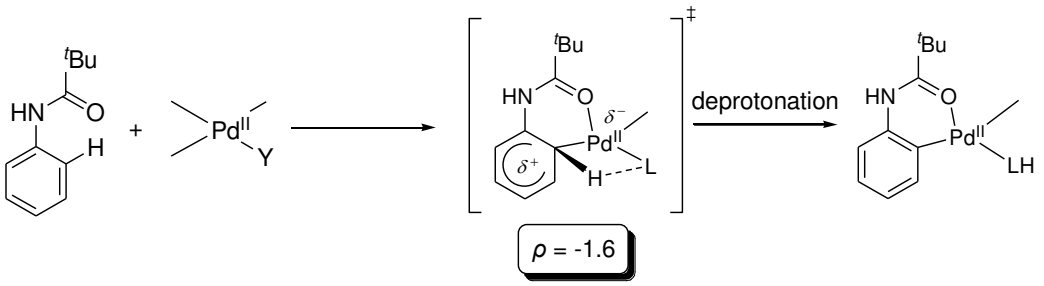

[3] Concerted Metalation Deprotonation (CMD)

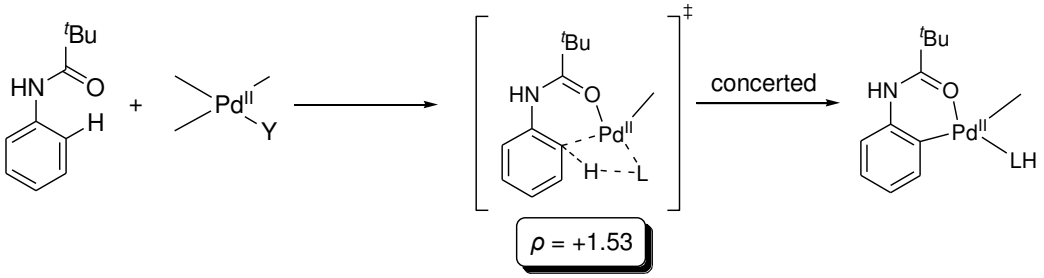

[4] Formation of agostic C-H complex

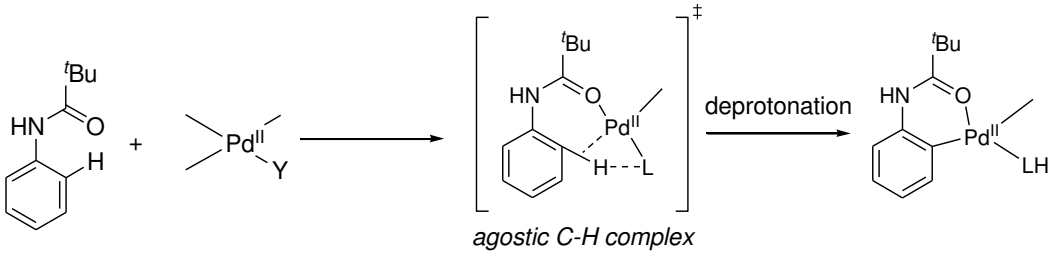

Experimental and theoretical research has formulated several mechanistic pathways for the directing group-assisted *ortho*-C–H activation; namely (1) oxidative addition (OA) with electron-rich low-valent transition metals;[21] (2) electrophilic metalation at electron-deficient late transition metal centers *via* the Wheland intermediate;[19] (3) ambiphilic Metal Ligand Activation (AMLA), also known as Concerted Metalation-Deprotonation (CMD);[22] and (4) formation of a C–H agostic complex followed by the deprotonation with an coordinated auxiliary ligand[20] (Scheme 3.10).

Oxidative addition occurs with an electron-rich metal [e.g. Ir(I), Rh(I) and Ru(0)][60] that reacts with a C–H bond to form a M–C and M–H bond *via* a three-membered transition state (Scheme 3.10, [1]). However, oxidative addition seems implausible for the Pd(II)-mediated C–H bond cleavage. In this work, ^{1}H NMR analysis of the cyclometalation of 2-phenylpyridine with $Pd(OAc)_2$ in methanol at room temperature did not reveal any strongly shielded hydride ligand, which are characterized by upfield chemical shift (δ_H = 0 to -60 ppm). Therefore, oxidative addition is not a possible pathway for the Pd-catalyzed C–H acylation.

Ryabov and co-workers studied the mechanism of C–H cyclopalladation of *N,N*-dimethylbenzylamine in the presence of $Pd(OAc)_2$. Detailed kinetic studies by

Ryabov and co-workers revealed that the electrophilic C–H bond cleavage should involve a cationic Wheland intermediate. The authors reported the Hammett correlation study, and a linear relationship (ρ = -1.6) with Hammett σ_{meta} constant was observed. An electrophilic C–H cyclopalladation with substantial positive charge development on the arene ring (Wheland intermediate) was proposed[19b] (Scheme 3.10, [2]).

In this work, a linear Hammett correlation with the *meta*-substituted pivalanilides was observed for the Pd-catalyzed C–H acylation. A linear free energy relationship (R = 0.96) with the ρ^+ value of -0.74 was established. The small negative ρ^+ value implies only a small extent of positive charge build-up at the C–H activation transition state. However, when compared to the ρ value of -1.6 reported by Ryabov and co-workers in the $Pd(OAc)_2$ mediated C–H activation of *N*,*N*-dimethylenzylamine,[19] our ρ^+ value was too small to support a Wheland intermediate in the Pd-catalyzed C–H acylation. It should be noted that the rate-limiting Wheland intermediate formation in electrophilic aromatic substitutions (e.g. chlorination and bromination) are associated with much larger negative ρ value (-8 to -12).[61]

The concerted metalation deprotonation (CMD) mechanism was reported by

Fagnou and co-workers in their studies on Pd-catalyzed direct arylation on perfluorobenzenes with aryl halide (Scheme 3.10, [3]).[22] Interestingly, the reactions proceeds faster for electron-deficient arenes; this is in contrast with a purely electrophilic metalation mechanism. The term "concerted" is used to describe the process that the hydrogen is abstracted by the coordinated base (L) at the same time as the M–C bond is formed. The faster reaction of electron-deficient arenes is therefore due to greater acidity of the C–H bond. In particular, it was found that the $Pd(OAc)_2$-catalyzed coupling of pyridine *N*-oxides and aryl bromides exhibited a linear Hammett correlation with a positive slope (ρ = +1.53).[22c] The observed positive Hammett correlation implied the developing negative charge at the CMD transition state. Obviously, the negative free energy Hammett correlation observed in our work indicated that the CMD pathway may not be tenable.

Recently, Davies and Macgregor reported a computational study of $Pd(OAc)_2$ mediated C–H activation of *N*,*N*-dimethylbenzylamine (DMBA) and suggested that the C–H cleavage should go through an agostic C–H complex rather than the Wheland intermediate (Scheme 3.10, [4]).[20] The calculation results revealed a rate-determining formation of an agostic C–H complex, followed by facile deprotonation by the coordinated acetate ligand *via* highly ordered six-membered

transition state. The transition state involving predominant charge-transfer from the C–H bond to the Pd(II) center with little C–H cleavage. The author suggested the C–H activation mechanism should involve a very small extent of positive charge built-up in the transition state.[20a] Moreover, the calculated activation energies for C–H activation changed when different C-4 substituted DMBA were employed in the computational study. For example, the activation energy for 4-Cl-DMBA (E = +15.0 kcal mol^{-1}) was calculated to be higher than those for 4-Me-DMBA (E = +13.2 kcal mol^{-1}) and 4-H-DMBA (E = +14.2 kcal mol^{-1}). The author suggested that these findings should be consistent to a negative free energy Hammett correlation. Apparently, our Hammett correlation results on Pd-catalyzed C–H acylation of pivalanilides are compatitbale with the agostic C–H complex formation pathway. The small negative ρ^+ value obtained in our work is more consistent with the C–H agostic complex formation mechanism.

3.3.4 The carbon–carbon formation step

Pd-catalyzed *ortho*-C–H functionalization for C–C bond formation has been attracting considerable attention. In particular, C–C bond formation reactions such as alkenylation, alkylation, alkynylation, arylation and carbonylation have been extensively investigated.[18] While Pd(0)/Pd(II) catalysis is very common in the

reaction with aryl halide,[4] the Pd(II)-catalyzed *ortho*-C–H functionalization may operate *via* three possible manifolds (Scheme 3.11): (1) Pd(II)/Pd(0) pathway,[23a,b,c] (2) Pd(II)/Pd(IV) or (3) $Pd(II)_2/Pd(III)_2$ pathway.

Scheme 3.11 Different catalytic pathways in Pd-catalyzed C–H functionalization for C–C bond formations

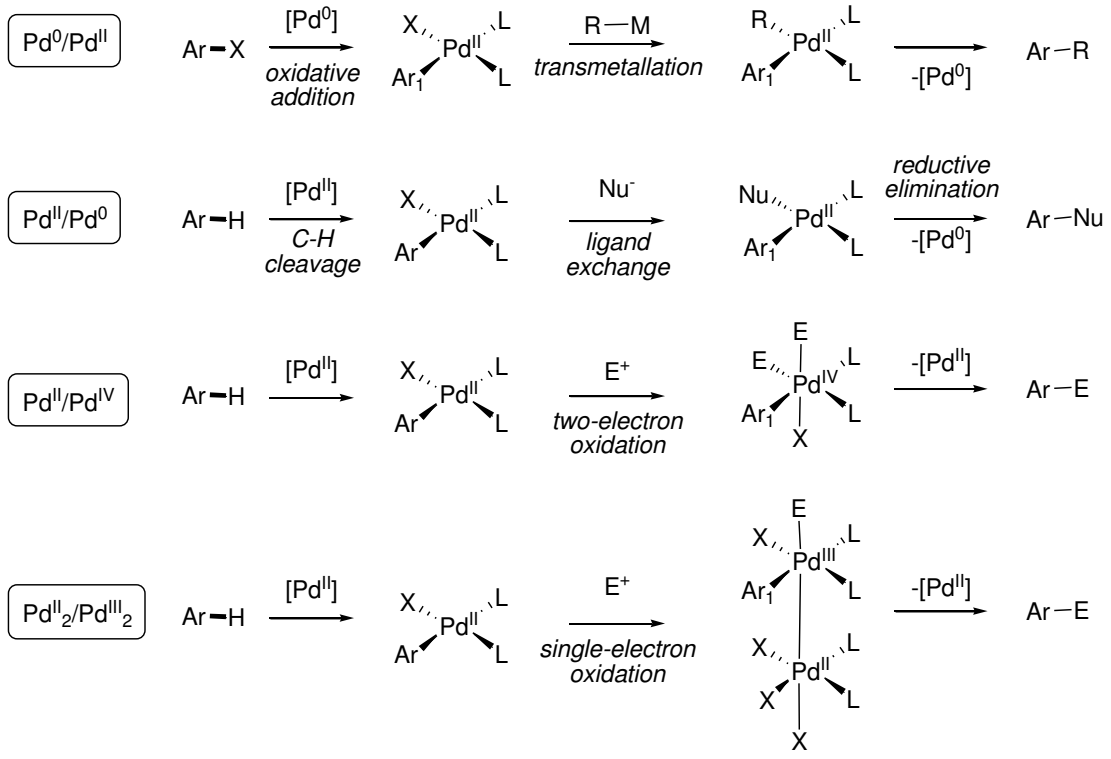

The Pd(II)/Pd(0) pathway involves a redox neutral process (typically nucleophilic C=C bond insertion into cyclopalladated complexes), followed by a reductive process (reductive elimination or β-hydride elimination) to release the coupled product. Generally, *ortho*-C–H alkenylations such as aforementioned reaction

reported by Miura (Chapter 1.4) was believed to proceed *via* Pd(II)/Pd(0) pathway.[17] While insertion of C=C bond into arylpalladium(II) complexes have been extensively investigated, the analogous addition of C=O bond are less documented. Lu and co-workers reported a related example of Pd-catalyzed intermolecular cyclization of 2-arylethynylanilines with aldehydes for the synthesis of substituted 3-hydroxymethyl indoles (Scheme 3.12).[62] The authors suggested the reaction should be initiated by (1) an intramolecular aminopalladation of 2-ethynylanilines to form the indolylpalladium(II) complexes, (2) followed by nucleophilic-type insertion of aldehydes into the Pd–C bond of indolylpalladium(II) complexes to produce the Pd(II)-alkoxide intermediate, and finally (3) the product is released by protonlysis.

Scheme 3.12 Nucleophilic-type insertion of aldehydes into the Pd–C bond of arylpalladium(II) complexes (Lu and co-workers)

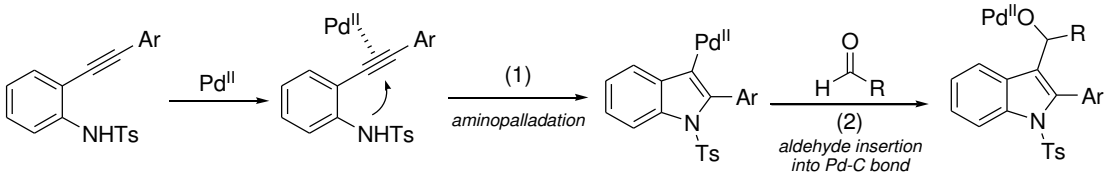

To evaluate the viability of the nucleophilic-type insertion of aldehydes into the Pd–C bond of the arylpalladium(II) complexes, we examined the stoichiometric acylation of **8a** with aldehydes in the absence of TBHP. When **8a-Pd** (0.1 mmol) was

treated with **2a** (0.3 mmol), AcOH (20 equiv) in toluene (1 mL) at 80 ^{o}C in the absence of TBHP (Scheme 3.13), no coupled ketone **9a** was obtained. Since no coupled products were obtained under non-oxidative conditions, nucleophilic-type Pd(II)/Pd(0) pathway is unlikely to be operative.

Scheme 3.13 Stoichiometric acylation of **8a-Pd** in the absence of TBHP

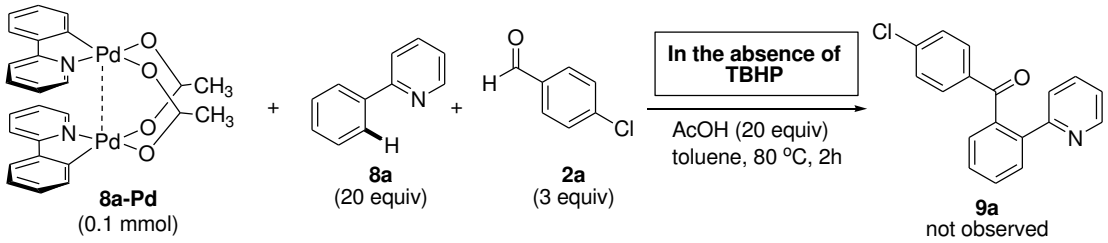

Scheme 3.14 Catalytic C–H functionalization based on Pd(II)/Pd(IV) pathway

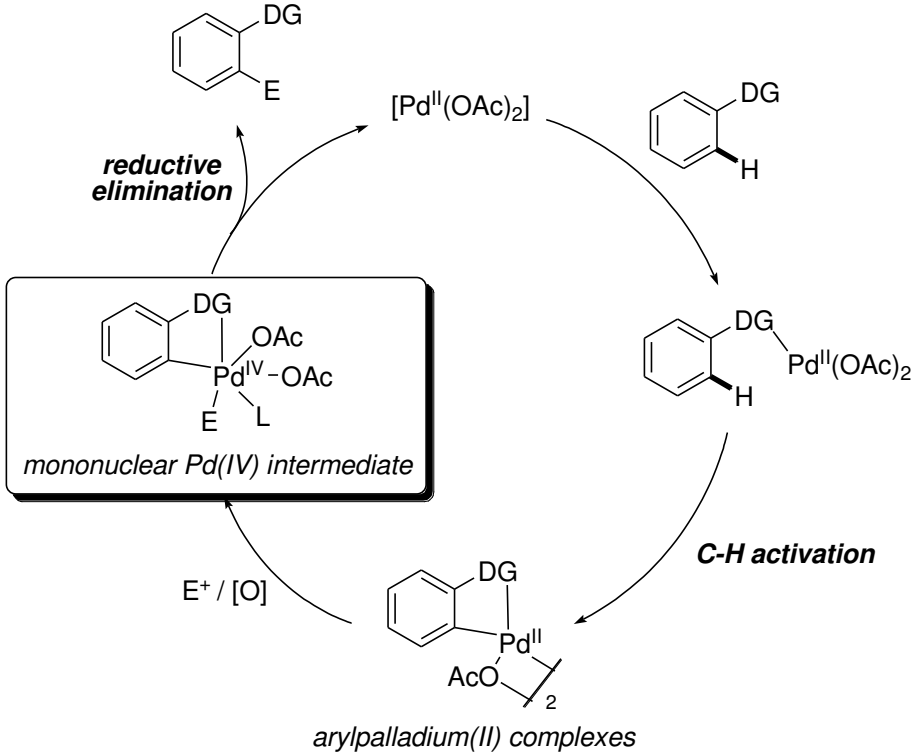

Scheme 3.15 Synthesis and characterization of a trimethylpalladium(IV) complex [(N~N)Pd$(CH_3)_2$] (N~N = 2-2'-biprridine) with methyl iodide (Canty and co-workers)

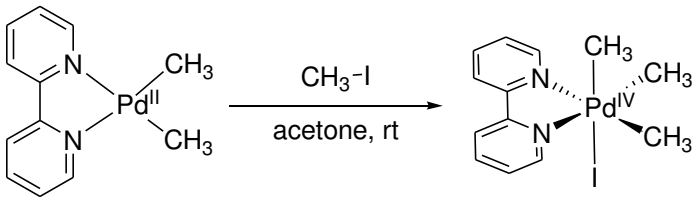

Scheme 3.16 Some selected examples of mononuclear Organopalladium Pd(IV) complexes with X-ray characterization

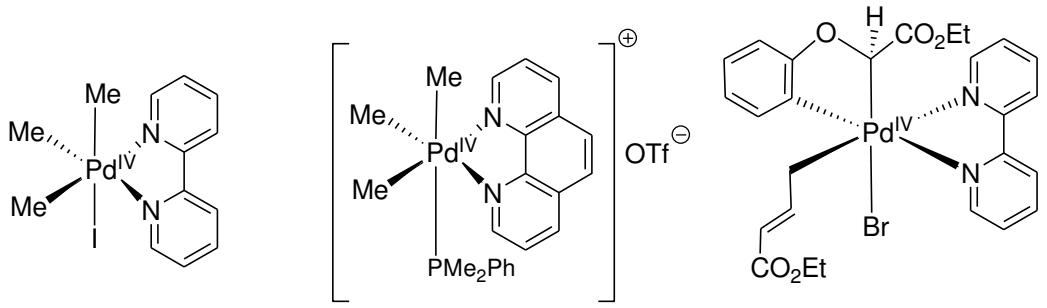

Canty (1986) ***Canty*** (2000) ***Malinakova*** (2007)

Tanaka (1996) ***Ritter*** (2008) ***Sanford*** (2005)

Pd(II)/Pd(IV) pathways have been widely accepted for many Pd(II)-catalyzed oxidative C–H couplings with strong electrophilic reagents (Scheme 3.14). It is believed that oxidation of arylpalladium(II) complexes with the electrophilic reagents

such as organohalides and diaryliodonium(III) salts would afford mononuclear Pd(IV) complexes. The first well-defined molecular structure of Pd(IV) complex was reported by Canty and co-workers.[63a] According to Canty and co-workers, oxidation of $[(N\sim N)Pd(CH_3)_2]$ (N~N = 2-2'-biprridine) with methyl iodide produced trialkylpalladium(IV) complex $[(N\sim N)Pd(CH_3)_3I]$ (Scheme 3.15). Since then, many mononuclear organopalladium(IV) complexes have been prepared and structurally characterized. Some representative examples are shown in the Scheme 3.16.[63]

Scheme 3.17 C–O, C–C and C–Cl bond formations from mononuclear Pd(IV) complexes (Sanford and co-workers)

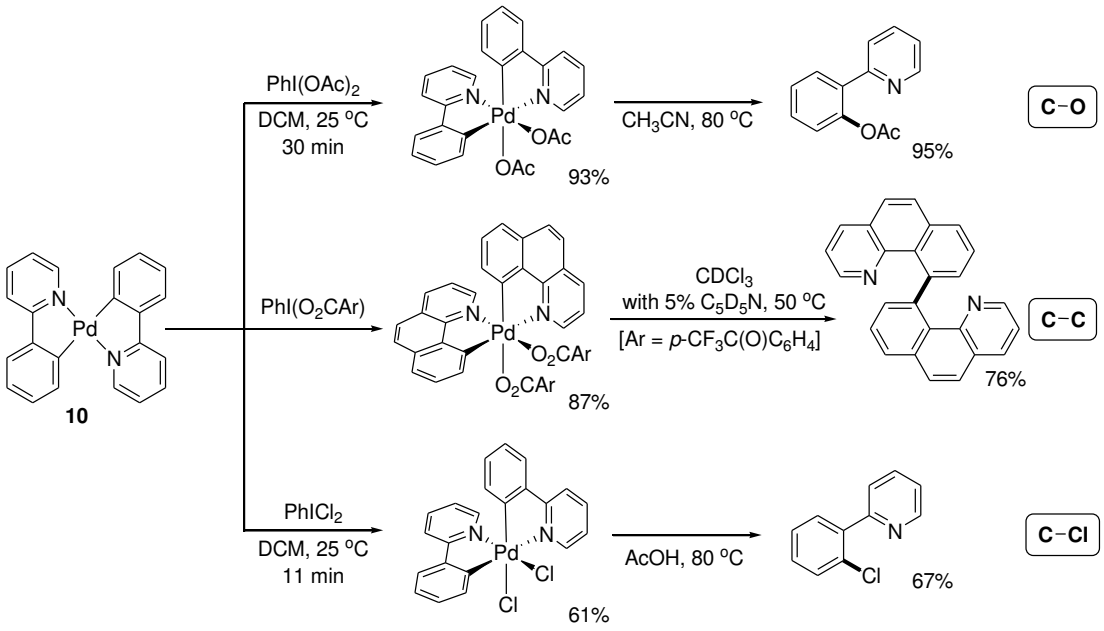

In 2005, Sanford and co-workers reported formation of a series Pd(IV) complexes by reacting [Pd(2-phenylpyridine)$_2$] complex **10** with oxidants such as PhI(OAc)$_2$[52a] and PhICl$_2$[52d]. Accodring to Sanford and co-workers, the Pd(IV) complexes have been structurally characterized and was found to undergo reductive elimination to form C–C[52a], C–O[52a] and C–Cl[52d] bonds (Scheme 3.17).

Scheme 3.18 Evaluate the possible involvement of mononuclear Pd(IV) in the C–H acylation

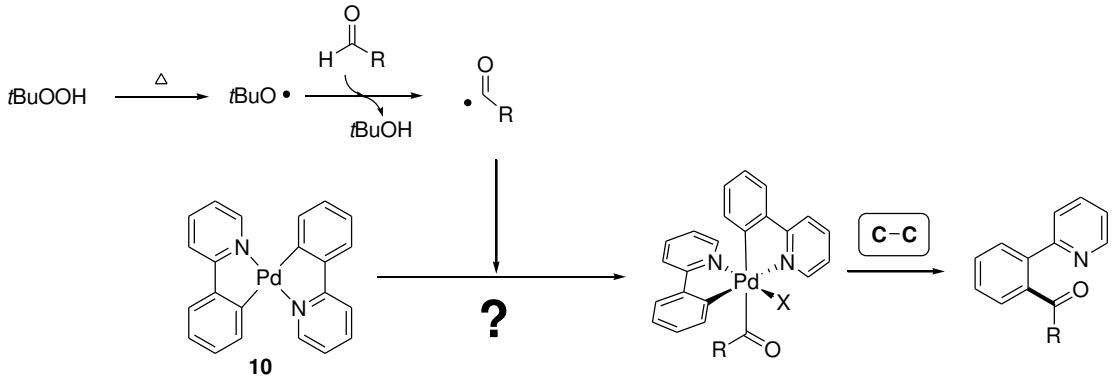

Scheme 3.19 Stoichiometric acylation of mononuclear Pd(II) complex

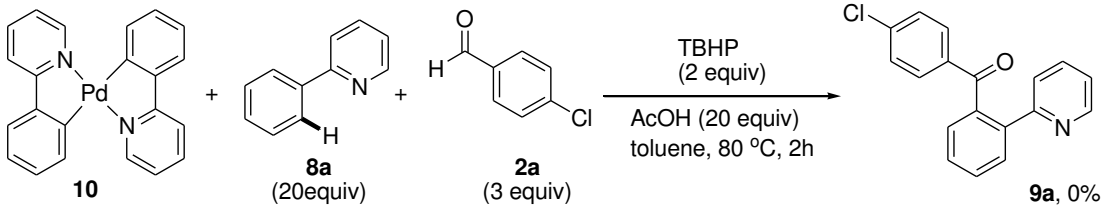

To evaluate the possible involvement of mononuclear arylpalladium(IV) complexes in the C–H acylation (Scheme 3.18), **10** was subjected to the

stoichiometric acylation conditions: **10** (0.1 mmol), **8a** (2 mmol) **2a** (0.3 mmol), TBHP (0.3 mmol), AcOH (20 equiv) in toluene (1 mL) at 80 ^{o}C failed to furnish any coupled ketone **9a** with complete recovery of the starting complex **10** (Scheme 3.19). This result argued against the intermediacy of the mononuclear Pd (IV) intermediates for the C–H acylation reaction.

In 2009, bimetallic Pd catalysis concerning Pd(III)–Pd(III) complexes was proposed by Ritter and co-workers,[53] and it is considered as a mechanistic alternative to the Pd(II)/Pd(IV) pathway.

Cyclopalladation of benzo[*h*]quinoline afforded a palladacycles in a form of dinuclear Pd(II)–Pd(II) complexes. The Pd nuclei were held in proximity by bridging acetate ligands. Subsequent reaction of the dinuclear palladacycles with the oxidant $PhICl_2$ afforded a dinuclear Pd(III)–Pd(III) complexes, which was structurally characterized at -30 ^{o}C (Scheme 3.20).[53a] By warming to room temperature reductive elimination of aryl chloride was completed (94% yield) within 2 h. According to Ritter and co-workers, the metal-metal redox synergy of the Pd(III)–Pd(III) unit may offers a lower activation barrier for the C–H functionalization.[53e]

Scheme 3.20 Characterization of a bimetallic Pd(III) intermediate (Ritter and co-workers)

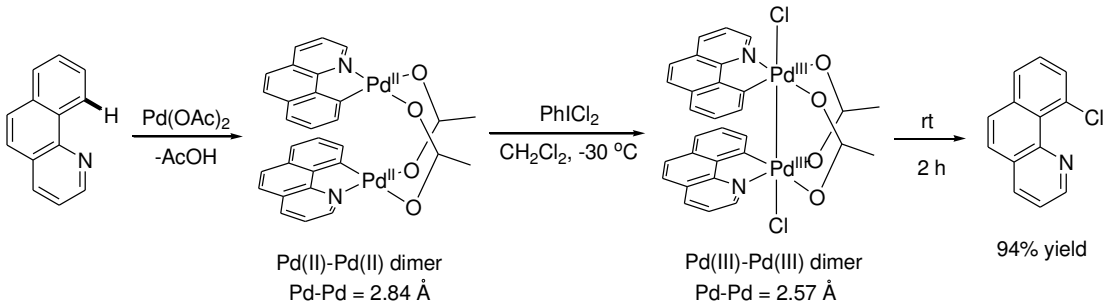

By simple qualitative orbital analysis, the lack of reactivity of mononuclear complex **10** could be attributed to the forbidden orbital interaction between acyl radical's SOMO and the complex's HOMO (d_{xy}). Notably, those active catalysts for C–H acylation are dinuclear Pd(II)–Pd(II) complexes with an open clamshell structure. The open clamshell structure characterized by the Pd–Pd bond distances of around 2.8–2.9 Å, which is much shorter than the van der Waal's radii of 3.26 Å, suggesting that d^8-d^8 interaction is operative.[64] The mixing of oribitals along the Pd–Pd axis results a weak bonding (bond order ~ 0.1). Therefore, we proposed that the HOMO of the clamshell dimer would be d_z^2 σ^* Pd–Pd anti-bonding oribital, which may interact favourably with the SOMO of acyl radical (Scheme 3.21).

Scheme 3.21 Oribital enerygy level diagram for interaction along metal-metal axis of dinuclear Pd(II)–Pd(II) complexes

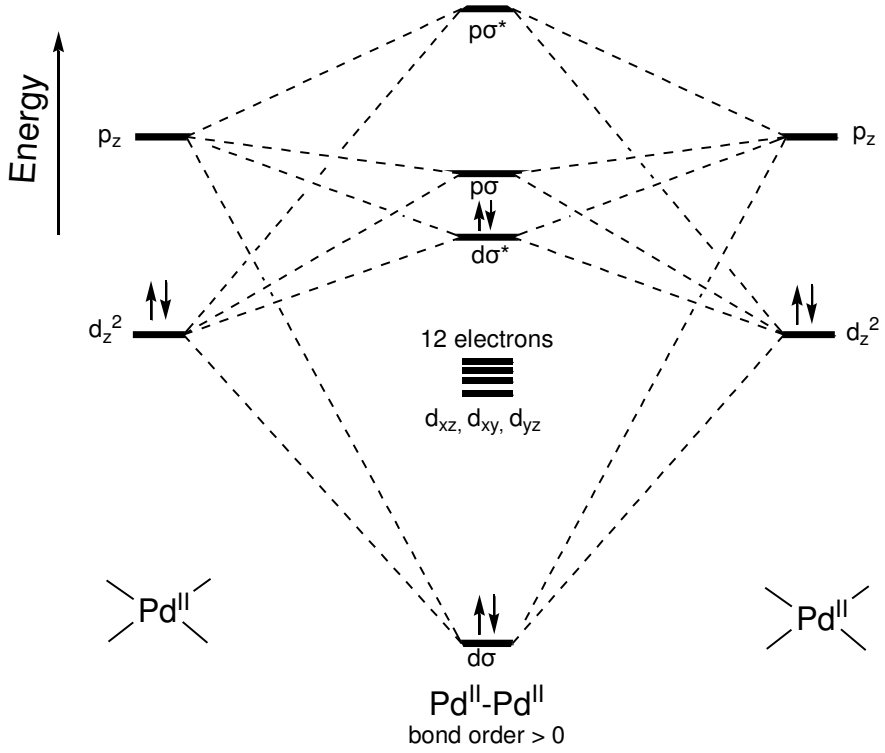

In this work, we prepared some dinuclear [(benzo[*h*]quinoline)Pd(μ-L)]$_2$ complexes with different bridging ligands (L) [L = carboxylates, succinimide and bicyclic guanidine (hpp)]. In general, the [(benzo[*h*]quinoline)Pd(μ-L)]$_2$ complexes were prepared by ligand substitution reactions of [(benzo[*h*]quinoline)Pd(μ-OAc)]$_2$ (**13b**) or [(benzo[*h*]quinoline)Pd(μ-Cl)]$_2$ (**13f**) (Scheme 3.22). X-ray crystallographic analysis revealed the Pd–Pd distances were varied from 2.80 to 3.27 Å (Scheme 3.23).

Scheme 3.22 Synthesis of dinuclear [(benzo[*h*]quinoline)Pd(μ-L)]$_2$ complexes

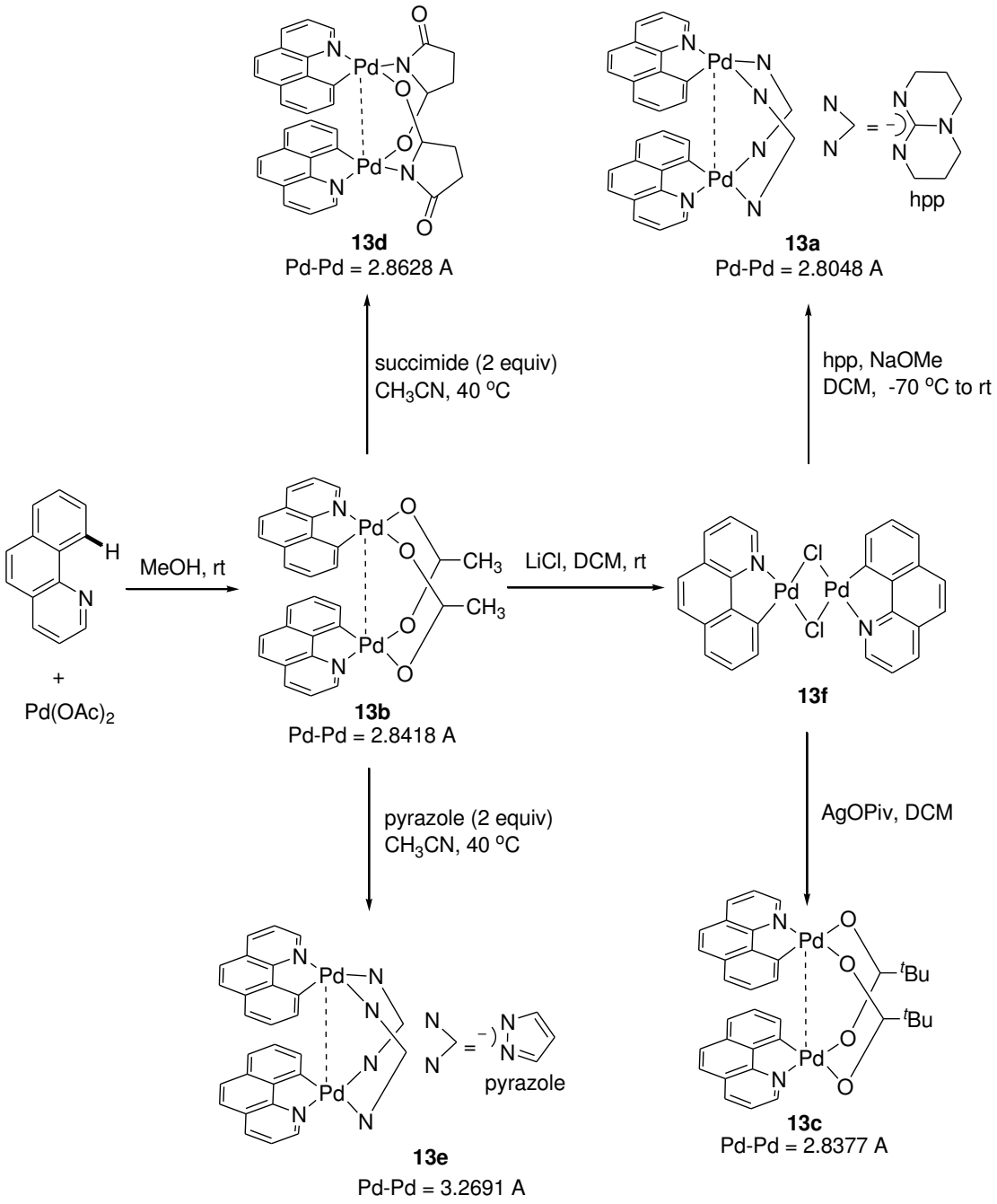

Scheme 3.23 Molecular structures of [(benzo[*h*]quinoline)Pd(μ-hpp)]$_2$ and [(benzo[*h*]quinoline)Pd(μ-OPiv)]$_2$ determined by X-ray diffraction study

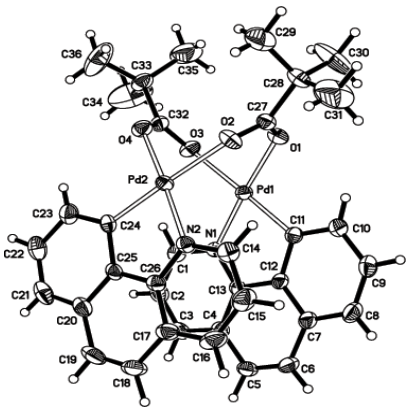

≡

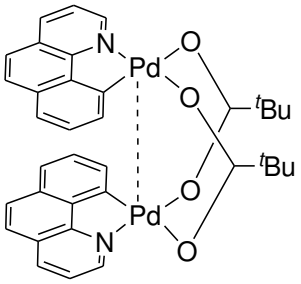

13c
Pd-Pd = 2.8377 A

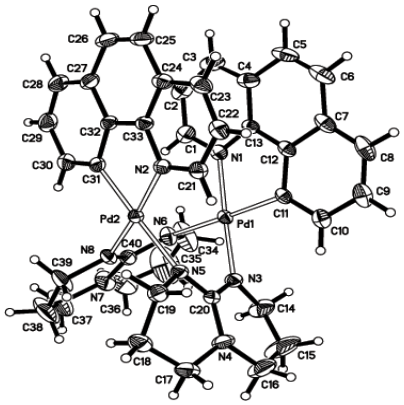

≡

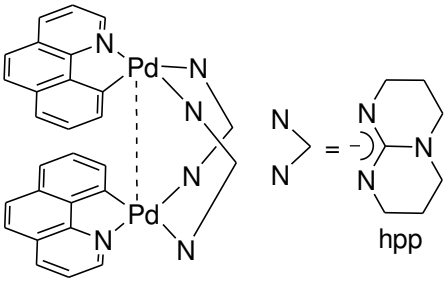

13a
Pd-Pd = 2.8048 A

The catalytic activities of these dinuclear arylpalladium(II) complexes towards C–H acylation were examined (Scheme 3.24). With **13a** as catalyst, **9a** was obtained in 81% yield (Scheme 3.24, entry 1). When **13b** was used, the yield of **9a** was improved to 88% (entry 2). Notably, when employing [(Bzq)Pd(μ-pyrazol-1-yl)]$_2$ (**13e**) as catalyst, which is characteristic by a long Pd–Pd distance (3.27 Å), the product yield diminished to 30% (entry 5). The lower catalytic activity of **13e** may be

associated with the weaker Pd(III)–Pd(III) bonding at the radical coupling step.

Notably, no product yields were formed with the planner $[(Bzq)Pd(Cl)]_2$ (**13f**) under the reaction condition (entry 6). This result led us to conclude that oxidation of the dinuclear palladium(II) complexes to dinuclear Pd(III)–Pd(III) complexes is probably associated by the product formation.

Scheme 3.24 C–H acylation of 2-phenylpyridine catalyzed by a series of dinuclear Pd(II)–Pd(II) complexes

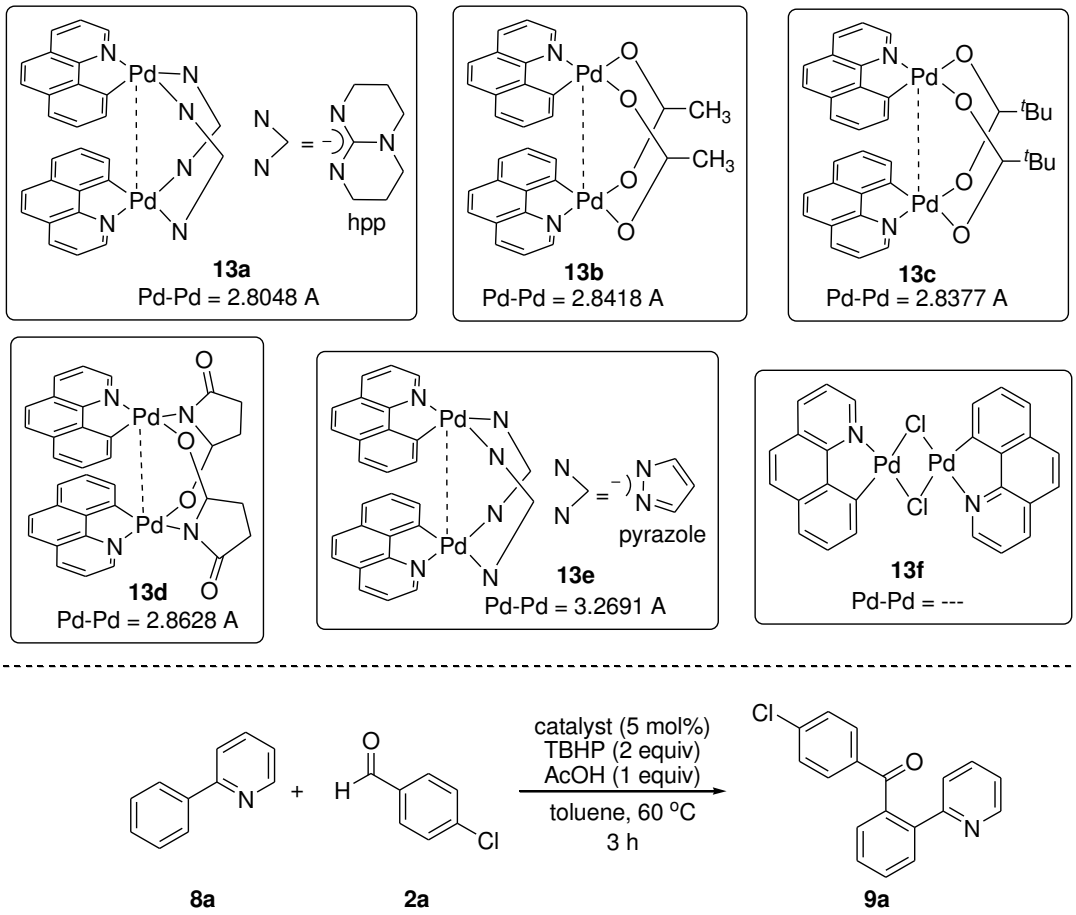

entry	Pd complexes	Pd–Pd (Å)	yield (%)[b]
1	[(benzo[*h*]quinoline)Pd(μ-hpp)]$_2$ (**13a**)	2.8048	81
2	[(benzo[*h*]quinoline)Pd(μ-OAc)]$_2$ (**13b**)	2.8418	88
3	[(benzo[*h*]quinoline)Pd(μ-OPiv)]$_2$ (**13c**)	2.8377	95
4	[(benzo[*h*]quinoline)Pd(μ-succinimide)]$_2$ (**13d**)	2.8628	86
5	[(benzo[*h*]quinoline)Pd(μ-pyrazole)]$_2$ (**13e**)	3.2691	30
6	[(benzo[*h*]quinoline)Pd(μ-Cl)]$_2$ (**13f**)	---	0

[a]Reaction conditions: **8a** (0.2 mmol), **2a** (0.6 mmol), catalyst (5 mol%), TBHP (0.5 mmol), AcOH (0.2 mmol), ascorbic acid and toluene (1 mL) under air at 60 °C for 3 h. [b]Yields were determined by GC-FID with tetradecane as internal standard.

3.3.5 Proposed Mechanism

Scheme 3.25 Proposed catalytic cycle

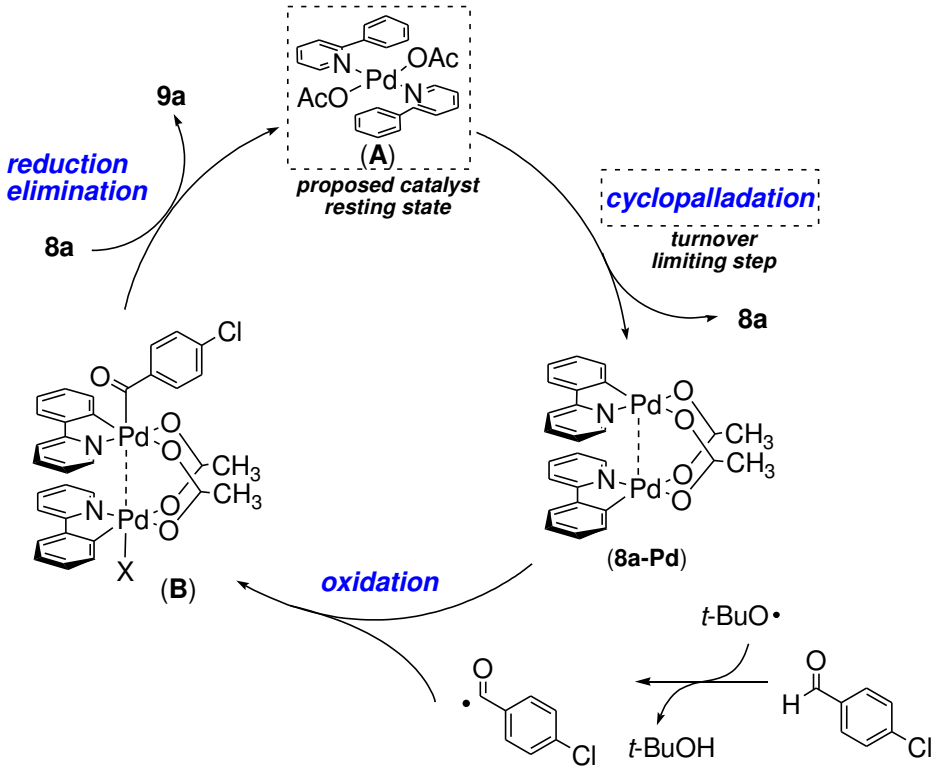

Based on our mechanistic studies, a plausible catalytic cycle for the Pd-catalyzed *othro*-C–H acylation is depicted in Scheme 3.25. We proposed that the catalyst resting state during C–H acylation is most likely the mononuclear complex **A**. The reaction was probably initiated by dissociation of **8a** from **A**, followed by turnover-limiting *ortho*-C-H activation to give **8a-Pd**. The intermediacy of **8a-Pd** is supported by our stoichiometric reaction study. The intermediacy of the acyl radicals was confirmed by radical scavengers study and TEMPO trapping. It is likely that the acyl radicals would couple with the dinuclear **8a-Pd** to give bimetallic Pd(III) intermediates **(B)**.

Subsequently, C–C bond formation through reductive elimination affords the *ortho*-acylation of **8a** and regenerates the catalyst resting state **(A)** for the next catalytic run.

3.4 Summary on mechanistic results

The Pd(II)-catalyzed C–H acylation of 2-phenylpyridine (**8a**) with 4-chlorobenzaldehyde (**2a**) revealed an experimental rate law: rate = k[**8a**]$^{-1}$[**Pd**]^{2}. The inverse first-order dependence of [**8a**] suggests that the turnover-limiting step should involve substrate dissociation. The second-order dependence on [**Pd**] suggests the involvement of dinuclear palladium complex in the turnover-limiting step.

With **8a**-d_5 as substrate, significant primary kinetic isotope effect (k_H / k_D = 5.6) revealed the C–H bond cleavage is a turnover-limiting step. A Hammett correlation study on a series of *meta*-substituted pivalanilides (**6**) revealed a small ρ^+ value of -0.74, and the C–H cleavage was proposed to proceed through an agnostic C–H complex formation.

The arylpalladium(II) complexes **8a-Pd** is competent to both the catalytic and stoichiometric acylation reaction. The catalytic C–H acylation was suppressed by radical scavengers such as ascorbic acid in a dose-dependent manner. When 2,2,6,6-tetramethylpiperidine *N*-oxide (TEMPO) was employed as additives, the ketones formation was completely suppressed and the 2,2,6,6-tetramethyl -piperidino-4-chlorobenzoate was isolated. These finding are compatible to intermediacy of carboradicals in the reaction. The catalytic acylation is probably

mediated by coupling of the carboradicals with the arylpalladium(II) complexes. We prepared some dinuclear [(benzo[*h*]quinoline)Pd(μ-L)]$_2$ complexes and studied their catalytic activity towards C–H acylation. The result led us to conclude that oxidation of the dinuclear arylpalladium(II) complexes to dinuclear Pd(III)–Pd(III) complexes is probably associated by the product formation.

3.5 Experimental section

All the solvents were freshly distilled and dried according to the standard methods prior to use. d_5-**8a**, substituted pivalanilides, complexes **8a-Pd**,[29d] **10**,[28a] **13b**,[28a] **13d**,[28a] **13f**[28a] were prepared according to literature. Aldehydes were obtained commercially and purified by vacuum distillation if necessary. 4.8M TBHP in DCE is prepared by the reported procedure. All the reaction were performed in 8 mL-vials equipped with Teflon liner cap. The reaction kinetics were measured using the method of initial rate. In each experiment, the reaction was monitored to < 25% conversion. Each experiment was run in triplicate, and all kinetic data represents an average of these three runs. Error analysis was conducted by taking the average and standard deviation of the obtained initial rates. Linear regression was performed by using least squares fit equations.

Thin layer chromatography was performed on silica gel plates. Flash column chromatography was performed on silica gel (Merck, 230-400 mesh). ^{1}H and ^{13}C NMR spectra were recorded on a Bruker DPX-400 MHz spectrometer. The chemical shift (δ) values are given in ppm and are referenced to residual solvent peaks; carbon multiplicities were determined by DEPT-135 and DEPT-90 experiments. Coupling constants (*J*) were reported in hertz (Hz). Multiplicity abbreviations are: s = singlet, d= doublet, t = triplet, q = quartet, m = multiplet, dt = doublet of triplets, td = triplet of doublets, and br = broad. Mass spectra and high resolution mass spectra (HRMS) were obtained on a VG MICROMASS Fison VG platform, a Finnigan Model Mat 95 ST instrument, or a Bruker APEX 47e FT-ICR mass spectrometer. Infra-red spectra were obtained by a Bruker Vector 22 FT-IR spectrometer. Optical rotations were recorded on a Perkin-Elmer 341 polarimeter in a 10 mm cell. Melting points were

measured on a BUCHI Melting Point B-545 machine. X-ray crystallographic study was performed by a Brüker CCD area detector diffractometer. GC-MS experiments were performed with HP 5973 GC system using a HP5-MS column (25 m × 0.25 mm). The GC yields were obtained by the signal ratio of authentic samples/tetradecane calibration standard from HP 6890 GC-FID system.

3.5.1 Kinetic experiments on reaction rate order

Rate profile measurements with 2-phenylpyridine (**8a**)

A 100 mL Schlenk tube containing a magnetic stir bar was charged with **8a** (1 mmol), 4-chlorobenzaldehyde **2a** (3 mmol), $Pd(OAc)_2$ (0.05 mmol), TBHP (2 mmol), AcOH(0.875 mmol), and internal standard tetradecane in toluene (5 mL). The reaction tube was capped with a rubber septum, then stirred at 60 ^{o}C. At the indicated time points, a small aliquot (< 10 μL) was removed from the vial and subjected to GC-FID analysis to determine the product (**9a**) yield.

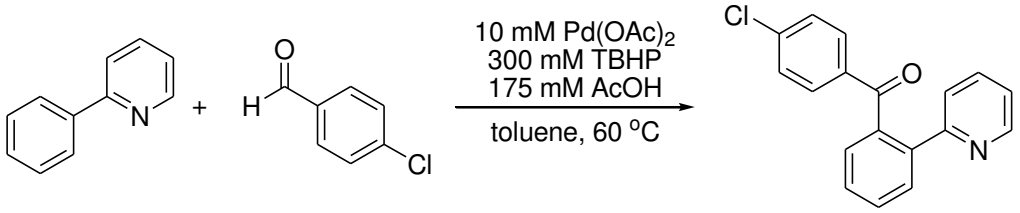

8a (200 mM) **2a** (600 mM) **9a**

time	yield of **9a** (%)	time	yield of **9a** (%)
5	10	60	63
10	16	70	71
15	23	80	78
20	28	90	82
25	33	110	88
30	38	130	93
35	42	220	96
40	48		

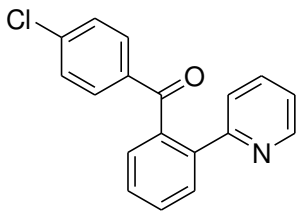

9a

^{1}H NMR (400 MHz, $CDCl_3$): δ_H 8.64 (d, J = 4.8, 2H), 8.42 (d, J = 4.6, 1H), 7.90 (d, J = 4.8, 2H), 7.71 (d, J = 4.6, 1H), 7.43 (m, 3H), 7.30 (m, 1H), 7.09 (m, 2H).

General procedures for the kinetic experiment on rate order

Kinetic experiments were run in a 8-mL vial sealed with Teflon-lined caps. Each data point represents a reaction in an individual vial, with each vial containing a constant concentration of substrate, catalyst, oxidant and acid. The vials were each sequentially charged with substrate **8a** (added as a 2 M stock solution in toluene), aldehyde **2a** (added as a 1 M stock solution in toluene), $Pd(OAc)_2$ (added as a 0.1 M stock solution in toluene), TBHP (added as a 5 M stock solution in DCE), AcOH, and the resulting mixtures were diluted to a total volume of 1mL of toluene. The reaction mixtures were stirred at room temperature for 5 min to ensure complete mixing of all stock solutions. The vials were then heated to 60 ^{o}C for various amounts of time with **8a** conversion being kept below 30%. The reactions were then quenched by immersing the reaction mixtures into an ice-water bath for 5 min. The amount of **9a** being formed was determined by gas chromatography.

Rate order for [**8a**]

The reaction were performed according to the general procedures with varing concentrations of **8a** (80 mM, 120 mM, 200 mM, 240 mM, 300 mM) and fixed concentrations of **2a** (600 mM), $Pd(OAc)_2$ (10 mM), TBHP (300 mM), AcOH (175 mM) in toluene (1 mL).

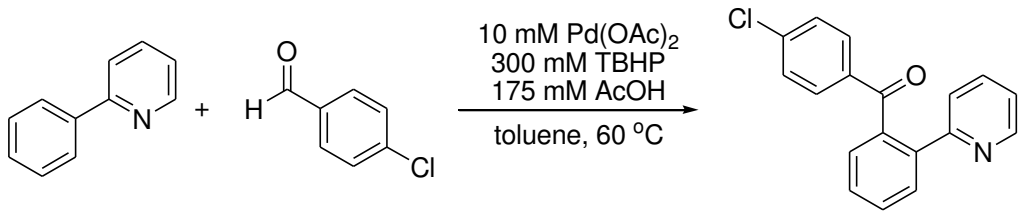

8a (80 - 300 mM) **2a** (600 mM) **9a**

entry	**8a**		trial 1	trail 2	trail 3	Std.	average rate
	C(mM)	V(μL)	[**9a**] (mM)	[**9a**] (mM)	[**9a**] (mM)	Dev.	(mM/min)
1	80	40	2.89	3.09	3.42	0.27	3.13
2	120	60	2.99	2.77	2.96	0.12	2.91
3	200	100	1.85	1.81	2.06	0.13	1.91
4	240	120	2.03	1.29	1.22	0.45	1.51
5	300	150	1.00	0.80	0.58	0.21	0.79

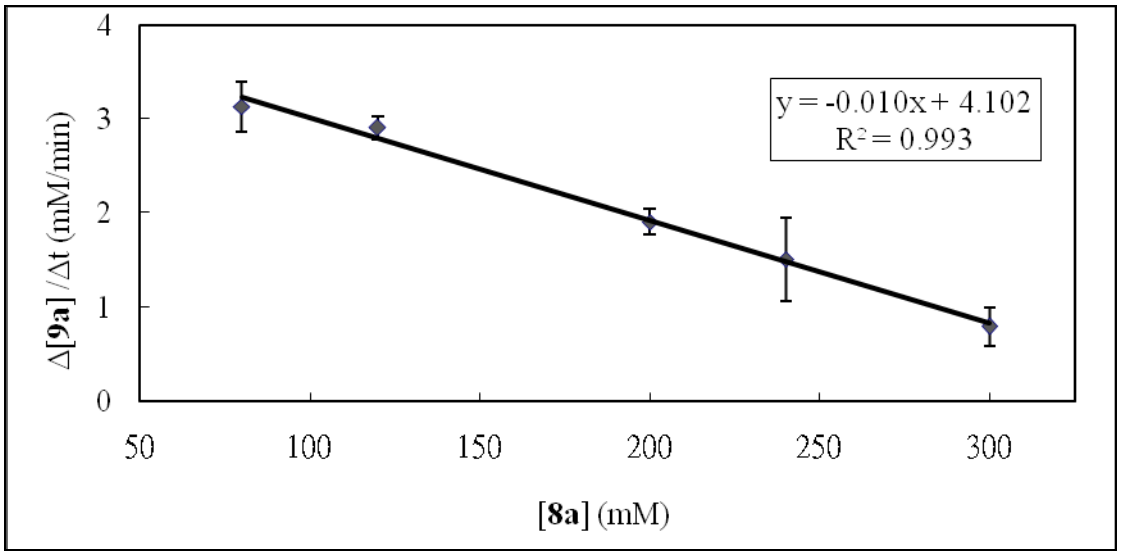

The first-order kinetics of [**8a**] was further verified by plotting the log of (Δ[**9a**] /Δt) versus log [**8a**].

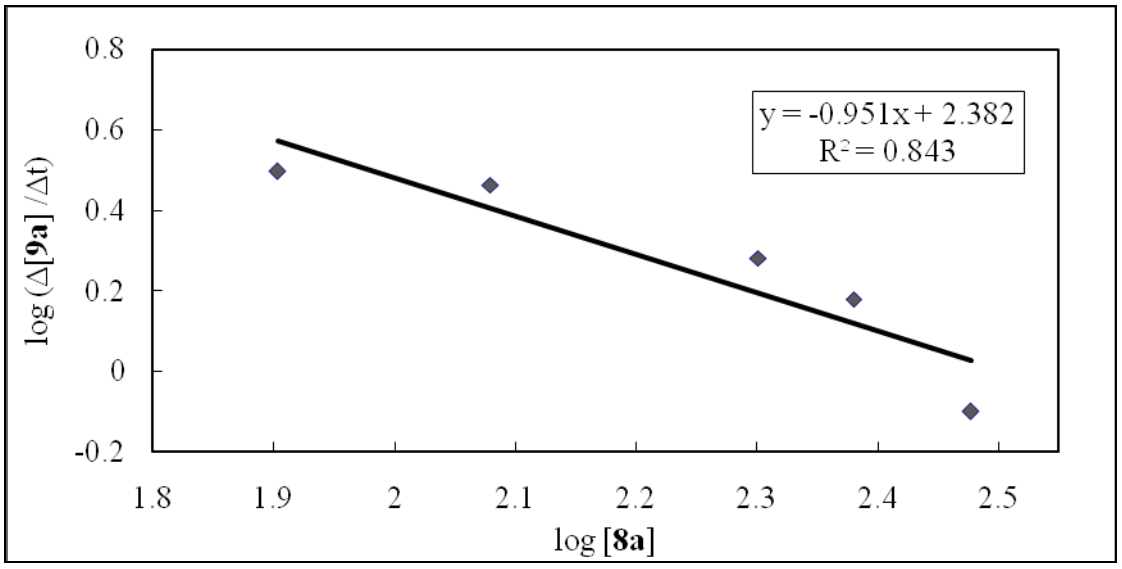

Rate order for [**2a**]

The reaction were performed according to the general procedures with varing concentrations of **2a** (400 mM, 450 mM, 500 mM, 550 mM, 600 mM, 650 mM) and fixed concentrations of **8a** (200 mM), $Pd(OAc)_2$ (10 mM), TBHP (300 mM), AcOH (175 mM) in toluene (1 mL).

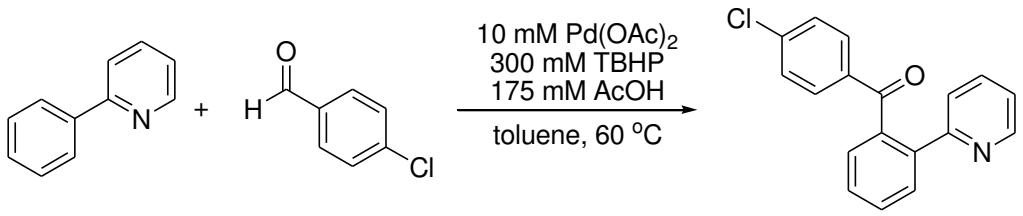

8a (200 mM) **2a** (400 - 650 mM) **9a**

entry	**2a**		trial 1 [**9a**] (mM)	trail 2 [**9a**] (mM)	trail 3 [**9a**] (mM)	Std. Dev.	average rate (mM/min)
	C(mM)	V(μL)					
1	400	400	2.35	2.33	1.52	0.47	2.07
2	450	450	2.38	2.66	1.83	0.42	2.29
3	500	500	1.49	1.82	2.03	0.27	1.78
4	550	550	2.29	2.58	2.20	0.20	2.36
5	600	600	2.13	2.73	1.85	0.45	2.23
6	650	650	1.85	1.67	1.69	0.10	1.74

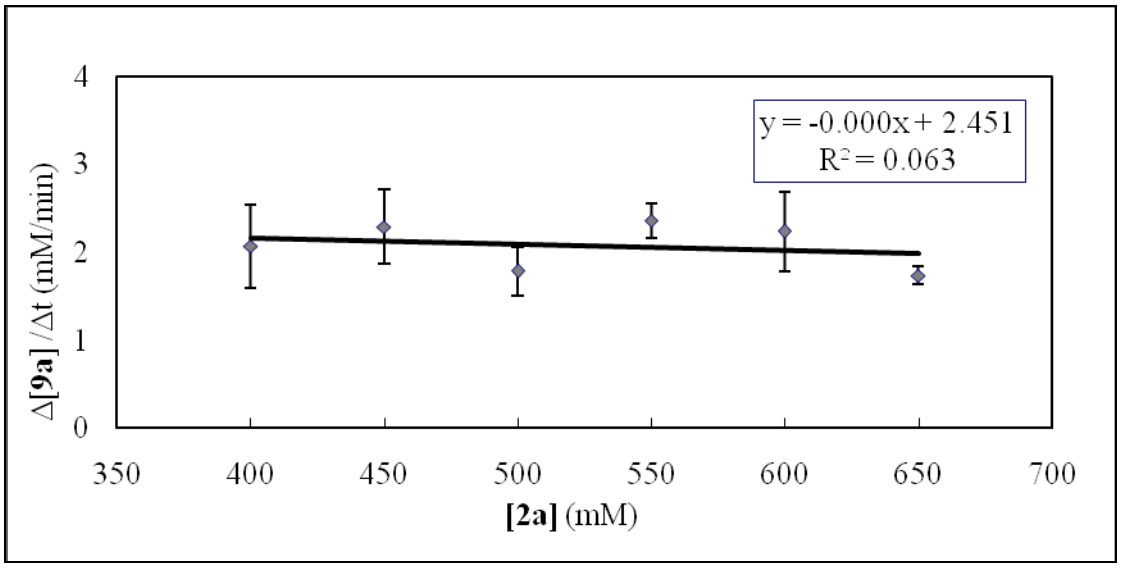

The zero-order kinetics of [**2a**] was further verified by plotting the log of (Δ[**9a**] /Δt) versus log [**2a**].

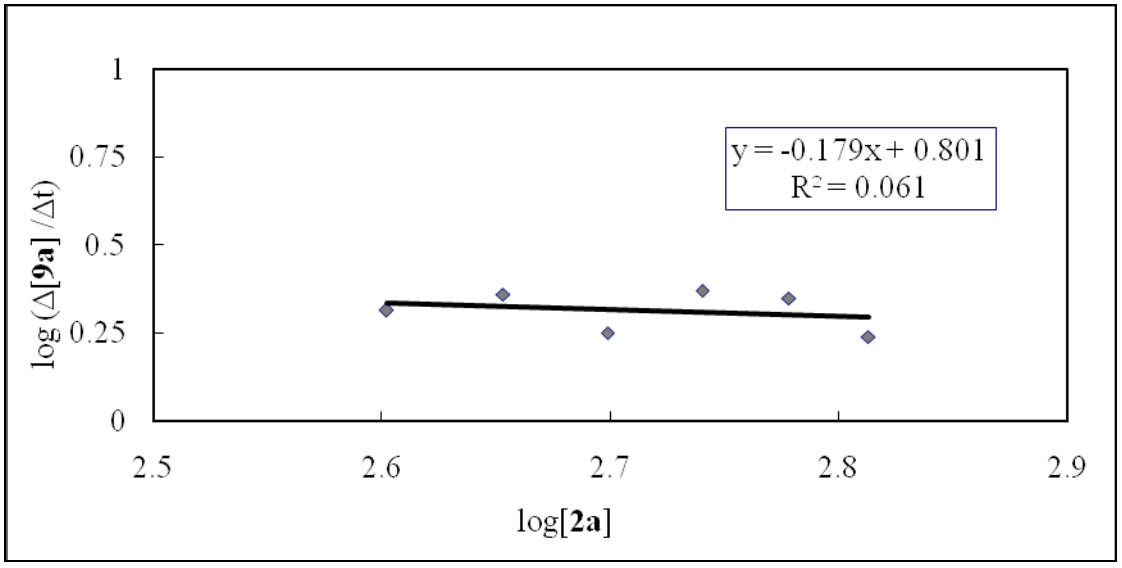

Rate order for [TBHP]

The reaction were performed according to the general procedures with varing concentrations of TBHP (300 mM, 350 mM, 400 mM, 450 mM, 500 mM, 600 mM) and fixed concentrations of **8a** (200 mM), $Pd(OAc)_2$ (10 mM), **2a** (600 mM), AcOH (175 mM) in toluene (1 mL).

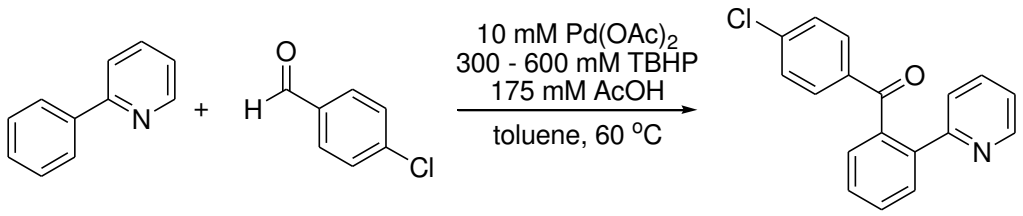

8a (200 mM) **2a** (600 mM) **9a**

entry	TBHP		trial 1	trail 2	trail 3	Std. Dev.	average
	C(mM)	V(μL)	[**9a**] (mM)	[**9a**] (mM)	[**9a**] (mM)		rate (mM/min)
1	300	60	1.03	1.01	1.25	0.13	1.10
2	350	70	1.40	1.03	1.15	0.19	1.19
3	400	80	0.85	1.12	1.23	0.19	1.06
4	450	90	1.01	1.42	1.11	0.21	1.18
5	500	100	0.87	0.79	1.07	0.14	0.91
6	600	110	1.01	0.93	1.34	0.22	1.09

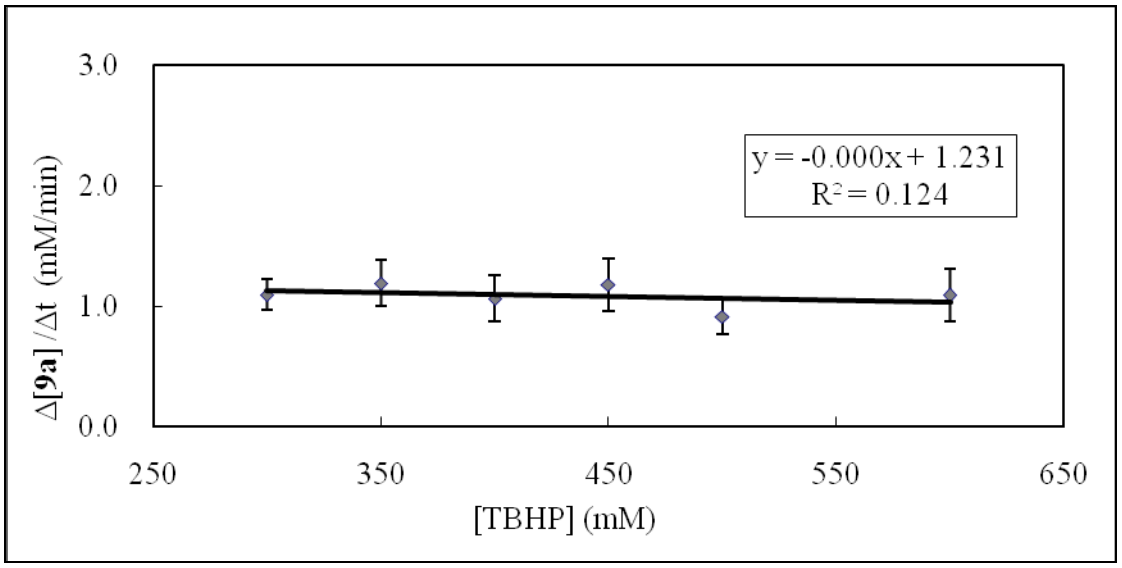

The zero-order kinetics of [TBHP] was further verified by plotting the log of (Δ[**9a**] /Δt) versus log [TBHP].

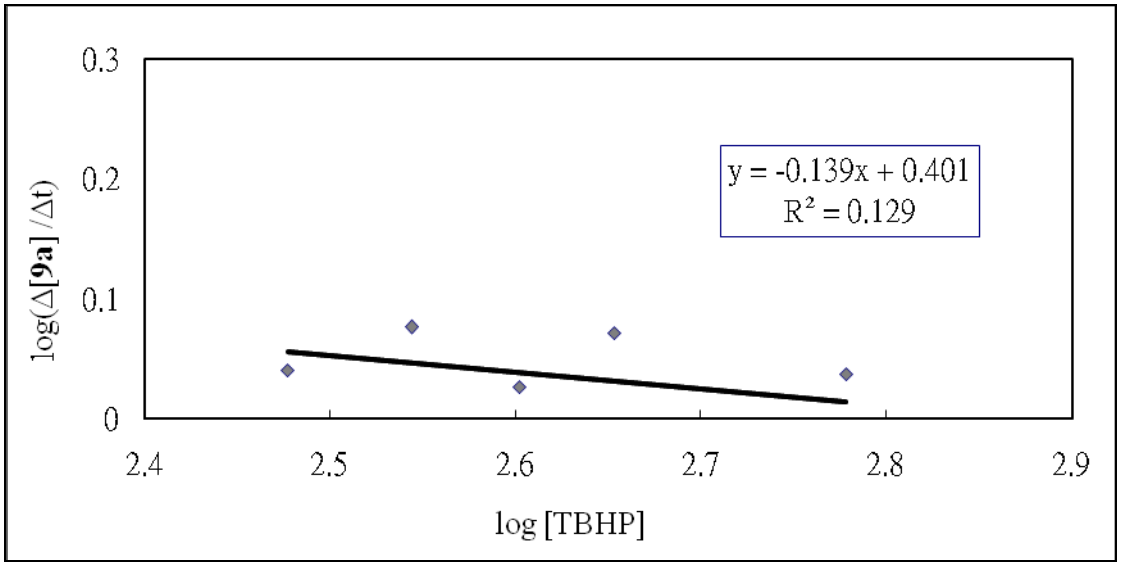

Rate order for [$Pd(OAc)_2$]

The reaction were performed according to the general procedures with varing concentrations of $Pd(OAc)_2$ (2.5 mM, 5 mM, 7.5 mM, 10 mM, 15 mM) and fixed concentrations of **8a** (200 mM), TBHP (300 mM), **2a** (600 mM), AcOH (175 mM) in toluene (1 mL).

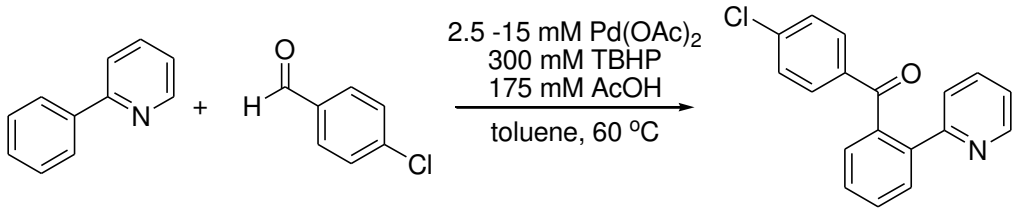

8a (200 mM) **2a** (600 mM) **9a**

entry	$Pd(OAc)_2$		trial 1 [**9a**] (mM)	trail 2 [**9a**] (mM)	trail 3 [**9a**] (mM)	Std. Dev.	average rate (mM/min)
	C(mM)	V(μL)					
1	2.5	25	0.11	0.08	0.14	0.03	0.11
2	5	50	0.16	0.06	0.24	0.09	0.15
3	7.5	75	0.25	0.55	0.29	0.16	0.36
4	10	100	1.15	1.25	1.55	0.20	1.32
5	15	150	3.32	3.20	2.56	0.41	3.03

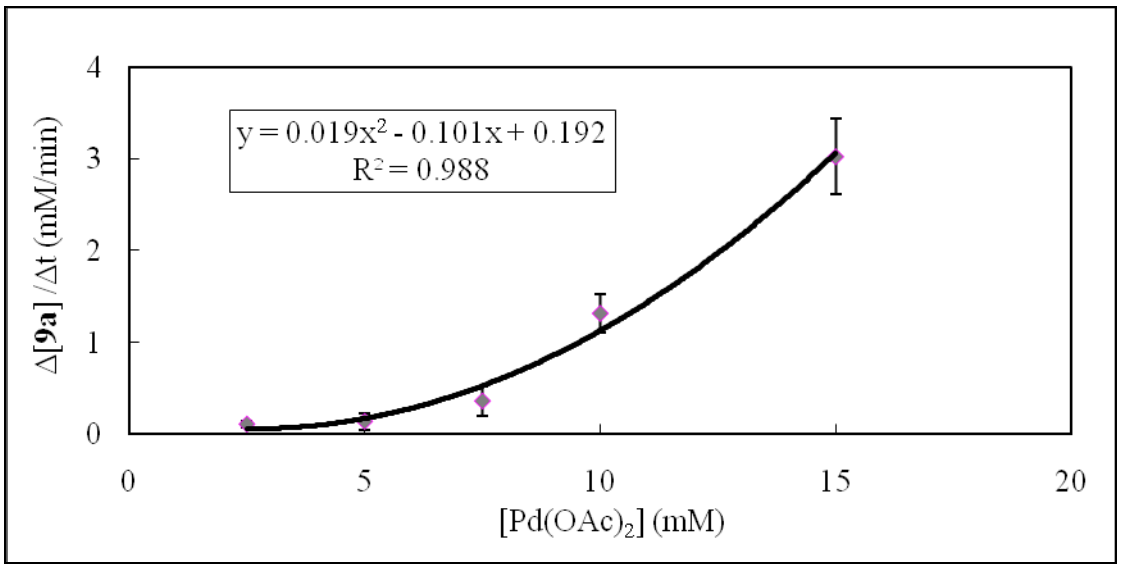

The second-order kinetics of $[Pd(OAc)_2]$ was further verified by plotting the log of (Δ[**9a**] /Δt) versus log $[Pd(OAc)_2]$.

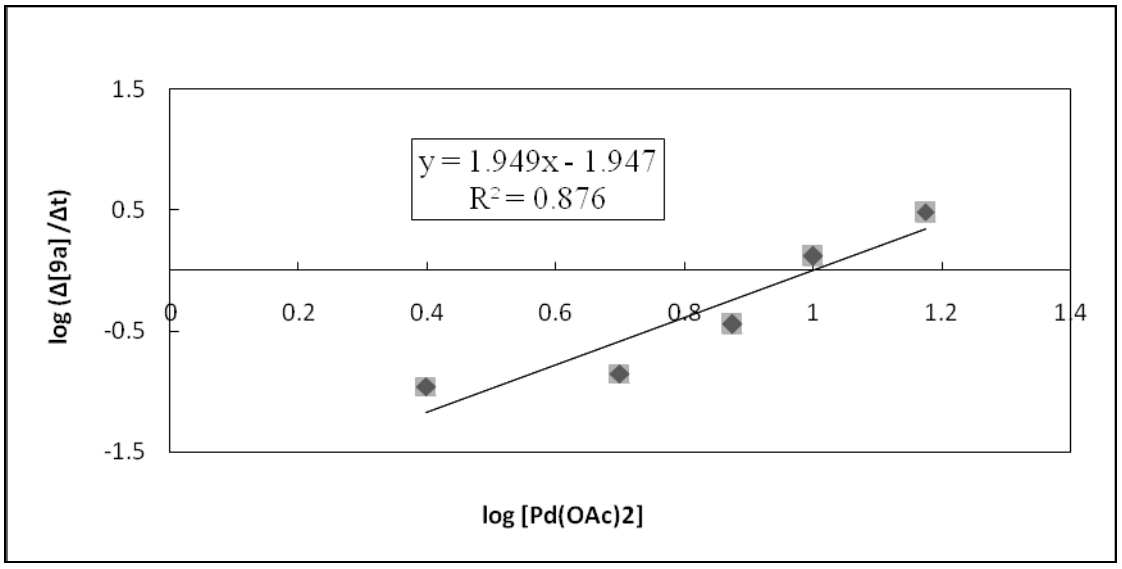

3.5.2 Kinetic isotope effect experiments

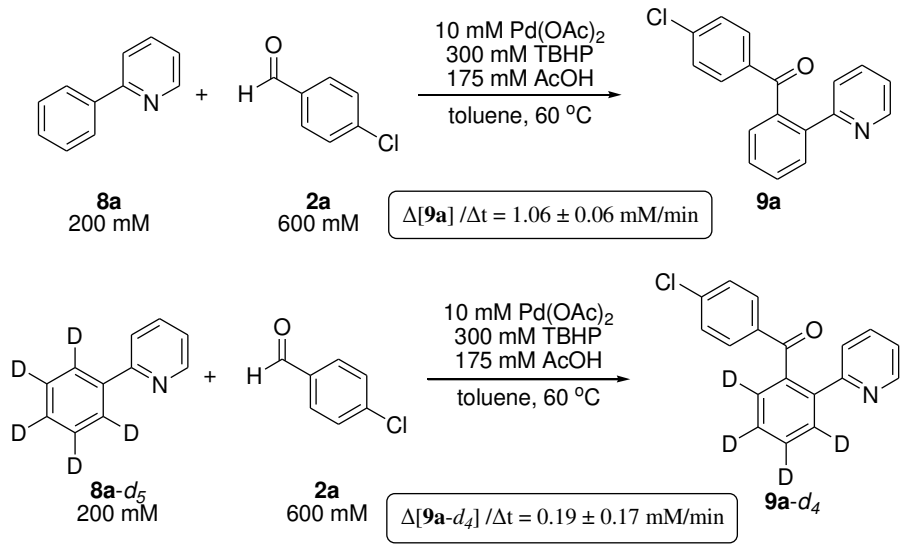

k_H / k_D = 5.6

A 8 mL-vial equipped with a magnetic stir bar was charged with a mixture of 2-phenylpyridine (**8a**) (200 mM), $Pd(OAc)_2$ (10 mM), **2a** (600 mM), TBHP(300 mM), AcOH (175 mM), toluene (1 mL). The vial was sealed with a Teflon liner cap. The reaction mixture was stirred at 60 °C for 10 minutes. The reactions were then quenched by immersing the reaction mixtures into an ice-water bath for 5 min. The amount of **9a** being formed was determined by gas chromatography. The reaction was repeated for three times, and an average kinetic isotope effect (KIE) of k_H/k_D = 5.6 based on initial reaction rate measurement (conversion of 20%) was obtained.

entry	k_H (mM/min)	k_D (mM/min)	k_H/k_D
1	1.10	0.17	6.47
2	0.99	0.21	4.71
3	1.09	0.20	5.45
			average k_H / k_D = 5.6

3.5.3 Hammett correlation study

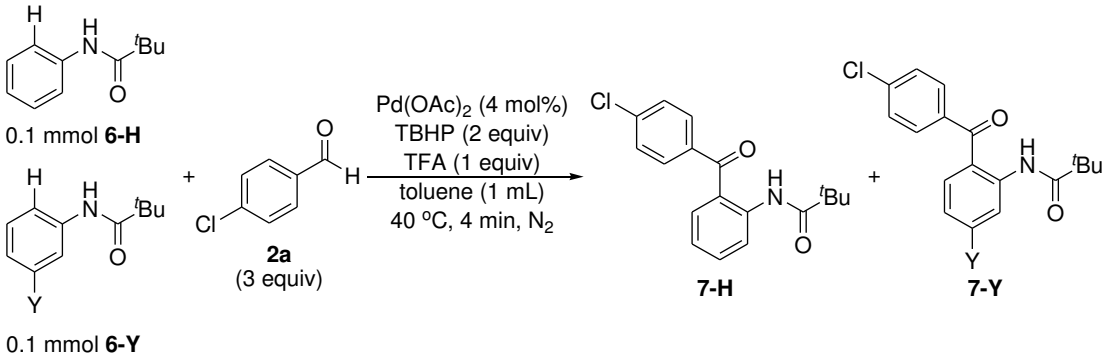

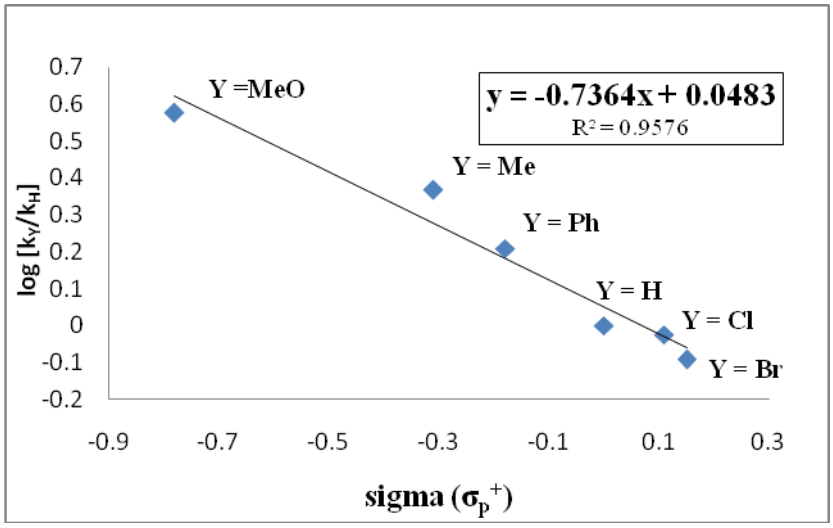

A 10 mL Schlenk-type test tube (with a Quick-fit stopper and side arm) equipped with a magnetic stir bar was charged with an equimolar amount of competitive pivalanilides **6** (0.2 mmol in total), $Pd(OAc)_2$ (4 mol%), 4-chlorobenzaldehyde **2a** (6 mmol), TBHP (0.4 mmol), TFA (0.2 mmol) in toluene (1mL) under nitrogen atmosphere at 40 °C for 4 min (around 10-20 % of pivalanilide conversion). The reaction mixture was cooled with ice-bath and quenched by saturated sodium bisulfate solution (2 mL). The resulting residue was analyzed by GC/FID for determination of conversion using a calibration curve (3 points) with tetradecane (0.1 mmol) as the internal standard. Each result was triplicated and an average value was reported in each case.

3.5.4 Radical trapping experiment

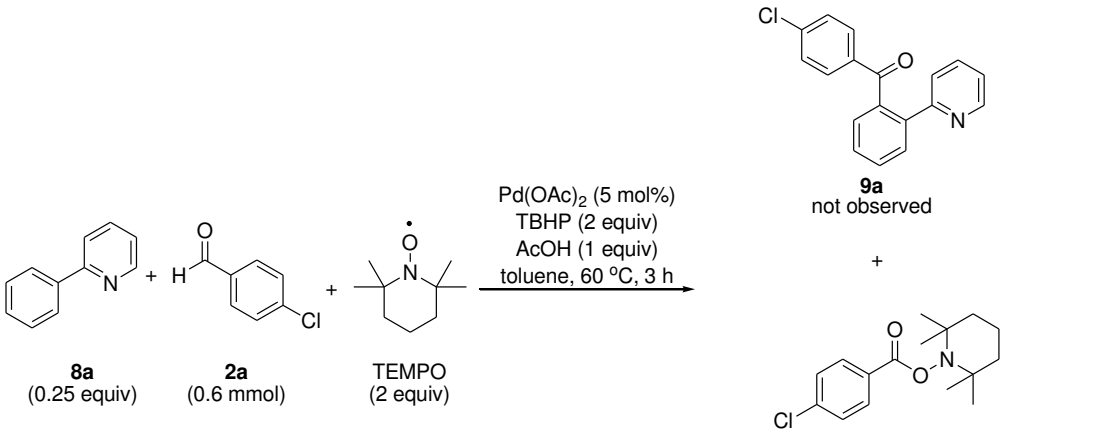

A mixture of **8a** (0.25 mmol), **2a** (0.6 mmol), $Pd(OAc)_2$ (5 mol%), TBHP (2 equiv), AcOH (1 equiv) and TEMPO (0.40 mmol) was dissolved in toluene (1 mL). The mixture was sealed in an 8 mL-vial and was heated in a stirred oil bath at 60 °C for 3 h. The reaction mixture was cooled to room temperature. Solvent was removed in *vacuo*. The crude product was purified by flash column chromatorgraphy.

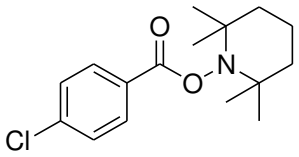

4-chlorobenzoate-2,2,6,6-tetramethylpiperidine
65% yield

^{1}H NMR (400 MHz, $CDCl_3$): δ_H 7.98 (d, J = 8, 2H), 7.41 (d, J = 8, 2H), 4.91 (internal standard = CH_2Br_2), 1.58 (m, 6H), 1.24 (s, 6H), 1.08 (s, 6H).

3.5.5 Synthesis of dinuclear [(benzo[*h*]quinoline)Pd(μ-L)]$_2$ complexes

Synthesis of **13a**

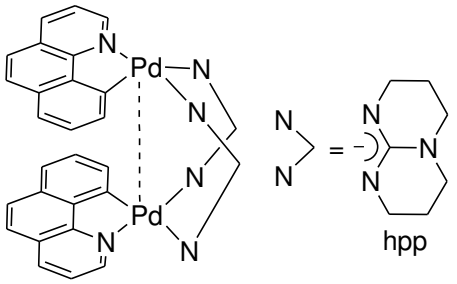

13a

To a mixture of **13f** (0.5 mmol) in DCM (20 mL) at -70 ^{o}C was added NaOMe (1 equiv) and hpp (1 equiv). The reaction solution was warmed to room temperature for 12 h. Solvent was removed in vacuo and the residue was dissolved in CH_2Cl_2 (15 mL) and filtered through Celite. Following removal of solvent in vacuo, the residue was triturated with ether to afford compound **13a** as a organge solid (35% yield). ^{1}H NMR (400 MHz, $CDCl_3$): δ_H 9.54 (d, J = 5.2, 1H), 8.22 (d, J = 5.2, 1H), 7.72 (d, J = 8.7, 1H), 7.57 (m, 2H), 7.45 (m, 2H), 7.23 (m, 1H), 3.86 (m, 1H), 3.65 (m, 1H), 3.25 (m, 6H), 2.09 (m, 2H), 1.97 (m, 2H).

Synthesis of **13c**

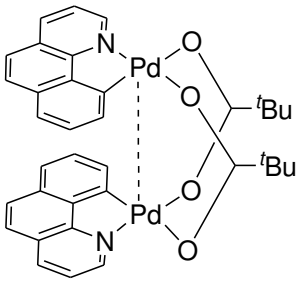

13c

To a mixture of **13f** (0.5 mmol) in DCM (20 mL) at room temperature was added AgOPiv (1 equiv). The reaction solution was heated to room temperature for 12 h. Solvent was removed in vacuo and the residue was dissolved in CH_2Cl_2 (15 mL) and

filtered through Celite. Following removal of solvent in vacuo, the residue was triturated with hexane to afford compound **13c** as a organge solid (88% yield). ^{1}H NMR (400 MHz, $CDCl_3$): δ_H 7.76 (d, J = 5.2, 1H), 7.41 (d, J = 5.2, 1H), 7.21 (m, 3H), 7.05 (d, J = 4.7, 1H), 6,98 (d, J = 4.8, 1H), 6.45 (m, 1H), 1.38 (s, 9H).

Synthesis of **13e**

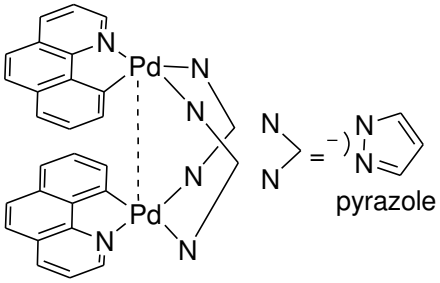

13e

To a mixture of **13b** (0.5 mmol) in CH_3CN (40 mL) at room temperature was added pyrazole (2 equiv). The reaction solution was heated to 40 ºC, at which temperature it was stirred for 2 h. Solvent was removed in vacuo and the residue was dissolved in CH_2Cl_2 (15 mL) and filtered through Celite. Following removal of solvent in vacuo, the residue was triturated with Et_2O to afford compound **13e** as a pale yellow solid (60% yield). ^{1}H NMR (400 MHz, $CDCl_3$):δ_H 8.53 (d, J = 5.3, 1H), 8.21 (d, J = 5.3, 1H), 7.85 (m, 1H), 7.73 (m, 2H), 7.55 (m, 2H), 7.38 (m, 2H), 6.46 (m, 1H).

Chapter 4

Copper-catalyzed cross-dehydrogenative coupling of N-arylacrylamides with chloroform using tert-butyl peroxybenzoate as oxidant for the synthesis of trichloromethylated 2-oxindoles

4.1 Background

Selective trichloromethylation of hydrocarbons is of fundamental interest for organic synthesis. While trichloromethyl groups are found in a vast number of bioactive natural products[65] (e.g. dysamide, barbamide, muironolide and neodysidenin), trichloromethylated hydrocarbons are useful precursors to other functionalized molecules (Scheme 4.1). For example, trichloromethylcarbinols can be transformed to α-substituted carboxylic acids[66] (Jocic reaction); other functionalized molecules including 2-imino-4-thiazolidinones are accessible with an appropriate choice of nucleophiles (Scheme 4.2).[67] Conventionally, deprotonation of chloroform with strong alkaline is commonly employed to generate $^{-}CCl_3$ anion for nucleophilic trichloromethylation of electrophilic substrates (e.g. aldehydes, enones).[68] However, side-reactions such as dichlorocarbene formation and Carnizarro reactions for aldehyde substrates remain a major drawback of this approach.[69] Notably, these drawbacks have been resolved by the use of trichloromethyl silane (CCl_3-TMS) as

precursors for the $^{-}CCl_3$ anion.[70] Recently, Zakarian and co-workers reported a ruthenium-catalyzed radical trichloromethylation of *N*-acyloxalidinones with $BrCCl_3$ as radical precursor.[71] Alternatively, Walsh and co-workers described an enzymatic approach for regioselective trichlorination of leucine for synthesis of barbamide.[72]

Scheme 4.1 Bioactive natural products containing trichloromethylated moiety

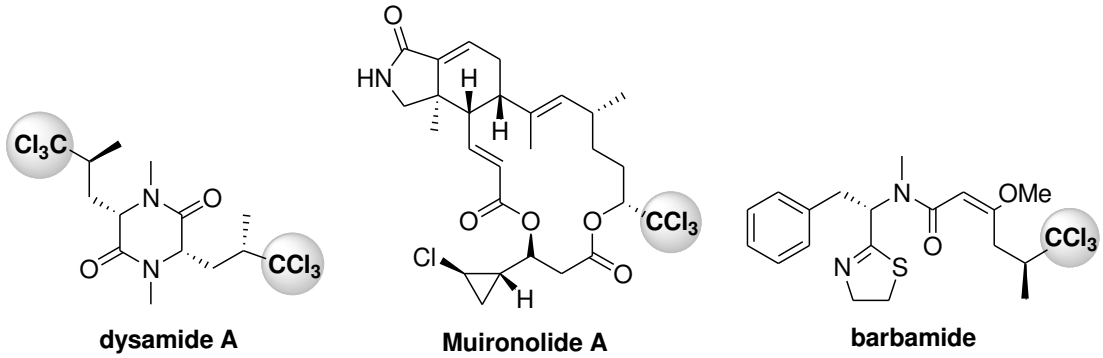

Scheme 4.2 Transformations of trichloromethylcarbinols into different functionalized molecules

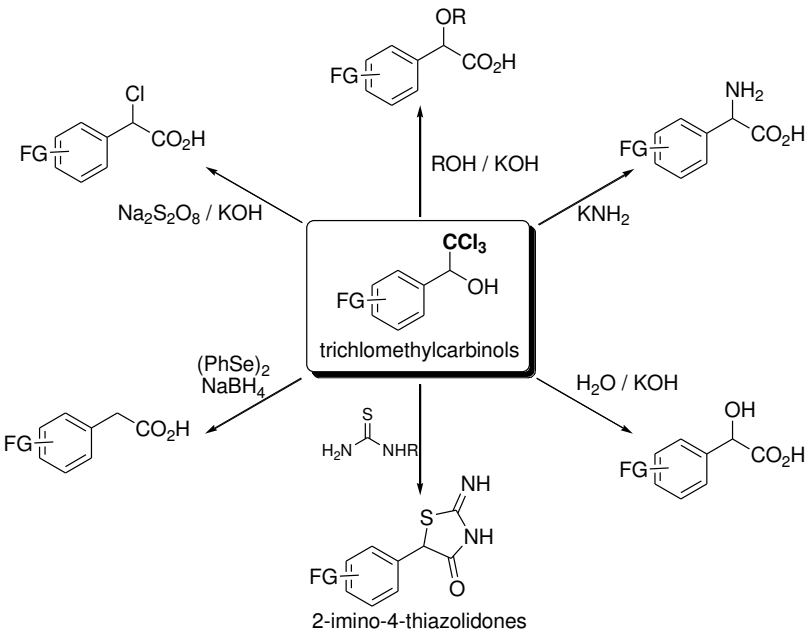

In *chapter 2*, we described the Pd-catalyzed *intermolecular* cross-dehydrogenative coupling of arenes with aldehydes using *tert*-butyl hydroperoxide as oxidant to afford aryl ketones in excellent chemo- and regioselectivity. In *chapter 3*, it was found that the regioselectivity of the coupling reaction is controlled by cyclopalladation assisted by *ortho*-coordinating groups, and the C–C bond coupling is probably mediated by reaction of acyl radicals (•C(O)R) with the arylpalladium(II) complexes. In addition, our previous investigations implicated that arylpalladium(II) complexes would couple with carboradicals such as $•CO_2Et$, •Ar, $•CH(COR)_2$ to achieve ethoxycarbonylation[29d], arylation[27d] and alkylation[25] of arene C–H bonds. Prompted by these results, we envisioned that the analogous cross-coupling reaction of arylpalladium(II) complexes with trichloromethyl radicals ($•CCl_3$) would lead to the formation of trichlomethylated arenes.

It is known that heat decomposition of TBHP with hemolytic O–O bond cleavage would generate *tert*-butoxy radicals,[56] which should react with the chloroform by hydrogen atom abstraction to give trichloromethyl radicals ($•CCl_3$).[73] As depicted in Scheme 4.3, cyclopalladated complex **8a-Pd** (0.1 mmol) was treated with TBHP (0.2 mmol) in chloroform (1 mL) at 120 ^oC for 2 h, it was failed to afford any

trichloromethylated arenes.

Scheme 4.3 Stoichiometric reaction of cyclopalladated complex **8a-Pd** with trichlomethyl radicals

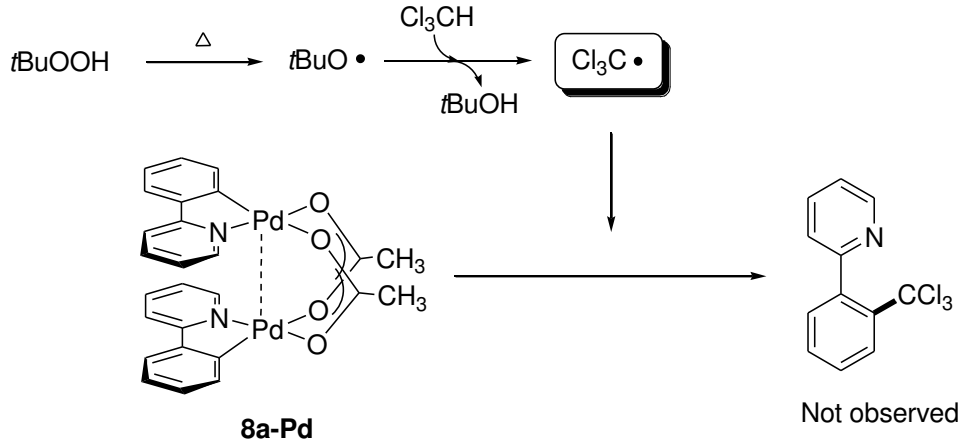

While *intermolecular* CDC reactions mediated by carboradicals remain challenging,[74] *intramolecular* radical-mediated C–C coupling reactions should be plausible. Pioneered by Gulder and co-workers,[75a] regioselective tandem radical bromination/radical-mediated arylative cyclization of *N*-arylacrylamides to form 3,3-disubstituted oxindoles was achieved. With different radicals (e.g. phosphoryl, acyl, aryl, azido), various functionalized oxindoles can be prepared by the tandem radical C=C addition/aryl cyclization reactions (Scheme 4.4).[75]

Scheme 4.4 Overview of radical cyclizations of *N*-arylacrylamides with different radicals

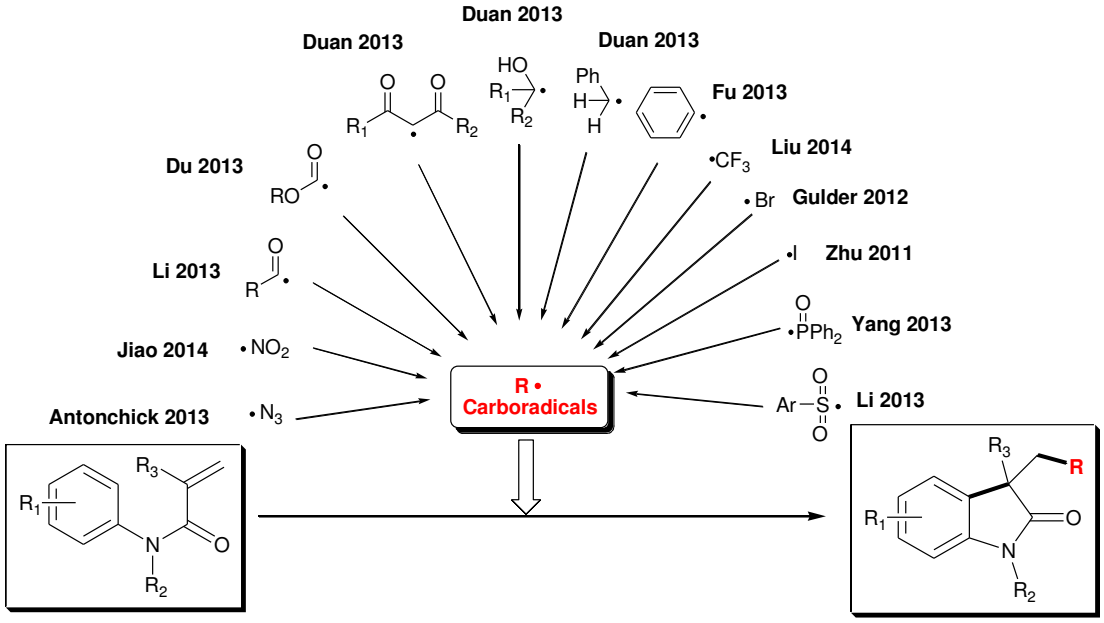

In this work, we investigated the Cu-catalyzed cross-dehydrogenative coupling of *N*-arylacrylamides with chloroform to afford oxindoles. This coupling reaction is believed to proceed by cascade $\bullet CCl_3$ radical addition to C=C bond and aryl cyclization.[76]

4.2 Results and discussion

At the outset, we studied the coupling of *N*-methyl-*N*-phenylmethacrylamide (**11a**) and chloroform as a model reaction. When **11a** (0.2 mmol) was treated with TBHP (2 equiv.) and chloroform (1 mL) at 120 ^{o}C for 3 h. In our initial study, oxindole **12a** was isolated in 30% yield (Scheme 4.5). The molecular structure of **12a** was confirmed by single-crystal-X-ray diffraction study (Figure 4.1).

Scheme 4.5 Preliminary study

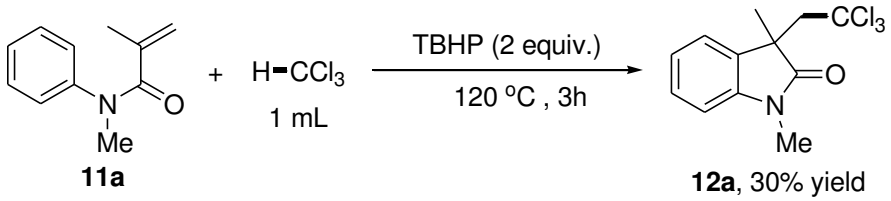

11a **12a**, 30% yield

Figure 4.1 Molecular structure of 3-(2,2,2-trichloroethyl)-1,3-dimethylindolin-2-one (**12a**)

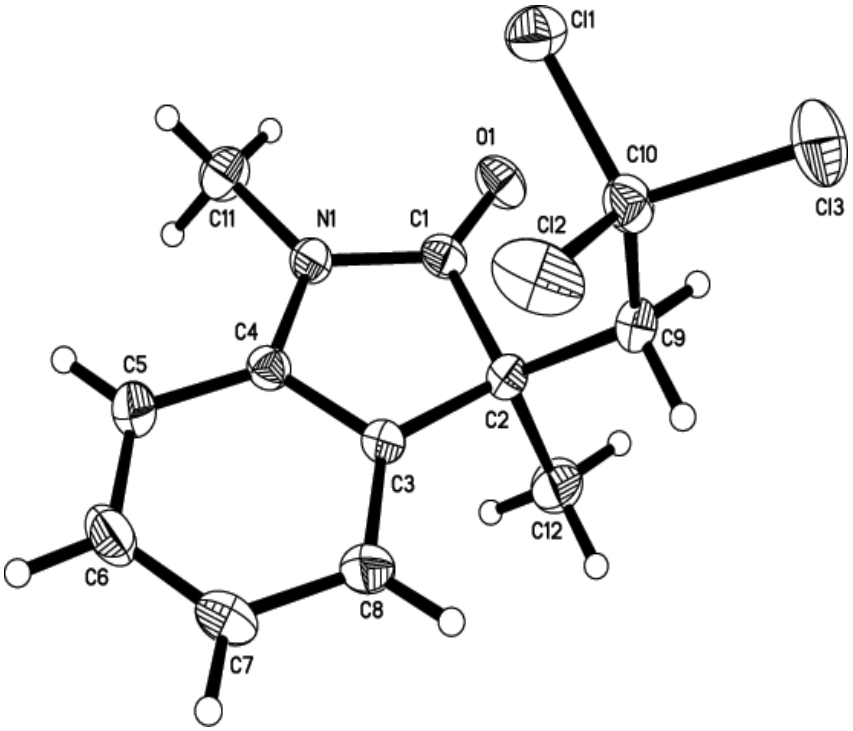

Table 4.1 Selected bond distances and angles for **12a**

bond distances [Å]	
C(9)-C(10)	1.512(3)
C(10)-Cl(11)	1.762(2)
C(2)-C(3)	1.508(3)
C(1)-O(1)	1.214(2)
bond angles [^{o}]	
C(3)-C(2)-C(1)	102.00(14)
C(9)-C(10)-Cl(1)	113.39(13)

Table 4.2 Crystal data and structure refinement for **12a**

Empirical formula	$C_{12}H_{12}Cl_3NO$	
Formula weight	292.58	
Temperature	296(2) K	
Wavelength	0.71073 Å	
Crystal system	Monoclinic	
Space group	P2(1)/n	
Unit cell dimensions	a = 8.9464(3)(5) Å	□= 90°.
	b = 15.2283(4) Å	□= 98°.
	c = 10.0810(3) Å	□= 90°.
Volume	1359.6(7) $Å^3$	
Z	4	
Density (calculated)	1.429 mg/m^3	
Absorption coefficient	0.258 mm^{-1}	
F(000)	600	
Crystal size	0.40 x 0.36 x 0.34 mm^3	
Theta range for data collection	2.44 to 27.63°.	
Index ranges	-10<=h<=11,-15<=k<=19	
Reflections collected	24145	
Independent reflections	3146 [R(int) = 0.0456]	
Completeness to theta = 27.31°	99.6 %	
Absorption correction	Semi-empirical from equivalents	
Max. and min. transmission	0.7456 and 0.6371	
Refinement method	Full-matrix least-squares on F^2	
Data / restraints / parameters	3146 / 0 / 194	
Goodness-of-fit on F^2	1.003	
Final R indices [I>2sigma(I)]	R1 = 0.0542, wR2 = 0.1113	
R indices (all data)	R1 = 0.0860, wR2 = 0.1280	
Largest diff. peak and hole	0.510 and -0.447 $e.Å^{-3}$	

4.2.1 Reaction optimization

We surmised that the oxindole formation was mediated by trichloromethyl radicals. It is known that heat decomposition of TBHP with homolytic O–O bond cleavage would generate *tert*-butoxy radicals,[56] which should react with the chloroform by hydrogen atom abstraction to give trichloromethyl radicals. Therefore, we began by examining the effect of a range of peroxy oxidants known for their hydrogen atom abstraction reactivity (Table 4.3). While employing inorganic peroxy compounds such as $K_2S_2O_8$, OXONE, $(NH_4)_2(S_2O_8)$ failed to effect oxindole formation from **11a** (entries 2–7), the analogous reaction with di-*tert*-butyl peroxide (DTBP) and BPO (2 equiv) as oxidants produced the desired **12a** in 35% and 22% yields (entries 2 and 3), respectively. To our delight, *tert*-butyl peroxybenzoate (TBPB) was found to be the most effective oxidant for the trichloromethylation of **11a** with the oxindole being obtained in 68% yield (entry 4).

Table 4.3 Effect of peroxy oxidants[a]

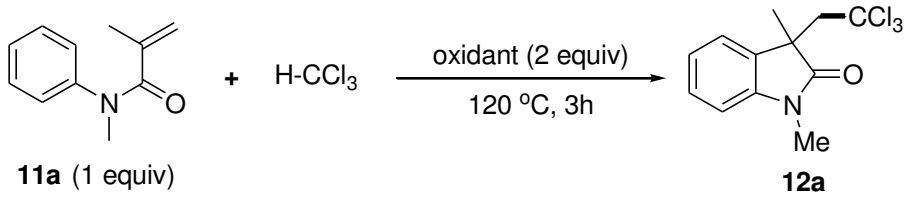

11a (1 equiv) **12a**

entry	oxidant (2 equiv)	yield (%)[b]
1	TBHP	30
2	DTBP	25
3	BPO	22
4	TBPB	68
5	oxone	trace
6	$K_2S_2O_8$	trace
7	$(NH_4)_2S_2O_8$	trace

[a]Reaction conditions: **11a** (0.25 mmol), oxidant (0.5 mmol) in $CHCl_3$ (1 mL) at 120 °C for 3 h. [b] GC-FID yield with tetradecane (10 μL) as internal standard.

Metal salts such as $CuCl_2$ and $FeCl_3$ were reported to catalyze the generation of trichloromethyl radicals from CCl_4 or $CHCl_3$ for radical addition to alkenes;[73b] an oxidation-reduction mechanism was suggested.[76] During our optimization study, we found that employing copper salts as additives would further improve the yield of the trichloromethylation reaction (Table 4.4). For instance, treating **11a** (0.2 mmol) with TBPB (2 equiv) and Cu_2O (5 mol%) in chloroform (1 mL) at 120 °C for 3 h afforded **12a** in 80% yield (entry 1). Notably, employing $CuBr_2$ (5 mol%) as additive for the

trichloromethylation of **11a** furnished **12a** in 87% yield (entry 2). However, the analogous reaction with $Cu(OAc)_2 \cdot H_2O$ as additive gave **12a** in only 55% yield (entry 3). Employing other metal salts such as $FeCl_3$ and $AgNO_3$ as additives failed to afford better results (entries 4 and 5).

Table 4.4 Effect of metal catalysts[a]

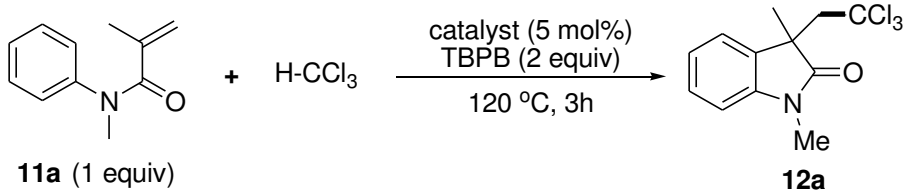

11a (1 equiv) **12a**

entry	catalyst (5 mol%)	yield (%)[b]
1	Cu_2O	80
2	$CuBr_2$	87
3	$Cu(OAc)_2 \cdot H_2O$	55
4	$FeCl_3$	40
5	$AgNO_3$	55

[a]Reaction conditions: **11a** (0.25 mmol), catalyst (5 mol%), TBPB (0.5 mmol) in $CHCl_3$ (1 mL) at 120 °C for 3 h. [b] GC-FID yield with tetradecane (10 μL) as internal standard.

Temperature effect on the trichloromethylation reaction was also investigated (Table 4.3). By TLC monitoring, the reaction was found to be completed in 3 h at 120 ^{o}C (entry 2). When the reaction was performed at 100 ^{o}C, a slighltly diminished yield (85%) was obtained (entry 2). At 80 ^{o}C, the reaction only produced **3a** in 63% yield (entry 3). No **12a** formation was detected after 18 h if the reaction was performed at 50 ^{o}C (entry 4).

Table 4.5 Effect of temperature and reaction time[a]

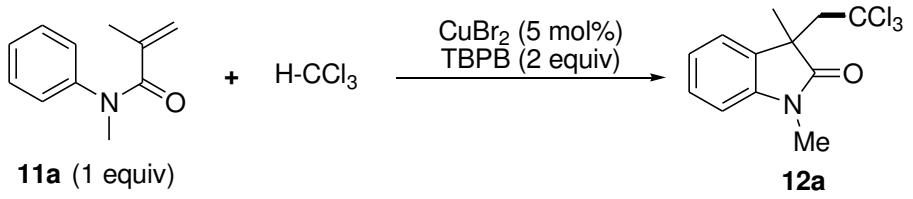

11a (1 equiv) **12a**

entry	temp (^{o}C)	time (h)	yield (%)[b]
1	120	3	87
2	100	3	85
3	80	3	63
4	50	18	trace

[a]Reaction conditions: **11a** (0.25 mmol), $CuBr_2$ (5 mol%), TBPB (0.5 mmol) in $CHCl_3$ (1 mL). [b] GC-FID yield with tetradecane (10 μL) as internal standard.

4.2.2 Scope and limitation

With the optimized conditions in hand, the scope of the cross-dehydrogenative coupling reaction was examined (Table 4.6). Acrylamides bearing electron-withdrawing (halogen, acetyl, CF_3) and -donating (MeO, EtO and Me) substituents on the arenes are effective substrates for the trichloromethylative coupling reaction with the corresponding oxindoles (**12a** – **12h**) being formed in 60–86% yields. It is noteworthy that halogen atoms are tolerated, and thus further functionalization of the product oxindoles by conventional cross-coupling reactions is feasible. Acrylamides with disubstituted aryl groups are effective substrates, and the oxindole products (**12i** and **12j**) were obtained in 67–92% yields.

Apparently, reactions of substrates bearing electron-withdrawing groups afforded the oxindoles in better yields.[77] For instance, trichloromethylation of acrylamides bearing bromo and acetyl group gave **12f** and **12h** in 86 and 81% yields. For those bearing methoxy group, the analogous reactions furnished **12b** in only 60% yield. For the *meta*-substituted acrylamides, the coupling reactions with chloroform produced mixtures of regioisomers (~1 : 1.7). In most cases, products derived from cyclization at the more hindered site were preferred.[78] We found that the α-substituted acrylamides such as those containing a phenyl and a benzyl group are effective

substrates for the coupling reaction, and **12n** and **12o** were formed in 60 and 74% yields. However, the acrylamide derivative without any α-substituents failed to undergo the coupling reaction, and no oxindoles were obtained. We hypothesized that the α-substituent is probably key to stabilize the carboradicals formed by addition of the $\bullet CCl_3$ radical to the C=C bond. Consistent with this notion, the cinnamic acid-derived acrylamide was found to undergo trichloromethyl radical-mediated cyclization to give dihydroquinolinone **12q** in 78% yield. Evidently, the regioselectivity of the radical addition is directed to the formation of a benzyl radical, which then proceeded to cyclization with the arene.

The dependence of the *N*-substituents was also observed; reactions with *N*-benzyl substituted acrylamides afforded the oxindole **12r** in 34% yield versus 85% yield for the *N*-methyl derivative. Notably, reaction with NH-free substrates failed to produce the desired oxindole **12s**, and extensive substrate decomposition was observed. Interestingly, acrylamide derived from 2-aminopyridine can be converted to aza-oxindole **12t** in 85% yield. This finding is compatible with some earlier findings that heteroaromatic nucleus are excellent substrates for radical substitution reactions.[79]

Table 4.6 Substrate scope study for the Cu-catalyzed cross-dehydrogenative coupling *N*-arylacrylamides with chloroform[a,b]

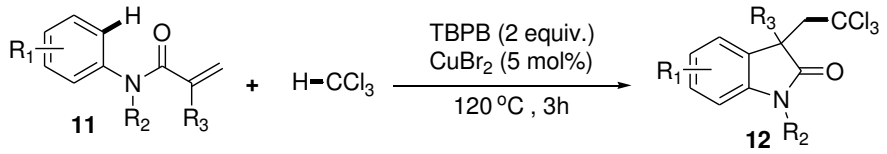

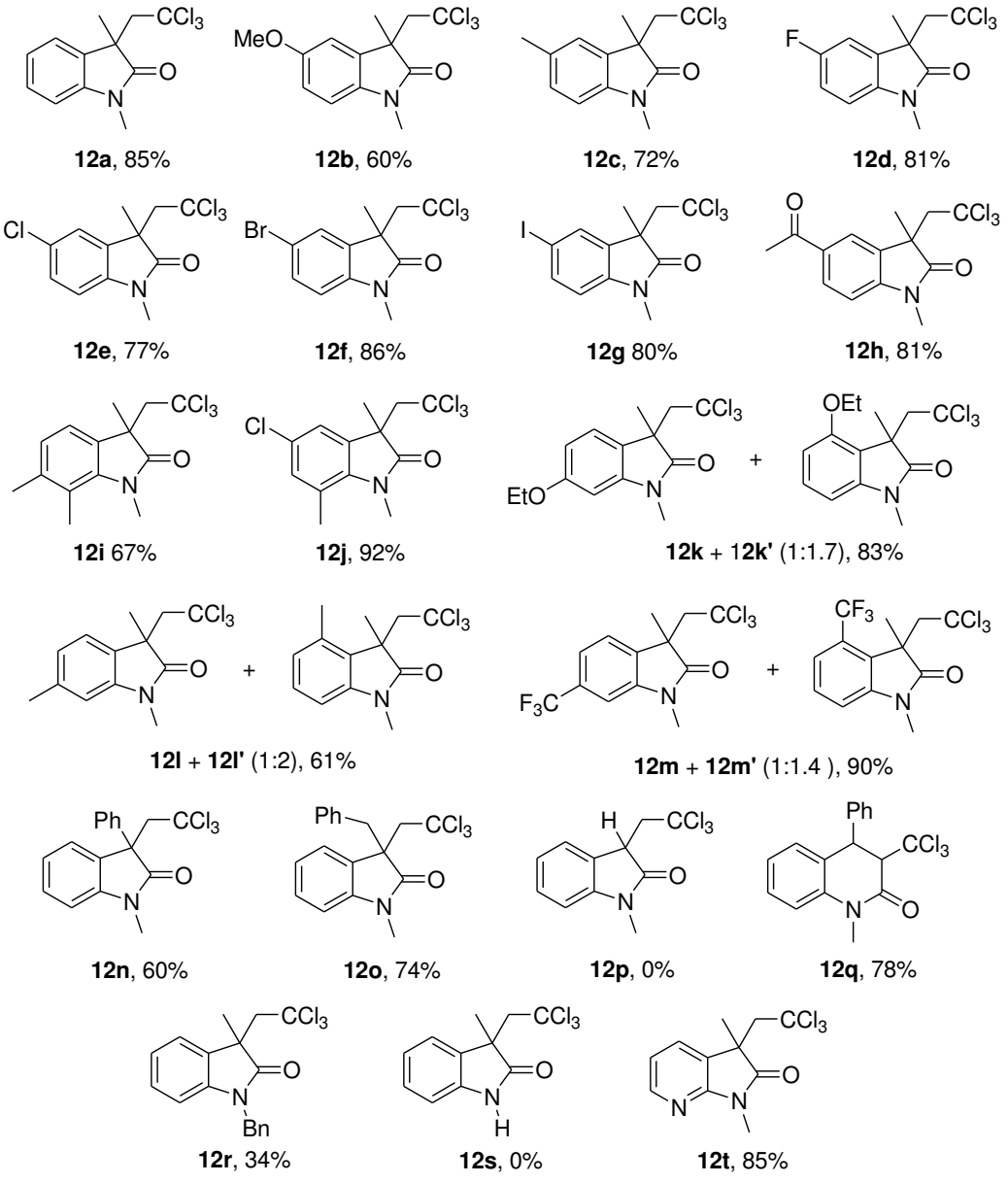

[a] Reaction conditions: **11** (0.2 mmol), TBPB (2 equiv.), $CuBr_2$ (5 mol%) in $CHCl_3$ (1 mL) at 120 °C for 3 h. [b] Isolated yields.

4.2.3 Synthetic applications

Having established the catalytic direct acylation reaction, we hoped to explore the synthetic versatility of this reaction by transforming the trichloromethyl group on the oxindoles to other functional groups (Scheme 4.6). For example, reductive dechlorination of **12a** has been achieved by treating the sample with tributyltin hydride in toluene at 100 ^{o}C; the monohalide product **13a** was obtained in 66% yield.[80] We found that when **12a** was treated with *t*-BuOK (3 equiv.) in toluene at 100 ^{o}C, 1-chloroalkyne **14a** was obtained in 60% yield. According to the literature, 1-chloroalkynes are useful building blocks for cross coupling reactions (e.g. Cadiot-Chodkiewicz coupling).[81]

Scheme 4.6 Synthetic modification of the trichloromethyl moiety

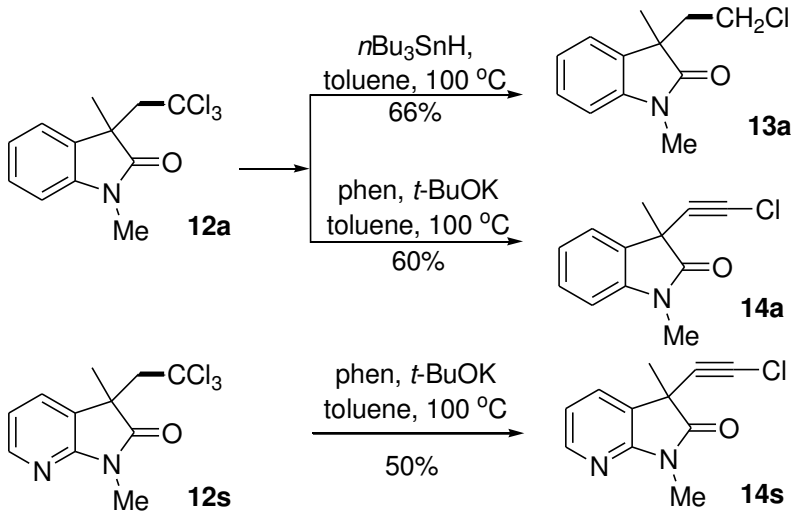

4.2.4 Mechanistic study

As illustrated in Scheme 4.7, to test our mechanistic hypothesis on trichloromethyl radical-mediated cyclization, we performed the trichloromethylation of **11a** in the presence of radical scavengers such as ascorbic acid and 2,6-di-*tert*-butyl-4-methyl phenol (BHT), a significant drop of the product yields was observed in a dose-dependent manner. Notably, with 2 equiv. of BHT, only a trace quantity of **12a** was detected. To our delight, our GC-MS analysis of the reaction treated with BHT revealed the BHT-trapped adduct of trichloromethyl radical [2-(trichloromethoxy)-1,3-di-*tert*-butyl-5-methylbenzene].

Scheme 4.7 Radical trapping experiment

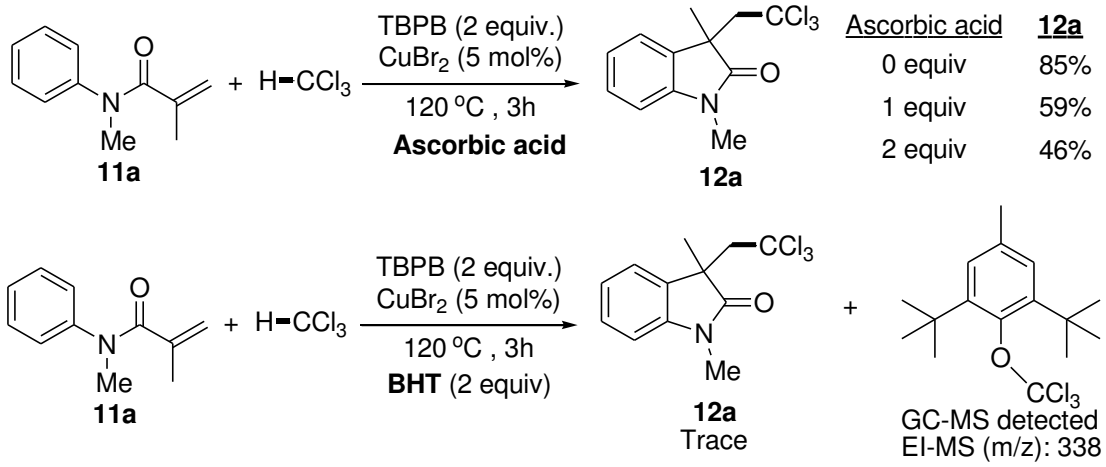

4.2.5 Proposed mechanism

A plausible mechanism for the trichloromethylation is depicted in Scheme 4.8. The reaction is likely to be initiated by Cu(II)-mediated decomposition of TBPB to form some $Cu^{III}(OBz)$ species and *tert*-butoxy radicals. The *tert*-butoxy radicals would undergo hydrogen atom abstraction with chloroform to give $\bullet CCl_3$ radicals, which would react with the C=C bond of **11a** to form carboradical **A**. Subsequent radical addition to the arene should afford radical intermediate **B**, which should then react with $Cu^{III}(OBz)$ species to produce the oxindole product **12a** with the regeneration of the Cu^{II} catalyst.

Scheme 4.8 Proposed mechanism

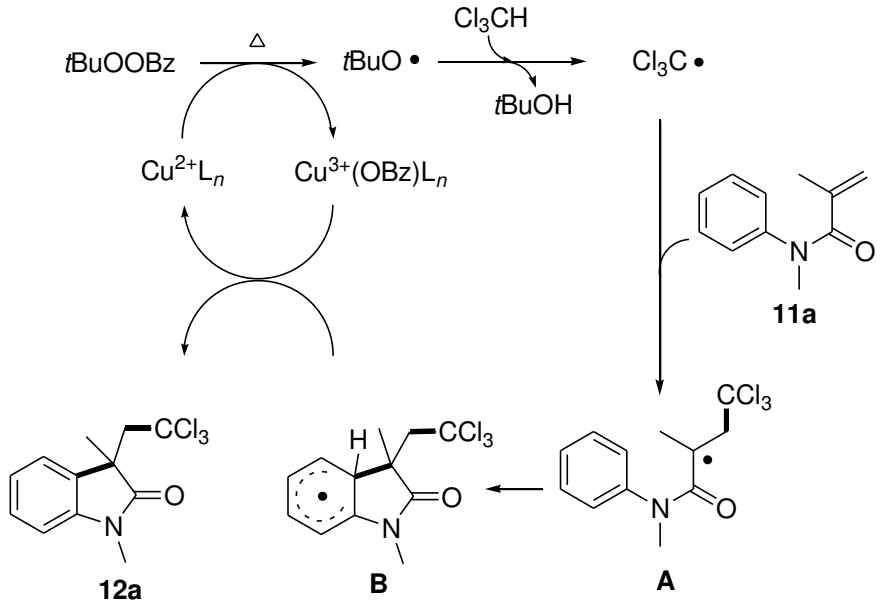

4.3 Concluding summary

In summary, a Cu-catalyzed cross-dehydrogenative coupling of *N*-arylacrylamides with chloroform is achieved using *tert*-butyl peroxybenzoate as oxidant, and trichloromethylated oxindoles were obtained in excellent yield and regioselectivity. This reaction should proceed by cascade addition of $\bullet CCl_3$ radicals and aryl cyclization.

4.4 Experimental section

All the solvents were freshly distilled and dried according to the standard methods prior to use. All experiments were conducted under undegassed atmosphere unless otherwise specified. Anilines were purified by vacuum distillation if necessary. Other reagents were used as received from commercial suppliers without purification.

Thin layer chromatography was performed on silica gel plates. Flash column chromatography was performed on silica gel (Merck, 230-400 mesh). Gas chromatography-mass spectrometry (GC-MS) was performed on a 6890N-GC (Agilent Technology). ^{1}H and ^{13}C NMR spectra were recorded on a Bruker DPX-400 MHz spectrometer. The chemical shift (δ) values are given in ppm and are referenced to residual solvent peaks; carbon multiplicities were determined by DEPT-135 and DEPT-90 experiments. Coupling constants (*J*) were reported in hertz (Hz). Multiplicity abbreviations are: s = singlet, d= doublet, t = triplet, q = quartet, m = multiplet, dt = doublet of triplets, td = triplet of doublets, and br = broad. Mass spectra and high resolution mass spectra (HRMS) were obtained on a VG MICROMASS Fison VG platform, a Finnigan Model Mat 95 ST instrument, or a Bruker APEX 47e FT-ICR mass spectrometer. Infra-red spectra were obtained by a Bruker Vector 22 FT-IR spectrometer. Optical rotations were recorded on a Perkin-Elmer 341 polarimeter in a 10 mm cell. Melting points were measured on a BUCHI Melting Point B-545 machine. X-ray crystallographic study was performed by a Brüker CCD area detector diffractometer.

4.4.1 General procedures for preparation of *N*-arylacrylamides

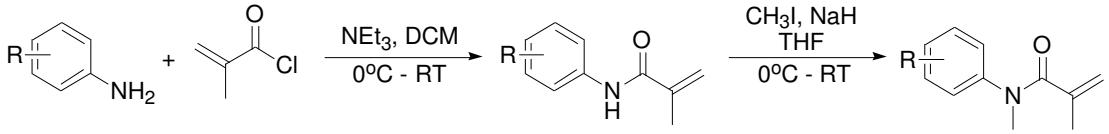

S1 S2 S3 1

Aminobenzene **S1** (10.00 mmol, 1.0 equiv) was dissolved in DCM (30 mL) under nitrogen. NEt_3 (12.00 mmol, 1.2 equiv) was added to the reaction flask at 0 ^oC. Acid chloride **S2** (12.00 mmol, 1.2 equiv) was added slowly to the mixture and the reaction was monitored by TLC. After completion of the reaction, aqueous $NaHCO_3$ (25 mL) was added. The crude product was extracted with DCM (3 x 50 mL). The combined organic layers were washed with 1M HCl (3 x 20 mL) and brine (3 x 20 mL) and dried over Na_2SO_4. Solvent was removed in *vacuo*. The crude product was purified by flash column chromatography.

Purified amide **S3** (8.00 mmol, 1.0 equiv) was dissolved in THF (50 mL) at 0 ^oC. NaH (10.40 mmol, 1.3 equiv) was in three portions and the mixture was stirred for further 15 min. CH_3I (32.00 mmol, 4.0 equiv) was added slowly and the reaction mixture was stirred until completion as monitored by TLC. THF was removed in *vacuo*. Water (30 mL) was added to the mixture and the crude product was extracted with EtOAc (3 x 40 mL). The combined organic layers were washed with brine (3 x 20 mL) and dried over Na_2SO_4. Solvent was removed in *vacuo*. The crude product **11** was purified by flash column chromatography.

4.4.2 General procedures for the preparation of trichloromethylated oxindole derivatives

A mixture of substrate **11** (0.20 mmol), $CuBr_2$ (0.01 mmol, 5 mol%) and TBPB

(0.40 mmol) was dissolved in chloroform (1 mL). The mixture was sealed in an 8 mL-vial and was heated in a stirred oil bath at 120 ^{o}C for 3 h. The reaction mixture was cooled to room temperature. Solvent was removed in *vacuo*. EtOAc (6 mL) was added to redissolve the crude mixture. 1M NaOH (1 mL) was added to neutralize the benzoic acid produced during the reaction and the crude product was extracted with EtOAc (3 x 6 mL). The combined organic layer was dried over Na_2SO_4 and solvent was removed in *vacuo*. The crude product was purified by flash column chromatorgraphy.

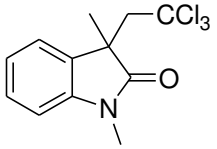

12a, 85%

Yellow solid; Eluent: *n*-hexane/EtOAc 6:1; ^{1}H NMR (400 MHz, $CDCl_3$): δ_H 7.32 (m, 2H), 7.06 (t, *J* = 7.4 Hz, 1H), 6.88 (d, *J* = 7.6 Hz, 1H), 3.69 (d, *J* = 15.2 Hz, 1H), 3.34 (d, *J* = 15.2 Hz, 1H), 3.23 (s, 3H), 1.40 (s, 3H); ^{13}C NMR (100 MHz, $CDCl_3$): δ_C 178.60 (C=O), 143.28 (Ar C), 129.57 (Ar C), 128.49 (Ar C-H), 125.64 (Ar C-H), 122.00 (Ar C-H), 108.38 (Ar C-H), 96.14 (CCl_3), 59.88 (CH_2), 47.97 (C), 26.83 (NCH_3), 26.56 (CH_3); HRMS (ESI): calcd. for $C_{12}H_{13}NOCl_3$: 292.0063, found: 292.0060.

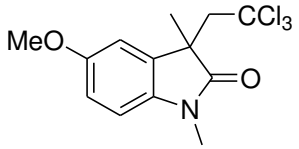

12b, 60%

Yellow solid; Eluent: *n*-hexane/EtOAc 7:3; ^{1}H NMR (400 MHz, $CDCl_3$): δ_H 6.97 (s, 1H), 6.84 (d, *J* = 10.8 Hz, 1H), 6.78 (d, *J* = 8.4 Hz, 1H), 3.79 (s, 3H), 3.69 (d, *J* = 15.2

Hz, 1H), 3.31 (d, *J* = 15.2 Hz, 1H), 3.21 (s, 3H), 1.38 (s, 3H); ^{13}C NMR (100 MHz, $CDCl_3$): δ_C 178.25 (C=O), 155.58 (Ar C), 136.91 (Ar C), 130.96 (Ar C), 113.27 (Ar C-H), 112.81 (Ar C-H), 108.62 (Ar C-H), 96.12 (CCl_3), 59.82 (CH_2), 55.90 (OCH_3), 48.37 (C), 26.91 (NCH_3), 26.65 (CH_3); HRMS (ESI): calcd. for $C_{13}H_{15}NO_2Cl_3$: 322.0162, found: 322.0163.

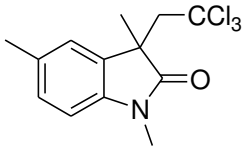

12c, 72%

White solid; Eluent: *n*-hexane/EtOAc 8:2; ^{1}H NMR (400 MHz, $CDCl_3$): δ_H 7.16 (s, 3H), 7.09 (d, *J* = 8 Hz, 1H), 6.76 (d, *J* = 7.6 Hz, 1H), 3.67 (d, *J* = 15.2 Hz, 1H), 3.30 (d, *J* = 15.2 Hz, 1H), 3.20 (s, 3H), 2.33 (s, 3H), 1.37 (s, 3H); ^{13}C NMR (100 MHz, $CDCl_3$): δ_C 178.54 (C=O), 140.90 (Ar C), 131.48 (Ar C), 129.59 (Ar C), 128.74 (Ar C-H), 126.40 (Ar C-H), 108.10 (Ar C-H), 96.22 (CCl_3) , 59.84 (CH_2), 48.02 (C), 26.88 (CH_3), 26.60 (CH_3), 21.16 (CH_3); HRMS (ESI): calcd. for $C_{13}H_{15}NOCl_3$: 306.0214, found: 306.0205.

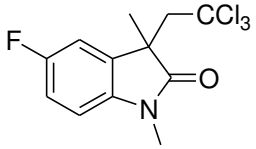

12d, 81%

Pale yellow solid; Eluent: *n*-hexane/EtOAc 8:2; ^{1}H NMR (400 MHz, $CDCl_3$): δ_H 7.10 (m, 1H), 7.01 (m, 1H), 6.79 (m, 1H), 3.69 (d, *J* = 15.2 Hz, 1H), 3.31 (d, *J* = 15.6 Hz, 1H), 3.22 (s, 3H), 1.39 (s, 3H); ^{13}C NMR (100 MHz, $CDCl_3$): δ_C 178.22 (C=O), 158.89 (d, *J* = 241 Hz, Ar C-F), 139.24 (Ar C), 131.26 (d, *J* = 8 Hz, Ar C), 114.86 (d, *J* = 23 Hz, Ar C-H), 113.68 (d, *J* = 24 Hz, Ar C-H), 108.85 (d, *J* = 8 Hz, Ar C-H),

95.89 (CCl_3), 59.78 (CH_2), 48.36 (C), 26.75 (NCH_3), 26.71 (CH_3); ^{19}F NMR (376 MHz, $CDCl_3$): δ_F -120.94; HRMS (ESI): calcd. for $C_{12}H_{12}NOFCl_3$: 309.9963, found: 309.9966.

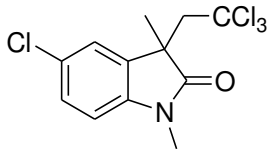

12e, 77%

White solid; Eluent: *n*-hexane/EtOAc 8:2; ^1H NMR (400 MHz, $CDCl_3$): δ_H 7.33 (m, 1H), 7.28 (m, 1H), 6.80 (d, J = 8.4 Hz, 1H), 3.69 (d, J = 15.6 Hz, 1H), 3.31 (d, J = 15.6 Hz, 1H), 3.22 (s, 3H), 1.39 (s, 3H); ^{13}C NMR (100 MHz, $CDCl_3$): δ_C 178.11 (C=O), 141.84 (Ar C), 131.30 (Ar C), 128.48 (Ar C-H), 127.52 (Ar C), 126.07 (Ar C-H), 109.35 (Ar C-H), 95.85 (CCl_3), 59.75 (CH_2), 48.14 (C), 26.72 (CH_3).

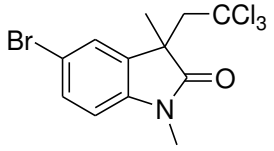

12f, 86%

White solid; Eluent: *n*-hexane/EtOAc 85:15; ^1H NMR (400 MHz, $CDCl_3$): δ_H 7.43 (m, 2H), 6.75 (d, J = 8.0 Hz, 1H), 3.68 (d, J = 15.2 Hz, 1H), 3.30 (d, J = 15.2 Hz, 1H), 3.21 (s, 3H), 1.39 (s, 3H); ^{13}C NMR (100 MHz, $CDCl_3$): δ_C 177.98 (C=O), 142.32 (Ar C), 131.70 (Ar C), 131.36 (Ar C-H), 128.81 (Ar C-H), 114.72 (Ar C), 109.88 (Ar C-H), 95.86 (CCl_3), 59.76 (CH_2), 48.08 (C), 26.71 (CH_3).

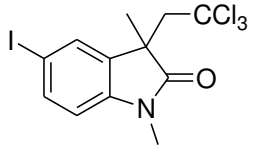

12g 80%

White solid; Eluent: *n*-hexane/EtOAc 8:2; ^1H NMR (400 MHz, $CDCl_3$): δ_H 7.61 (m,

2H), 6.65 (d, *J* = 8 Hz, 1H), 3.66 (d, *J* = 15.2 Hz, 1H), 3.29 (d, *J* = 15.2 Hz, 1H), 3.19 (s, 3H), 1.37 (s, 3H); ^{13}C NMR (100 MHz, $CDCl_3$): δ_C 177.84 (C=O), 143.00 (Ar C), 137.30 (Ar C-H), 134.40 (Ar C-H), 132.07 (Ar C), 110.47 (Ar C-H), 95.89 (CCl_3), 84.42 (Ar C), 59.76 (CH_2), 47.91 (C), 26.69 (CH_3), 26.64 (CH_3); HRMS (ESI): calcd. for $C_{12}H_{11}NOCl_3I$: 416.8951, found: 416.8961.

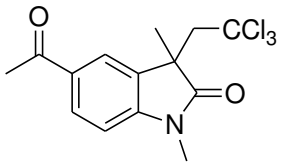

12h, 81%

Pale yellow solid; Eluent: *n*-hexane/EtOAc 65:35; ^{1}H NMR (400 MHz, $CDCl_3$): δ_H 8.00 (s, 1H), 7.95 (d, *J* = 8.2 Hz, 1H), 6.91 (d, *J* = 8.4 Hz, 1H), 3.69 (d, *J* = 15.2 Hz, 1H), 3.38 (d, *J* = 15.2 Hz, 1H), 3.26 (s, 3H), 2.57 (s, 3H), 1.41 (s, 3H); ^{13}C NMR (100 MHz, $CDCl_3$): δ_C 196.67 (Ar C=O), 178.93 (C=O), 147.52 (Ar C), 131.69 (Ar C), 130.44 (Ar C-H), 129.88 (Ar C), 125.60 (Ar C-H), 107.86 (Ar C-H), 95.88 (CCl_3), 59.75 (CH_2), 47.74 (C), 26.82 (CH_3), 26.67 (CH_3), 26.39 (CH_3); HRMS (ESI): calcd. for $C_{14}H_{15}NO_2Cl_3$: 334.0168, found: 334.0153.

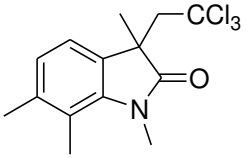

12i 67%

Yellow oil; Eluent: *n*-hexane/EtOAc 8:2; ^{1}H NMR (400 MHz, $CDCl_3$): δ_H 7.06 (d, *J* = 7.6 Hz, 1H), 6.86 (d, *J* = 7.6 Hz, 1H), 3.66 (d, *J* = 15.2 Hz, 1H), 3.53 (s, 3H), 3.28 (d, *J* = 15.2 Hz, 1H), 2.47 (s, 3H), 2.30 (s, 3H), 1.35 (s, 3H); ^{13}C NMR (100 MHz, $CDCl_3$): δ_C 179.93 (C=O), 141.40 (Ar C), 138.27 (Ar C), 127.96 (Ar C), 123.76 (Ar C-H), 122.86 (Ar C-H), 119.17 (Ar C), 96.27 (CCl_3), 60.00 (CH_2), 47.13 (C), 30.95

(CH_3), 27.41 (CH_3), 21.00 (CH_3), 14.31 (CH_3).

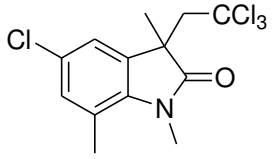

12j, 92%

White solid; Eluent: *n*-hexane/EtOAc 7:3; ^{1}H NMR (400 MHz, $CDCl_3$): δ_H 7.14 (s, 1H), 7.02 (s, 1H), 3.66 (d, *J* = 15.2 Hz, 1H), 3.49 (s, 3H), 3.27 (d, *J* = 15.2 Hz, 1H), 2.56 (2, 3H), 1.37 (s, 3H); ^{13}C NMR (100 MHz, $CDCl_3$): δ_C 178.87 (C=O), 139.77 (Ar C), 131.95 (Ar C), 131.72 (Ar C-H), 127.05 (Ar C), 123.65 (Ar C-H), 121.52 (Ar C), 95.87 (CCl_3), 59.96 (CH_2), 47.55 (C), 29.98 (CH_3), 27.06 (CH_3), 18.90 (CH_3); HRMS (ESI): calcd. for $C_{13}H_{14}NOCl_4$: 339.9824, found: 339.9822.

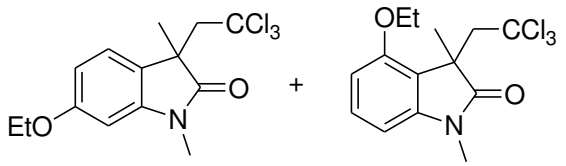

12k + **12k'** (1:1.7), 83%

ellow oil; Eluent: *n*-hexane/EtOAc 8:2; ^{1}H NMR for **2k** (400 MHz, $CDCl_3$): δ_H 7.20 (d, *J* = 8 Hz, 1H), 6.55 (m, 1H), 6.45 (d, *J* = 2.4 Hz, 1H), 4.05 (q, *J* = 7.2 Hz, 2H), 3.65 (d, *J* = 15.2 Hz, 1H), 3.28 (d, *J* = 15.2 Hz, 1H), 3.19 (s, 3H), 1.43 (t, *J* = 6.8 Hz, 3H), 1.36 (s, 3H); ^{13}C NMR for **2k** (100 MHz, $CDCl_3$): δ_C 179.32 (C=O), 159.83 (Ar C), 144.48 (Ar C), 126.28 (Ar C-H), 121.07 (Ar C), 106.70 (Ar C-H), 96.62 (Ar C-H), 96.28 (CCl_3), 63.71(OCH_2), 59.87 (CH_2), 47.54 (C), 26.94 (CH_3), 26.56 (CH_3), 14.83 (CH_3); ^{1}H NMR for **2k'** (400 MHz, $CDCl_3$): δ_H 7.24 (m, 1H), 6.53 (m, 2H), 4.14 (m, 1H), 4.00 (m, 1H), 3.56 (q, *J* = 15.2 Hz, 2H), 3.20 (s, 3H), 1.44 (m, 6H); ^{13}C NMR for **2k'** (100 MHz, $CDCl_3$): δ_C 179.01 (C=O), 156.29 (Ar C), 144.24 (Ar C), 129.78 (Ar C-H), 115.75 (Ar C), 106.14 (Ar C-H), 101.47 (Ar C-H), 96.69 (CCl_3), 63.33 (OCH_2),

58.16 (CH_2), 47.73 (C), 26.75 (CH_3), 23.59 (CH_3), 14.93 (CH_3); HRMS (ESI): calcd. for $C_{14}H_{17}NO_2Cl_3$: 336.0319, found: 336.0299.

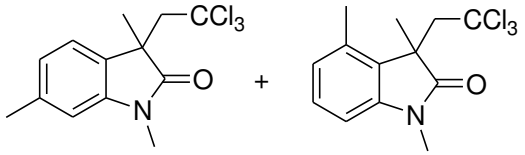

12l + **12l'** (1:2), 61%

Yellow solid; Eluent: *n*-hexane/EtOAc 85:15; ^{1}H NMR (400 MHz, $CDCl_3$): δ_H 7.21 (t, *J* = 7.4 Hz, 1H) , 6.87 (d, *J* = 7.2 Hz, 0.34H), 6.82 (d, *J* = 8 Hz, 0.67H), 6.71 (m, 1H), 3.65 (m, 1H), 3.47 (d, *J* = 15.2 Hz, 0.71H), 3.30 (d, *J* = 15.6 Hz, 0.37H), 3.21 (s, 3H), 2.44 (s, 2H), 2.39 (s, 1H), 1.46 (s, 2H), 1.36 (s, 1H); ^{13}C NMR (100 MHz, $CDCl_3$): δ_C 178.96 (C=O), 178.47 (C=O), 143.46 (Ar C), 143.32 (Ar C), 138.65 (Ar C), 135.87 (Ar C), 128.43 (Ar C-H), 127.10 (Ar C-H), 126.54 (Ar C-H), 125.41 (Ar C-H), 125.03 (Ar C-H), 122.60 (Ar C-H), 109.31 (Ar C-H), 106.13 (Ar C-H), 96.26 (CCl_3), 96.18 (CCl_3), 59.87 (CH_2), 58.59 (CH_2), 48.38 (C), 47.78 (C), 26.94 (CH_3), 26.64 (CH_3), 26.52 (CH_3), 23.83 (CH_3), 21.85 (CH_3), 19.28 (CH_3); HRMS (ESI): calcd. for $C_{13}H_{15}NOCl_3$: 306.0214, found: 306.0209.

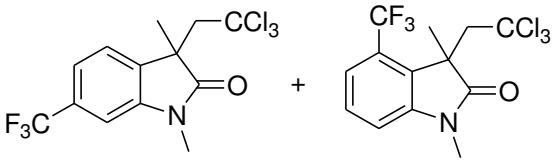

12m + **12m'** (1:1.4), 90%

Yellow oil; Eluent: *n*-hexane/EtOAc 8:2; ^{1}H NMR (400 MHz, $CDCl_3$): δ_H 7.46 (m, 1H), 7.32 (m, 1H), 7.06 (m, 1H), 3.70 (d, *J* = 15.2 Hz, 1H), 3.57 (s, 1H), 3.36 (d, *J* = 15.2 Hz, 1H), 3.25 (s, 3H), 1.45 (m, 3H); ^{13}C NMR (100 MHz, $CDCl_3$): 178.25 (C=O), 177.98 (C=O), 144.64 (Ar C), 143.83 (Ar C), 133.52 (Ar C), 131.18 (Ar C), 130.86 (Ar C), 129.38 (Ar C-H), 128.58 (Ar C), 128.25 (Ar C), 126.79 (Ar C), 125.91(Ar

C-H), 125.45 (Ar C), 125.29 (Ar C), 122.73 (Ar C), 120.58 (Ar C-H), 120.53 (Ar C-H), 120.48 (Ar C-H), 120.43 (Ar C-H), 119.05 (Ar C-H), 119.01 (Ar C-H), 111.81 (Ar C-H), 105.24 (Ar C-H), 105.21 (Ar C-H), 95.92 (C), 95.79 (C), 59.72 (CH_2), 59.62 (CH_2), 59.58 (CH_2), 48.84 (C), 47.98 (C), 26.94 (CH_3), 26.73(CH_3), 24.32(CH_3), 24.30(CH_3); ^{19}F NMR (376 MHz, $CDCl_3$): δ_F 57.42, 62.35; HRMS (ESI): calcd. for $C_{13}H_{11}NOCl_3F_3$: 358.9858, found: 358.9852.

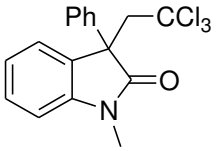

12n, 60%

Yellow solid; Eluent: *n*-hexane/EtOAc 15:1; ^1H NMR (400 MHz, $CDCl_3$): δ_H 7.50 (d, *J* = 7.6 Hz, 1H), 7.39 (m, 3H), 7.29 (m, 3H), 7.13 (t, *J* = 7.2 Hz, 1H), 6.93 (d, *J* = 8 Hz, 1H), 4.25 (d, *J* = 15.2 Hz, 1H), 3.73 (d, *J* = 15.2 Hz, 1H), 3.22 (s, 3H); ^{13}C NMR (100 MHz, $CDCl_3$): δ_C 176.79 (C=O), 144.31 (Ar C), 139.44 (Ar C), 129.13 (Ar C-H), 128.85 (Ar C-H), 128.83 (Ar C), 127.93 (Ar C-H), 126.87 (Ar C), 126.62 (Ar C-H), 121.81 (Ar C-H), 108.69 (Ar C-H), 96.02 (CCl_3), 60.01 (CH_2), 55.73 (C), 26.88 (CH_3); HRMS (ESI): calcd. for $C_{17}H_{15}NOCl_3$: 354.0214, found: 354.0215.

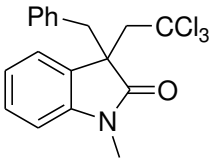

12o, 74%

White solid; Eluent: *n*-hexane/EtOAc 6:1; ^1H NMR (400 MHz, $CDCl_3$): δ_H 7.37 (m, 1H, Ar C-H), 7.21 (m, 1H, Ar C-H), 7.04 (m, 4H, Ar C-H), 6.75 (m, 2H, Ar C-H), 6.57 (m, 1H, Ar C-H), 3.88 (d, *J* = 15.2 Hz, 1H, CH_2), 3.49 (d, *J* = 15.2 Hz, 1H, CH_2), 3.03 (q, *J* = 12.4 Hz, 2H, CH_2), 2.91 (s, 3H, NCH_3); ^{13}C NMR (100 MHz, $CDCl_3$): δ_C

177.12 (C=O), 143.94 (Ar C), 133.61 (Ar C), 130.17 (Ar C-H), 128.59 (Ar C-H), 127.45 (Ar C-H), 127.02 (Ar C-H), 126.96 (Ar C-H), 126.42 (Ar C), 121.39 (Ar C-H), 108.05 (Ar C-H), 96.22 (CCl_3), 58.78 (CH_2), 53.98 (C), 45.93 (CH_2), 26.12 (NCH_3); HRMS (ESI): calcd. for $C_{18}H_{17}NOCl_3$: 368.0370, found: 368.0368.

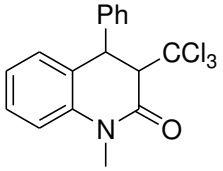

12q, 78%

Yellow oil; Eluent: *n*-hexane/EtOAc 8:2; ^{1}H NMR (400 MHz, $CDCl_3$): δ_H 7.28 (m, 5H), 7.10 (m, 2H), 7.02 (m, 2H), 4.94 (s, 1H), 3.90 (s, 1H), 3.51 (s, 3H); ^{13}C NMR (100 MHz, $CDCl_3$): δ_C 162.22 (C=O), 140.91 (Ar C), 139.78 (Ar C), 129.54 (Ar C-H), 129.23 (Ar C-H), 128.57 (Ar C-H), 127.55 (Ar C-H), 127.11 (Ar C-H), 125.07 (Ar C), 124.23 (Ar C-H), 114.98 (Ar C-H), 97.78 (CCl_3), 67.45 (CH_3), 45.62 (C-H), 30.66 (C-H); HRMS (ESI): calcd. for $C_{17}H_{15}NOCl_3$: 354.0214, found: 354.0202.

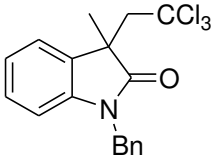

12r, 34%

Pale yellow solid; Eluent: *n*-hexane/Et_2O 9:1; ^{1}H NMR (400 MHz, $CDCl_3$): δ_H 7.28 (m, 7H), 7.03 (t, *J* = 7.6 Hz, 1H), 6.82 (d, *J* = 7.6 Hz, 1H), 4.98 (d, *J* = 15.6 Hz, 1H), 4.88 (d, *J* = 15.2 Hz, 1H), 3.75 (d, *J* = 15.2 Hz, 1H), 3.38 (d, *J* = 15.2 Hz, 1H), 1.45 (s, 3H); ^{13}C NMR (100 MHz, $CDCl_3$): δ_C 178.61 (C=O), 142.49 (Ar C), 135.64 (Ar C), 129.65 (Ar C), 128.73 (Ar C-H), 128.35 (Ar C-H), 127.69 (Ar C-H), 125.75 (Ar C-H), 122.00 (Ar C-H), 109.42 (Ar C-H), 96.13 (CCl_3), 59.69 (CH_2), 48.06 (C), 44.23 (CH_2), 27.56 (CH_3); HRMS (ESI): calcd. for $C_{18}H_{17}NOCl_3$: 368.0370, found: 368.0372.

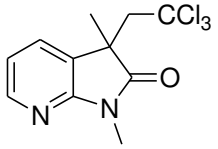

12t, 85%

White solid; Eluent: *n*-hexane/EtOAc 8:2; ^{1}H NMR (400 MHz, $CDCl_3$): δ_H 8.20 (m, 1H), 7.58 (d, *J* = 7.2 Hz, 1H), 6.94 (m, 1H), 3.71 (m, 1H), 3.33 (m, 1H), 3.28 (s, 3H), 1.39 (s, 3H); ^{13}C NMR (100 MHz, $CDCl_3$): δ_C 178.32 (C=O), 156.50 (Ar C), 147.48 (Ar C-H), 133.24 (Ar C-H), 124.01 (Ar C), 117.69 (Ar C-H), 95.86 (CCl_3), 59.43 (CH_2), 47.60 (C), 26.38 (CH_3), 25.73 (CH_3).

4.4.3 General procedures for the reductive dechlorination of trichloromethylated oxindole derivatives

To a solution of **2a** (0.1 mmol) in toluene (2 mL) under nitrogen tributyltin hydride (0.3 mmol) and AIBN (10 mol%) was added. The mixture was sealed in an 8 mL-vial and was heated in a stirred oil bath at 100 ^{o}C for 12 h. The reaction mixture was cooled to room temperature. Solvent was removed in *vacuo*. The residue was dissolved in MeCN (5 mL) and washed with hexane (6 x 5 mL) to remove all tin compounds. The combined organic layer was dried over Na_2SO_4 and solvent was removed in *vacuo*. The crude product was purified by flash column chromatorgraphy.

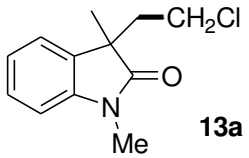

13a

Colorless oil; Eluent: *n*-hexane/EtOAc 8:2; ^{1}H NMR (400 MHz, $CDCl_3$): δ_H 7.30 (t, *J* = 7.6 Hz, 1H), 7.19 (d, *J* = 6.8 Hz, 1H), 7.09 (t, *J* = 7.2 Hz, 1H), 6.86 (d, *J* = 8 Hz, 1H), 3.22 (s, 3H), 3.16 (m, 2H), 2.44 (m, 1H), 2.21 (m, 1H), 1.39 (s, 3H); ^{13}C NMR

(100 MHz, $CDCl_3$): δ_C 179.50 (C=O), 143.15 (Ar C), 132.49 (Ar C), 128.28 (Ar C-H), 122.77 (Ar C-H), 122.59 (Ar C-H), 108.30 (Ar C-H), 47.48 (C), 40.73 (CH_2), 39.99 (CH_2), 26.30 (CH_3), 23.98 (CH_3); HRMS (ESI): calcd. for $C_{12}H_{15}ClNO$: 224.0837, found: 224.0833.

4.4.4 General procedures for the preparation of 1-chloroalkyne (4) with trichloromethylated oxindole derivatives

A mixture of trichloromethylated oxindole derivatives **2** (0.20 mmol), phenanthroline (40 mol%) and *t*-BuOK (0.60 mmol) was dissolved in toluene (2 mL). The mixture was sealed in an 8 mL-vial and was heated in a stirred oil bath at 100 ^oC for 12 h. The reaction mixture was cooled to room temperature. Solvent was removed in *vacuo*. The crude product was purified by flash column chromatorgraphy.

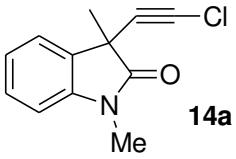

14a

White oil; Eluent: *n*-hexane/EtOAc 8:2; ^1H NMR (400 MHz, $CDCl_3$): δ_H 7.33 (m, 2H), 7.14 (t, J = 7.6 Hz, 1H), 6.85 (d, J = 8 Hz, 1H), 3.23 (s, 3H), 1.65 (s, 3H); ^{13}C NMR (100 MHz, $CDCl_3$): δ_C 175.31 (C=O), 142.31 (Ar C), 131.55 (Ar C), 128.91 (Ar C-H), 123.30 (Ar C-H), 123.26 (Ar C-H), 108.56 (Ar C-H), 67.67 (C≡C), 61.11 (C≡C), 42.98 (C), 26.69 (CH_3), 25.24 (CH_3); HRMS (ESI): calcd. for $C_{12}H_{11}NOCl$: 220.0524, found: 220.0514.

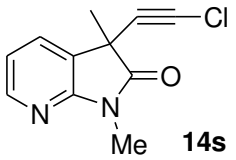

14s

White solid; Eluent: *n*-hexane/EtOAc 8:2; ^{1}H NMR (400 MHz, $CDCl_3$): δ_H 8.22 (dd, *J* = 5.2, 1.6 Hz, 1H), 7.58 (dd, *J* = 7.2, 1.6 Hz, 1H), 7.01 (m, 1H), 3.31 (s, 3H), 1.66 (s, 3H); ^{13}C NMR (100 MHz, $CDCl_3$): δ_C 174.78 (C=O), 155.78 (Ar C), 147.81 (Ar C-H), 130.71 (Ar C-H), 126.12 (Ar C), 118.78 (Ar C-H), 66.62 (C≡C), 61.84 (C≡C), 42.57 (C), 25.83 (CH_3), 24.74 (CH_3); HRMS (ESI): calcd. for $C_{11}H_{10}N_2OCl$: 221.0454, found: 221.0469.

Chapter 5

Conclusion

The catalytic regioselective C–C bond formation *via* C–H / C–H bond cross coupling of two hydrocarbon substrates has been explored. With the use of aldehydes and chloroform, we developed the Pd- and Cu-catalyzed direct carbo-functionalization of arenes. In our study, aldehydes and chloroform were found to be transformed to carboradicals, which are the key intermediates for the cross coupling reactions.

In *Chapter 2*, we initially demonstrated that using $Pd(OAc)_2$ as catalyst, C–H coupling of acetophenone *O*-methyloximes with aldehydes was achieved and 1,2-diacylbenzenes were obtained in up to 95% yields. The Pd-catalyzed coupling exhibits excellent *ortho*-selectivity, which are difficult to achieve by conventional Friedel-Crafts acylation. Apart from good regioselectivity, methoxy, sulfonyl, halogen and amide were well tolerated. Both aliphatic and heteroaromatic aldehydes were effectively coupled to the oximes. Moreover, we demonstrated the transformation of acylated arenes **3a**, **3c** and **3o** towards phthalazines in good yields respectively. The

Pd-catalyzed coupling reaction was also successfully extended to the acylation of anilides to furnish 2-aminobenzophenones under mild conditions (40 ^{o}C, 3 h). This acylation of anilides also exhibited excellent *ortho*-selectivity and functional group tolerance. Notably, aldehydes containing heteroaromatic rings and strained cyclopropanes have been successful coupled to the anilides.

To develop broadly applicable catalytic C–H acylations, we performed a detailed investigation on the mechanism of the Pd-catalyzed *ortho*-C–H acylation of 2-phenylpyridine with 4-chlorobenzaldehyde. Our kinetic studies revealed an experimental rate law being rate = k[**8a**]$^{-1}$[**Pd**]^{2}. The inverse first-order dependence of [**8a**] suggests that the turnover-limiting step should involve substrate dissociation. The second-order dependence on [**Pd**] suggests the involvement of dinuclear palladium complexes in the turnover-limiting step. Primary kinetic isotope effect (k_H / k_D = 5.6) was observed; it revealed that the C–H bond cleavage is a turnover-limiting step. A linear free energy Hammett correlation study on a series of *meta*-substituted pivalanilides (**6**) revealed a small ρ^{+} value of -0.74. The arylpalladium(II) complexes **8a-Pd** was found to be competent to both the catalytic and stoichiometric acylation reactions. The catalytic C–H acylation was suppressed by radical scavengers such as ascorbic acid in a dose-dependent manner. When 2,2,6,6-tetramethylpiperidine

N-oxide (TEMPO) was employed as additives, the ketones formation was completely suppressed and the 2,2,6,6-tetramethyl-piperidino-4-chlorobenzoate was isolated. These findings are compatible to intermediacy of carboradicals in the reaction. Based on our results, we proposed the catalytic acylation is mediated by coupling of acyl radicals with **8a-Pd**. In this work, we prepared some dinuclear [(benzo[*h*]quinoline)Pd(μ-L)]$_2$ complexes and studied their catalytic activity towards C–H acylation. The result led us to conclude that oxidation of the dinuclear arylpalladium(II) complexes to dinuclear Pd(III)–Pd(III) complexes is probably associated by the product formation.

In *Chapter 4*, we achieved the synthesis of trichloromethylated 2-oxindoles *via* Cu-catalyzed C–H / C–H bond coupling of *N*-arylacrylamides with chloroform and the trichloromethylated 2-oxindoles were obtained in up to 92% yield. The reaction showed excellent functional group tolerance and regioselectivity. To demonstrate the synthetic versatility of this reaction, the trichloromethyl group on the oxindoles **15a** has been transformed to monochloromethyl (**16a**) and 1-chloroalkynes (**17a**) in good yields respectively. We performed the trichloromethylation in the presence of radical scavengers such as ascorbic acid and 2,6-di-*tert*-butyl-4-methyl phenol (BHT), a significant drop of the product yields was observed in a dose-dependent manner. More

importantly, our GC-MS analysis of the reaction treated with BHT revealed the BHT-trapped adduct of $\bullet CCl_3$ radical [2-(trichloromethoxy)-1,3-di-*tert*-butyl-5-methylbenzene]. These findings are compatible to intermediacy of carboradicals in the reaction. Based on these results, we proposed the reaction proceed by cascade C=C bond addition of $\bullet CCl_3$ radicals, followed by aryl cyclization.

Appendices

CHAPTER 2
Figure A001 ^{1}H NMR spectrum of **3a**

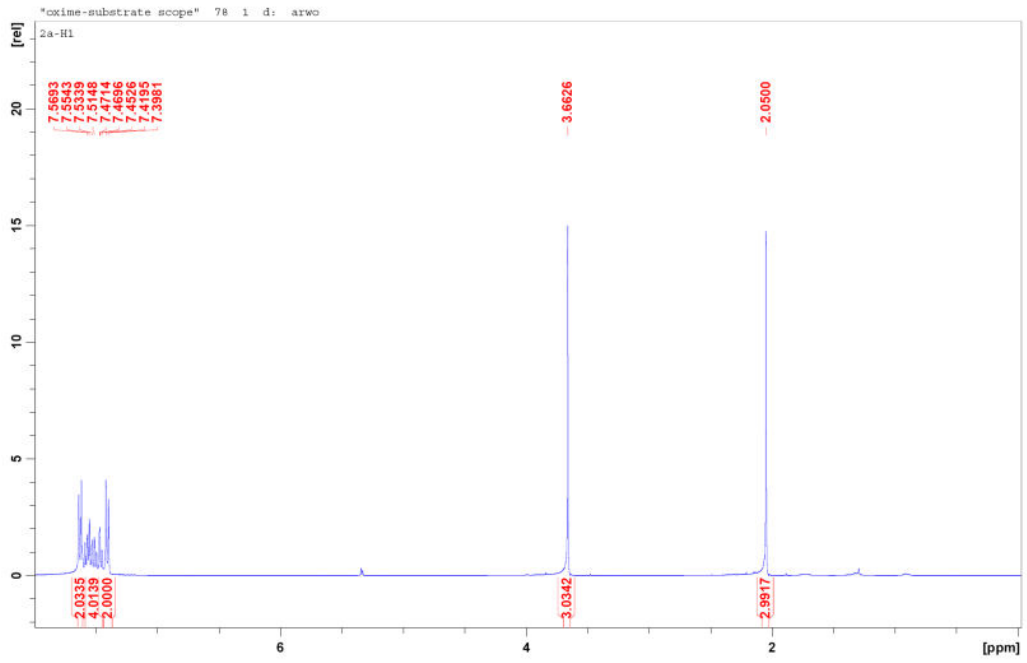

Figure A002 ^{13}C NMR spectrum of **3a**

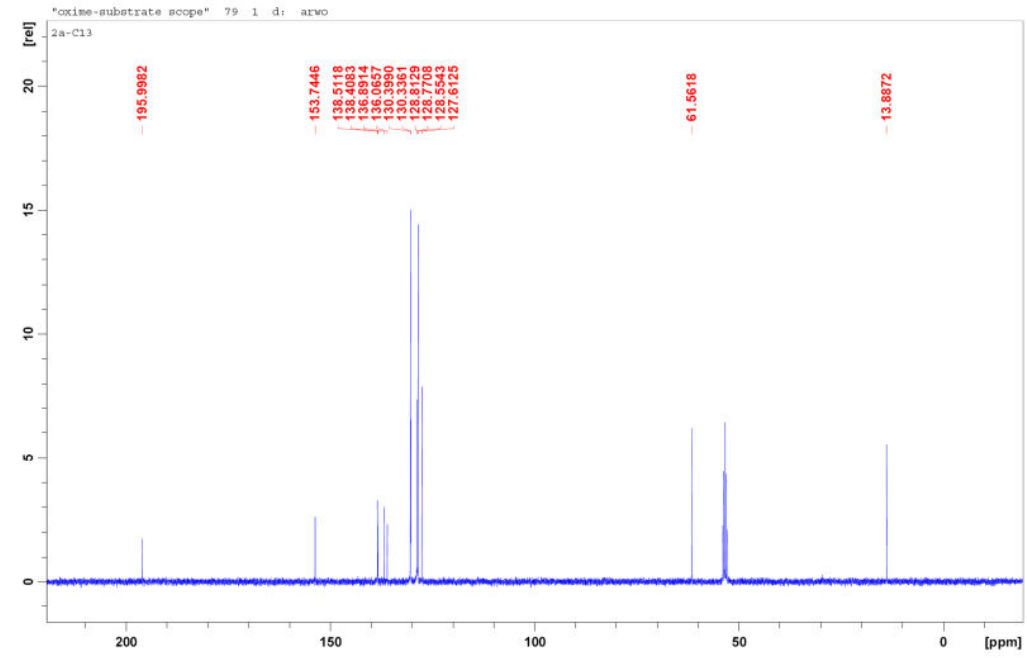

Figure A003 ^{1}H NMR spectrum of **3b**

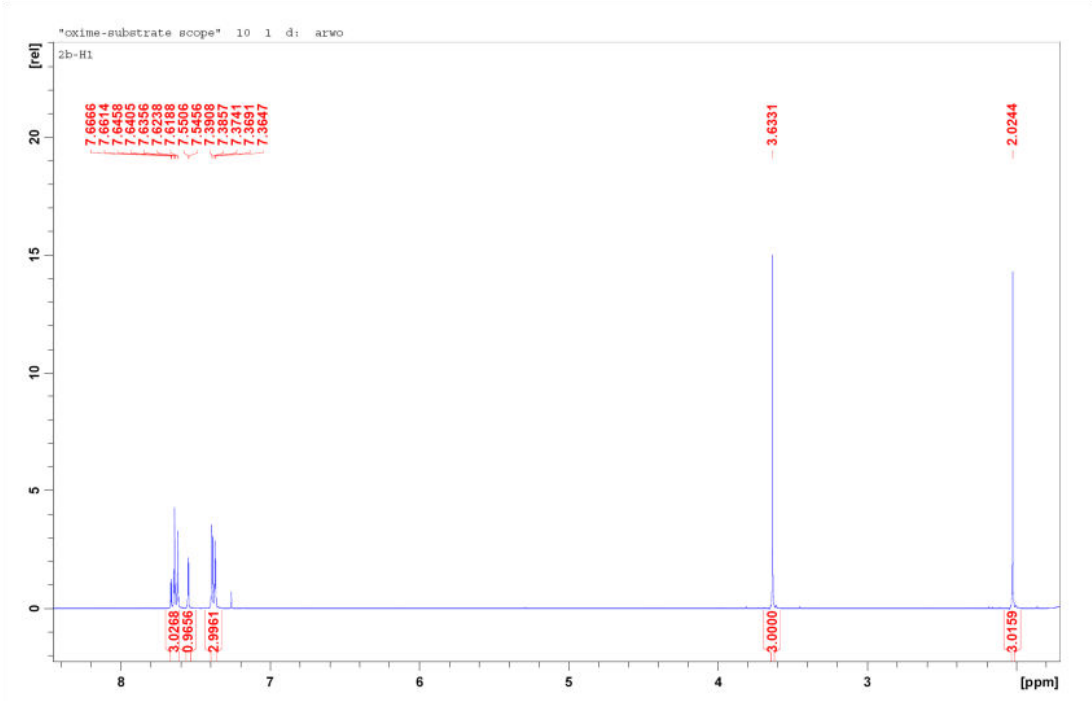

Figure A004 ^{13}C NMR spectrum of **3b**

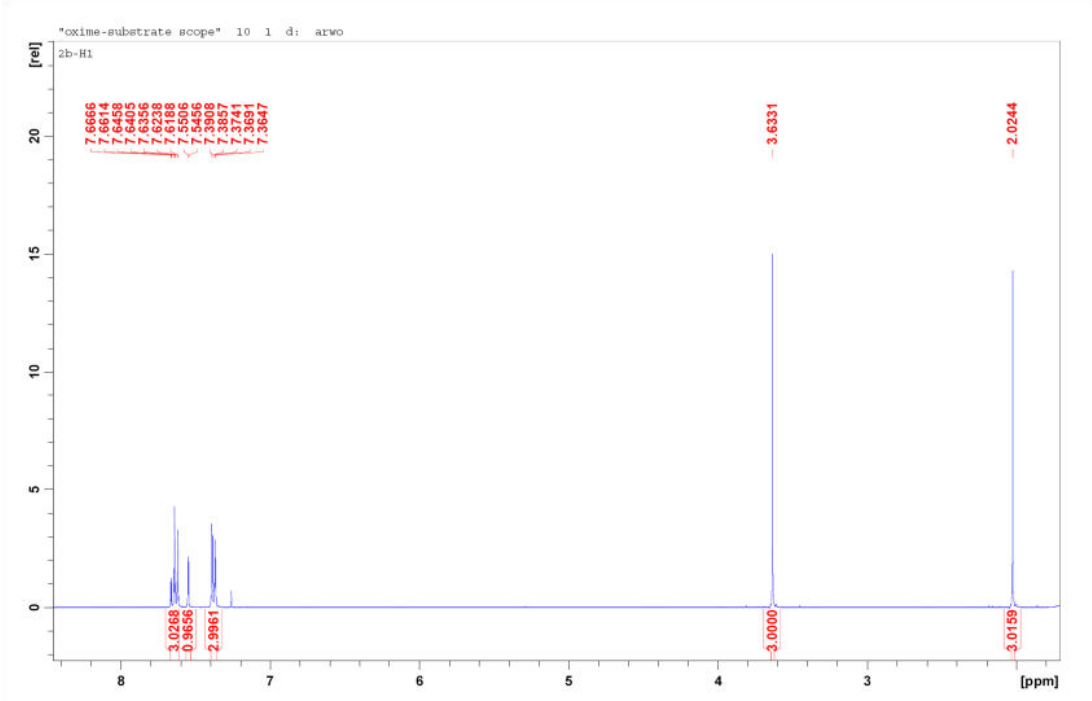

Figure A005 [1]H NMR spectrum of **3c**

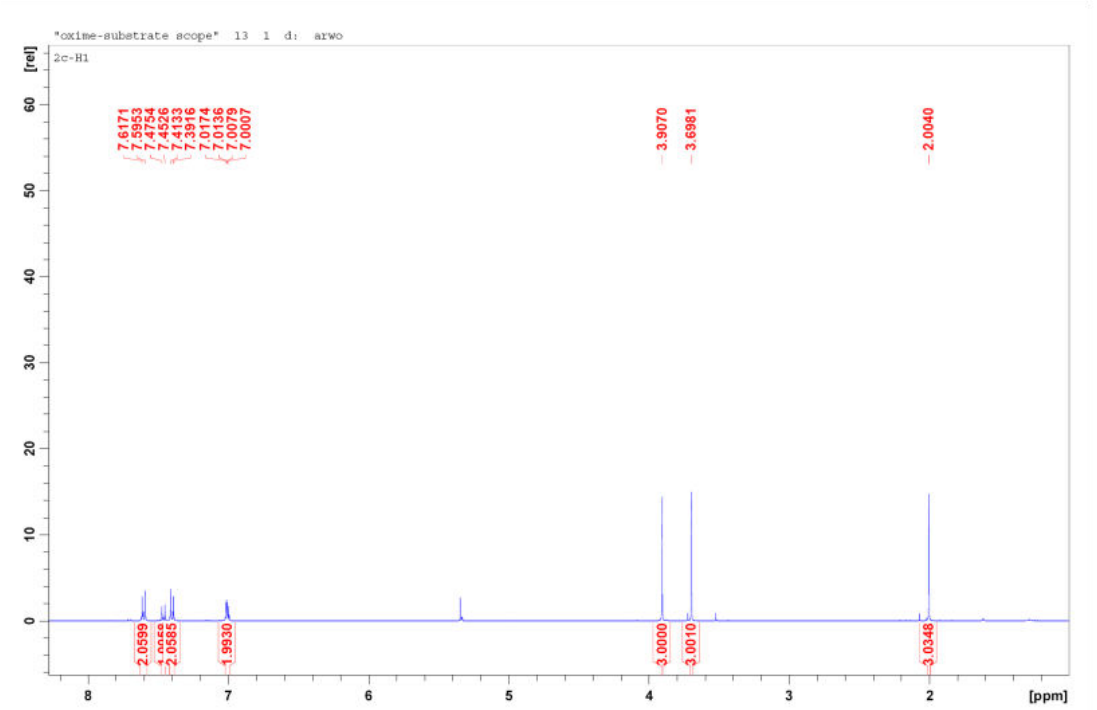

Figure A006 [13]C NMR spectrum of **3c**

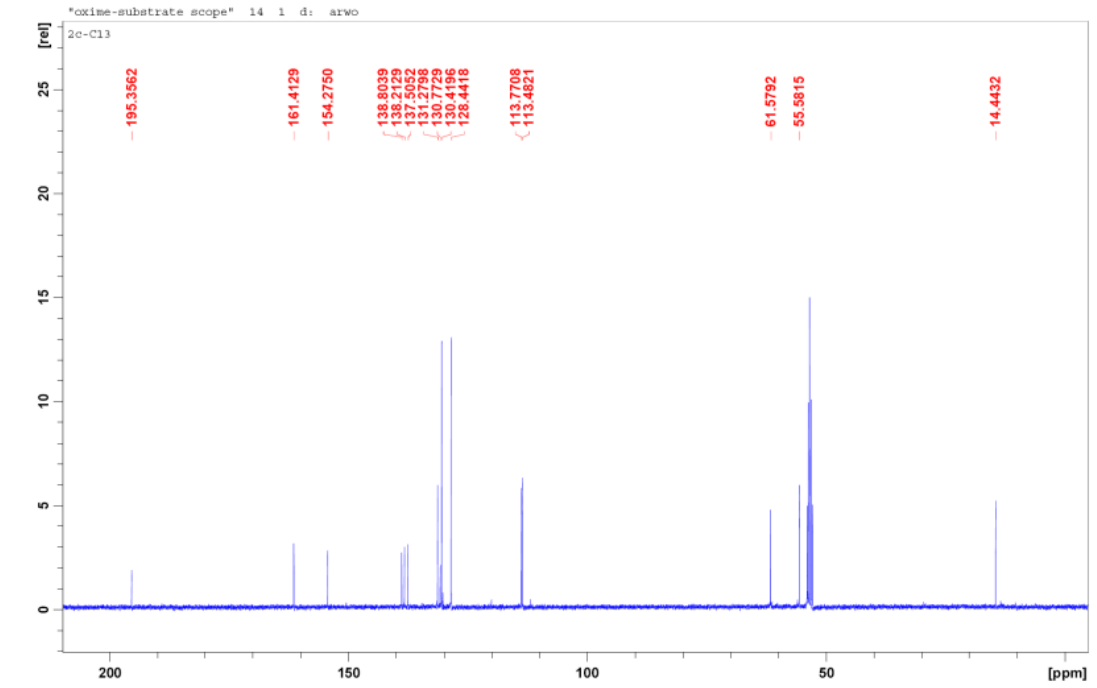

Figure A007 [1]H NMR spectrum of **3d**

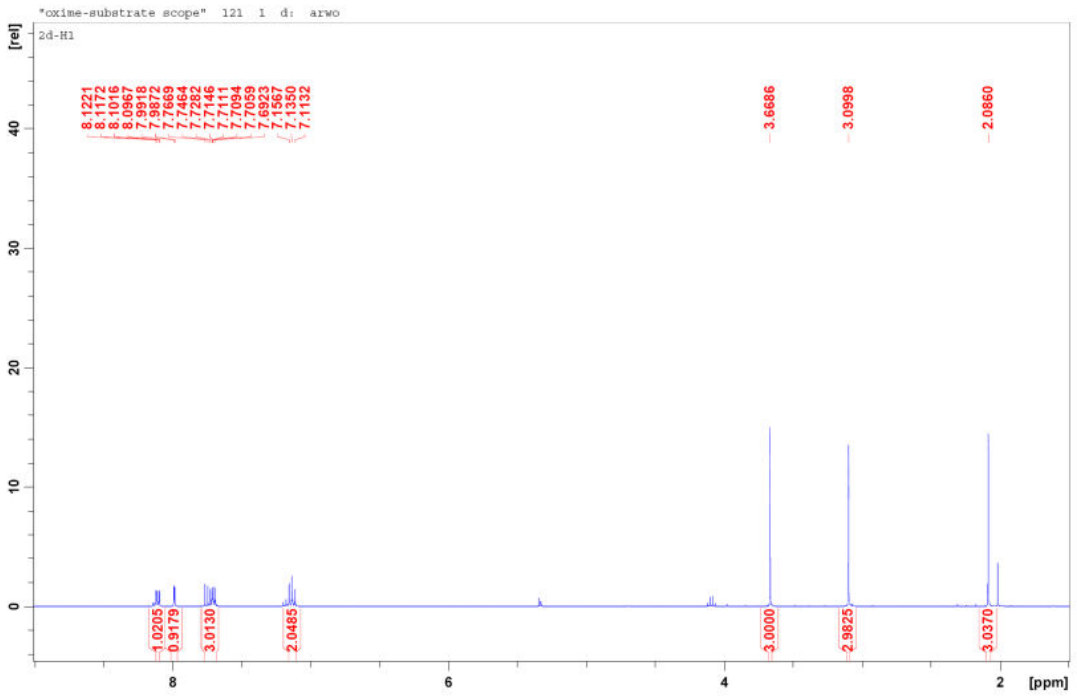

Figure A008 [13]C NMR spectrum of **3d**

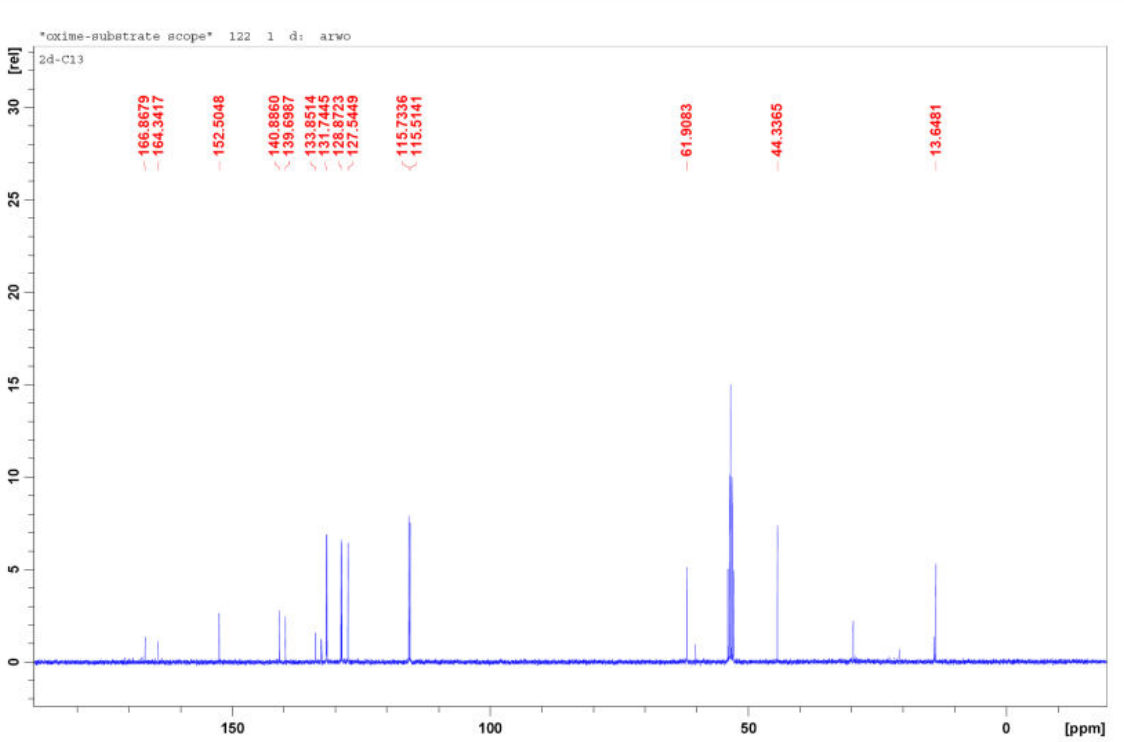

Figure A009 [1]H NMR spectrum of **3e**

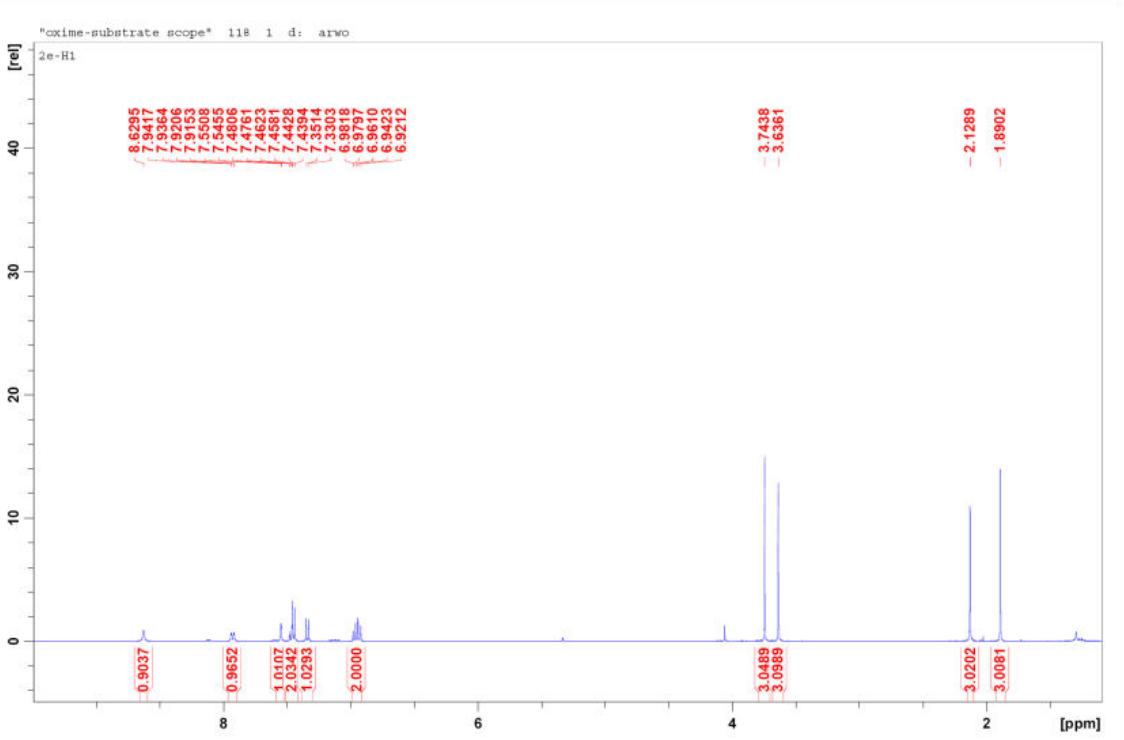

Figure A010 [13]C NMR spectrum of **3e**

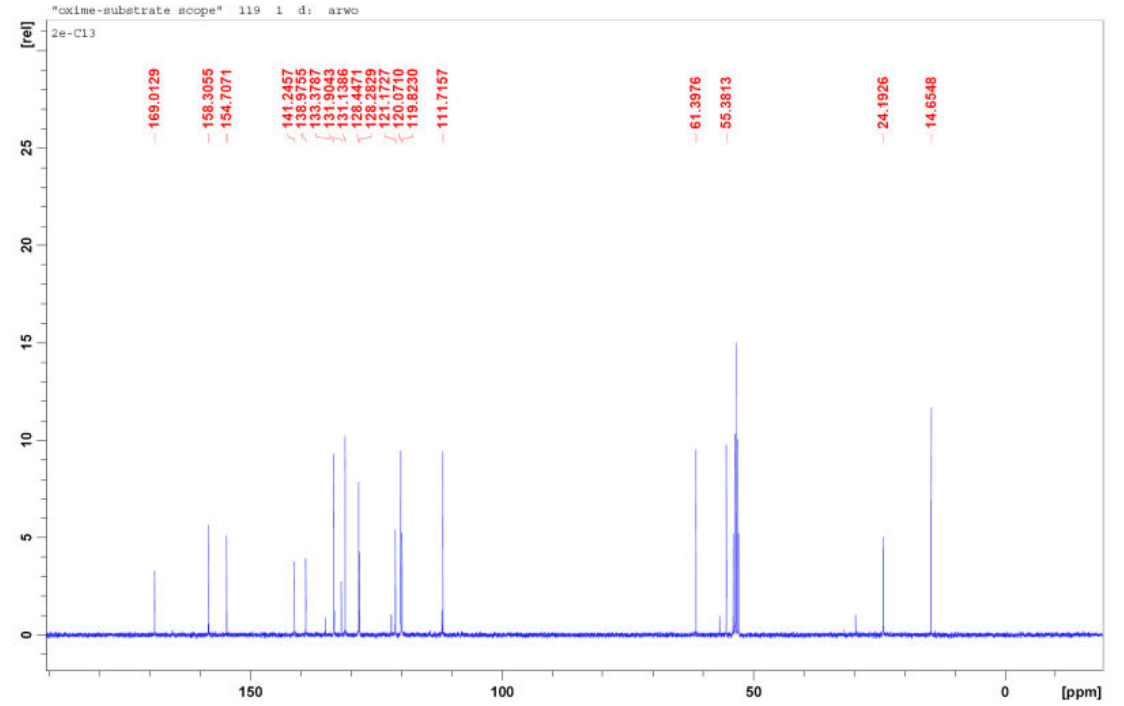

Figure A011 [1]H NMR spectrum of **3f**

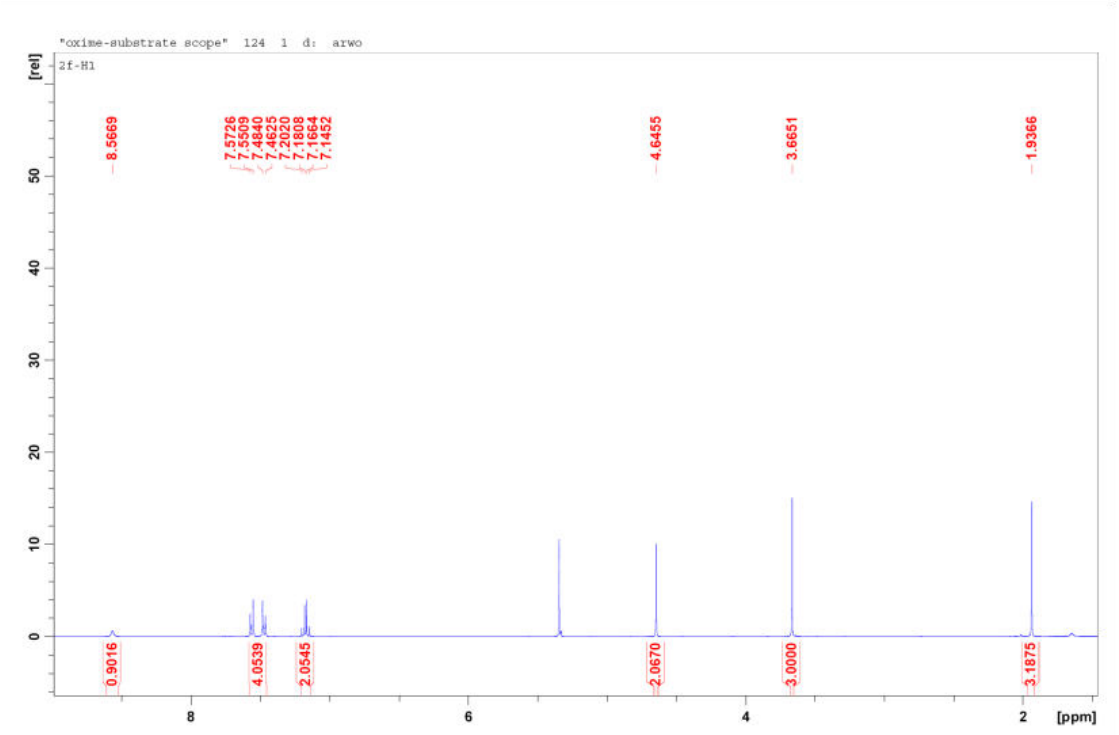

Figure A012 [13]C NMR spectrum of **3f**

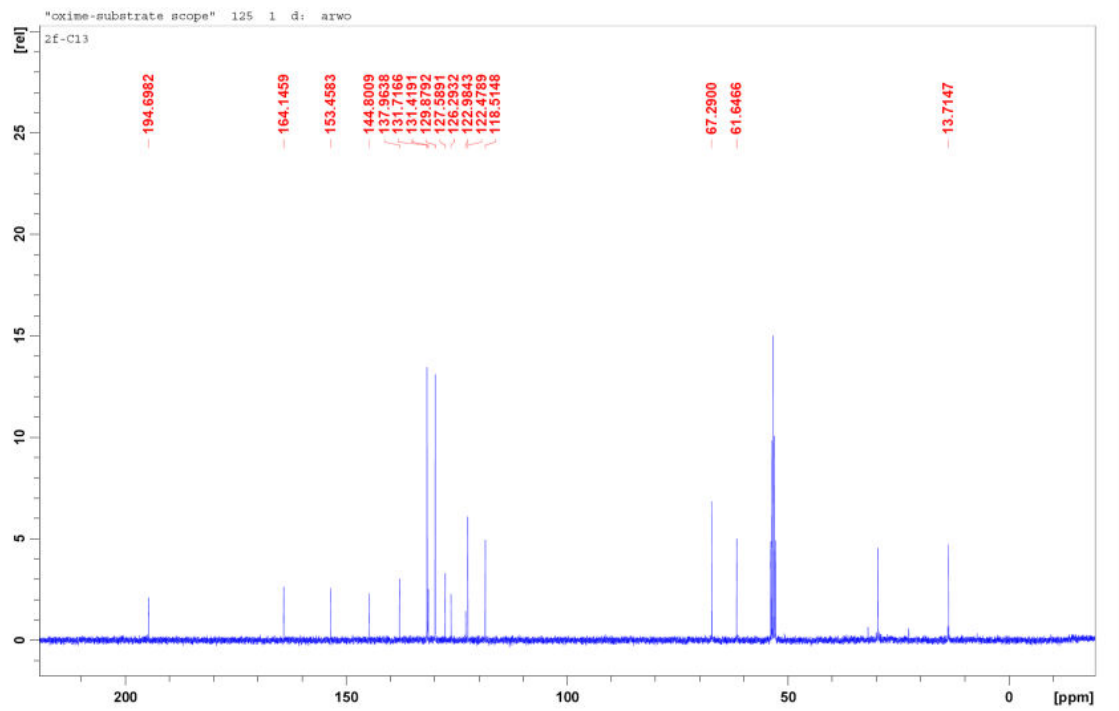

Figure A013 [1]H NMR spectrum of **3g**

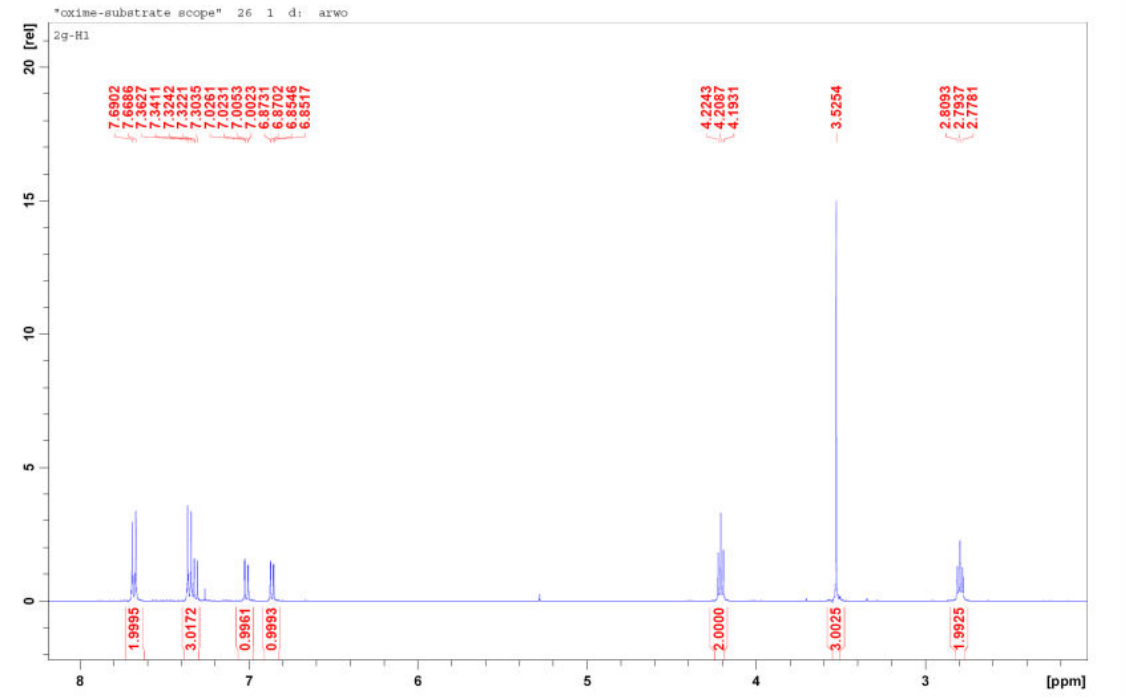

Figure A014 [13]C NMR spectrum of **3g**

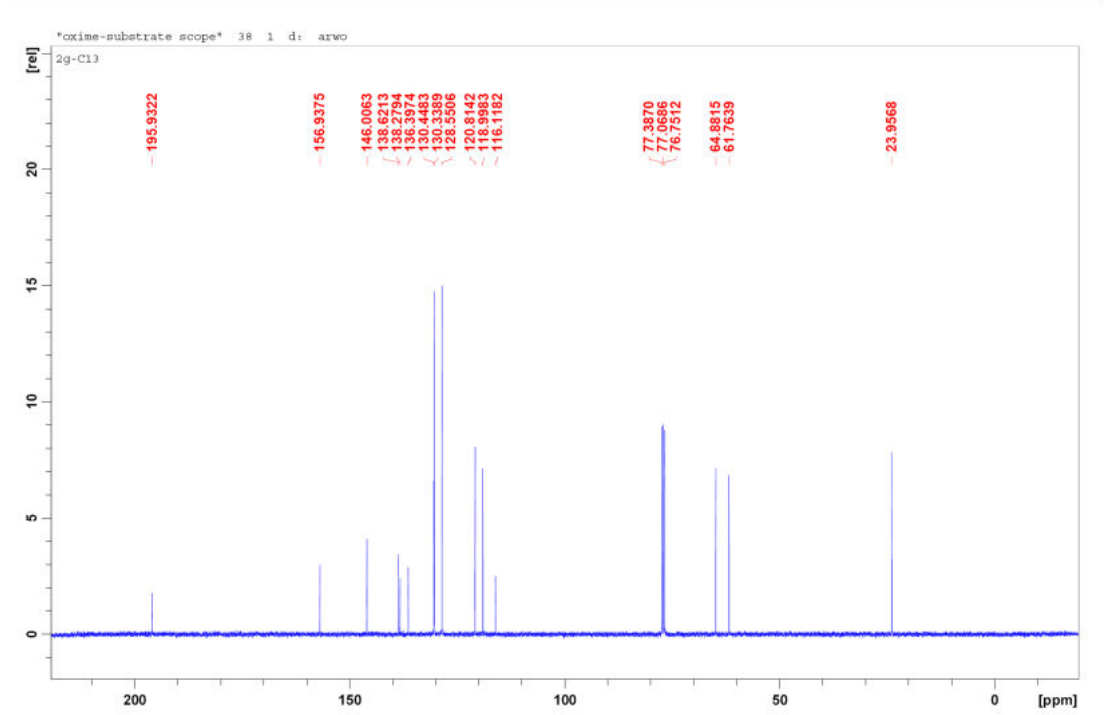

Figure A015 [1]H NMR spectrum of **3h**

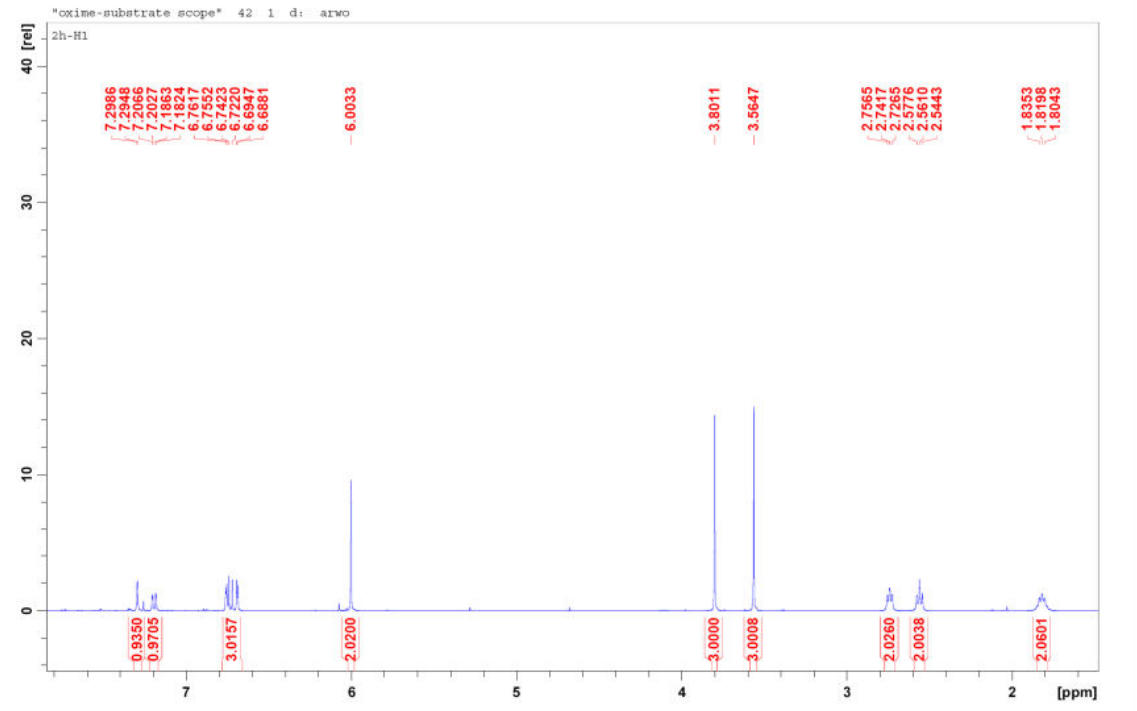

Figure A016 [13]C NMR spectrum of **3h**

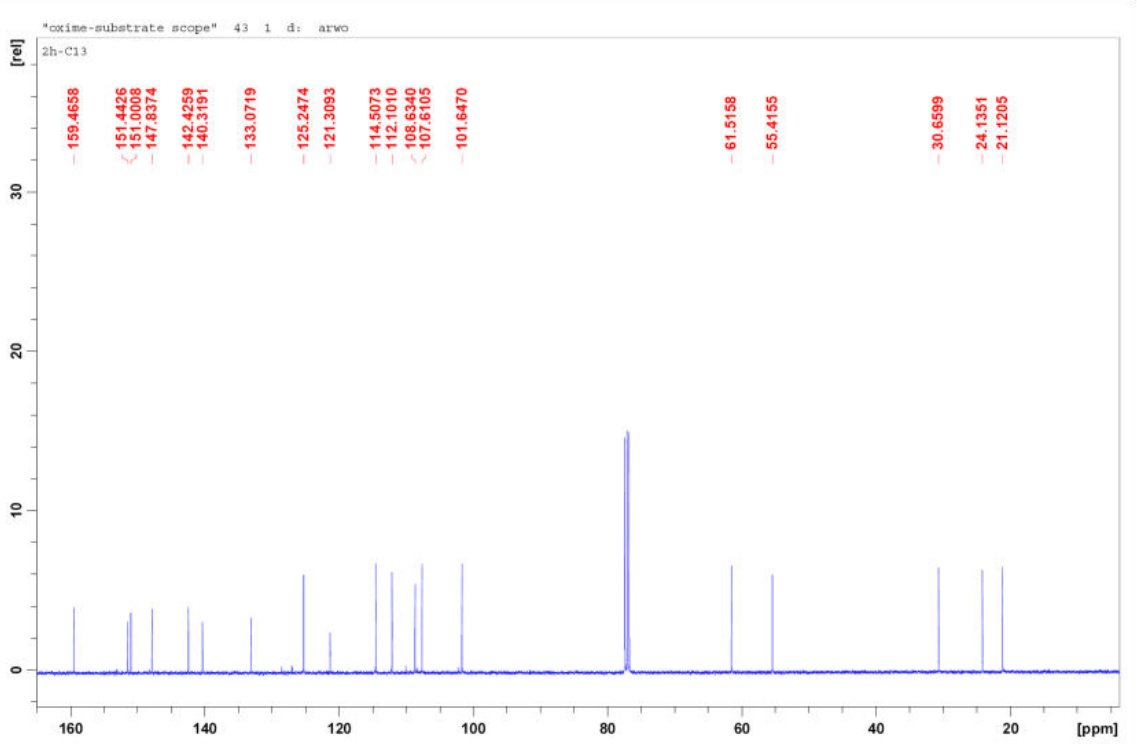

Figure A017 [1]H NMR spectrum of **3i**

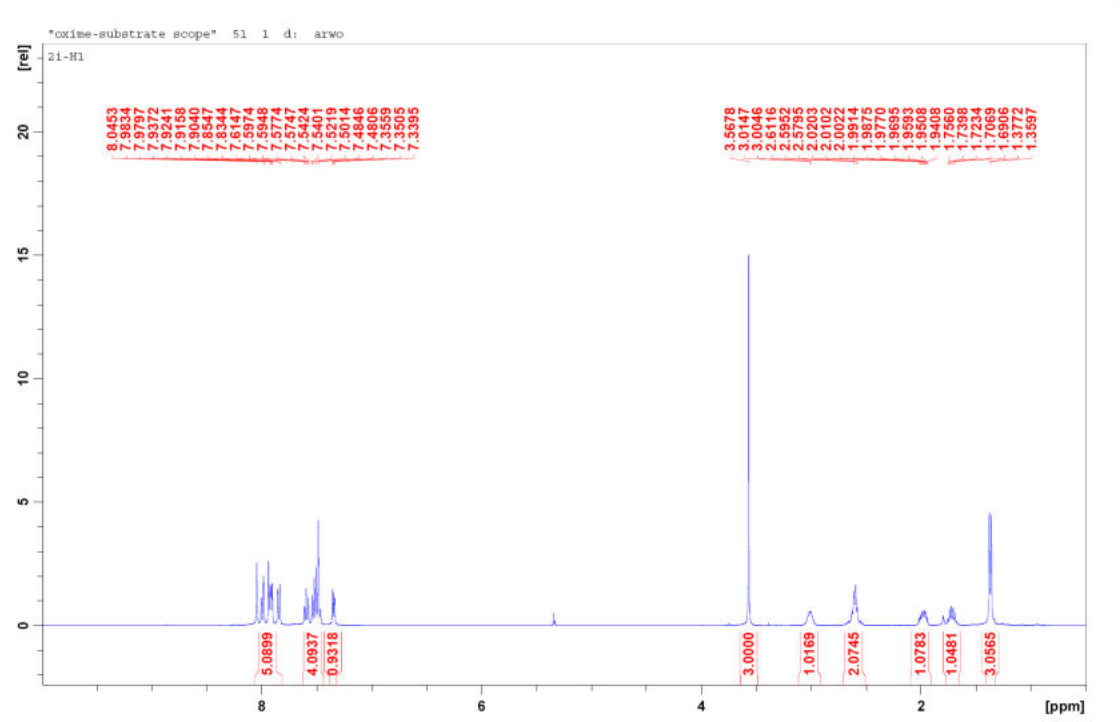

Figure A018 [13]C NMR spectrum of **3i**

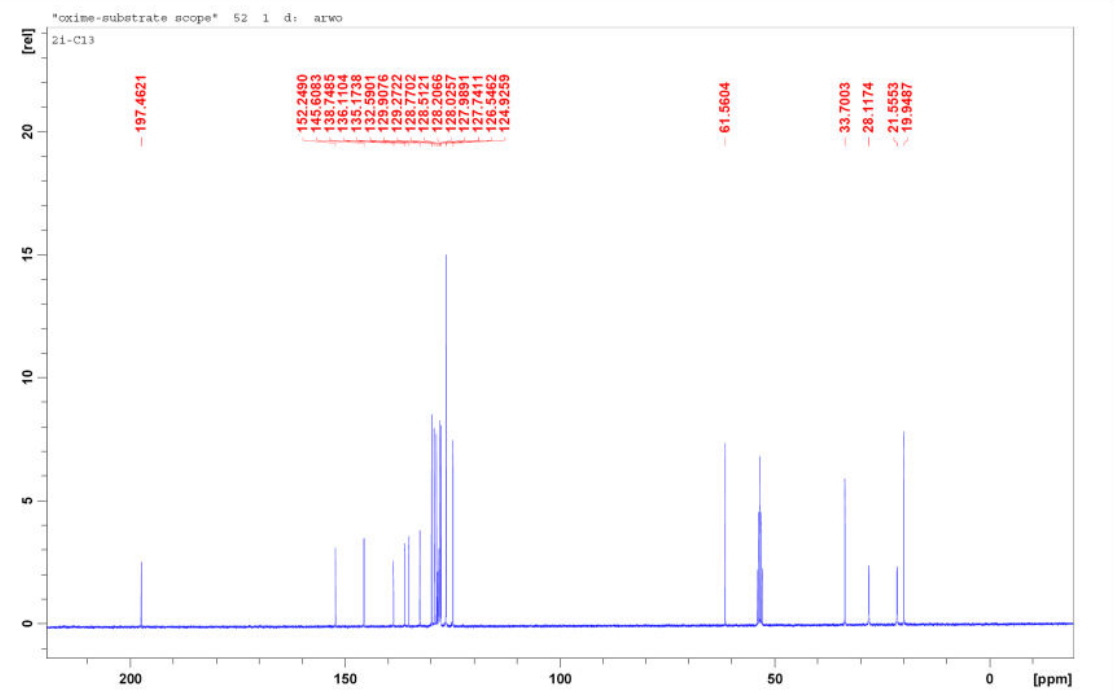

Figure A019 [1]H NMR spectrum of **3j**

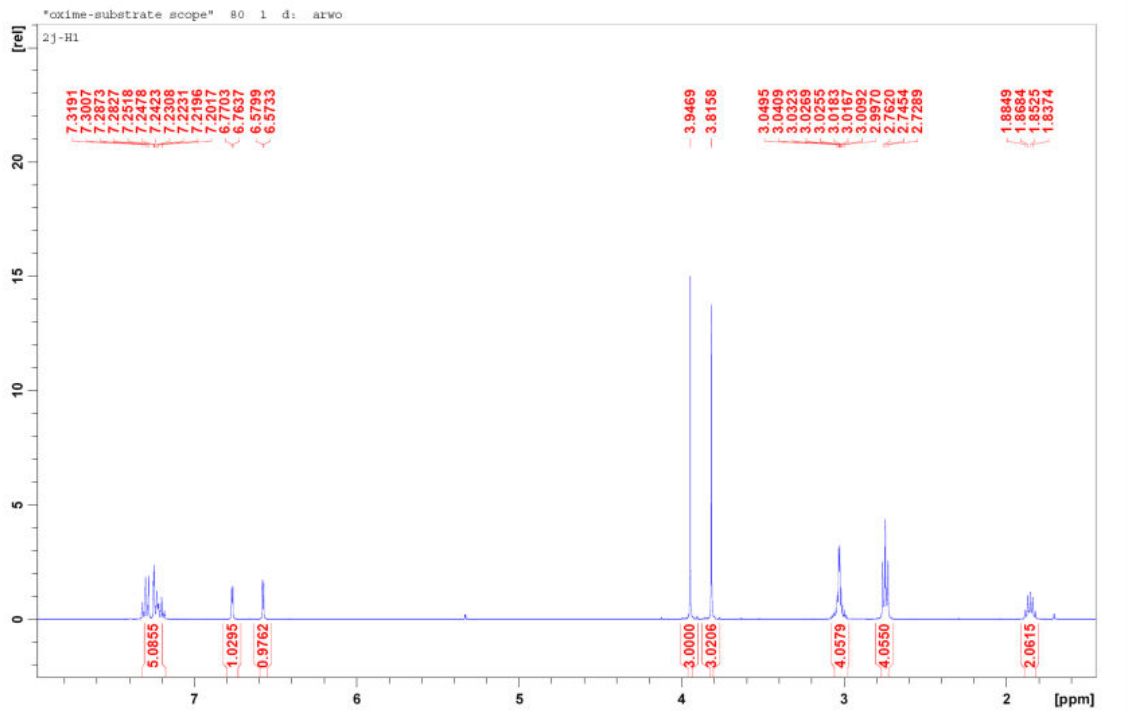

Figure A020 [13]C NMR spectrum of **3j**

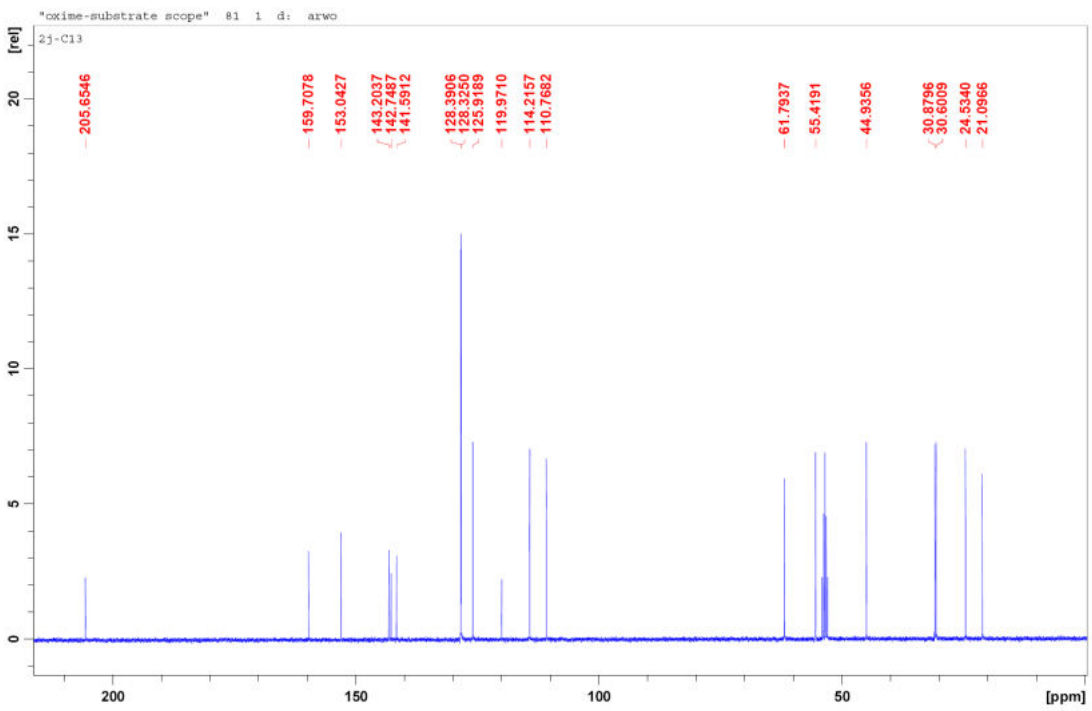

Figure A021 [1]H NMR spectrum of **3k**

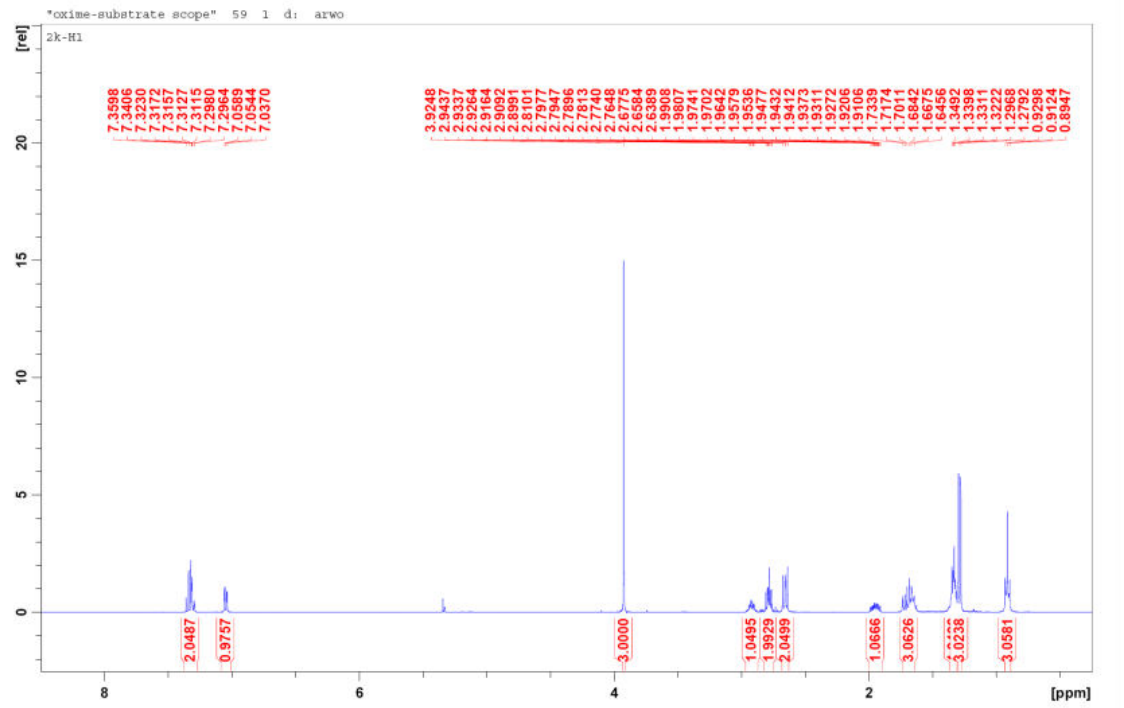

Figure A022 [13]C NMR spectrum of **3k**

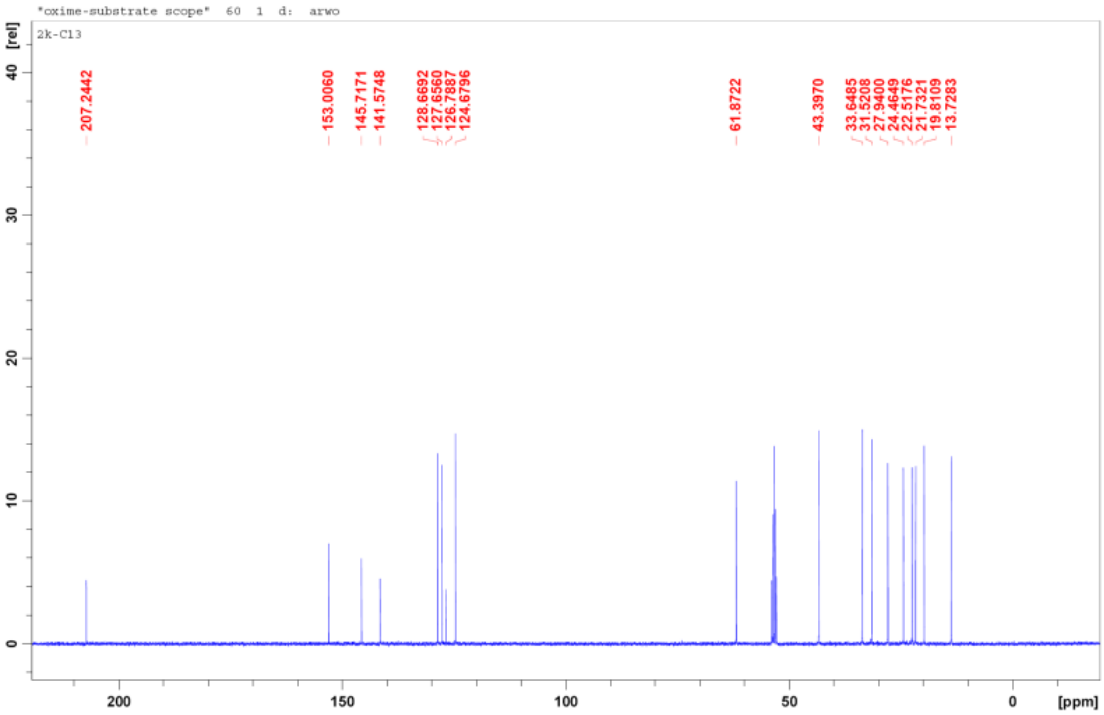

Figure A023 [1]H NMR spectrum of **3l**

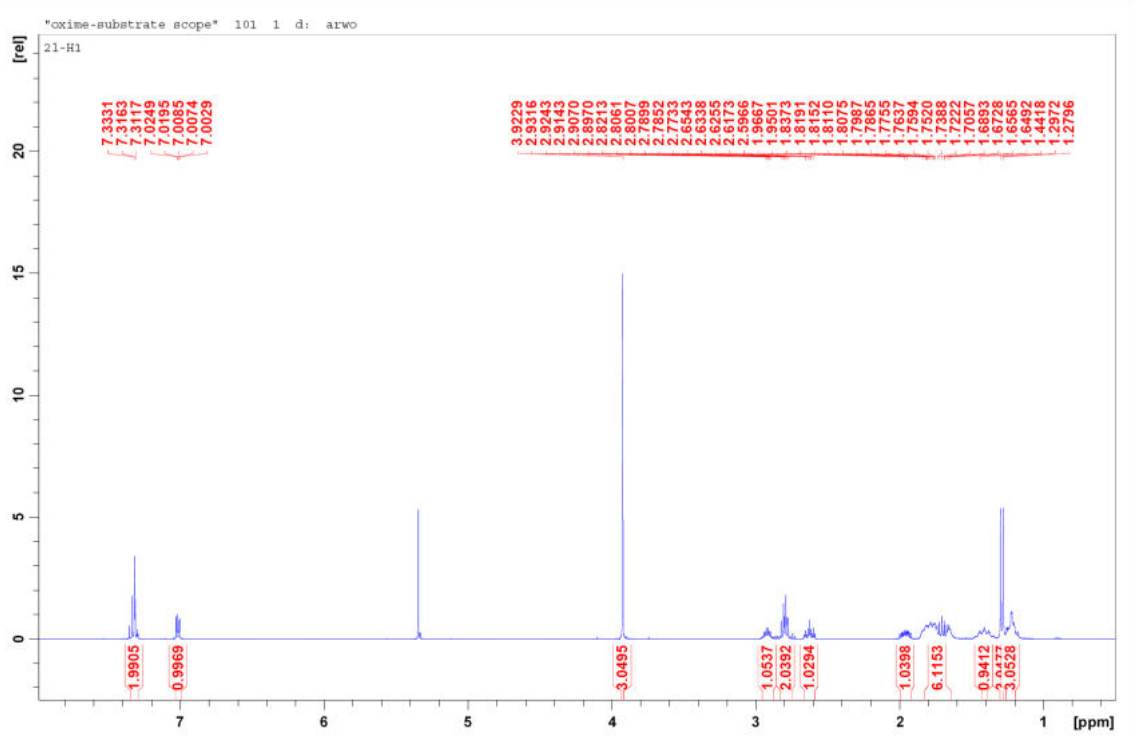

Figure A024 [13]C NMR spectrum of **3l**

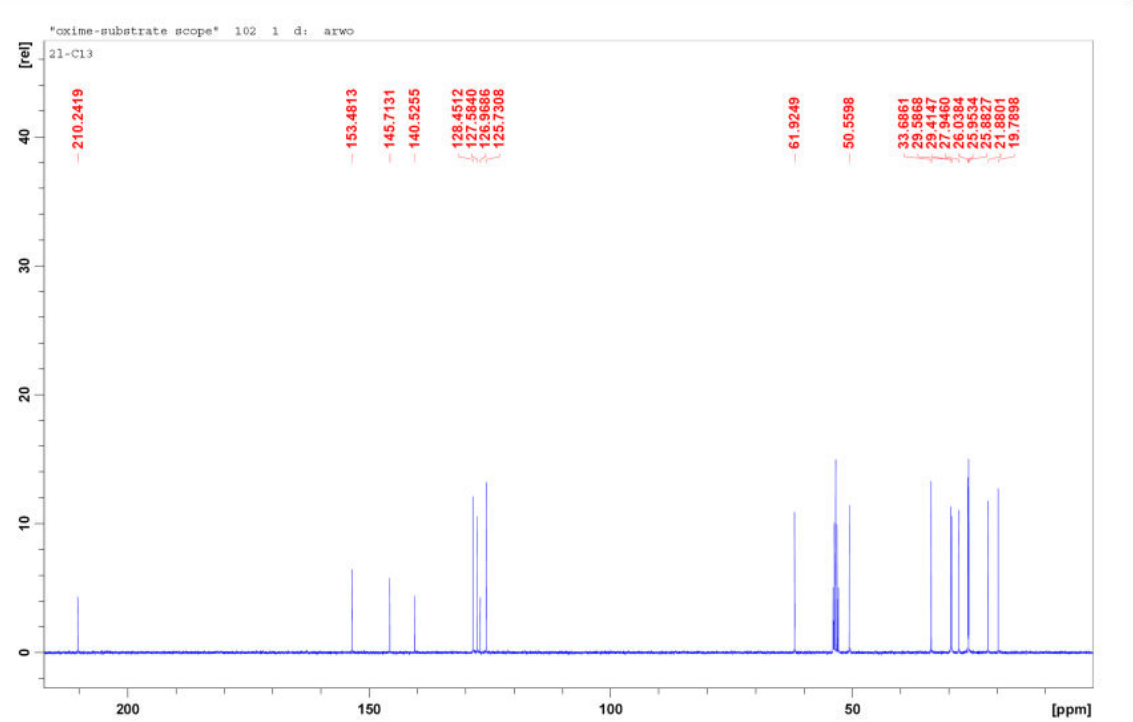

Figure A025 [1]H NMR spectrum of **3m**

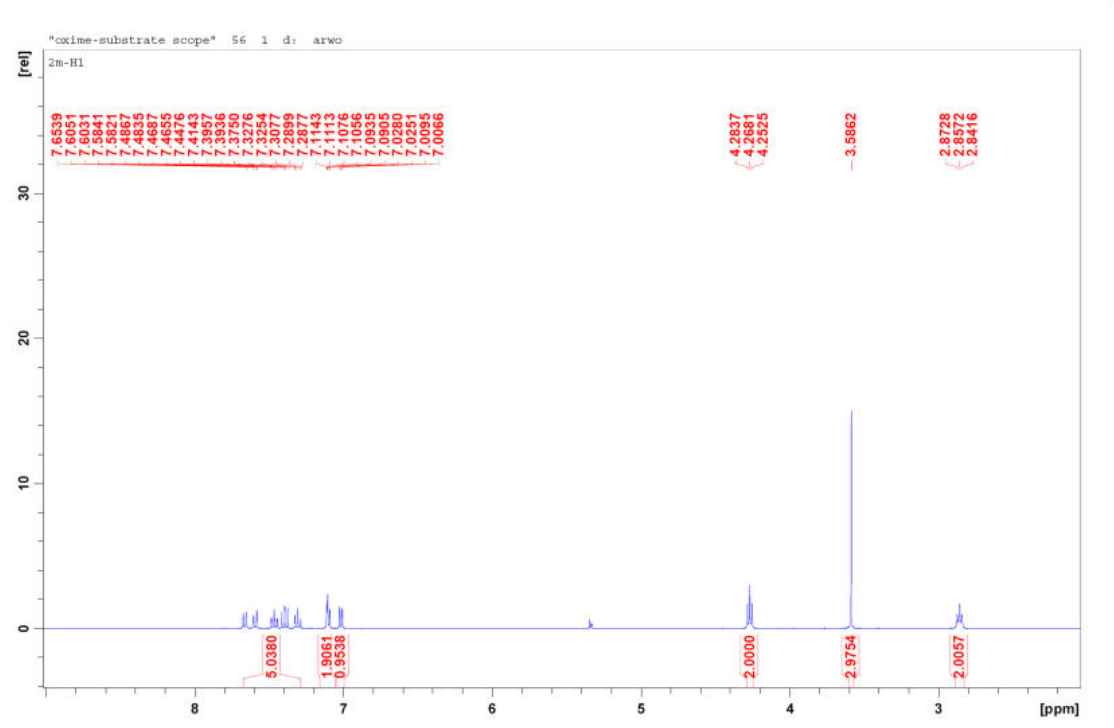

Figure A026 [13]C NMR spectrum of **3m**

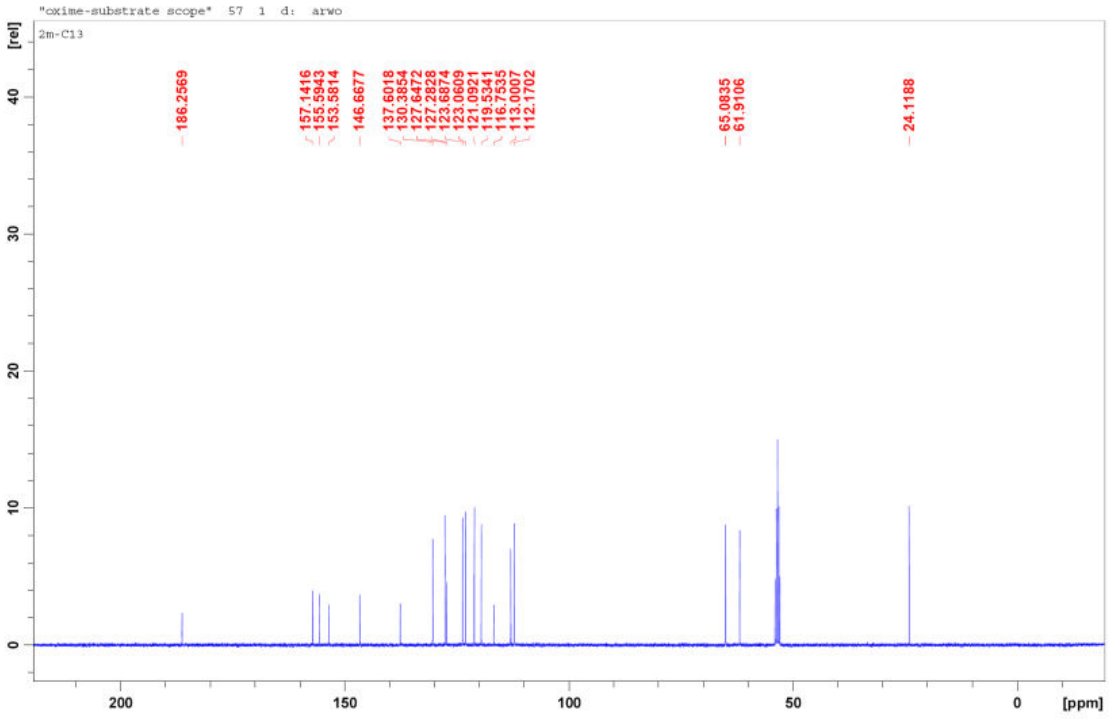

Figure A027 [1]H NMR spectrum of **3n**

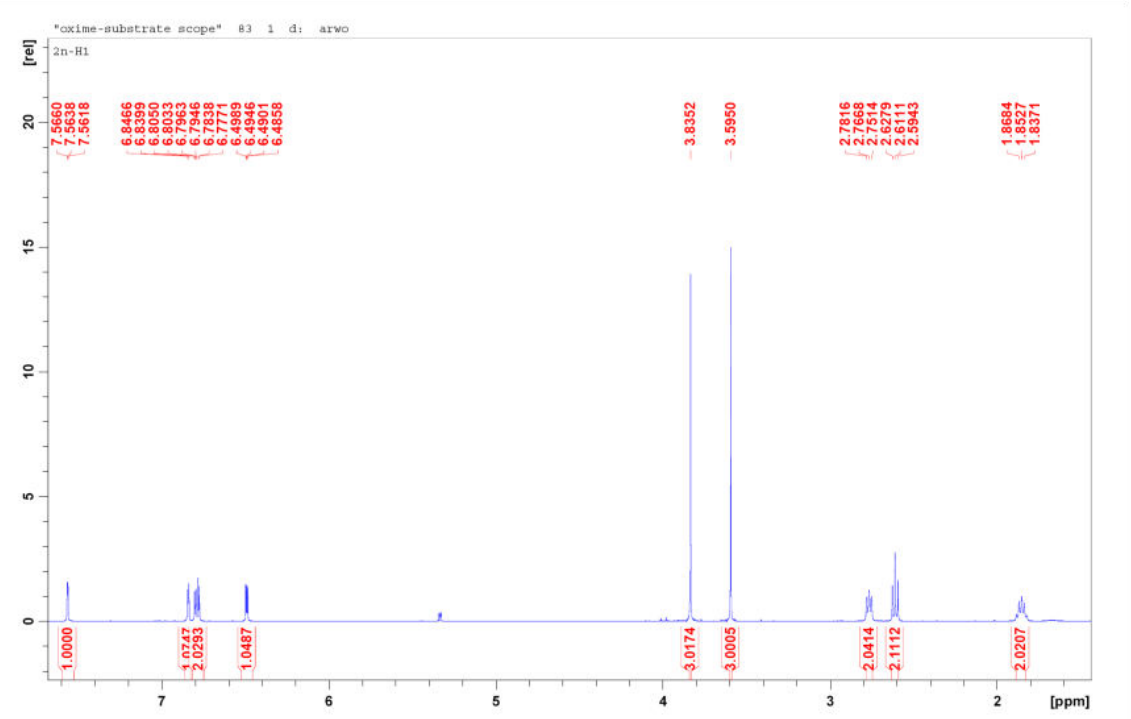

Figure A028 [13]C NMR spectrum of **3n**

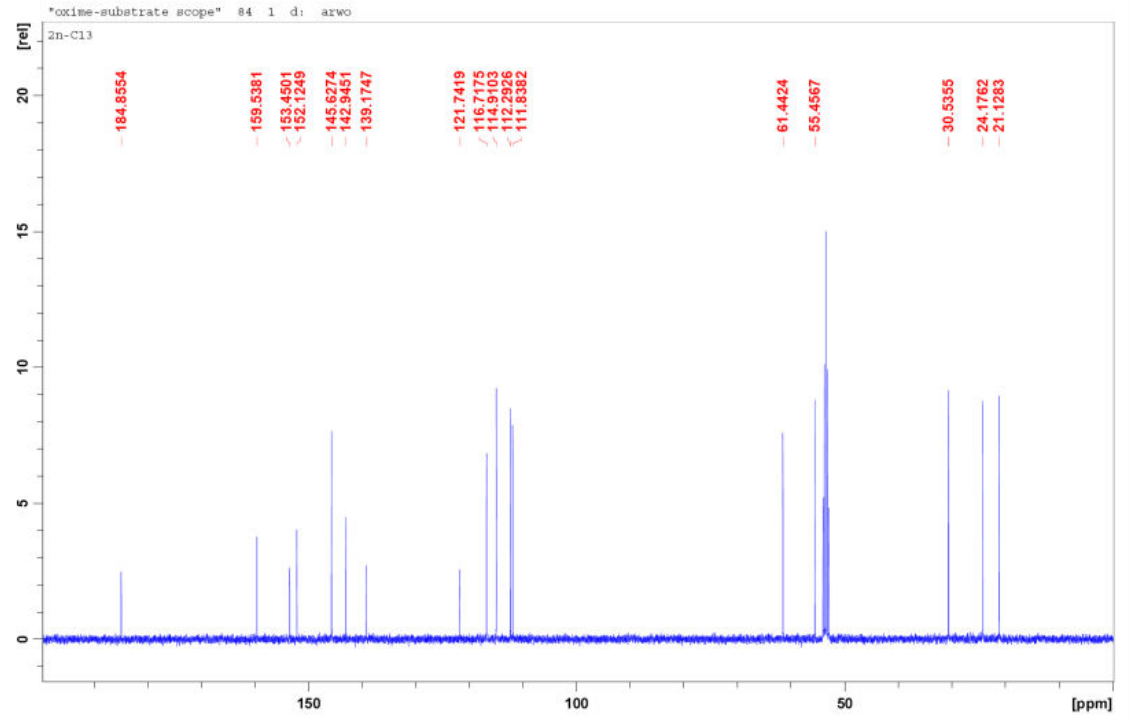

Figure A029 [1]H NMR spectrum of **3o**

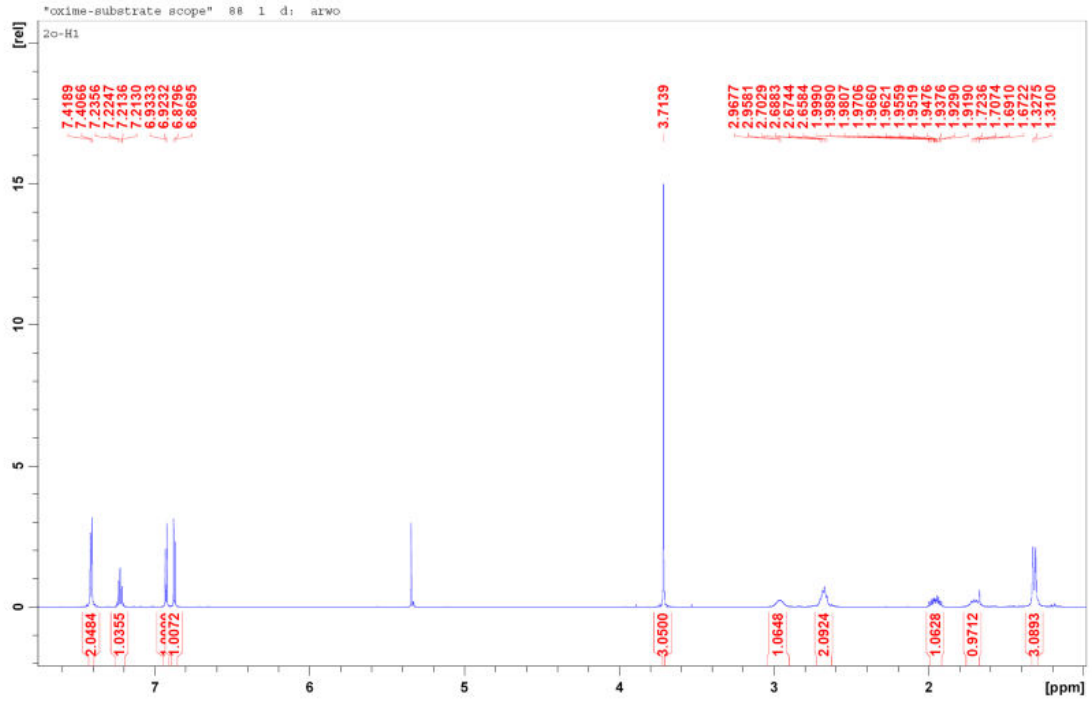

Figure A030 [13]C NMR spectrum of **3o**

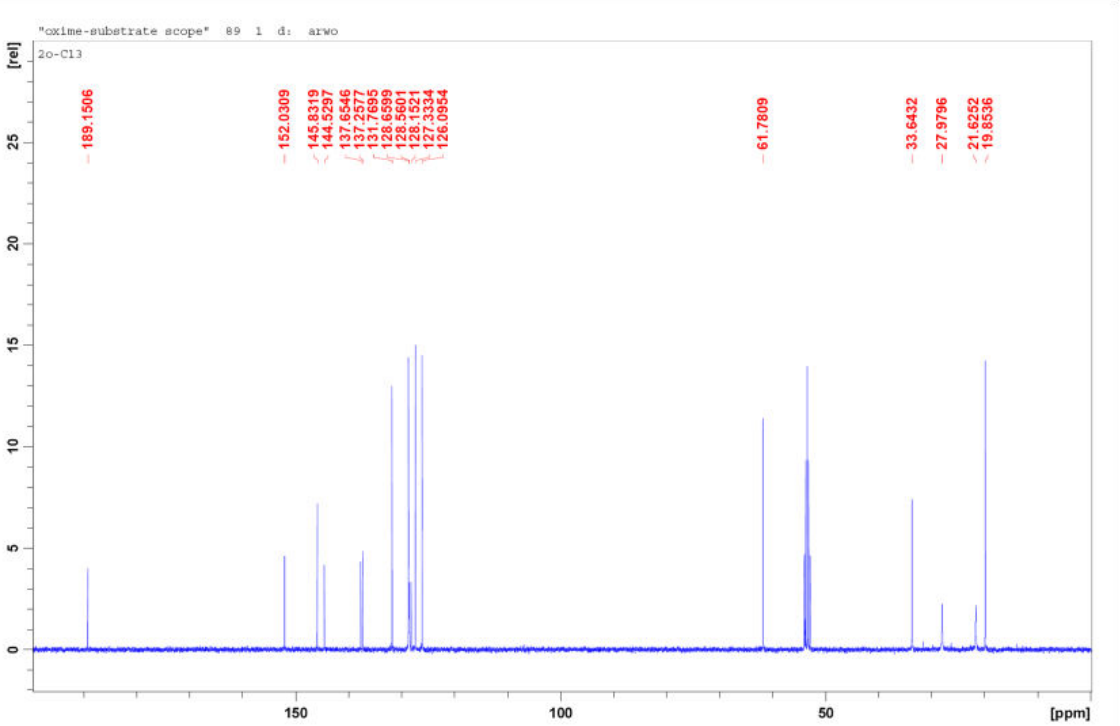

Figure A031 [1]H NMR spectrum of **3p**

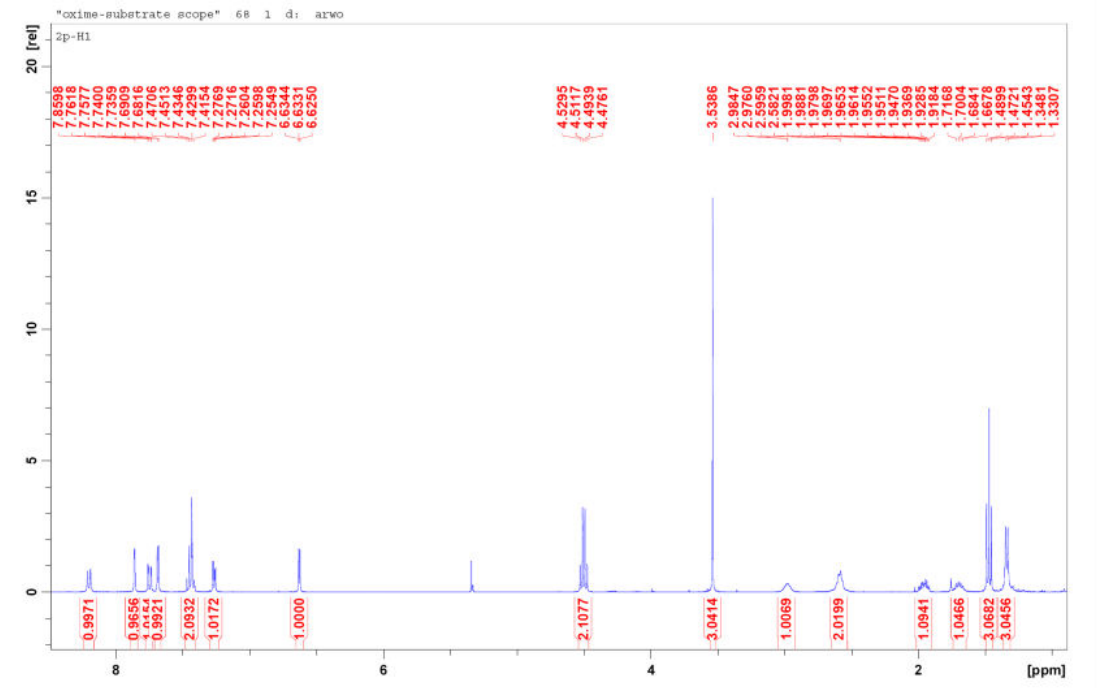

Figure A032 [13]C NMR spectrum of **3p**

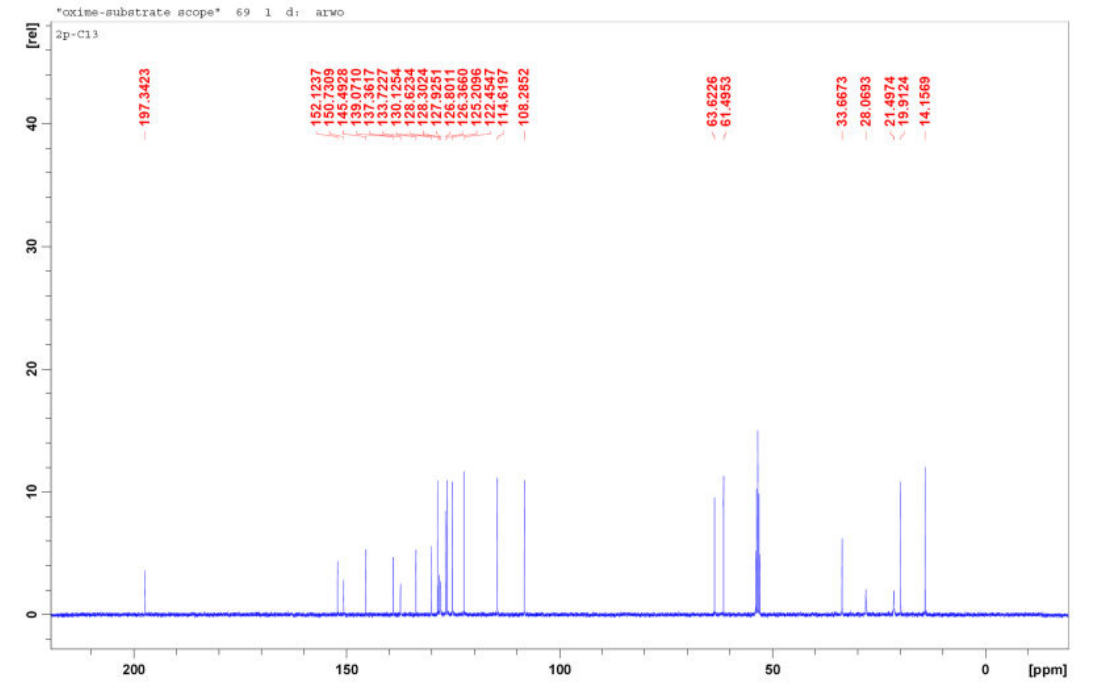

Figure A033 [1]H NMR spectrum of **3q**

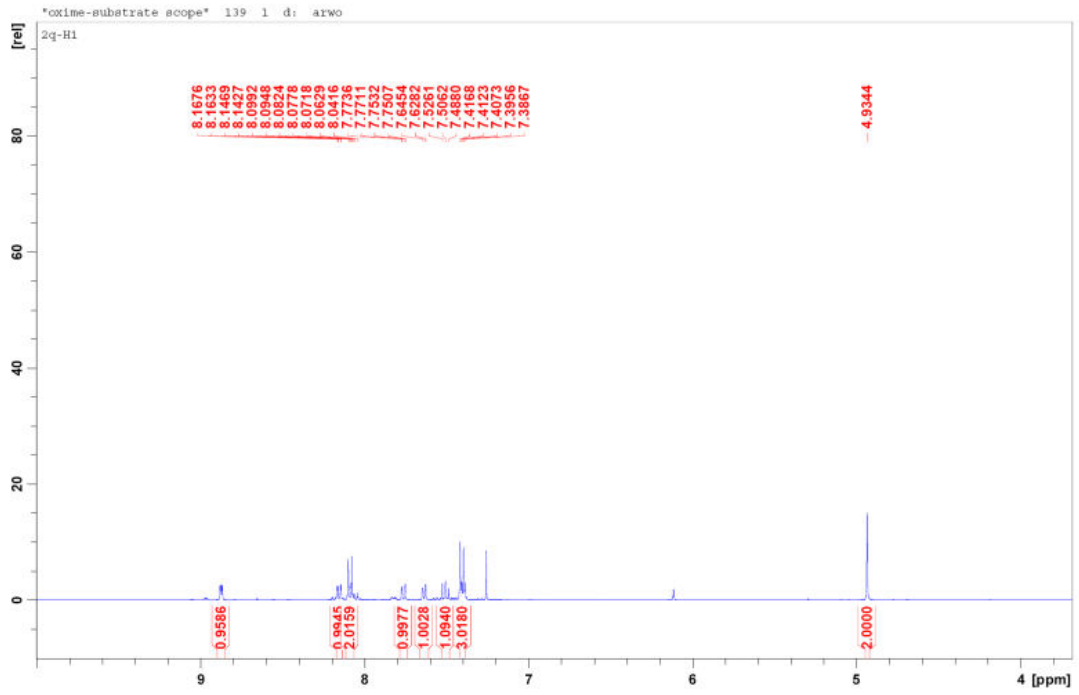

Figure A034 [13]C NMR spectrum of **3q**

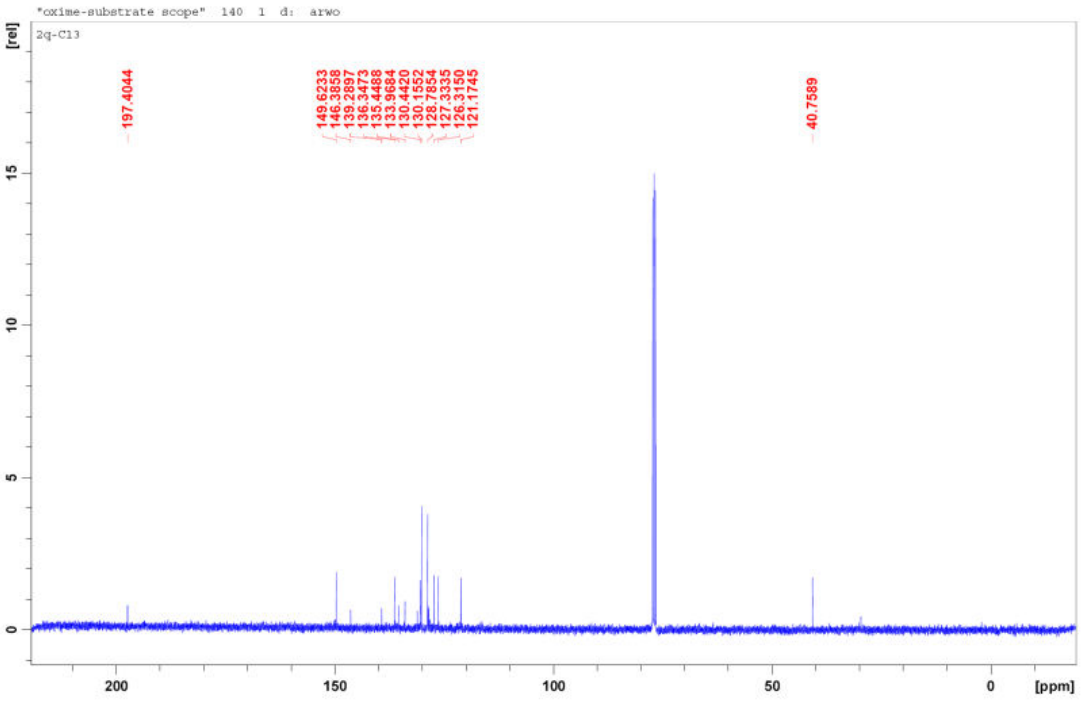

Figure A035 ^{1}H NMR spectrum of **4a**

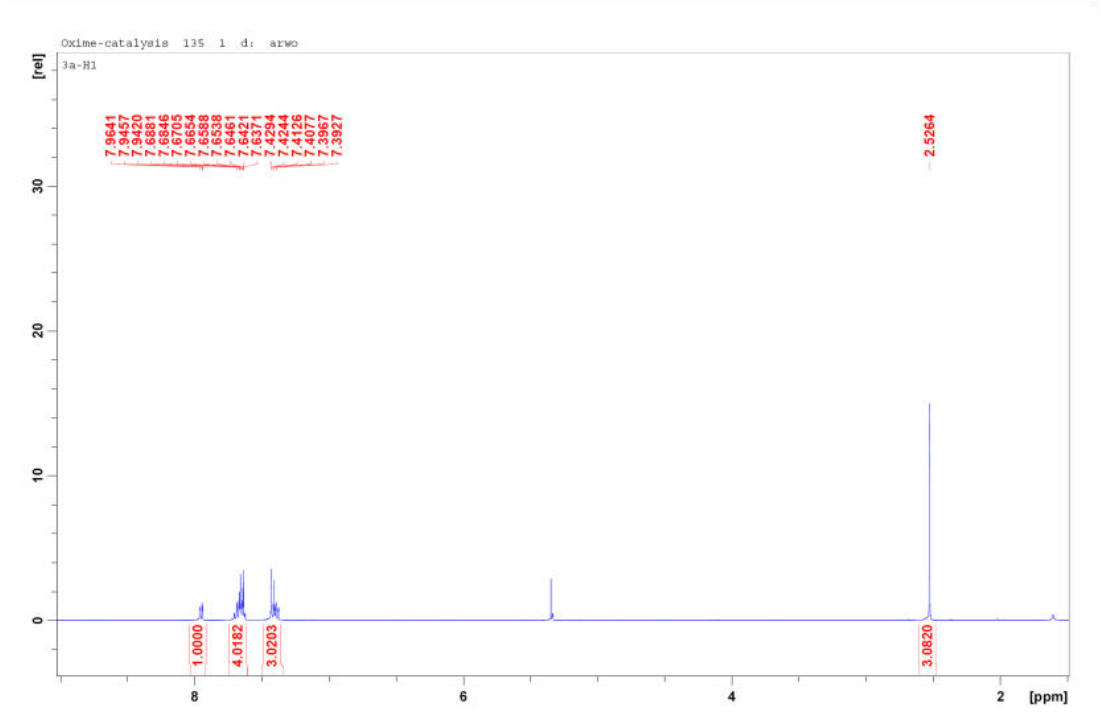

Figure A036 ^{13}C NMR spectrum of **4a**

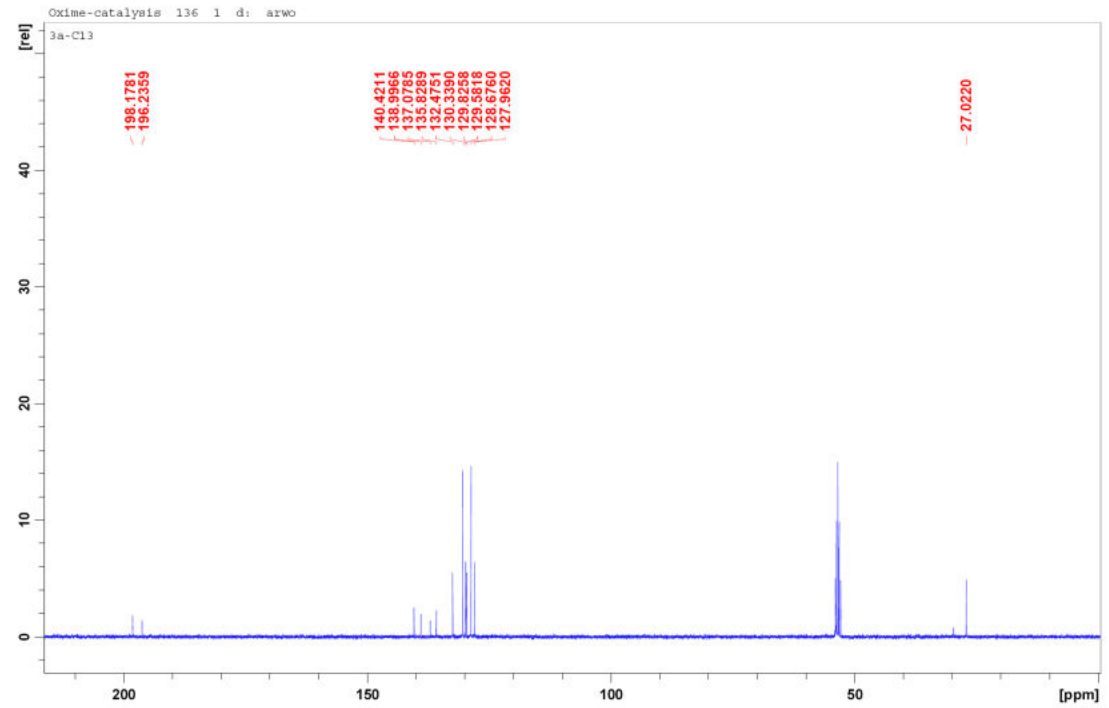

Figure A037 [1]H NMR spectrum of **4c**

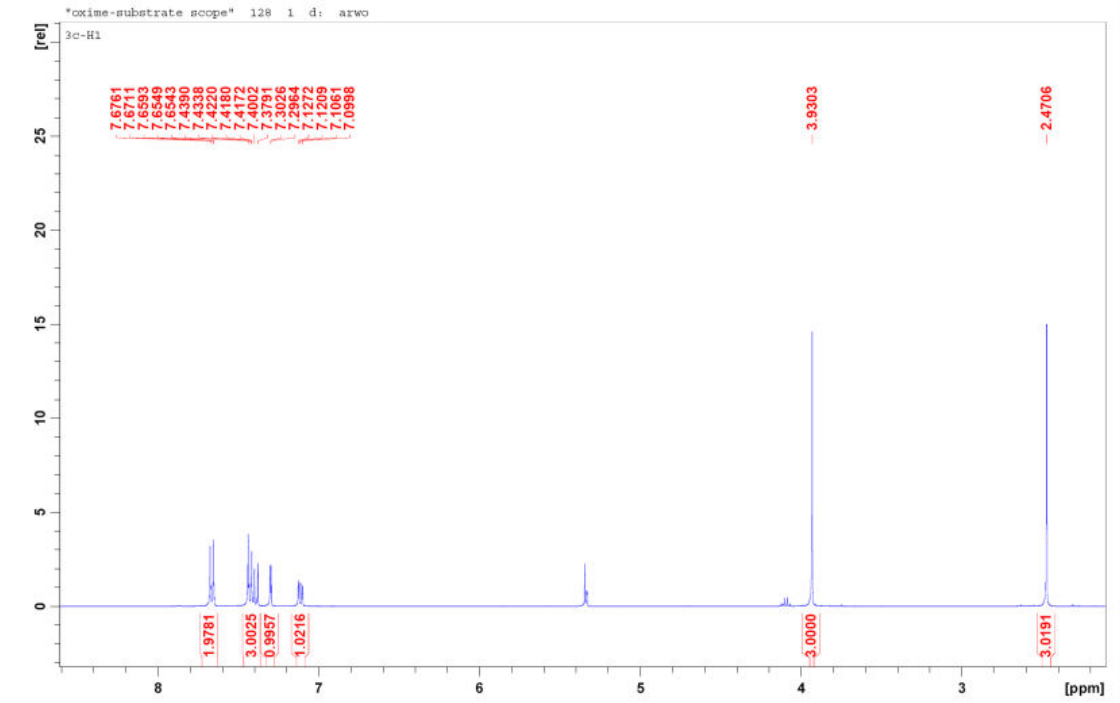

Figure A038 [13]C NMR spectrum of **4c**

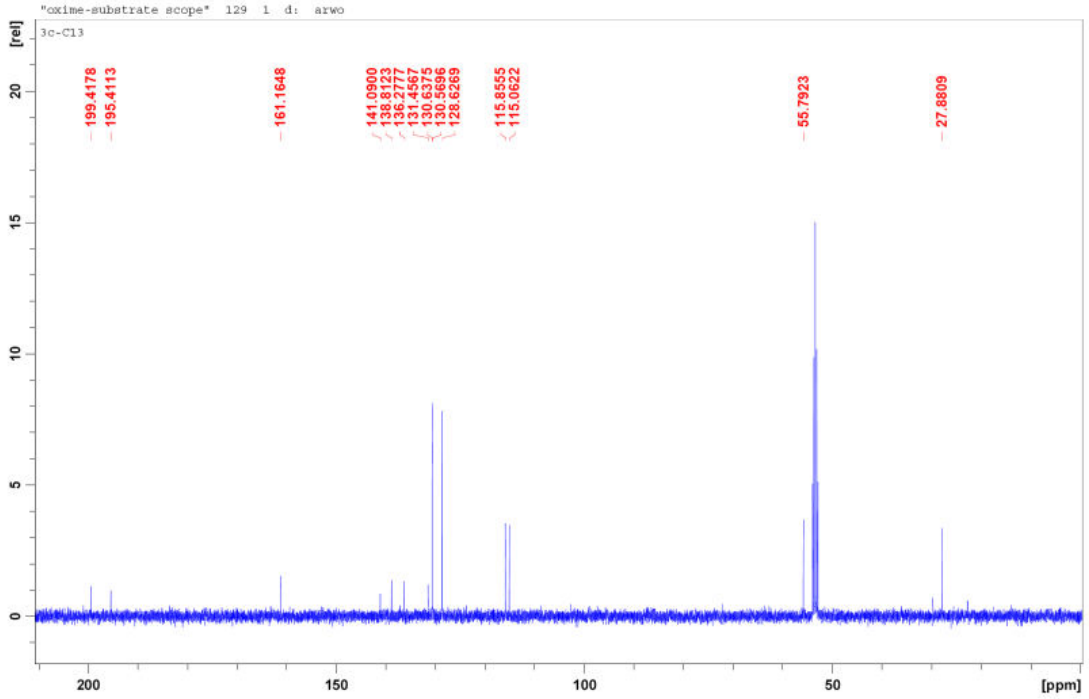

Figure A039 [1]H NMR spectrum of **4o**

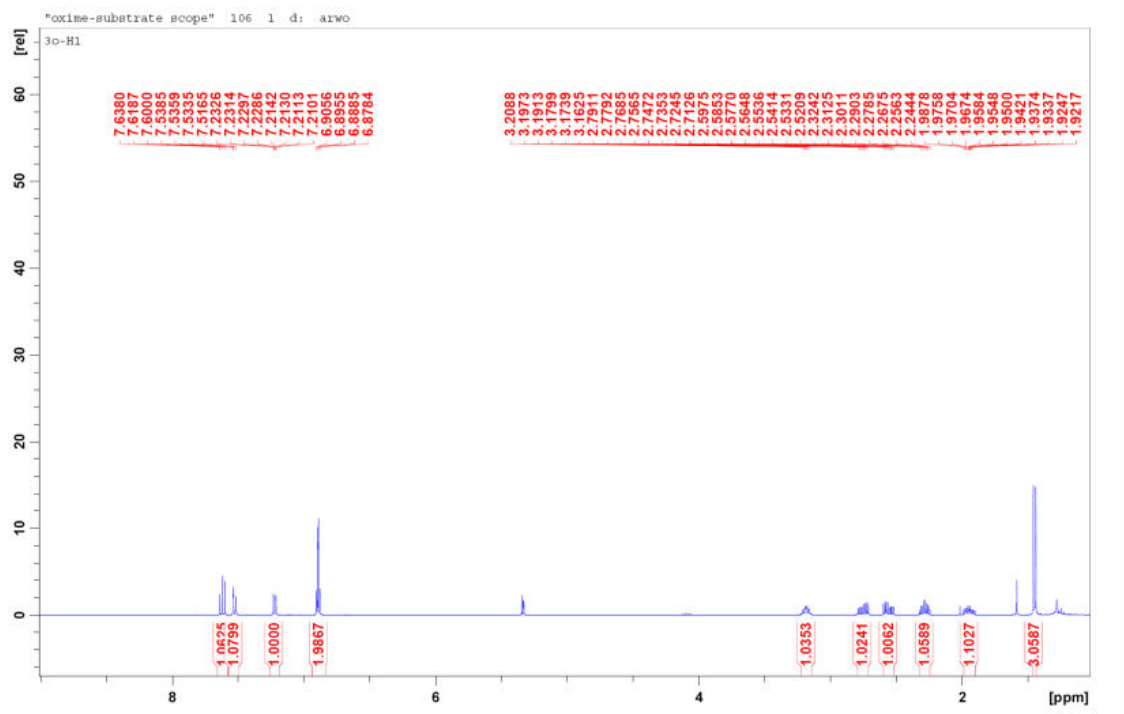

Figure A040 [13]C NMR spectrum of **4o**

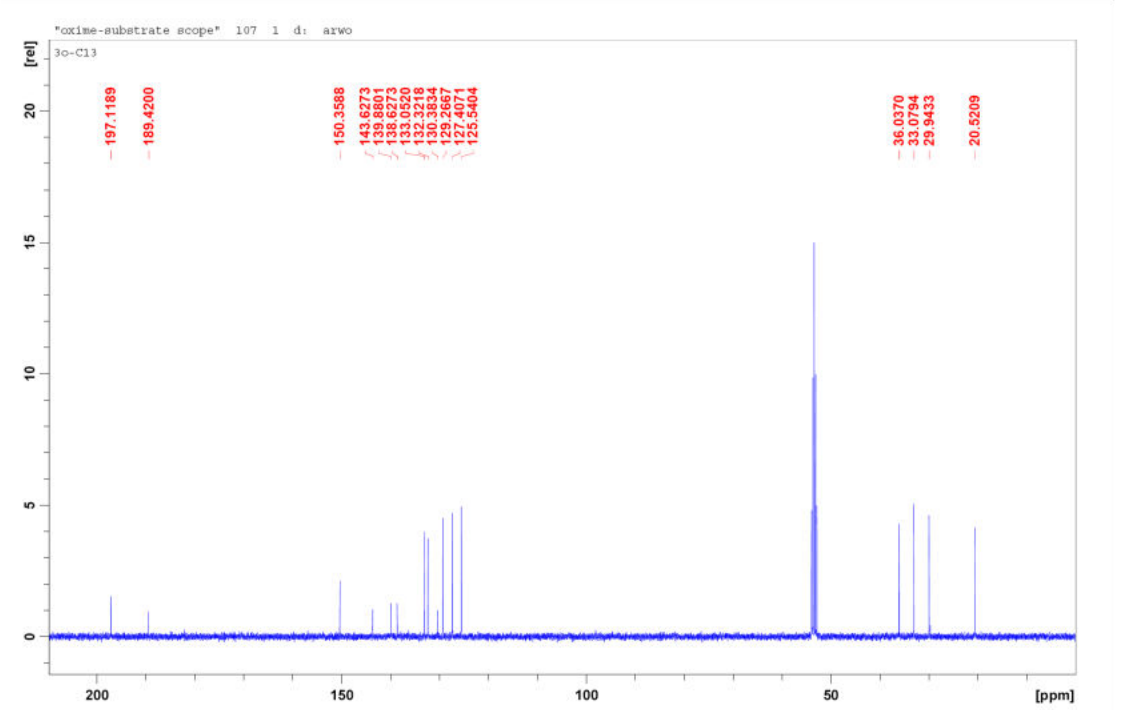

Figure A041 [1]H NMR spectrum of **5a**

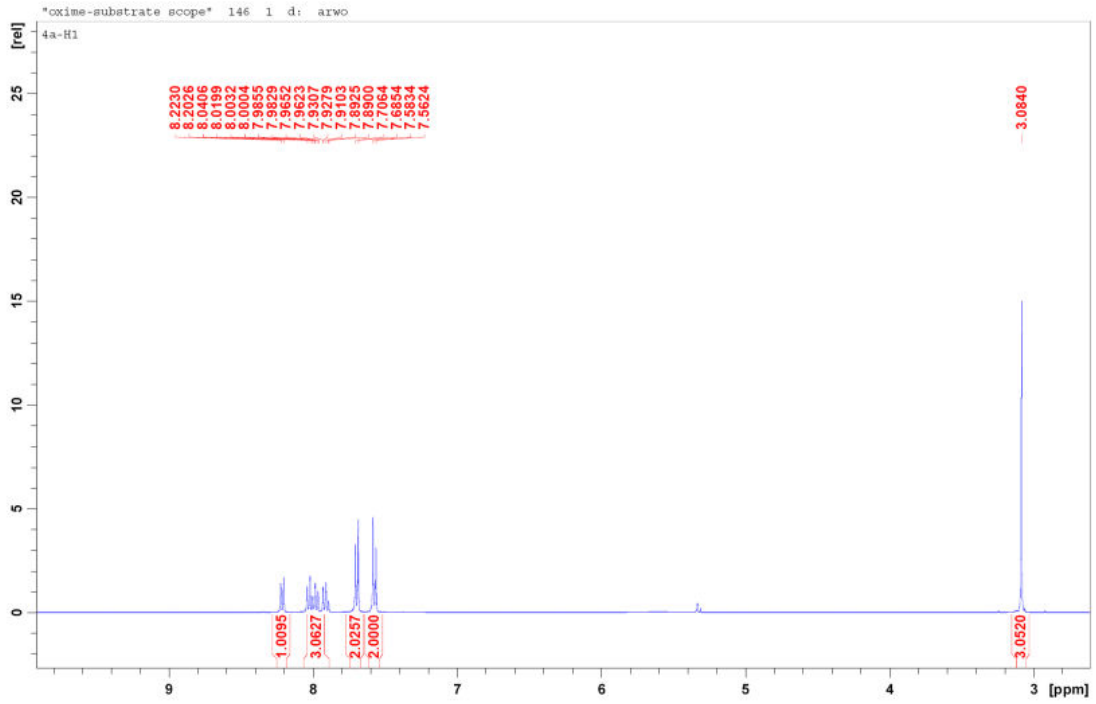

Figure A042 [13]C NMR spectrum of **5a**

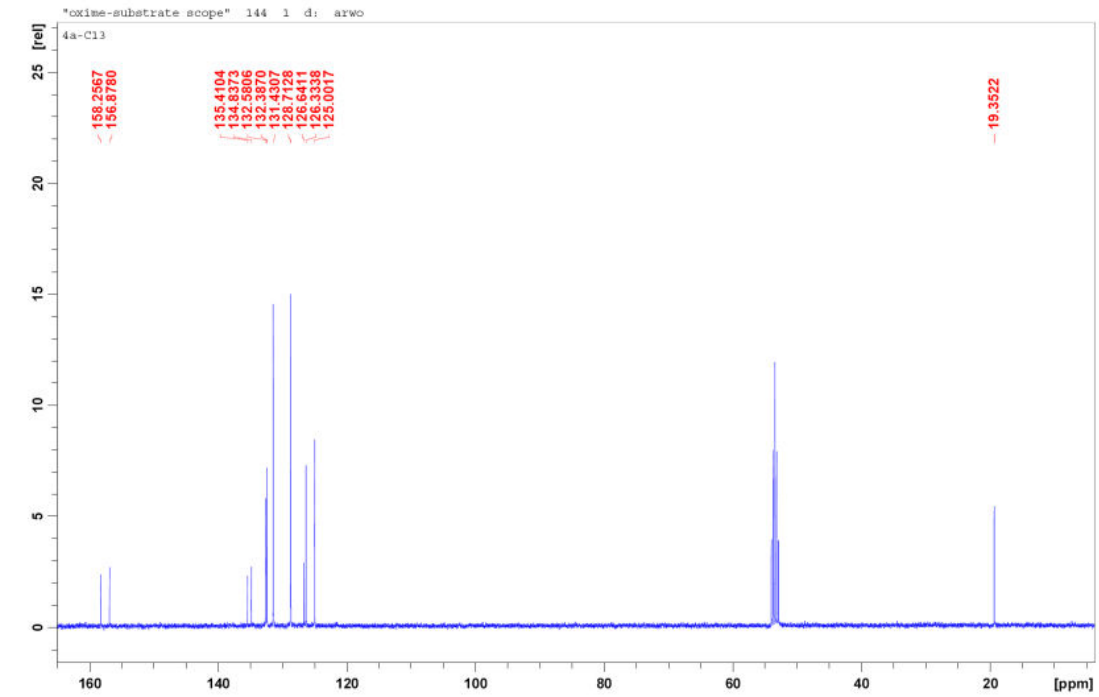

Figure A043 [1]H NMR spectrum of **5c**

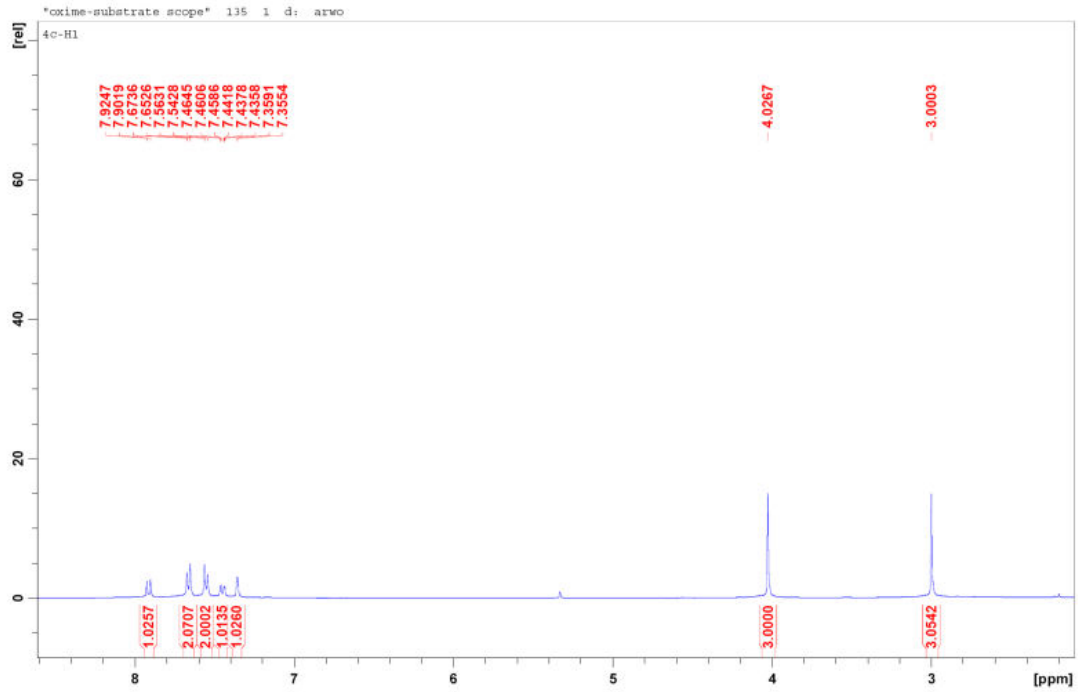

Figure A044 [13]C NMR spectrum of **5c**

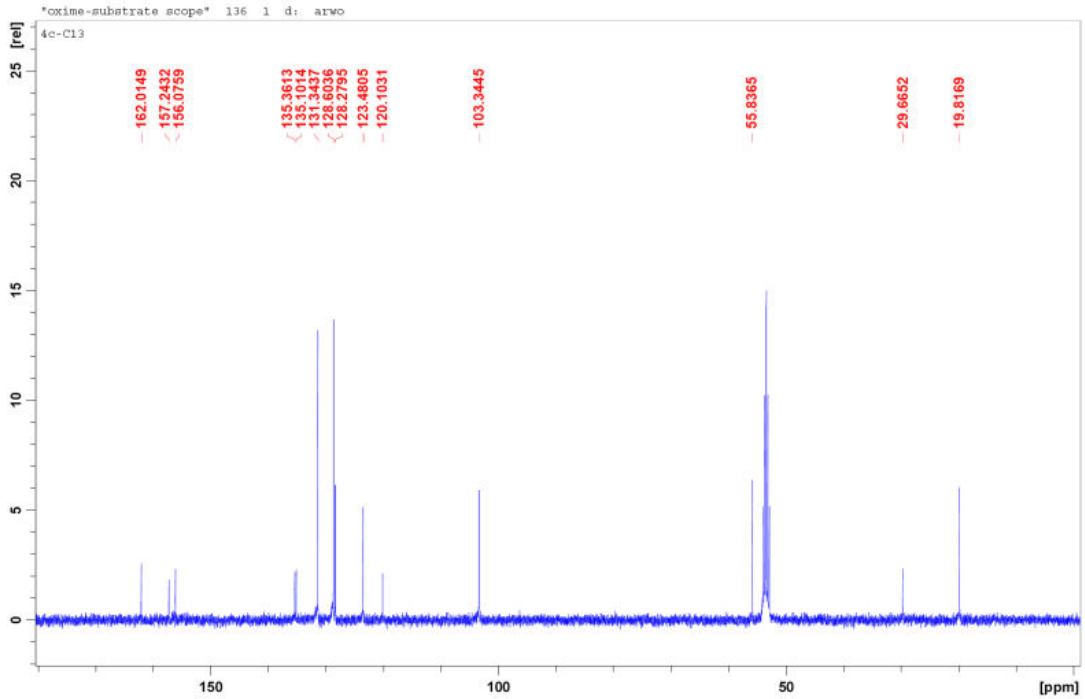

Figure A045 [1]H NMR spectrum of **5o**

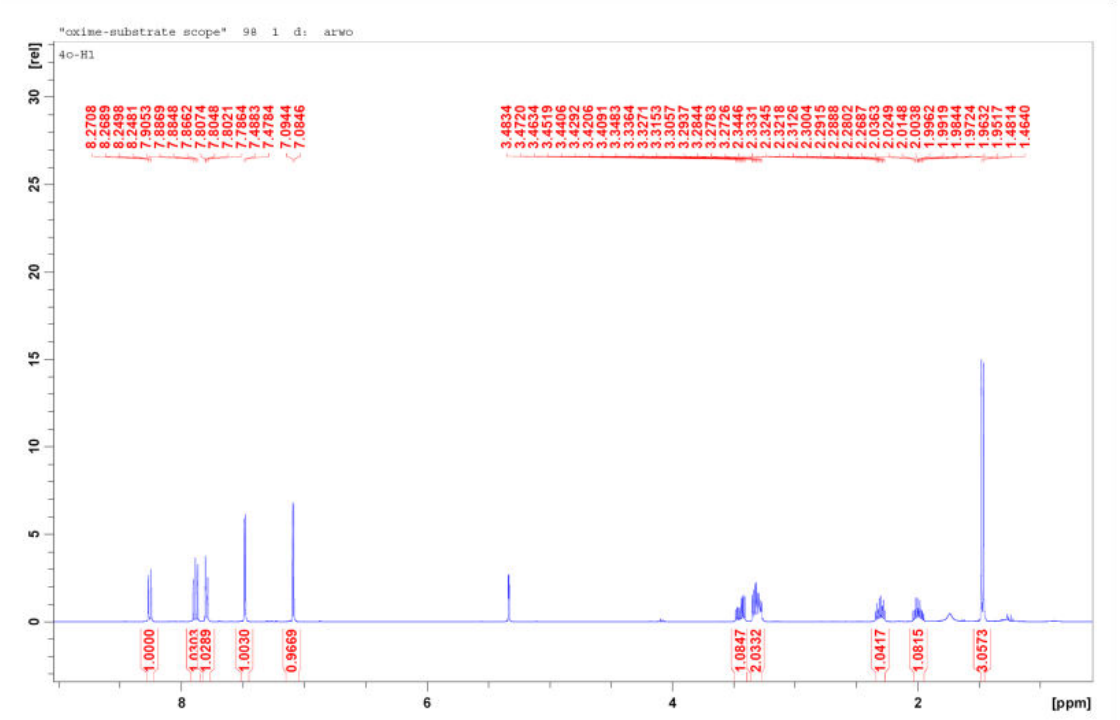

Figure A046 [13]C NMR spectrum of **5o**

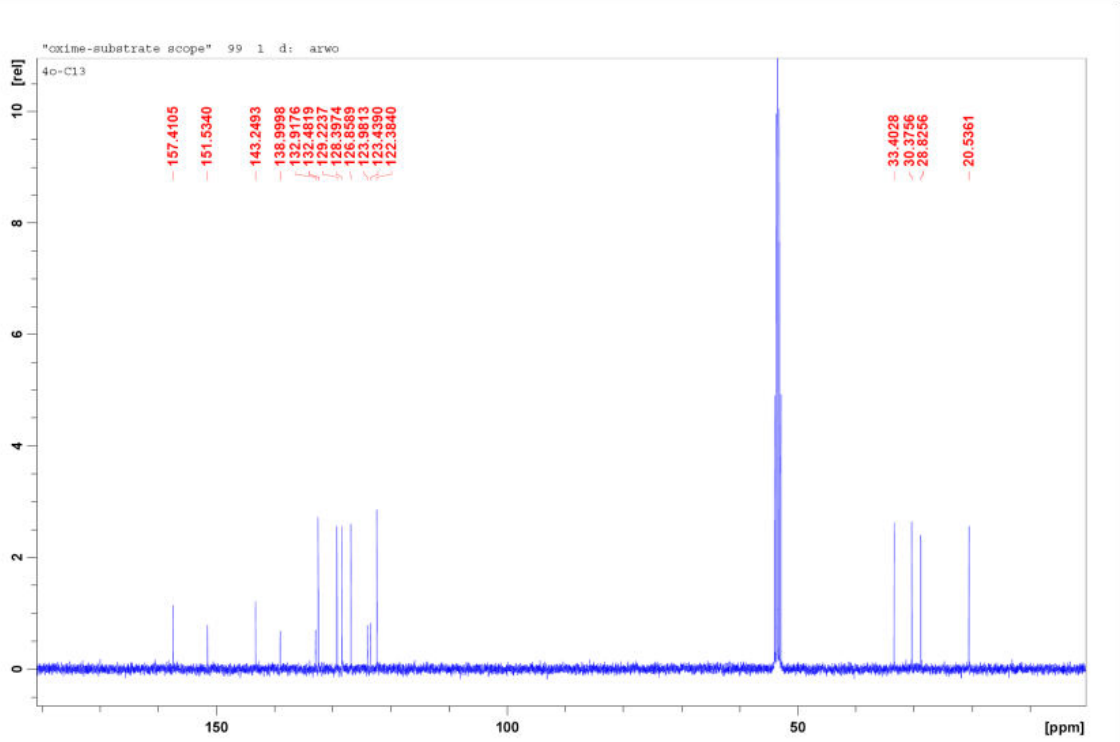

CHAPTER 3

Figure A047 [1]H NMR spectrum of **7a**

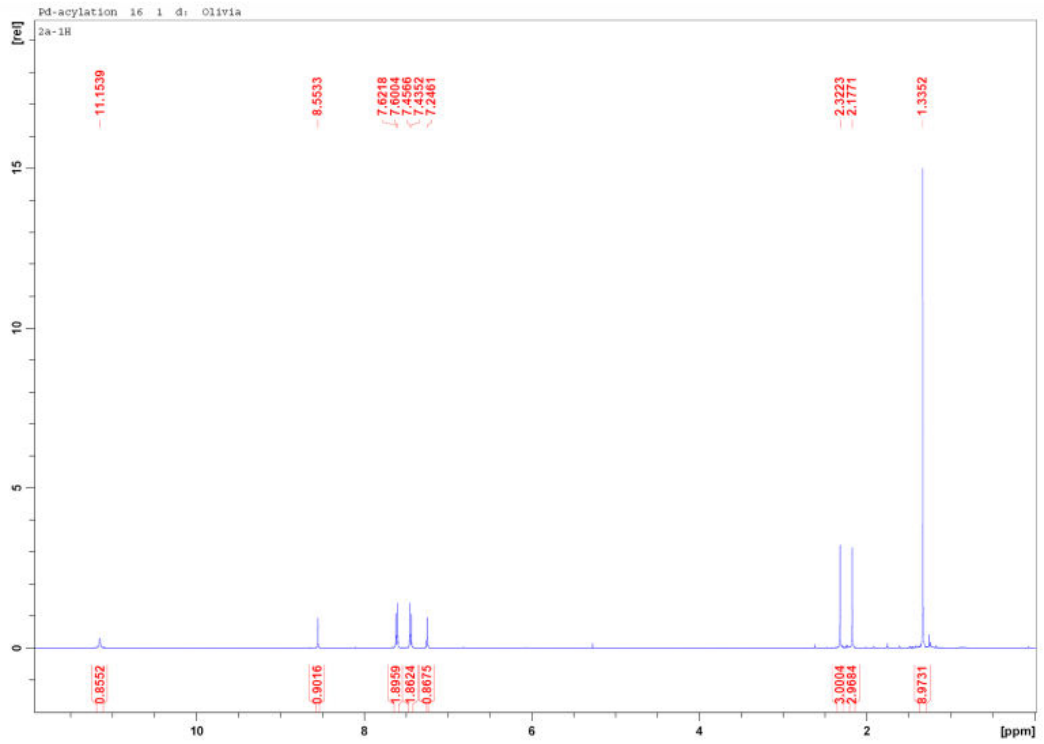

Figure A048 [13]C NMR spectrum of **7a**

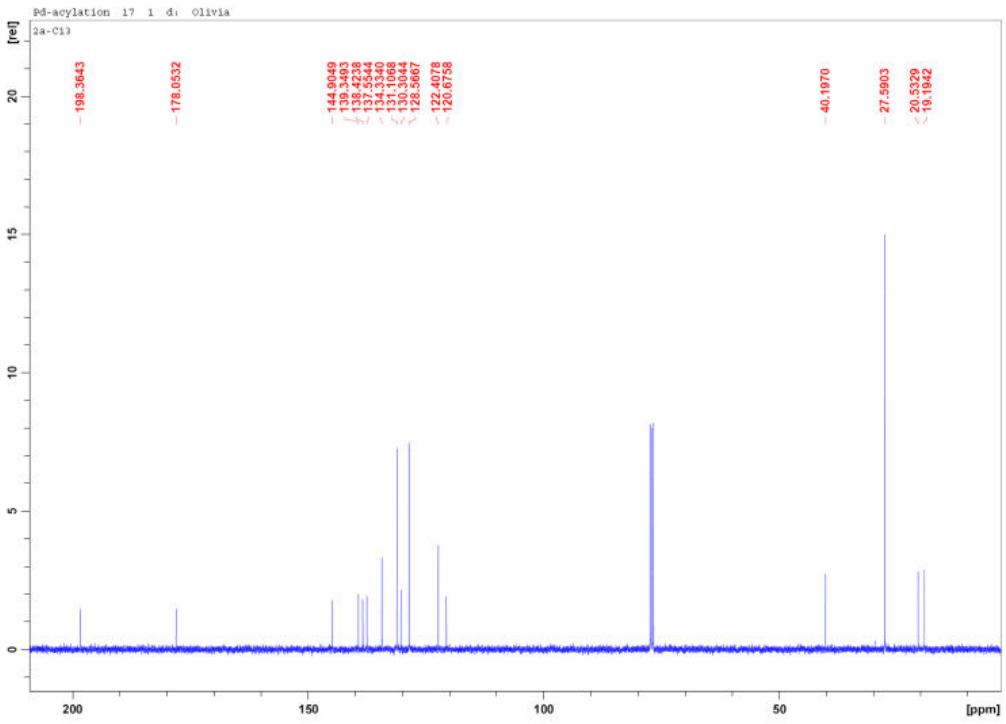

Figure A049 [1]H NMR spectrum of **7b**

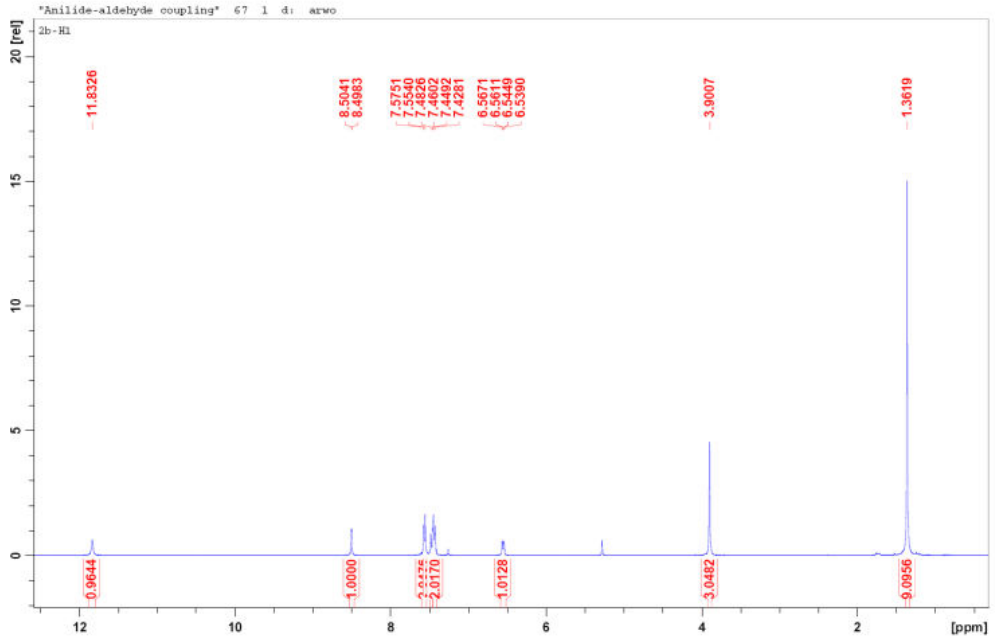

Figure A050 [13]C NMR spectrum of **7b**

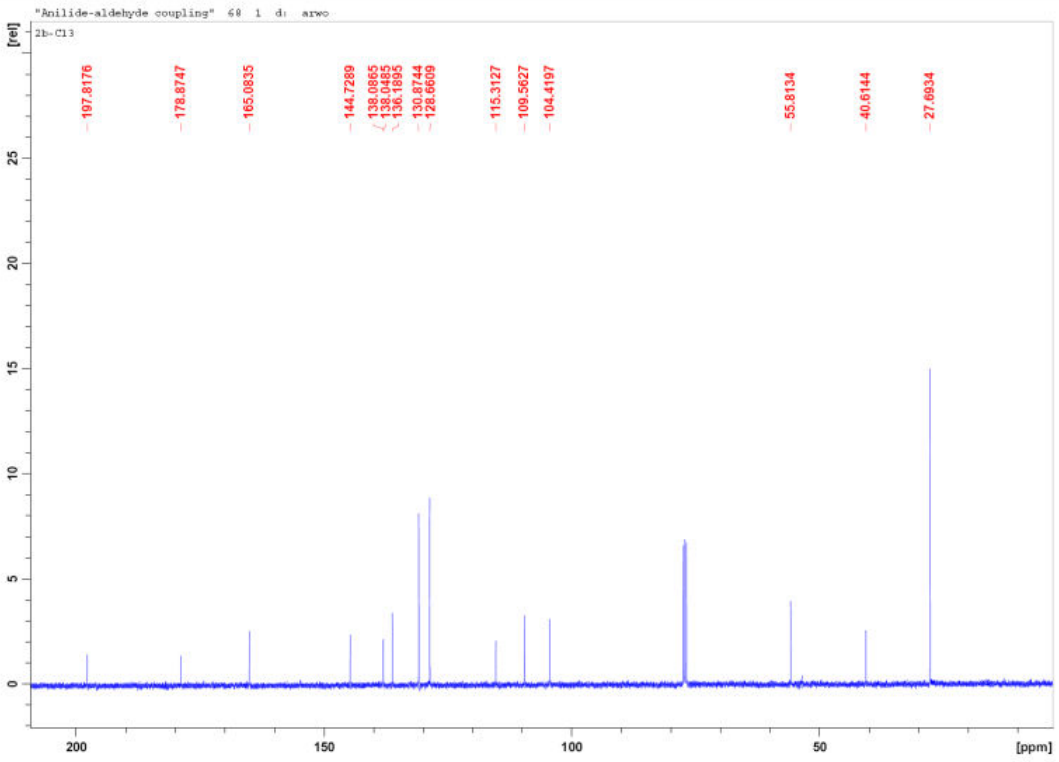

Figure A051 [1]H NMR spectrum of **7c**

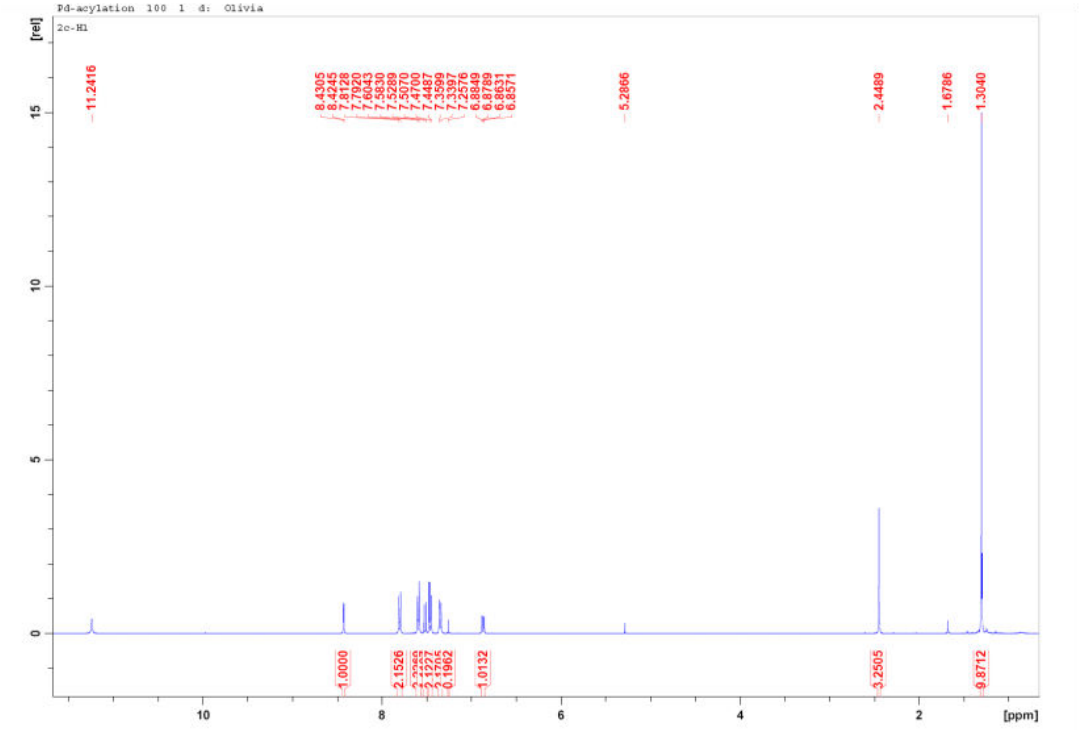

Figure A052 [13]C NMR spectrum of **7c**

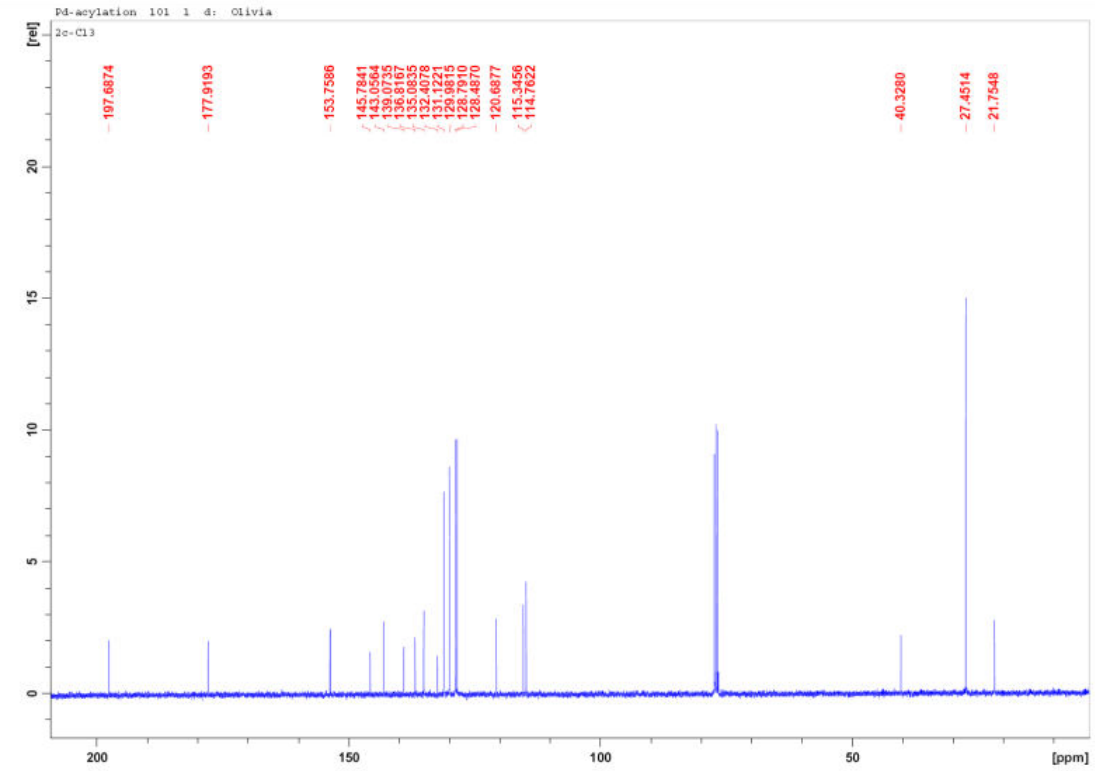

Figure A053 [1]H NMR spectrum of **7d**

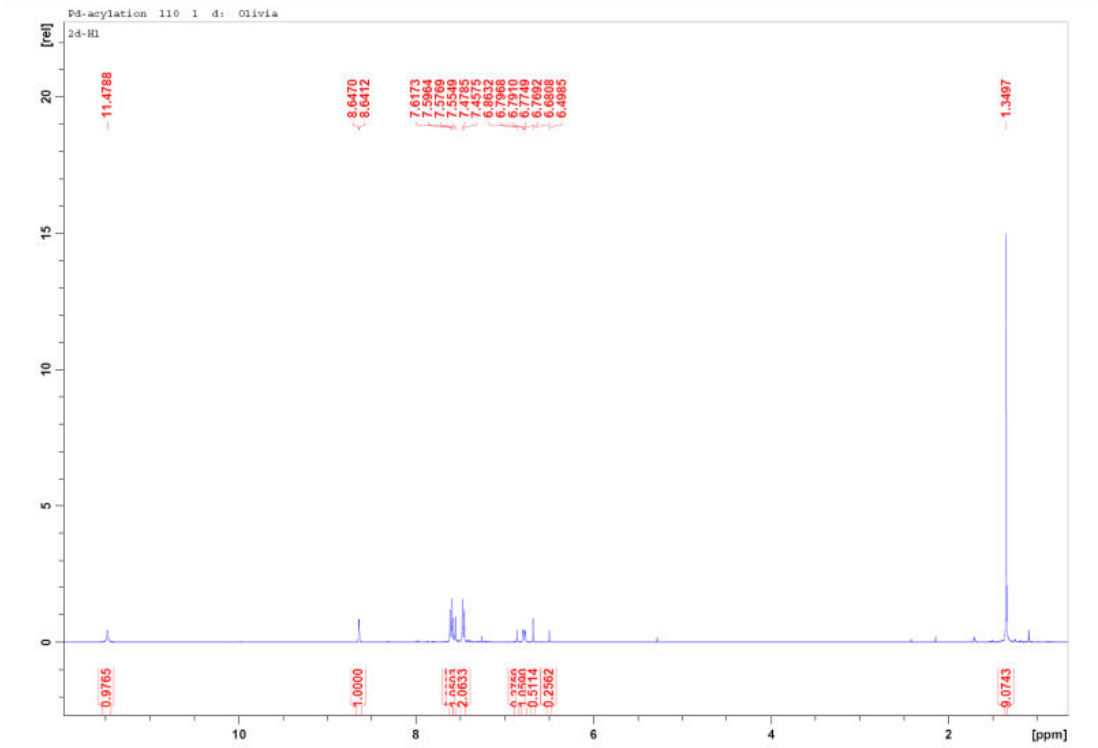

Figure A054 [13]C NMR spectrum of **7d**

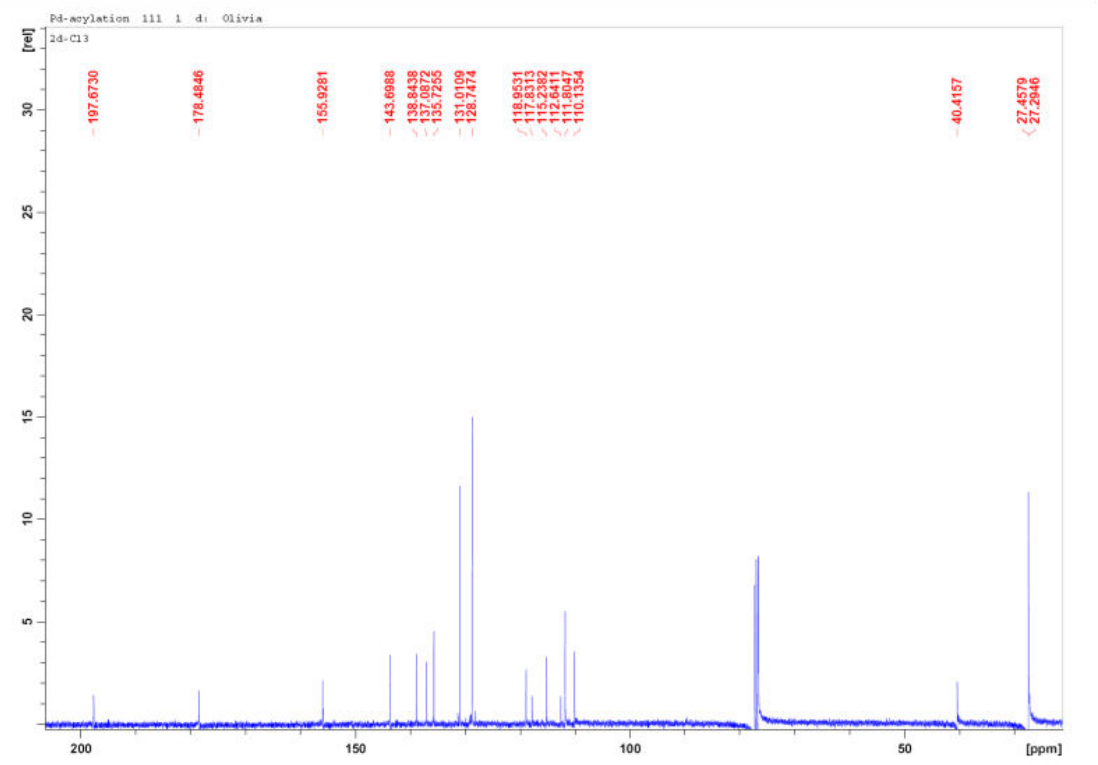

Figure A055 [1]H NMR spectrum of **7e**

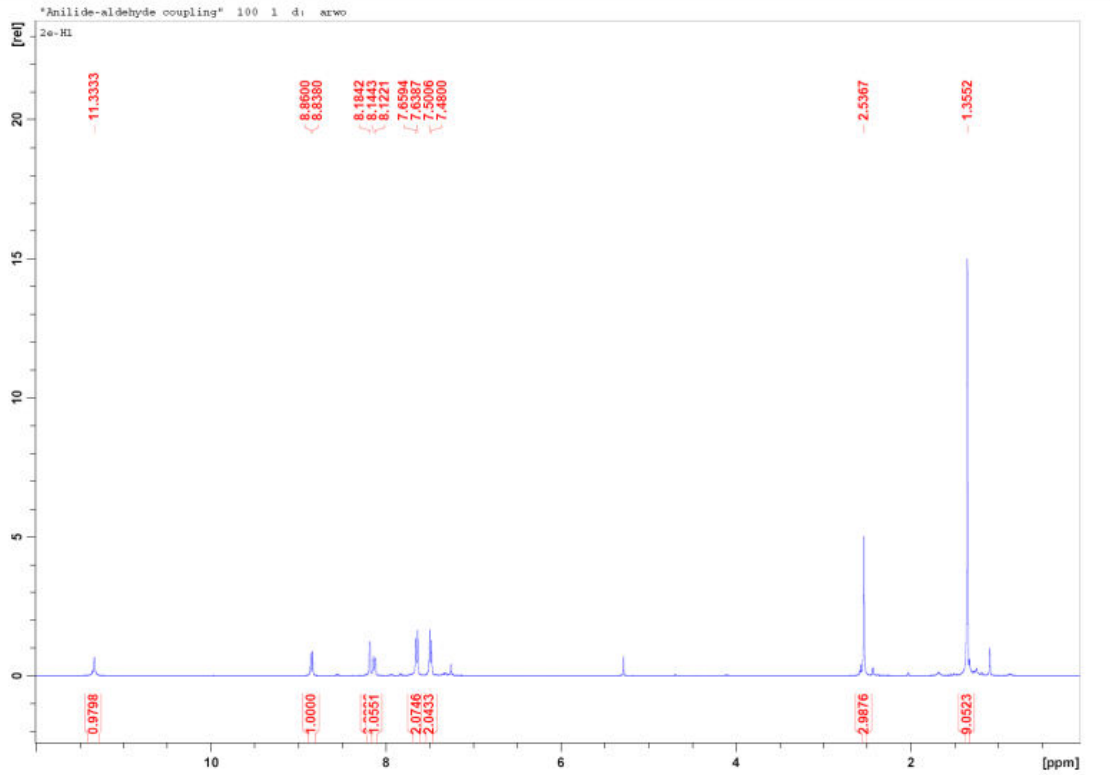

Figure A056 [13]C NMR spectrum of **7e**

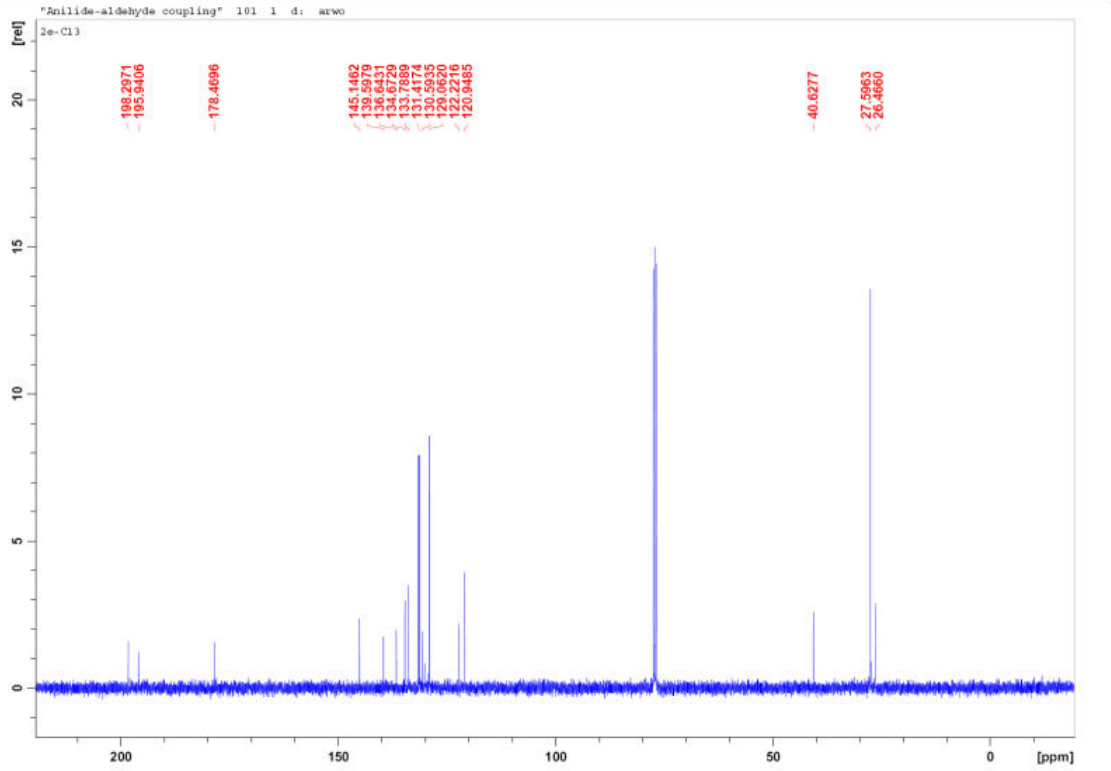

Figure A057 [1]H NMR spectrum of **7f**

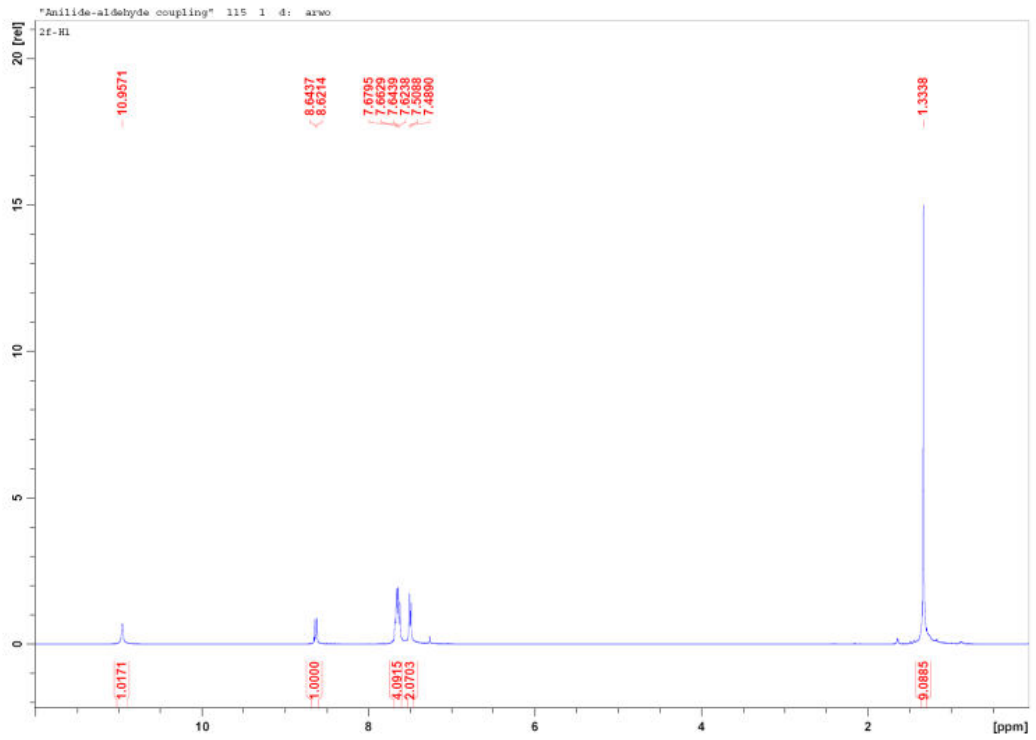

Figure A058 [13]C NMR spectrum of **7f**

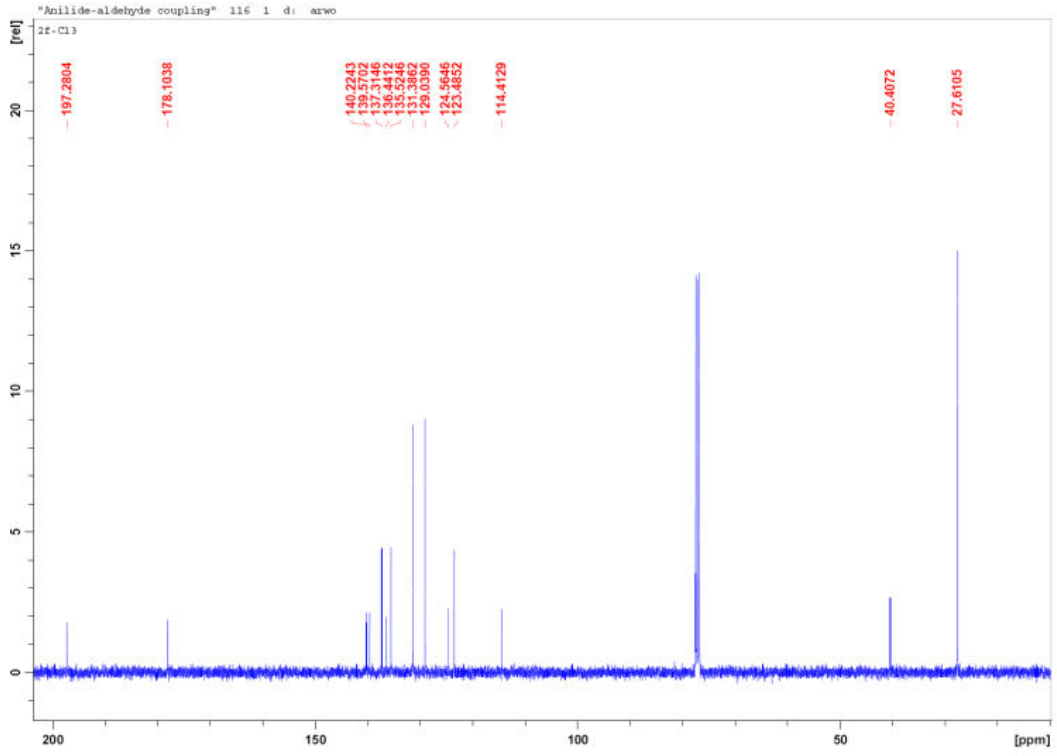

Figure A059 [1]H NMR spectrum of **7g**

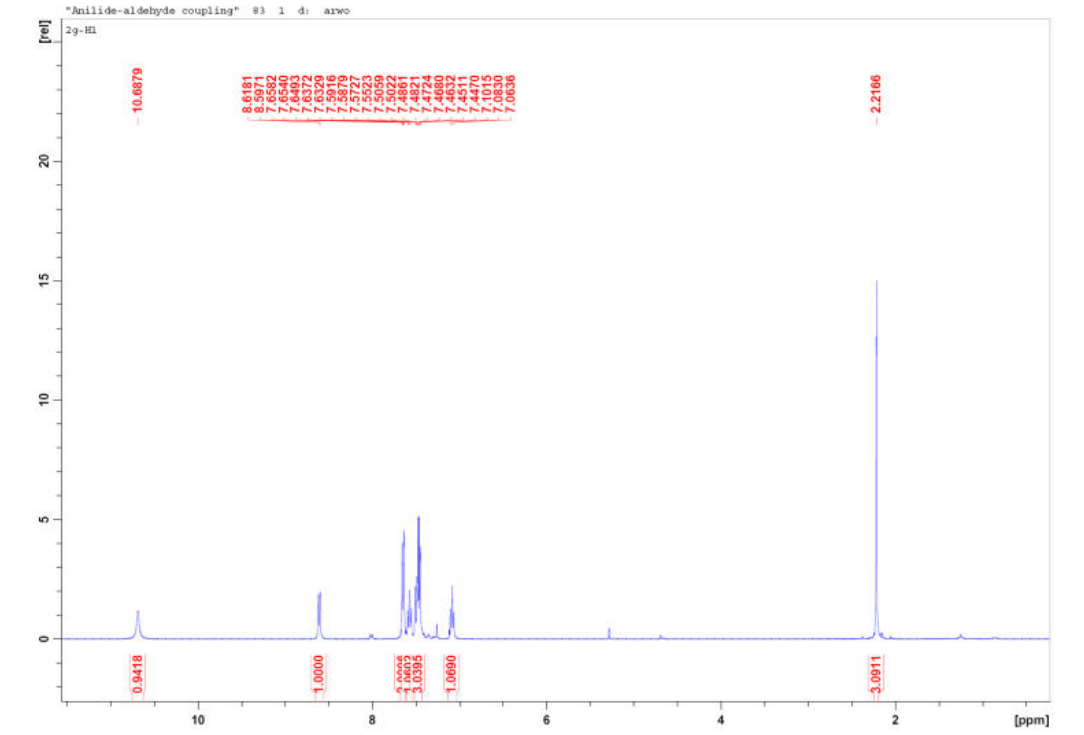

Figure A060 [13]C NMR spectrum of **7g**

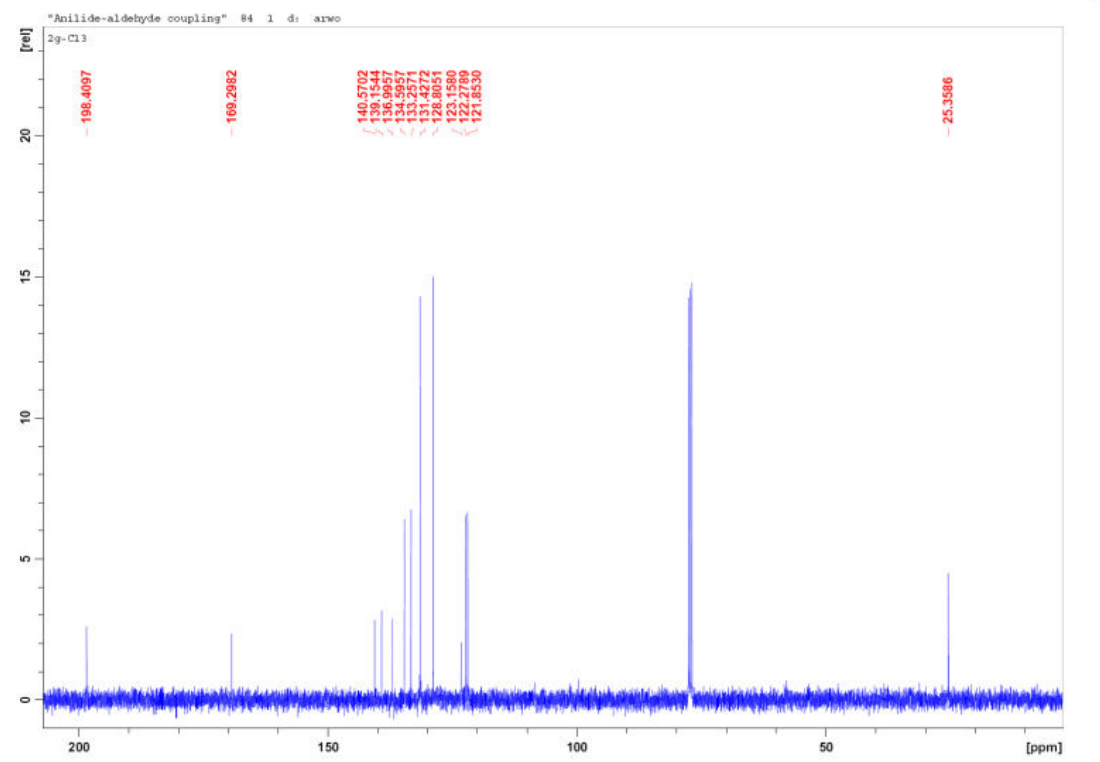

Figure A061 [1]H NMR spectrum of **7h**

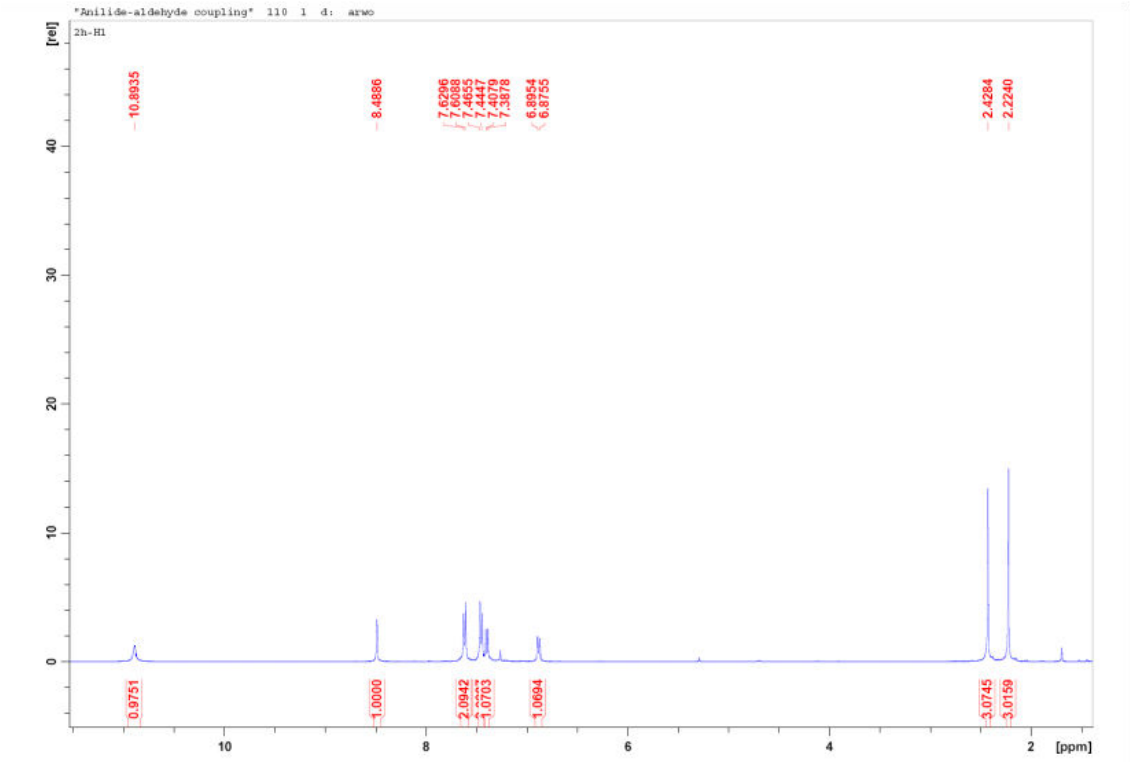

Figure A062 [13]C NMR spectrum of **7h**

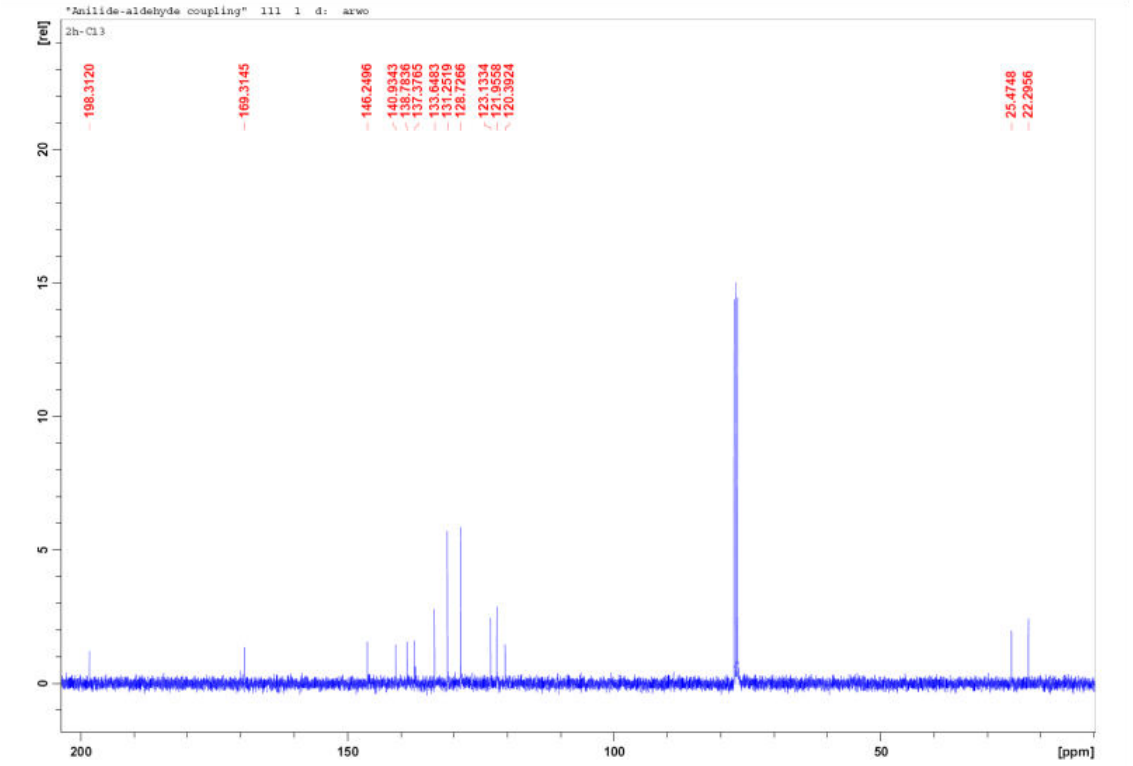

Figure A063 [1]H NMR spectrum of **7i**

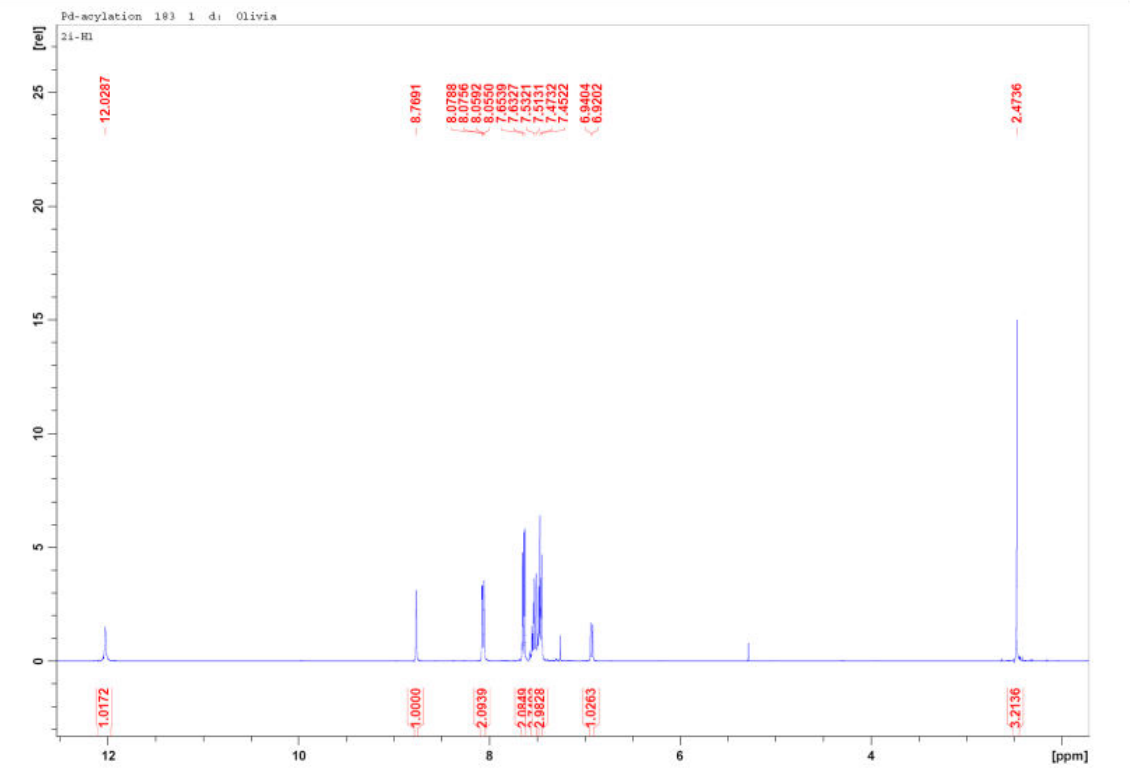

Figure A064 [13]C NMR spectrum of **7i**

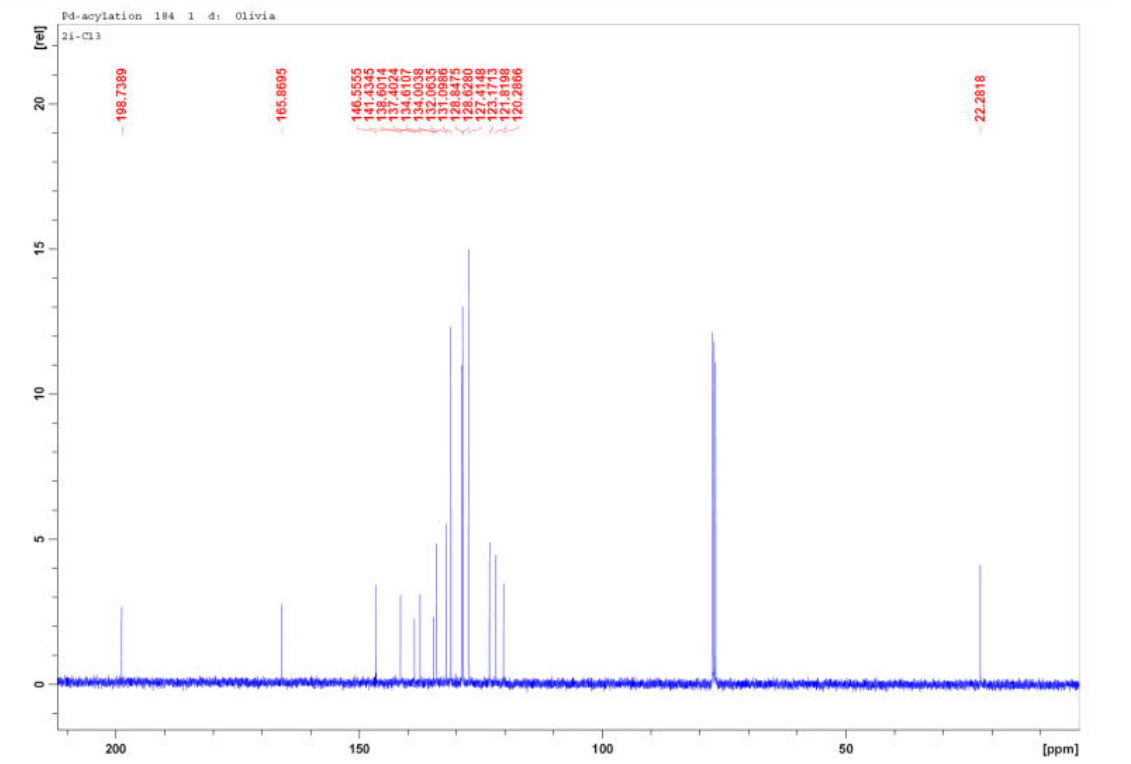

Figure A065 [1]H NMR spectrum of **7j**

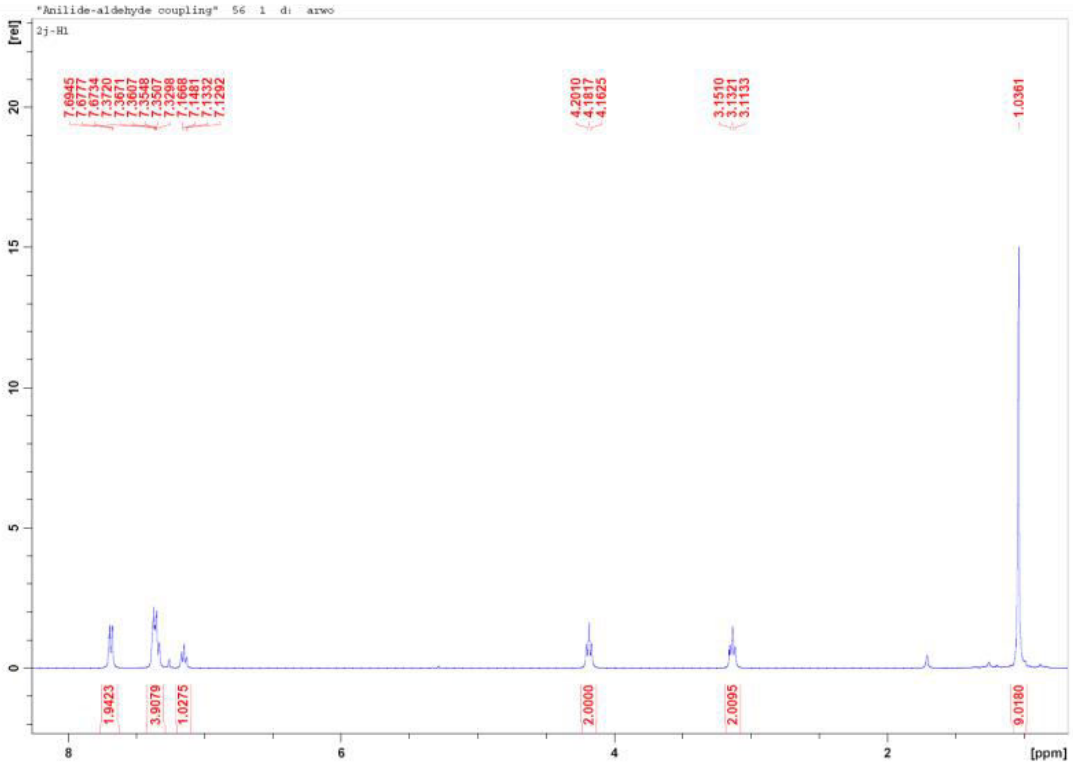

Figure A066 [13]C NMR spectrum of **7j**

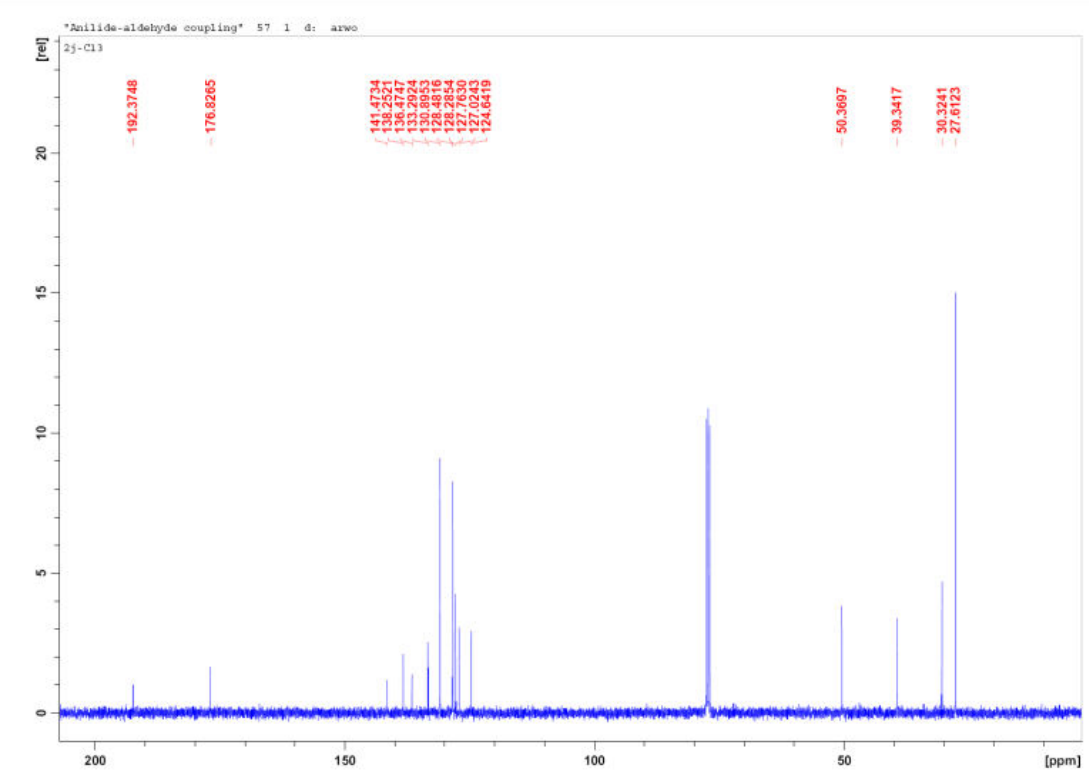

Figure A067 [1]H NMR spectrum of **7k**

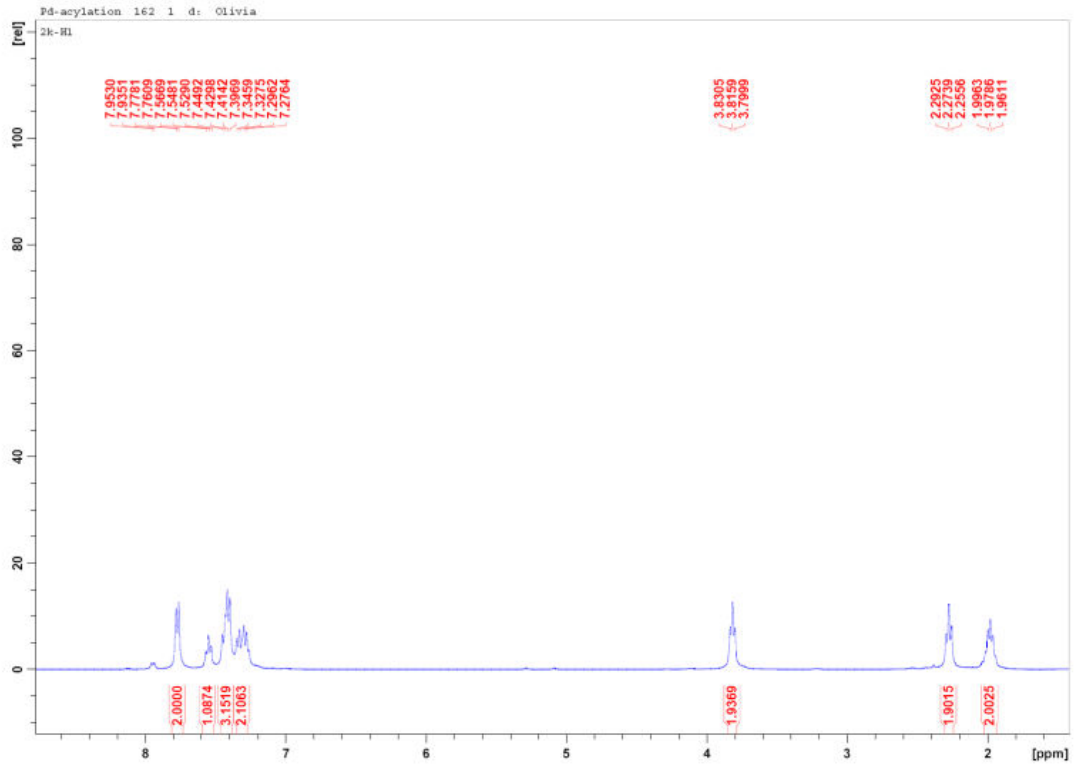

Figure A068 [13]C NMR spectrum of **7k**

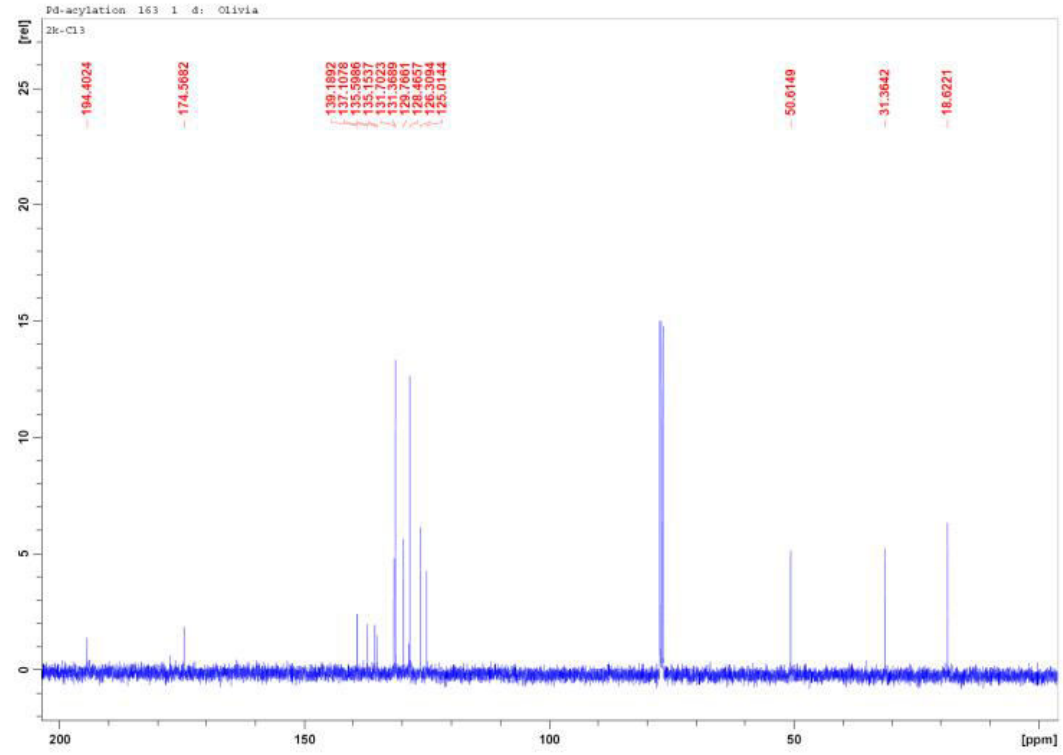

Figure A069 [1]H NMR spectrum of **7l**

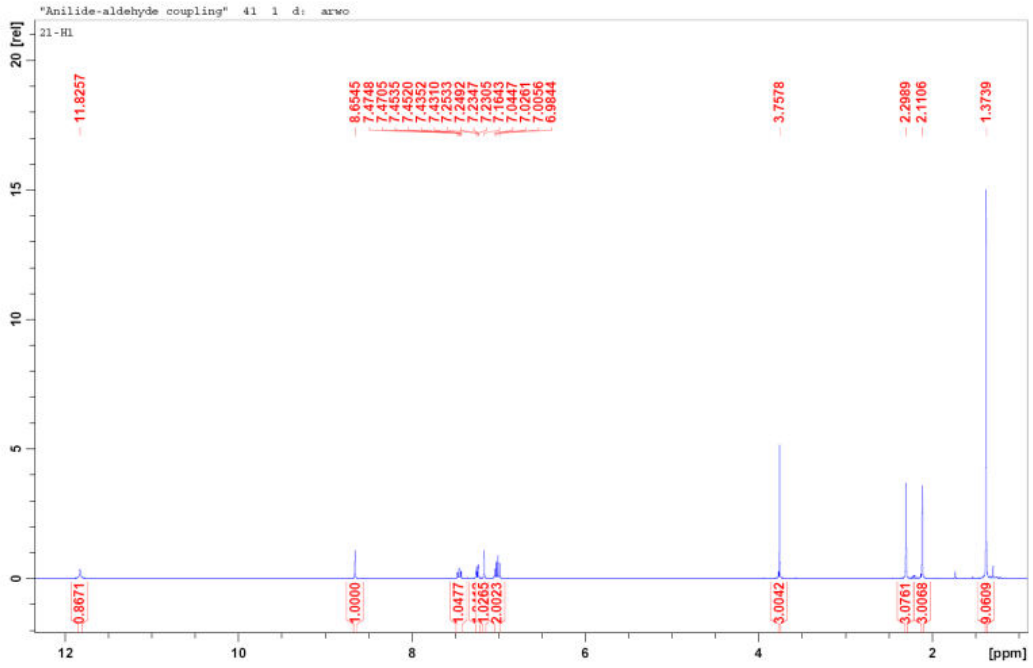

Figure A070 [13]C NMR spectrum of **7l**

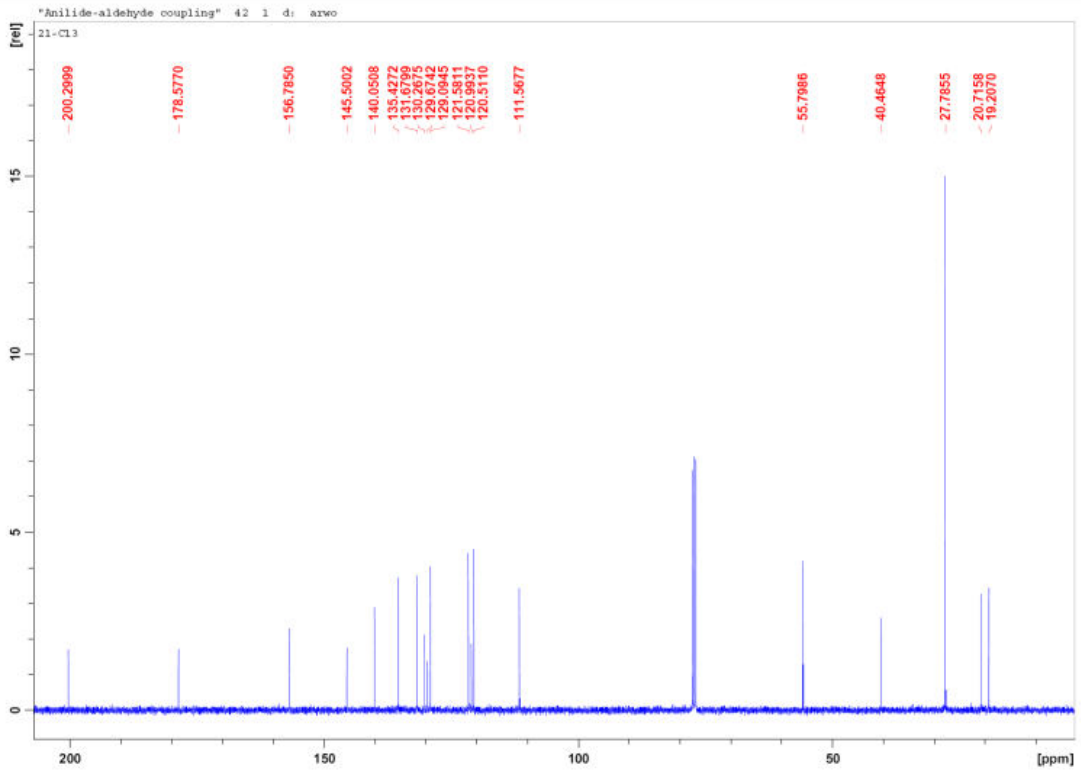

Figure A071 [1]H NMR spectrum of **7m**

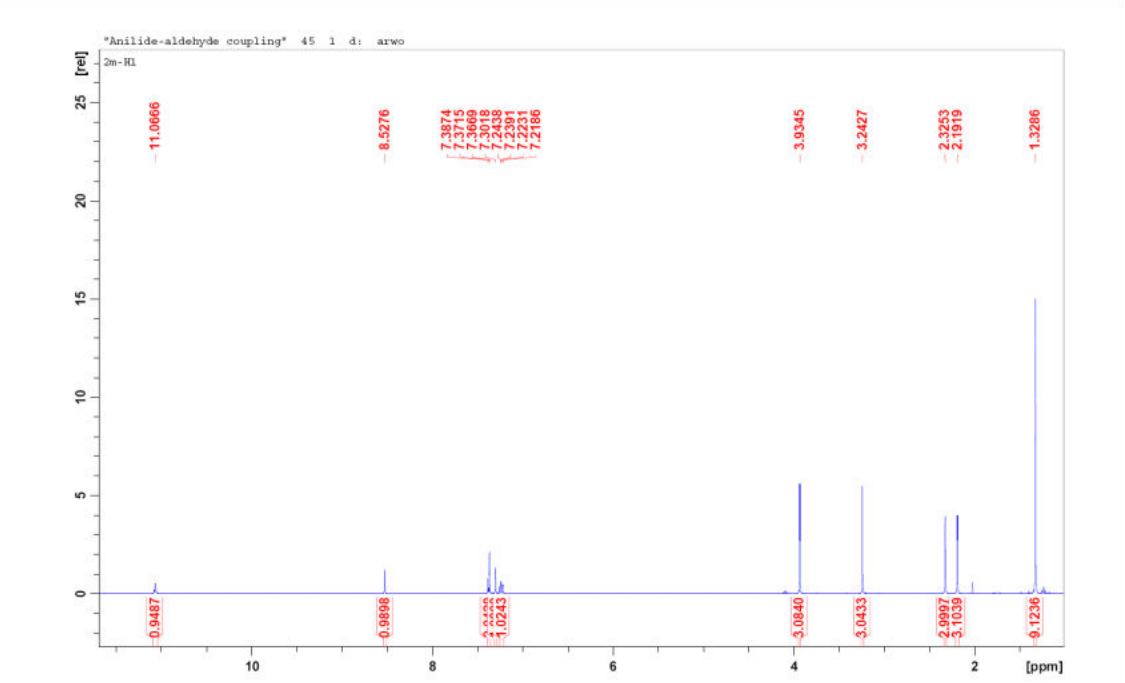

Figure A072 [13]C NMR spectrum of **7m**

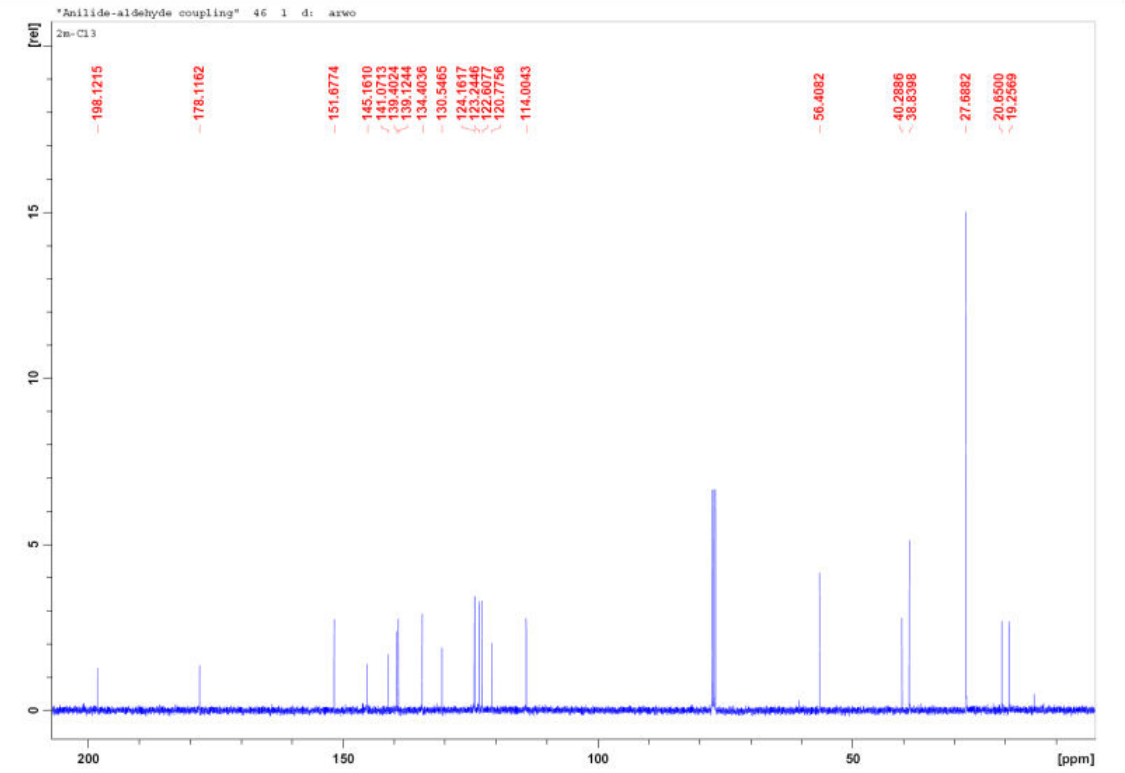

Figure A073 [1]H NMR spectrum of **7n**

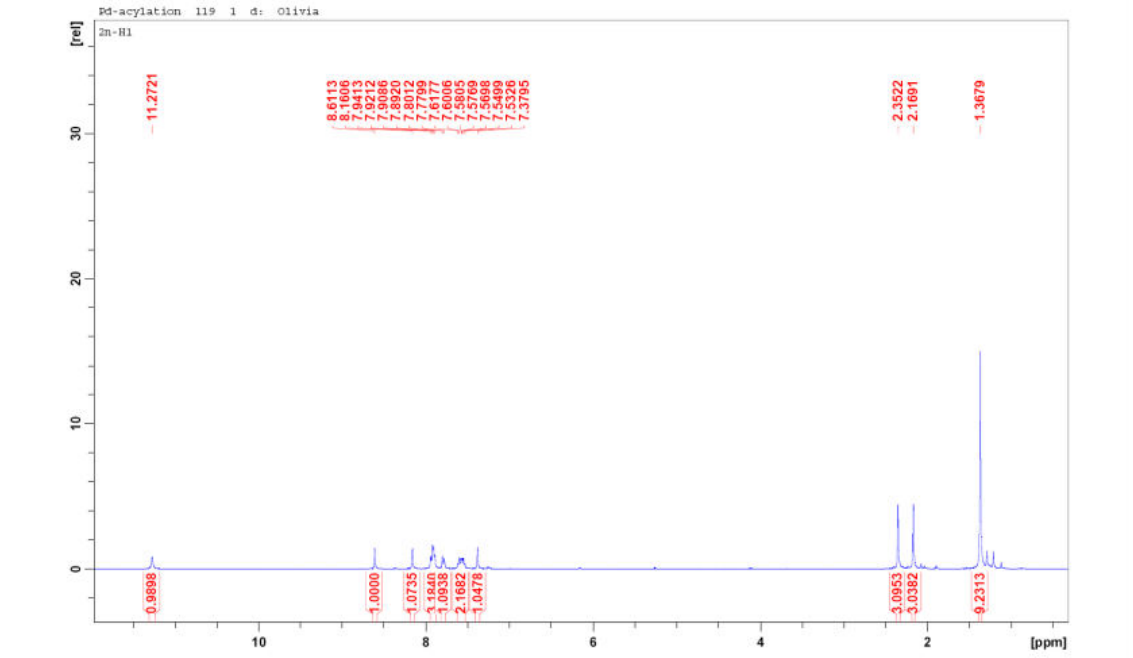

Figure A074 [13]C NMR spectrum of **7n**

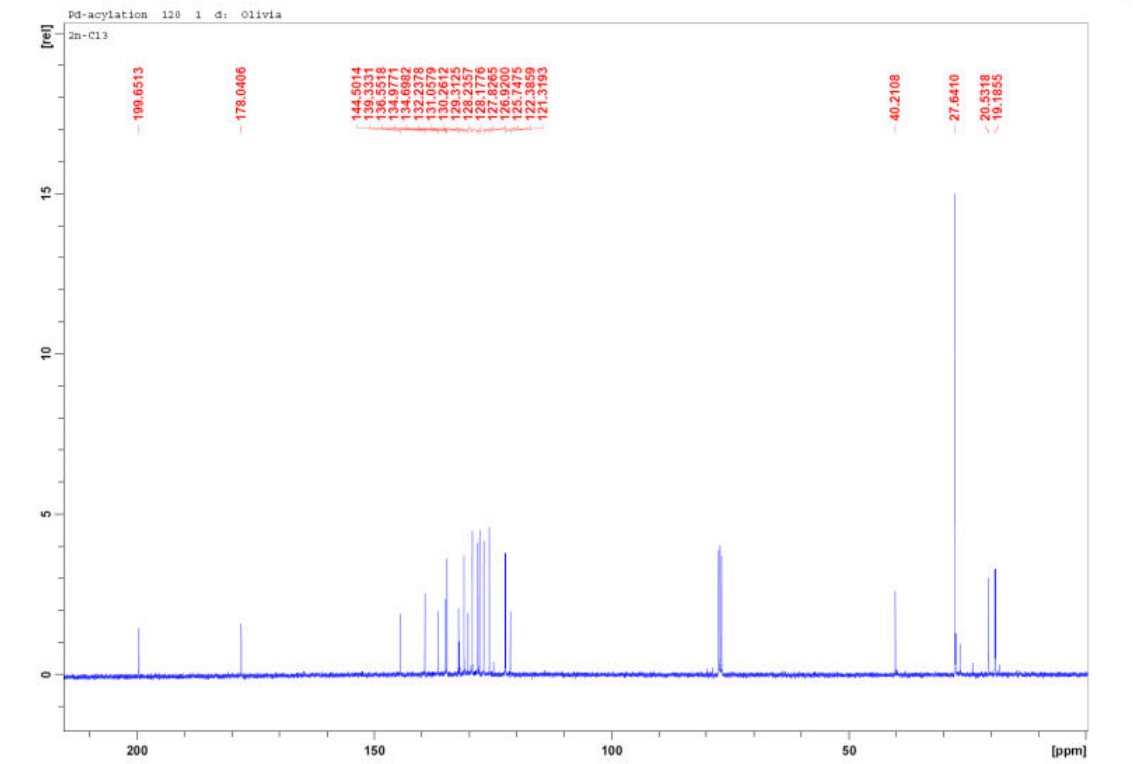

Figure A075 [1]H NMR spectrum of **7o**

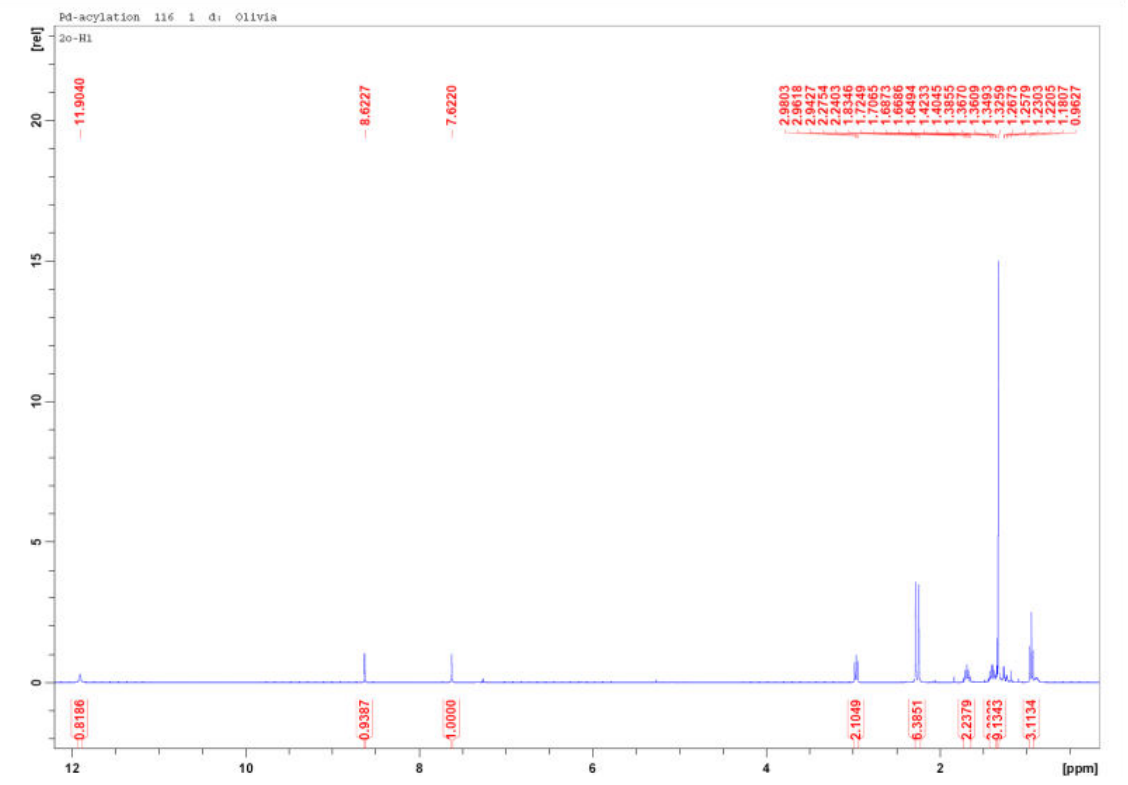

Figure A076 [13]C NMR spectrum of **7o**

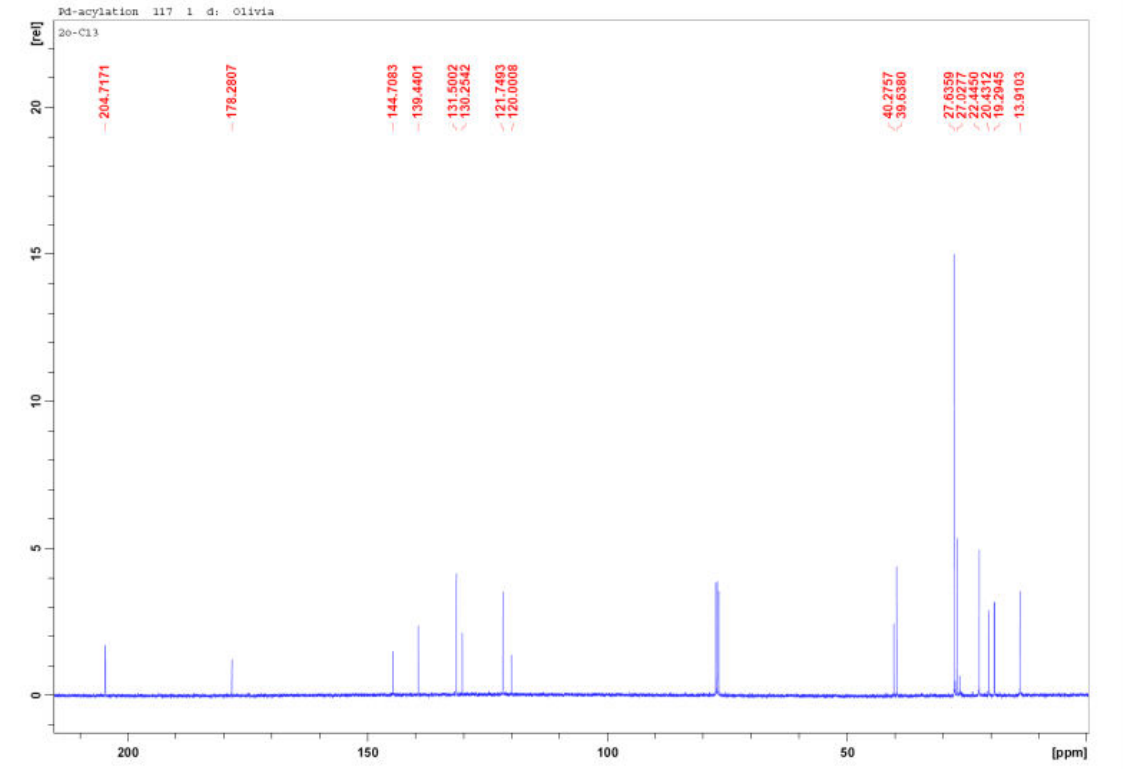

Figure A077 [1]H NMR spectrum of **7p**

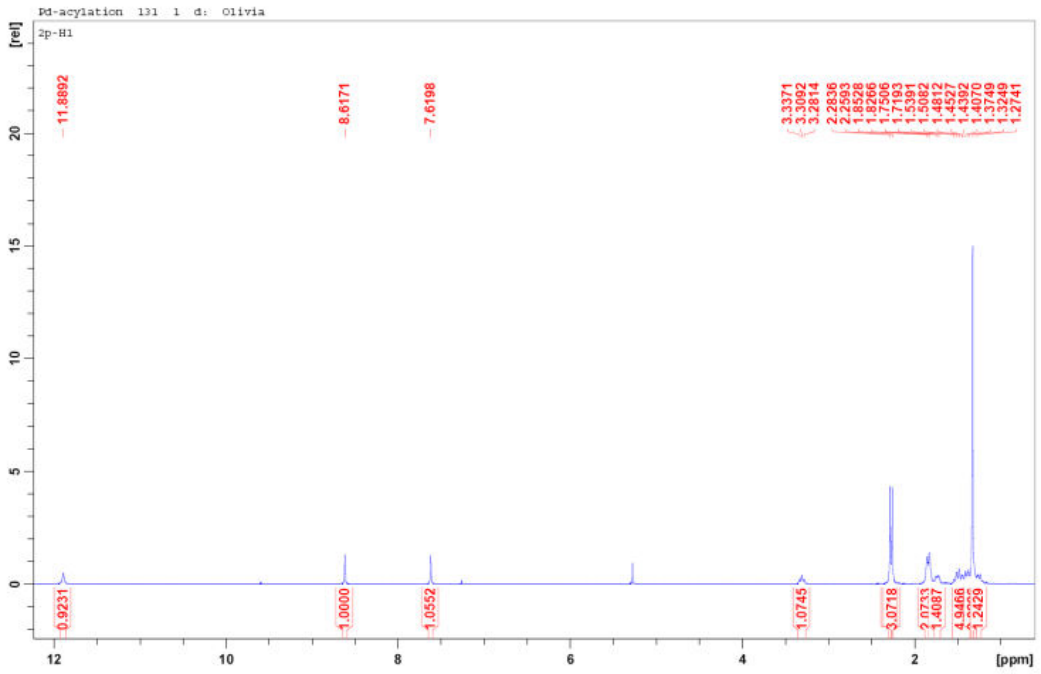

Figure A078 [13]C NMR spectrum of **7p**

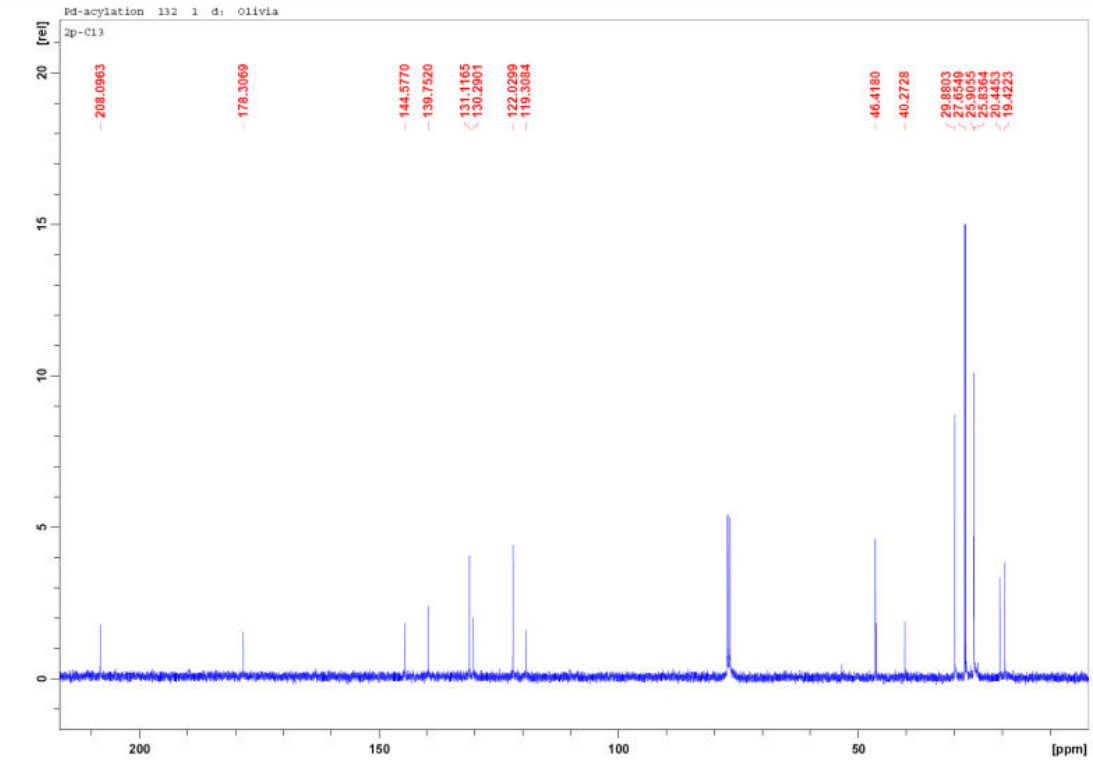

Figure A079 [1]H NMR spectrum of **7q**

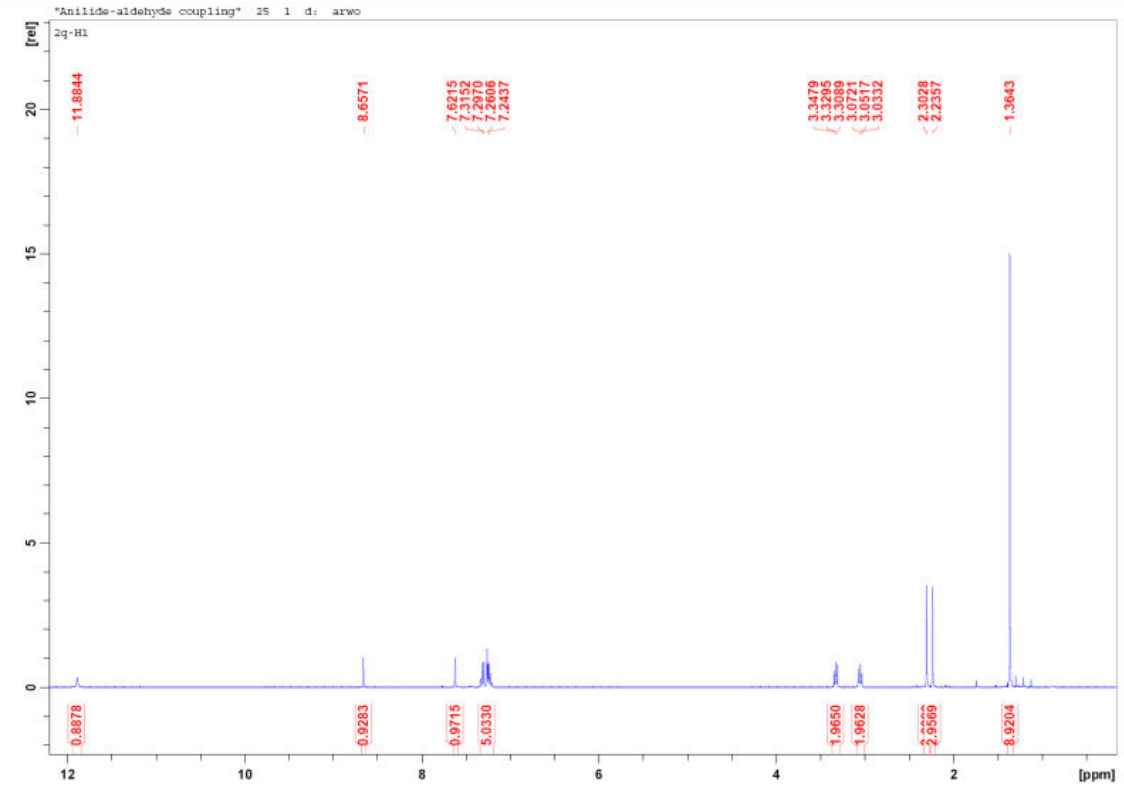

Figure A080 [13]C NMR spectrum of **7q**

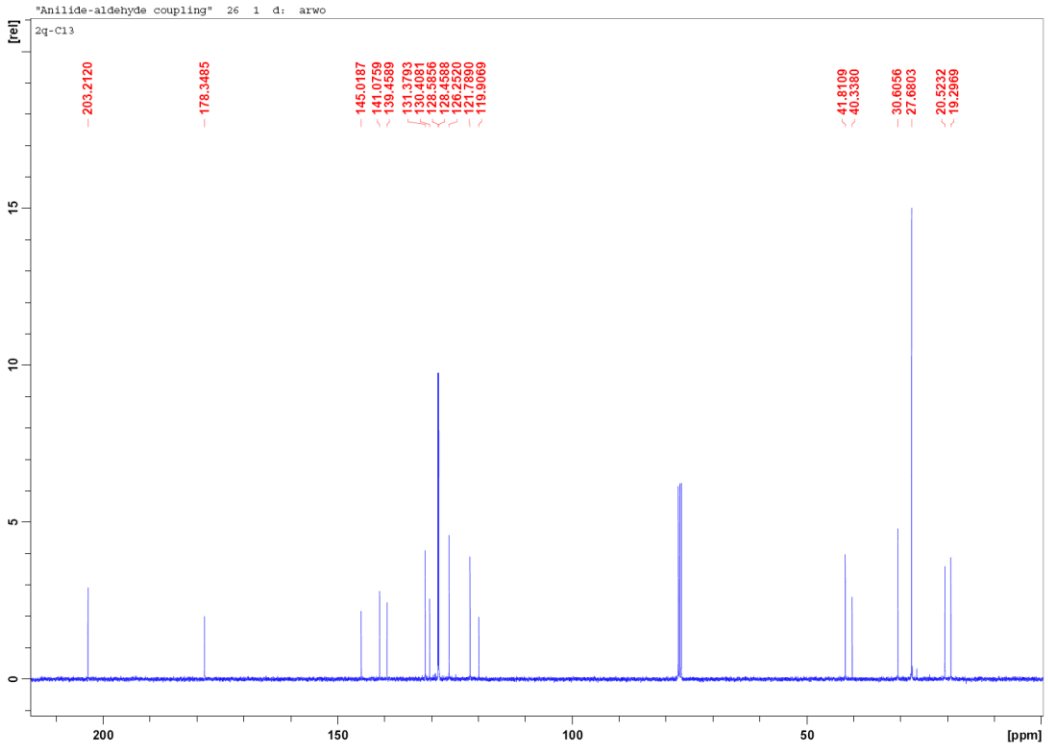

Figure A081 [1]H NMR spectrum of **7r**

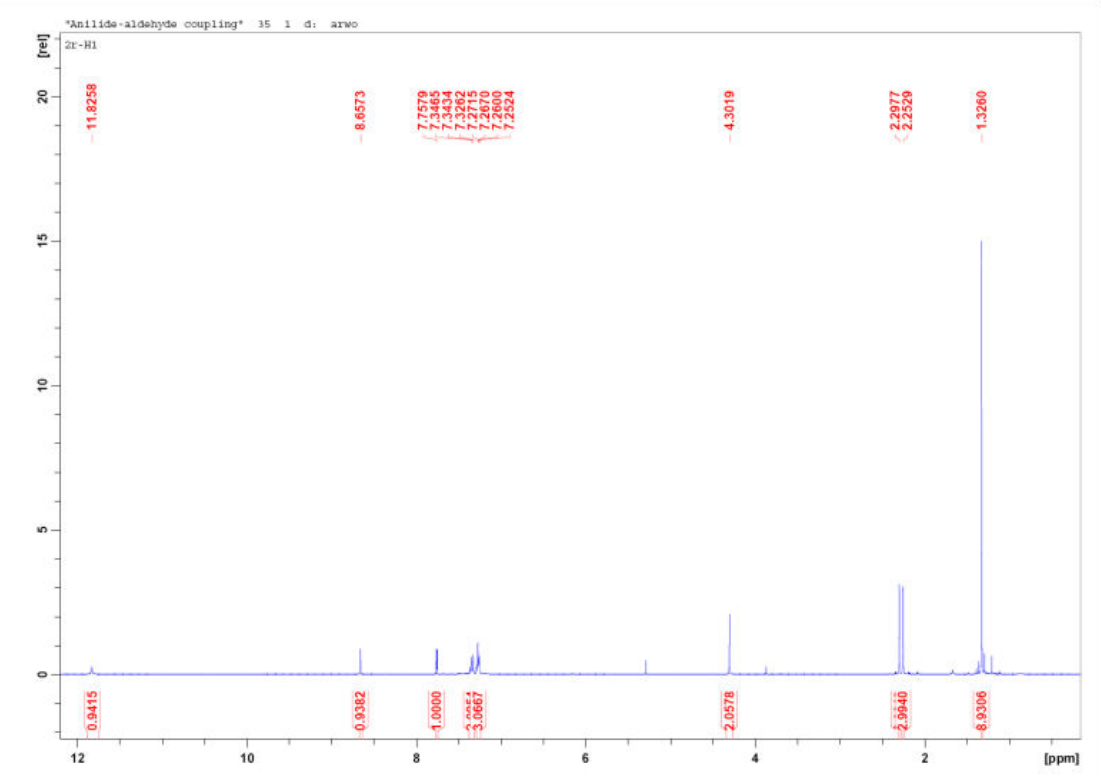

Figure A082 [13]C NMR spectrum of **7r**

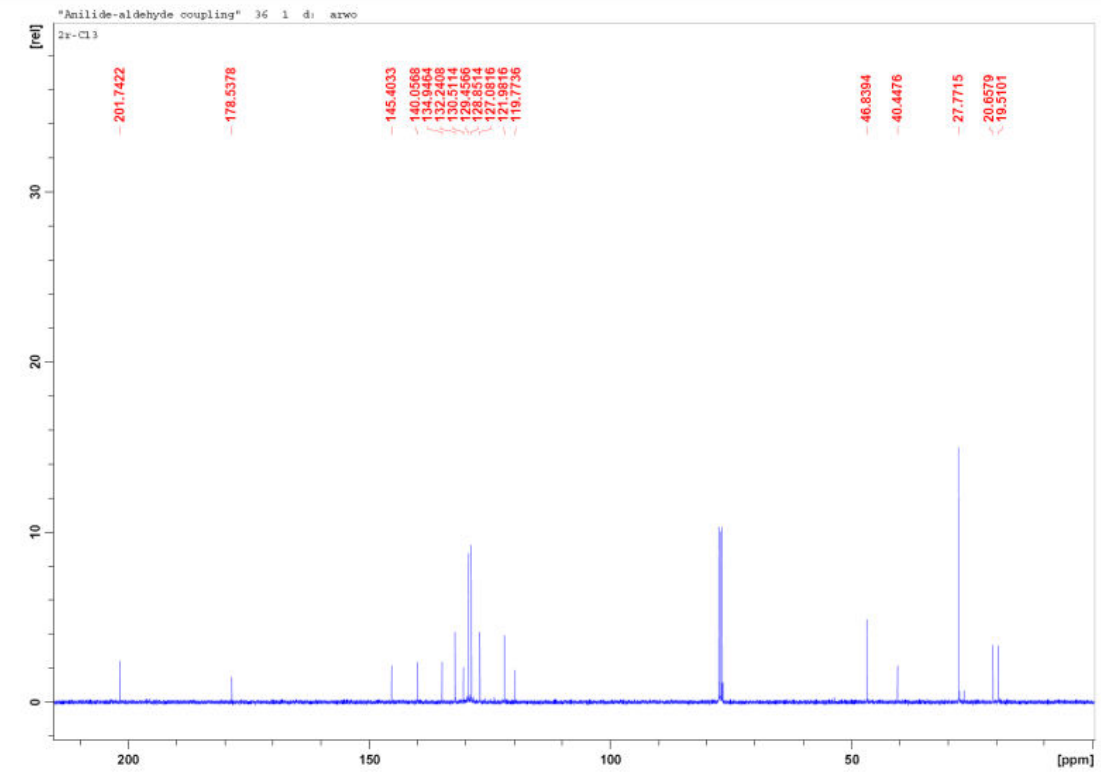

Figure A083 [1]H NMR spectrum of **7s**

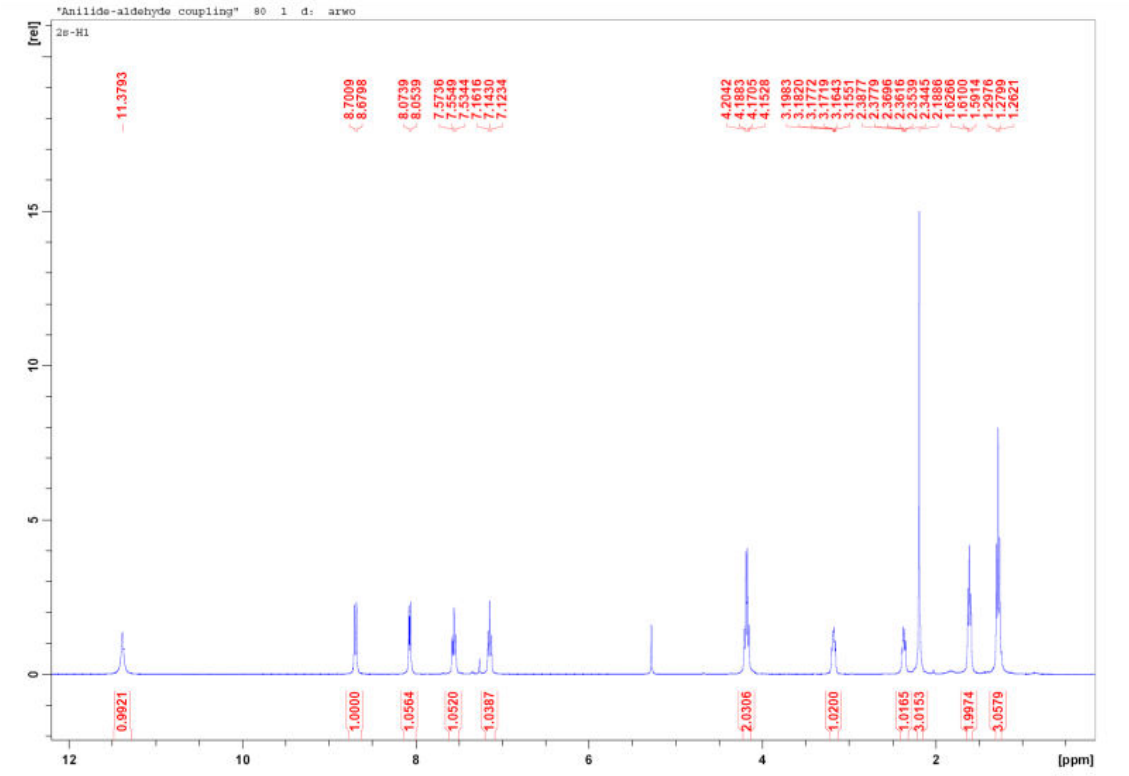

Figure A084 [13]C NMR spectrum of **7s**

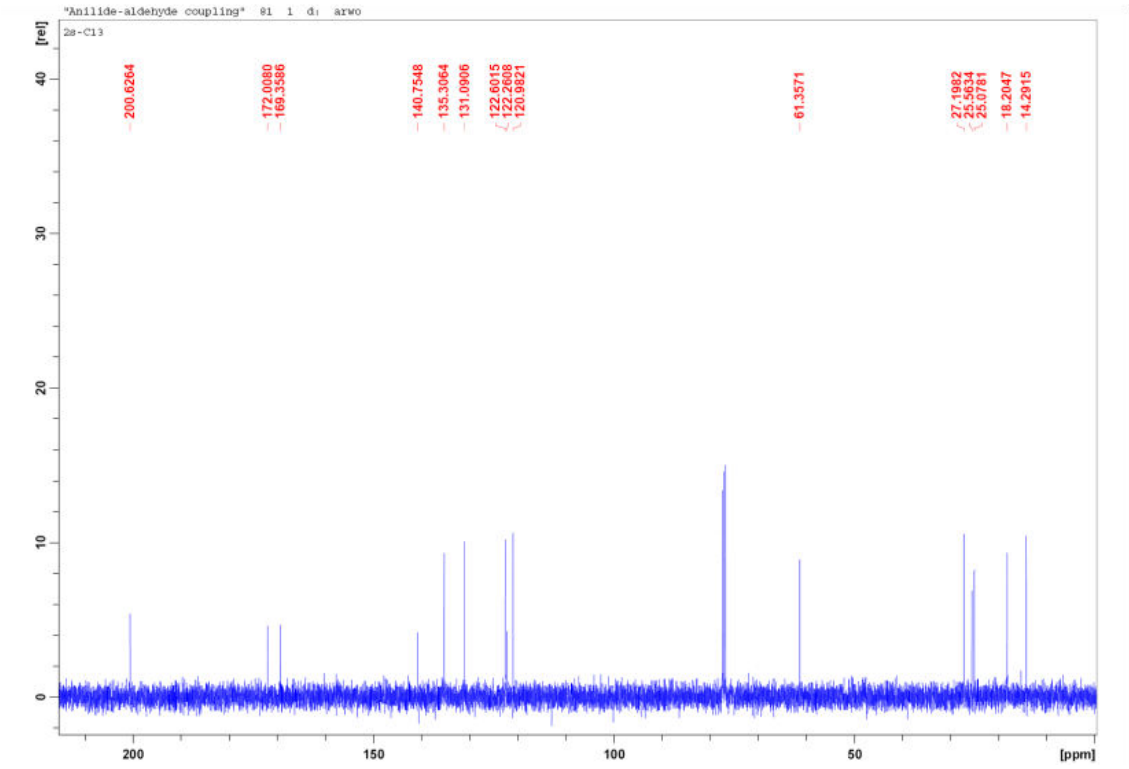

Figure A085 [1]H NMR spectrum of **7t**

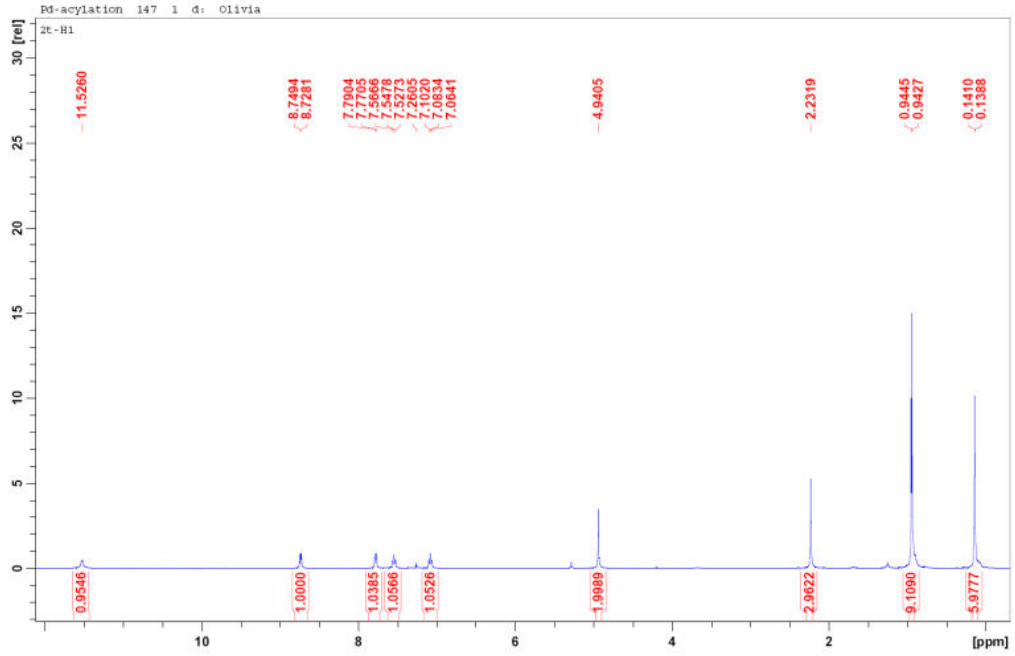

Figure A086 [13]C NMR spectrum of **7t**

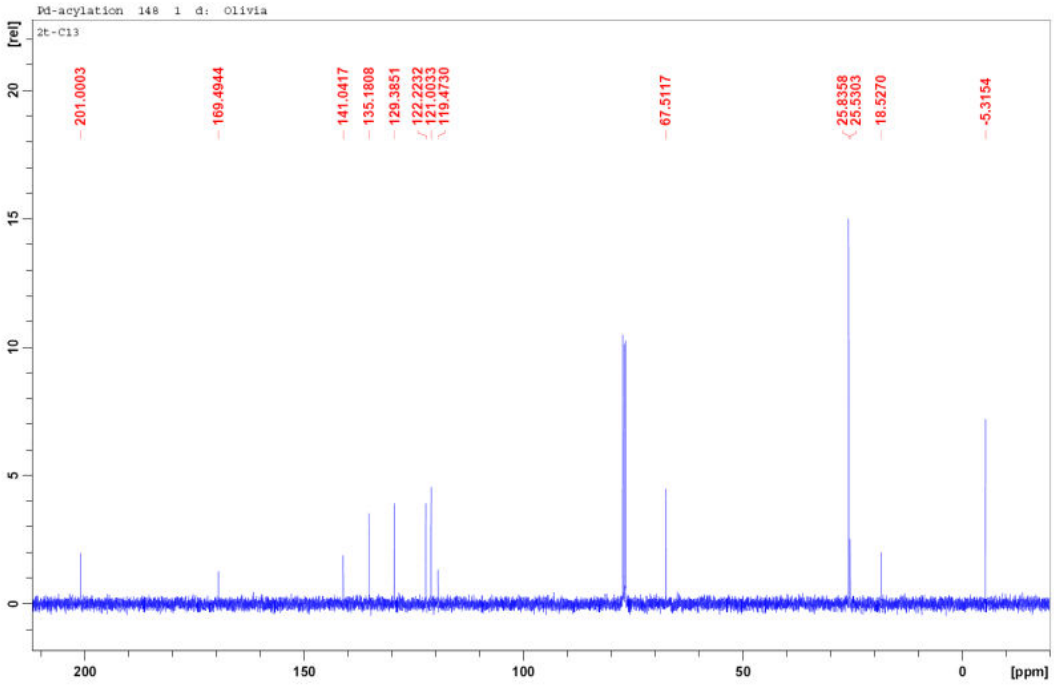

Figure A087 [1]H NMR spectrum of **7u**

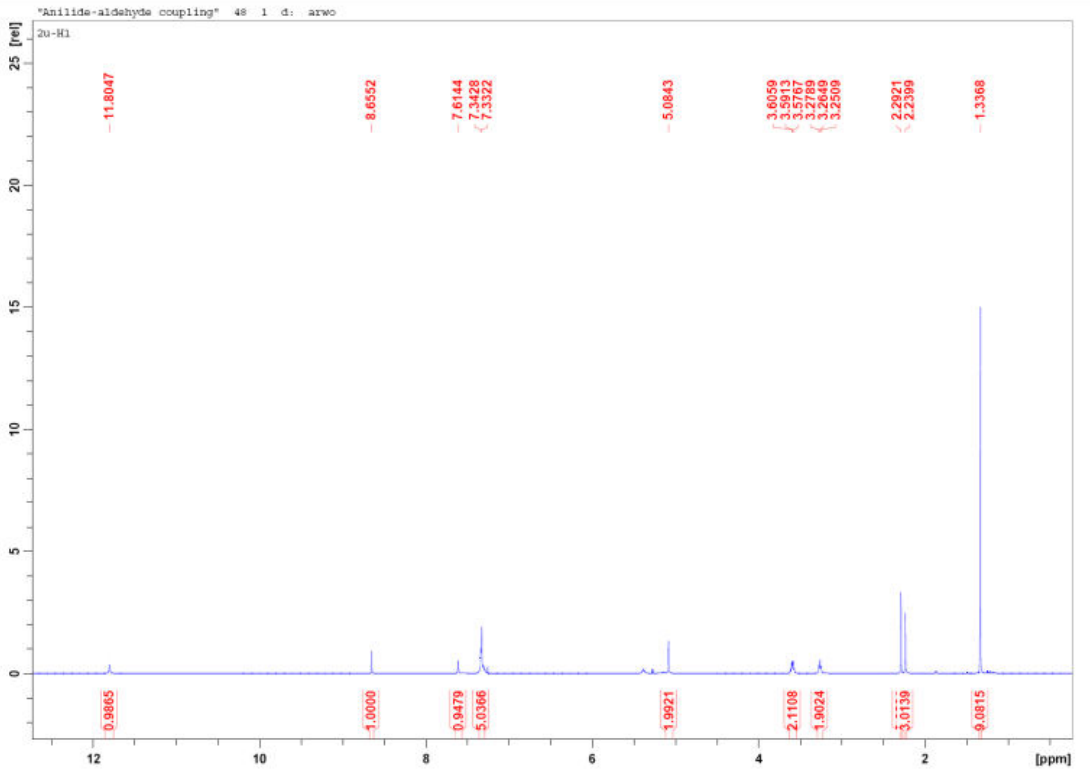

Figure A088 [13]C NMR spectrum of **7u**

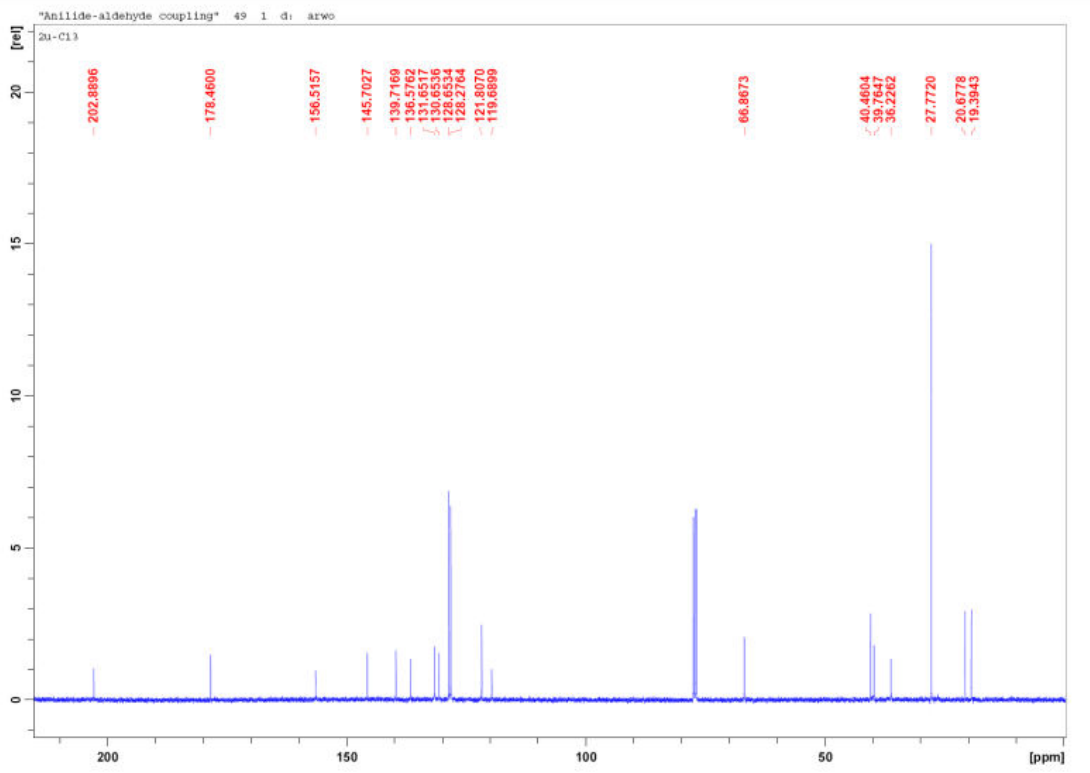

Figure A089 [1]H NMR spectrum of **7v**

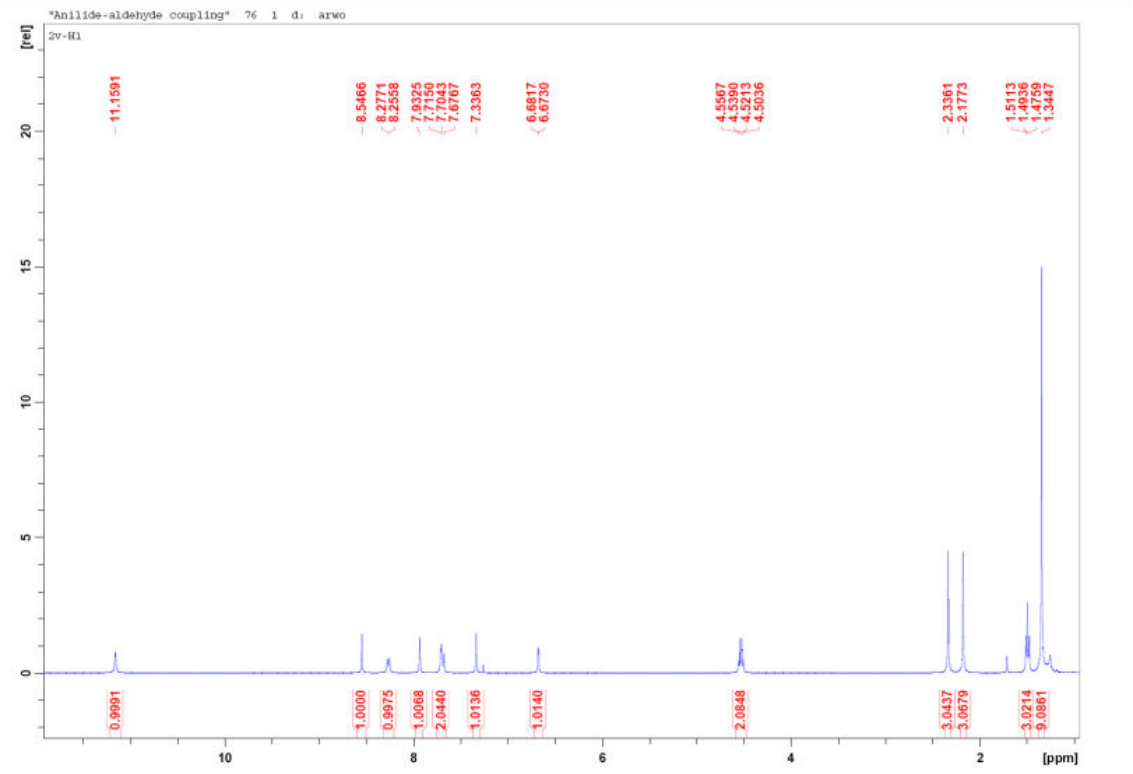

Figure A090 [13]C NMR spectrum of **7v**

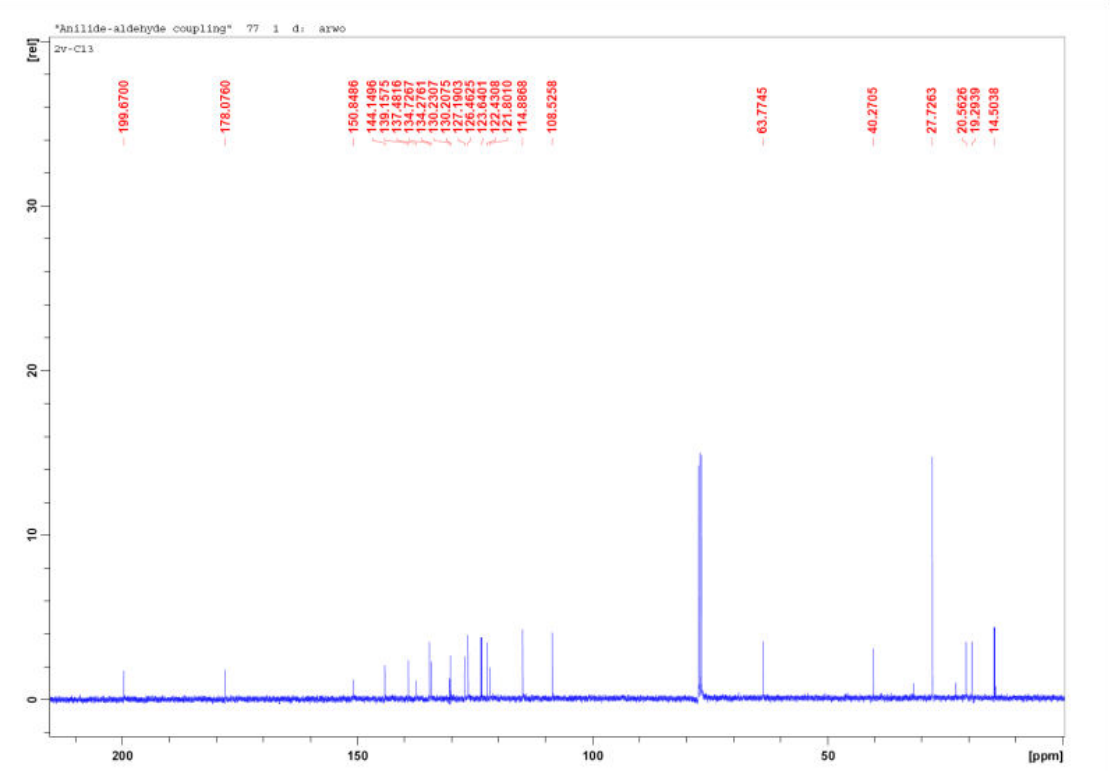

Figure A091 [1]H NMR spectrum of **7w**

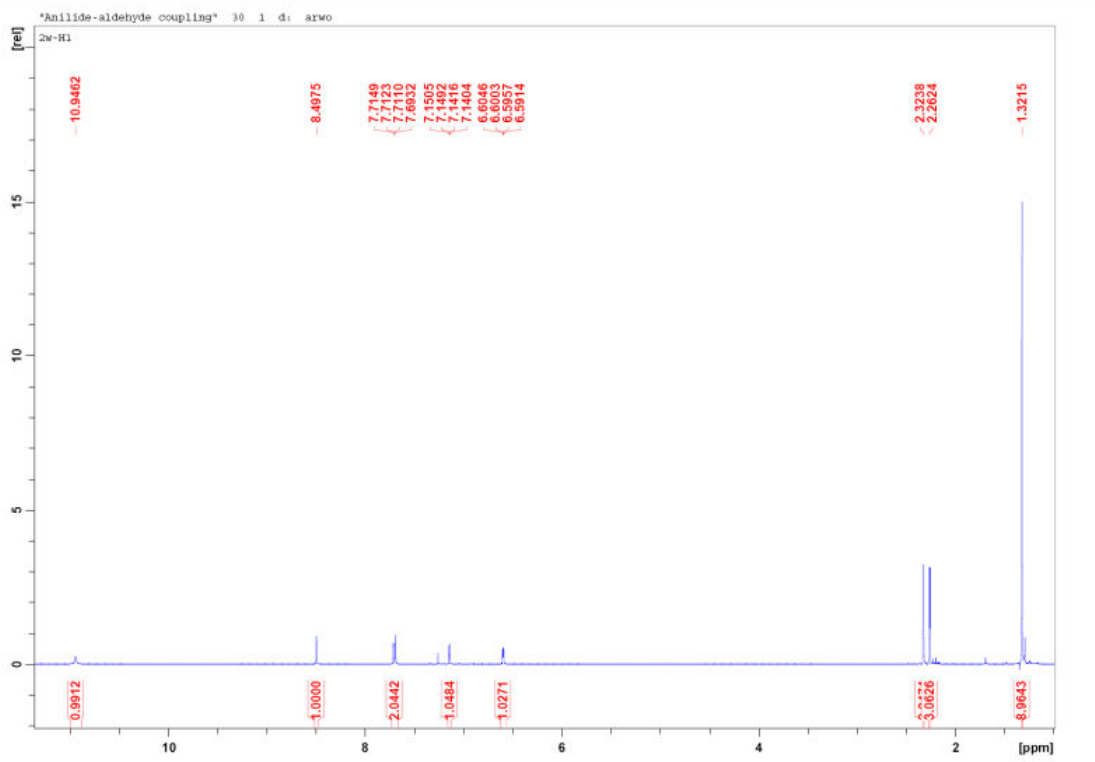

Figure A092 [13]C NMR spectrum of **7w**

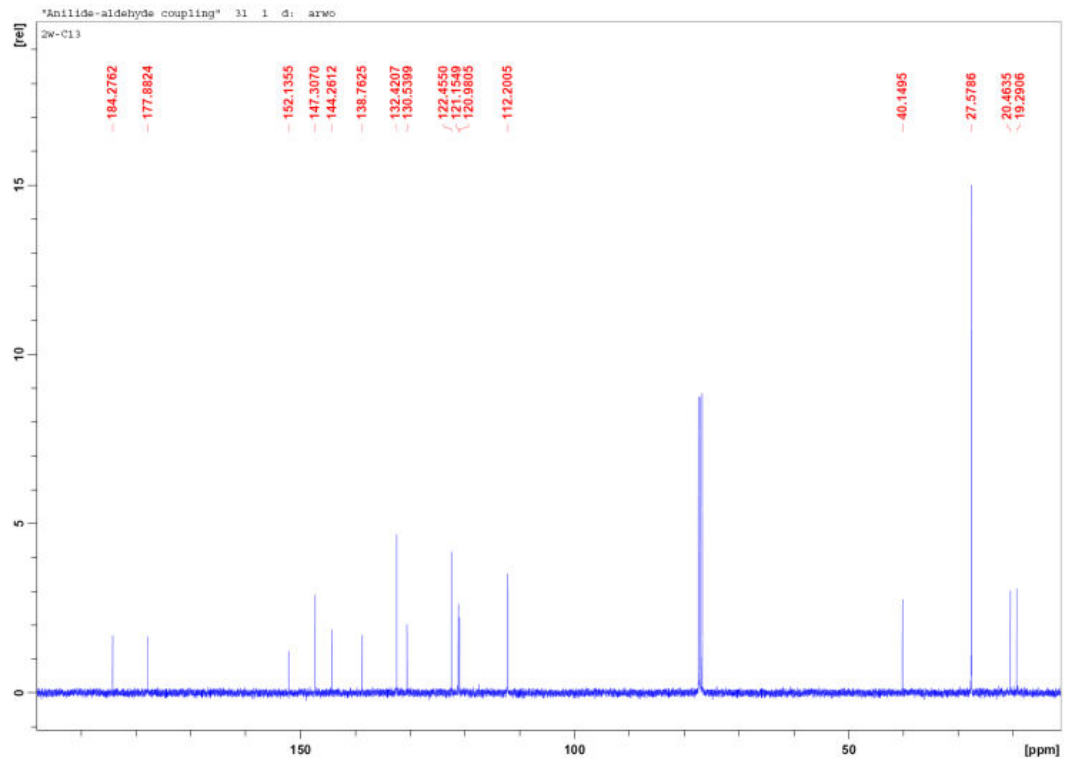

Figure A093 [1]H NMR spectrum of **7x**

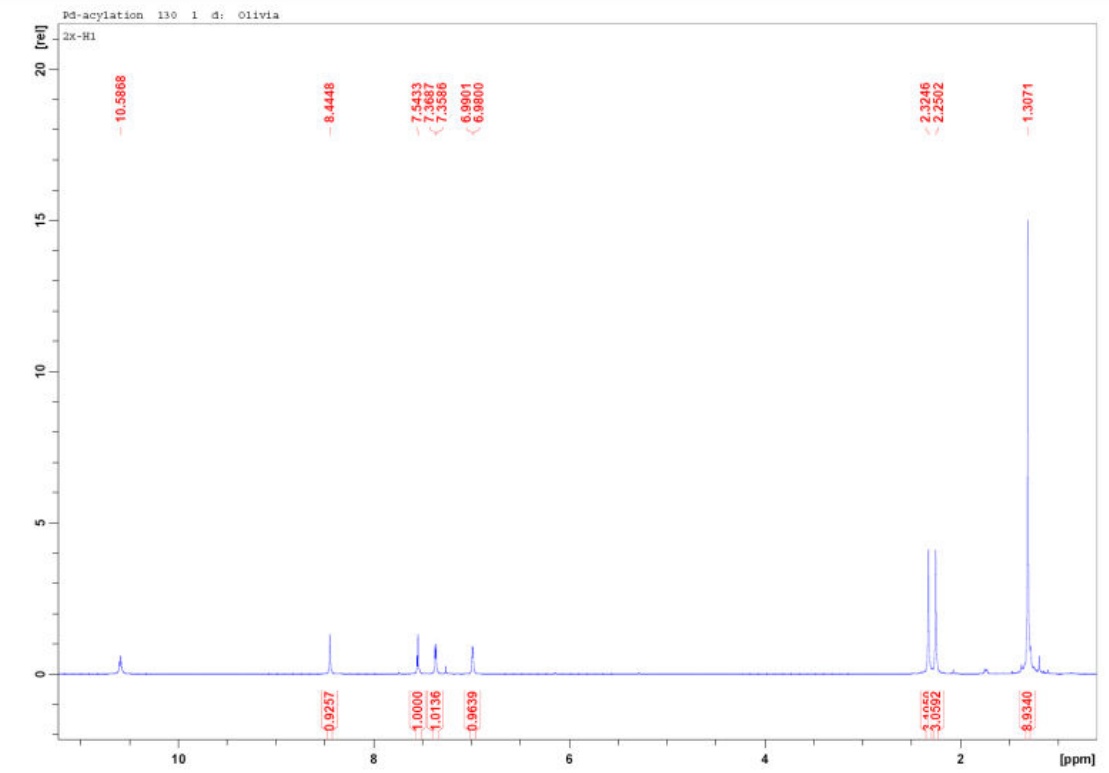

Figure A094 [13]C NMR spectrum of **7x**

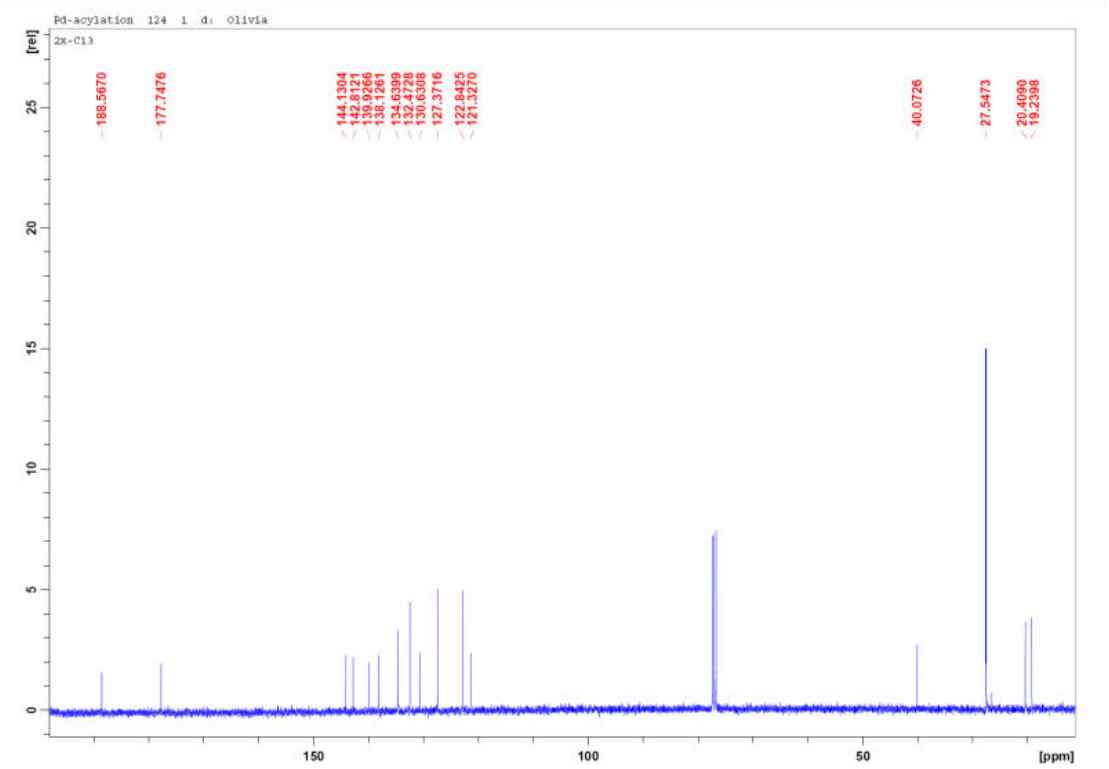

Figure A095 [1]H NMR spectrum of **7y**

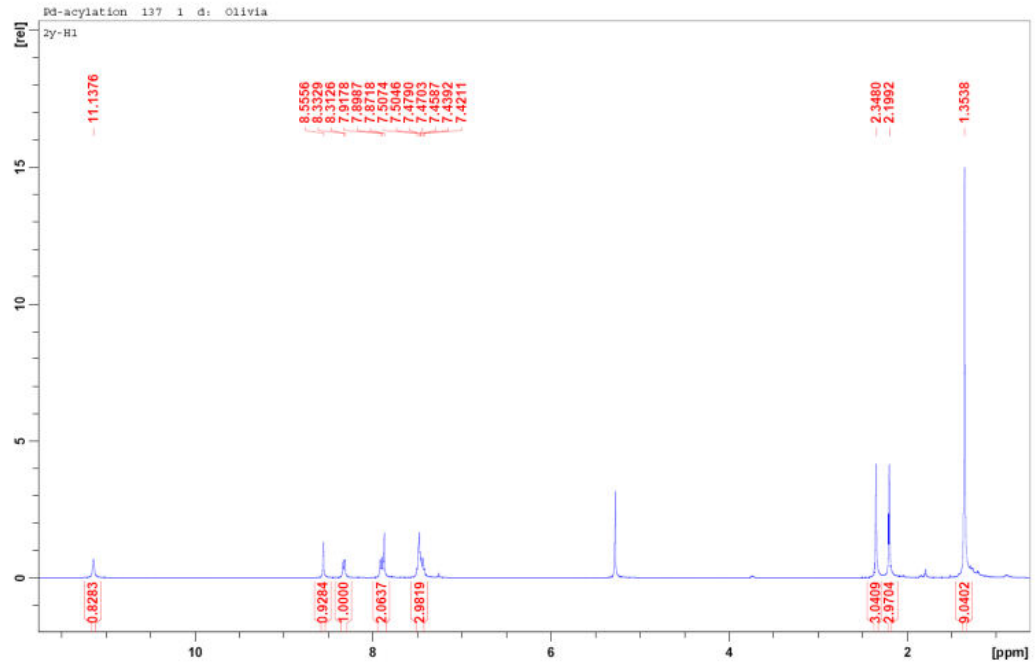

Figure A096 [13]C NMR spectrum of **7y**

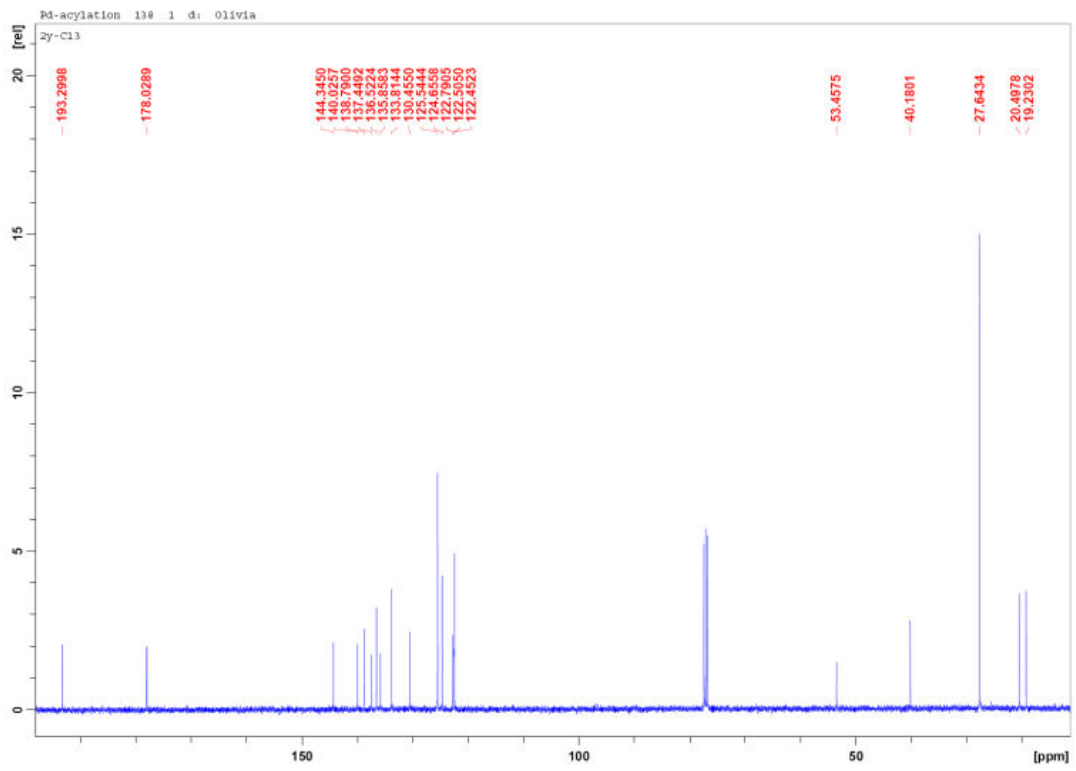

Figure A097 1H NMR spectrum of **9a**

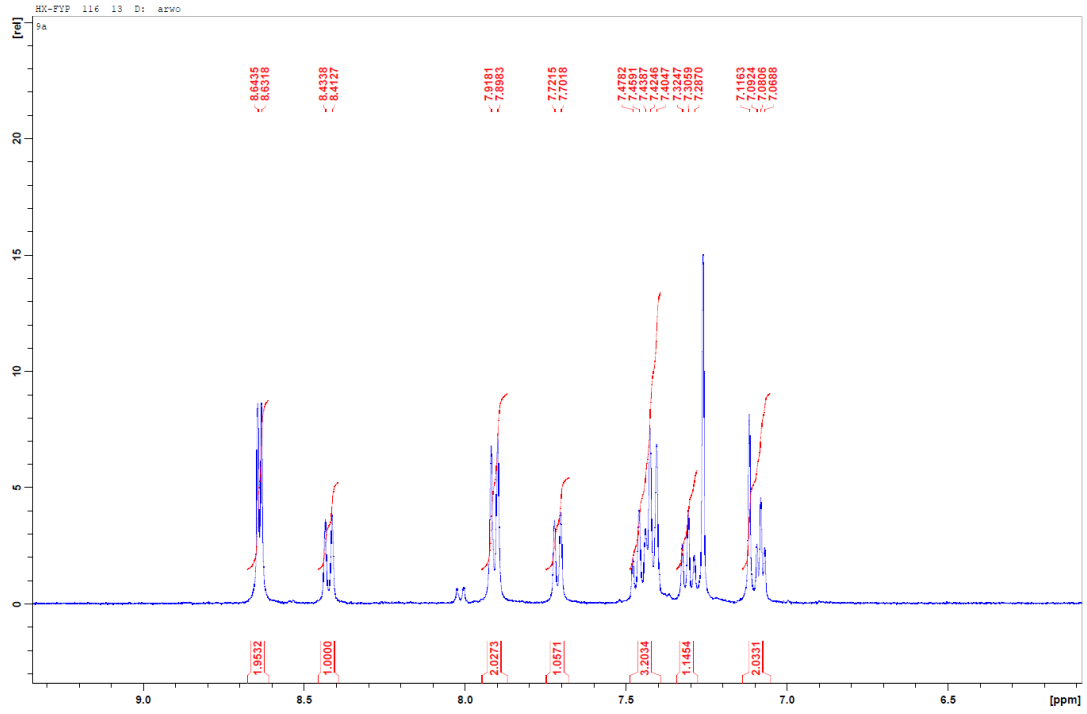

Figure A098 [1]H NMR spectrum of 4-chlorobenzoate-2,2,6,6-tetramethylpiperidine

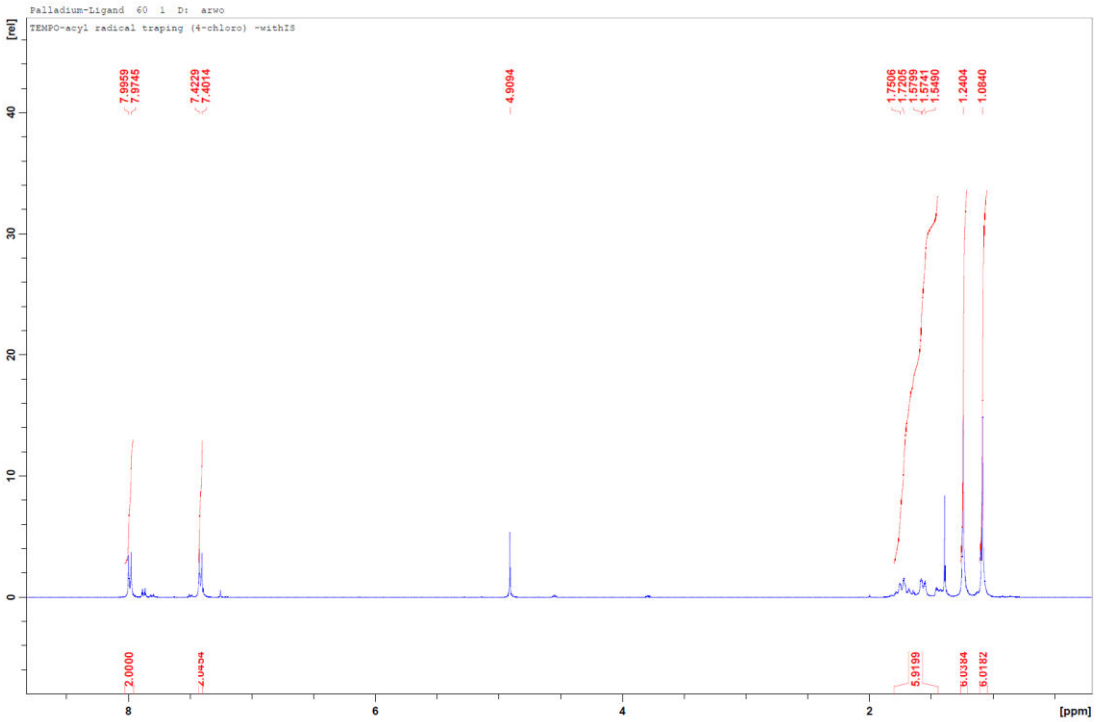

Figure A099 ^{1}H NMR spectrum of **13a**

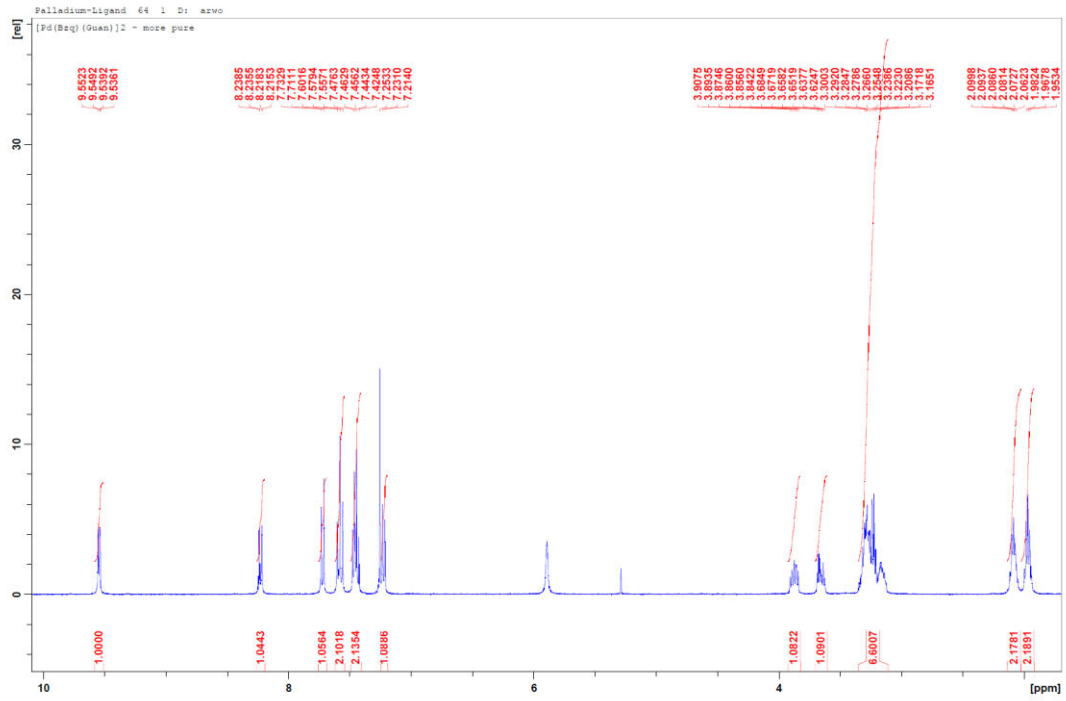

Figure A100 ^{1}H NMR spectrum of **13c**

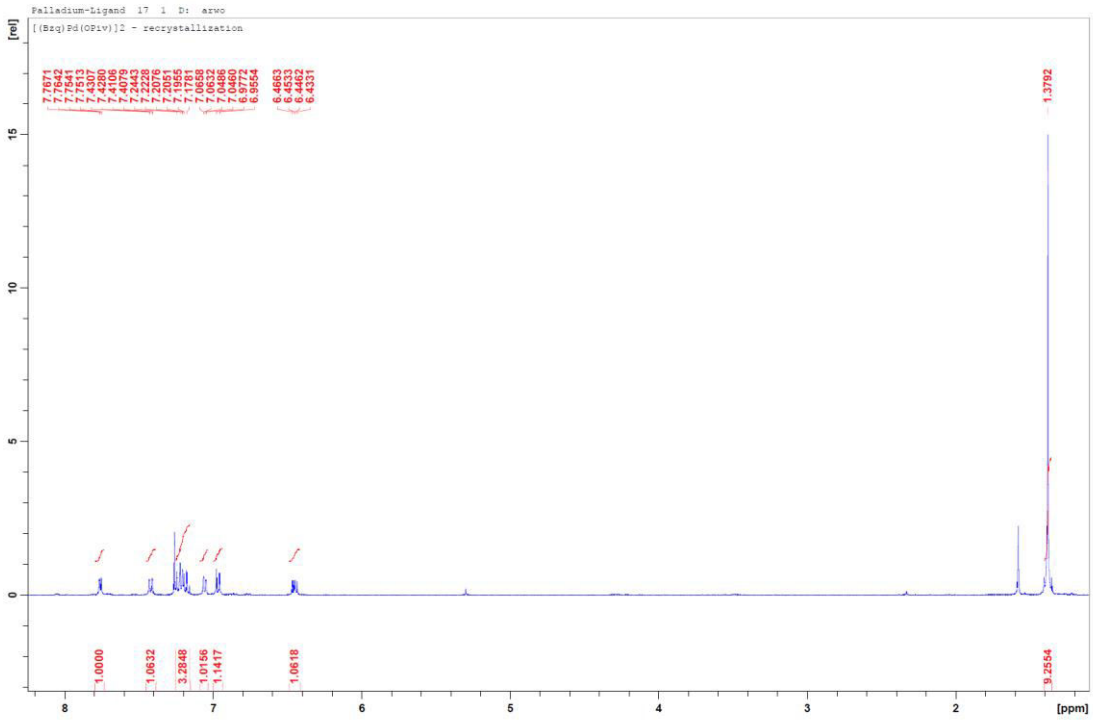

Figure A101 ^{1}H NMR spectrum of **13e**

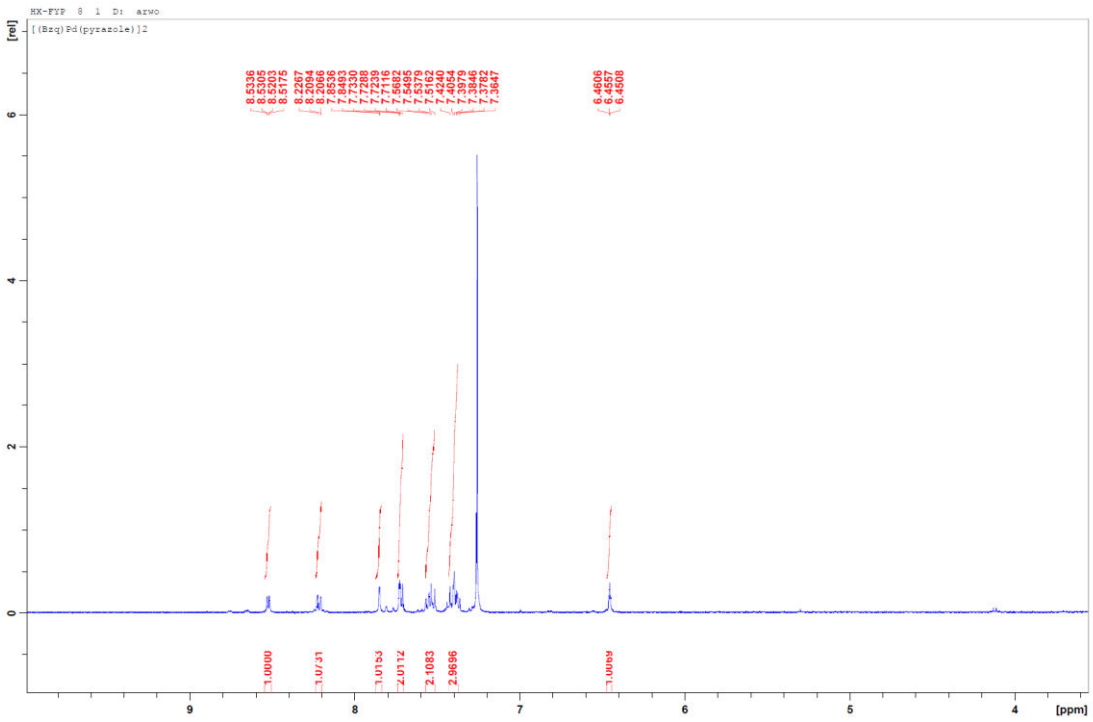

CHAPTER 4

Figure A102 [1]H NMR spectrum of **15a**

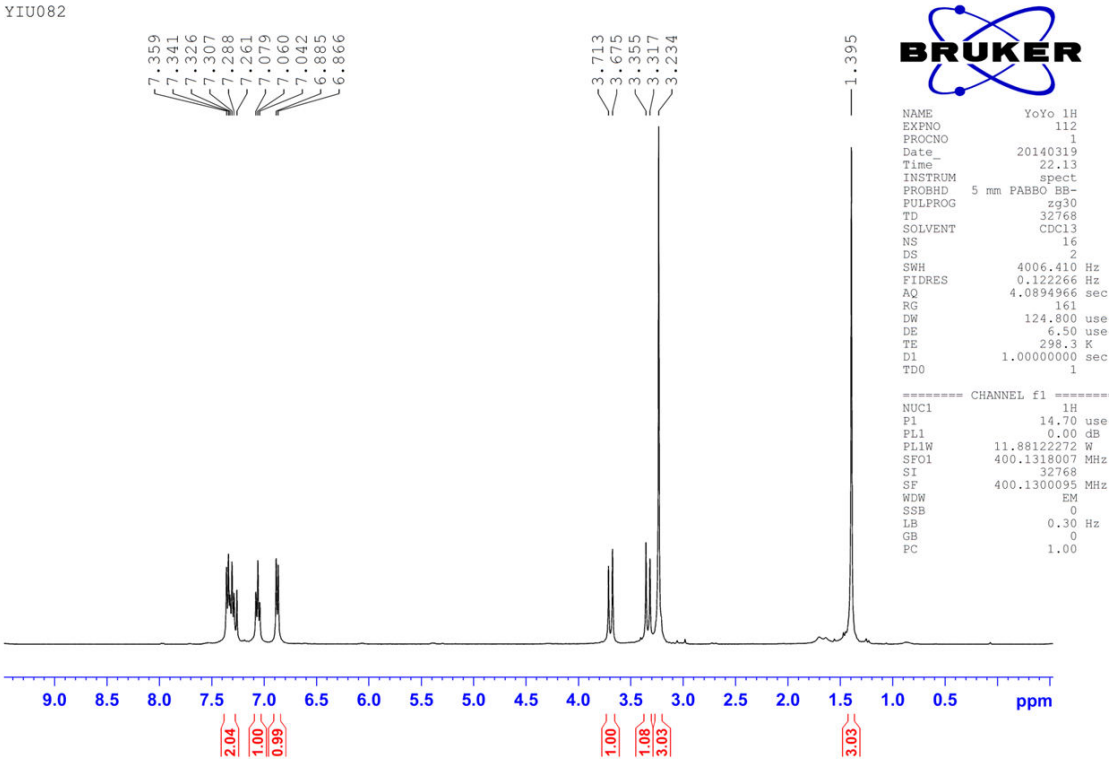

Figure A103 [13]C NMR spectrum of **15a**

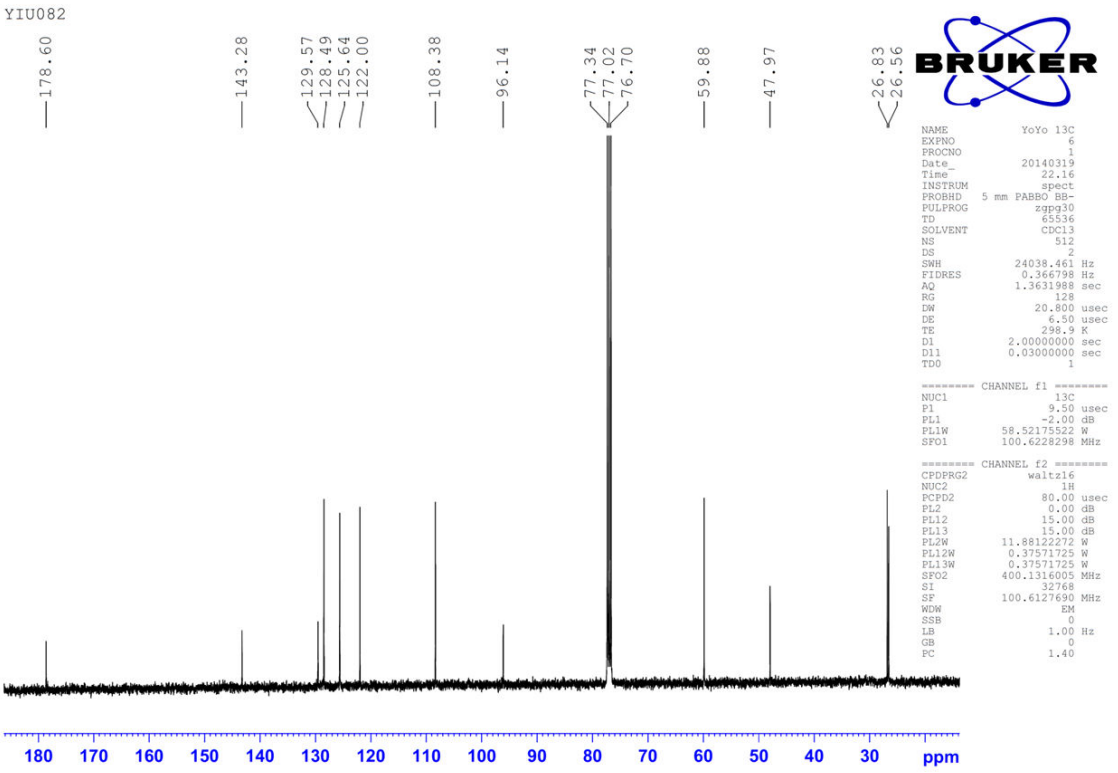

Figure A104 [1]H NMR spectrum of **15b**

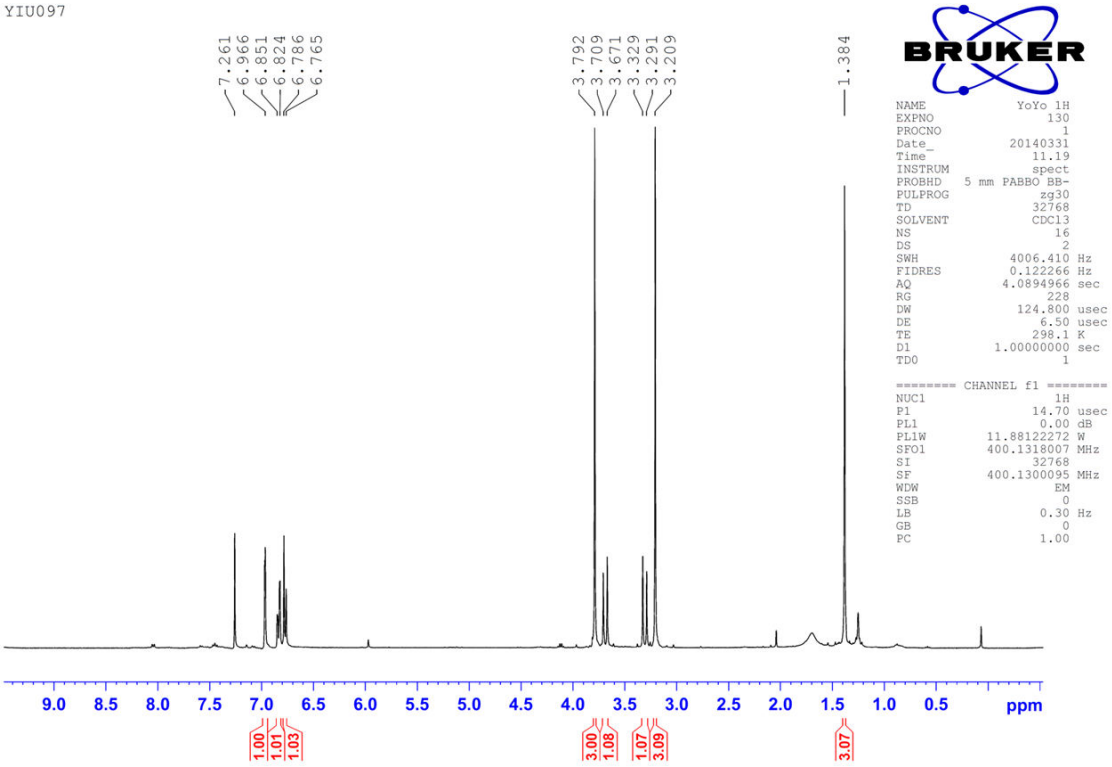

Figure A105 [13]C NMR spectrum of **15b**

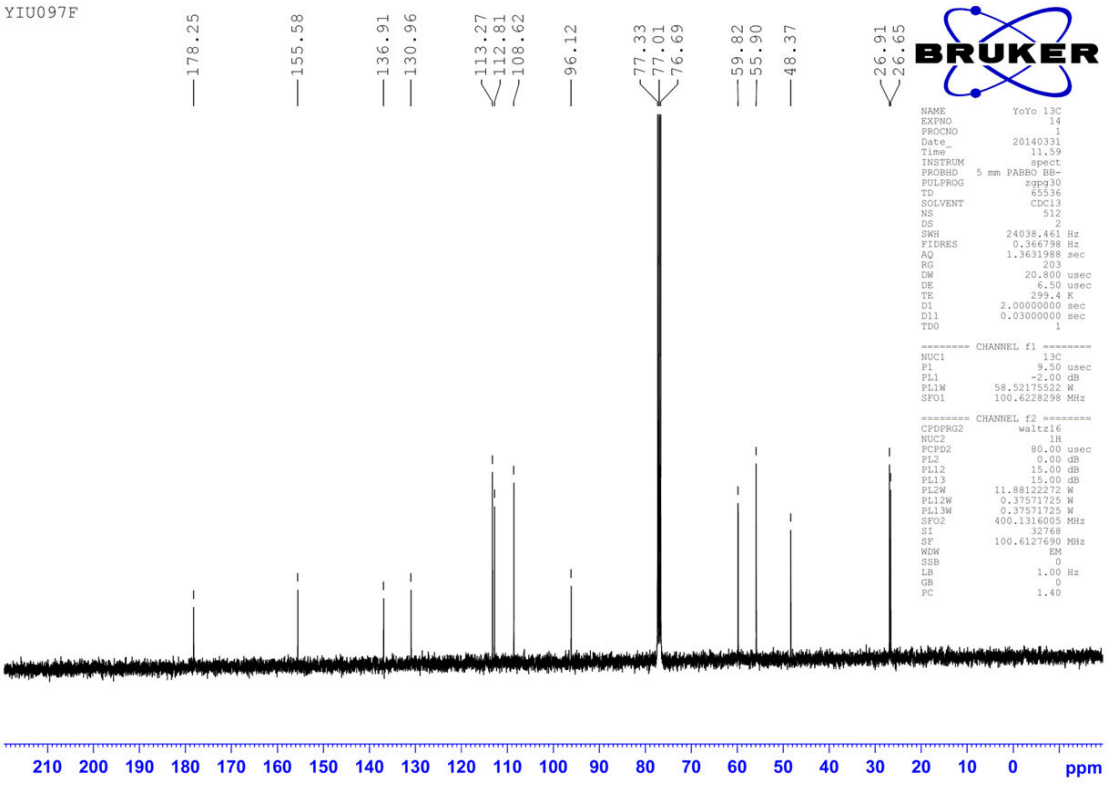

Figure A106 [1]H NMR spectrum of **15c**

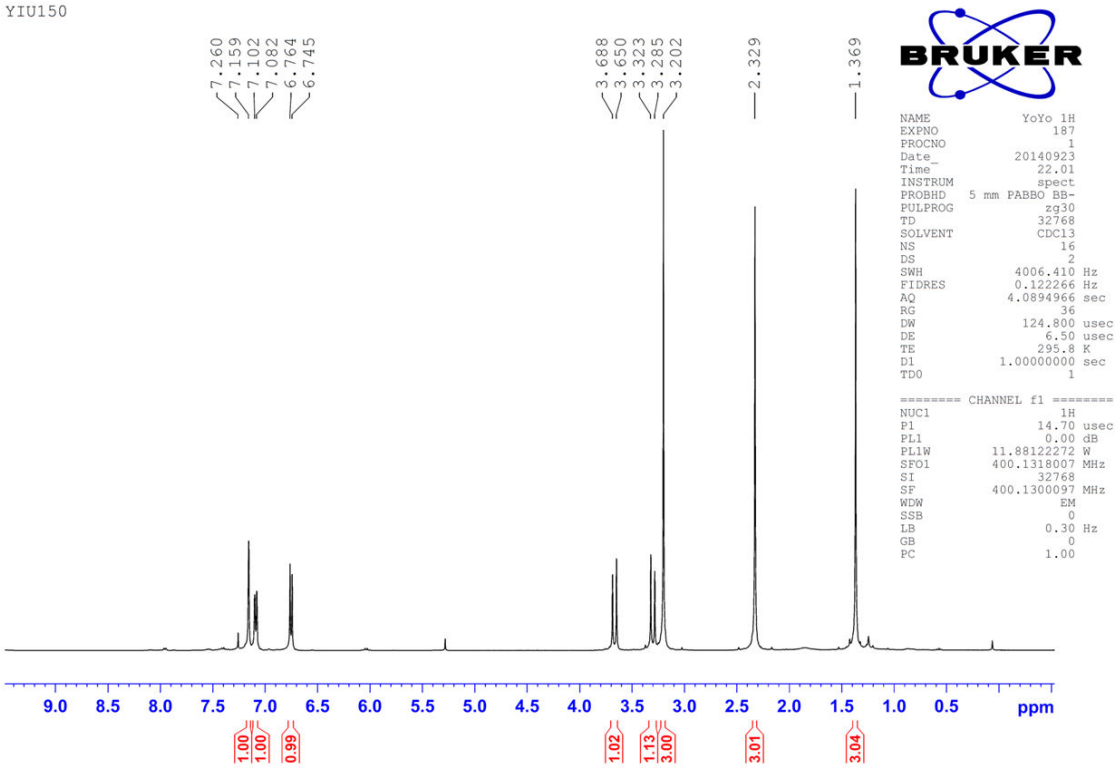

Figure A107 [13]C NMR spectrum of **15c**

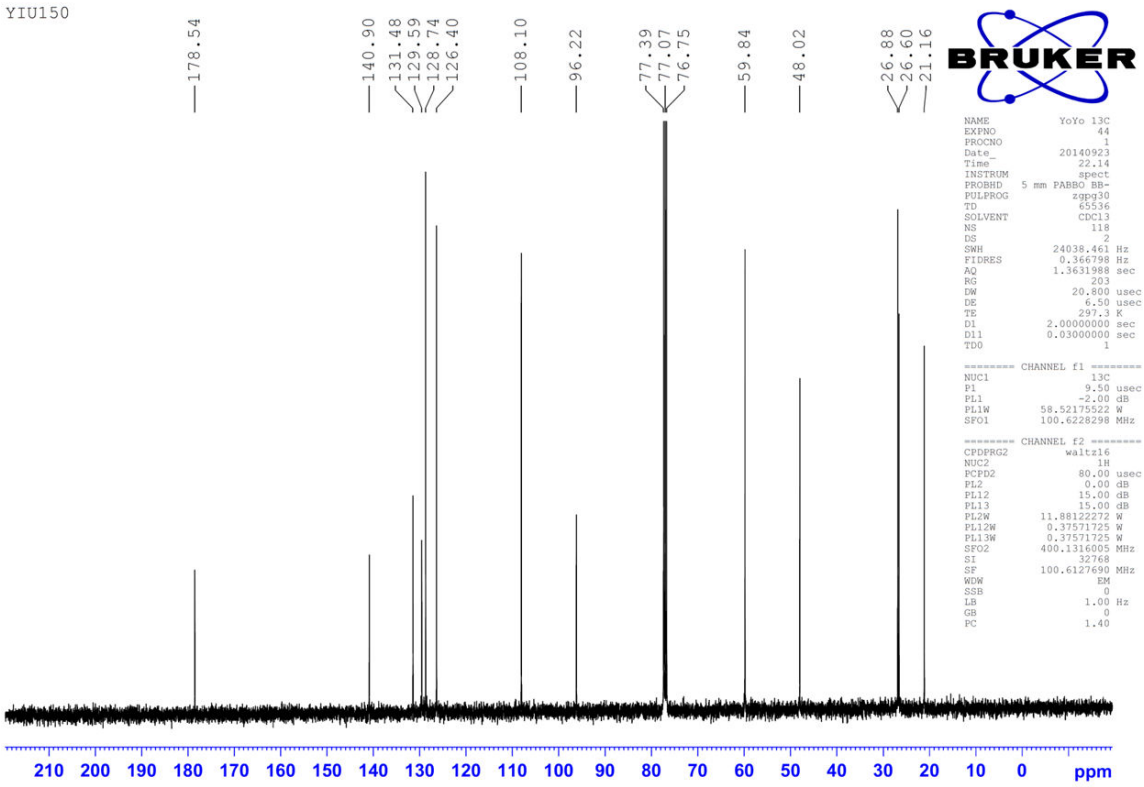

Figure A108 [1]H NMR spectrum of **15d**

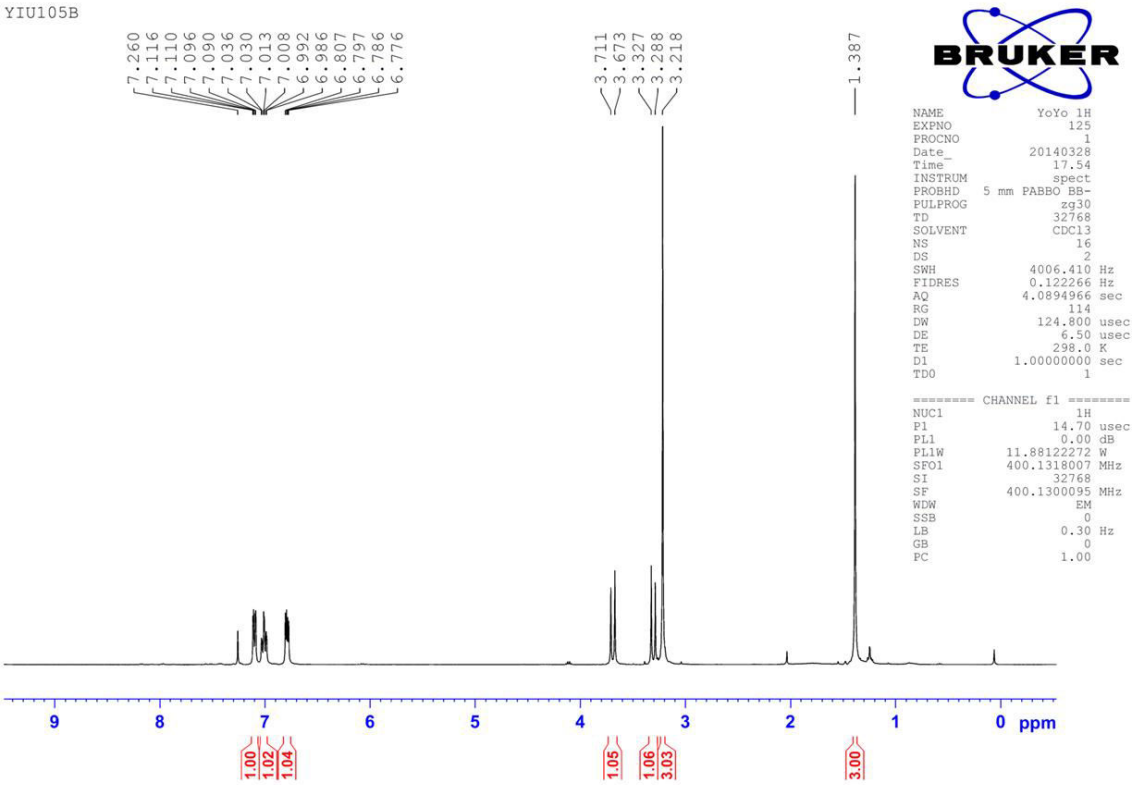

Figure A109 [13]C NMR spectrum of **15d**

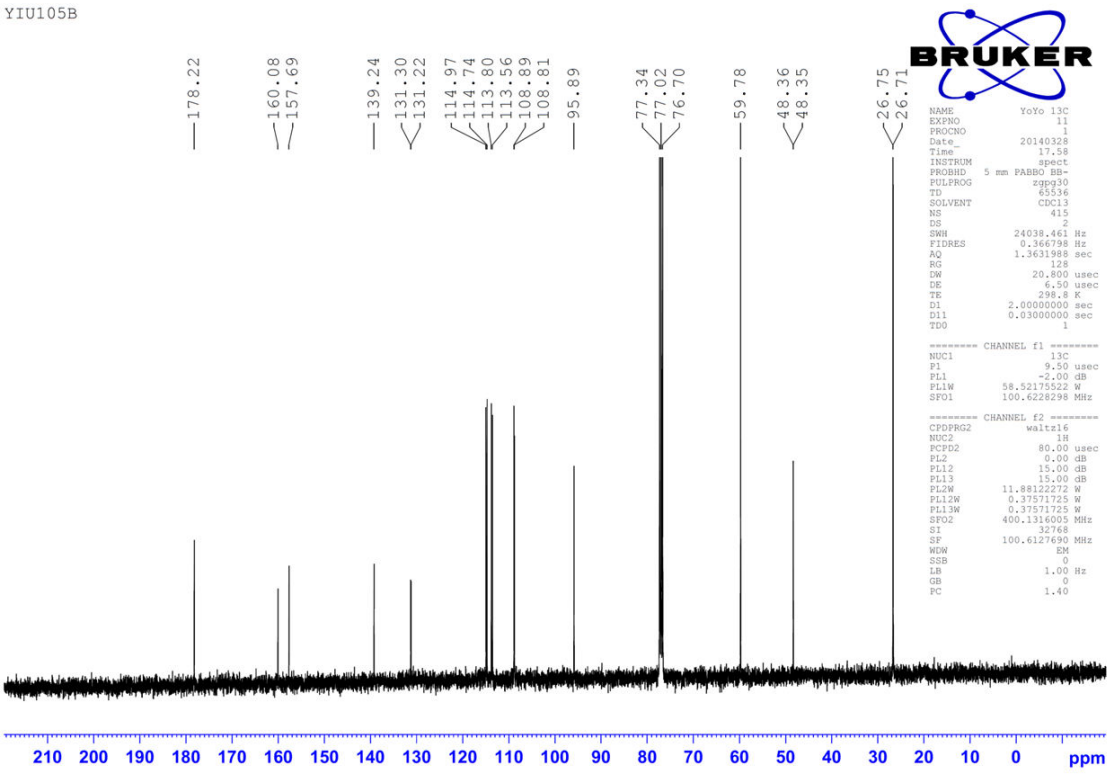

Figure A110 [1]H NMR spectrum of **15e**

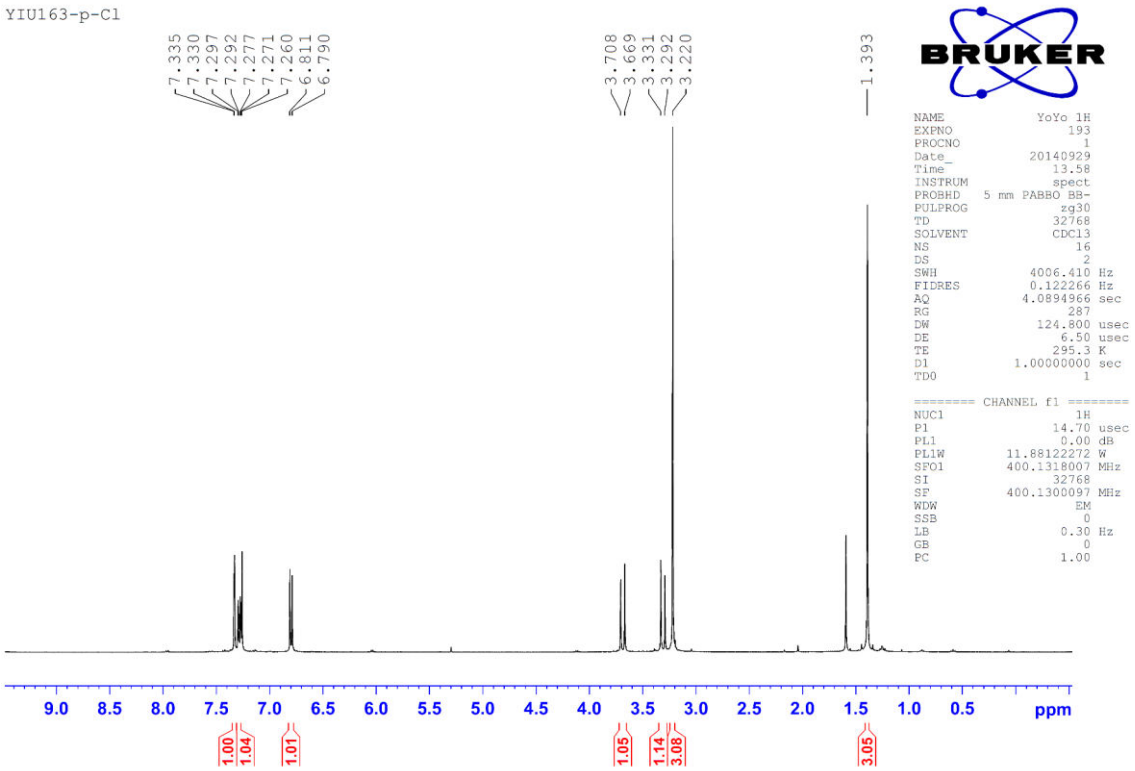

Figure A111 [13]C NMR spectrum of **15e**

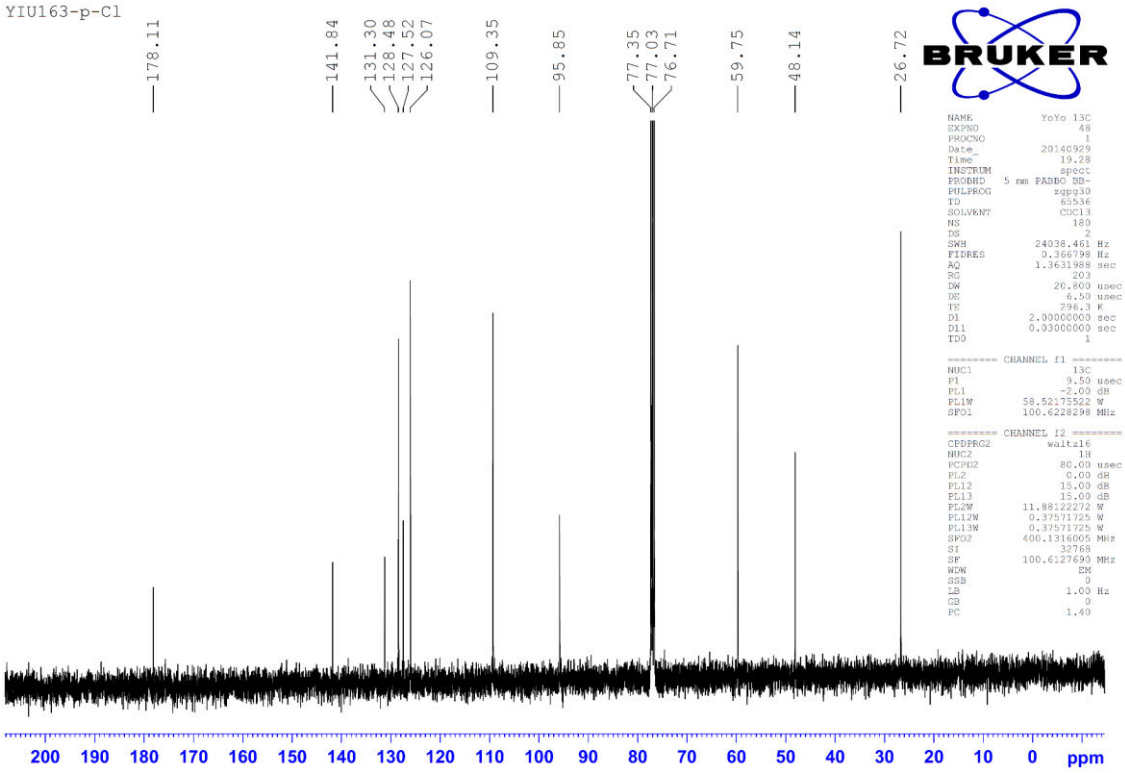

Figure A112 [1]H NMR spectrum of **15f**

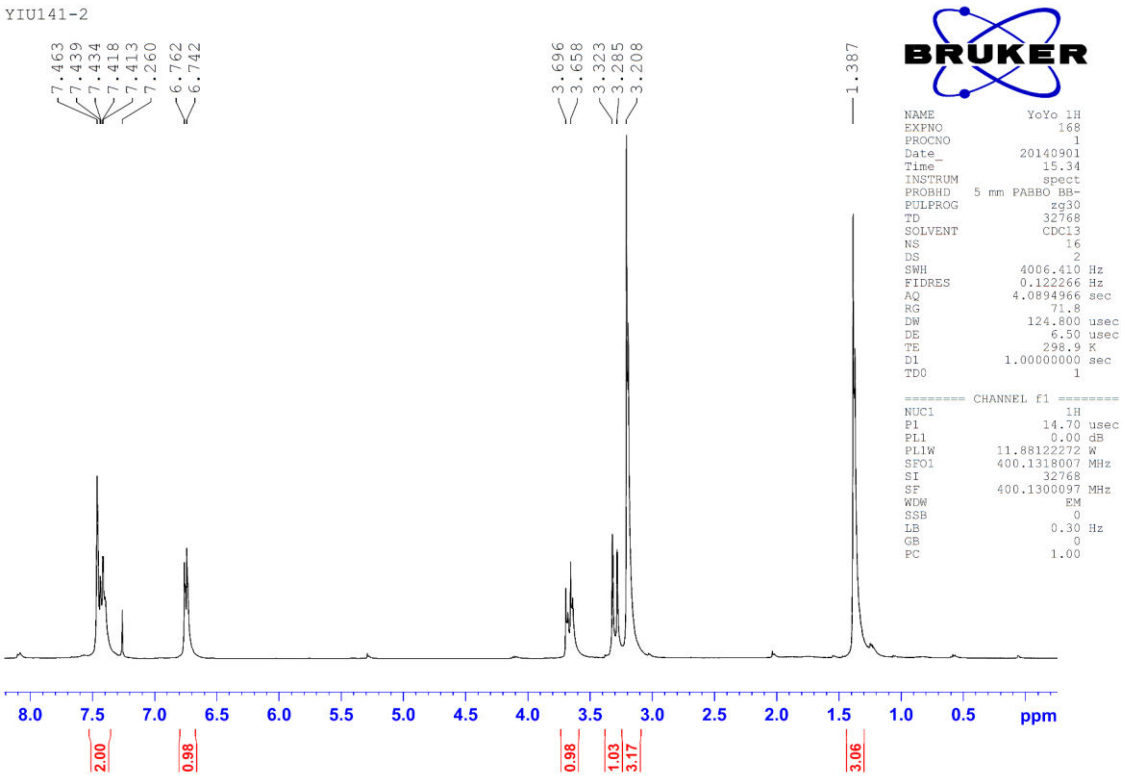

Figure A113 [13]C NMR spectrum of **15f**

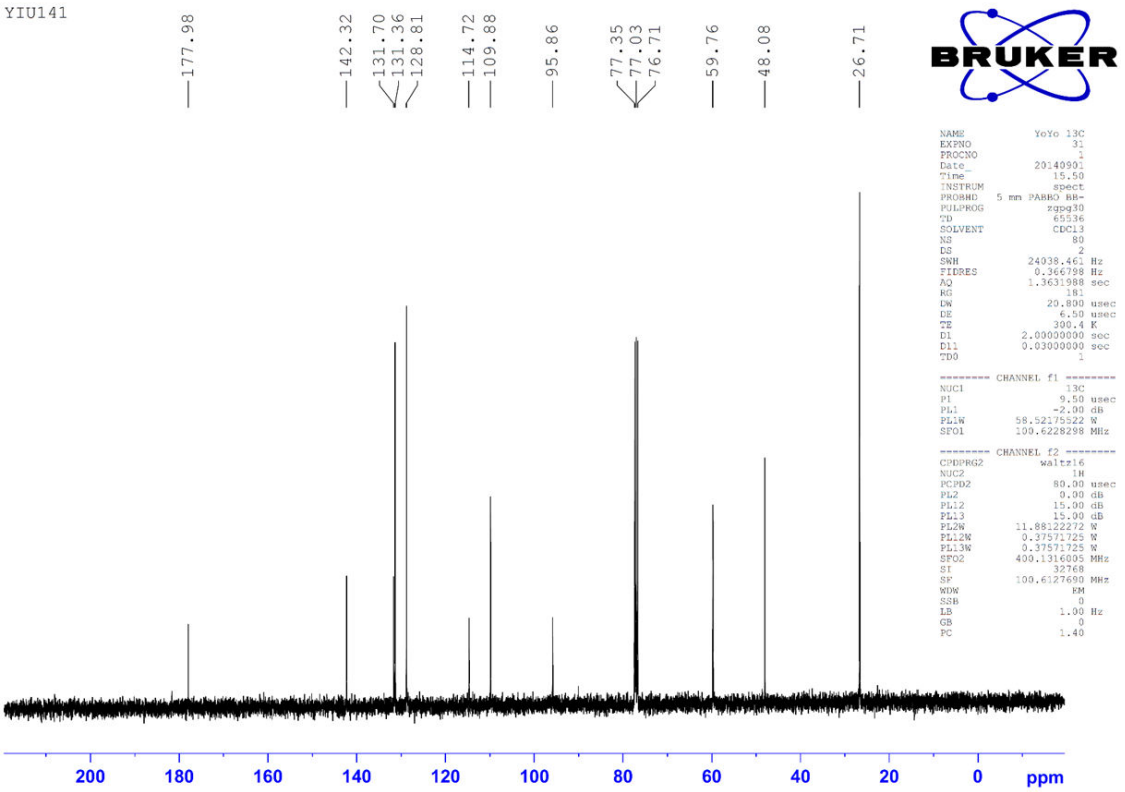

Figure A114 [1]H NMR spectrum of **15g**

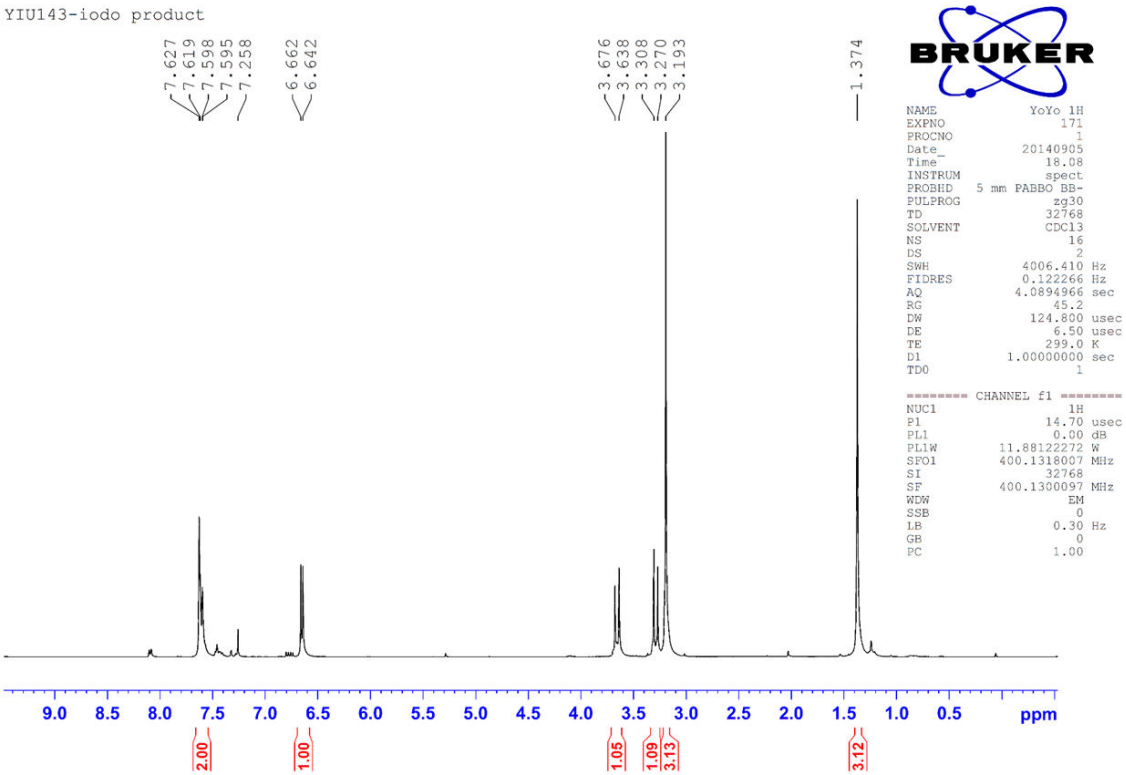

Figure A115 [13]C NMR spectrum of **15g**

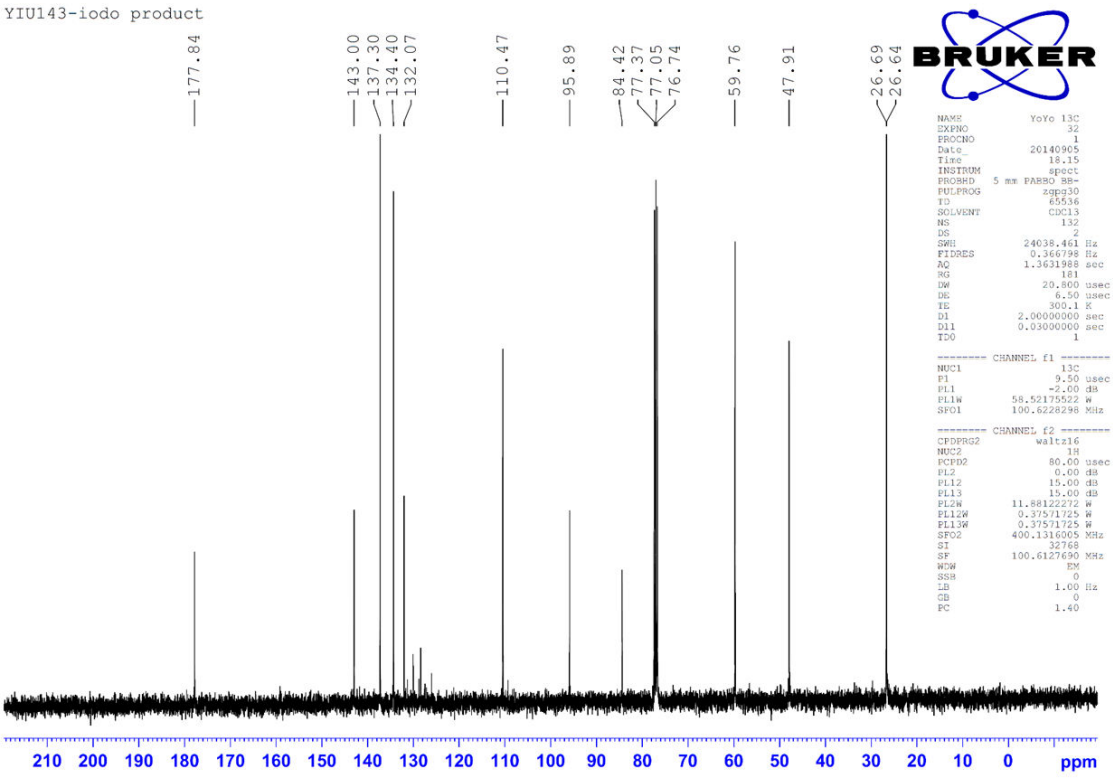

Figure A116 [1]H NMR spectrum of **15h**

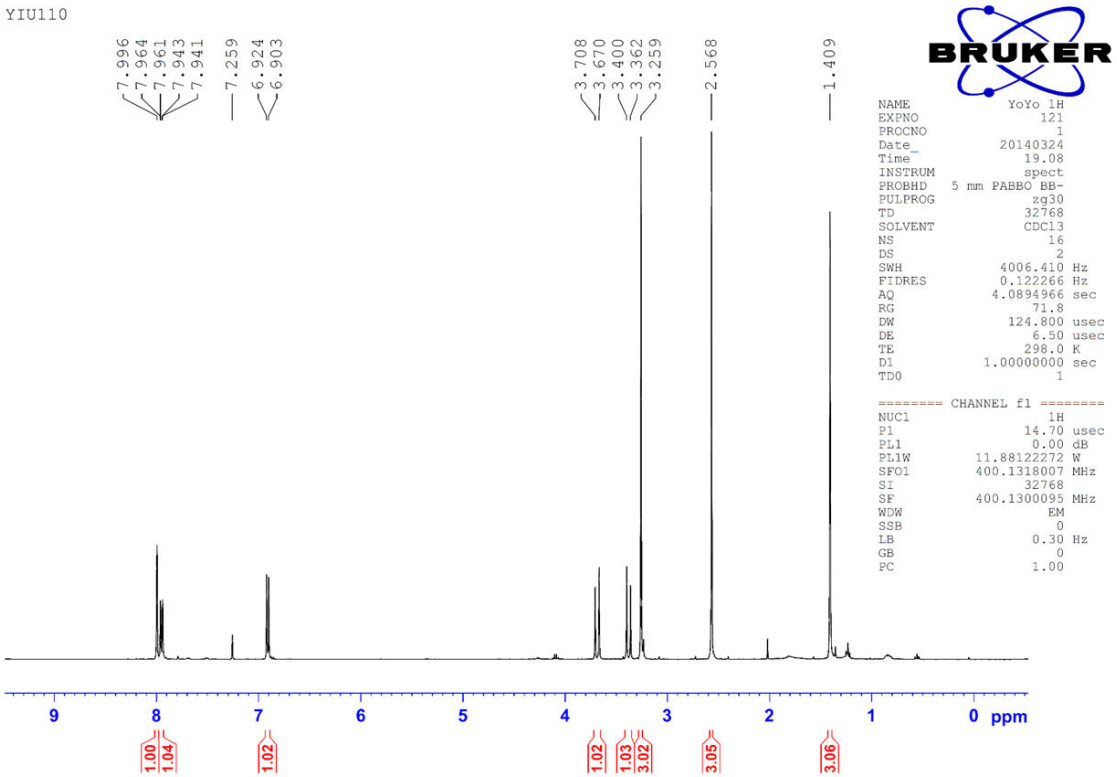

Figure A117 [13]C NMR spectrum of **15h**

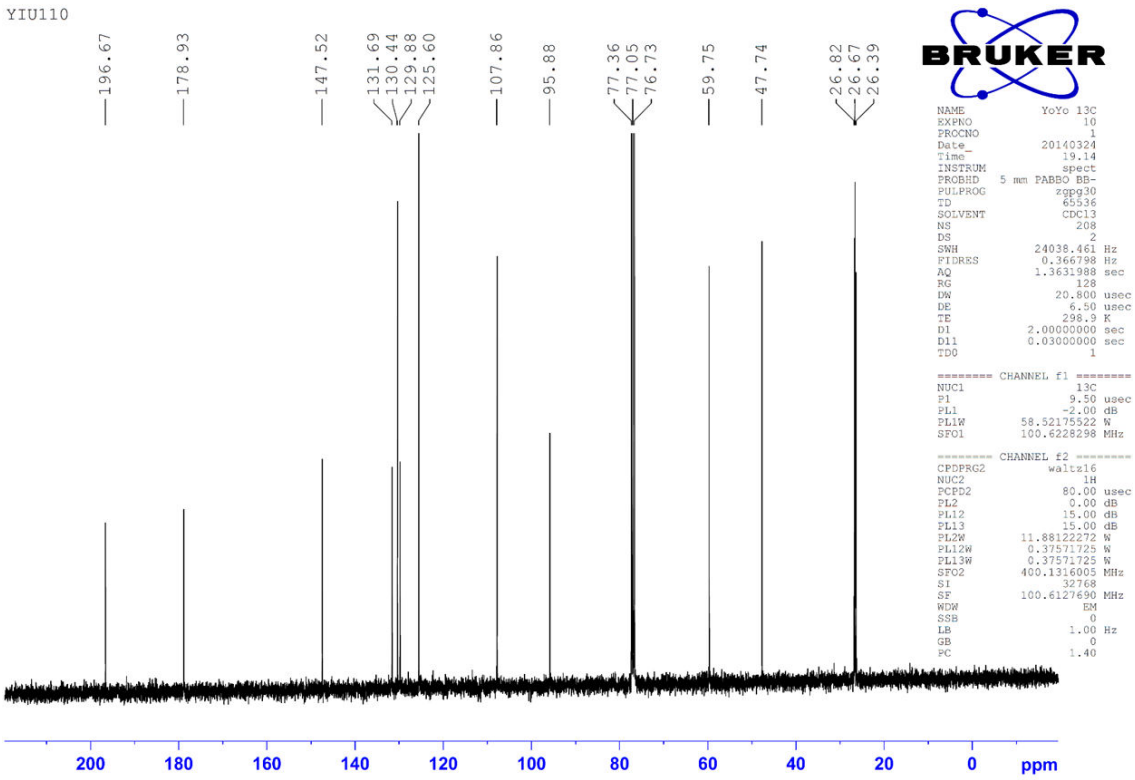

Figure A118 ^{1}H NMR spectrum of **15i**

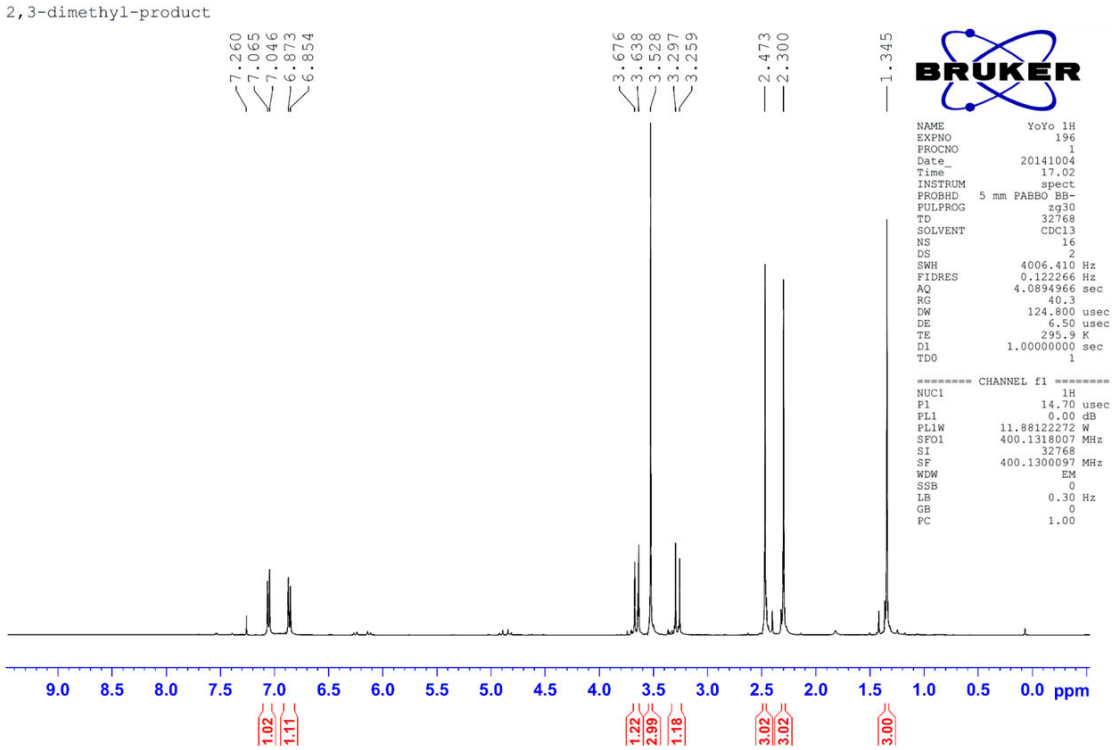

Figure A119 ^{13}C NMR spectrum of **15i**

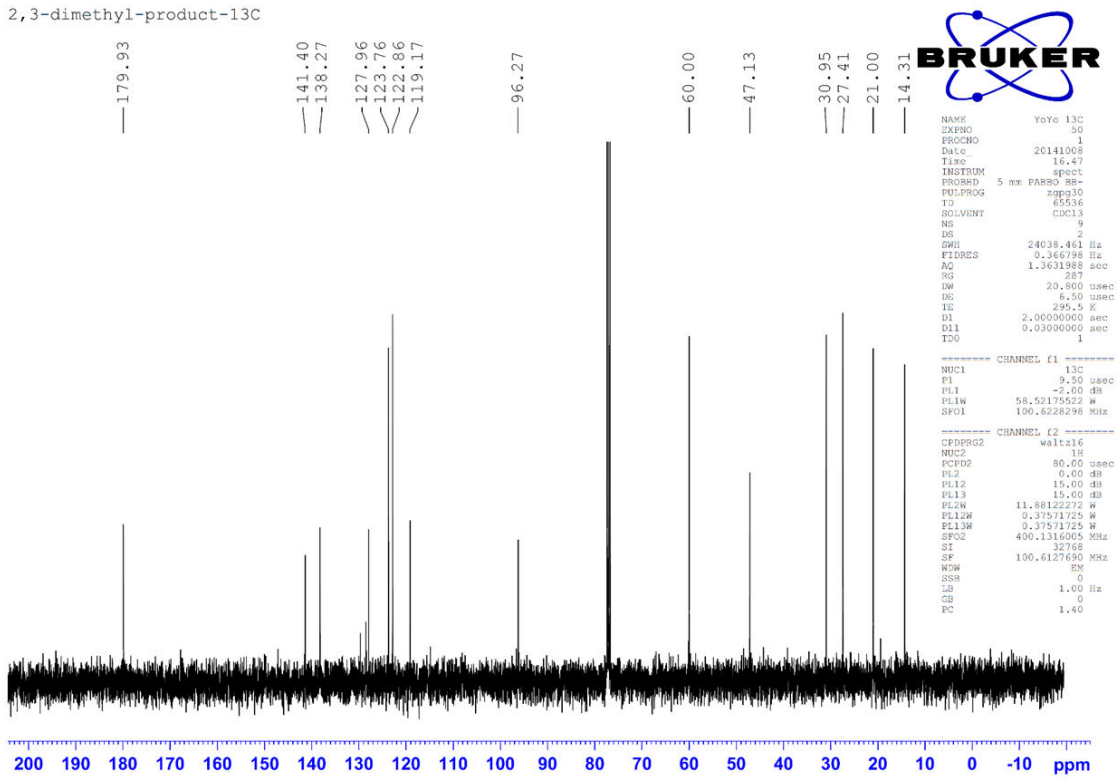

Figure A120 [1]H NMR spectrum of **15j**

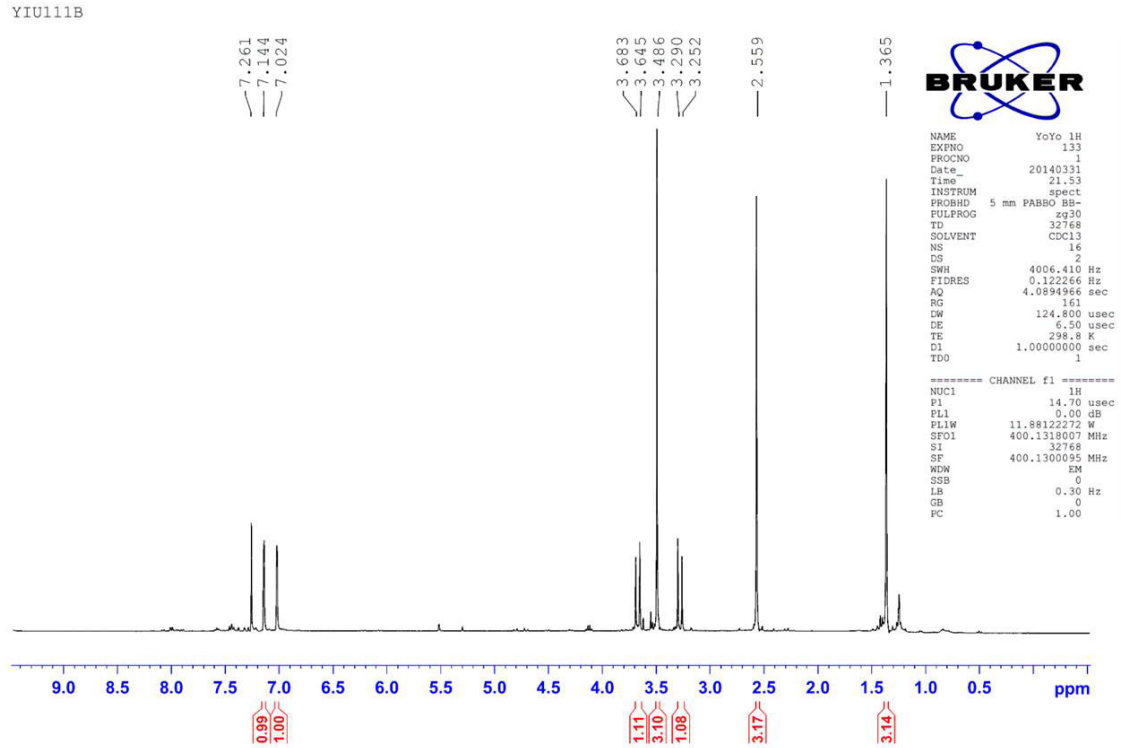

Figure A121 [13]C NMR spectrum of **15j**

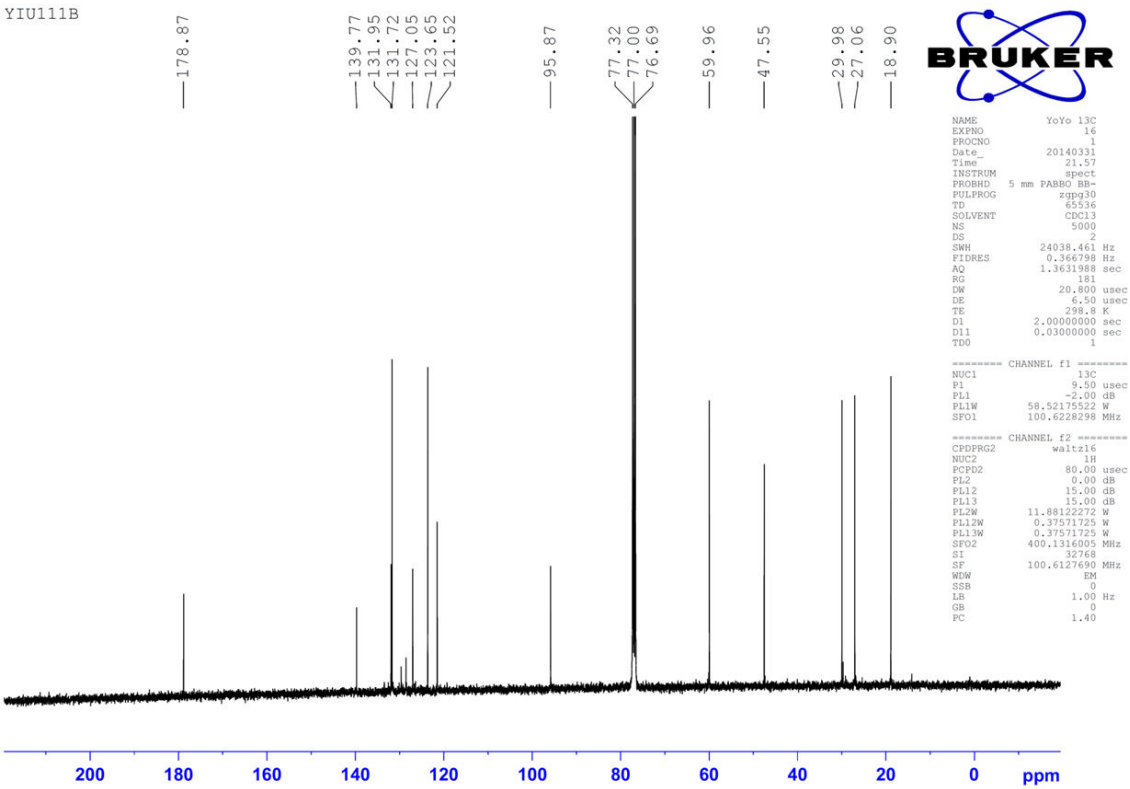

Figure A122 [1]H NMR spectrum of **15k + 15k'**

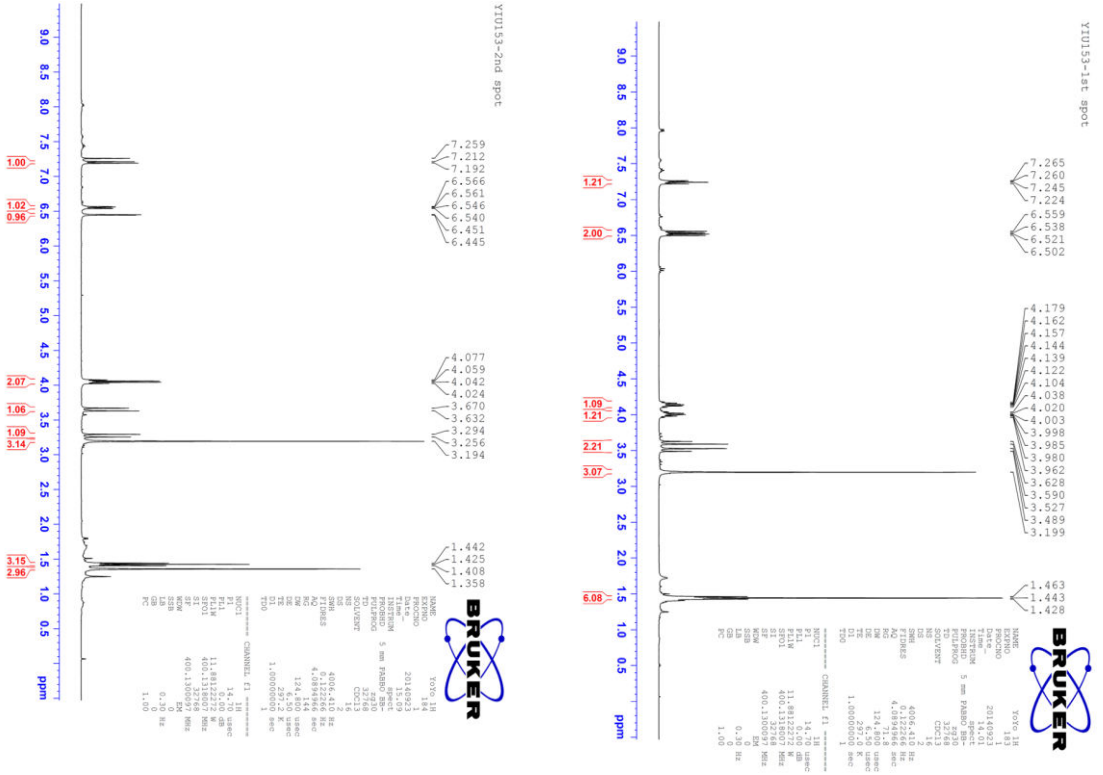

Figure A123 [13]C NMR spectrum of **15k + 15k'**

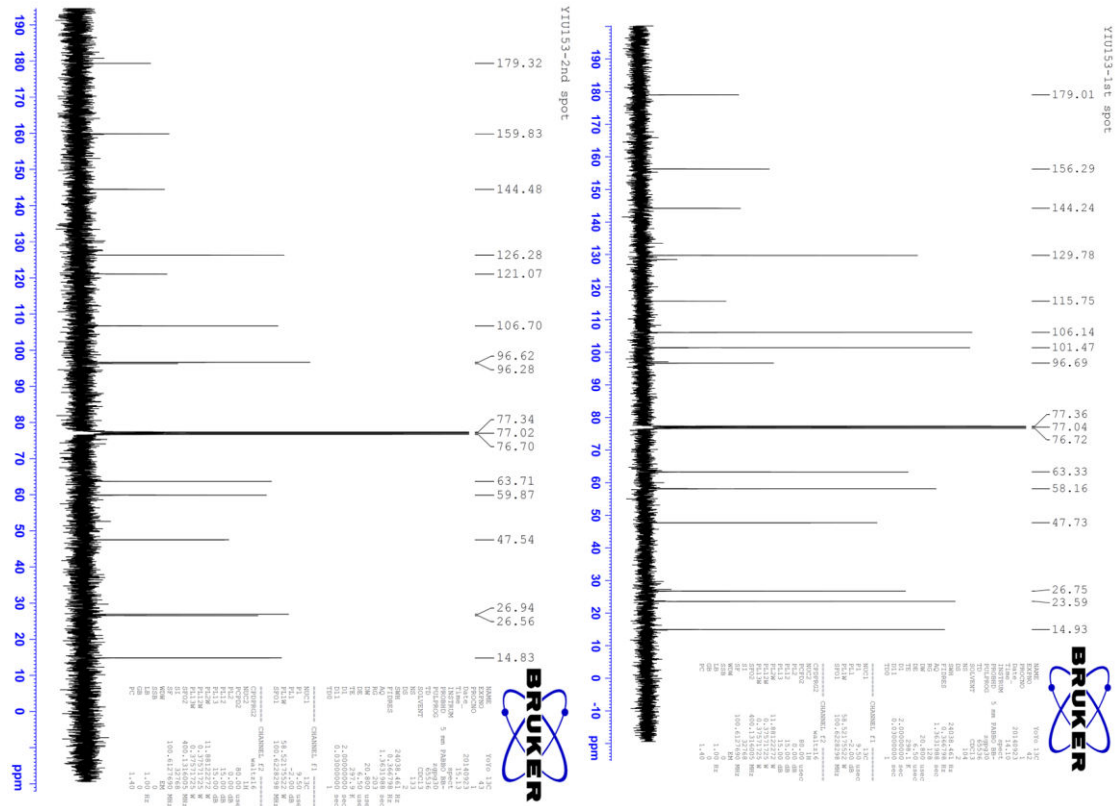

Figure A124 [1]H NMR spectrum of **15l + 15l'**

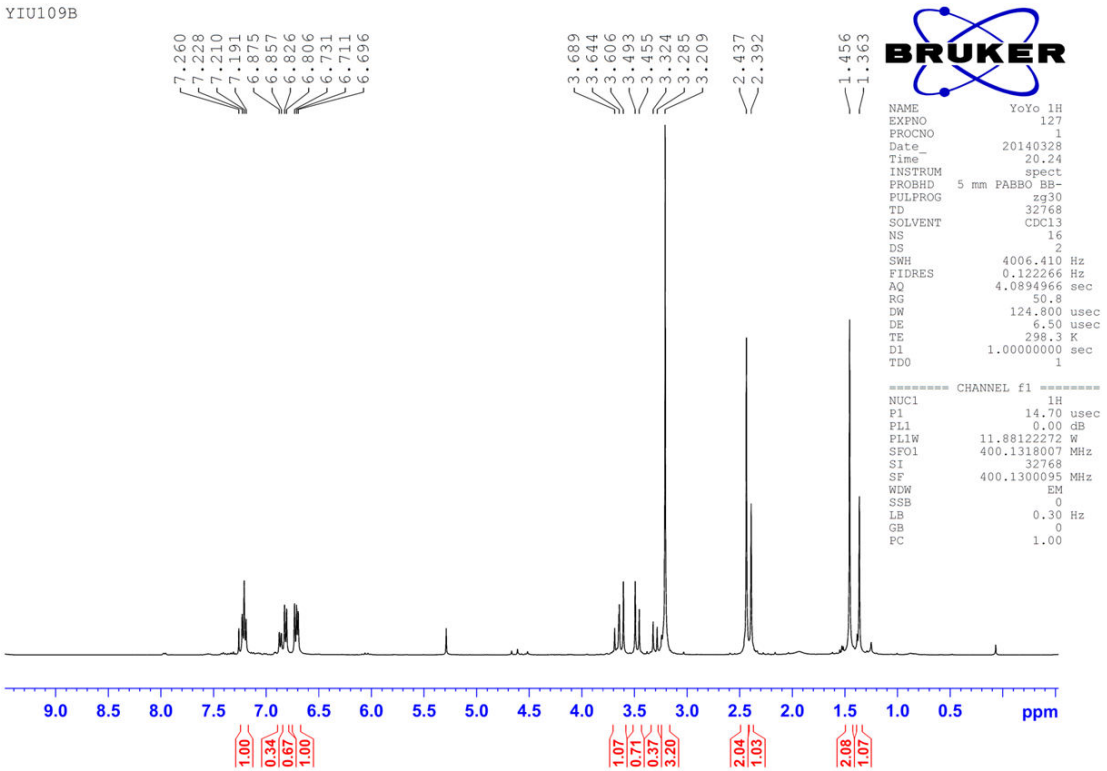

Figure A125 [13]C NMR spectrum of **15l + 15l'**

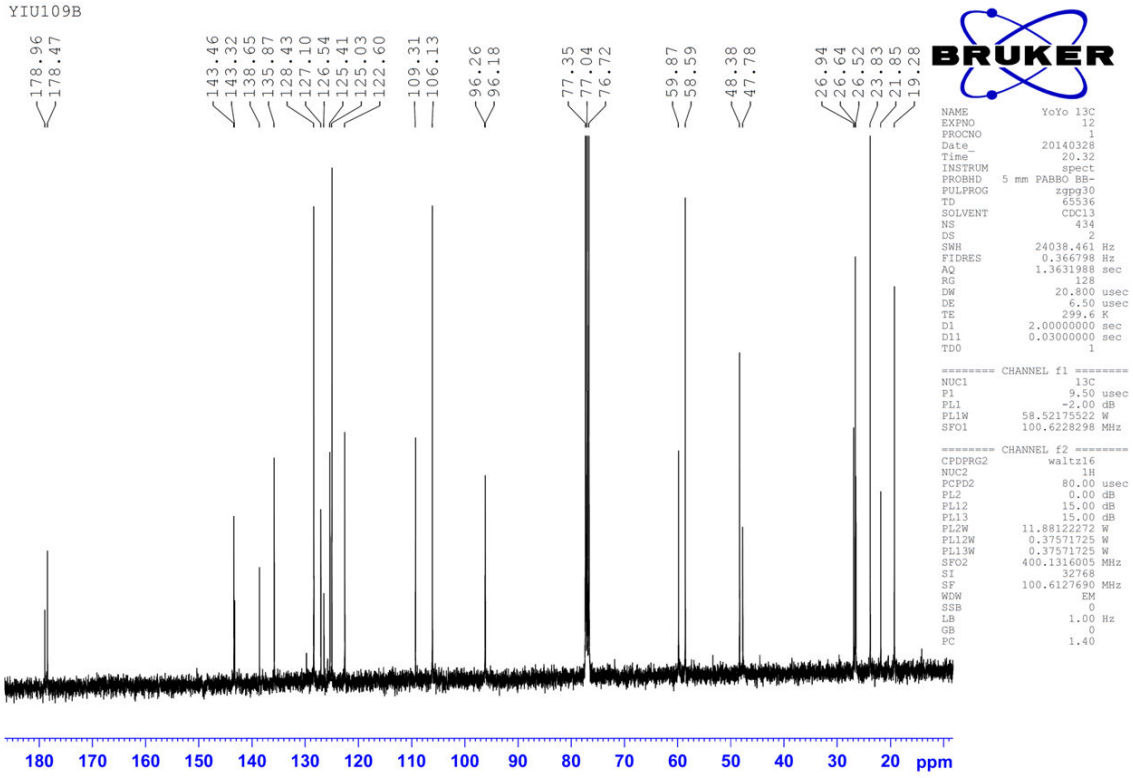

Figure A126 [1]H NMR spectrum of **15m + 15m'**

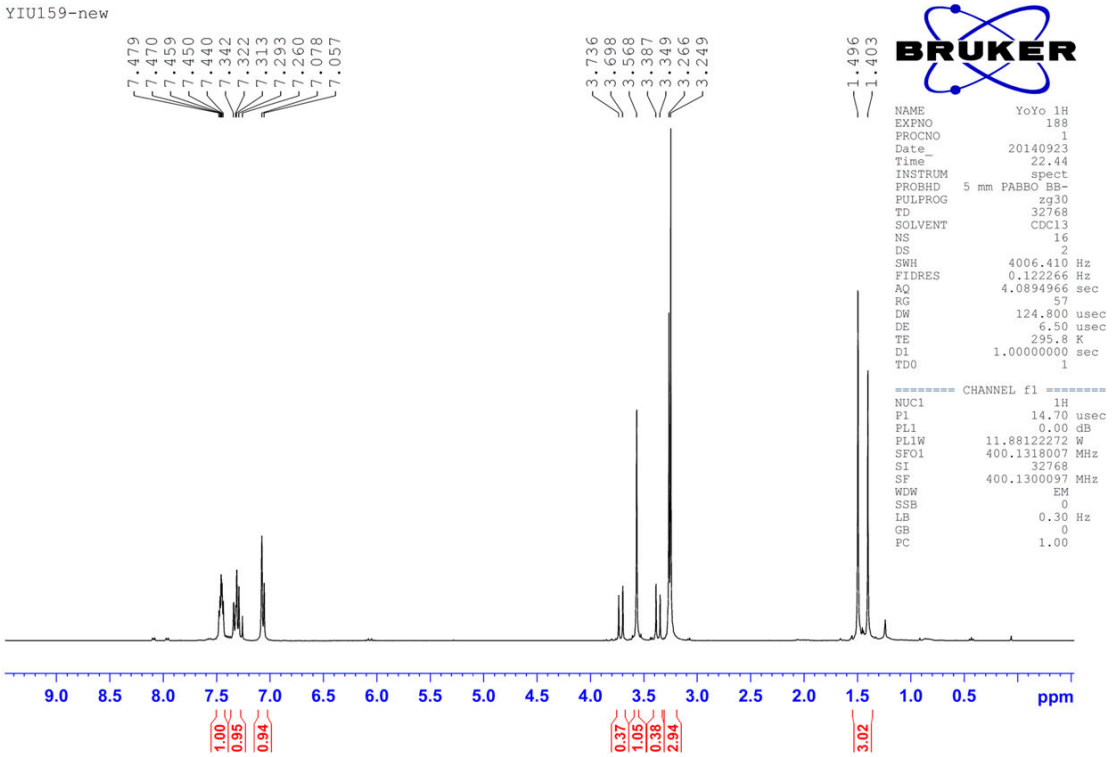

Figure A127 [13]C NMR spectrum of **15m + 15m'**

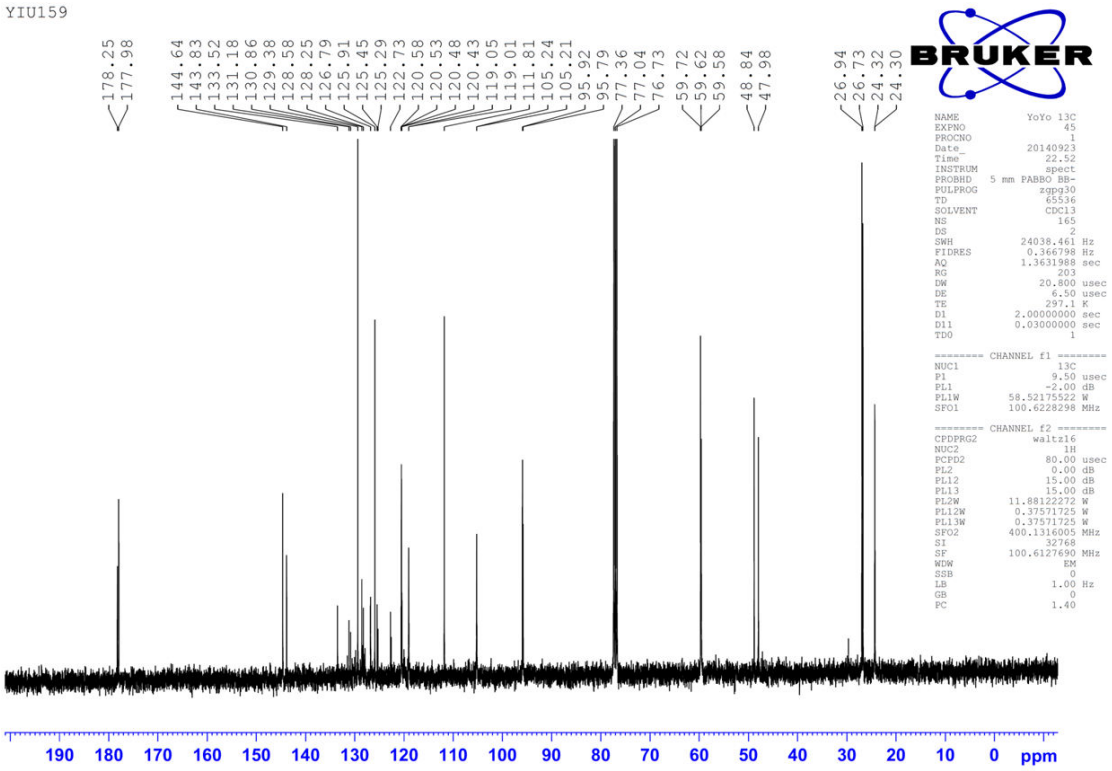

Figure A128 [1]H NMR spectrum of **15n**

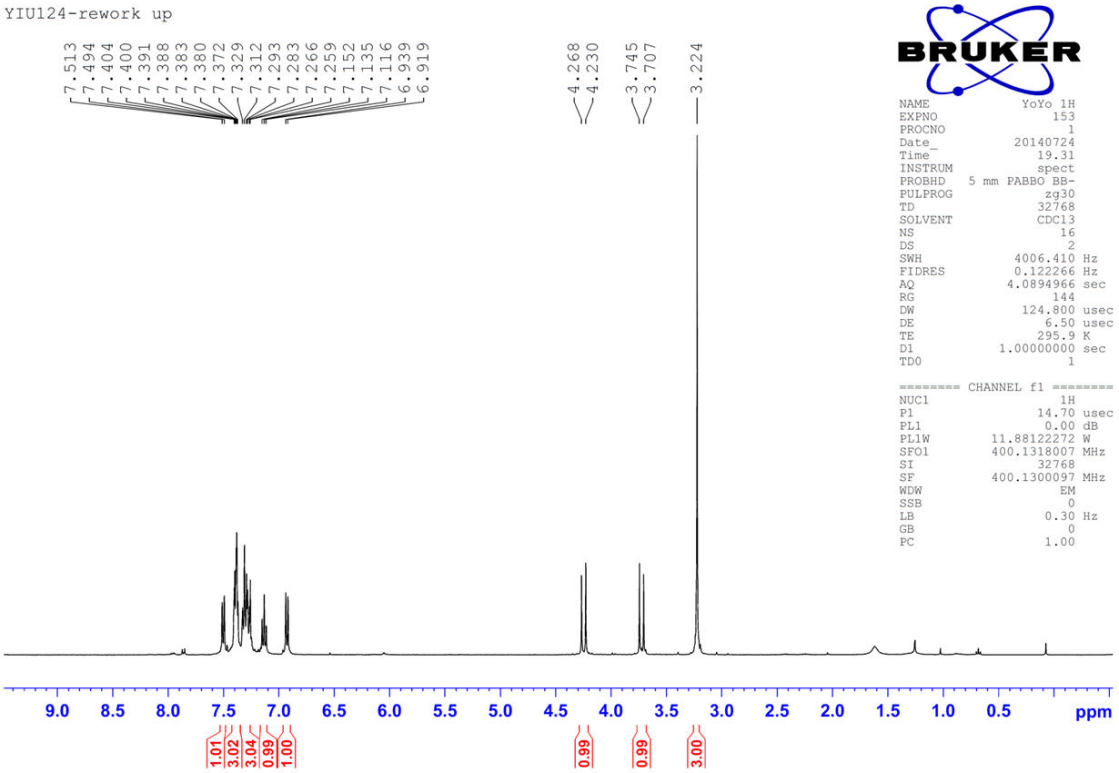

Figure A129 [13]C NMR spectrum of **15n**

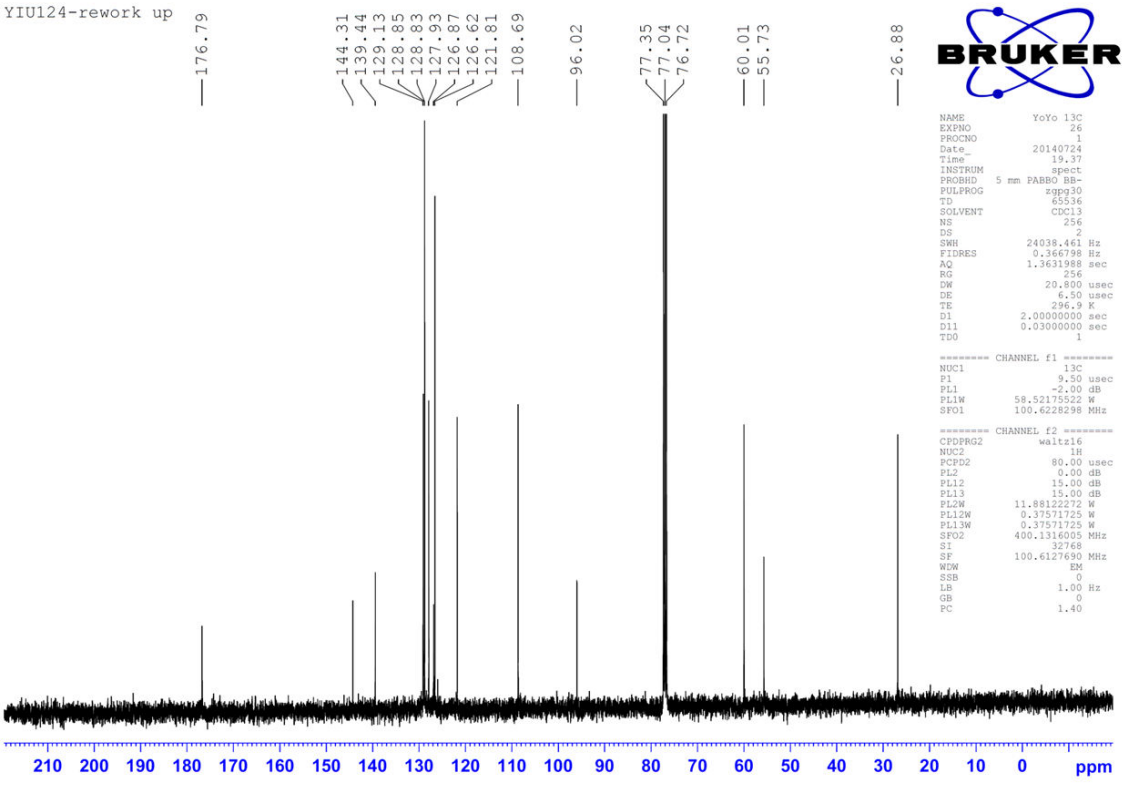

Figure A130 [1]H NMR spectrum of **15o**

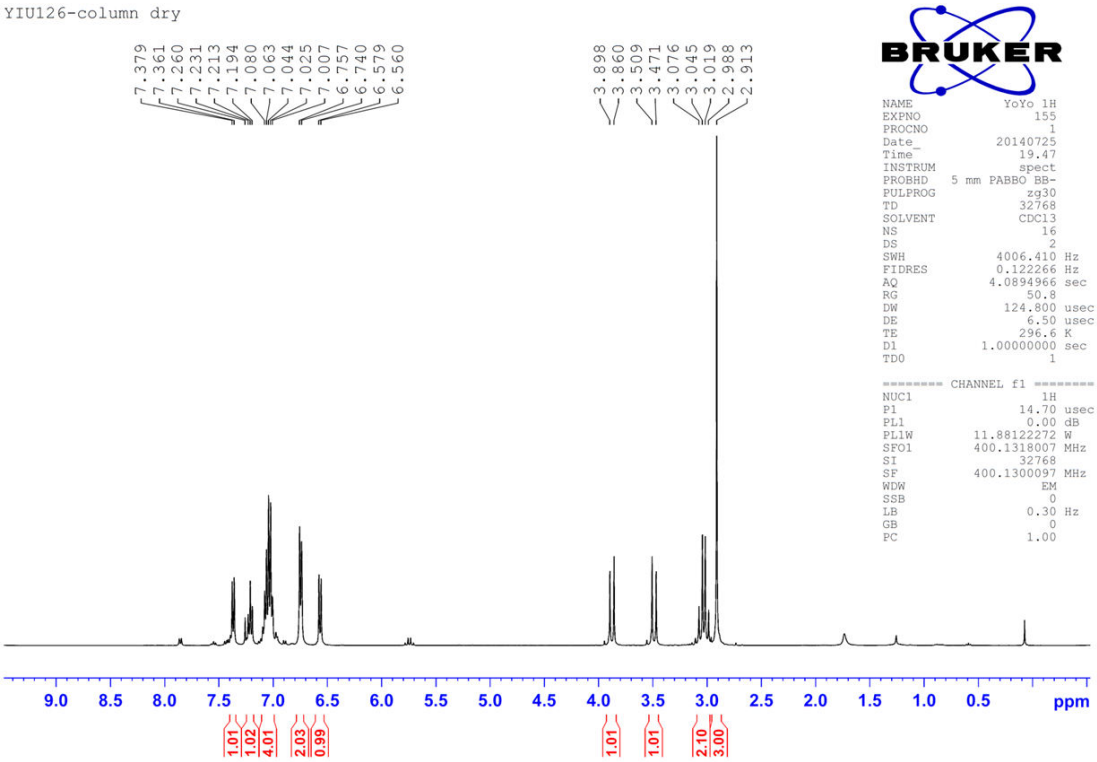

Figure A131 [13]C NMR spectrum of **15o**

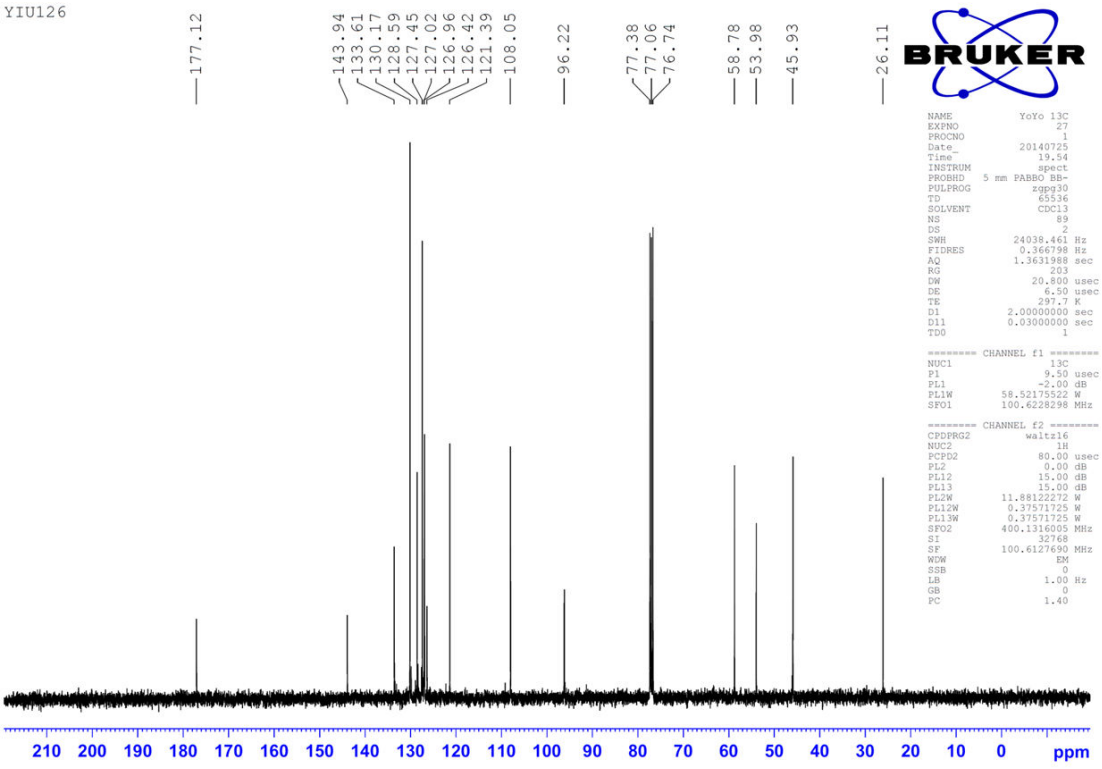

Figure A132 [1]H NMR spectrum of **15q**

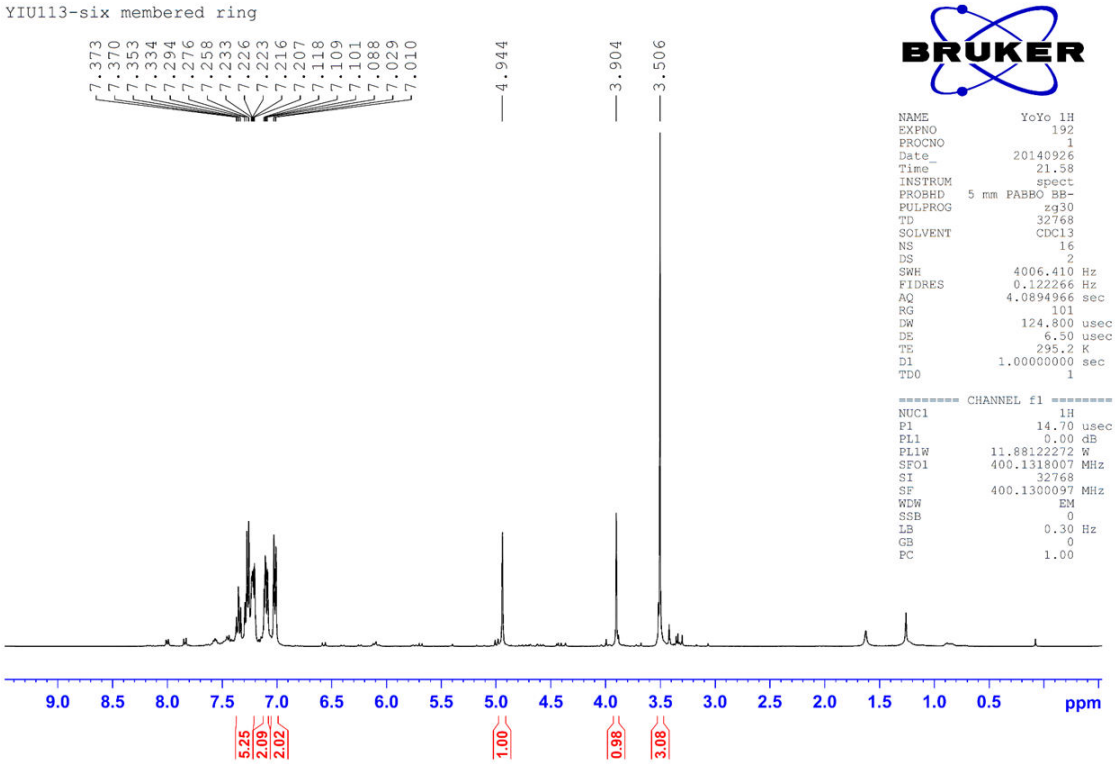

Figure A133 [13]C NMR spectrum of **15q**

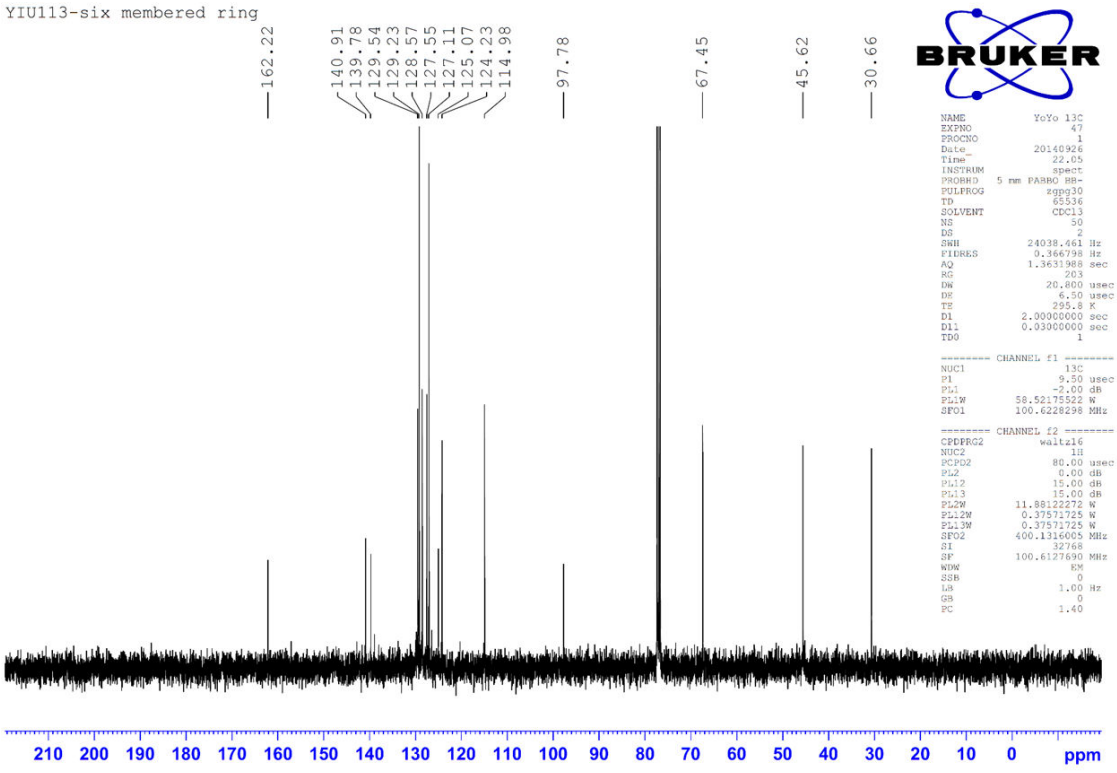

Figure A134 [1]H NMR spectrum of **15r**

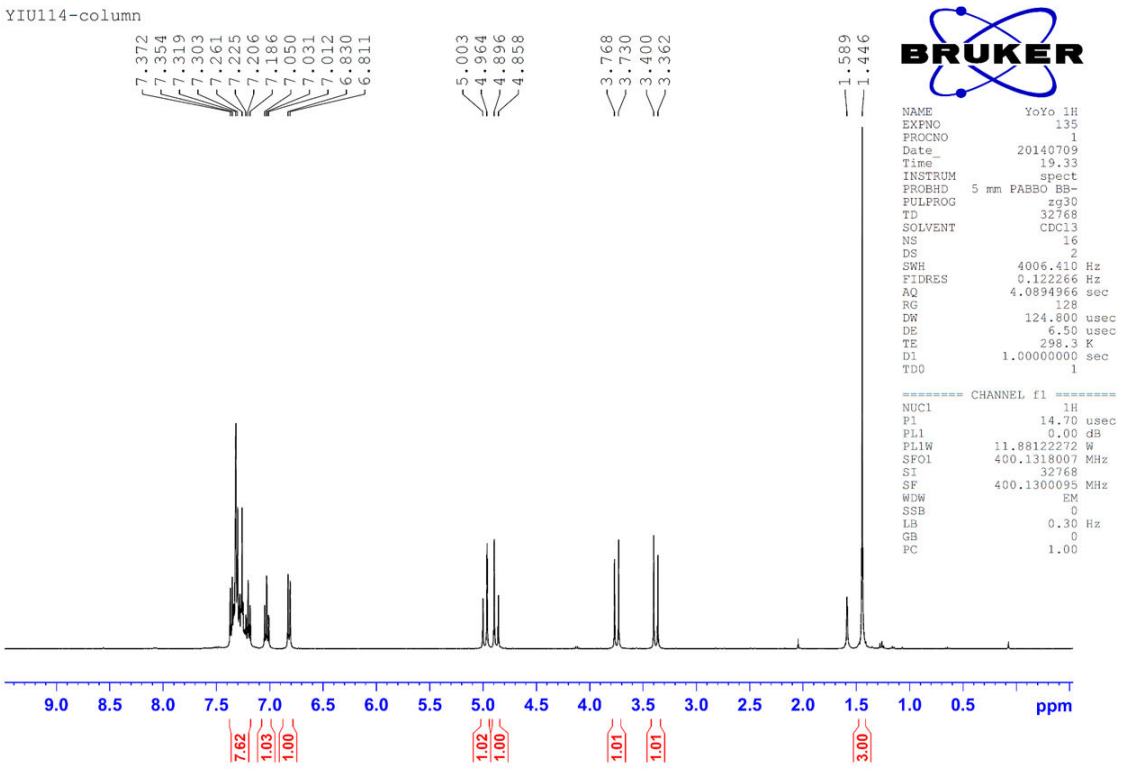

Figure A135 [13]C NMR spectrum of **15r**

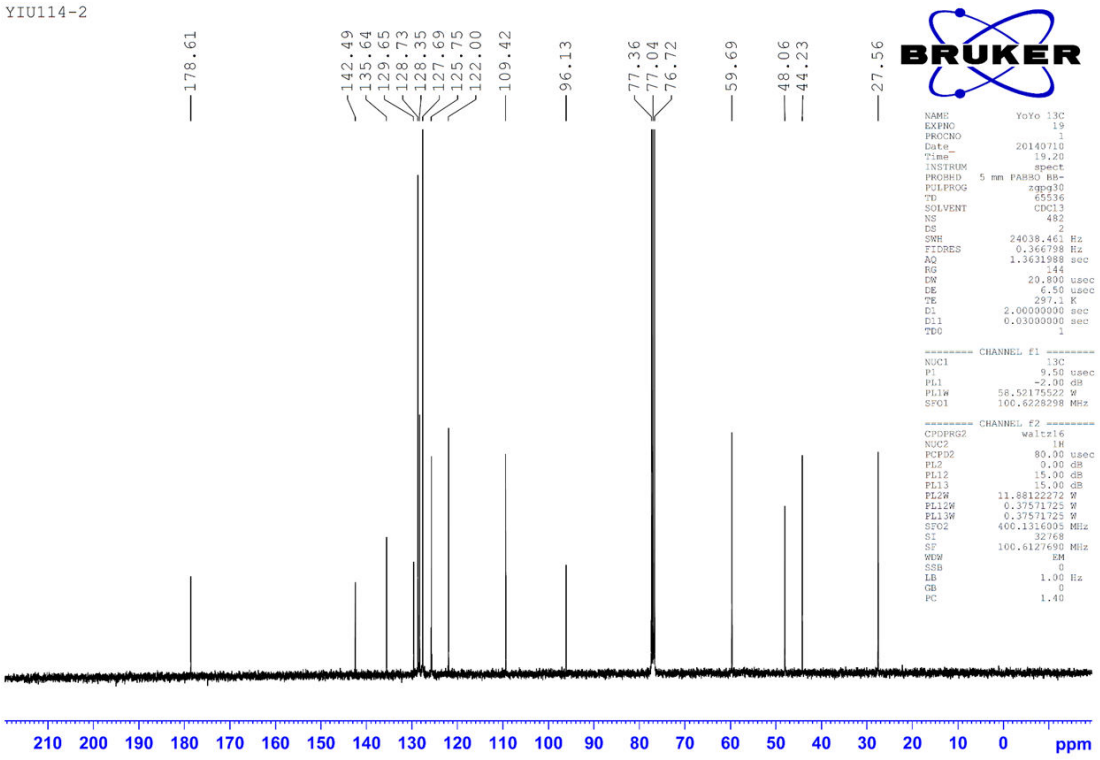

Figure A136 [1]H NMR spectrum of **15t**

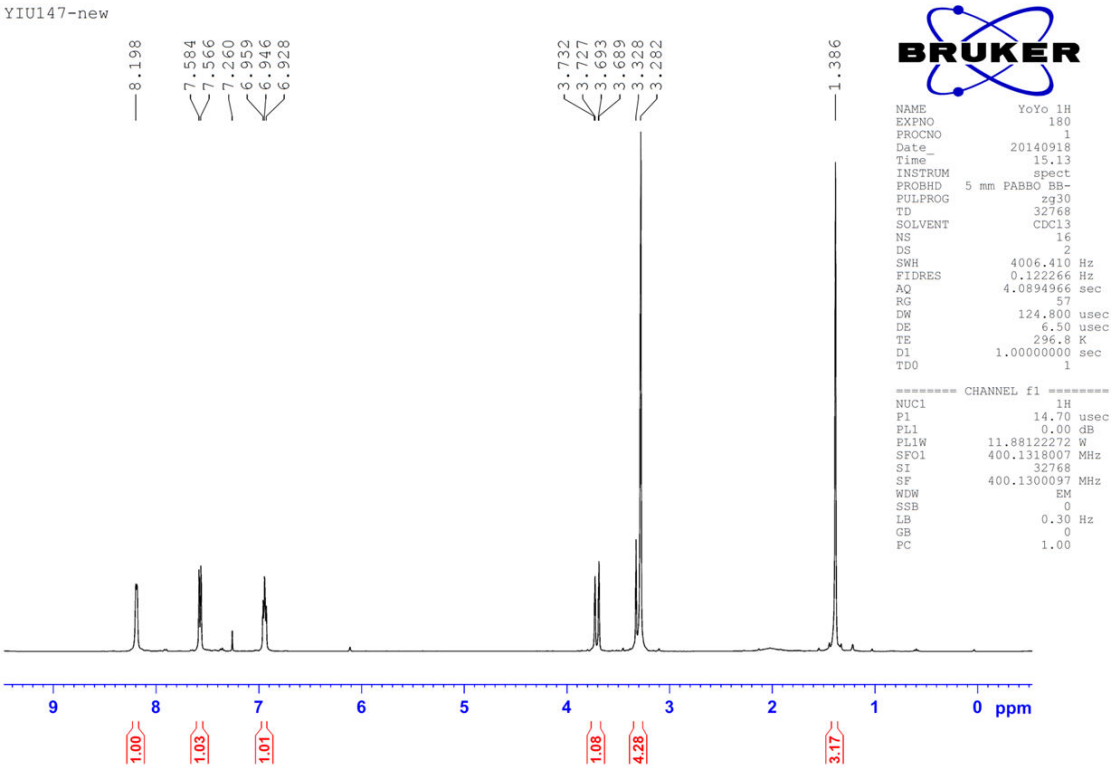

Figure A137 [13]C NMR spectrum of **15t**

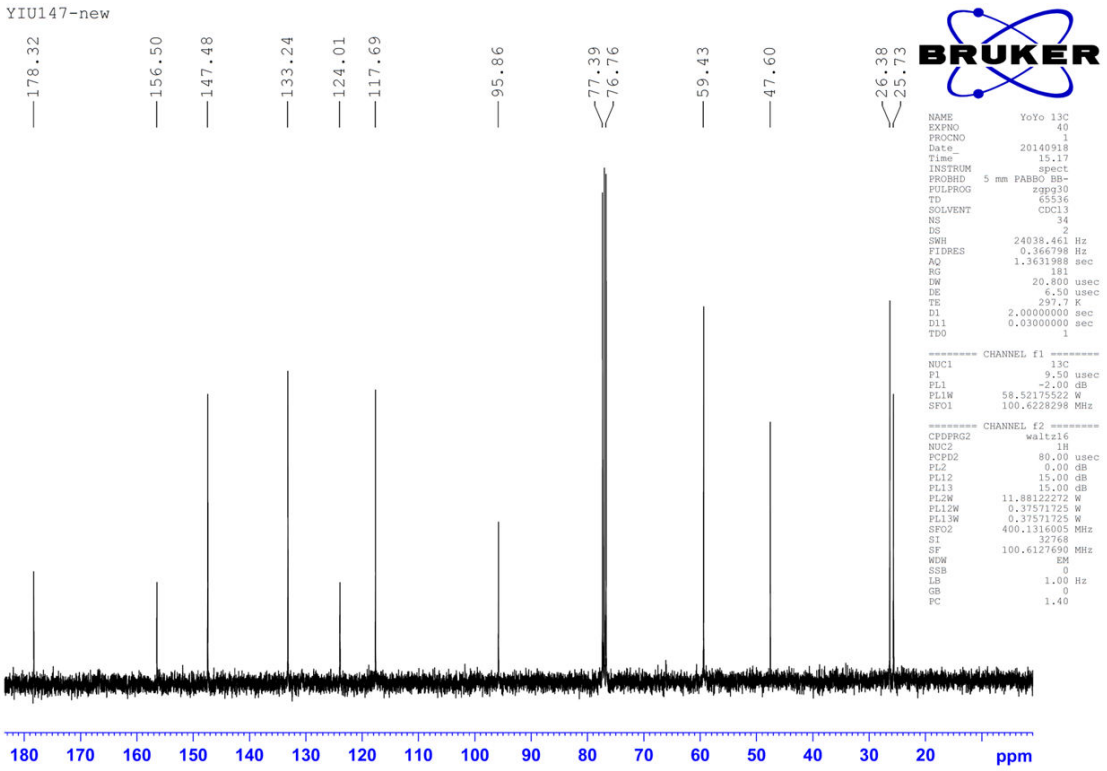

Figure A138 [1]H NMR spectrum of **16a**

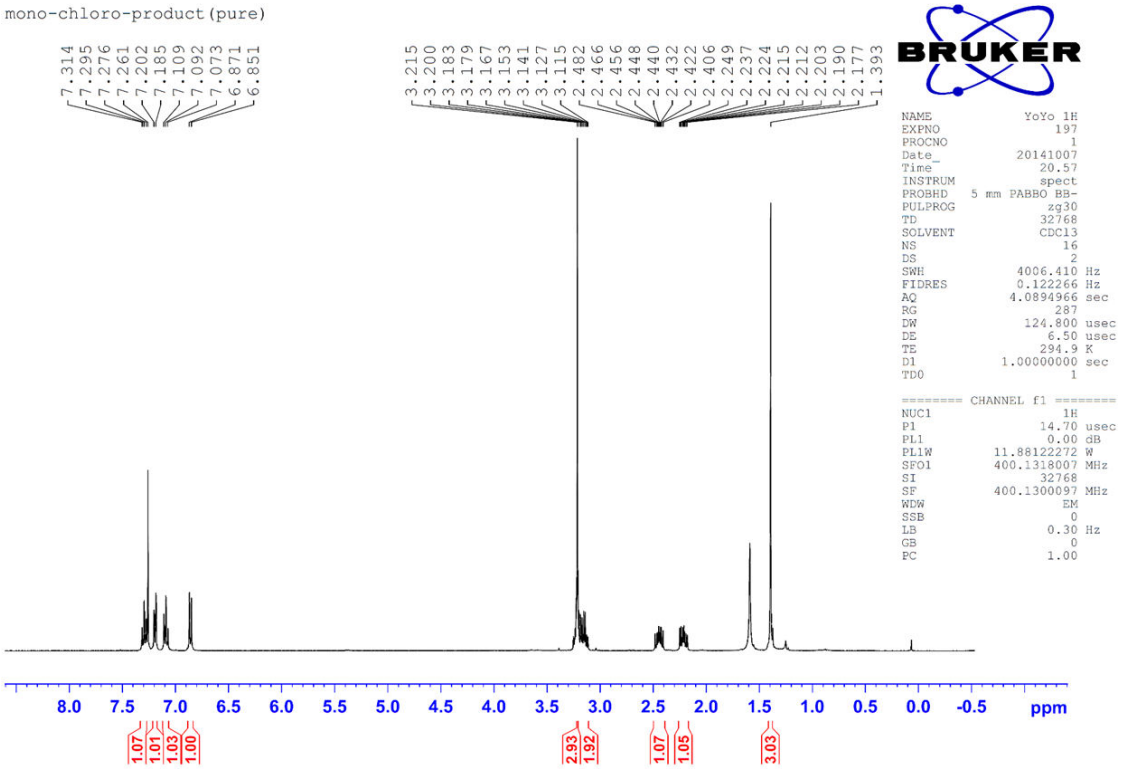

Figure A139 [13]C NMR spectrum of **16a**

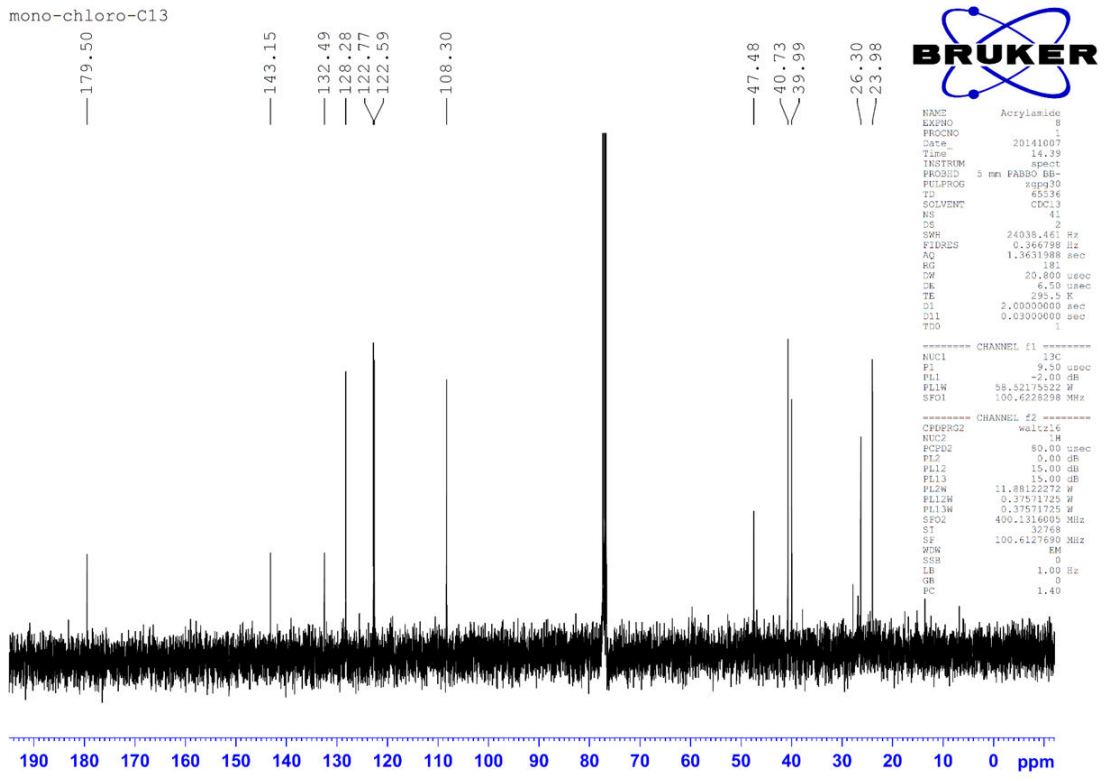

Figure A140 [1]H NMR spectrum of **17a**

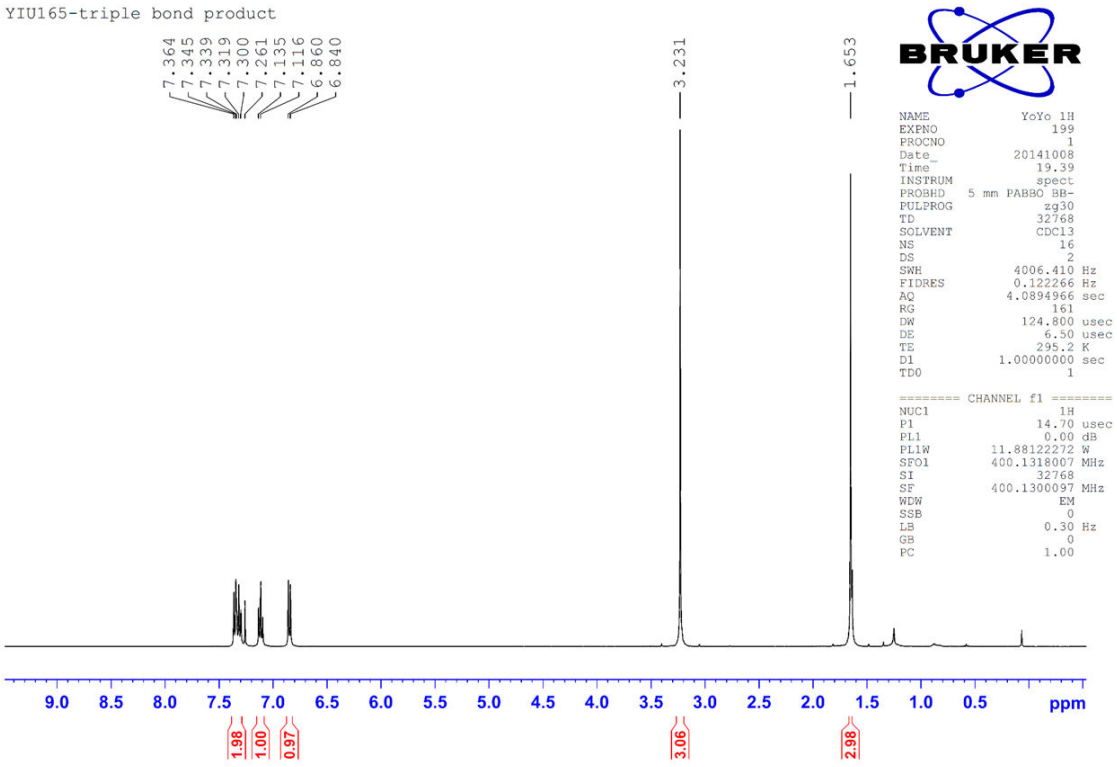

Figure A141 [13]C NMR spectrum of **17a**

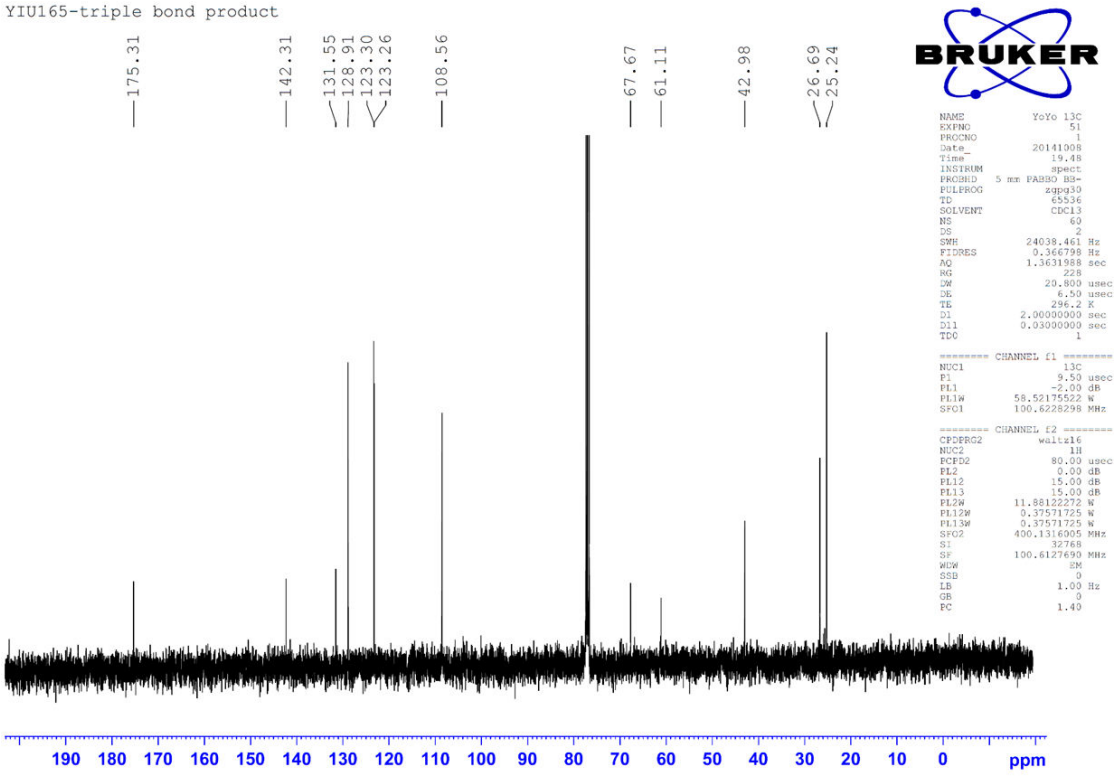

Figure A142 [1]H NMR spectrum of **17s**

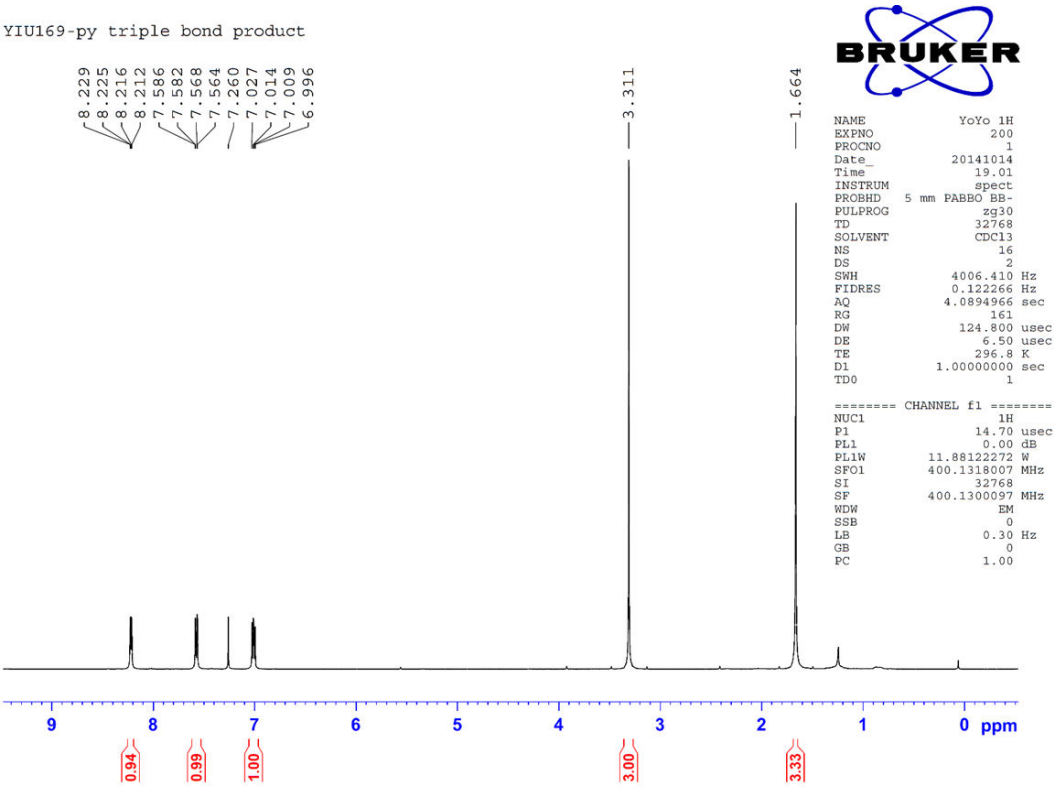

Figure A143 [13]C NMR spectrum of **17s**

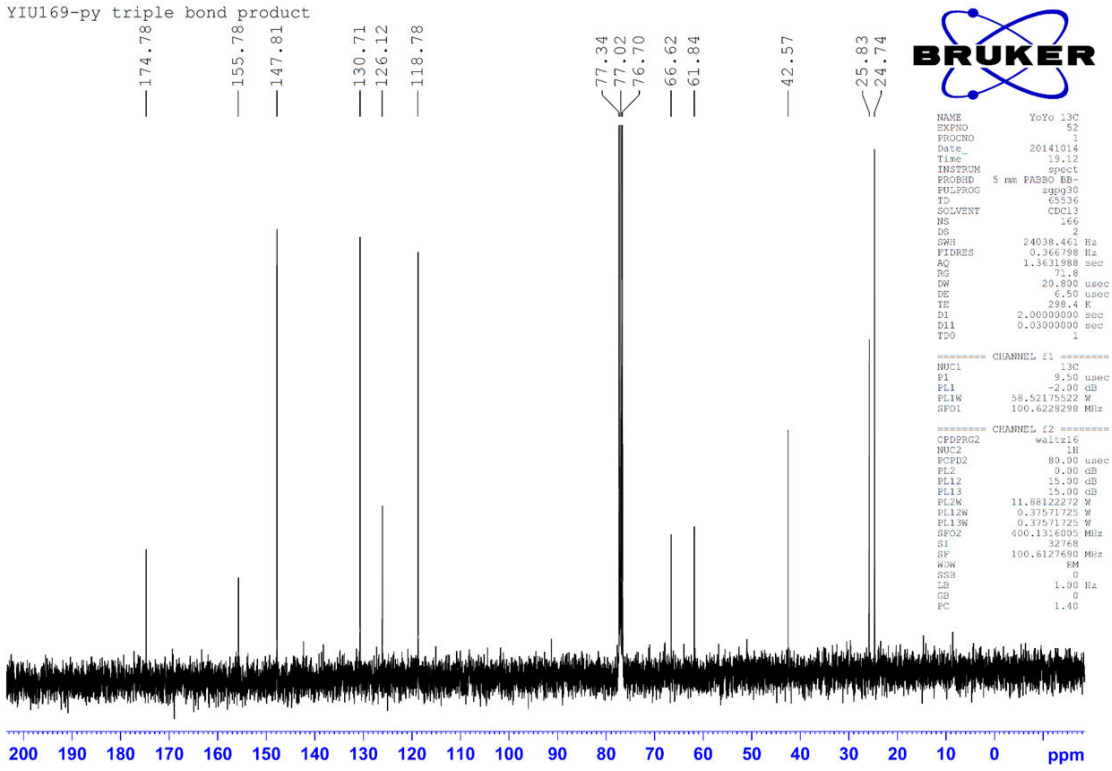

Figure A144 Molecular structure of **3a**

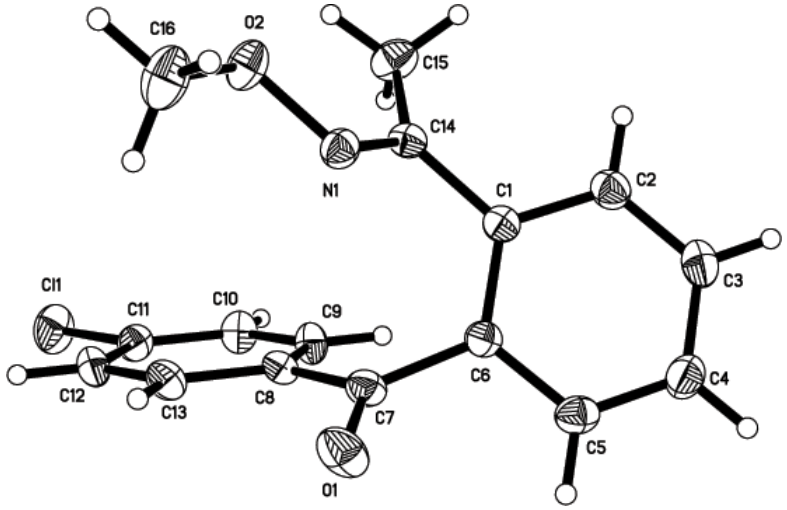

Table A01 Atomic coordinates (x 10^4) and equivalent isotropic displacement parameters ($Å^2$ x 10^3) for **3a**. U(eq) is defined as one third of the trace of the orthogonalized U^{ij} tensor.

	x	y	z	U(eq)
Cl(1)	4183(1)	5208(1)	3081(1)	93(1)
O(1)	8133(2)	3672(2)	5560(2)	83(1)
O(2)	7802(2)	2059(2)	3329(1)	68(1)
N(1)	7696(2)	2054(2)	4161(1)	54(1)
C(1)	6611(2)	1689(2)	5252(2)	48(1)
C(2)	6259(2)	915(2)	5640(2)	60(1)
C(3)	6228(3)	872(2)	6450(2)	69(1)
C(4)	6543(3)	1599(3)	6902(2)	69(1)
C(5)	6885(2)	2371(2)	6531(2)	61(1)
C(6)	6913(2)	2432(2)	5708(2)	48(1)
C(7)	7257(3)	3303(2)	5353(2)	54(1)
C(8)	6481(2)	3747(2)	4775(2)	47(1)
C(9)	5331(2)	3570(2)	4749(2)	57(1)
C(10)	4623(3)	4016(2)	4232(2)	64(1)
C(11)	5075(3)	4644(2)	3734(2)	58(1)
C(12)	6211(3)	4843(2)	3742(2)	63(1)

C(13)	6911(3)	4391(2)	4266(2)	62(1)
C(14)	6757(2)	1699(2)	4383(2)	49(1)
C(16)	8861(3)	2463(3)	3137(2)	92(1)
C(15)	5870(2)	1324(2)	3844(2)	73(1)

Table A02 Bond lengths [Å] and angles [°] for **3a**.

Cl(1)-C(11)	1.738(3)
O(1)-C(7)	1.217(3)
O(2)-N(1)	1.410(3)
O(2)-C(16)	1.419(4)
N(1)-C(14)	1.278(3)
C(1)-C(2)	1.391(4)
C(1)-C(6)	1.397(4)
C(1)-C(14)	1.477(4)
C(2)-C(3)	1.370(4)
C(2)-H(2A)	0.9300
C(3)-C(4)	1.376(4)
C(3)-H(3A)	0.9300
C(4)-C(5)	1.371(4)
C(4)-H(4A)	0.9300
C(5)-C(6)	1.393(4)
C(5)-H(5A)	0.9300
C(6)-C(7)	1.487(4)
C(7)-C(8)	1.490(4)
C(8)-C(9)	1.376(4)
C(8)-C(13)	1.384(4)
C(9)-C(10)	1.377(4)
C(9)-H(9A)	0.9300
C(10)-C(11)	1.367(4)
C(10)-H(10A)	0.9300
C(11)-C(12)	1.366(4)
C(12)-C(13)	1.384(4)
C(12)-H(12A)	0.9300
C(13)-H(13A)	0.9300
C(14)-C(15)	1.493(4)
C(16)-H(16A)	0.9600
C(16)-H(16B)	0.9600
C(16)-H(16C)	0.9600
C(15)-H(15A)	0.9600
C(15)-H(15B)	0.9600

C(15)-H(15C) 0.9600

N(1)-O(2)-C(16) 108.0(2)
C(14)-N(1)-O(2) 111.8(2)
C(2)-C(1)-C(6) 118.3(3)
C(2)-C(1)-C(14) 120.8(3)
C(6)-C(1)-C(14) 120.7(3)
C(3)-C(2)-C(1) 121.1(3)
C(3)-C(2)-H(2A) 119.4
C(1)-C(2)-H(2A) 119.4
C(2)-C(3)-C(4) 120.6(3)
C(2)-C(3)-H(3A) 119.7
C(4)-C(3)-H(3A) 119.7
C(5)-C(4)-C(3) 119.2(3)
C(5)-C(4)-H(4A) 120.4
C(3)-C(4)-H(4A) 120.4
C(4)-C(5)-C(6) 121.1(3)
C(4)-C(5)-H(5A) 119.4
C(6)-C(5)-H(5A) 119.4
C(5)-C(6)-C(1) 119.5(3)
C(5)-C(6)-C(7) 117.7(3)
C(1)-C(6)-C(7) 122.7(3)
O(1)-C(7)-C(6) 120.6(3)
O(1)-C(7)-C(8) 120.2(3)
C(6)-C(7)-C(8) 119.1(2)
C(9)-C(8)-C(13) 118.1(3)
C(9)-C(8)-C(7) 122.3(3)
C(13)-C(8)-C(7) 119.5(3)
C(8)-C(9)-C(10) 121.3(3)
C(8)-C(9)-H(9A) 119.3
C(10)-C(9)-H(9A) 119.3
C(11)-C(10)-C(9) 119.2(3)
C(11)-C(10)-H(10A) 120.4
C(9)-C(10)-H(10A) 120.4
C(12)-C(11)-C(10) 121.5(3)
C(12)-C(11)-Cl(1) 119.2(3)

C(10)-C(11)-Cl(1) 119.3(3)
C(11)-C(12)-C(13) 118.6(3)
C(11)-C(12)-H(12A) 120.7
C(13)-C(12)-H(12A) 120.7
C(12)-C(13)-C(8) 121.3(3)
C(12)-C(13)-H(13A) 119.3
C(8)-C(13)-H(13A) 119.3
N(1)-C(14)-C(1) 113.3(2)
N(1)-C(14)-C(15) 125.3(3)
C(1)-C(14)-C(15) 121.4(3)
O(2)-C(16)-H(16A) 109.5
O(2)-C(16)-H(16B) 109.5
H(16A)-C(16)-H(16B) 109.5
O(2)-C(16)-H(16C) 109.5
H(16A)-C(16)-H(16C) 109.5
H(16B)-C(16)-H(16C) 109.5
C(14)-C(15)-H(15A) 109.5
C(14)-C(15)-H(15B) 109.5
H(15A)-C(15)-H(15B) 109.5
C(14)-C(15)-H(15C) 109.5
H(15A)-C(15)-H(15C) 109.5
H(15B)-C(15)-H(15C) 109.5

Symmetry transformations used to generate equivalent atoms:

Table A03 Anisotropic displacement parameters ($Å^2 x\ 10^3$) for **3a**. The anisotropic displacement factor exponent takes the form: $-2\pi^2[\ h^2 a^{*2} U^{11} + ... + 2\ h\ k\ a^*\ b^*\ U^{12}\ ]$

U^{11}	U^{22}	U^{33}	U^{23}	U^{13}	U^{12}
Cl(1)100(1)	97(1)	84(1)	28(1)	-14(1)	23(1)
O(1)74(2)	67(2)	109(2)	4(1)	-36(1)	-18(1)
O(2)54(1)	95(2)	55(1)	9(1)	4(1)	-5(1)
N(1)55(2)	57(2)	50(2)	1(1)	-2(1)	4(1)
C(1)42(2)	49(2)	53(2)	-1(2)	1(1)	4(1)
C(2)60(2)	55(2)	67(2)	-1(2)	4(2)	-5(2)
C(3)70(2)	61(2)	76(3)	18(2)	9(2)	3(2)
C(4)79(2)	76(3)	53(2)	6(2)	-1(2)	12(2)
C(5)58(2)	63(2)	61(2)	-10(2)	-10(2)	9(2)
C(6)47(2)	47(2)	50(2)	-1(2)	-9(1)	4(1)
C(7)54(2)	49(2)	60(2)	-5(2)	-8(2)	-4(2)
C(8)48(2)	38(2)	56(2)	-3(2)	-2(1)	-3(1)
C(9)54(2)	55(2)	63(2)	15(2)	3(2)	5(2)
C(10)49(2)	72(2)	70(2)	11(2)	2(2)	5(2)
C(11)62(2)	56(2)	55(2)	4(2)	-4(2)	14(2)
C(12)78(3)	49(2)	62(2)	11(2)	0(2)	-8(2)
C(13)57(2)	55(2)	73(2)	-1(2)	-2(2)	-12(2)
C(14)43(2)	47(2)	56(2)	-6(2)	3(1)	-1(1)
C(16)60(2)	132(3)	82(3)	20(2)	13(2)	-10(2)
C(15)59(2)	93(3)	66(2)	-13(2)	-6(2)	-13(2)

Table A04 Hydrogen coordinates (x 10^4) and isotropic displacement parameters ($Å^2$x 10^3) for **3a**.

	x	y	z	U(eq)
H(2A)	6041	417	5345	73
H(3A)	5991	347	6698	83
H(4A)	6525	1566	7451	83
H(5A)	7101	2863	6835	73
H(9A)	5027	3140	5087	69
H(10A)	3847	3892	4223	77
H(12A)	6508	5274	3401	76
H(13A)	7685	4523	4277	74
H(16A)	8952	2476	2572	137
H(16B)	9469	2123	3369	137
H(16C)	8877	3065	3339	137
H(15A)	6111	1394	3304	109
H(15B)	5165	1639	3923	109
H(15C)	5762	700	3958	109

Table A05 Torsion angles [°] for **3a**.

C(16)-O(2)-N(1)-C(14)	179.9(3)
C(6)-C(1)-C(2)-C(3)	-1.2(4)
C(14)-C(1)-C(2)-C(3)	173.6(3)
C(1)-C(2)-C(3)-C(4)	0.2(5)
C(2)-C(3)-C(4)-C(5)	0.4(5)
C(3)-C(4)-C(5)-C(6)	0.2(5)
C(4)-C(5)-C(6)-C(1)	-1.3(4)
C(4)-C(5)-C(6)-C(7)	178.0(3)
C(2)-C(1)-C(6)-C(5)	1.8(4)
C(14)-C(1)-C(6)-C(5)	-173.0(2)
C(2)-C(1)-C(6)-C(7)	-177.5(2)
C(14)-C(1)-C(6)-C(7)	7.7(4)
C(5)-C(6)-C(7)-O(1)	51.7(4)
C(1)-C(6)-C(7)-O(1)	-129.1(3)
C(5)-C(6)-C(7)-C(8)	-124.8(3)
C(1)-C(6)-C(7)-C(8)	54.4(4)
O(1)-C(7)-C(8)-C(9)	-153.9(3)
C(6)-C(7)-C(8)-C(9)	22.6(4)
O(1)-C(7)-C(8)-C(13)	23.1(4)
C(6)-C(7)-C(8)-C(13)	-160.4(3)
C(13)-C(8)-C(9)-C(10)	0.1(4)
C(7)-C(8)-C(9)-C(10)	177.2(3)
C(8)-C(9)-C(10)-C(11)	0.3(5)
C(9)-C(10)-C(11)-C(12)	-0.5(5)
C(9)-C(10)-C(11)-Cl(1)	179.9(2)
C(10)-C(11)-C(12)-C(13)	0.3(5)
Cl(1)-C(11)-C(12)-C(13)	179.8(2)
C(11)-C(12)-C(13)-C(8)	0.2(5)
C(9)-C(8)-C(13)-C(12)	-0.3(4)
C(7)-C(8)-C(13)-C(12)	-177.5(3)
O(2)-N(1)-C(14)-C(1)	-179.5(2)
O(2)-N(1)-C(14)-C(15)	0.5(4)
C(2)-C(1)-C(14)-N(1)	-132.7(3)
C(6)-C(1)-C(14)-N(1)	41.9(4)

C(2)-C(1)-C(14)-C(15)	47.3(4)
C(6)-C(1)-C(14)-C(15)	-138.0(3)

Symmetry transformations used to generate equivalent atoms:

Figure A145 Molecular structure of **7a**

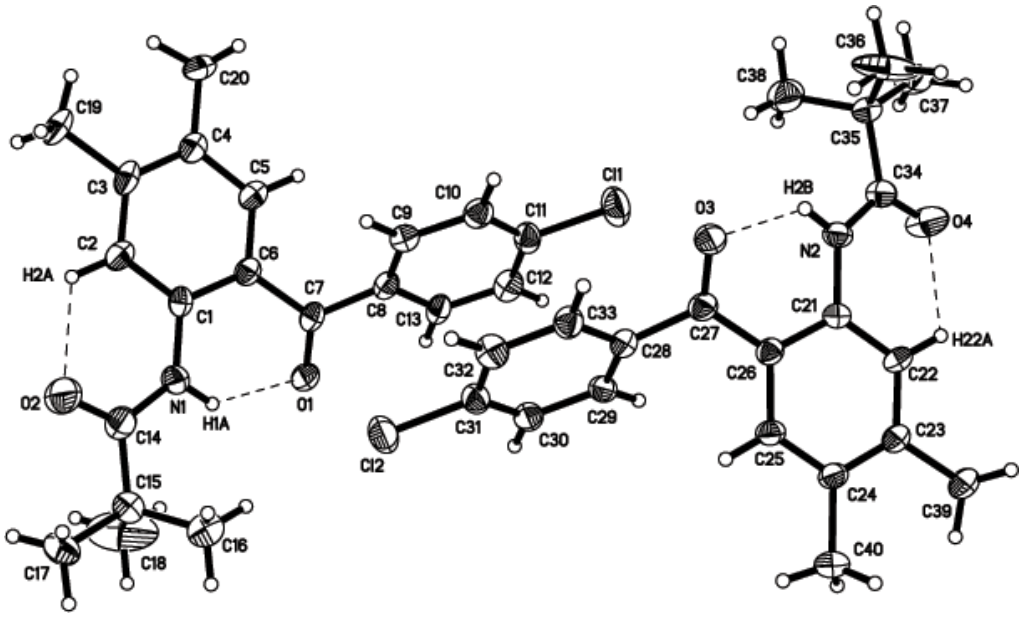

Table A06 Atomic coordinates (x 10^4) and equivalent isotropic displacement parameters (Å^{2}x 10^3) for **7a**. U(eq) is defined as one third of the trace of the orthogonalized U^{ij} tensor.

	x	y	z	U(eq)
Cl(1)	1742(1)	575(1)	2076(1)	116(1)
O(1)	2644(1)	5457(1)	774(1)	86(1)
O(2)	5150(1)	7651(2)	1581(1)	139(1)
N(1)	4046(1)	6580(1)	1159(1)	74(1)
C(1)	4321(1)	5475(2)	1054(1)	64(1)
C(2)	5063(1)	5334(2)	1047(1)	75(1)
C(3)	5325(1)	4254(2)	916(1)	73(1)
C(4)	4835(1)	3285(2)	782(1)	72(1)
C(5)	4110(1)	3419(2)	817(1)	69(1)
C(6)	3836(1)	4496(2)	957(1)	61(1)
C(7)	3052(1)	4571(2)	975(1)	65(1)
C(8)	2743(1)	3537(2)	1233(1)	63(1)
C(9)	3227(1)	2817(2)	1803(1)	71(1)
C(10)	2920(1)	1917(2)	2067(1)	76(1)
C(11)	2124(1)	1724(2)	1752(1)	75(1)

C(12)	1622(1)	2434(2)	1201(1)	81(1)
C(13)	1934(1)	3347(2)	951(1)	70(1)
C(14)	4438(1)	7586(2)	1407(1)	85(1)
C(15)	3963(1)	8642(2)	1449(1)	89(1)
C(16)	3596(3)	8313(4)	2005(3)	164(2)
C(17)	4558(2)	9618(4)	1846(3)	132(2)
C(18)	3344(3)	9096(6)	738(3)	271(4)
C(16')	3152(2)	8367(5)	1433(3)	136(2)
C(17')	4447(4)	9445(6)	2060(3)	198(3)
C(18')	3757(3)	9193(4)	680(2)	116(2)
C(19)	6139(1)	4154(2)	930(1)	97(1)
C(20)	5077(1)	2105(2)	597(1)	97(1)
Cl(2)	3102(1)	5665(1)	2732(1)	107(1)
O(3)	2384(1)	712(1)	4075(1)	90(1)
O(4)	-18(1)	-1660(1)	3467(1)	116(1)
N(2)	1061(1)	-532(1)	3832(1)	67(1)
C(21)	769(1)	556(1)	3952(1)	55(1)
C(22)	74(1)	622(2)	4053(1)	63(1)
C(23)	-205(1)	1677(2)	4193(1)	64(1)
C(24)	220(1)	2697(2)	4237(1)	65(1)
C(25)	899(1)	2627(2)	4118(1)	63(1)
C(26)	1191(1)	1580(2)	3969(1)	57(1)
C(27)	1953(1)	1576(2)	3902(1)	65(1)
C(28)	2217(1)	2636(2)	3624(1)	61(1)
C(29)	1698(1)	3313(2)	3050(1)	63(1)
C(30)	1972(1)	4247(2)	2768(1)	69(1)
C(31)	2760(1)	4484(2)	3076(1)	72(1)
C(32)	3290(1)	3823(2)	3639(1)	81(1)
C(33)	3014(1)	2892(2)	3896(1)	74(1)
C(34)	670(1)	-1548(2)	3589(1)	70(1)
C(35)	1142(1)	-2553(2)	3468(1)	73(1)
C(36)	1808(3)	-2927(4)	4156(2)	163(2)
C(37)	558(2)	-3584(3)	3094(2)	111(2)
C(38)	1429(2)	-2232(4)	2878(2)	117(2)
C(36')	2037(3)	-2303(4)	3875(4)	140(3)
C(37')	958(3)	-3640(4)	3800(3)	165(2)

C(38')	924(3)	-2599(6)	2662(2)	164(3)
C(39)	-966(1)	1705(2)	4297(1)	93(1)
C(40)	-38(1)	3865(2)	4420(1)	96(1)

Table A07 Bond lengths [Å] and angles [°] for **7a**.

Cl(1)-C(11)	1.735(2)
O(1)-C(7)	1.230(2)
O(2)-C(14)	1.224(2)
N(1)-C(14)	1.343(2)
N(1)-C(1)	1.410(2)
N(1)-H(1A)	0.8600
C(1)-C(2)	1.393(2)
C(1)-C(6)	1.401(2)
C(2)-C(3)	1.391(3)
C(2)-H(2A)	0.9300
C(3)-C(4)	1.389(3)
C(3)-C(19)	1.507(3)
C(4)-C(5)	1.385(2)
C(4)-C(20)	1.514(3)
C(5)-C(6)	1.405(3)
C(5)-H(5A)	0.9300
C(6)-C(7)	1.473(2)
C(7)-C(8)	1.493(3)
C(8)-C(9)	1.387(2)
C(8)-C(13)	1.388(2)
C(9)-C(10)	1.378(3)
C(9)-H(9A)	0.9300
C(10)-C(11)	1.367(2)
C(10)-H(10A)	0.9300
C(11)-C(12)	1.371(2)
C(12)-C(13)	1.381(3)
C(12)-H(12A)	0.9300
C(13)-H(13A)	0.9300
C(14)-C(15)	1.519(3)
C(15)-C(17')	1.491(6)
C(15)-C(18)	1.496(5)
C(15)-C(16')	1.527(5)
C(15)-C(17)	1.540(4)
C(15)-C(18')	1.540(5)

C(15)-C(16)	1.559(5)
C(16)-H(16A)	0.9600
C(16)-H(16B)	0.9600
C(16)-H(16C)	0.9600
C(17)-H(17A)	0.9600
C(17)-H(17B)	0.9600
C(17)-H(17C)	0.9600
C(18)-H(18A)	0.9600
C(18)-H(18B)	0.9600
C(18)-H(18C)	0.9600
C(16')-H(16D)	0.9600
C(16')-H(16E)	0.9600
C(16')-H(16F)	0.9600
C(17')-H(17D)	0.9600
C(17')-H(17E)	0.9600
C(17')-H(17F)	0.9600
C(18')-H(18D)	0.9600
C(18')-H(18E)	0.9600
C(18')-H(18F)	0.9600
C(19)-H(19A)	0.9600
C(19)-H(19B)	0.9600
C(19)-H(19C)	0.9600
C(20)-H(20A)	0.9600
C(20)-H(20B)	0.9600
C(20)-H(20C)	0.9600
Cl(2)-C(31)	1.746(2)
O(3)-C(27)	1.229(2)
O(4)-C(34)	1.207(2)
N(2)-C(34)	1.351(2)
N(2)-C(21)	1.417(2)
N(2)-H(2B)	0.8600
C(21)-C(22)	1.387(2)
C(21)-C(26)	1.403(2)
C(22)-C(23)	1.386(2)
C(22)-H(22A)	0.9300
C(23)-C(24)	1.391(2)

C(23)-C(39)	1.511(3)
C(24)-C(25)	1.379(3)
C(24)-C(40)	1.514(3)
C(25)-C(26)	1.395(2)
C(25)-H(25A)	0.9300
C(26)-C(27)	1.475(2)
C(27)-C(28)	1.494(3)
C(28)-C(33)	1.383(2)
C(28)-C(29)	1.385(2)
C(29)-C(30)	1.394(3)
C(29)-H(29A)	0.9300
C(30)-C(31)	1.362(2)
C(30)-H(30A)	0.9300
C(31)-C(32)	1.371(2)
C(32)-C(33)	1.366(3)
C(32)-H(32A)	0.9300
C(33)-H(33A)	0.9300
C(34)-C(35)	1.525(3)
C(35)-C(38')	1.472(5)
C(35)-C(36)	1.476(4)
C(35)-C(37')	1.510(5)
C(35)-C(38)	1.512(4)
C(35)-C(36')	1.546(5)
C(35)-C(37)	1.568(4)
C(36)-H(36A)	0.9600
C(36)-H(36B)	0.9600
C(36)-H(36C)	0.9600
C(37)-H(37A)	0.9600
C(37)-H(37B)	0.9600
C(37)-H(37C)	0.9600
C(38)-H(38A)	0.9600
C(38)-H(38B)	0.9600
C(38)-H(38C)	0.9600
C(36')-H(36D)	0.9600
C(36')-H(36E)	0.9600
C(36')-H(36F)	0.9600

C(37')-H(37D) 0.9600
C(37')-H(37E) 0.9600
C(37')-H(37F) 0.9600
C(38')-H(38D) 0.9600
C(38')-H(38E) 0.9600
C(38')-H(38F) 0.9600
C(39)-H(39A) 0.9600
C(39)-H(39B) 0.9600
C(39)-H(39C) 0.9600
C(40)-H(40A) 0.9600
C(40)-H(40B) 0.9600
C(40)-H(40C) 0.9600
C(14)-N(1)-C(1) 130.35(16)
C(14)-N(1)-H(1A) 114.8
C(1)-N(1)-H(1A) 114.8
C(2)-C(1)-C(6) 119.33(18)
C(2)-C(1)-N(1) 121.67(17)
C(6)-C(1)-N(1) 119.00(16)
C(3)-C(2)-C(1) 121.90(18)
C(3)-C(2)-H(2A) 119.1
C(1)-C(2)-H(2A) 119.1
C(4)-C(3)-C(2) 119.51(17)
C(4)-C(3)-C(19) 121.16(19)
C(2)-C(3)-C(19) 119.33(18)
C(5)-C(4)-C(3) 118.46(18)
C(5)-C(4)-C(20) 120.08(17)
C(3)-C(4)-C(20) 121.46(17)
C(4)-C(5)-C(6) 123.10(17)
C(4)-C(5)-H(5A) 118.5
C(6)-C(5)-H(5A) 118.5
C(1)-C(6)-C(5) 117.58(16)
C(1)-C(6)-C(7) 122.54(17)
C(5)-C(6)-C(7) 119.85(16)
O(1)-C(7)-C(6) 121.59(17)
O(1)-C(7)-C(8) 119.37(16)
C(6)-C(7)-C(8) 119.03(15)

C(9)-C(8)-C(13) 117.86(17)
C(9)-C(8)-C(7) 122.37(14)
C(13)-C(8)-C(7) 119.45(15)
C(10)-C(9)-C(8) 121.28(16)
C(10)-C(9)-H(9A) 119.4
C(8)-C(9)-H(9A) 119.4
C(11)-C(10)-C(9) 119.18(17)
C(11)-C(10)-H(10A) 120.4
C(9)-C(10)-H(10A) 120.4
C(10)-C(11)-C(12) 121.36(19)
C(10)-C(11)-Cl(1) 118.98(14)
C(12)-C(11)-Cl(1) 119.64(14)
C(11)-C(12)-C(13) 119.01(16)
C(11)-C(12)-H(12A) 120.5
C(13)-C(12)-H(12A) 120.5
C(12)-C(13)-C(8) 121.22(16)
C(12)-C(13)-H(13A) 119.4
C(8)-C(13)-H(13A) 119.4
O(2)-C(14)-N(1) 121.1(2)
O(2)-C(14)-C(15) 121.40(19)
N(1)-C(14)-C(15) 117.53(17)
C(17')-C(15)-C(18) 121.5(4)
C(17')-C(15)-C(14) 111.4(3)
C(18)-C(15)-C(14) 117.7(3)
C(17')-C(15)-C(16') 113.9(4)
C(18)-C(15)-C(16') 71.4(3)
C(14)-C(15)-C(16') 115.2(3)
C(17')-C(15)-C(17) 21.8(4)
C(18)-C(15)-C(17) 109.9(3)
C(14)-C(15)-C(17) 107.1(2)
C(16')-C(15)-C(17) 130.9(3)
C(17')-C(15)-C(18') 111.7(4)
C(18)-C(15)-C(18') 31.6(3)
C(14)-C(15)-C(18') 100.8(2)
C(16')-C(15)-C(18') 102.7(3)
C(17)-C(15)-C(18') 92.4(3)

C(17')-C(15)-C(16) 82.6(4)
C(18)-C(15)-C(16)110.8(3)
C(14)-C(15)-C(16)106.2(2)
C(16')-C(15)-C(16) 41.5(3)
C(17)-C(15)-C(16)104.2(3)
C(18')-C(15)-C(16)142.2(3)
C(15)-C(16)-H(16A)109.5
C(15)-C(16)-H(16B)109.5
H(16A)-C(16)-H(16B)109.5
C(15)-C(16)-H(16C)109.5
H(16A)-C(16)-H(16C)109.5
H(16B)-C(16)-H(16C)109.5
C(15)-C(17)-H(17A)109.5
C(15)-C(17)-H(17B)109.5
H(17A)-C(17)-H(17B)109.5
C(15)-C(17)-H(17C)109.5
H(17A)-C(17)-H(17C)109.5
H(17B)-C(17)-H(17C)109.5
C(15)-C(18)-H(18A)109.5
C(15)-C(18)-H(18B)109.5
H(18A)-C(18)-H(18B)109.5
C(15)-C(18)-H(18C)109.5
H(18A)-C(18)-H(18C)109.5
H(18B)-C(18)-H(18C)109.5
C(15)-C(16')-H(16D)109.5
C(15)-C(16')-H(16E)109.5
H(16D)-C(16')-H(16E)109.5
C(15)-C(16')-H(16F)109.5
H(16D)-C(16')-H(16F)109.5
H(16E)-C(16')-H(16F)109.5
C(15)-C(17')-H(17D)109.5
C(15)-C(17')-H(17E)109.5
H(17D)-C(17')-H(17E)109.5
C(15)-C(17')-H(17F)109.5
H(17D)-C(17')-H(17F)109.5
H(17E)-C(17')-H(17F)109.5

C(15)-C(18')-H(18D)109.5
C(15)-C(18')-H(18E)109.5
H(18D)-C(18')-H(18E)109.5
C(15)-C(18')-H(18F)109.5
H(18D)-C(18')-H(18F)109.5
H(18E)-C(18')-H(18F)109.5
C(3)-C(19)-H(19A)109.5
C(3)-C(19)-H(19B)109.5
H(19A)-C(19)-H(19B)109.5
C(3)-C(19)-H(19C)109.5
H(19A)-C(19)-H(19C)109.5
H(19B)-C(19)-H(19C)109.5
C(4)-C(20)-H(20A)109.5
C(4)-C(20)-H(20B)109.5
H(20A)-C(20)-H(20B)109.5
C(4)-C(20)-H(20C)109.5
H(20A)-C(20)-H(20C)109.5
H(20B)-C(20)-H(20C)109.5
C(34)-N(2)-C(21)128.95(15)
C(34)-N(2)-H(2B) 115.5
C(21)-N(2)-H(2B) 115.5
C(22)-C(21)-C(26)119.75(16)
C(22)-C(21)-N(2)120.99(15)
C(26)-C(21)-N(2)119.26(15)
C(23)-C(22)-C(21)121.44(17)
C(23)-C(22)-H(22A)119.3
C(21)-C(22)-H(22A)119.3
C(22)-C(23)-C(24)119.68(17)
C(22)-C(23)-C(39)119.53(17)
C(24)-C(23)-C(39)120.79(17)
C(25)-C(24)-C(23)118.44(17)
C(25)-C(24)-C(40)119.61(17)
C(23)-C(24)-C(40)121.94(17)
C(24)-C(25)-C(26)123.23(17)
C(24)-C(25)-H(25A)118.4
C(26)-C(25)-H(25A)118.4

C(25)-C(26)-C(21)117.41(16)
C(25)-C(26)-C(27)119.46(16)
C(21)-C(26)-C(27)122.92(16)
O(3)-C(27)-C(26)121.10(17)
O(3)-C(27)-C(28)118.73(17)
C(26)-C(27)-C(28)120.17(15)
C(33)-C(28)-C(29)118.25(17)
C(33)-C(28)-C(27)119.37(15)
C(29)-C(28)-C(27)122.07(14)
C(28)-C(29)-C(30)120.68(15)
C(28)-C(29)-H(29A)119.7
C(30)-C(29)-H(29A)119.7
C(31)-C(30)-C(29)118.42(16)
C(31)-C(30)-H(30A)120.8
C(29)-C(30)-H(30A)120.8
C(30)-C(31)-C(32)122.33(18)
C(30)-C(31)-Cl(2)118.48(14)
C(32)-C(31)-Cl(2)119.20(14)
C(33)-C(32)-C(31)118.49(17)
C(33)-C(32)-H(32A)120.8
C(31)-C(32)-H(32A)120.8
C(32)-C(33)-C(28)121.75(16)
C(32)-C(33)-H(33A)119.1
C(28)-C(33)-H(33A)119.1
O(4)-C(34)-N(2) 122.26(18)
O(4)-C(34)-C(35)121.33(17)
N(2)-C(34)-C(35)116.41(16)
C(38')-C(35)-C(37')115.4(4)
C(36)-C(35)-C(38)110.7(3)
C(36)-C(35)-C(34)113.1(2)
C(38)-C(35)-C(34)110.2(2)
C(38')-C(35)-C(36')109.2(4)
C(37')-C(35)-C(36')108.3(3)
C(36)-C(35)-C(37)111.8(3)
C(38)-C(35)-C(37)102.4(3)
C(34)-C(35)-C(37)108.04(19)

C(35)-C(36)-H(36A)109.5
C(35)-C(36)-H(36B)109.5
H(36A)-C(36)-H(36B)109.5
C(35)-C(36)-H(36C)109.5
H(36A)-C(36)-H(36C)109.5
H(36B)-C(36)-H(36C)109.5
C(35)-C(37)-H(37A)109.5
C(35)-C(37)-H(37B)109.5
H(37A)-C(37)-H(37B)109.5
C(35)-C(37)-H(37C)109.5
H(37A)-C(37)-H(37C)109.5
H(37B)-C(37)-H(37C)109.5
C(35)-C(38)-H(38A)109.5
C(35)-C(38)-H(38B)109.5
H(38A)-C(38)-H(38B)109.5
C(35)-C(38)-H(38C)109.5
H(38A)-C(38)-H(38C)109.5
H(38B)-C(38)-H(38C)109.5
H(36E)-C(36')-H(36F)109.5
C(35)-C(37')-H(37D)109.5
C(35)-C(37')-H(37E)109.5
H(37D)-C(37')-H(37E)109.5
C(35)-C(37')-H(37F)109.5
H(37D)-C(37')-H(37F)109.5
H(37E)-C(37')-H(37F)109.5
H(38D)-C(38')-H(38E)109.5
H(38D)-C(38')-H(38F)109.5
H(38E)-C(38')-H(38F)109.5
C(23)-C(39)-H(39A)109.5
C(23)-C(39)-H(39B)109.5
H(39A)-C(39)-H(39B)109.5
C(23)-C(39)-H(39C)109.5
H(39A)-C(39)-H(39C)109.5
H(39B)-C(39)-H(39C)109.5
C(24)-C(40)-H(40A)109.5
C(24)-C(40)-H(40B)109.5

H(40A)-C(40)-H(40B)109.5
C(24)-C(40)-H(40C)109.5
H(40A)-C(40)-H(40C)109.5
H(40B)-C(40)-H(40C)109.5

Symmetry transformations used to generate equivalent atoms:

Table A08 Anisotropic displacement parameters ($Å^2 x\ 10^3$) for **7a**. The anisotropic displacement factor exponent takes the form: $-2\pi^2[h^2 a^{*2} U^{11} + ... + 2 h k a^* b^* U^{12}]$

U^{11}	U^{22}	U^{33}	U^{23}	U^{13}	U^{12}
Cl(1)139(1)	97(1)	128(1)	-14(1)	72(1)	-46(1)
O(1)63(1)	86(1)	113(1)	11(1)	41(1)	12(1)
O(2)84(1)	117(1)	213(2)	-55(1)	57(1)	-24(1)
N(1)61(1)	76(1)	87(1)	-4(1)	31(1)	-7(1)
C(1)57(1)	77(1)	59(1)	1(1)	24(1)	-2(1)
C(2)60(1)	90(1)	81(1)	7(1)	35(1)	-5(1)
C(3)52(1)	100(1)	71(1)	14(1)	28(1)	4(1)
C(4)62(1)	90(1)	71(1)	9(1)	33(1)	12(1)
C(5)60(1)	77(1)	72(1)	1(1)	29(1)	-3(1)
C(6)51(1)	71(1)	61(1)	2(1)	23(1)	-1(1)
C(7)48(1)	81(1)	66(1)	-7(1)	23(1)	-3(1)
C(8)53(1)	75(1)	65(1)	-11(1)	29(1)	-5(1)
C(9)57(1)	77(1)	79(1)	-5(1)	27(1)	0(1)
C(10)80(1)	78(1)	73(1)	-2(1)	32(1)	3(1)
C(11)82(1)	74(1)	76(1)	-15(1)	42(1)	-18(1)
C(12)61(1)	103(2)	79(1)	-24(1)	29(1)	-25(1)
C(13)58(1)	87(1)	64(1)	-4(1)	26(1)	-4(1)
C(14)75(1)	91(2)	87(1)	-14(1)	32(1)	-15(1)
C(15)90(1)	78(1)	105(1)	-5(1)	45(1)	-3(1)
C(16)222(4)	110(4)	246(4)	-11(3)	181(3)	1(4)
C(17)151(3)	65(3)	206(4)	-38(3)	101(3)	-19(3)
C(18)177(5)	341(7)	155(5)	-102(5)	-73(4)	174(5)
C(16')134(3)	108(4)	213(5)	13(4)	117(3)	31(3)
C(17')126(5)	270(7)	142(4)	-139(4)	-2(4)	16(5)
C(18')101(4)	85(3)	135(4)	28(3)	23(3)	44(3)
C(19)62(1)	129(2)	110(1)	12(1)	45(1)	7(1)
C(20)83(1)	93(2)	124(2)	1(1)	53(1)	16(1)
Cl(2)135(1)	83(1)	119(1)	-2(1)	70(1)	-27(1)
O(3)64(1)	77(1)	135(1)	25(1)	47(1)	18(1)
O(4)68(1)	102(1)	174(1)	-59(1)	44(1)	-14(1)

N(2)57(1)	60(1)	87(1)	-4(1)	32(1)	5(1)
C(21)56(1)	54(1)	58(1)	-1(1)	24(1)	8(1)
C(22)62(1)	60(1)	74(1)	-3(1)	35(1)	4(1)
C(23)58(1)	74(1)	64(1)	3(1)	29(1)	10(1)
C(24)73(1)	63(1)	67(1)	-1(1)	36(1)	11(1)
C(25)67(1)	54(1)	69(1)	2(1)	30(1)	3(1)
C(26)54(1)	60(1)	61(1)	1(1)	26(1)	7(1)
C(27)56(1)	66(1)	72(1)	-1(1)	25(1)	3(1)
C(28)51(1)	67(1)	65(1)	-1(1)	25(1)	0(1)
C(29)61(1)	63(1)	66(1)	0(1)	26(1)	2(1)
C(30)77(1)	67(1)	62(1)	1(1)	28(1)	7(1)
C(31)81(1)	65(1)	78(1)	-11(1)	41(1)	-12(1)
C(32)63(1)	90(1)	84(1)	-1(1)	23(1)	-13(1)
C(33)61(1)	79(1)	77(1)	5(1)	24(1)	2(1)
C(34)63(1)	63(1)	80(1)	-10(1)	25(1)	1(1)
C(35)79(1)	62(1)	87(1)	-4(1)	44(1)	7(1)
C(36)180(4)	113(3)	105(3)	-6(3)	-32(3)	98(3)
C(37)136(3)	77(3)	145(3)	-38(2)	83(2)	-5(2)
C(38)140(3)	105(3)	126(3)	4(2)	74(2)	25(3)
C(36')106(4)	64(3)	228(7)	-7(4)	45(4)	60(3)
C(37')279(5)	51(3)	268(5)	-10(3)	216(4)	-12(4)
C(38')194(5)	222(6)	56(3)	-32(3)	31(3)	116(5)
C(39)86(1)	92(2)	124(1)	6(1)	68(1)	15(1)
C(40)116(1)	74(1)	119(1)	0(1)	69(1)	23(1)

Table A09 Hydrogen coordinates (x 10^4) and isotropic displacement parameters (Å^2 x 10^3) for **7a**.

	x	y	z	U(eq)
H(1A)	3548	6615	1046	89
H(2A)	5392	5980	1132	90
H(5A)	3790	2764	744	82
H(9A)	3769	2944	2012	85
H(10A)	3250	1447	2453	92
H(12A)	1081	2302	998	97
H(13A)	1596	3844	586	83
H(16A)	3212	7706	1795	247
H(16B)	3346	8988	2102	247
H(16C)	4005	8042	2461	247
H(17A)	4820	9862	1541	198
H(17B)	4940	9329	2311	198
H(17C)	4283	10270	1935	198
H(18A)	2973	8487	496	407
H(18B)	3589	9353	420	407
H(18C)	3075	9741	842	407
H(16D)	2935	7695	1126	204
H(16E)	2808	9024	1234	204
H(16F)	3203	8210	1928	204
H(17D)	4352	9285	2493	298
H(17E)	4306	10240	1908	298
H(17F)	4997	9329	2174	298
H(18D)	3372	8718	305	173
H(18E)	4225	9243	588	173
H(18F)	3546	9963	668	173
H(19A)	6235	3359	834	145
H(19B)	6524	4386	1409	145
H(19C)	6178	4653	555	145
H(20A)	5594	2161	601	145
H(20B)	4706	1864	114	145
H(20C)	5083	1542	960	145

H(2B)	1556	-547	3927	81
H(22A)	-211	-58	4026	76
H(25A)	1177	3312	4137	75
H(29A)	1162	3142	2850	76
H(30A)	1625	4697	2380	82
H(32A)	3825	4004	3842	98
H(33A)	3372	2419	4263	88
H(36A)	2156	-2278	4365	244
H(36B)	2092	-3545	4044	244
H(36C)	1610	-3203	4505	244
H(37A)	28	-3290	2871	166
H(37B)	598	-4157	3463	166
H(37C)	690	-3938	2720	166
H(38A)	1804	-1606	3054	176
H(38B)	989	-1988	2436	176
H(38C)	1675	-2899	2767	176
H(36D)	2117	-1485	3989	211
H(36E)	2296	-2521	3562	211
H(36F)	2251	-2747	4327	211
H(37D)	1278	-3654	4325	248
H(37E)	1069	-4318	3573	248
H(37F)	411	-3637	3714	248
H(38D)	1188	-1983	2525	246
H(38E)	363	-2504	2402	246
H(38F)	1077	-3340	2536	246
H(39A)	-1078	2493	4388	139
H(39B)	-914	1223	4713	139
H(39C)	-1389	1415	3858	139
H(40A)	327	4459	4421	144
H(40B)	-49	3826	4902	144
H(40C)	-556	4050	4055	144

Table A10 Torsion angles [°] for **7a**.

C(14)-N(1)-C(1)-C(2)	-14.8(3)
C(14)-N(1)-C(1)-C(6)	164.85(19)
C(6)-C(1)-C(2)-C(3)	2.7(3)
N(1)-C(1)-C(2)-C(3)	-177.60(16)
C(1)-C(2)-C(3)-C(4)	0.6(3)
C(1)-C(2)-C(3)-C(19)	-178.92(16)
C(2)-C(3)-C(4)-C(5)	-3.0(3)
C(19)-C(3)-C(4)-C(5)	176.49(16)
C(2)-C(3)-C(4)-C(20)	176.77(17)
C(19)-C(3)-C(4)-C(20)	-3.8(3)
C(3)-C(4)-C(5)-C(6)	2.2(3)
C(20)-C(4)-C(5)-C(6)	-177.53(16)
C(2)-C(1)-C(6)-C(5)	-3.4(2)
N(1)-C(1)-C(6)-C(5)	176.88(14)
C(2)-C(1)-C(6)-C(7)	178.53(15)
N(1)-C(1)-C(6)-C(7)	-1.1(2)
C(4)-C(5)-C(6)-C(1)	1.0(2)
C(4)-C(5)-C(6)-C(7)	179.10(16)
C(1)-C(6)-C(7)-O(1)	30.3(2)
C(5)-C(6)-C(7)-O(1)	-147.69(17)
C(1)-C(6)-C(7)-C(8)	-150.65(16)
C(5)-C(6)-C(7)-C(8)	31.4(2)
O(1)-C(7)-C(8)-C(9)	-144.27(18)
C(6)-C(7)-C(8)-C(9)	36.7(3)
O(1)-C(7)-C(8)-C(13)	29.0(3)
C(6)-C(7)-C(8)-C(13)	-150.05(17)
C(13)-C(8)-C(9)-C(10)	2.0(3)
C(7)-C(8)-C(9)-C(10)	175.40(18)
C(8)-C(9)-C(10)-C(11)	0.8(3)
C(9)-C(10)-C(11)-C(12)	-2.5(3)
C(9)-C(10)-C(11)-Cl(1)	178.96(15)
C(10)-C(11)-C(12)-C(13)	1.3(3)
Cl(1)-C(11)-C(12)-C(13)	179.78(15)
C(11)-C(12)-C(13)-C(8)	1.7(3)

C(9)-C(8)-C(13)-C(12)	-3.3(3)
C(7)-C(8)-C(13)-C(12)	-176.88(17)
C(1)-N(1)-C(14)-O(2)	0.5(3)
C(1)-N(1)-C(14)-C(15)	179.34(17)
O(2)-C(14)-C(15)-C(17')	-31.5(4)
N(1)-C(14)-C(15)-C(17')	149.7(4)
O(2)-C(14)-C(15)-C(18)	115.5(4)
N(1)-C(14)-C(15)-C(18)	-63.3(4)
O(2)-C(14)-C(15)-C(17)	-8.9(3)
N(1)-C(14)-C(15)-C(17)	172.3(3)
O(2)-C(14)-C(15)-C(16)	-119.7(3)
N(1)-C(14)-C(15)-C(16)	61.5(3)
C(34)-N(2)-C(21)-C(22)	20.8(3)
C(34)-N(2)-C(21)-C(26)	-159.30(17)
C(26)-C(21)-C(22)-C(23)	-1.9(2)
N(2)-C(21)-C(22)-C(23)	178.03(14)
C(21)-C(22)-C(23)-C(24)	-0.3(2)
C(21)-C(22)-C(23)-C(39)	179.87(15)
C(22)-C(23)-C(24)-C(25)	1.9(2)
C(39)-C(23)-C(24)-C(25)	-178.29(15)
C(22)-C(23)-C(24)-C(40)	-177.36(15)
C(39)-C(23)-C(24)-C(40)	2.5(2)
C(23)-C(24)-C(25)-C(26)	-1.4(2)
C(40)-C(24)-C(25)-C(26)	177.89(15)
C(24)-C(25)-C(26)-C(21)	-0.8(2)
C(24)-C(25)-C(26)-C(27)	-175.65(15)
C(22)-C(21)-C(26)-C(25)	2.3(2)
N(2)-C(21)-C(26)-C(25)	-177.56(14)
C(22)-C(21)-C(26)-C(27)	177.04(15)
N(2)-C(21)-C(26)-C(27)	-2.9(2)
C(25)-C(26)-C(27)-O(3)	149.70(17)
C(21)-C(26)-C(27)-O(3)	-24.9(2)
C(25)-C(26)-C(27)-C(28)	-29.9(2)
C(21)-C(26)-C(27)-C(28)	155.53(15)
O(3)-C(27)-C(28)-C(33)	-32.6(3)
C(26)-C(27)-C(28)-C(33)	146.98(17)

O(3)-C(27)-C(28)-C(29)	140.97(18)
C(26)-C(27)-C(28)-C(29)	-39.4(3)
C(33)-C(28)-C(29)-C(30)	-1.7(3)
C(27)-C(28)-C(29)-C(30)	-175.36(17)
C(28)-C(29)-C(30)-C(31)	-0.6(3)
C(29)-C(30)-C(31)-C(32)	1.4(3)
C(29)-C(30)-C(31)-Cl(2)	-179.18(14)
C(30)-C(31)-C(32)-C(33)	0.3(3)
Cl(2)-C(31)-C(32)-C(33)	-179.16(16)
C(31)-C(32)-C(33)-C(28)	-2.8(3)
C(29)-C(28)-C(33)-C(32)	3.5(3)
C(27)-C(28)-C(33)-C(32)	177.27(18)
C(21)-N(2)-C(34)-O(4)	-3.3(3)
C(21)-N(2)-C(34)-C(35)	176.05(16)
O(4)-C(34)-C(35)-C(36)	-117.9(3)
N(2)-C(34)-C(35)-C(36)	62.8(3)
O(4)-C(34)-C(35)-C(38)	117.6(2)
N(2)-C(34)-C(35)-C(38)	-61.8(2)
O(4)-C(34)-C(35)-C(37)	6.4(3)
N(2)-C(34)-C(35)-C(37)	-172.9(2)

Symmetry transformations used to generate equivalent atoms:

Table A11 Hydrogen bonds for ccw6 [Å and °].

D-H...A	d(D-H)	d(H...A)	d(D...A)	<(DHA)
(1A)...O(1)	0.86	2.03	2.7183(18)	136.4
N(2)-H(2B)...O(3)	0.86	2.04	2.7068(18)	133.9
C(2)-H(2A)...O(2)	0.93	2.23	2.833(3)	121.9
C(22)-H(22A)...O(4)	0.93	2.24	2.832(2)	120.6

Symmetry transformations used to generate equivalent atoms:

Figure A146 Molecular structure of **15a**

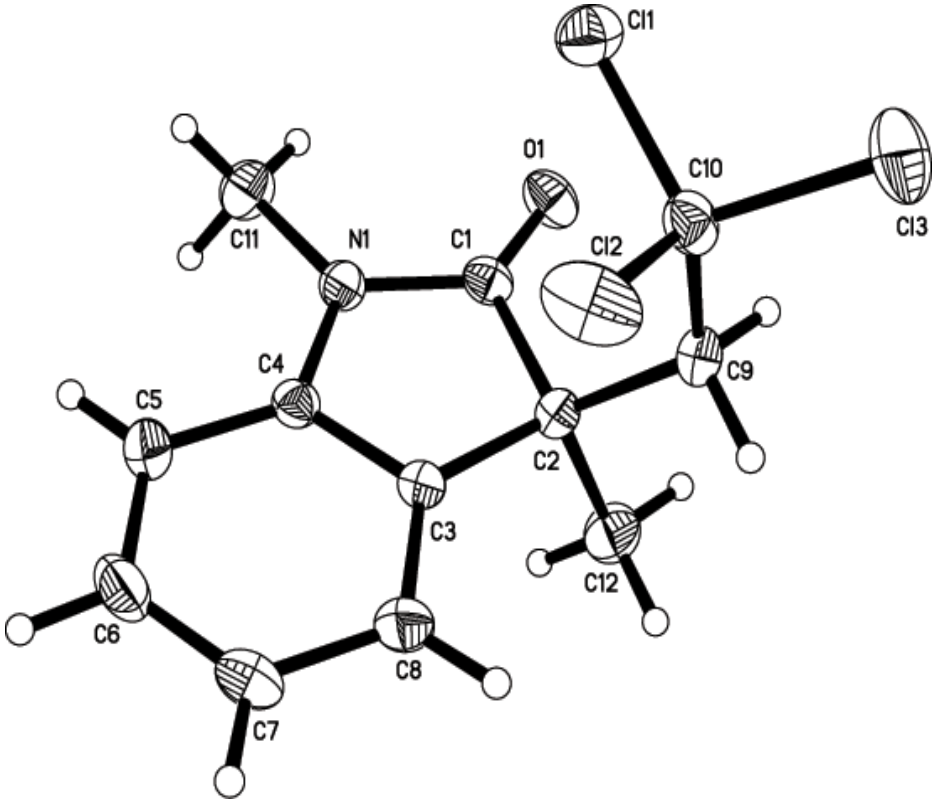

Table A12 Atomic coordinates (x 10^4) and equivalent isotropic displacement parameters ($Å^2$ x 10^3) for **15a**. U(eq) is defined as one third of the trace of the orthogonalized U^{ij} tensor.

	x	y	z	U(eq)
Cl(1)	3651(1)	132(1)	3147(1)	67(1)
Cl(2)	1097(1)	649(1)	1303(1)	97(1)
Cl(3)	4087(1)	944(1)	681(1)	105(1)
O(1)	4524(2)	1580(1)	5490(1)	61(1)
N(1)	2095(2)	1234(1)	5783(1)	46(1)
C(1)	3172(2)	1593(1)	5123(2)	45(1)
C(2)	2369(2)	2075(1)	3883(2)	45(1)
C(3)	735(2)	1856(1)	3937(2)	44(1)
C(4)	642(2)	1383(1)	5094(2)	43(1)
C(5)	-726(2)	1139(2)	5462(2)	59(1)
C(6)	-2015(2)	1391(2)	4631(3)	70(1)

C(7)	-1938(2)	1865(2)	3488(3)	72(1)
C(8)	-559(2)	2104(2)	3130(2)	62(1)
C(9)	3044(2)	1868(1)	2596(2)	52(1)
C(10)	2948(2)	956(2)	1998(2)	56(1)
C(11)	2409(3)	768(2)	7053(2)	67(1)
C(12)	2633(3)	3066(2)	4156(3)	70(1)

Table A13 Bond lengths [Å] and angles [°] for **15a**.

Cl(1)-C(10)	1.762(2)
Cl(2)-C(10)	1.767(2)
Cl(3)-C(10)	1.784(2)
O(1)-C(1)	1.214(2)
N(1)-C(1)	1.360(2)
N(1)-C(4)	1.403(2)
N(1)-C(11)	1.456(3)
C(1)-C(2)	1.538(2)
C(2)-C(3)	1.508(3)
C(2)-C(9)	1.538(3)
C(2)-C(12)	1.546(3)
C(3)-C(8)	1.372(3)
C(3)-C(4)	1.382(3)
C(4)-C(5)	1.380(3)
C(5)-C(6)	1.380(3)
C(5)-H(5A)	0.93(2)
C(6)-C(7)	1.370(4)
C(6)-H(6A)	0.91(2)
C(7)-C(8)	1.382(3)
C(7)-H(7A)	0.94(2)
C(8)-H(8A)	0.93(2)
C(9)-C(10)	1.512(3)
C(9)-H(9A)	0.9700
C(9)-H(9B)	0.9700
C(11)-H(11C)	0.94(3)
C(11)-H(11B)	0.88(2)
C(11)-H(11A)	0.97(3)
C(12)-H(12C)	0.95(2)
C(12)-H(12B)	0.96(2)
C(12)-H(12A)	0.93(3)
C(1)-N(1)-C(4)	111.33(14)
C(1)-N(1)-C(11)	124.28(16)
C(4)-N(1)-C(11)	124.39(17)
O(1)-C(1)-N(1)	126.11(17)

O(1)-C(1)-C(2)	125.84(18)
N(1)-C(1)-C(2)	107.92(15)
C(3)-C(2)-C(1)	102.00(14)
C(3)-C(2)-C(9)	118.91(15)
C(1)-C(2)-C(9)	113.21(15)
C(3)-C(2)-C(12)	109.52(17)
C(1)-C(2)-C(12)	106.20(16)
C(9)-C(2)-C(12)	106.37(17)
C(8)-C(3)-C(4)	119.84(18)
C(8)-C(3)-C(2)	131.20(18)
C(4)-C(3)-C(2)	108.70(15)
C(5)-C(4)-C(3)	121.94(17)
C(5)-C(4)-N(1)	128.17(17)
C(3)-C(4)-N(1)	109.87(16)
C(4)-C(5)-C(6)	117.3(2)
C(4)-C(5)-H(5A)	119.4(13)
C(6)-C(5)-H(5A)	123.3(13)
C(7)-C(6)-C(5)	121.3(2)
C(7)-C(6)-H(6A)	118.7(14)
C(5)-C(6)-H(6A)	119.9(14)
C(6)-C(7)-C(8)	120.7(2)
C(6)-C(7)-H(7A)	119.2(15)
C(8)-C(7)-H(7A)	120.0(15)
C(3)-C(8)-C(7)	118.8(2)
C(3)-C(8)-H(8A)	118.1(13)
C(7)-C(8)-H(8A)	123.0(13)
C(10)-C(9)-C(2)	121.18(17)
C(10)-C(9)-H(9A)	107.0
C(2)-C(9)-H(9A)	107.0
C(10)-C(9)-H(9B)	107.0
C(2)-C(9)-H(9B)	107.0
H(9A)-C(9)-H(9B)	106.8
C(9)-C(10)-Cl(1)	113.39(13)
C(9)-C(10)-Cl(2)	113.47(15)
Cl(1)-C(10)-Cl(2)	107.43(12)
C(9)-C(10)-Cl(3)	107.48(15)

Cl(1)-C(10)-Cl(3)107.05(11)
Cl(2)-C(10)-Cl(3)107.71(11)
N(1)-C(11)-H(11C)111.2(15)
N(1)-C(11)-H(11B)108.7(17)
H(11C)-C(11)-H(11B)116(2)
N(1)-C(11)-H(11A)108.5(16)
H(11C)-C(11)-H(11A)107(2)
H(11B)-C(11)-H(11A)104(2)
C(2)-C(12)-H(12C)110.6(14)
C(2)-C(12)-H(12B)106.4(13)
H(12C)-C(12)-H(12B)109.5(19)
C(2)-C(12)-H(12A)111.1(17)
H(12C)-C(12)-H(12A)107(2)
H(12B)-C(12)-H(12A)112(2)

Symmetry transformations used to generate equivalent atoms:

Table A14 Anisotropic displacement parameters ($Å^2 x\ 10^3$) for **15a**. The anisotropic displacement factor exponent takes the form: $-2\pi^2[h^2 a^{*2} U^{11} + ... + 2 h k a^* b^* U^{12}]$

U^{11}	U^{22}	U^{33}	U^{23}	U^{13}	U^{12}
Cl(1)84(1)	57(1)	60(1)	-1(1)	6(1)	10(1)
Cl(2)71(1)	108(1)	101(1)	-40(1)	-24(1)	11(1)
Cl(3)130(1)	133(1)	62(1)	-7(1)	52(1)	13(1)
O(1)42(1)	83(1)	56(1)	-10(1)	0(1)	6(1)
N(1)48(1)	54(1)	37(1)	5(1)	8(1)	7(1)
C(1)46(1)	48(1)	41(1)	-9(1)	4(1)	6(1)
C(2)48(1)	42(1)	44(1)	5(1)	9(1)	1(1)
C(3)42(1)	44(1)	47(1)	4(1)	9(1)	6(1)
C(4)45(1)	42(1)	43(1)	-2(1)	9(1)	5(1)
C(5)59(1)	60(1)	63(1)	5(1)	23(1)	0(1)
C(6)42(1)	78(2)	93(2)	-4(1)	21(1)	1(1)
C(7)44(1)	84(2)	87(2)	6(1)	1(1)	15(1)
C(8)53(1)	70(1)	63(1)	16(1)	5(1)	16(1)
C(9)57(1)	55(1)	47(1)	8(1)	15(1)	-1(1)
C(10)55(1)	70(1)	43(1)	-2(1)	10(1)	6(1)
C(11)77(2)	78(2)	45(1)	16(1)	5(1)	9(1)
C(12)80(2)	48(1)	83(2)	-2(1)	18(1)	-6(1)

Table A15 Hydrogen coordinates (x 10^4) and isotropic displacement parameters ($Å^2$x 10^3) for **15a**.

	x	y	z	U(eq)
H(5A)	-740(20)	840(14)	6260(20)	62(6)
H(6A)	-2940(30)	1269(15)	4860(20)	72(7)
H(7A)	-2840(30)	2001(16)	2920(20)	85(8)
H(8A)	-470(20)	2422(14)	2360(20)	67(6)
H(9A)	2574	2265	1908	63
H(9B)	4105	2024	2766	63
H(11C)	2010(30)	195(18)	6980(20)	94(9)
H(11B)	3380(30)	815(16)	7350(20)	85(8)
H(11A)	1910(30)	1075(18)	7710(30)	105(9)
H(12C)	3680(20)	3202(15)	4250(20)	71(7)
H(12B)	2110(20)	3371(14)	3390(20)	67(6)
H(12A)	2300(30)	3232(17)	4950(30)	91(8)

Table A16 Torsion angles [°] for **15a**.

C(4)-N(1)-C(1)-O(1)	178.81(18)
C(11)-N(1)-C(1)-O(1)	-0.2(3)
C(4)-N(1)-C(1)-C(2)	2.8(2)
C(11)-N(1)-C(1)-C(2)	-176.26(18)
O(1)-C(1)-C(2)-C(3)	179.79(18)
N(1)-C(1)-C(2)-C(3)	-4.18(19)
O(1)-C(1)-C(2)-C(9)	50.8(3)
N(1)-C(1)-C(2)-C(9)	-133.15(16)
O(1)-C(1)-C(2)-C(12)	-65.5(2)
N(1)-C(1)-C(2)-C(12)	110.49(18)
C(1)-C(2)-C(3)-C(8)	178.2(2)
C(9)-C(2)-C(3)-C(8)	-56.5(3)
C(12)-C(2)-C(3)-C(8)	66.0(3)
C(1)-C(2)-C(3)-C(4)	4.18(19)
C(9)-C(2)-C(3)-C(4)	129.46(18)
C(12)-C(2)-C(3)-C(4)	-108.03(19)
C(8)-C(3)-C(4)-C(5)	0.9(3)
C(2)-C(3)-C(4)-C(5)	175.64(18)
C(8)-C(3)-C(4)-N(1)	-177.61(18)
C(2)-C(3)-C(4)-N(1)	-2.8(2)
C(1)-N(1)-C(4)-C(5)	-178.4(2)
C(11)-N(1)-C(4)-C(5)	0.7(3)
C(1)-N(1)-C(4)-C(3)	0.0(2)
C(11)-N(1)-C(4)-C(3)	179.02(18)
C(3)-C(4)-C(5)-C(6)	-0.4(3)
N(1)-C(4)-C(5)-C(6)	177.8(2)
C(4)-C(5)-C(6)-C(7)	-0.2(4)
C(5)-C(6)-C(7)-C(8)	0.3(4)
C(4)-C(3)-C(8)-C(7)	-0.7(3)
C(2)-C(3)-C(8)-C(7)	-174.2(2)
C(6)-C(7)-C(8)-C(3)	0.2(4)
C(3)-C(2)-C(9)-C(10)	-54.0(2)
C(1)-C(2)-C(9)-C(10)	65.6(2)
C(12)-C(2)-C(9)-C(10)	-178.10(18)

C(2)-C(9)-C(10)-Cl(1)	-53.5(2)
C(2)-C(9)-C(10)-Cl(2)	69.5(2)
C(2)-C(9)-C(10)-Cl(3)	-171.57(14)

Symmetry transformations used to generate equivalent atoms:

Table A17 Hydrogen bonds for **15a** [Å and °].

D-H...A	d(D-H)	d(H...A)	d(D...A)	<(DHA)
C(11)-H(11B)...O(1)	0.88(2)	2.54(3)	2.904(3)	105.3(18)

Symmetry transformations used to generate equivalent atoms:

Figure A147 Molecular structure of **13a**

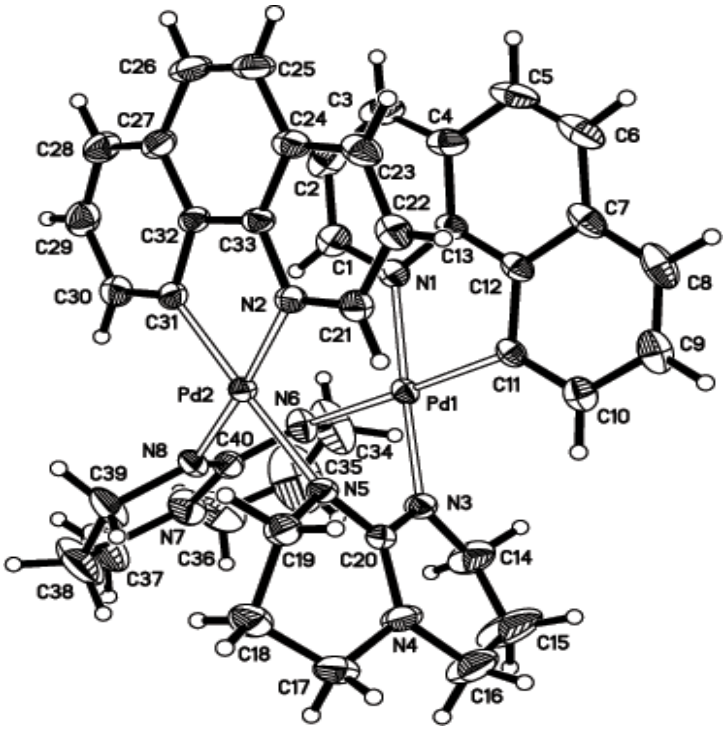

Table A18 Atomic coordinates (x 104) and equivalent isotropic displacement parameters ($Å^2$x 103) for **13a**. U(eq) is defined as one third of the trace of the orthogonalized Uij tensor.

	x	y	z	U(eq)
Pd(1)	5327(1)	7282(1)	2282(1)	42(1)
Pd(2)	4057(1)	5615(1)	2117(1)	42(1)
N(1)	6142(1)	6168(2)	2894(1)	50(1)
N(2)	4698(1)	4377(1)	1633(1)	45(1)
N(3)	4544(1)	8254(2)	1584(1)	53(1)
N(4)	3445(1)	8469(2)	626(1)	76(1)
N(5)	3752(1)	6654(2)	1169(1)	48(1)
N(6)	4664(1)	7709(2)	3133(1)	62(1)
N(7)	3427(2)	8213(2)	3539(1)	86(1)
N(8)	3473(1)	6746(2)	2682(1)	55(1)
C(1)	6136(2)	5804(2)	3564(1)	66(1)
C(2)	6660(2)	4912(3)	3868(2)	83(1)
C(3)	7180(2)	4381(3)	3474(2)	88(1)

C(4)	7197(2)	4738(2)	2769(2)	71(1)
C(5)	7713(2)	4249(2)	2285(2)	86(1)
C(6)	7694(2)	4659(3)	1619(2)	84(1)
C(7)	7161(1)	5592(2)	1334(2)	65(1)
C(8)	7126(2)	6082(3)	644(2)	80(1)
C(9)	6566(2)	6926(3)	414(1)	75(1)
C(10)	6009(2)	7325(2)	845(1)	60(1)
C(11)	6021(1)	6913(2)	1537(1)	45(1)
C(12)	6618(1)	6057(2)	1776(1)	49(1)
C(13)	6656(1)	5642(2)	2488(1)	46(1)
C(14)	4657(2)	9513(2)	1608(2)	95(1)
C(15)	4305(3)	10100(3)	964(3)	168(2)
C(16)	3653(3)	9671(3)	510(2)	120(1)
C(17)	2613(2)	8169(3)	314(2)	86(1)
C(18)	2361(2)	6990(3)	523(2)	86(1)
C(19)	3092(2)	6215(2)	629(2)	64(1)
C(20)	3916(1)	7790(2)	1145(1)	49(1)
C(21)	4857(1)	4346(2)	964(1)	55(1)
C(22)	5374(2)	3512(2)	727(2)	64(1)
C(23)	5749(2)	2707(2)	1203(2)	66(1)
C(24)	5600(1)	2702(2)	1918(1)	56(1)
C(25)	5952(2)	1907(2)	2466(2)	71(1)
C(26)	5768(2)	1961(2)	3135(2)	75(1)
C(27)	5221(2)	2819(2)	3346(2)	62(1)
C(28)	5039(2)	2950(3)	4044(2)	77(1)
C(29)	4546(2)	3847(3)	4197(2)	77(1)
C(30)	4206(2)	4661(2)	3670(1)	65(1)
C(31)	4361(1)	4582(2)	2970(1)	49(1)
C(32)	4876(1)	3645(2)	2822(1)	49(1)
C(33)	5060(1)	3560(2)	2113(1)	47(1)
C(34)	5089(2)	8558(3)	3632(2)	139(1)
C(35)	4599(3)	9336(4)	3967(3)	217(2)
C(36)	3796(3)	9104(4)	3993(2)	122(1)
C(37)	2559(2)	8009(5)	3539(3)	144(2)
C(38)	2154(2)	7366(4)	2967(4)	170(2)
C(39)	2597(2)	6542(4)	2643(2)	96(1)

C(40)	3865(1)	7540(2)	3108(1)	55(1)

Table A19 Bond lengths [Å] and angles [°] for **13a**.

Pd(1)-C(11)	1.985(2)
Pd(1)-N(3)	2.0165(18)
Pd(1)-N(1)	2.0591(18)
Pd(1)-N(6)	2.126(2)
Pd(1)-Pd(2)	2.8048(2)
Pd(2)-C(31)	1.989(2)
Pd(2)-N(8)	2.0120(19)
Pd(2)-N(2)	2.0587(18)
Pd(2)-N(5)	2.1317(17)
N(1)-C(1)	1.327(3)
N(1)-C(13)	1.365(3)
N(2)-C(21)	1.323(3)
N(2)-C(33)	1.367(3)
N(3)-C(20)	1.324(3)
N(3)-C(14)	1.451(3)
N(4)-C(20)	1.382(3)
N(4)-C(17)	1.438(4)
N(4)-C(16)	1.442(4)
N(5)-C(20)	1.328(3)
N(5)-C(19)	1.450(3)
N(6)-C(40)	1.320(3)
N(6)-C(34)	1.449(4)
N(7)-C(40)	1.396(3)
N(7)-C(36)	1.403(5)
N(7)-C(37)	1.445(4)
N(8)-C(40)	1.308(3)
N(8)-C(39)	1.446(3)
C(1)-C(2)	1.396(4)
C(1)-H(1A)	0.9300
C(2)-C(3)	1.358(5)
C(2)-H(2A)	0.9300
C(3)-C(4)	1.389(5)
C(3)-H(3A)	0.9300
C(4)-C(13)	1.408(3)

C(4)-C(5)	1.450(4)
C(5)-C(6)	1.331(5)
C(5)-H(5A)	0.9300
C(6)-C(7)	1.429(4)
C(6)-H(6A)	0.9300
C(7)-C(8)	1.404(4)
C(7)-C(12)	1.414(3)
C(8)-C(9)	1.355(4)
C(8)-H(8A)	0.9300
C(9)-C(10)	1.391(4)
C(9)-H(9A)	0.9300
C(10)-C(11)	1.379(3)
C(10)-H(10A)	0.9300
C(11)-C(12)	1.407(3)
C(12)-C(13)	1.410(3)
C(14)-C(15)	1.422(5)
C(14)-H(14A)	0.9700
C(14)-H(14B)	0.9700
C(15)-C(16)	1.349(6)
C(15)-H(15A)	0.9700
C(15)-H(15B)	0.9700
C(16)-H(16A)	0.9700
C(16)-H(16B)	0.9700
C(17)-C(18)	1.482(5)
C(17)-H(17A)	0.9700
C(17)-H(17B)	0.9700
C(18)-C(19)	1.479(4)
C(18)-H(18A)	0.9700
C(18)-H(18B)	0.9700
C(19)-H(19A)	0.9700
C(19)-H(19B)	0.9700
C(21)-C(22)	1.396(3)
C(21)-H(21A)	0.9300
C(22)-C(23)	1.360(4)
C(22)-H(22A)	0.9300
C(23)-C(24)	1.402(4)

C(23)-H(23A)	0.9300
C(24)-C(33)	1.409(3)
C(24)-C(25)	1.424(4)
C(25)-C(26)	1.339(4)
C(25)-H(25A)	0.9300
C(26)-C(27)	1.428(4)
C(26)-H(26A)	0.9300
C(27)-C(28)	1.397(4)
C(27)-C(32)	1.415(3)
C(28)-C(29)	1.365(4)
C(28)-H(28A)	0.9300
C(29)-C(30)	1.408(4)
C(29)-H(29A)	0.9300
C(30)-C(31)	1.379(3)
C(30)-H(30A)	0.9300
C(31)-C(32)	1.420(3)
C(32)-C(33)	1.414(3)
C(34)-C(35)	1.412(4)
C(34)-H(34A)	0.9700
C(34)-H(34B)	0.9700
C(35)-C(36)	1.353(6)
C(35)-H(35A)	0.9700
C(35)-H(35B)	0.9700
C(36)-H(36A)	0.9700
C(36)-H(36B)	0.9700
C(37)-C(38)	1.382(7)
C(37)-H(37A)	0.9700
C(37)-H(37B)	0.9700
C(38)-C(39)	1.388(6)
C(38)-H(38A)	0.9700
C(38)-H(38B)	0.9700
C(39)-H(39A)	0.9700
C(39)-H(39B)	0.9700

C(11)-Pd(1)-N(3)	92.15(8)
C(11)-Pd(1)-N(1)	82.31(8)

N(3)-Pd(1)-N(1) 173.30(8)
C(11)-Pd(1)-N(6) 175.77(8)
N(3)-Pd(1)-N(6) 90.71(8)
N(1)-Pd(1)-N(6) 95.03(8)
C(11)-Pd(1)-Pd(2) 106.10(6)
N(3)-Pd(1)-Pd(2) 85.25(5)
N(1)-Pd(1)-Pd(2) 92.64(5)
N(6)-Pd(1)-Pd(2) 77.24(5)
C(31)-Pd(2)-N(8) 92.05(9)
C(31)-Pd(2)-N(2) 82.35(8)
N(8)-Pd(2)-N(2) 174.33(7)
C(31)-Pd(2)-N(5) 177.12(8)
N(8)-Pd(2)-N(5) 90.77(8)
N(2)-Pd(2)-N(5) 94.84(7)
C(31)-Pd(2)-Pd(1) 103.21(6)
N(8)-Pd(2)-Pd(1) 85.01(5)
N(2)-Pd(2)-Pd(1) 95.40(5)
N(5)-Pd(2)-Pd(1) 77.61(5)
C(1)-N(1)-C(13) 119.3(2)
C(1)-N(1)-Pd(1) 128.39(17)
C(13)-N(1)-Pd(1) 111.49(14)
C(21)-N(2)-C(33) 118.46(19)
C(21)-N(2)-Pd(2) 128.95(15)
C(33)-N(2)-Pd(2) 112.24(14)
C(20)-N(3)-C(14) 120.0(2)
C(20)-N(3)-Pd(1) 122.41(14)
C(14)-N(3)-Pd(1) 117.47(18)
C(20)-N(4)-C(17) 122.7(2)
C(20)-N(4)-C(16) 121.5(2)
C(17)-N(4)-C(16) 113.5(2)
C(20)-N(5)-C(19) 116.62(18)
C(20)-N(5)-Pd(2) 123.46(15)
C(19)-N(5)-Pd(2) 116.11(15)
C(40)-N(6)-C(34) 119.6(2)
C(40)-N(6)-Pd(1) 124.36(16)
C(34)-N(6)-Pd(1) 112.86(18)

C(40)-N(7)-C(36)	122.7(3)
C(40)-N(7)-C(37)	120.7(3)
C(36)-N(7)-C(37)	116.6(3)
C(40)-N(8)-C(39)	122.1(2)
C(40)-N(8)-Pd(2)	122.55(15)
C(39)-N(8)-Pd(2)	115.04(19)
N(1)-C(1)-C(2)	121.3(3)
N(1)-C(1)-H(1A)	119.3
C(2)-C(1)-H(1A)	119.3
C(3)-C(2)-C(1)	120.3(3)
C(3)-C(2)-H(2A)	119.9
C(1)-C(2)-H(2A)	119.9
C(2)-C(3)-C(4)	119.7(3)
C(2)-C(3)-H(3A)	120.1
C(4)-C(3)-H(3A)	120.1
C(3)-C(4)-C(13)	117.8(3)
C(3)-C(4)-C(5)	125.8(3)
C(13)-C(4)-C(5)	116.3(3)
C(6)-C(5)-C(4)	121.6(3)
C(6)-C(5)-H(5A)	119.2
C(4)-C(5)-H(5A)	119.2
C(5)-C(6)-C(7)	122.4(3)
C(5)-C(6)-H(6A)	118.8
C(7)-C(6)-H(6A)	118.8
C(8)-C(7)-C(12)	116.9(2)
C(8)-C(7)-C(6)	125.2(3)
C(12)-C(7)-C(6)	117.8(3)
C(9)-C(8)-C(7)	120.3(2)
C(9)-C(8)-H(8A)	119.8
C(7)-C(8)-H(8A)	119.8
C(8)-C(9)-C(10)	121.5(3)
C(8)-C(9)-H(9A)	119.2
C(10)-C(9)-H(9A)	119.2
C(11)-C(10)-C(9)	121.6(2)
C(11)-C(10)-H(10A)	119.2
C(9)-C(10)-H(10A)	119.2

C(10)-C(11)-C(12) 116.3(2)
C(10)-C(11)-Pd(1) 131.84(17)
C(12)-C(11)-Pd(1) 111.89(16)
C(11)-C(12)-C(13) 117.3(2)
C(11)-C(12)-C(7) 123.2(2)
C(13)-C(12)-C(7) 119.5(2)
N(1)-C(13)-C(4) 121.5(2)
N(1)-C(13)-C(12) 116.29(18)
C(4)-C(13)-C(12) 122.2(2)
C(15)-C(14)-N(3) 114.2(3)
C(15)-C(14)-H(14A) 108.7
N(3)-C(14)-H(14A) 108.7
C(15)-C(14)-H(14B) 108.7
N(3)-C(14)-H(14B) 108.7
H(14A)-C(14)-H(14B) 107.6
C(16)-C(15)-C(14) 122.6(4)
C(16)-C(15)-H(15A) 106.7
C(14)-C(15)-H(15A) 106.7
C(16)-C(15)-H(15B) 106.7
C(14)-C(15)-H(15B) 106.7
H(15A)-C(15)-H(15B) 106.6
C(15)-C(16)-N(4) 115.8(3)
C(15)-C(16)-H(16A) 108.3
N(4)-C(16)-H(16A) 108.3
C(15)-C(16)-H(16B) 108.3
N(4)-C(16)-H(16B) 108.3
H(16A)-C(16)-H(16B) 107.4
N(4)-C(17)-C(18) 113.4(2)
N(4)-C(17)-H(17A) 108.9
C(18)-C(17)-H(17A) 108.9
N(4)-C(17)-H(17B) 108.9
C(18)-C(17)-H(17B) 108.9
H(17A)-C(17)-H(17B) 107.7
C(19)-C(18)-C(17) 109.0(2)
C(19)-C(18)-H(18A) 109.9
C(17)-C(18)-H(18A) 109.9

C(19)-C(18)-H(18B)109.9
C(17)-C(18)-H(18B)109.9
H(18A)-C(18)-H(18B)108.3
N(5)-C(19)-C(18) 112.7(2)
N(5)-C(19)-H(19A)109.1
C(18)-C(19)-H(19A)109.1
N(5)-C(19)-H(19B)109.1
C(18)-C(19)-H(19B)109.1
H(19A)-C(19)-H(19B)107.8
N(3)-C(20)-N(5) 120.86(19)
N(3)-C(20)-N(4) 120.4(2)
N(5)-C(20)-N(4) 118.66(19)
N(2)-C(21)-C(22) 122.9(2)
N(2)-C(21)-H(21A)118.6
C(22)-C(21)-H(21A)118.6
C(23)-C(22)-C(21)119.2(3)
C(23)-C(22)-H(22A)120.4
C(21)-C(22)-H(22A)120.4
C(22)-C(23)-C(24)120.1(2)
C(22)-C(23)-H(23A)119.9
C(24)-C(23)-H(23A)119.9
C(23)-C(24)-C(33)117.3(2)
C(23)-C(24)-C(25)125.5(2)
C(33)-C(24)-C(25)117.1(2)
C(26)-C(25)-C(24)121.4(2)
C(26)-C(25)-H(25A)119.3
C(24)-C(25)-H(25A)119.3
C(25)-C(26)-C(27)122.6(2)
C(25)-C(26)-H(26A)118.7
C(27)-C(26)-H(26A)118.7
C(28)-C(27)-C(32)117.3(2)
C(28)-C(27)-C(26)124.9(2)
C(32)-C(27)-C(26)117.7(3)
C(29)-C(28)-C(27)120.0(3)
C(29)-C(28)-H(28A)120.0
C(27)-C(28)-H(28A)120.0

C(28)-C(29)-C(30)122.0(3)
C(28)-C(29)-H(29A)119.0
C(30)-C(29)-H(29A)119.0
C(31)-C(30)-C(29)120.9(3)
C(31)-C(30)-H(30A)119.5
C(29)-C(30)-H(30A)119.5
C(30)-C(31)-C(32)116.2(2)
C(30)-C(31)-Pd(2)131.89(19)
C(32)-C(31)-Pd(2)111.77(16)
C(33)-C(32)-C(27)119.1(2)
C(33)-C(32)-C(31)117.36(19)
C(27)-C(32)-C(31)123.5(2)
N(2)-C(33)-C(24) 122.0(2)
N(2)-C(33)-C(32)115.95(19)
C(24)-C(33)-C(32)122.0(2)
C(35)-C(34)-N(6) 117.5(3)
C(35)-C(34)-H(34A)107.9
N(6)-C(34)-H(34A)107.9
C(35)-C(34)-H(34B)107.9
N(6)-C(34)-H(34B)107.9
H(34A)-C(34)-H(34B)107.2
C(36)-C(35)-C(34)121.3(4)
C(36)-C(35)-H(35A)107.0
C(34)-C(35)-H(35A)107.0
C(36)-C(35)-H(35B)107.0
C(34)-C(35)-H(35B)107.0
H(35A)-C(35)-H(35B)106.7
C(35)-C(36)-N(7) 116.7(3)
C(35)-C(36)-H(36A)108.1
N(7)-C(36)-H(36A)108.1
C(35)-C(36)-H(36B)108.1
N(7)-C(36)-H(36B)108.1
H(36A)-C(36)-H(36B)107.3
C(38)-C(37)-N(7) 115.9(3)
C(38)-C(37)-H(37A)108.3
N(7)-C(37)-H(37A)108.3

C(38)-C(37)-H(37B)108.3
N(7)-C(37)-H(37B)108.3
H(37A)-C(37)-H(37B)107.4
C(37)-C(38)-C(39)118.8(4)
C(37)-C(38)-H(38A)107.6
C(39)-C(38)-H(38A)107.6
C(37)-C(38)-H(38B)107.6
C(39)-C(38)-H(38B)107.6
H(38A)-C(38)-H(38B)107.1
C(38)-C(39)-N(8) 117.0(3)
C(38)-C(39)-H(39A)108.0
N(8)-C(39)-H(39A)108.0
C(38)-C(39)-H(39B)108.0
N(8)-C(39)-H(39B)108.0
H(39A)-C(39)-H(39B)107.3
N(8)-C(40)-N(6) 120.9(2)
N(8)-C(40)-N(7) 119.2(2)
N(6)-C(40)-N(7) 120.0(2)

Symmetry transformations used to generate equivalent atoms:

Table A20 Anisotropic displacement parameters ($Å^2 x\ 10^3$)for **13a**. The anisotropic displacement factor exponent takes the form: $-2\pi^2[\ h^2 a^{*2} U^{11} + ... + 2\ h\ k\ a^*\ b^*\ U^{12}\ ]$

U^{11}	U^{22}	U^{33}	U^{23}	U^{13}	U^{12}
Pd(1)34(1)	43(1)	50(1)	-6(1)	8(1)	-3(1)
Pd(2)36(1)	38(1)	53(1)	3(1)	6(1)	-1(1)
N(1)41(1)	53(1)	52(1)	-3(1)	-3(1)	-9(1)
N(2)41(1)	38(1)	55(1)	-2(1)	3(1)	-4(1)
N(3)47(1)	37(1)	72(1)	4(1)	5(1)	0(1)
N(4)65(1)	57(1)	98(2)	31(1)	-13(1)	1(1)
N(5)38(1)	46(1)	57(1)	8(1)	-1(1)	-1(1)
N(6)62(1)	61(1)	68(1)	-22(1)	25(1)	-11(1)
N(7)93(1)	81(2)	97(2)	-22(1)	51(1)	14(1)
N(8)41(1)	57(1)	71(1)	1(1)	19(1)	6(1)
C(1)61(1)	73(2)	57(1)	2(1)	-10(1)	-16(1)
C(2)80(2)	86(2)	71(2)	22(2)	-27(1)	-23(2)
C(3)62(2)	62(2)	123(2)	18(2)	-36(2)	-5(1)
C(4)46(1)	50(1)	107(2)	-2(1)	-18(1)	-4(1)
C(5)43(1)	54(1)	151(3)	-21(2)	-14(2)	11(1)
C(6)46(1)	75(2)	131(2)	-43(2)	10(2)	4(1)
C(7)39(1)	67(1)	88(2)	-36(1)	9(1)	-7(1)
C(8)56(1)	110(2)	77(2)	-49(2)	27(1)	-19(1)
C(9)64(1)	110(2)	54(1)	-24(1)	15(1)	-21(2)
C(10)51(1)	77(2)	51(1)	-10(1)	6(1)	-9(1)
C(11)34(1)	49(1)	52(1)	-12(1)	5(1)	-6(1)
C(12)34(1)	50(1)	62(1)	-16(1)	3(1)	-7(1)
C(13)33(1)	41(1)	63(1)	-8(1)	-2(1)	-3(1)
C(14)112(2)	39(1)	124(3)	5(2)	-8(2)	-11(2)
C(15)200(4)	64(2)	208(4)	61(2)	-70(4)	-41(3)
C(16)128(3)	69(2)	146(3)	51(2)	-24(3)	-14(2)
C(17)63(2)	86(2)	101(2)	22(2)	-8(2)	18(2)
C(18)54(1)	94(2)	100(2)	12(2)	-13(2)	1(2)
C(19)54(1)	61(1)	72(2)	4(1)	-5(1)	-8(1)
C(20)40(1)	43(1)	63(1)	9(1)	10(1)	5(1)

C(21)50(1)	55(1)	60(1)	0(1)	9(1)	-3(1)
C(22)57(1)	68(2)	69(1)	-9(1)	16(1)	-2(1)
C(23)53(1)	57(1)	88(2)	-18(1)	12(1)	4(1)
C(24)47(1)	42(1)	76(2)	-6(1)	-1(1)	-1(1)
C(25)65(1)	45(1)	98(2)	4(1)	1(1)	15(1)
C(26)77(2)	46(1)	95(2)	18(1)	-5(2)	10(1)
C(27)62(1)	49(1)	72(2)	14(1)	-2(1)	-6(1)
C(28)81(2)	75(2)	71(2)	28(1)	4(1)	3(2)
C(29)81(2)	91(2)	59(1)	16(1)	14(1)	-7(2)
C(30)62(1)	72(2)	62(1)	9(1)	15(1)	0(1)
C(31)41(1)	49(1)	56(1)	7(1)	3(1)	-6(1)
C(32)44(1)	39(1)	60(1)	6(1)	-1(1)	-5(1)
C(33)41(1)	37(1)	59(1)	1(1)	-1(1)	-1(1)
C(34)108(2)	155(3)	167(3)	-112(2)	59(2)	-50(2)
C(35)221(5)	227(4)	227(4)	-180(3)	109(4)	-87(4)
C(36)123(3)	136(3)	113(2)	-51(2)	39(2)	27(3)
C(37)93(2)	179(4)	181(3)	-51(3)	79(2)	23(3)
C(38)71(2)	128(3)	327(7)	-41(4)	80(3)	12(2)
C(39)43(1)	153(3)	96(2)	-6(2)	24(1)	6(2)
C(40)60(1)	51(1)	61(1)	1(1)	27(1)	9(1)

Table A21 Hydrogen coordinates (x 10^4) and isotropic displacement parameters ($Å^2$ x 10^3) for **13a**.

	x	y	z	U(eq)
H(1A)	5775	6149	3837	79
H(2A)	6653	4681	4342	100
H(3A)	7524	3781	3676	106
H(5A)	8066	3634	2444	103
H(6A)	8040	4325	1329	101
H(8A)	7488	5826	344	95
H(9A)	6553	7245	-44	91
H(10A)	5619	7884	662	72
H(14A)	4413	9823	2006	114
H(14B)	5243	9681	1704	114
H(15A)	4149	10874	1105	202
H(15B)	4746	10208	682	202
H(16A)	3765	9748	20	143
H(16B)	3176	10152	550	143
H(17A)	2562	8206	-207	103
H(17B)	2240	8744	463	103
H(18A)	2129	7038	966	103
H(18B)	1943	6676	148	103
H(19A)	2928	5447	774	77
H(19B)	3294	6131	174	77
H(21A)	4613	4904	637	66
H(22A)	5461	3508	250	76
H(23A)	6105	2158	1054	79
H(25A)	6318	1339	2357	85
H(26A)	6005	1419	3475	90
H(28A)	5254	2425	4404	92
H(29A)	4432	3923	4665	92
H(30A)	3872	5260	3794	78
H(34A)	5444	8135	4008	167
H(34B)	5443	9020	3375	167
H(35A)	4872	9437	4461	260

H(35B)	4618	10087	3730	260
H(36A)	3483	9817	3876	146
H(36B)	3748	8899	4486	146
H(37A)	2497	7608	3983	173
H(37B)	2286	8761	3544	173
H(38A)	1917	7913	2596	204
H(38B)	1699	6964	3132	204
H(39A)	2355	6486	2138	115
H(39B)	2525	5788	2862	115

Table A22 Torsion angles [°] for **13a**.

C(11)-Pd(1)-Pd(2)-C(31)	107.40(9)
N(3)-Pd(1)-Pd(2)-C(31)	-161.73(9)
N(1)-Pd(1)-Pd(2)-C(31)	24.64(9)
N(6)-Pd(1)-Pd(2)-C(31)	-69.92(9)
C(11)-Pd(1)-Pd(2)-N(8)	-161.67(8)
N(3)-Pd(1)-Pd(2)-N(8)	-70.79(8)
N(1)-Pd(1)-Pd(2)-N(8)	115.57(8)
N(6)-Pd(1)-Pd(2)-N(8)	21.01(8)
C(11)-Pd(1)-Pd(2)-N(2)	24.01(8)
N(3)-Pd(1)-Pd(2)-N(2)	114.88(8)
N(1)-Pd(1)-Pd(2)-N(2)	-58.75(7)
N(6)-Pd(1)-Pd(2)-N(2)	-153.31(8)
C(11)-Pd(1)-Pd(2)-N(5)	-69.78(8)
N(3)-Pd(1)-Pd(2)-N(5)	21.10(8)
N(1)-Pd(1)-Pd(2)-N(5)	-152.54(7)
N(6)-Pd(1)-Pd(2)-N(5)	112.90(8)
C(11)-Pd(1)-N(1)-C(1)	-176.9(2)
N(3)-Pd(1)-N(1)-C(1)	-142.5(6)
N(6)-Pd(1)-N(1)-C(1)	6.4(2)
Pd(2)-Pd(1)-N(1)-C(1)	-71.0(2)
C(11)-Pd(1)-N(1)-C(13)	-7.45(14)
N(3)-Pd(1)-N(1)-C(13)	27.0(7)
N(6)-Pd(1)-N(1)-C(13)	175.86(14)
Pd(2)-Pd(1)-N(1)-C(13)	98.44(13)
C(31)-Pd(2)-N(2)-C(21)	-178.32(19)
N(8)-Pd(2)-N(2)-C(21)	-169.6(6)
N(5)-Pd(2)-N(2)-C(21)	2.30(19)
Pd(1)-Pd(2)-N(2)-C(21)	-75.68(18)
C(31)-Pd(2)-N(2)-C(33)	-5.27(14)
N(8)-Pd(2)-N(2)-C(33)	3.5(8)
N(5)-Pd(2)-N(2)-C(33)	175.35(14)
Pd(1)-Pd(2)-N(2)-C(33)	97.38(13)
C(11)-Pd(1)-N(3)-C(20)	85.45(19)
N(1)-Pd(1)-N(3)-C(20)	51.3(7)

N(6)-Pd(1)-N(3)-C(20)	-97.66(19)
Pd(2)-Pd(1)-N(3)-C(20)	-20.53(18)
C(11)-Pd(1)-N(3)-C(14)	-98.5(2)
N(1)-Pd(1)-N(3)-C(14)	-132.6(6)
N(6)-Pd(1)-N(3)-C(14)	78.4(2)
Pd(2)-Pd(1)-N(3)-C(14)	155.6(2)
C(31)-Pd(2)-N(5)-C(20)	-138.5(15)
N(8)-Pd(2)-N(5)-C(20)	53.10(17)
N(2)-Pd(2)-N(5)-C(20)	-126.10(17)
Pd(1)-Pd(2)-N(5)-C(20)	-31.63(16)
C(31)-Pd(2)-N(5)-C(19)	64.3(15)
N(8)-Pd(2)-N(5)-C(19)	-104.16(17)
N(2)-Pd(2)-N(5)-C(19)	76.64(17)
Pd(1)-Pd(2)-N(5)-C(19)	171.12(17)
C(11)-Pd(1)-N(6)-C(40)	-172.7(11)
N(3)-Pd(1)-N(6)-C(40)	54.7(2)
N(1)-Pd(1)-N(6)-C(40)	-121.8(2)
Pd(2)-Pd(1)-N(6)-C(40)	-30.23(19)
C(11)-Pd(1)-N(6)-C(34)	27.6(12)
N(3)-Pd(1)-N(6)-C(34)	-104.9(2)
N(1)-Pd(1)-N(6)-C(34)	78.5(2)
Pd(2)-Pd(1)-N(6)-C(34)	170.1(2)
C(31)-Pd(2)-N(8)-C(40)	80.8(2)
N(2)-Pd(2)-N(8)-C(40)	72.2(8)
N(5)-Pd(2)-N(8)-C(40)	-99.74(19)
Pd(1)-Pd(2)-N(8)-C(40)	-22.25(18)
C(31)-Pd(2)-N(8)-C(39)	-93.1(2)
N(2)-Pd(2)-N(8)-C(39)	-101.7(7)
N(5)-Pd(2)-N(8)-C(39)	86.3(2)
Pd(1)-Pd(2)-N(8)-C(39)	163.8(2)
C(13)-N(1)-C(1)-C(2)	1.6(3)
Pd(1)-N(1)-C(1)-C(2)	170.35(19)
N(1)-C(1)-C(2)-C(3)	-1.3(4)
C(1)-C(2)-C(3)-C(4)	0.8(4)
C(2)-C(3)-C(4)-C(13)	-0.8(4)
C(2)-C(3)-C(4)-C(5)	-179.6(3)

C(3)-C(4)-C(5)-C(6)	-179.2(3)
C(13)-C(4)-C(5)-C(6)	2.0(4)
C(4)-C(5)-C(6)-C(7)	-0.8(4)
C(5)-C(6)-C(7)-C(8)	178.4(3)
C(5)-C(6)-C(7)-C(12)	-2.3(4)
C(12)-C(7)-C(8)-C(9)	-2.8(4)
C(6)-C(7)-C(8)-C(9)	176.6(3)
C(7)-C(8)-C(9)-C(10)	-0.5(4)
C(8)-C(9)-C(10)-C(11)	2.5(4)
C(9)-C(10)-C(11)-C(12)	-1.0(3)
C(9)-C(10)-C(11)-Pd(1)	-179.66(19)
N(3)-Pd(1)-C(11)-C(10)	7.8(2)
N(1)-Pd(1)-C(11)-C(10)	-176.0(2)
N(6)-Pd(1)-C(11)-C(10)	-124.7(11)
Pd(2)-Pd(1)-C(11)-C(10)	93.5(2)
N(3)-Pd(1)-C(11)-C(12)	-170.91(15)
N(1)-Pd(1)-C(11)-C(12)	5.31(14)
N(6)-Pd(1)-C(11)-C(12)	56.6(12)
Pd(2)-Pd(1)-C(11)-C(12)	-85.23(14)
C(10)-C(11)-C(12)-C(13)	178.53(19)
Pd(1)-C(11)-C(12)-C(13)	-2.5(2)
C(10)-C(11)-C(12)-C(7)	-2.5(3)
Pd(1)-C(11)-C(12)-C(7)	176.43(17)
C(8)-C(7)-C(12)-C(11)	4.4(3)
C(6)-C(7)-C(12)-C(11)	-175.0(2)
C(8)-C(7)-C(12)-C(13)	-176.7(2)
C(6)-C(7)-C(12)-C(13)	3.9(3)
C(1)-N(1)-C(13)-C(4)	-1.6(3)
Pd(1)-N(1)-C(13)-C(4)	-172.10(16)
C(1)-N(1)-C(13)-C(12)	178.7(2)
Pd(1)-N(1)-C(13)-C(12)	8.2(2)
C(3)-C(4)-C(13)-N(1)	1.1(3)
C(5)-C(4)-C(13)-N(1)	-180.0(2)
C(3)-C(4)-C(13)-C(12)	-179.2(2)
C(5)-C(4)-C(13)-C(12)	-0.3(3)
C(11)-C(12)-C(13)-N(1)	-4.0(3)

C(7)-C(12)-C(13)-N(1)	177.00(19)
C(11)-C(12)-C(13)-C(4)	176.3(2)
C(7)-C(12)-C(13)-C(4)	-2.7(3)
C(20)-N(3)-C(14)-C(15)	-25.2(5)
Pd(1)-N(3)-C(14)-C(15)	158.6(3)
N(3)-C(14)-C(15)-C(16)	27.0(7)
C(14)-C(15)-C(16)-N(4)	-13.2(8)
C(20)-N(4)-C(16)-C(15)	-3.4(6)
C(17)-N(4)-C(16)-C(15)	159.9(4)
C(20)-N(4)-C(17)-C(18)	-8.4(4)
C(16)-N(4)-C(17)-C(18)	-171.5(3)
N(4)-C(17)-C(18)-C(19)	-31.8(4)
C(20)-N(5)-C(19)-C(18)	-43.5(3)
Pd(2)-N(5)-C(19)-C(18)	115.3(2)
C(17)-C(18)-C(19)-N(5)	57.8(3)
C(14)-N(3)-C(20)-N(5)	-172.9(3)
Pd(1)-N(3)-C(20)-N(5)	3.1(3)
C(14)-N(3)-C(20)-N(4)	10.5(4)
Pd(1)-N(3)-C(20)-N(4)	-173.52(18)
C(19)-N(5)-C(20)-N(3)	-175.4(2)
Pd(2)-N(5)-C(20)-N(3)	27.5(3)
C(19)-N(5)-C(20)-N(4)	1.3(3)
Pd(2)-N(5)-C(20)-N(4)	-155.84(18)
C(17)-N(4)-C(20)-N(3)	-157.3(3)
C(16)-N(4)-C(20)-N(3)	4.5(4)
C(17)-N(4)-C(20)-N(5)	26.0(4)
C(16)-N(4)-C(20)-N(5)	-172.2(3)
C(33)-N(2)-C(21)-C(22)	0.4(3)
Pd(2)-N(2)-C(21)-C(22)	173.08(17)
N(2)-C(21)-C(22)-C(23)	-1.5(4)
C(21)-C(22)-C(23)-C(24)	1.5(4)
C(22)-C(23)-C(24)-C(33)	-0.5(3)
C(22)-C(23)-C(24)-C(25)	179.9(2)
C(23)-C(24)-C(25)-C(26)	-179.4(3)
C(33)-C(24)-C(25)-C(26)	1.0(4)
C(24)-C(25)-C(26)-C(27)	-0.9(4)

C(25)-C(26)-C(27)-C(28)	-176.7(3)
C(25)-C(26)-C(27)-C(32)	-0.9(4)
C(32)-C(27)-C(28)-C(29)	0.0(4)
C(26)-C(27)-C(28)-C(29)	175.9(3)
C(27)-C(28)-C(29)-C(30)	0.1(5)
C(28)-C(29)-C(30)-C(31)	-0.1(4)
C(29)-C(30)-C(31)-C(32)	-0.1(4)
C(29)-C(30)-C(31)-Pd(2)	-175.1(2)
N(8)-Pd(2)-C(31)-C(30)	0.2(2)
N(2)-Pd(2)-C(31)-C(30)	179.3(2)
N(5)-Pd(2)-C(31)-C(30)	-168.2(14)
Pd(1)-Pd(2)-C(31)-C(30)	85.6(2)
N(8)-Pd(2)-C(31)-C(32)	-175.01(15)
N(2)-Pd(2)-C(31)-C(32)	4.13(15)
N(5)-Pd(2)-C(31)-C(32)	16.6(16)
Pd(1)-Pd(2)-C(31)-C(32)	-89.65(15)
C(28)-C(27)-C(32)-C(33)	178.6(2)
C(26)-C(27)-C(32)-C(33)	2.4(3)
C(28)-C(27)-C(32)-C(31)	-0.2(4)
C(26)-C(27)-C(32)-C(31)	-176.4(2)
C(30)-C(31)-C(32)-C(33)	-178.6(2)
Pd(2)-C(31)-C(32)-C(33)	-2.6(2)
C(30)-C(31)-C(32)-C(27)	0.2(3)
Pd(2)-C(31)-C(32)-C(27)	176.27(18)
C(21)-N(2)-C(33)-C(24)	0.7(3)
Pd(2)-N(2)-C(33)-C(24)	-173.21(16)
C(21)-N(2)-C(33)-C(32)	179.20(19)
Pd(2)-N(2)-C(33)-C(32)	5.3(2)
C(23)-C(24)-C(33)-N(2)	-0.6(3)
C(25)-C(24)-C(33)-N(2)	179.0(2)
C(23)-C(24)-C(33)-C(32)	-179.1(2)
C(25)-C(24)-C(33)-C(32)	0.6(3)
C(27)-C(32)-C(33)-N(2)	179.15(19)
C(31)-C(32)-C(33)-N(2)	-2.0(3)
C(27)-C(32)-C(33)-C(24)	-2.3(3)
C(31)-C(32)-C(33)-C(24)	176.6(2)

C(40)-N(6)-C(34)-C(35)	-12.5(5)
Pd(1)-N(6)-C(34)-C(35)	148.2(4)
N(6)-C(34)-C(35)-C(36)	18.6(7)
C(34)-C(35)-C(36)-N(7)	-14.1(7)
C(40)-N(7)-C(36)-C(35)	3.7(6)
C(37)-N(7)-C(36)-C(35)	-176.8(4)
C(40)-N(7)-C(37)-C(38)	-17.0(6)
C(36)-N(7)-C(37)-C(38)	163.5(4)
N(7)-C(37)-C(38)-C(39)	29.4(8)
C(37)-C(38)-C(39)-N(8)	-27.3(7)
C(40)-N(8)-C(39)-C(38)	12.2(5)
Pd(2)-N(8)-C(39)-C(38)	-173.9(4)
C(39)-N(8)-C(40)-N(6)	-180.0(3)
Pd(2)-N(8)-C(40)-N(6)	6.5(3)
C(39)-N(8)-C(40)-N(7)	0.0(4)
Pd(2)-N(8)-C(40)-N(7)	-173.48(18)
C(34)-N(6)-C(40)-N(8)	-177.3(3)
Pd(1)-N(6)-C(40)-N(8)	24.3(3)
C(34)-N(6)-C(40)-N(7)	2.7(4)
Pd(1)-N(6)-C(40)-N(7)	-155.66(19)
C(36)-N(7)-C(40)-N(8)	-178.1(3)
C(37)-N(7)-C(40)-N(8)	2.4(4)
C(36)-N(7)-C(40)-N(6)	1.9(4)
C(37)-N(7)-C(40)-N(6)	-177.6(3)

Symmetry transformations used to generate equivalent atoms:

Figure A148 Molecular structure of **13c**

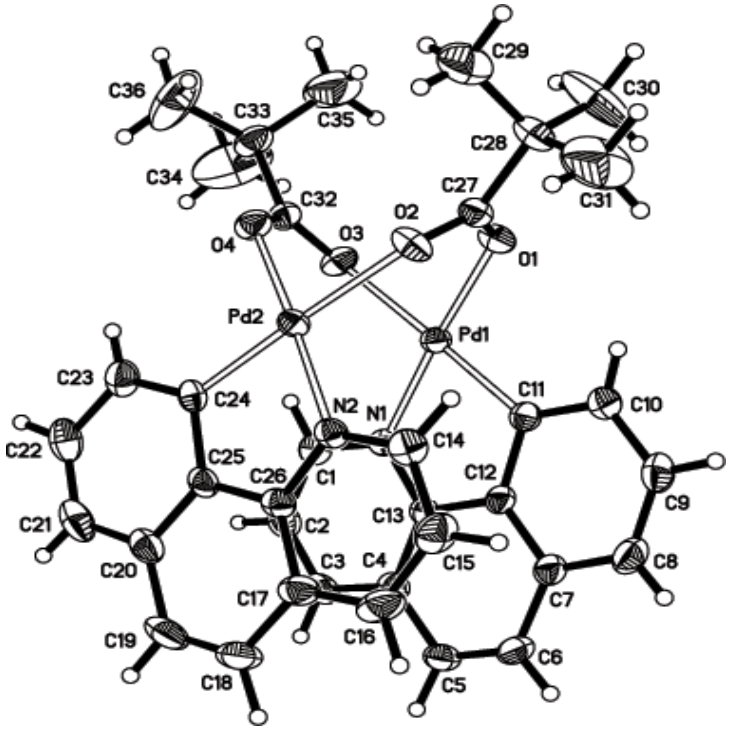

Table A23 Atomic coordinates (x 10^4) and equivalent isotropic displacement parameters ($Å^2$x 10^3) for **13c**. U(eq) is defined as one third of the trace of the orthogonalized U^{ij} tensor.

	x	y	z	U(eq)
Pd(1)	2427(1)	3677(1)	4263(1)	33(1)
Pd(2)	2625(1)	6166(1)	3318(1)	34(1)
O(1)	1825(1)	5218(2)	4719(1)	43(1)
O(2)	1737(1)	6887(2)	3800(1)	48(1)
O(3)	3322(1)	4871(2)	4809(1)	45(1)
O(4)	3240(1)	7087(2)	4165(1)	46(1)
N(1)	2958(1)	2077(2)	3762(1)	35(1)
N(2)	2074(1)	5124(2)	2464(1)	35(1)
C(1)	3636(1)	1933(3)	3789(1)	44(1)
C(2)	3928(1)	883(3)	3358(2)	51(1)
C(3)	3523(1)	-26(3)	2884(1)	49(1)
C(4)	2802(1)	130(3)	2830(1)	41(1)
C(5)	2303(2)	-723(3)	2340(1)	49(1)

C(6)	1626(2)	-493(3)	2331(1)	52(1)
C(7)	1349(1)	606(3)	2795(1)	44(1)
C(8)	649(2)	922(4)	2802(2)	55(1)
C(9)	446(1)	2003(4)	3269(2)	57(1)
C(10)	927(1)	2843(3)	3737(2)	49(1)
C(11)	1627(1)	2592(3)	3747(1)	36(1)
C(12)	1827(1)	1456(3)	3272(1)	36(1)
C(13)	2546(1)	1194(2)	3284(1)	33(1)
C(14)	1394(1)	5018(3)	2309(1)	46(1)
C(15)	1079(2)	4103(4)	1756(2)	57(1)
C(16)	1483(2)	3254(4)	1348(2)	59(1)
C(17)	2207(2)	3344(3)	1492(1)	48(1)
C(18)	2683(2)	2546(3)	1111(2)	61(1)
C(19)	3373(2)	2734(4)	1289(2)	64(1)
C(20)	3661(2)	3723(3)	1872(1)	49(1)
C(21)	4363(2)	3988(4)	2083(2)	62(1)
C(22)	4576(1)	4952(4)	2643(2)	60(1)
C(23)	4107(1)	5668(4)	3037(2)	52(1)
C(24)	3412(1)	5455(3)	2856(1)	37(1)
C(25)	3198(1)	4487(3)	2259(1)	37(1)
C(26)	2479(1)	4303(3)	2061(1)	37(1)
C(27)	1601(1)	6441(3)	4392(1)	38(1)
C(28)	1108(1)	7458(3)	4760(1)	50(1)
C(29)	1350(2)	9120(5)	4780(3)	113(1)
C(30)	1053(2)	6890(6)	5492(2)	128(2)
C(31)	419(2)	7420(7)	4299(3)	126(2)
C(32)	3449(1)	6290(3)	4714(1)	39(1)
C(33)	3870(2)	7194(3)	5320(1)	54(1)
C(34)	4478(3)	6209(6)	5628(3)	155(2)
C(35)	3458(3)	7263(6)	5921(2)	158(2)
C(36)	4118(3)	8706(5)	5114(3)	129(1)

Table A24 Bond lengths [Å] and angles [°] for **13c**.

Pd(1)-C(11)	1.963(2)
Pd(1)-N(1)	2.0268(19)
Pd(1)-O(1)	2.0325(16)
Pd(1)-O(3)	2.1632(16)
Pd(1)-Pd(2)	2.8377(2)
Pd(2)-C(24)	1.966(2)
Pd(2)-N(2)	2.0262(18)
Pd(2)-O(4)	2.0328(16)
Pd(2)-O(2)	2.1573(18)
O(1)-C(27)	1.260(3)
O(2)-C(27)	1.249(3)
O(3)-C(32)	1.252(3)
O(4)-C(32)	1.264(3)
N(1)-C(1)	1.323(3)
N(1)-C(13)	1.357(3)
N(2)-C(14)	1.326(3)
N(2)-C(26)	1.365(3)
C(1)-C(2)	1.387(4)
C(1)-H(1A)	0.95(3)
C(2)-C(3)	1.359(4)
C(2)-H(2A)	0.9300
C(3)-C(4)	1.404(4)
C(3)-H(3A)	0.9300
C(4)-C(13)	1.390(3)
C(4)-C(5)	1.449(4)
C(5)-C(6)	1.335(4)
C(5)-H(5A)	0.95(3)
C(6)-C(7)	1.439(4)
C(6)-H(6A)	0.87(3)
C(7)-C(8)	1.396(4)
C(7)-C(12)	1.411(3)
C(8)-C(9)	1.374(4)
C(8)-H(8A)	0.84(3)
C(9)-C(10)	1.400(4)

C(9)-H(9A)	0.91(3)
C(10)-C(11)	1.382(3)
C(10)-H(10A)	0.89(3)
C(11)-C(12)	1.414(3)
C(12)-C(13)	1.420(3)
C(14)-C(15)	1.384(4)
C(14)-H(14A)	0.93(3)
C(15)-C(16)	1.381(4)
C(15)-H(15A)	0.93(3)
C(16)-C(17)	1.406(4)
C(16)-H(16A)	0.9300
C(17)-C(26)	1.401(3)
C(17)-C(18)	1.425(4)
C(18)-C(19)	1.355(5)
C(18)-H(18A)	0.98(3)
C(19)-C(20)	1.445(4)
C(19)-H(19A)	0.9300
C(20)-C(21)	1.395(4)
C(20)-C(25)	1.402(4)
C(21)-C(22)	1.364(5)
C(21)-H(21A)	0.84(3)
C(22)-C(23)	1.399(4)
C(22)-H(22A)	0.91(3)
C(23)-C(24)	1.369(4)
C(23)-H(23A)	0.82(3)
C(24)-C(25)	1.418(3)
C(25)-C(26)	1.414(3)
C(27)-C(28)	1.532(3)
C(28)-C(30)	1.489(4)
C(28)-C(29)	1.491(5)
C(28)-C(31)	1.505(5)
C(29)-H(29A)	0.9600
C(29)-H(29B)	0.9600
C(29)-H(29C)	0.9600
C(30)-H(30A)	0.9600
C(30)-H(30B)	0.9600

C(30)-H(30C)	0.9600
C(31)-H(31A)	0.9600
C(31)-H(31B)	0.9600
C(31)-H(31C)	0.9600
C(32)-C(33)	1.530(3)
C(33)-C(36)	1.448(5)
C(33)-C(35)	1.484(6)
C(33)-C(34)	1.506(6)
C(34)-H(34A)	0.9600
C(34)-H(34B)	0.9600
C(34)-H(34C)	0.9600
C(35)-H(35A)	0.9600
C(35)-H(35B)	0.9600
C(35)-H(35C)	0.9600
C(36)-H(36A)	0.9600
C(36)-H(36B)	0.9600
C(36)-H(36C)	0.9600

C(11)-Pd(1)-N(1)	82.69(9)
C(11)-Pd(1)-O(1)	92.75(8)
N(1)-Pd(1)-O(1)	175.40(7)
C(11)-Pd(1)-O(3)	178.59(8)
N(1)-Pd(1)-O(3)	96.28(7)
O(1)-Pd(1)-O(3)	88.27(7)
C(11)-Pd(1)-Pd(2)	101.66(6)
N(1)-Pd(1)-Pd(2)	94.75(5)
O(1)-Pd(1)-Pd(2)	85.57(5)
O(3)-Pd(1)-Pd(2)	77.43(4)
C(24)-Pd(2)-N(2)	82.60(9)
C(24)-Pd(2)-O(4)	93.28(8)
N(2)-Pd(2)-O(4)	175.36(8)
C(24)-Pd(2)-O(2)	177.87(8)
N(2)-Pd(2)-O(2)	95.34(7)
O(4)-Pd(2)-O(2)	88.76(7)
C(24)-Pd(2)-Pd(1)	103.51(7)
N(2)-Pd(2)-Pd(1)	94.40(5)

O(4)-Pd(2)-Pd(1)	84.45(5)
O(2)-Pd(2)-Pd(1)	76.02(5)
C(27)-O(1)-Pd(1)	120.48(15)
C(27)-O(2)-Pd(2)	125.20(16)
C(32)-O(3)-Pd(1)	123.17(15)
C(32)-O(4)-Pd(2)	122.45(15)
C(1)-N(1)-C(13)	118.4(2)
C(1)-N(1)-Pd(1)	128.03(16)
C(13)-N(1)-Pd(1)	113.04(15)
C(14)-N(2)-C(26)	118.6(2)
C(14)-N(2)-Pd(2)	128.12(17)
C(26)-N(2)-Pd(2)	112.81(15)
N(1)-C(1)-C(2)	121.7(2)
N(1)-C(1)-H(1A)	114.8(17)
C(2)-C(1)-H(1A)	123.4(17)
C(3)-C(2)-C(1)	120.5(3)
C(3)-C(2)-H(2A)	119.7
C(1)-C(2)-H(2A)	119.7
C(2)-C(3)-C(4)	119.0(2)
C(2)-C(3)-H(3A)	120.5
C(4)-C(3)-H(3A)	120.5
C(13)-C(4)-C(3)	117.2(2)
C(13)-C(4)-C(5)	117.2(2)
C(3)-C(4)-C(5)	125.6(2)
C(6)-C(5)-C(4)	121.0(2)
C(6)-C(5)-H(5A)	121.5(16)
C(4)-C(5)-H(5A)	117.2(16)
C(5)-C(6)-C(7)	122.8(2)
C(5)-C(6)-H(6A)	122.1(19)
C(7)-C(6)-H(6A)	115.0(19)
C(8)-C(7)-C(12)	117.4(2)
C(8)-C(7)-C(6)	125.5(2)
C(12)-C(7)-C(6)	117.1(2)
C(9)-C(8)-C(7)	120.3(3)
C(9)-C(8)-H(8A)	119(2)
C(7)-C(8)-H(8A)	121(2)

C(8)-C(9)-C(10) 121.7(3)
C(8)-C(9)-H(9A) 121.2(19)
C(10)-C(9)-H(9A) 117.1(19)
C(11)-C(10)-C(9) 120.5(3)
C(11)-C(10)-H(10A) 117(2)
C(9)-C(10)-H(10A) 122(2)
C(10)-C(11)-C(12) 117.1(2)
C(10)-C(11)-Pd(1) 130.94(19)
C(12)-C(11)-Pd(1) 111.73(17)
C(7)-C(12)-C(11) 123.0(2)
C(7)-C(12)-C(13) 119.9(2)
C(11)-C(12)-C(13) 117.1(2)
N(1)-C(13)-C(4) 123.0(2)
N(1)-C(13)-C(12) 114.92(19)
C(4)-C(13)-C(12) 122.0(2)
N(2)-C(14)-C(15) 122.5(3)
N(2)-C(14)-H(14A) 118.7(17)
C(15)-C(14)-H(14A) 118.5(17)
C(16)-C(15)-C(14) 119.4(3)
C(16)-C(15)-H(15A) 120.6(19)
C(14)-C(15)-H(15A) 119.4(19)
C(15)-C(16)-C(17) 119.9(3)
C(15)-C(16)-H(16A) 120.1
C(17)-C(16)-H(16A) 120.1
C(26)-C(17)-C(16) 116.7(3)
C(26)-C(17)-C(18) 117.6(3)
C(16)-C(17)-C(18) 125.7(3)
C(19)-C(18)-C(17) 120.9(3)
C(19)-C(18)-H(18A) 121.8(16)
C(17)-C(18)-H(18A) 117.0(16)
C(18)-C(19)-C(20) 122.2(3)
C(18)-C(19)-H(19A) 118.9
C(20)-C(19)-H(19A) 118.9
C(21)-C(20)-C(25) 117.1(2)
C(21)-C(20)-C(19) 125.6(3)
C(25)-C(20)-C(19) 117.4(3)

C(22)-C(21)-C(20) 120.4(3)
C(22)-C(21)-H(21A) 119(2)
C(20)-C(21)-H(21A) 120(2)
C(21)-C(22)-C(23) 121.9(3)
C(21)-C(22)-H(22A) 123.8(18)
C(23)-C(22)-H(22A) 114.3(19)
C(24)-C(23)-C(22) 120.5(3)
C(24)-C(23)-H(23A) 118(2)
C(22)-C(23)-H(23A) 121(2)
C(23)-C(24)-C(25) 117.0(2)
C(23)-C(24)-Pd(2) 131.1(2)
C(25)-C(24)-Pd(2) 111.80(17)
C(20)-C(25)-C(26) 119.9(2)
C(20)-C(25)-C(24) 123.2(2)
C(26)-C(25)-C(24) 116.9(2)
N(2)-C(26)-C(17) 122.9(2)
N(2)-C(26)-C(25) 115.1(2)
C(17)-C(26)-C(25) 122.0(2)
O(2)-C(27)-O(1) 126.3(2)
O(2)-C(27)-C(28) 117.5(2)
O(1)-C(27)-C(28) 116.1(2)
C(30)-C(28)-C(29) 110.3(3)
C(30)-C(28)-C(31) 111.5(3)
C(29)-C(28)-C(31) 106.9(3)
C(30)-C(28)-C(27) 111.8(3)
C(29)-C(28)-C(27) 109.3(3)
C(31)-C(28)-C(27) 106.9(3)
C(28)-C(29)-H(29A) 109.5
C(28)-C(29)-H(29B) 109.5
H(29A)-C(29)-H(29B) 109.5
C(28)-C(29)-H(29C) 109.5
H(29A)-C(29)-H(29C) 109.5
H(29B)-C(29)-H(29C) 109.5
C(28)-C(30)-H(30A) 109.5
C(28)-C(30)-H(30B) 109.5
H(30A)-C(30)-H(30B) 109.5

C(28)-C(30)-H(30C)109.5
H(30A)-C(30)-H(30C)109.5
H(30B)-C(30)-H(30C)109.5
C(28)-C(31)-H(31A)109.5
C(28)-C(31)-H(31B)109.5
H(31A)-C(31)-H(31B)109.5
C(28)-C(31)-H(31C)109.5
H(31A)-C(31)-H(31C)109.5
H(31B)-C(31)-H(31C)109.5
O(3)-C(32)-O(4) 126.1(2)
O(3)-C(32)-C(33) 118.3(2)
O(4)-C(32)-C(33) 115.6(2)
C(36)-C(33)-C(35)114.1(4)
C(36)-C(33)-C(34)109.0(4)
C(35)-C(33)-C(34)101.9(4)
C(36)-C(33)-C(32)114.2(3)
C(35)-C(33)-C(32)107.7(3)
C(34)-C(33)-C(32)109.2(3)
C(33)-C(34)-H(34A)109.5
C(33)-C(34)-H(34B)109.5
H(34A)-C(34)-H(34B)109.5
C(33)-C(34)-H(34C)109.5
H(34A)-C(34)-H(34C)109.5
H(34B)-C(34)-H(34C)109.5
C(33)-C(35)-H(35A)109.5
C(33)-C(35)-H(35B)109.5
H(35A)-C(35)-H(35B)109.5
C(33)-C(35)-H(35C)109.5
H(35A)-C(35)-H(35C)109.5
H(35B)-C(35)-H(35C)109.5
C(33)-C(36)-H(36A)109.5
C(33)-C(36)-H(36B)109.5
H(36A)-C(36)-H(36B)109.5
C(33)-C(36)-H(36C)109.5
H(36A)-C(36)-H(36C)109.5
H(36B)-C(36)-H(36C)109.5

Symmetry transformations used to generate equivalent atoms:

Table A25 Anisotropic displacement parameters ($Å^2$ x 10^3)for **13c**. The anisotropic displacement factor exponent takes the form: $-2\pi^2[h^2a^{*2}U^{11} + ... + 2 h k a^* b^* U^{12}]$

U^{11}	U^{22}	U^{33}	U^{23}	U^{13}	U^{12}
Pd(1)37(1)	30(1)	32(1)	-2(1)	5(1)	-1(1)
Pd(2)39(1)	38(1)	25(1)	0(1)	6(1)	-1(1)
O(1)53(1)	41(1)	37(1)	0(1)	13(1)	9(1)
O(2)55(1)	55(1)	37(1)	4(1)	17(1)	14(1)
O(3)51(1)	39(1)	42(1)	-2(1)	-6(1)	-8(1)
O(4)61(1)	44(1)	32(1)	-2(1)	1(1)	-11(1)
N(1)38(1)	32(1)	36(1)	1(1)	4(1)	1(1)
N(2)37(1)	40(1)	27(1)	3(1)	3(1)	1(1)
C(1)39(1)	46(1)	46(1)	4(1)	2(1)	2(1)
C(2)42(1)	54(1)	60(2)	4(1)	15(1)	10(1)
C(3)57(1)	42(1)	53(1)	0(1)	22(1)	12(1)
C(4)52(1)	34(1)	38(1)	3(1)	13(1)	0(1)
C(5)67(2)	41(1)	43(1)	-10(1)	18(1)	-4(1)
C(6)64(2)	49(1)	44(1)	-11(1)	7(1)	-19(1)
C(7)49(1)	44(1)	39(1)	0(1)	9(1)	-11(1)
C(8)44(1)	63(2)	57(2)	-5(1)	0(1)	-18(1)
C(9)35(1)	70(2)	67(2)	-3(2)	11(1)	-9(1)
C(10)41(1)	48(1)	59(2)	-8(1)	14(1)	-2(1)
C(11)41(1)	32(1)	37(1)	3(1)	7(1)	-1(1)
C(12)39(1)	33(1)	37(1)	1(1)	7(1)	-6(1)
C(13)40(1)	27(1)	32(1)	4(1)	9(1)	-3(1)
C(14)44(1)	53(1)	42(1)	4(1)	2(1)	2(1)
C(15)44(1)	70(2)	53(2)	1(1)	-9(1)	-8(1)
C(16)77(2)	57(2)	40(1)	-5(1)	-10(1)	-14(2)
C(17)67(2)	44(1)	33(1)	-2(1)	5(1)	-4(1)
C(18)91(2)	52(2)	43(1)	-16(1)	17(1)	-5(2)
C(19)95(2)	53(2)	51(1)	-6(1)	38(1)	12(2)
C(20)59(1)	44(1)	48(1)	8(1)	23(1)	7(1)
C(21)57(2)	67(2)	68(2)	15(1)	34(1)	18(1)
C(22)36(1)	78(2)	67(2)	17(2)	13(1)	4(1)

C(23)43(1)	63(2)	50(2)	5(1)	5(1)	-7(1)
C(24)37(1)	40(1)	35(1)	9(1)	10(1)	-1(1)
C(25)46(1)	37(1)	31(1)	6(1)	13(1)	0(1)
C(26)48(1)	36(1)	27(1)	5(1)	6(1)	1(1)
C(27)37(1)	43(1)	34(1)	-3(1)	5(1)	2(1)
C(28)57(1)	54(1)	43(1)	4(1)	19(1)	19(1)
C(29)128(2)	76(2)	151(4)	-27(2)	72(3)	9(2)
C(30)174(3)	152(3)	74(2)	45(2)	80(2)	99(3)
C(31)82(2)	147(4)	145(4)	-33(3)	0(3)	59(2)
C(32)39(1)	42(1)	36(1)	-5(1)	1(1)	-6(1)
C(33)66(2)	52(1)	41(1)	-5(1)	-7(1)	-18(1)
C(34)174(4)	139(5)	120(5)	-27(3)	-99(3)	3(4)
C(35)248(6)	133(5)	104(3)	-68(2)	68(3)	-90(4)
C(36)139(3)	131(3)	102(3)	23(3)	-40(3)	-86(2)

Table A26 Hydrogen coordinates (x 10^4) and isotropic displacement parameters ($Å^2$x 10^3) for **13c**.

	x	y	z	U(eq)
H(1A)	3898(14)	2610(30)	4118(14)	55(8)
H(2A)	4406	801	3393	61
H(3A)	3719	-742	2601	59
H(5A)	2479(14)	-1370(30)	1995(15)	51(8)
H(6A)	1318(14)	-1060(30)	2066(14)	51(8)
H(8A)	345(15)	440(40)	2527(16)	71(10)
H(9A)	-10(15)	2180(40)	3298(15)	66(9)
H(10A)	802(17)	3620(40)	4012(17)	74(10)
H(14A)	1117(14)	5490(30)	2611(15)	56(8)
H(15A)	605(16)	3960(30)	1704(16)	64(9)
H(16A)	1277	2624	979	71
H(18A)	2490(14)	1790(30)	752(14)	53(8)
H(19A)	3670	2209	1026	76
H(21A)	4660(17)	3540(40)	1868(17)	75(11)
H(22A)	5025(15)	5210(30)	2784(14)	60(8)
H(23A)	4238(16)	6280(30)	3355(17)	64(10)
H(29A)	1789	9195	5074	170
H(29B)	1020	9774	4972	170
H(29C)	1397	9461	4307	170
H(30A)	1497	6953	5776	192
H(30B)	898	5819	5472	192
H(30C)	729	7530	5700	192
H(31A)	94	8048	4512	189
H(31B)	256	6357	4253	189
H(31C)	468	7831	3838	189
H(34A)	4742	6769	6010	232
H(34B)	4763	5991	5266	232
H(34C)	4316	5240	5803	232
H(35A)	3711	7825	6309	237
H(35B)	3366	6216	6070	237
H(35C)	3029	7792	5771	237

H(36A)	4374	9205	5519	194
H(36B)	3732	9354	4933	194
H(36C)	4411	8562	4752	194

Table A27 Torsion angles [°] for **13c**.

C(11)-Pd(1)-Pd(2)-C(24)	-102.36(10)
N(1)-Pd(1)-Pd(2)-C(24)	-18.86(9)
O(1)-Pd(1)-Pd(2)-C(24)	165.75(8)
O(3)-Pd(1)-Pd(2)-C(24)	76.53(8)
C(11)-Pd(1)-Pd(2)-N(2)	-18.92(9)
N(1)-Pd(1)-Pd(2)-N(2)	64.58(8)
O(1)-Pd(1)-Pd(2)-N(2)	-110.82(7)
O(3)-Pd(1)-Pd(2)-N(2)	159.97(7)
C(11)-Pd(1)-Pd(2)-O(4)	165.59(9)
N(1)-Pd(1)-Pd(2)-O(4)	-110.90(7)
O(1)-Pd(1)-Pd(2)-O(4)	73.70(7)
O(3)-Pd(1)-Pd(2)-O(4)	-15.51(7)
C(11)-Pd(1)-Pd(2)-O(2)	75.50(9)
N(1)-Pd(1)-Pd(2)-O(2)	159.00(7)
O(1)-Pd(1)-Pd(2)-O(2)	-16.40(7)
O(3)-Pd(1)-Pd(2)-O(2)	-105.61(7)
C(11)-Pd(1)-O(1)-C(27)	-84.50(18)
N(1)-Pd(1)-O(1)-C(27)	-77.2(9)
O(3)-Pd(1)-O(1)-C(27)	94.52(18)
Pd(2)-Pd(1)-O(1)-C(27)	17.00(17)
C(24)-Pd(2)-O(2)-C(27)	102(2)
N(2)-Pd(2)-O(2)-C(27)	117.8(2)
O(4)-Pd(2)-O(2)-C(27)	-60.0(2)
Pd(1)-Pd(2)-O(2)-C(27)	24.58(18)
C(11)-Pd(1)-O(3)-C(32)	75(3)
N(1)-Pd(1)-O(3)-C(32)	118.6(2)
O(1)-Pd(1)-O(3)-C(32)	-60.8(2)
Pd(2)-Pd(1)-O(3)-C(32)	25.07(18)
C(24)-Pd(2)-O(4)-C(32)	-89.1(2)
N(2)-Pd(2)-O(4)-C(32)	-61.8(10)
O(2)-Pd(2)-O(4)-C(32)	90.2(2)
Pd(1)-Pd(2)-O(4)-C(32)	14.13(19)
C(11)-Pd(1)-N(1)-C(1)	178.1(2)
O(1)-Pd(1)-N(1)-C(1)	170.8(8)

O(3)-Pd(1)-N(1)-C(1)	-0.9(2)
Pd(2)-Pd(1)-N(1)-C(1)	76.9(2)
C(11)-Pd(1)-N(1)-C(13)	6.36(15)
O(1)-Pd(1)-N(1)-C(13)	-1.0(10)
O(3)-Pd(1)-N(1)-C(13)	-172.66(14)
Pd(2)-Pd(1)-N(1)-C(13)	-94.82(14)
C(24)-Pd(2)-N(2)-C(14)	-179.8(2)
O(4)-Pd(2)-N(2)-C(14)	152.6(8)
O(2)-Pd(2)-N(2)-C(14)	0.8(2)
Pd(1)-Pd(2)-N(2)-C(14)	77.1(2)
C(24)-Pd(2)-N(2)-C(26)	8.02(16)
O(4)-Pd(2)-N(2)-C(26)	-19.6(10)
O(2)-Pd(2)-N(2)-C(26)	-171.40(15)
Pd(1)-Pd(2)-N(2)-C(26)	-95.06(15)
C(13)-N(1)-C(1)-C(2)	-1.7(4)
Pd(1)-N(1)-C(1)-C(2)	-173.03(19)
N(1)-C(1)-C(2)-C(3)	0.7(4)
C(1)-C(2)-C(3)-C(4)	1.0(4)
C(2)-C(3)-C(4)-C(13)	-1.6(4)
C(2)-C(3)-C(4)-C(5)	178.3(3)
C(13)-C(4)-C(5)-C(6)	-0.3(4)
C(3)-C(4)-C(5)-C(6)	179.8(3)
C(4)-C(5)-C(6)-C(7)	0.6(4)
C(5)-C(6)-C(7)-C(8)	178.6(3)
C(5)-C(6)-C(7)-C(12)	0.0(4)
C(12)-C(7)-C(8)-C(9)	-1.2(4)
C(6)-C(7)-C(8)-C(9)	-179.8(3)
C(7)-C(8)-C(9)-C(10)	1.5(5)
C(8)-C(9)-C(10)-C(11)	-0.7(5)
C(9)-C(10)-C(11)-C(12)	-0.4(4)
C(9)-C(10)-C(11)-Pd(1)	173.8(2)
N(1)-Pd(1)-C(11)-C(10)	179.6(2)
O(1)-Pd(1)-C(11)-C(10)	-1.0(2)
O(3)-Pd(1)-C(11)-C(10)	-137(3)
Pd(2)-Pd(1)-C(11)-C(10)	-87.1(2)
N(1)-Pd(1)-C(11)-C(12)	-5.94(16)

O(1)-Pd(1)-C(11)-C(12)	173.47(16)
O(3)-Pd(1)-C(11)-C(12)	38(3)
Pd(2)-Pd(1)-C(11)-C(12)	87.43(16)
C(8)-C(7)-C(12)-C(11)	0.1(4)
C(6)-C(7)-C(12)-C(11)	178.8(2)
C(8)-C(7)-C(12)-C(13)	-179.5(2)
C(6)-C(7)-C(12)-C(13)	-0.7(3)
C(10)-C(11)-C(12)-C(7)	0.7(3)
Pd(1)-C(11)-C(12)-C(7)	-174.60(18)
C(10)-C(11)-C(12)-C(13)	-179.7(2)
Pd(1)-C(11)-C(12)-C(13)	4.9(3)
C(1)-N(1)-C(13)-C(4)	1.0(3)
Pd(1)-N(1)-C(13)-C(4)	173.62(17)
C(1)-N(1)-C(13)-C(12)	-177.9(2)
Pd(1)-N(1)-C(13)-C(12)	-5.3(2)
C(3)-C(4)-C(13)-N(1)	0.6(3)
C(5)-C(4)-C(13)-N(1)	-179.3(2)
C(3)-C(4)-C(13)-C(12)	179.5(2)
C(5)-C(4)-C(13)-C(12)	-0.4(3)
C(7)-C(12)-C(13)-N(1)	179.9(2)
C(11)-C(12)-C(13)-N(1)	0.3(3)
C(7)-C(12)-C(13)-C(4)	0.9(3)
C(11)-C(12)-C(13)-C(4)	-178.6(2)
C(26)-N(2)-C(14)-C(15)	0.2(4)
Pd(2)-N(2)-C(14)-C(15)	-171.5(2)
N(2)-C(14)-C(15)-C(16)	0.4(4)
C(14)-C(15)-C(16)-C(17)	-0.9(4)
C(15)-C(16)-C(17)-C(26)	0.7(4)
C(15)-C(16)-C(17)-C(18)	-179.4(3)
C(26)-C(17)-C(18)-C(19)	-1.1(4)
C(16)-C(17)-C(18)-C(19)	179.0(3)
C(17)-C(18)-C(19)-C(20)	0.9(5)
C(18)-C(19)-C(20)-C(21)	-179.4(3)
C(18)-C(19)-C(20)-C(25)	0.5(4)
C(25)-C(20)-C(21)-C(22)	0.0(4)
C(19)-C(20)-C(21)-C(22)	179.9(3)

C(20)-C(21)-C(22)-C(23)	1.9(5)
C(21)-C(22)-C(23)-C(24)	-2.0(5)
C(22)-C(23)-C(24)-C(25)	0.1(4)
C(22)-C(23)-C(24)-Pd(2)	175.8(2)
N(2)-Pd(2)-C(24)-C(23)	177.1(3)
O(4)-Pd(2)-C(24)-C(23)	-5.0(3)
O(2)-Pd(2)-C(24)-C(23)	-167(2)
Pd(1)-Pd(2)-C(24)-C(23)	-90.1(2)
N(2)-Pd(2)-C(24)-C(25)	-6.95(16)
O(4)-Pd(2)-C(24)-C(25)	170.90(16)
O(2)-Pd(2)-C(24)-C(25)	9(2)
Pd(1)-Pd(2)-C(24)-C(25)	85.83(16)
C(21)-C(20)-C(25)-C(26)	178.3(2)
C(19)-C(20)-C(25)-C(26)	-1.6(3)
C(21)-C(20)-C(25)-C(24)	-2.0(4)
C(19)-C(20)-C(25)-C(24)	178.2(2)
C(23)-C(24)-C(25)-C(20)	1.9(4)
Pd(2)-C(24)-C(25)-C(20)	-174.62(18)
C(23)-C(24)-C(25)-C(26)	-178.3(2)
Pd(2)-C(24)-C(25)-C(26)	5.1(3)
C(14)-N(2)-C(26)-C(17)	-0.4(3)
Pd(2)-N(2)-C(26)-C(17)	172.57(18)
C(14)-N(2)-C(26)-C(25)	179.7(2)
Pd(2)-N(2)-C(26)-C(25)	-7.3(2)
C(16)-C(17)-C(26)-N(2)	0.0(4)
C(18)-C(17)-C(26)-N(2)	-180.0(2)
C(16)-C(17)-C(26)-C(25)	179.9(2)
C(18)-C(17)-C(26)-C(25)	-0.1(4)
C(20)-C(25)-C(26)-N(2)	-178.7(2)
C(24)-C(25)-C(26)-N(2)	1.6(3)
C(20)-C(25)-C(26)-C(17)	1.4(3)
C(24)-C(25)-C(26)-C(17)	-178.3(2)
Pd(2)-O(2)-C(27)-O(1)	-21.2(3)
Pd(2)-O(2)-C(27)-C(28)	159.58(17)
Pd(1)-O(1)-C(27)-O(2)	-3.7(3)
Pd(1)-O(1)-C(27)-C(28)	175.57(16)

O(2)-C(27)-C(28)-C(30)	-173.7(3)
O(1)-C(27)-C(28)-C(30)	7.0(4)
O(2)-C(27)-C(28)-C(29)	-51.2(3)
O(1)-C(27)-C(28)-C(29)	129.4(3)
O(2)-C(27)-C(28)-C(31)	64.1(4)
O(1)-C(27)-C(28)-C(31)	-115.2(3)
Pd(1)-O(3)-C(32)-O(4)	-24.4(4)
Pd(1)-O(3)-C(32)-C(33)	152.97(19)
Pd(2)-O(4)-C(32)-O(3)	1.2(4)
Pd(2)-O(4)-C(32)-C(33)	-176.32(17)
O(3)-C(32)-C(33)-C(36)	167.2(3)
O(4)-C(32)-C(33)-C(36)	-15.1(4)
O(3)-C(32)-C(33)-C(35)	-64.9(4)
O(4)-C(32)-C(33)-C(35)	112.8(3)
O(3)-C(32)-C(33)-C(34)	45.0(4)
O(4)-C(32)-C(33)-C(34)	-137.4(3)

Symmetry transformations used to generate equivalent atoms:

Figure A149 Molecular structure of [(acetanilide)Pd(TFA)]$_a$ (**13g**)

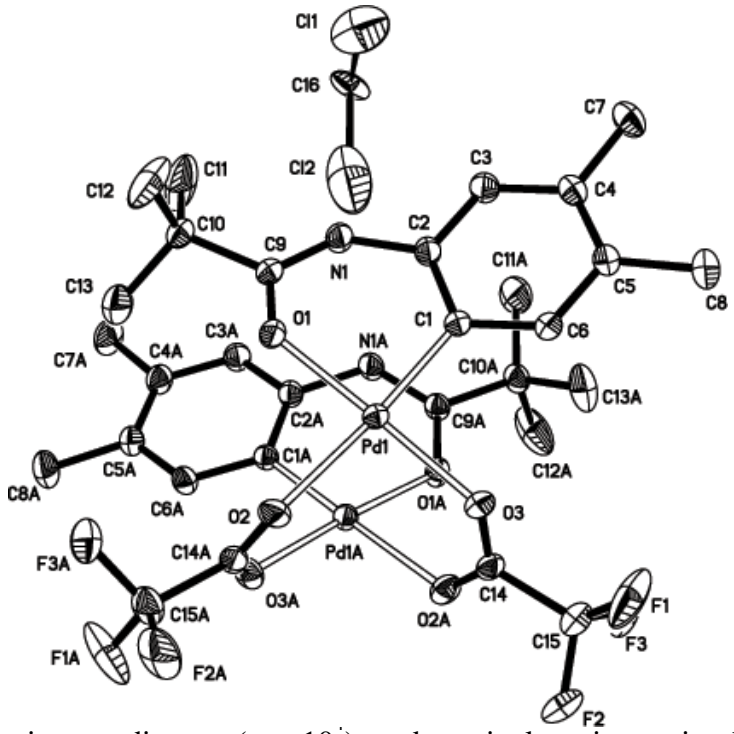

Table A28 Atomic coordinates (x $10^{\cdot}$) and equivalent isotropic displacement parameters ($Å^2$ x 10^3) for **13g**. U(eq) is defined as one third of the trace of the orthogonalized U^{ij} tensor.

	x	y	z	U(eq)
Pd(1)	996(1)	6123(1)	2483(1)	41(1)
O(1)	876(2)	5153(2)	1751(1)	52(1)
O(2)	357(2)	7380(2)	1819(1)	55(1)
O(3)	1147(2)	7192(2)	3207(1)	56(1)
N(1)	1048(2)	3501(2)	2236(1)	57(1)
C(1)	1637(2)	4945(2)	3025(1)	41(1)
C(2)	1571(2)	3848(2)	2834(1)	49(1)
C(3)	2050(3)	3022(3)	3220(2)	60(1)
C(4)	2613(2)	3250(3)	3801(2)	57(1)
C(5)	2693(2)	4334(3)	3999(1)	53(1)
C(6)	2210(2)	5164(3)	3610(1)	48(1)
C(7)	3103(3)	2302(4)	4195(2)	84(1)
C(8)	3287(3)	4653(4)	4627(2)	80(1)

C(9)	807(2)	4121(2)	1736(1)	47(1)
C(10)	483(2)	3575(3)	1106(1)	55(1)
C(11)	164(6)	2411(5)	1129(2)	138(3)
C(12)	1273(4)	3696(5)	818(2)	127(2)
C(13)	-337(4)	4210(5)	719(2)	102(2)
C(14)	483(2)	7537(2)	3386(1)	48(1)
C(15)	770(2)	8244(3)	3962(2)	71(1)
F(1)	1636(3)	8439(5)	4185(2)	145(2)
F(2)	296(4)	9187(4)	3904(2)	112(2)
F(3)	472(4)	7737(4)	4418(2)	119(2)
F(1')	1334(4)	9120(4)	3872(3)	87(2)
F(2')	116(4)	8722(6)	4129(3)	127(2)
F(3')	1359(5)	7703(6)	4420(3)	107(2)
C(16)	0	-423(3)	2500	85(2)
Cl(1)	1205(3)	-101(4)	2421(2)	171(1)
Cl(2)	-277(3)	1049(6)	2511(2)	304(5)

Table A29 Bond lengths [Å] and angles [°] for **13g**.

Pd(1)-C(1)	1.951(3)
Pd(1)-O(1)	2.001(2)
Pd(1)-O(3)	2.054(2)
Pd(1)-O(2)	2.165(2)
Pd(1)-Pd(1)#1	3.0153(4)
O(1)-C(9)	1.248(4)
O(2)-C(14)#1	1.231(4)
O(3)-C(14)	1.249(4)
N(1)-C(9)	1.324(4)
N(1)-C(2)	1.430(4)
N(1)-H(1A)	0.8600
C(1)-C(2)	1.387(4)
C(1)-C(6)	1.393(4)
C(2)-C(3)	1.389(4)
C(3)-C(4)	1.384(4)
C(3)-H(3A)	0.9300
C(4)-C(5)	1.378(5)
C(4)-C(7)	1.512(5)
C(5)-C(6)	1.398(4)
C(5)-C(8)	1.509(5)
C(6)-H(6A)	0.9300
C(7)-H(7A)	0.9600
C(7)-H(7B)	0.9600
C(7)-H(7C)	0.9600
C(8)-H(8A)	0.9600
C(8)-H(8B)	0.9600
C(8)-H(8C)	0.9600
C(9)-C(10)	1.528(4)
C(10)-C(11)	1.488(7)
C(10)-C(13)	1.509(6)
C(10)-C(12)	1.514(7)
C(11)-H(11A)	0.9600
C(11)-H(11B)	0.9600
C(11)-H(11C)	0.9600

C(12)-H(12A)	0.9600
C(12)-H(12B)	0.9600
C(12)-H(12C)	0.9600
C(13)-H(13A)	0.9600
C(13)-H(13B)	0.9600
C(13)-H(13C)	0.9600
C(14)-O(2)#1	1.231(4)
C(14)-C(15)	1.522(4)
C(15)-F(1)	1.279(5)
C(15)-F(2')	1.285(7)
C(15)-F(2)	1.329(5)
C(15)-F(3')	1.335(6)
C(15)-F(3)	1.382(6)
C(15)-F(1')	1.404(6)
C(16)-Cl(2)#1	1.825(7)
C(16)-Cl(2)	1.825(7)
C(16)-Cl(1)	1.910(5)
C(16)-Cl(1)#1	1.910(5)
C(16)-H(16)	0.9398
Cl(1)-Cl(2)#1	2.003(8)
Cl(2)-Cl(2)#1	0.849(9)
Cl(2)-Cl(1)#1	2.003(8)

C(1)-Pd(1)-O(1)	90.82(10)
C(1)-Pd(1)-O(3)	91.46(10)
O(1)-Pd(1)-O(3)	176.58(9)
C(1)-Pd(1)-O(2)	174.44(11)
O(1)-Pd(1)-O(2)	84.83(8)
O(3)-Pd(1)-O(2)	92.74(8)
C(1)-Pd(1)-Pd(1)#1	107.65(8)
O(1)-Pd(1)-Pd(1)#1	99.31(7)
O(3)-Pd(1)-Pd(1)#1	82.42(7)
O(2)-Pd(1)-Pd(1)#1	76.54(6)
C(9)-O(1)-Pd(1)	126.29(19)
C(14)#1-O(2)-Pd(1)	125.5(2)
C(14)-O(3)-Pd(1)	123.35(19)

C(9)-N(1)-C(2)	126.6(3)
C(9)-N(1)-H(1A)	116.7
C(2)-N(1)-H(1A)	116.7
C(2)-C(1)-C(6)	116.9(3)
C(2)-C(1)-Pd(1)	121.06(19)
C(6)-C(1)-Pd(1)	122.0(2)
C(1)-C(2)-C(3)	120.4(3)
C(1)-C(2)-N(1)	123.4(3)
C(3)-C(2)-N(1)	116.2(3)
C(4)-C(3)-C(2)	122.2(3)
C(4)-C(3)-H(3A)	118.9
C(2)-C(3)-H(3A)	118.9
C(5)-C(4)-C(3)	118.3(3)
C(5)-C(4)-C(7)	122.7(3)
C(3)-C(4)-C(7)	119.0(3)
C(4)-C(5)-C(6)	119.3(3)
C(4)-C(5)-C(8)	121.8(3)
C(6)-C(5)-C(8)	118.9(3)
C(1)-C(6)-C(5)	122.8(3)
C(1)-C(6)-H(6A)	118.6
C(5)-C(6)-H(6A)	118.6
C(4)-C(7)-H(7A)	109.5
C(4)-C(7)-H(7B)	109.5
H(7A)-C(7)-H(7B)	109.5
C(4)-C(7)-H(7C)	109.5
H(7A)-C(7)-H(7C)	109.5
H(7B)-C(7)-H(7C)	109.5
C(5)-C(8)-H(8A)	109.5
C(5)-C(8)-H(8B)	109.5
H(8A)-C(8)-H(8B)	109.5
C(5)-C(8)-H(8C)	109.5
H(8A)-C(8)-H(8C)	109.5
H(8B)-C(8)-H(8C)	109.5
O(1)-C(9)-N(1)	122.7(3)
O(1)-C(9)-C(10)	117.2(3)
N(1)-C(9)-C(10)	120.1(3)

C(11)-C(10)-C(13) 106.3(4)
C(11)-C(10)-C(12) 113.9(5)
C(13)-C(10)-C(12) 108.1(4)
C(11)-C(10)-C(9) 113.3(3)
C(13)-C(10)-C(9) 108.9(3)
C(12)-C(10)-C(9) 106.3(3)
C(10)-C(11)-H(11A) 109.5
C(10)-C(11)-H(11B) 109.5
H(11A)-C(11)-H(11B) 109.5
C(10)-C(11)-H(11C) 109.5
H(11A)-C(11)-H(11C) 109.5
H(11B)-C(11)-H(11C) 109.5
C(10)-C(12)-H(12A) 109.5
C(10)-C(12)-H(12B) 109.5
H(12A)-C(12)-H(12B) 109.5
C(10)-C(12)-H(12C) 109.5
H(12A)-C(12)-H(12C) 109.5
H(12B)-C(12)-H(12C) 109.5
C(10)-C(13)-H(13A) 109.5
C(10)-C(13)-H(13B) 109.5
H(13A)-C(13)-H(13B) 109.5
C(10)-C(13)-H(13C) 109.5
H(13A)-C(13)-H(13C) 109.5
H(13B)-C(13)-H(13C) 109.5
O(2)#1-C(14)-O(3) 130.8(3)
O(2)#1-C(14)-C(15) 115.3(3)
O(3)-C(14)-C(15) 113.9(3)
F(1)-C(15)-F(2') 125.3(4)
F(1)-C(15)-F(2) 109.9(4)
F(2')-C(15)-F(3') 112.5(5)
F(1)-C(15)-F(3) 106.8(4)
F(2)-C(15)-F(3) 100.1(4)
F(2')-C(15)-F(1') 104.4(5)
F(3')-C(15)-F(1') 100.8(5)
F(1)-C(15)-C(14) 117.3(4)
F(2')-C(15)-C(14) 116.6(4)

F(2)-C(15)-C(14) 112.2(3)
F(3')-C(15)-C(14) 111.5(4)
F(3)-C(15)-C(14) 108.9(3)
F(1')-C(15)-C(14) 109.5(4)
Cl(2)#1-C(16)-Cl(2)26.9(3)
Cl(2)#1-C(16)-Cl(1)64.8(2)
Cl(2)-C(16)-Cl(1) 91.7(3)
Cl(2)#1-C(16)-Cl(1)#191.7(3)
Cl(2)-C(16)-Cl(1)#164.8(2)
Cl(1)-C(16)-Cl(1)#1156.5(4)
Cl(2)#1-C(16)-H(16)118.2
Cl(2)-C(16)-H(16) 109.4
Cl(1)-C(16)-H(16) 114.2
Cl(1)#1-C(16)-H(16)76.0
C(16)-Cl(1)-Cl(2)#155.6(2)
Cl(2)#1-Cl(2)-C(16)76.56(15)
Cl(2)#1-Cl(2)-Cl(1)#1136.1(2)
C(16)-Cl(2)-Cl(1)#159.6(2)

Symmetry transformations used to generate equivalent atoms:
#1 -x,y,-z+1/2

Table A30 Anisotropic displacement parameters ($Å^2 x\ 10^3$) for **13g**. The anisotropic displacement factor exponent takes the form: $-2\pi^2[h^2 a^{*2} U^{11} + ... + 2 h k a^* b^* U^{12}]$

U^{11}	U^{22}	U^{33}	U^{23}	U^{13}	U^{12}
Pd(1)53(1)	33(1)	37(1)	-2(1)	10(1)	5(1)
O(1)74(1)	44(1)	36(1)	-1(1)	13(1)	7(1)
O(2)69(1)	42(1)	55(1)	10(1)	19(1)	11(1)
O(3)66(1)	44(1)	53(1)	-14(1)	7(1)	6(1)
N(1)81(2)	33(1)	46(1)	-6(1)	2(1)	-1(1)
C(1)44(1)	37(1)	40(1)	-2(1)	10(1)	2(1)
C(2)59(2)	42(2)	41(1)	0(1)	6(1)	1(1)
C(3)79(2)	40(2)	53(2)	2(1)	6(2)	4(2)
C(4)59(2)	58(2)	50(2)	7(1)	6(1)	9(2)
C(5)53(1)	60(2)	43(1)	1(1)	7(1)	4(1)
C(6)51(1)	46(2)	43(1)	-6(1)	8(1)	3(1)
C(7)98(3)	75(2)	65(2)	22(2)	1(2)	24(2)
C(8)81(2)	95(3)	51(2)	-5(2)	-6(2)	3(2)
C(9)55(1)	40(1)	42(1)	-6(1)	10(1)	3(1)
C(10)68(2)	51(2)	44(1)	-12(1)	11(1)	0(2)
C(11)245(7)	89(3)	61(2)	-27(2)	11(3)	-60(4)
C(12)95(3)	204(5)	91(2)	-85(3)	40(2)	-26(3)
C(13)102(3)	128(4)	57(2)	-24(2)	-8(2)	22(3)
C(14)71(2)	31(1)	42(1)	-3(1)	14(1)	0(1)
C(15)85(2)	67(2)	57(2)	-20(2)	16(2)	2(2)
F(1) 68(2)	241(5)	124(3)	-126(3)	23(2)	-37(3)
F(2)150(4)	83(2)	95(3)	-49(2)	23(3)	25(3)
F(3)185(5)	123(4)	47(2)	-14(2)	30(2)	-38(4)
F(1')89(4)	72(3)	86(4)	-42(3)	2(3)	-24(3)
F(2')96(3)	174(6)	133(4)	-114(3)	71(3)	-52(4)
F(3')128(6)	126(6)	50(3)	-20(3)	-2(3)	-14(5)
C(16)64(3)	25(2)	135(5)	0	-23(3)	0
Cl(1)209(3)	135(3)	208(3)	-3(3)	120(2)	-16(3)
Cl(2)133(3)	665(15)	128(3)	39(5)	62(3)	124(4)

Table A31 Hydrogen coordinates (x 10^4) and isotropic displacement parameters (Å^{2}x 10^3) for **13g**.

	x	y	z	U(eq)
H(1A)	873	2819	2198	68
H(3A)	1991	2292	3083	72
H(6A)	2274	5895	3747	57
H(7A)	2962	1619	3971	125
H(7B)	2900	2258	4559	125
H(7C)	3760	2426	4306	125
H(8A)	3571	4001	4841	120
H(8B)	2908	4999	4852	120
H(8C)	3758	5161	4589	120
H(11A)	664	1970	1372	207
H(11B)	-35	2116	721	207
H(11C)	-344	2397	1308	207
H(12A)	1801	3291	1056	191
H(12B)	1431	4465	808	191
H(12C)	1087	3407	409	191
H(13A)	-163	4969	687	152
H(13B)	-835	4180	906	152
H(13C)	-533	3886	318	152
H(16)	0	-746	2876	102

Table A32 Torsion angles [°] for **13g**.

C(1)-Pd(1)-O(1)-C(9)	30.5(3)
O(3)-Pd(1)-O(1)-C(9)	162.2(14)
O(2)-Pd(1)-O(1)-C(9)	-153.0(3)
Pd(1)#1-Pd(1)-O(1)-C(9)	-77.6(3)
C(1)-Pd(1)-O(2)-C(14)#1	127.3(10)
O(1)-Pd(1)-O(2)-C(14)#1	88.8(2)
O(3)-Pd(1)-O(2)-C(14)#1	-93.7(2)
Pd(1)#1-Pd(1)-O(2)-C(14)#1	-12.1(2)
C(1)-Pd(1)-O(3)-C(14)	-112.7(2)
O(1)-Pd(1)-O(3)-C(14)	115.6(15)
O(2)-Pd(1)-O(3)-C(14)	71.0(2)
Pd(1)#1-Pd(1)-O(3)-C(14)	-5.0(2)
O(1)-Pd(1)-C(1)-C(2)	-19.5(3)
O(3)-Pd(1)-C(1)-C(2)	163.1(3)
O(2)-Pd(1)-C(1)-C(2)	-57.8(11)
Pd(1)#1-Pd(1)-C(1)-C(2)	80.6(3)
O(1)-Pd(1)-C(1)-C(6)	157.9(3)
O(3)-Pd(1)-C(1)-C(6)	-19.5(3)
O(2)-Pd(1)-C(1)-C(6)	119.6(9)
Pd(1)#1-Pd(1)-C(1)-C(6)	-102.0(2)
C(6)-C(1)-C(2)-C(3)	0.8(5)
Pd(1)-C(1)-C(2)-C(3)	178.4(3)
C(6)-C(1)-C(2)-N(1)	-176.8(3)
Pd(1)-C(1)-C(2)-N(1)	0.7(5)
C(9)-N(1)-C(2)-C(1)	22.5(6)
C(9)-N(1)-C(2)-C(3)	-155.3(4)
C(1)-C(2)-C(3)-C(4)	-0.5(6)
N(1)-C(2)-C(3)-C(4)	177.3(4)
C(2)-C(3)-C(4)-C(5)	0.2(6)
C(2)-C(3)-C(4)-C(7)	179.3(4)
C(3)-C(4)-C(5)-C(6)	-0.3(5)
C(7)-C(4)-C(5)-C(6)	-179.3(4)
C(3)-C(4)-C(5)-C(8)	179.6(4)
C(7)-C(4)-C(5)-C(8)	0.5(6)

C(2)-C(1)-C(6)-C(5)	-0.9(5)
Pd(1)-C(1)-C(6)-C(5)	-178.4(3)
C(4)-C(5)-C(6)-C(1)	0.7(5)
C(8)-C(5)-C(6)-C(1)	-179.2(3)
Pd(1)-O(1)-C(9)-N(1)	-18.6(5)
Pd(1)-O(1)-C(9)-C(10)	165.1(2)
C(2)-N(1)-C(9)-O(1)	-12.7(6)
C(2)-N(1)-C(9)-C(10)	163.5(3)
O(1)-C(9)-C(10)-C(11)	-163.5(4)
N(1)-C(9)-C(10)-C(11)	20.1(6)
O(1)-C(9)-C(10)-C(13)	-45.5(5)
N(1)-C(9)-C(10)-C(13)	138.1(4)
O(1)-C(9)-C(10)-C(12)	70.7(4)
N(1)-C(9)-C(10)-C(12)	-105.7(4)
Pd(1)-O(3)-C(14)-O(2)#1	-3.1(5)
Pd(1)-O(3)-C(14)-C(15)	175.2(2)
O(2)#1-C(14)-C(15)-F(1)	-179.2(4)
O(3)-C(14)-C(15)-F(1)	2.2(5)
O(2)#1-C(14)-C(15)-F(2')	-8.8(6)
O(3)-C(14)-C(15)-F(2')	172.6(5)
O(2)#1-C(14)-C(15)-F(2)	-50.4(5)
O(3)-C(14)-C(15)-F(2)	131.0(4)
O(2)#1-C(14)-C(15)-F(3')	122.3(5)
O(3)-C(14)-C(15)-F(3')	-56.3(5)
O(2)#1-C(14)-C(15)-F(3)	59.5(4)
O(3)-C(14)-C(15)-F(3)	-119.1(4)
O(2)#1-C(14)-C(15)-F(1')	-127.1(4)
O(3)-C(14)-C(15)-F(1')	54.3(4)
Cl(2)-C(16)-Cl(1)-Cl(2)#1	1.1(4)
Cl(1)#1-C(16)-Cl(1)-Cl(2)#1	0.56(19)
Cl(1)-C(16)-Cl(2)-Cl(2)#1	-2.1(7)
Cl(1)#1-C(16)-Cl(2)-Cl(2)#1	177.6(8)
Cl(2)#1-C(16)-Cl(2)-Cl(1)#1	-177.6(8)
Cl(1)-C(16)-Cl(2)-Cl(1)#1	-179.78(8)

Symmetry transformations used to generate equivalent atoms: #1 -x,y,-z+1/2

Figure A150 Molecular structure of [(8-methyl-quinoline)Pd(OAc)]$_a$ (**13h**)

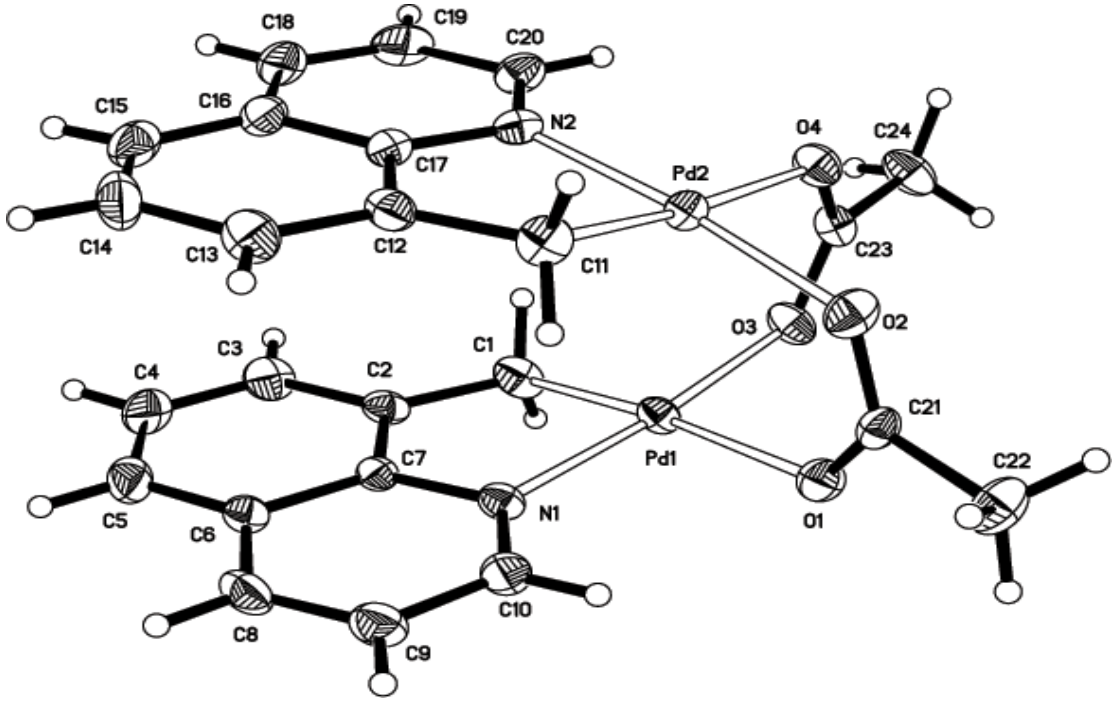

Table A33 Atomic coordinates (x 10^4) and equivalent isotropic displacement parameters (Å^2 x 10^3) for **13h**. U(eq) is defined as one third of the trace of the orthogonalized U^{ij} tensor.

	x	y	z	U(eq)
Pd(1)	5793(1)	5447(1)	5027(1)	42(1)
Pd(2)	6741(1)	5536(1)	6796(1)	40(1)
N(1)	6432(2)	3901(4)	4448(3)	44(1)
N(2)	6114(2)	3993(4)	7373(3)	45(1)
C(1)	4874(3)	4099(5)	5163(4)	56(1)
C(2)	5217(3)	2750(5)	4954(4)	48(1)
C(3)	4815(4)	1531(5)	5113(4)	66(2)
C(4)	5202(4)	344(5)	4890(5)	71(2)
C(5)	5997(5)	309(6)	4485(4)	68(2)
C(6)	6446(3)	1483(5)	4326(4)	50(1)
C(7)	6037(3)	2704(5)	4572(3)	42(1)
C(8)	7261(4)	1581(5)	3923(4)	61(2)

C(9)	7621(4)	2795(6)	3790(4)	65(2)
C(10)	7193(3)	3934(5)	4071(4)	55(1)
C(11)	7670(3)	4195(5)	6655(5)	54(2)
C(12)	7311(3)	2838(5)	6827(4)	50(1)
C(13)	7688(3)	1644(6)	6657(5)	65(2)
C(14)	7271(5)	429(5)	6860(6)	81(2)
C(15)	6472(4)	427(6)	7217(5)	68(2)
C(16)	6083(4)	1583(6)	7429(4)	58(2)
C(17)	6482(3)	2788(5)	7218(4)	41(1)
C(18)	5241(4)	1671(6)	7805(5)	71(2)
C(19)	4889(4)	2850(7)	7963(5)	70(2)
C(20)	5342(3)	4028(5)	7760(4)	55(1)
O(1)	6786(2)	6865(3)	4727(3)	53(1)
O(2)	7467(2)	6942(3)	6126(3)	57(1)
O(3)	5056(2)	6859(3)	5684(3)	54(1)
O(4)	5745(2)	6928(3)	7076(3)	54(1)
C(21)	7370(3)	7248(4)	5256(4)	43(1)
C(22)	8031(3)	8165(6)	4831(5)	67(2)
C(23)	5154(3)	7249(5)	6531(4)	44(1)
C(24)	4475(3)	8142(6)	6927(5)	69(2)

Table A34 Bond lengths [Å] and angles [°] for **13h**.

Pd(1)-C(1)	1.996(5)
Pd(1)-N(1)	2.023(4)
Pd(1)-O(3)	2.053(3)
Pd(1)-O(1)	2.164(3)
Pd(1)-Pd(2)	2.8902(5)
Pd(2)-C(11)	2.005(5)
Pd(2)-N(2)	2.011(4)
Pd(2)-O(2)	2.048(3)
Pd(2)-O(4)	2.143(3)
N(1)-C(10)	1.315(6)
N(1)-C(7)	1.368(6)
N(2)-C(20)	1.335(7)
N(2)-C(17)	1.361(6)
C(1)-C(2)	1.490(7)
C(1)-H(1A)	0.9700
C(1)-H(1B)	0.9700
C(2)-C(3)	1.399(7)
C(2)-C(7)	1.404(7)
C(3)-C(4)	1.377(8)
C(3)-H(3A)	0.9300
C(4)-C(5)	1.379(9)
C(4)-H(4A)	0.9300
C(5)-C(6)	1.395(8)
C(5)-H(5A)	0.9300
C(6)-C(8)	1.410(8)
C(6)-C(7)	1.430(7)
C(8)-C(9)	1.360(8)
C(8)-H(8A)	0.9300
C(9)-C(10)	1.387(8)
C(9)-H(9A)	0.9300
C(10)-H(10A)	0.9300
C(11)-C(12)	1.498(7)
C(11)-H(11A)	0.9700
C(11)-H(11B)	0.9700

C(12)-C(13)	1.361(7)
C(12)-C(17)	1.422(7)
C(13)-C(14)	1.417(8)
C(13)-H(13A)	0.9300
C(14)-C(15)	1.358(10)
C(14)-H(14A)	0.9300
C(15)-C(16)	1.348(8)
C(15)-H(15A)	0.9300
C(16)-C(17)	1.399(7)
C(16)-C(18)	1.433(9)
C(18)-C(19)	1.328(8)
C(18)-H(18A)	0.9300
C(19)-C(20)	1.414(8)
C(19)-H(19A)	0.9300
C(20)-H(20A)	0.9300
O(1)-C(21)	1.243(6)
O(2)-C(21)	1.261(6)
O(3)-C(23)	1.254(6)
O(4)-C(23)	1.248(6)
C(21)-C(22)	1.516(7)
C(22)-H(22A)	0.9600
C(22)-H(22B)	0.9600
C(22)-H(22C)	0.9600
C(23)-C(24)	1.505(7)
C(24)-H(24A)	0.9600
C(24)-H(24B)	0.9600
C(24)-H(24C)	0.9600

C(1)-Pd(1)-N(1)	83.11(18)
C(1)-Pd(1)-O(3)	90.82(18)
N(1)-Pd(1)-O(3)	173.55(15)
C(1)-Pd(1)-O(1)	174.2(2)
N(1)-Pd(1)-O(1)	93.78(15)
O(3)-Pd(1)-O(1)	92.45(13)
C(1)-Pd(1)-Pd(2)	108.55(17)
N(1)-Pd(1)-Pd(2)	96.04(11)

O(3)-Pd(1)-Pd(2) 83.81(10)
O(1)-Pd(1)-Pd(2) 76.57(10)
C(11)-Pd(2)-N(2) 83.23(18)
C(11)-Pd(2)-O(2) 90.47(18)
N(2)-Pd(2)-O(2) 173.14(16)
C(11)-Pd(2)-O(4) 175.1(2)
N(2)-Pd(2)-O(4) 93.90(15)
O(2)-Pd(2)-O(4) 92.57(14)
C(11)-Pd(2)-Pd(1) 106.01(18)
N(2)-Pd(2)-Pd(1) 93.54(11)
O(2)-Pd(2)-Pd(1) 85.55(11)
O(4)-Pd(2)-Pd(1) 78.11(10)
C(10)-N(1)-C(7) 119.4(4)
C(10)-N(1)-Pd(1) 126.8(3)
C(7)-N(1)-Pd(1) 113.4(3)
C(20)-N(2)-C(17) 118.6(4)
C(20)-N(2)-Pd(2) 126.3(4)
C(17)-N(2)-Pd(2) 114.3(3)
C(2)-C(1)-Pd(1) 109.6(3)
C(2)-C(1)-H(1A) 109.8
Pd(1)-C(1)-H(1A) 109.8
C(2)-C(1)-H(1B) 109.8
Pd(1)-C(1)-H(1B) 109.8
H(1A)-C(1)-H(1B) 108.2
C(3)-C(2)-C(7) 116.8(4)
C(3)-C(2)-C(1) 127.0(4)
C(7)-C(2)-C(1) 116.1(4)
C(4)-C(3)-C(2) 121.4(5)
C(4)-C(3)-H(3A) 119.3
C(2)-C(3)-H(3A) 119.3
C(3)-C(4)-C(5) 121.3(5)
C(3)-C(4)-H(4A) 119.3
C(5)-C(4)-H(4A) 119.3
C(4)-C(5)-C(6) 120.5(5)
C(4)-C(5)-H(5A) 119.7
C(6)-C(5)-H(5A) 119.7

C(5)-C(6)-C(8)	126.0(5)
C(5)-C(6)-C(7)	117.3(5)
C(8)-C(6)-C(7)	116.7(5)
N(1)-C(7)-C(2)	116.2(4)
N(1)-C(7)-C(6)	121.3(4)
C(2)-C(7)-C(6)	122.5(4)
C(9)-C(8)-C(6)	120.0(5)
C(9)-C(8)-H(8A)	120.0
C(6)-C(8)-H(8A)	120.0
C(8)-C(9)-C(10)	119.9(5)
C(8)-C(9)-H(9A)	120.0
C(10)-C(9)-H(9A)	120.0
N(1)-C(10)-C(9)	122.6(5)
N(1)-C(10)-H(10A)	118.7
C(9)-C(10)-H(10A)	118.7
C(12)-C(11)-Pd(2)	108.6(3)
C(12)-C(11)-H(11A)	110.0
Pd(2)-C(11)-H(11A)	110.0
C(12)-C(11)-H(11B)	110.0
Pd(2)-C(11)-H(11B)	110.0
H(11A)-C(11)-H(11B)	108.4
C(13)-C(12)-C(17)	116.1(5)
C(13)-C(12)-C(11)	127.6(5)
C(17)-C(12)-C(11)	116.3(4)
C(12)-C(13)-C(14)	121.5(5)
C(12)-C(13)-H(13A)	119.3
C(14)-C(13)-H(13A)	119.3
C(15)-C(14)-C(13)	120.5(5)
C(15)-C(14)-H(14A)	119.8
C(13)-C(14)-H(14A)	119.8
C(16)-C(15)-C(14)	120.3(5)
C(16)-C(15)-H(15A)	119.8
C(14)-C(15)-H(15A)	119.8
C(15)-C(16)-C(17)	119.7(6)
C(15)-C(16)-C(18)	123.9(5)
C(17)-C(16)-C(18)	116.3(5)

N(2)-C(17)-C(16) 123.0(5)
N(2)-C(17)-C(12) 115.1(4)
C(16)-C(17)-C(12) 121.8(5)
C(19)-C(18)-C(16) 120.4(5)
C(19)-C(18)-H(18A) 119.8
C(16)-C(18)-H(18A) 119.8
C(18)-C(19)-C(20) 120.2(5)
C(18)-C(19)-H(19A) 119.9
C(20)-C(19)-H(19A) 119.9
N(2)-C(20)-C(19) 121.5(5)
N(2)-C(20)-H(20A) 119.3
C(19)-C(20)-H(20A) 119.3
C(21)-O(1)-Pd(1) 128.9(3)
C(21)-O(2)-Pd(2) 122.7(3)
C(23)-O(3)-Pd(1) 124.5(3)
C(23)-O(4)-Pd(2) 127.5(3)
O(1)-C(21)-O(2) 125.9(4)
O(1)-C(21)-C(22) 117.9(5)
O(2)-C(21)-C(22) 116.2(4)
C(21)-C(22)-H(22A) 109.5
C(21)-C(22)-H(22B) 109.5
H(22A)-C(22)-H(22B) 109.5
C(21)-C(22)-H(22C) 109.5
H(22A)-C(22)-H(22C) 109.5
H(22B)-C(22)-H(22C) 109.5
O(4)-C(23)-O(3) 125.8(4)
O(4)-C(23)-C(24) 117.7(5)
O(3)-C(23)-C(24) 116.4(5)
C(23)-C(24)-H(24A) 109.5
C(23)-C(24)-H(24B) 109.5
H(24A)-C(24)-H(24B) 109.5
C(23)-C(24)-H(24C) 109.5
H(24A)-C(24)-H(24C) 109.5
H(24B)-C(24)-H(24C) 109.5

Symmetry transformations used to generate equivalent atoms:

Table A35 Anisotropic displacement parameters ($Å^2$x 10^3)for **13h**. The anisotropic displacement factor exponent takes the form: $-2\pi^2[h^2a^{*2}U^{11} + ... + 2 h k a^* b^* U^{12}]$

U^{11}	U^{22}	U^{33}	U^{23}	U^{13}	U^{12}
Pd(1)35(1)	46(1)	44(1)	-9(1)	2(1)	-1(1)
Pd(2)34(1)	42(1)	45(1)	3(1)	2(1)	-1(1)
N(1)39(2)	50(2)	43(2)	-7(2)	5(2)	-1(2)
N(2)42(2)	57(2)	37(2)	5(2)	2(2)	-3(2)
C(1)38(2)	70(3)	61(3)	-18(3)	0(3)	-10(2)
C(2)49(2)	58(3)	36(2)	-8(2)	-5(2)	-9(2)
C(3)67(3)	68(3)	63(3)	-10(3)	-11(3)	-30(2)
C(4)91(4)	56(3)	67(4)	2(3)	0(3)	-39(3)
C(5)100(4)	48(3)	57(4)	-4(3)	-21(3)	-4(3)
C(6)63(3)	48(3)	39(2)	-4(2)	-5(2)	2(2)
C(7)51(2)	42(2)	32(2)	-5(2)	-8(2)	-12(2)
C(8)65(3)	63(3)	55(3)	-16(3)	5(3)	21(3)
C(9)68(3)	71(3)	57(3)	-6(3)	14(3)	14(3)
C(10)52(3)	55(3)	57(3)	-2(3)	15(2)	-8(2)
C(11)35(2)	62(3)	67(4)	4(3)	9(3)	7(2)
C(12)53(2)	53(3)	46(3)	-7(3)	-5(3)	7(2)
C(13)54(3)	68(3)	72(4)	-5(3)	4(3)	10(3)
C(14)116(5)	43(3)	83(4)	-7(3)	-33(5)	16(3)
C(15)89(4)	56(3)	60(4)	10(3)	-17(3)	-23(3)
C(16)75(3)	50(3)	48(3)	6(2)	-8(3)	-10(3)
C(17)37(2)	46(2)	40(3)	3(2)	-3(2)	-6(2)
C(18)92(4)	57(3)	63(4)	9(3)	11(3)	-32(3)
C(19)51(3)	101(4)	58(4)	5(3)	23(3)	-16(3)
C(20)49(3)	63(3)	54(3)	10(3)	12(2)	2(3)
O(1)51(2)	55(2)	54(2)	0(2)	5(2)	-10(2)
O(2)44(2)	64(2)	64(2)	10(2)	1(2)	-13(2)
O(3)44(2)	60(2)	60(2)	-18(2)	0(2)	9(2)
O(4)49(2)	55(2)	58(2)	-9(2)	2(2)	9(1)
C(21)40(2)	41(2)	50(3)	8(2)	7(2)	-2(2)
C(22)47(3)	74(3)	81(4)	23(3)	-5(3)	-15(2)

C(23)28(2)	45(2)	59(3)	-10(2)	6(2)	0(2)
C(24)56(3)	78(3)	74(4)	-30(3)	7(3)	10(3)

Table A36 Hydrogen coordinates (x 10^4) and isotropic displacement parameters ($Å^2$x 10^3) for **13h**.

	x	y	z	U(eq)
H(1A)	4649	4123	5809	68
H(1B)	4419	4302	4721	68
H(3A)	4275	1522	5375	79
H(4A)	4922	-450	5014	86
H(5A)	6236	-503	4317	82
H(8A)	7552	815	3748	73
H(9A)	8153	2861	3512	78
H(10A)	7455	4754	3988	66
H(11A)	7909	4244	6015	65
H(11B)	8116	4376	7114	65
H(13A)	8231	1625	6402	78
H(14A)	7546	-373	6748	97
H(15A)	6193	-375	7316	82
H(18A)	4941	899	7939	85
H(19A)	4343	2900	8208	84
H(20A)	5098	4847	7900	66
H(22A)	7904	8324	4168	101
H(22B)	8578	7758	4883	101
H(22C)	8031	8994	5172	101
H(24A)	4614	8383	7574	104
H(24B)	3943	7683	6919	104
H(24C)	4436	8930	6542	104

Table A37 Torsion angles [°] for **13h**.

C(1)-Pd(1)-Pd(2)-C(11)	89.9(2)
N(1)-Pd(1)-Pd(2)-C(11)	5.16(19)
O(3)-Pd(1)-Pd(2)-C(11)	178.68(18)
O(1)-Pd(1)-Pd(2)-C(11)	-87.30(18)
C(1)-Pd(1)-Pd(2)-N(2)	5.93(19)
N(1)-Pd(1)-Pd(2)-N(2)	-78.80(15)
O(3)-Pd(1)-Pd(2)-N(2)	94.71(16)
O(1)-Pd(1)-Pd(2)-N(2)	-171.26(15)
C(1)-Pd(1)-Pd(2)-O(2)	179.11(18)
N(1)-Pd(1)-Pd(2)-O(2)	94.38(15)
O(3)-Pd(1)-Pd(2)-O(2)	-92.11(13)
O(1)-Pd(1)-Pd(2)-O(2)	1.92(14)
C(1)-Pd(1)-Pd(2)-O(4)	-87.32(18)
N(1)-Pd(1)-Pd(2)-O(4)	-172.05(15)
O(3)-Pd(1)-Pd(2)-O(4)	1.46(14)
O(1)-Pd(1)-Pd(2)-O(4)	95.49(13)
C(1)-Pd(1)-N(1)-C(10)	176.3(5)
O(3)-Pd(1)-N(1)-C(10)	-164.0(12)
O(1)-Pd(1)-N(1)-C(10)	1.2(4)
Pd(2)-Pd(1)-N(1)-C(10)	-75.7(4)
C(1)-Pd(1)-N(1)-C(7)	-10.8(3)
O(3)-Pd(1)-N(1)-C(7)	9.0(16)
O(1)-Pd(1)-N(1)-C(7)	174.1(3)
Pd(2)-Pd(1)-N(1)-C(7)	97.3(3)
C(11)-Pd(2)-N(2)-C(20)	176.1(5)
O(2)-Pd(2)-N(2)-C(20)	-160.4(12)
O(4)-Pd(2)-N(2)-C(20)	0.1(5)
Pd(1)-Pd(2)-N(2)-C(20)	-78.2(4)
C(11)-Pd(2)-N(2)-C(17)	-13.7(4)
O(2)-Pd(2)-N(2)-C(17)	9.9(15)
O(4)-Pd(2)-N(2)-C(17)	170.4(3)
Pd(1)-Pd(2)-N(2)-C(17)	92.1(3)
N(1)-Pd(1)-C(1)-C(2)	10.5(4)
O(3)-Pd(1)-C(1)-C(2)	-167.3(4)

O(1)-Pd(1)-C(1)-C(2)	68.2(18)
Pd(2)-Pd(1)-C(1)-C(2)	-83.5(4)
Pd(1)-C(1)-C(2)-C(3)	169.3(5)
Pd(1)-C(1)-C(2)-C(7)	-9.5(6)
C(7)-C(2)-C(3)-C(4)	-1.0(8)
C(1)-C(2)-C(3)-C(4)	-179.9(6)
C(2)-C(3)-C(4)-C(5)	-1.1(10)
C(3)-C(4)-C(5)-C(6)	2.6(10)
C(4)-C(5)-C(6)-C(8)	179.8(6)
C(4)-C(5)-C(6)-C(7)	-1.8(8)
C(10)-N(1)-C(7)-C(2)	-178.3(5)
Pd(1)-N(1)-C(7)-C(2)	8.2(5)
C(10)-N(1)-C(7)-C(6)	2.0(7)
Pd(1)-N(1)-C(7)-C(6)	-171.5(4)
C(3)-C(2)-C(7)-N(1)	-178.0(5)
C(1)-C(2)-C(7)-N(1)	1.0(6)
C(3)-C(2)-C(7)-C(6)	1.7(7)
C(1)-C(2)-C(7)-C(6)	-179.3(5)
C(5)-C(6)-C(7)-N(1)	179.4(5)
C(8)-C(6)-C(7)-N(1)	-2.1(7)
C(5)-C(6)-C(7)-C(2)	-0.3(7)
C(8)-C(6)-C(7)-C(2)	178.2(5)
C(5)-C(6)-C(8)-C(9)	178.7(6)
C(7)-C(6)-C(8)-C(9)	0.4(8)
C(6)-C(8)-C(9)-C(10)	1.4(9)
C(7)-N(1)-C(10)-C(9)	-0.2(8)
Pd(1)-N(1)-C(10)-C(9)	172.4(4)
C(8)-C(9)-C(10)-N(1)	-1.5(9)
N(2)-Pd(2)-C(11)-C(12)	12.9(4)
O(2)-Pd(2)-C(11)-C(12)	-164.3(4)
O(4)-Pd(2)-C(11)-C(12)	68(2)
Pd(1)-Pd(2)-C(11)-C(12)	-78.8(4)
Pd(2)-C(11)-C(12)-C(13)	168.9(5)
Pd(2)-C(11)-C(12)-C(17)	-11.5(6)
C(17)-C(12)-C(13)-C(14)	0.1(9)
C(11)-C(12)-C(13)-C(14)	179.7(6)

C(12)-C(13)-C(14)-C(15)	1.1(11)
C(13)-C(14)-C(15)-C(16)	-3.4(11)
C(14)-C(15)-C(16)-C(17)	4.4(10)
C(14)-C(15)-C(16)-C(18)	179.8(7)
C(20)-N(2)-C(17)-C(16)	1.2(7)
Pd(2)-N(2)-C(17)-C(16)	-169.9(4)
C(20)-N(2)-C(17)-C(12)	-178.5(5)
Pd(2)-N(2)-C(17)-C(12)	10.5(5)
C(15)-C(16)-C(17)-N(2)	177.2(5)
C(18)-C(16)-C(17)-N(2)	1.4(8)
C(15)-C(16)-C(17)-C(12)	-3.2(8)
C(18)-C(16)-C(17)-C(12)	-179.0(5)
C(13)-C(12)-C(17)-N(2)	-179.4(5)
C(11)-C(12)-C(17)-N(2)	0.9(7)
C(13)-C(12)-C(17)-C(16)	1.0(8)
C(11)-C(12)-C(17)-C(16)	-178.7(5)
C(15)-C(16)-C(18)-C(19)	-177.5(6)
C(17)-C(16)-C(18)-C(19)	-2.0(9)
C(16)-C(18)-C(19)-C(20)	0.0(10)
C(17)-N(2)-C(20)-C(19)	-3.3(8)
Pd(2)-N(2)-C(20)-C(19)	166.6(4)
C(18)-C(19)-C(20)-N(2)	2.7(9)
C(1)-Pd(1)-O(1)-C(21)	-151.8(16)
N(1)-Pd(1)-O(1)-C(21)	-94.6(4)
O(3)-Pd(1)-O(1)-C(21)	83.7(4)
Pd(2)-Pd(1)-O(1)-C(21)	0.7(4)
C(11)-Pd(2)-O(2)-C(21)	100.6(4)
N(2)-Pd(2)-O(2)-C(21)	77.3(14)
O(4)-Pd(2)-O(2)-C(21)	-83.3(4)
Pd(1)-Pd(2)-O(2)-C(21)	-5.4(4)
C(1)-Pd(1)-O(3)-C(23)	104.4(4)
N(1)-Pd(1)-O(3)-C(23)	84.8(14)
O(1)-Pd(1)-O(3)-C(23)	-80.4(4)
Pd(2)-Pd(1)-O(3)-C(23)	-4.2(4)
C(11)-Pd(2)-O(4)-C(23)	-146.5(19)
N(2)-Pd(2)-O(4)-C(23)	-92.3(4)

O(2)-Pd(2)-O(4)-C(23)	85.4(4)
Pd(1)-Pd(2)-O(4)-C(23)	0.5(4)
Pd(1)-O(1)-C(21)-O(2)	-5.3(7)
Pd(1)-O(1)-C(21)-C(22)	174.5(3)
Pd(2)-O(2)-C(21)-O(1)	7.9(7)
Pd(2)-O(2)-C(21)-C(22)	-171.9(3)
Pd(2)-O(4)-C(23)-O(3)	-4.0(7)
Pd(2)-O(4)-C(23)-C(24)	173.6(3)
Pd(1)-O(3)-C(23)-O(4)	6.1(7)
Pd(1)-O(3)-C(23)-C(24)	-171.4(3)

Symmetry transformations used to generate equivalent atoms.

REFERENCES

Chapter 1

1. (a) Clayden, J.; Greeves, N.; Warren, S. *Organic Chemistry*; *2nd Ed.*; Oxford University Press Inc.: New York, 2012. (b) Ding, K.; Dai, L.-X. *Organic Chemistry – Breakthroughs and Perspectives*; Wiley-VCH: Weinheim, 2012.
2. (a) Yamaguchi, J.; Yamaguchi, A. D.; Itami, K. *Angew. Chem. Int. Ed.* **2012**, *51*, 8960. (b) Lloyd-Jones, G. C. *Angew. Chem. Int. Ed.* **2002**, *41*, 953. b) Chida, N.; Ohtsuka, M.; Ogawa, S. *J. Org. Chem.* **1993**, *58*, 4441.
3. (a) Bandini. M.; Umani-Ronchi, A., *Catalytic Asymmetric Friedel-Crafts Alkylations*; Wiley-VCH: Weinheim, 2009. (b) Ackermann, L., *Modern Arylation Methods*; Wiley-VCH: Weinheim, 2009.
4. (a) Diederich, F.; Stang, P. J. *Metal-catalyzed Cross-coupling Reactions*; Wiley-VCH: Weinheim, 1998. (b) Magano, J.; Dunetz, J. R. *Chem. Rev.* **2011**, *111*, 2177. (*44*, 4442. (c) Daugulis, O., *Top. Curr. Chem.*, **2010**, *292*, 57.
5. Nicolaou, K. C.; Bulger, P. G.; Sarlah, D. *Angew. Chem. Int. Ed.* **2005**.
6. (a) Ackermann, L.; Vicente, R.; Kapdi, A. R. *Angew. Chem. Int. Ed.* **2009**, *48*, 9792. (b) Godula, K.; Sames, D. *Science*, **2006**, *312*, 67. (c) Dick, A. R.; Sanford, M. S. *Tetrahedron* **2006**, *62*, 2439. (d) Ritleng, V.; Sirlin, C.; Pfeffer, M. *Chem. Rev.* **2002**, *102*, 1731.
7. Bergman, R. G. *Nature*, **2007**, *446*, 391.
8. (a) Anslyn, E. V.; Dougherty. D. A., *Modern Physical Organic Chemistry*; Murdzek, J., Ed.; University Science Book: USA, 2006. (b) Blanksby, S. J.; Ellison, G. B. *Acc. Chem. Res.* **2003**, *36*, 255.
9. Labinger, J. A.; Bercaw, J. E. *Nature*, **2002**, *417*, 507.
10. (a) Pesci, L. *Gazz. Chim. Ital.* **1892**, *33*, 373. (b) Volhard, J. *Justus Liebigs Ann. Chem.* **1892**, *267*, 172. (c) Dimroth, O. *Ber. Dtsch. Chem. Ges.* **1898**, *31*, 2154. (d) Kharasch, M. S.; Isbell, H. S. *J. Am. Chem. Soc.*, **1931**, *53*, 3053.
11. (a) Moritani, I.; Fujiwara, Y. *Tetrahedron Lett.* **1967**, *8*, 1119. (b) Fujiwara, Y.; Asano, R.; Moritani, I.; Teranishi, S. *J. Org. Chem.* **1967**, *41*, 1681. (c) Fuchita, Y.; Hiraki, K.; Kamogawa, Y.; Suenaga, M.; Togoh, K.; Fujiwara, Y. *Bull. Chem. Soc. Jpn.* **1989**, *62*, 1081.
12. Kleiman, J. P.; Dubeck, M. *J. Am. Chem. Soc.* **1963**, *85*, 1544.
13. Cope, A. C.; Siekman, R. W. *J. Am. Chem. Soc.* **1965**, *87*, 3272.
14. (a) For a review, see: Jain, V. K.; Jain, L. *Coord. Chem. Rev.* **2005**, *249*, 3057. (b) Wan, X.; Ma, Z.; Li, B.; Zhang, K.; Cao, S.; Zhang, S.; Shi, Z. *J. Am. Chem. Soc.*

2006 *128*, 7416. (c) Horino, H.; Inoue, N. *J. Org. Chem.* **1981**, *46*, 4416. (d) Peterson, D. L.; Keuseman, K. J.; Kataeva, N. A.; Kuzimina, L. G.; Howard, J. A. K.; Dunina, V. V.; Smoliakova, I. P. *J. Organomet. Chem.* **2002**, *654*, 66. (e) Churchill, M. R.; Wasserman, H. J.; Young, G. J. *Inorg. Chem.* **1980**, *19,* 762. (f) Cope, A. C.; Friedrich, E. C. *J. Am. Chem. Soc.* **1968**, *90*, 909. (g) Ryabov, A. D.; Sakodinskaya, I. K.; Yatsimirsky, A. K. *J. Chem. Soc., Dalton Trans.* **1985**, 2629. (h) Kasahara, A. Bull. Chem. Soc. Jap. 1968, 41, 1272. (i) Constable, E. C.; Leese, T. A. *J. Organomet. Chem.* **1987**, *335*, 293. (j) Refer to Appendice in this thesis.

15. Fahey, D. R. *J. Organometal. Chem.* **1971**, *27*, 283.
16. Tremont, S. J.; Rahman, H. U. *J. Am. Chem. Soc.* **1984**, *106*, 5759.
17. Miura, M.; Tusda, T.; Satoh, T.; Pivsa-Art, S.; Nomura, M. *J. Org. Chem.* **1998**, *63*, 5211.
18. (a) Engle, K. M.; Mei, T. S.; Wasa, M.; Yu, J. Q. *Acc. Chem. Res.* **2012**, *45*, 788. (b) Lyons, T. W.; Sanford, M. S. *Chem. Rev.* **2010**, *110*, 1147. (c) Chen, X.; Engle, K. M.; Wang, D. H.; Yu, J. Q. *Angew. Chem. Int. Ed.* **2009**, *48*, 5094. (d) Xu, L. M.; Li, B. J.; Yang, Z.; Shi, Z. J. *Chem. Soc. Rev.* **2010**, *39*, 712. (e) Dupont, J.; Consorti, C. S.; Spence, J. *Chem. Rev.* **2005**, *105*, 2527.
19. (a) Ryabov, A. D. *Chem. Rev.* **1990**, *90*, 403.
20. (a) Davies, D. L.; Donald, S. M. A.; Macgregor, S. A. *J. Am. Chem. Soc.* **2005**, *127*, 13754. (b) Davies, D. L.; Donald, S. M. A.;Al-Duaij, O.; Macgregor, S. A.; Polleth, M. *J. Am. Chem. Soc.* **2006**, *128*, 4210.
21. (a) Canty, A. J.; van Koten, G. *Acc. Chem. Res.* **1995**, *28*, 406. (b) Bayler, A.; Canty, A. J.; Skelton, B. W.; White, A. H. *J. Organomet. Chem.* **2000**, *595*, 296. (c) Byers, P. K.; Canty, A. J.; Skelton, B. W.; White, A. H. *J. Chem. Soc., Chem. Commun.* **1986**, 1722.
22. (a) Lapointe, D.; Fagnou, K. *Chem. Lett.* **2010**, *39*, 1118. (b) Gorelsky, S. I.; Lapointe, D.; Fagnou, K. *J. Am. Chem. Soc.* **2008**, *130*, 10848. (c) Sun, H. Y.; Gorelsky, S. I.; Stuart, D. R.; Campeau, L. C. Fagnou, K. *J. Org. Chem.* **2010**, *75*, 8180. (d) Lafrance, M.; Fagnou, K. *J. Am. Chem. Soc.* **2006**, *128*, 16496.
23. (a) Boele, M. D. K.; van Strijdonck, G. P. F.; de Vries, A. H.; Kamer, P. C. J.; de Vries, J. G.; van Leeuwen, P. W. N. M. *J. Am. Chem. Soc.* **2002**, *124*, 1586. (b) Houlden, C. E.; Bailey, C. D.; Ford, J. G.; Gagne, M. R.; Lloyd-Jones, G. C.; Booker-Milburn, K. I. *J. Am. Chem. Soc.* **2008**, *130*, 10066. (c) Wang, C.; Ge, H. *Chem. Eur. J.* **2011**, *17*, 14371. (d) Zaitsev, V. G.; Daugulis, O. *J. Am. Chem. Soc.* **2005**, *127*, 4156.
24. (a) Chen, X.; Li, J. J.; Hao, X. S.; Goodhue, C. E.; Yu, J. Q. *J. Am. Chem. Soc.* **2006**, *128*, 78. (b) Chen, X.; Goodhue, C. E.; Yu, J. Q. *J. Am. Chem. Soc.* **2006**, *128*, 12634.

25. Chan, W. W.; Zhou, Z.; Yu, W. Y. *Chem. Commun.* **2013**, *49*, 8214.
26. Tobisu, M.; Ano, Y.; Chatani, N. *Org. Lett.* **2009**, *11*, 3250.
27. (a) Kalyani, D.; Deprez, N. R.; Desai, L. V.; Sanford, M. S. *J. Am. Chem. Soc.* **2005**, *127*, 7330. (b) Deprez, N. R.; Sanford, M. S. *Inorg. Chem.* **2007**, *46*, 1924. (c) Daugulis, O.; Zaitsev, V. G. *Angew. Chem., Int. Ed.* **2005**, *44*, 4046. (d) Yu, W. Y.; Sit, W. N.; Zhou, Z.; Chan, A. S. C. *Org. Lett.* **2009**, *11*, 3174. (e) Qian, C.; Lin, D.; Deng, Y.; Zhang, X.; Jiang, H.; Zheng, Wei. *Org. Biomol. Chem.* **2014**, *12*, 5866. (f) Li, D.; Xu, N.; Zhang, Y.; Wang, L. *Chem. Commun.* **2014**, *50*, 14862.
28. (a) Hull, K. L.; Sanford, M. S. *J. Am. Chem. Soc.* **2007**, *129*, 11904. (b) Li, B. J.; Tian, S. L.; Fang, Z.; Shi, Z. J. *Angew. Chem., Int. Ed.* **2008**, *47*, 1115. (c) Li, B. J.; Yang, S. D.; Shi, Z. J. *Synlett* **2008**, 949. (d) Brasche, G.; Garcıa-Fortanet, J.; Buchwald, S. L. *Org. Lett.* **2008**, *10*, 2207.
29. (a) Orito, K.; Horibata, A.; Nakamura, T.; Ushito, H.; Nagasaki, H.; Yuguchi, M.; Yamashita, S.; Tokuda, M. *J. Am. Chem. Soc.* **2004**, *126*, 14342. (b) Giri, R.; Yu, J. Q. *J. Am. Chem. Soc.* **2008**, *130*, 14082. (c) Houlden, C. E.; Hutchby, M.; Bailey, C. D.; Ford, J. G.; Tyler, S. N. G.; Gagne, M. R.; Lloyd-Jones, G. C.; Booker-Milburn, K. I. *Angew. Chem., Int. Ed.* **2009**, *48*, 1830. (d) Yu, W. Y.; Sit, W. N.; Lai, K. M.; Zhou, Z.; Chan, A. S. C. *J. Am. Chem. Soc.* **2008**, *130*, 3304.
30. (a) Yeung C. S.; Dong, V. M. *Chem. Rev.* **2011**, *111*, 1215. (b) Liu, C.; Zhang, H.; Shi W.; Lei, A. *Chem. Rev.* **2011**, *111*, 1780. (c) Yoo, W. J.; Li, C. J. *Top. Curr. Chem.* **2010**, *292*, 281. (d) Li, C.-J. *Acc. Chem. Res.* **2009**, *42*, 335. (e) Scheuermann C. J. *Chem. Asian J.* **2010**, *5*, 436. (f) Sarhan, A.; Bolm, C. *Chem. Soc. Rev.* **2009**, *38*, 2730. (g) Wu, Y.; Wang, J.; Mao, F.; Kwong, F. Y. *Chem. Asian J.* **2014**, *9*, 26. (h) Ashenhurst, J. A. *Chem. Soc. Rev.* **2010**, *39*, 540.

Chapter 2

31. Kotali, A.; Harris, P. A. *Org. Prep. Proced. Int.* **2003**, *35*, 583.
32. Baele, S. C.; Savage, J. C.; Wiesler, D.; Wiedstock, S. M.; Novotny, M. *Anal. Chem.* **1988**, *60*, 1765.
33. Kotali, A.; Tsoungas, P. G. *Tetrahedron Lett.* **1987**, *28*, 4321.
34. Kumar, S.; Kumar, D. *Synth. Commun.* **2008**, *38*, 3683.
35. Metlesics, W.; Anton, T.; Chaykovsky, M.; Toome, V.; Sternbach, L. H. *J. Org. Chem.* **1968**, *33*, 2874.
36. Desai, L. V.; Stowers, K. J.; Sanford, M. S. *J. Am. Chem. Soc.* **2008**, *130*, 13285.
37. For selected examples, see: (a) Yang, S.; Li, B.; Wan, X.; Shi, Z. *J. Am. Chem. Soc.* **2007**, *129*, 6066. (b) Chiong, H. A.; Pham, Q.-N.; Daugulis, O. *J. Am. Chem. Soc.* **2007**, *129*, 9879. (c) Giri, R.; Maugel, N.; Li, J.-J.; Wang, D.-H.; Breazzano,

S. P.; Saunders, L. B.; Yu, J.-Q. *J. Am. Chem. Soc.* **2007**, *129*, 3510. (d) Lazareva, A.; Daugulis, O. *Org. Lett.* **2006**, *8*, 5211. (e) Kalyani, D.; Dick, A. R.; Anani, W. Q.; Sanford, M. S. *Org. Lett.* **2006**, *8*, 2523. (f) Zaitev, V. G.; Shabashov, D.; Daugulis, O. *J. Am. Chem. Soc.* **2005**, *127*, 13154.

38. (a) Sundberg, R. J. *Indoles*; Academic Press: London, 1996. (b) Sundberg, R. J. *The Chemistry of Indoles*; Academic Press: New York, 1970.
39. Liou, J. P.; Wu, C.-W.; Hsieh, H.-P.; Chang, C.-Y.; Chen, C.-M.; Kuo, C.-C.; Chang, J.-Y. *J. Med. Chem.* **2007**, *50*, 4548.
40. Neufeldt, S. R.; Sanford, M. S. *Org. Lett.* **2010**, *12*, 532.
41. Pradhan, P. K.; Dey, S.; Jaisamkar, P.; Giri, V. S. *Synth. Commun.* **2005**, *35*, 913.
42. Mi, B. X.; Pang, P. F.; Gao, Z. Q.; Lee, C. S.; Lee, S. T.; Hong, H. L.; Chen, X. M.; Wong, M. S.; Xia, P. F.; Cheah, K. W.; Chen, C. H.; Huang, W. *Adv. Mater.* **2009**, *21*, 339.
43. (a) Austin, R. J.; Kaizerman, J.; Lucas, B.; McMinn, D. L.; Powers, J. PCT Int. App. WO 2009002469, 2008. (b) Tasker, A.; Zhang, D.; Pettus, L. H.; Rzasa, R. M.; Sham, K. K. C.; Xu, S.; Chakrabarti, P. P. PCT Int. App. WO 2008030466, 2008.
44. For reviews of 2-aminobenzophenones synthesis, see: a) Simpson, J. C. E.; Atkinson, C. M.; Schofield, K.; Stephenson, O. *J. Chem. Soc.* **1945**, 646. b) Walsh, D. A. *Synthesis* **1980**, 677.
45. Selected references on the synthesis and bioactivities, for acridine derivatives, see: a) Denny, W. A. *Med. Chem. Rev.* **2004**, 1, 257. b) Denny, W. A. *Curr. Med. Chem.* **2002**, *9*, 1655. c) Rogness, D. C.; Larock, R. C. *J. Org. Chem.* **2010**, *75*, 2289. For indazoles, see: Claramunt, R. M.; Lopez, C.; Lopez, A.; Perez-Medina, C.; Perez-Torralba, M.; Alkorta, I.; Elguero, J.; Escames, G.; Acuna-Castroviejo, D.; *Eur. J. Med. Chem.* **2011**, *46*, 1439. e) Kamal, A.; Devaiah, K. L. V.; Shankaraiah, N. D.; Reddy, R. *Mini-Rev. Med. Chem.* **2006**, *6*, 53. f) Councekker, C. M.; Eichman, C. C.; Wray, B. C.; Welin, E. R.; Stambuli, J. P. *Org. Synth.* **2011**, *88*, 33. For quinolines, see: g) Jose, M. C.; Elena, P. M.; Abdeloushid, S. C.; Elena, S. *Chem. Rev.* **2009**, *109*, 2652. h) Madapa, S.; Tusi, Z.; Batra, S. *Curr. Org. Chem.*, **2008**, *12*, 1116. i) Atechian, S.; Nock, N. R.; Norcross, D.; Ratni, H.; Thomas, A. W. J.; Verron, R. *Tetrahedron*, **2007**, *63*, 2811. For benzodiazepines, see: j) Bunin, B. A.; Plunkett, M. J.; Ellman, J. A. *Proc. Natl. Acad. Sci. U.S.A.* **1994**, *91*, 4708. k) Evans, B. E.; Rittle, K. E.; Bock, M. G.; DiPardo, R. M.; Freidinger, R. M.; Whitter, W. L.; Anderson, P. S.; Chang, R. S. L.; Lotti, V. J.; Cerino, D. J.; Chen, T. B. P.; Kling, J.; Springer, J. P.; Hirshfieldt J. *J. Med. Chem.* **1988**, *31*, 2235. l) Sternbach, L. H. *Angew. Chem. Int. Ed.* **1971**, *10*, 34.
46. a) Prasad, K.; Lee, G. L.; Chaudhary, A. M.; Girgis, J.; Streemke, J. W.; Repic, O.

Org. Process Res. Dev. **2003**, *7*, 723. b) Douglas, A. W.; Abramson, N. L.; Houpis, I. N.; Karady, S.; Molina, A.; Xavier, L. C.; Yasuda, N. *Tetrahedron Lett.* **1994**, *35*, 6807. c) Sugasawa, T.; Toyoda, T.; Adachi, M.; Sasakura, K. *J. Am. Chem Soc.* **1978**, *100*, 4842.

47. D. J. C. Constable, P. J. Dunn, J. D. Hayler, G. R. Humphrey, J. L. Leazer, R. J. Linderman, L. Lorenz, J. Manley, B. A. Pearlman, A. Wells, A. Zaks, T. Y. Zhang, *Green Chem.* **2007**, *9*, 411.
48. For selected examples of Pd-catalyzed *ortho*-C–H bond functionalizations of anilides, see a) Sun, K.; Li, Y.; Xiong, T.; Zhang, J.; Zhang, Q. *J. Am. Chem. Soc.* **2011**, *133*, 1694. b) Yeung, C. S.; Zhao, X.; Borduas, N.; Dong, V. M. *Chem. Sci.* **2010**, *1*, 331. c) Shabashov, D.; Daugulis, O. *J. Am. Chem. Soc.* **2010**, *132*, 3965. d) Rauf, W.; Thompson, A. L.; Brown, J. H. *Dalton Trans.* **2010**, *39*, 10414. e) Li, B. J.; Tian, S. L.; Fang, Z.; Shi, Z. *Angew. Chem. Int. Ed.* **2008**, 47, 1115.
49. Kingbury, W. D.; Boehm, J. C.; Jakas, D. R.; Holden, K. G.; Hecht, S. M.; Gallagher, G.; Caranfa, M. J.; McCabe, F. L.; Faucette, L. F.; Johnson, R. K.; Hertzberg, R. P, *J. Med. Chem.* **1991**, *34*, 98.
50. Jew, S.-S.; Kim, H.-J.; Kim, M. G.; Roh, E.-Y.; Hong, C. L.; Kim, J.-K.; Lee, J.-H.; Lee, H.; Park, H.-G. *Bioorg. Med. Chem. Lett.* **1999**, *9*, 3203.
51. (a) Donaruma, L. G. *J. Org. Chem.* **1957**, *22*, 1024. (b) Sharpless, K. B.; Verhoeven, T. R. *Aldrichimica Acta* **1979**, *12*, 63.

Chapter 3

52. (a) Racowski, J. M.; Dick, A. R.; Sanford, M. S. *J. Am. Chem. Soc.* **2009**, *131*, 10974. (b) Dick, A. R.; Kampf, J. W.; Sanford, M. S. *J. Am. Chem. Soc.* **2005**, *127*, 12790. (c) Stowers, K. J.; Sanford, M. S. *Org. Lett.* **2009**, *11*, 4584. (d) Whitfield, S. R.; Sanford, M. S. *J. Am. Chem. Soc.* **2007**, *129*, 15142. (e) Deprez, N. R.; Sanford, M. S. *J. Am. Chem. Soc.* **2009**, *131*, 11234. (f) Deprez, N. R.; Sanford, M. S. *Inorg. Chem.* **2007**, *46*, 1924.
53. (a) Powers, D. C.; Ritter, T. *Nature Chemistry* **2009**, *1*, 302. (b) Powers, D. C.; Geibel, M. A.; Klein, J. E. M.; Ritter, T. *J. Am. Chem. Soc.* **2009**, *131*, 17050. (c) Powers, D. C.; Benitez, D.; Tkatchouk, E.; Goddard III, W. A.; Ritter, T. *J. Am. Chem. Soc.* **2010**, *132*, 14092. (d) Powers, D. C.; Xiao, D. Y.; Geibel, M. A.; Ritter, T. *J. Am. Chem. Soc.* **2010**, *132*, 14536. For a revew, see: (e) Powers, D. C.; Ritter, T. *Acc. Chem. Res.* **2012**, *45*, 840.
54. (a) Selbin, J.; Abboud, K.; Walkins, S. F.; Gutierrez, M. A.; Fronczek, F. R. *J. Organomet. Chem.* **1983**, *241*, 259. (b) Ghedini, M.; Ricci, D.; DeMunno, G.; Viterbo, D.; Neve, F.; Armentano, S. *Chem. Mater.* **1991**, *3*, 65. (c) Teijido, B.; Fernandez, A.; Lopez-Torres, M.; Castro-Juiz, S.; Suarez, A.; Ortigueira, J. M.;

Vila, J. M.; Fernandez, J. J. *J. Organomet. Chem.* **2000**, 598, 71.

55. A recent study on ascorbic acid as radical scavenger, see: Warren, J. J.; Meyer, J. M. *J. Am. Chem. Soc.* **2010**, *132,* 7784.
56. (a) Chatgilialoglu, C.; Lunazzi, L.; Macciantelli, D.; Placucci, G. *J. Am. Chem. Soc*. **1984**, *106*, 5252. (b) Walling, C.; Mintz, M. J. *J. Am. Chem. Soc*. **1967**, *89*, 1515.
57. Bagryanskaya, E. G.; Marque, S. R. A. *Chem. Rev.* **2014**, *114*, 5011.
58. Chatgilialoglu, C.; Crich, D.; Komatsu, M.; Ryu, I. *Chem. Rev*. **1999**, *99*, 1991.
59. (a) Deeming, A. J.; Rothwell, I. P. *J. Organomet. Chem.* **1981**, *205*, 117. (b) Kurzeev, S. A.; Kazankov, G. M.; Ryabov, A. D. *Inorg. Chim. Acta.* **2002**, *340*, 192.
60. (a) Arockiam, P. B.; Bruneau, C.; Dixneuf, P. H. *Chem. Rev.* **2012**, *112*, 5879. (b) Song, G.; Wang, F.; Li, W. *Chem. Soc. Rev.* **2012**, *41*, 3651. (c) Lersch, M.; Tilset, M. *Chem. Rev.* **2005**, *105*, 2471.
61. (a) Brown, H. C.; Stock, L. M. *J. Am. Chem. Soc.* **1957**, *79*, 5171. (b) De La Mare, P. B. D. *J. Chem. Soc.* **1954**, 4450.
62. Han, X.; Lu, X. *Org. Lett.* **2010**, *12*, 3336.
63. (a) Byers, P. K.; Canty, A. J.; Skelton, B. W.; White, A. H. *J. Chem. Soc., Chem. Commun.* **1986**, 1722. (b) Baudoin, O. *Chem. Soc. Rev.* **2011**, *40*, 4902. (c) Xu, L.-M.; Li, B.-J.; Yang, Z.; Shi, Z.-J. *Chem. Soc. Rev.* **2010**, *39*, 712. (d) Canty, A. J. *Acc. Chem. Res.* **1992**, *25*, 83.
64. Bercaw, J. E.; Durrell, A. C.; Gray, H. B.; Green, J. C.; Hazari, N.; Labinger, J. A.; Winkler, J. R. *Inorg. Chem.* **2010**, *49*, 1801.

Chapter 4

65. (a) Gribble, G. W. *Heterocycles*, **2012**, *84*, 157. (b) Gribble, G. W. *Naturally Occurring Organohalogen Compounds –A Comprehensive Update*; in *Progress in the Chemistry of Organic Natural Products*; ed. A. D. Kinghorn, H. Falk and J. Kobayashi, Springer Wien New York, Vienna, 1st ed., **2010**, vol. 91.
66. (a) Reeve, W. *Synthesis* **1971**, *3*, 131. (b) Corey, E. J.; Link, J. O. *Tetrahedron Lett.* **1992**, *33*, 3431. (c) Cafiero, L. R.; Snowden, T. S. *Org. Lett.* **2008**, *10*, 3853. For a recent selected review, see: (d) Snowden, T. S. *ARKIVOC* **2012**, 24.
67. Blanchet, J.; Zhu, J. P. *Tetrahedron Lett.* **2004**, *45*, 4449.
68. Lee, G. M.; Weinreb, S. M. *J. Org. Chem.* **1990**, *55*, 1281.
69. (a) Fedorynski, M. *Tetrahedron* **1999**, *55*, 6329. (b) Jensen, A. B.; Lindhardt, A. T. *J. Org. Chem.* **2014**, *79*, 1174.
70. (a) Li, D.; Li, Y.; Chen, Z.; Shang, H.; Li, H.; Ren, X. *RSC Adv.* **2014**, *4*, 14254. (b) Kister, J.; Mioskowski, C. *J. Org. Chem.* **2007**, *72*, 3925. (c) Fujita, M.; Hiyama, T.

J. Am. Chem. Soc. **1985**, *107*, 4085.

71. (a) Zakarian, A. *Radical Haloalkylation*; in *Asymmetric Synthesis: More Methods and Applications*; ed. Christmann, M. and Brase, S. Wiley-VCH, Weinheim, Germany, 1st edn., **2012**, vol. 2, ch. 36, pp. 285-291. (b) Beaumont, S.; Ilardi, E. A.; Monroe, L. R.; Zakarian, A. *J. Am. Chem. Soc.* **2010**, *132*, 1482.
72. Galonic, D. P.; Vaillancourt, F. H.; Walsh, C. T. *J. Am. Chem. Soc.* **2006**, 128, 3900.
73. (a) Kharasch, M. S.; Jensen, E. V.; Urry, W. H.; *J. Am. Chem. Soc.* **1947**, 69, 1100. (b) Kharasch, M. S.; Reinmuth, O.; Urry, W. H. *J. Am. Chem. Soc.* **1947**, 69, 1105.
74. For selected examples of transition metal-catalyzed carboradical-mediated coupling, see: (a) Tellis, J. C.; Primer, D. N.; Molander, G. A. *Science* **2014**, *345*, 433. (b) Thuy-Boun, P. S.; Villa, G.; Dang, D.; Richardson, P.; Su, S.; Yu, J. Q. *J. Am. Chem. Soc.* **2013**, *135*, 17508. (c) Kalyani, D.; McMurtrey, K. B.; Neufeldt, S. R.; Sanford, M. S. *J. Am. Chem. Soc.* **2011**, *133*, 18566. (d) Duan, P.; Yang, Y.; Ben, R.; Yan, Y.; Dai, L.; Hong, M.; Wu, Y. D.; Wang, D.; Zhang, X.; Zhao, J. *Chem. Sci.* **2014**, *5*, 1574. (e) Park, J.; Kim, A.; Sharma, S.; Kim, M.; Park, E.; Jeon, Y.; Lee, Y.; Kwak, J. H.; Jung, Y. H.; Kim, I. S. *Org. Biomol. Chem.* **2013**, *11*, 2766.
75. (a) Fabry, D. C.; Stodulski, M.; Hoerner, S.; Gulder, T. *Chem. Eur. J.* **2012**, *18*, 10834. (b) Li, Y. M.; Sun, M.; Wang, H. L.; Tian, Q. P.; Yang, S. D. *Angew. Chem. Int. Ed.* **2013**, *52*, 3972. (c) Zhou, M. B.; Song, R. J.; Ouyang, X. H.; Liu, Y.; Wei, W. T.; Deng, G. B.; Li, J. H. *Chem. Sci.* **2013**, *4*, 2690. (d) Zhou, B.; Hou, W.; Yang, Y.; Feng, H. J.; Li, Y. C. *Org. Lett.* **2014**, *16*, 1322. (e) Matcha, K.; R.; Antonchick, A. P. *Angew. Chem. Int. Ed.* **2013**, *52*, 7985. (f) Wei, H. L.; Piou, T.; Dufour, J.; Neuville, L.; Zhu, J. P. *Org. Lett.* **2011**, *13*, 2244. For a review, see: (g) Chen, J. R.; Yu, X. Y.; Xiao, W. J. *Synthesis* **2015**, *47*, 604.
76. Lu, M. Z.; Loh, T. P. *Org. Lett.* **2014**, *16*, 4698.
77. Asscher, M.; Vofsi, D. *J. Chem. Soc.* **1963**, 1887.
78. (a) Shen, T.; Yuan, Y.; Song, S.; Jiao, N. *Chem. Commun.* **2014**, *50*, 4115. (b) Li, X.; Xu, X.; Hu, P.; Xiao, X.; Zhou, C. *J. Org. Chem.* **2013**, *78*, 7343. (c) Meng, Y.; Guo, L. N.; Wang, H.; Duan, X. H.; *Chem. Commun.* **2013**, *49*, 7540.
79. (a) Yang, F.; Klumphu, P.; Liang, Y. M.; Lipshutz, B. H. *Chem. Commun.* **2014**, *50*, 936. (b) Fu, W.; Xu, F.; Fu, Y.; Xu, C.; Li, S.; Zou, D. *Eur. J. Org. Chem.* **2014**, 709. (c) Wei, W.; Wen, J.; Yang, D.; Liu, X.; Guo, M.; Dong, R.; Wang, H. *J. Org. Chem.* **2014**, *79*, 4225.
80. (a) Duncton, M. A. J. *Med. Chem. Commun.* **2011**, ***2***, 1135. (b) Seiple, I. B.; Su, S.; Rodriguez, R. A.; Gianatassio, R.; Fujiwara, Y.; Sobel, A. L.; Baran, P. S. *J. Am. Chem. Soc.* **2010**, *132*, 13194.

81. Tiseni, P. S.; Peters, R. *Angew. Chem. Int. Ed.* **2007**, *46*, 5325.
82. (a) Nishihara, Y.; Ikegashira, K.; Hirabayashi, K.; Ando, J.; Mori, A.; Hiyama, T. *J. Org. Chem.* **2000**, *65*, 1780. (b) Christensen, M. A.; Rimmen, M.; Nielsen, M. B. *Synlett* **2013**, *24*, 2715.